Interdisciplinary Applied Mathematics 42

Heinz Schättler
Urszula Ledzewicz

Optimal Control for Mathematical Models of Cancer Therapies

An Application of Geometric Methods

Springer

Optimal Control for Mathematical Models of Cancer Therapies

Interdisciplinary Applied Mathematics

Problems in engineering, computational science, and the physical and biological sciences are using increasingly sophisticated mathematical techniques. Thus, the bridge between the mathematical sciences and other disciplines is heavily traveled. The correspondingly increased dialog between the disciplines has led to the establishment of the series: *Interdisciplinary Applied Mathematics*.

The purpose of this series is to meet the current and future needs for the interaction between various science and technology areas on the one hand and mathematics on the other. This is done, firstly, by encouraging the ways that mathematics may be applied in traditional areas, as well as point towards new and innovative areas of applications; and, secondly, by encouraging other scientific disciplines to engage in a dialog with mathematicians outlining their problems to both access new methods and suggest innovative developments within mathematics itself.

The series will consist of monographs and high-level texts from researchers working on the interplay between mathematics and other fields of science and technology.

More information about this series at http://www.springer.com/series/1390

Heinz Schättler • Urszula Ledzewicz

Optimal Control for Mathematical Models of Cancer Therapies

An Application of Geometric Methods

Springer

Heinz Schättler
Electrical and Systems
Engineering
Washington University
St. Louis, MO, USA

Urszula Ledzewicz
Mathematics and Statistics
Southern Illinois University Edwardsville
Edwardsville, IL, USA

ISSN 0939-6047 ISSN 2196-9973 (electronic)
Interdisciplinary Applied Mathematics
ISBN 978-1-4939-2971-9 ISBN 978-1-4939-2972-6 (eBook)
DOI 10.1007/978-1-4939-2972-6

Library of Congress Control Number: 2015944982

Mathematics Subject Classification (2010): 49K15, 92C50

Springer New York Heidelberg Dordrecht London

Printed on acid-free paper

Springer Science+Business Media LLC New York is part of Springer Science+Business Media (www.springer.com)

Preface

Cancer is a highly complex disease with a myriad of different manifestations. The reasons for this simply lie not only in the many types of different cells that exist in our bodies, but also in the facts that populations of tumor cells often are highly heterogeneous and, overall, tumor growth depends on many aspects such as interactions with its microenvironment, especially immune response and tumor vasculature. At the same time, there exist many commonalities across various types of cancer that allow for overarching principles to apply. The main treatments, i.e., surgery, chemotherapy, and radiotherapy, as well as more novel approaches that also include antiangiogenic treatments and immunotherapy, apply to a wide spectrum of this disease. Thus, there also exists uniformity that allows us to view the problem of cancer treatment from a more all-embracing perspective. All treatments, while killing cancer cells, also induce toxicity to the healthy cells and thus the natural question arises how therapeutic agents (various drugs, radiation dosages, antiangiogenic biological agents, cancer vaccines, etc.) should be given in order to balance the therapeutic benefits of treatment with its side effects. In order to answer this fundamental question, one needs to understand the processes by which cancer evolves and the effects that treatment has so that therapies can be administered in an optimal, i.e., best possible, way. This book addresses these questions using the methods of optimal control.

Optimal control is a well-researched mathematical field with many applications in engineering, economics, other fields in the sciences and, more recently, also in biology. It deals with the minimization of some performance index imposed on an underlying dynamical system subject to constraints. Controls simply are functions in time that describe allowable outside influences on the system. These induce a system response and, based on this response, an objective function is evaluated, which is taken as a performance measure for the behavior of the system. Optimal controls minimize this criterion. The scheduling of therapeutic agents over time has all the characteristics of such a problem. The aim is to minimize some objective related to tumor burden and quality of life of the patient while the underlying system follows the processes of tumor development and treatment interactions.

In this text, we shall apply the tools and methods from optimal control to analyze various minimally parameterized models that describe the dynamics of populations of cancer cells and elements of the tumor microenvironment under different anticancer therapies. In spite of their simplicity, the analysis of these models that capture the essence of the underlying biology sheds light on more general scenarios and, in many cases, leads to conclusions that confirm experimental studies and clinical data. For example, a treatment strategy for the application of chemotherapy known as "chemo-switch" in the medical literature corresponds to optimal controls that are of the type"bang-singular," and these are shown to be optimal in many of the models considered here.

Our focus is on qualitative information about the structure of treatment protocols. For example, for many tumors it is standard medical practice to give chemotherapy at maximum tolerated doses (MTD) with rest periods in between. These are simply needed for the healthy tissue to recover from the strong toxic attack. The questions we are interested in answering in this text are of the following type: Is this necessarily the best strategy? If not, under what conditions is such a strategy optimal? Are there situations when protocols of a different type should be favored? For example, in a metronomic scheduling of chemotherapeutic agents, i.e., a more or less continuous treatment at substantially reduced dose rates, toxic side effects of treatment are lower, and thus it is hoped that, by being able to give treatment over prolonged periods, better results may be achieved. More generally, the concept of a biologically optimal dose (BOD) as a dose which takes into account the current state of the underlying biological system is an important topic in the medical and pharmaceutical literature. Clinical trials explore the scheduling of therapeutic agents in medically guided, exhaustive, trial-and-error approaches of simple strategies. Hardly ever are more complicated or nonstandard protocols pursued in such research since, quite simply, complex protocols are difficult, if not impossible to test in a laboratory setting, or only at great cost. It is here that the analysis of mathematical models (*in silico*)—an alternative noninvasive procedure—may be of use by giving theoretical guidance as to the structure of treatment protocols or by establishing benchmarks for medically realizable protocols.

While the underlying topic of this text is medical, the tools and techniques that will be used are mathematical with some elementary dynamical systems theory and more advanced methods from optimal control theory at the core of the reasoning. Aside from its biomedical context, the analysis presented has an intrinsic value from the mathematical point of view as interesting and challenging scenarios appear in the analysis of the problem. These include multi-stable behaviors and stability boundaries, the presence of singular arcs in optimal syntheses, optimal chattering controls, and others. The text is written in a self-contained way emphasizing the application of mathematical tools presenting not only results, but also challenges and open questions. We are interested in—as far as this is possible—complete solutions covering a wide range of parameters in order to obtain robust qualitative conclusions. In our view, a qualitative understanding of the structure of all solutions (not just some isolated numerical computations) and their robustness, respectively sensitivity

properties, significantly enhances the understanding of the underlying system. In our analysis, we shall inductively progress from simpler mathematical models that view a tumor as a homogeneous agglomeration of sensitive cells to more complex structures that incorporate varying levels of resistance of the cancer cells and, eventually, to models for combination treatments that model important aspects of a tumor's microenvironment.

Our text is intended for a dual audience. On one hand, we illustrate the applicability of the tools and techniques of optimal control theory to a wide class of problems coming from one particular field. As such, we hope it will be of interest to researchers in mathematics and engineering to whom it introduces a fascinating area of potential applications. On the other hand, this text is also aimed at students and researchers in the applied sciences and the widely understood field of mathematical modeling of cancer treatment. An effort has been made to write the text in a self-contained way to make it accessible to these two possibly disjoint sets of target audiences. Hence, as much as feasible, we included the biomedical background to make the models intelligible to the nonexpert in the field. At the same time, we do not dwell on the theoretical basis for optimal control, but focus on the application of results. There exist several textbooks on optimal control, among them one written by us, where this material is developed, but in this book we only include a concise summary of the required theory in an appendix. Also, in order not to burden the readability for the novice to optimal control theory, some of the more technical computations have been relegated into an appendix. It is our opinion that a student with a solid background in calculus and ordinary differential equations is well prepared to follow the mathematical reasoning. More advanced topics, such as Lie brackets or stable manifolds, are introduced whenever needed in the text.

We would like to take the opportunity to thank our colleagues who have collaborated with us on various topics that form the core of our text. This especially includes Andrzej Swierniak who introduced us to this fascinating topic more than 15 years ago, Alberto d'Onofrio who throughout these years has been our go-to person when we needed some medical clarifications, and Helmut Maurer who helped us out with numerical computations whenever we had reached the end of the road with our methods. Our friend and mentor Avner Friedman has provided us with valuable feedback on several parts of the text. A special thanks also goes to Nicolas André and Eddy Pasquier who have provided us with a wealth of data and information about metronomic chemotherapy. Many of our graduate students have participated in this research over the past 10 years and have in one way or the other contributed to the material presented in this text. Thanks go to John Marriott, Yi Liu, Vignon Oussa, Jim Munden, Benjamin Cardwell, Mohammad Naghneian, Mozhdeh Sadat Faraji Mosalman, Mostafa Reisi Gahrooi, Sia Mahmoudian Dehkordi, Kenneth Bratton, and Behrooz Amini. We also would like to thank our universities, Washington University in St. Louis and Southern Illinois University Edwardsville, and the National Science Foundation that has supported our research at various stages for

by now a good 25 years. Finally, we would like to thank all the editors at Springer, especially Achi Dosanjh, Ana Inoa, Donna Chernyk, and Danielle Walker, who have been so helpful throughout the entire production process. Special thanks are due to a number of anonymous reviewers who carefully read an earlier version of our manuscript and gave us many excellent suggestions.

St. Louis, MO, USA Heinz Schättler
Edwardsville, IL, USA Urszula Ledzewicz
March 2015

Outline of the Chapters of the Text

The text is organized to proceed from simpler to more complex models, both from a modeling and mathematical perspective.

In the introductory Chapter 1, we summarize some of the more important facts that form the *biomedical background* for the mathematical models of cancer development and treatment considered. This includes a discussion of tumor development and the main treatment modalities: chemotherapy and radiotherapy. We also give a short introductory formulation of the principal models to be considered and analyzed in the text.

Cell cycle specific models for cancer chemotherapy are used to introduce some basic modeling premises and are considered in Chapter 2, both for single and multi-drug treatments. These models were originally formulated in the work of Swierniak and co-workers (e.g., [311, 313]) and, under the assumption of exponential growth of the tumor populations, are described by multi-input bilinear control systems. Such systems then will be optimized with the objective to minimize a weighted average of the tumor volume and the total amount of drugs given. The latter is included as an indirect way of measuring side effects. In this chapter, we also discuss the fundamental aspects of drug delivery (pharmacokinetics and pharmacodynamics) and the effects which the inclusion of such models has on optimal controls. This is an important topic to be considered in all mathematical models and will be revisited several times in the later chapters.

An implicit assumption made in Chapter 2 is that the tumor population is *homogeneous* and consists of chemotherapeutically sensitive cells. In this situation, clear answers can be given about the structure of optimal therapy protocols and they consist of maximum tolerated dose (MTD) applications of cytotoxic agents with rest periods, the common practice in medical treatments. However, in reality tumor populations are *heterogeneous* with varying chemotherapeutic sensitivities. These concepts will be incorporated into the modeling in Chapter 3. While this preserves the mathematical structure of multi-input bilinear control systems, now clear-cut answers as to the structure of optimal therapy protocols become elusive as, with increasing drug resistance, the harm done to healthy cells needs to be weighted against the tumor cell kill.

Throughout most of our text, we use as valuation for the effects of treatment an objective functional which is affine in the controls and states, a so-called L_1-type objective. Such a formulation reflects well the biological background. For example, if u denotes the dose rate of a chemotherapeutic agent, then the integral $\int_0^T u(t)dt$ represents the total dose administered, an important medical and pharmacological quantity. On the other hand, also objectives which are quadratic in the controls, so-called *L_2-type objectives*, are commonly used in optimal control formulations of biological models. Such an approach, with its inherent convexity, simplifies the analysis. In Chapter 4, we present the solution for such formulations, also including the analysis of sufficient conditions for local optimality, a topic which is mostly absent in these problem formulations in the literature. We compare solutions for this formulation with some of the solutions for the L_1-type objective functionals that were obtained in Chapter 2.

In the remaining chapters of the text, we consider models that incorporate the most important aspects of the tumor microenvironment, the *tumor vasculature* and *tumor immune system interactions*. In Chapter 5, we consider several models for angiogenic signaling that are based on a mathematical model proposed by Hahnfeldt et al. [116]. We analyze the optimal control problem how to administer an a priori given amount of antiangiogenic agents to minimize the tumor volume. For this problem, we give a complete synthesis of optimal controlled trajectories. Intuitively, such a synthesis acts like *a GPS system showing for every possible state of the system how optimal protocols are administered*, both qualitatively and quantitatively. This gives a global solution of the optimal control problem. Different from the models considered earlier, here it is better to spread the administration schedules of a given amount of agents in time, and this is achieved optimally by time-varying administration schedules defined by so-called singular controls. However, time-varying administration schedules are less practical. For this reason, in Chapter 6, we include an extensive discussion of practically realizable *suboptimal protocols*. In fact, for all the models considered here, excellent simple suboptimal protocols exist.

The model formulations in Chapters 5 and 6 only consider antiangiogenic treatments as a monotherapy procedure. This is an indirect approach that aims to shrink the tumor by depriving it of the vasculature it needs for a supply of oxygen and nutrients. As such, the treatment is only limiting the tumor's support mechanism without actually killing the cancer cells and generally such procedures are less effective. While antiangiogenic monotherapy thus is not considered a viable treatment option, it has become a staple of anticancer treatments in combination with radio- and chemotherapy. In this way, simultaneously two separate compartments of a tumor—the cancerous cells and the vasculature that supports it—are targeted. In Chapter 7, we consider models for such *combination therapies* and it will be seen that the optimal solutions computed in Chapter 5 for the monotherapy problem become the base on which the optimal solutions for the combination treatments are built.

In Chapter 8, then the second major component of a tumor's microenvironment, *tumor immune system interactions*, will be considered. This leads to the emergence of bistable systems with both benign and malignant situations present simultaneously. For various versions of a classical model by Stepanova [303], we formu-

late an optimal control problem whose solutions induce the state of the system to move from the malignant into the benign region. With the mitigating influence of the immune system present, optimal protocols become what are called *chemo-switch protocols* in the medical literature. Such protocols follow an initial phase of maximum tolerated dose treatment with administration schedules at significantly reduced doses. In this chapter, we also formulate a model that combines angiogenic signaling with tumor immune system interactions and analyze its properties under so-called *metronomic chemotherapy*. This is the almost continuous administration of chemotherapeutic agents at significantly lower dose rates than MTD, possibly with small interruptions to increase the efficacy of the drugs. The hope is that, in the absence of limiting side effects, it is possible to give chemotherapy over prolonged time intervals so that, because of the greatly extended time horizon, the overall effect may be improved when compared with repeated short MTD doses.

Finally, two appendices provide additional information which can be looked up, if desired, while reading the main text. A "short course" on geometric methods in optimal control is included as Appendix A, but we refer the interested reader to the literature for proofs of the results (e.g., [31, 38, 217, 292]). Also, in order to make the main text easier to read, some of the more technical mathematical proofs have been relegated into Appendix B.

Generally, we include a fair amount of information on the biomedical aspects and also are at times quite explicit in the mathematical reasoning to make the text accessible to readers from various backgrounds. We hope we accomplished this goal.

Contents

About the Authors

Heinz Schättler is a Professor of Electrical and Systems Engineering at Washington University in St. Louis. He holds a Master's degree in Mathematics from the University of Würzburg in Germany and a Ph.D. in Mathematics from Rutgers University. His main research area is optimal control theory where he has published extensively on applications of methods and tools from optimal control and dynamical systems theory to problems motivated by real life applications. Besides the medical topics that are the focus of this text, these include electric power systems as well as models in economics, physics, and electronics.

Urszula Ledzewicz is a Distinguished Research Professor in the Department of Mathematics and Statistics at Southern Illinois University Edwardsville. She specialized in optimal control theory at the University of Lodz, Poland, where she received a master's and doctorate in Applied Mathematics. Her research interests include optimal control and optimization, mathematical modeling and analysis of systems in biomedicine with special emphasis on mathematical models for cancer growth and treatments. She has been active in the field as an Associate Editor of numerous scientific journals focused on nonlinear analysis, dynamical systems, and mathematical biosciences.

The authors also have published the text *Geometric Optimal Control – Theory, Methods and Examples* (Springer, 2012) and were co-editors for *Mathematical Methods and Models in Biomedicine* (Springer, 2012).

Chapter 1
Cancer and Tumor Development: Biomedical Background

In this introductory chapter, we briefly describe the more important aspects of the medical and biological background for the mathematical models of cancer development and treatment that will be considered and analyzed in this text. Obviously, this merely constitutes a nonexperts' attempt to summarize the major structural features that motivate these models. We focus on the "big picture," with at times full disregard for the myriad and complex details. Yet, it is precisely this highly simplified overall understanding that has motivated much of the historical developments of cancer research and it still defines most current activities in the "search for a cure."

We begin with a brief timeline of the major stages of tumor development (Section 1.1) and, along the way, introduce some of the simpler pieces of the huge puzzle that is mathematical modeling of cancer (Section 1.2). We briefly discuss the main treatment modalities in Section 1.3 and close with posing important questions about the structure of treatment protocols as an optimal control problem (Section 1.4).

1.1 Tumor Development

1.1.1 The Cell Cycle and the Origins of Cancer

The building blocks of all life are cells and cells constantly reproduce in the cell cycle through cell division (see Figure 1.1), the main mechanism of our body that governs growth and development. The general term "cancer" refers to an enormously large family of high-mortality diseases, widely differing from each other in their individual aspects and manifestations, but all having in common a derangement of cellular proliferation that originated at some time in the past with mistakes in the process of cell duplication. In the transition from cell birth to cell division, each cell passes through a complex and tightly regulated sequence of molecular events that

H. Schättler, U. Ledzewicz, *Optimal Control for Mathematical Models of Cancer Therapies*, Interdisciplinary Applied Mathematics 42,
DOI 10.1007/978-1-4939-2972-6_1

is encoded in our DNA (deoxyribonucleic acid) and executed by proteins. In a first growth phase G_1, mainly the synthesis of enzymes that are needed for DNA replication is carried out and the cell grows in size. Embedded in the cell cycle are various check points (control mechanisms) set up to verify that these processes have been adequately completed before the next phase of the cell cycle commences. One such checkpoint is located at the end of the G_1 phase where it is checked whether DNA was damaged in the process and whether environmental conditions (e.g., supply of oxygen and nutrients) are adequate for cell duplication. At this point, decisions are made whether the cell should proceed with the cell cycle to division or delay division and enter a resting stage G_0. The latter is a phase in the cell cycle where the cell neither divides nor prepares for division and is also called the quiescent state. In fact, many cells are arrested in the cell cycle at the G_1-checkpoint. Otherwise, if conditions are right, the cell enters a phase S where DNA synthesis occurs. When it is complete, all of the chromosomes have been duplicated and each chromosome has two copies, essentially doubling the amount of DNA in the cell. After that a second growth phase G_2 commences in which the cell synthesizes further cellular components such as microtubules that are needed for mitosis. At the end of the G_2 phase, there is a second major check point to ensure the cell is ready for mitosis. If this checkpoint is passed, the cell enters phase M. Here cell growth stops and mitosis occurs. This is the orderly division of the mother cell into two daughter cells containing roughly equal shares of the cellular components and in itself is a highly complex process consisting of various subphases. During an intermediate checkpoint in mitosis, the metaphase checkpoint, it is verified that all the chromosomes are properly aligned on the mitotic spindle. If all checkpoints are passed, cell duplication commences. Ideally, the two daughter cells are genetically identical to each other and to their parent cell, but errors in mitosis can either lead to cell death through apoptosis or cause mutations which eventually might lead to cancer. Each of the two daughter cells then reenters the cell cycle and thus starting the entire process all over again.

Cell duplication is a tightly regulated molecular mechanism in which various types of proteins (the so-called *cyclins*) control the transitions through the phases of the cell cycle. Naturally, there exist many possibilities for things to go wrong in such a complex and lengthy chain of events—and this happens on a regular basis. Quite simply, as with any other highly complex system, this is unavoidable. Of course, as medical research has established, the chances for matters to go wrong are significantly higher if we live in an unhealthy environment or if cells are exposed to detrimental factors introduced into our bodies such as tobacco. But given the overall complexity of the process, life has developed many safeguard and rescue procedures specifically designed to deal with mistakes during cell duplication. At numerous checkpoints in the cell cycle, and only the most important ones were mentioned above, both external factors (e.g., environmental conditions related to the available amounts of oxygen and other nutrients) and internal factors (such as whether chromosomes have arrived to the mitotic plate in mitosis) are verified and, in theory, only if conditions are right, cells are allowed to pass from one phase into the next. All in all, the regulation of the cell cycle includes numerous control

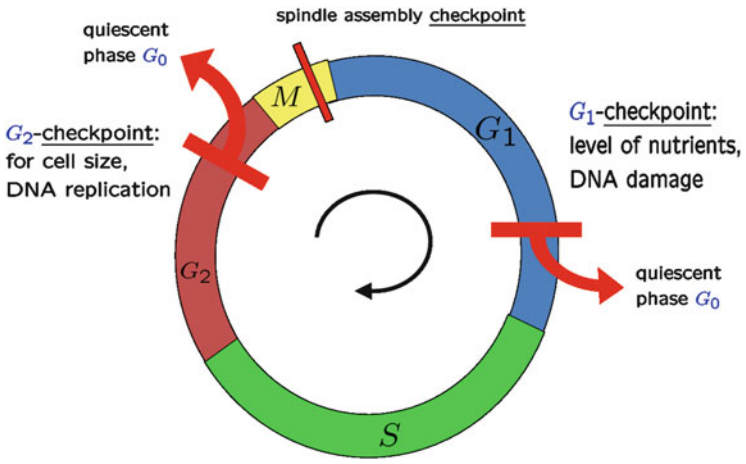

Fig. 1.1 Schematic representation of the cell cycle and its main check points.

mechanisms that detect and possibly repair genetic damage and are crucial for the survival of a cell.

Many of these mechanisms are connected with the actions of a specific protein, $p53$, that, because of its importance as a suppressor gene in the cell cycle, has been labeled "the guardian of the genome." It is involved in various functions within the regulatory mechanisms of the cell cycle: it activates DNA repair proteins when DNA has sustained damage, it induces cell arrest at the G_1-checkpoint holding the cell so that DNA repair proteins are given time to fix the damage and, if DNA damage proves to be irreparable, it initiates *apoptosis*. This is programmed death of the affected cell, itself again a complicated sequence of molecular mechanism. There exist several mechanisms which all under certain conditions initiate the command for a cell to self-destruct and then execute this procedure. In lay-person terms, cells die by suicide. The most important protein involved in these sequences of commands (molecular signaling pathways) is $p53$. In many forms of cancer, the disease can be traced to a series of mutations that occurred in cell duplication and had the effect to inhibit and disable these regulatory pathways. While dysfunctional cells (cells that do not fulfill their regular preprogrammed functions) which are produced in cell division simply will be eliminated from our body under normal circumstances, in the case of a cancerous cell these mechanisms become disabled and, in a weird sort of way, the cell becomes "immortal." Indeed, it is one of the important characteristics of a cancer cell, or "hallmarks" as medical researchers say, that, for whatever reason, it escapes the regulatory control mechanisms of the cell cycle that should eliminate it. Typically a so-called *cancer stem cell* is not caused just by a single mutation, but, being genetically unstable, in a sequence of progressive genetic changes which then enable these cells to undergo uncontrolled abnormal mitosis and increase the total number of cancer cells at that location.

Yet, even if the control mechanisms of the cell cycle prove ineffective, this does not necessarily mean that the medical disease that is called cancer has to develop. As with any complex system, the more checkpoints, the better. There exist additional mechanisms that lie outside of the cell cycle and enable the body to deal with renegade cells. One of these is activation of the immune system. It has been hypothesized for a long time, and also been backed up by medical evidence [72], that the immune system has the capability to control cancerous cells in early stages of the disease in a form of *immunosurveillance*. But, as cancer cells are part of our body, there are also situations when the immune system does not react or when its reaction simply is inadequate to overcome the initial cancerous growth. Still, if for whatever reason cancer cells do not duplicate, or grow so slowly that they never become a problem, the disease that generally is called cancer, does not materialize. In this sense, small 'tumors' are prevalent in all of us. For example, there are discussions about prostate cancer to the effect of whether screening and treatment (which has severe adverse side effects) should really be such an important part of prevention as they currently are. The argument is being made that for this generally very slowly growing tumor that mostly effects elderly men, it may simply be best to do nothing since the chances that tests based on PSA (prostate specific antigen) come up with false positives are actually unacceptably high, and, even if prostate cancer is present, no serious malignancy might develop in the patient's lifetime anyway. Clearly, for some patients this will not be valid, but current medical research does not give any indication as to where the boundary should be drawn.

Summarizing, mistakes in cell duplication are common, but no harm is done if any of the body's inherent control mechanisms succeeds in eliminating the initial dysfunctional cell. It is only if such *a cancerous cell persists, starts to duplicate, eventually escapes regulatory mechanisms, and growth gets out of control* that the disease that is called *cancer* occurs, i.e., the *"uncontrolled growth of abnormal cells in the body."* In more medical terms, in the paper [119] by Hanahan and Weinberg the following "hallmarks" of cancer are identified: "sustaining proliferative signaling, evading growth suppressors, resisting cell death, enabling replicative immortality, inducing angiogenesis, and activating invasion and metastasis."

1.1.2 A Rudimentary Classification of Tumors and their Development Stages

Medicine distinguishes over 200 types of cells that vastly differ in their numbers and functions [5]. For example, red blood cells transport oxygen and nutrients with over 2 million of them newly produced every second [288], brain cells consist of neurons (electrically excitable cells that receive, process and transmit information) and glia that support and protect the functions of neurons, plasma cells produce antibodies, gland cells secrete hormones, and other substances like saliva, and many more types of cells make up our bodies. Depending on which type of cell and which organ is affected, and possible variations of the mutations that actually occur, there

exist hundreds of types of cancers which in principle all exhibit different characteristics and are very different diseases with their own treatment options. But there are also common characteristics in their development and the word *tumor* (which is the Latin word for "being swollen" derived from *tumere*, "to swell") is commonly used for any abnormal growth of cells. In medicine, broadly one distinguishes between *solid tumors* that form a well-defined mass, grow in organs and can occur almost anywhere in the body (e.g., kidney, prostrate, etc.) and *liquid tumors* that occur in the blood (e.g., leukemia, glioma, lymphoma, and myeloma). Some models considered in this text (e.g., all those considered in Chapter 2) will be general, others will only be applicable for solid tumors and we give a brief description of the main phases of development of a solid tumor. These are avascular growth, tumor angiogenesis, and metastasis.

Avascular growth is the first stage of tumor growth. As it develops, a tumor needs a steady supply of oxygen and nutrients for cell duplication. Initially, this supply is adequately provided by the surrounding environment through diffusion. At the onset of the disease, since tumor cells are dysfunctional and do not partake in any kind of regular tasks, cells cluster together and form a coherent parasitical unit, often growing in a small spherical shape. Over time, cells toward the center become deprived of the necessary nutrients to divide further and develop a necrotic core of dead cells [8, 227]. Proliferating cells generally are only found in the outermost cell layers with a band of quiescent cells lying between these two regions [79]. Faced with a shortage of nutrients, tumor cells that enter the dormant or quiescent stage of the cell cycle trigger the release of vascular endothelial growth factor (VEGF) and other stimulating agents that promote the creation of a network of blood vessels and capillaries designed to provide the tumor with necessary nutrients, the *tumor vasculature*. The importance of this network in tumor development was already stressed in the early 1970s by J. Folkman [85, 86] who pointed to this vascular support system as a possible target of tumor treatment. It is now generally recognized that primary solid tumors require such a network in order to grow beyond 2 mm^3 in volume. The creation of this vascular network is called *tumor angiogenesis* after the Greek words $\alpha\nu\gamma\varepsilon\iota\sigma\nu$ (angeíon, "vessel, urn") and $\gamma\varepsilon\nu\varepsilon\sigma\iota\varsigma$ (genesis, "origin, source, beginning"). Tumor angiogenesis is sustained by various mechanisms: tumors coopt existing vessels, induce the formation of new vessels from pre-existing ones, and exploit endothelial precursors originating from the bone marrow [87, 89]. Overall, this is a complex process characterized by both proangiogenic agents such as VEGF and antiangiogenic chemicals that are released by the tumor in order to modulate the growth of the vessel network. A solid tumor thus deploys a sophisticated strategy based on reciprocal signaling between endothelial cells (which form the lining of the newly formed vessels and capillaries) and tumor cells to control its own growth through a balance of stimulatory and inhibitory mechanisms that are regulated through microenvironmental factors [90, 66]. It is the fact that endothelial cells have receptors that make them sensitive to inhibitors of inducers of angiogenesis that is one of the main modi operandi behind antiangiogenic therapies with simple disruptions of the signaling processes the other. All aim to deprive the tumor of the vasculature that it needs for vigorous growth by inhibiting and

destroying endothelial cells which provide the lining for the newly forming blood vessels. These cells thus are the main target of antiangiogenic therapies.

Once the tumor succeeds in developing its own vasculature, it has gained access to the needed supply of oxygen and nutrients via the blood stream and undergoes vigorous growth. In time, the size becomes large and incoherent enough that small parts of the tumor break off and travel through the bloodstream to other organs and parts of the body. This last stage of tumor development is called *metastasis* after the Greek word for "displacement" derived from $\mu\varepsilon\tau\alpha$ (meta, "next") and $\sigma\tau\alpha\sigma\iota\varsigma$ (stasis, "placement"). In the medical literature, the original tumor is called the primary tumor while the newly formed secondary tumor is called a secondary or metastatic tumor. Since the type of cancer is defined by the type of cell it originated with, the type of cancer on the secondary site is the same as in the original one. Metastasis, along with increased cell duplications and invasiveness, is one of the main characteristics of a *malignant* tumor. In contrast, a tumor that does not grow uncontrollably, does not invade neighboring tissues and does not spread throughout the body is called *benign*. If the cancer has spread to other parts of the body, survival chances are greatly diminished and treatment options are limited with chemotherapy remaining the predominant option.

1.1.3 The Tumor Microenvironment

Immense progress has been made in the fields of medicine and molecular biology which indicates that the great complexity of tumor behavior on the macroscopic level reflects the intricacy of its underlying deregulating biochemical mechanisms on the microscopic level. Other aspects contribute to this complexity as well. At an intercellular level, tumor cell populations act as ecosystems [102, 299] and many sources of complexity arise from internal cell-to-cell cooperative and competitive interactions [254]. Interactions, that are critically relevant for the survival of a cancer, are its relationships with external cell populations, such as blood vessels, lymphatic vessels, and with the cells of the immune system. The responses of tumor cells to these interactions are characterized by a considerable evolutionary ability via changes by means of mutations to enhance their survival in a hostile environment. Cancer thus is a disease with myriad manifestations whose macroscopic time course reflects complex, strongly nonlinear, inter- and intra-cellular phenomena. For all these reasons, the view of a tumor as a homogeneous collection of roughly equal and sensitive cells has been replaced with the understanding that *tumors are heterogeneous aggregations not only of cancer cells of various types of sensitivities, but also of many other types of healthy cells that make up its stroma*. This is the connective and functionally supportive framework that forms a tumor's microenvironment. Its main components comprise the tumor vasculature (e.g., endothelial cells), all kinds of cells of the innate immune system (T-cells, myeloid immune cells, macrophages, and many more), and fibroblast cells that form the intracellular matrix.

In this text, *we shall inductively progress from simpler mathematical models that view a tumor as a homogeneous agglomeration of sensitive cells to more complex structures that incorporate varying types of sensitivities of the cancer cells, the tumor vasculature, tumor immune system interactions, and eventually lead over to multi-compartment models for combination treatments that model important aspects of a tumor's microenvironment*.

1.2 Mathematical Models of Tumor Growth

Mathematical models for cancer development and treatment are often constructed in a modular way starting with pieces that broadly describe the major aspects of the disease and then adding increasingly more complex features as additional building blocks. One of the integral pieces in any such configuration becomes the model for tumor growth. In view of all the complexities that only were briefly touched upon above, it should be clear that it is not possible to devise one mathematical model that describes the full development of cancer in time. Naturally, existing models all have limited validity, limited both to specific stages in the tumor time line and also to specific forms of the disease. The recurrent question which model is more realistic simply is ill-posed and has no correct answer [227]. Populations of cancer cells of different types and/or in different conditions may behave very differently. Any macroscopic growth law that is derived by aggregating cell populations therefore has to mirror a set of phenomena that occur at the cellular scale including metabolic processes and cellular interactions that vary considerably from case to case [239, 254]. It should not be surprising at all that models of cancer growth are very diversified.

We introduce the main types of mathematical models that are commonly used to describe tumor growth. To begin with, a phenomenological model (i.e., a model according to our perception and interpretation of events) that describes the growth of a population of cells may simply be written in the general form

$$\dot{p} = pF(p) \tag{1.1}$$

where p denotes the size of the population (measured in terms of volume, number of cells, density of cells, etc.) and $F(\cdot)$ models its net proliferation rate, i.e., the difference between the proliferation rate $\pi = \pi(p)$ of the cells and their death rate $\mu = \mu(p)$ governed by apoptosis. Generally, it is difficult to infer the proliferation rate π and death rate μ separately from experimental data and thus often the net proliferation rate F is used.

1.2.1 Exponential Growth

Over a short time interval, and under relatively constant environmental conditions, it is reasonable to assume that the proliferation and death rates are constant and in

such a case the growth law becomes exponential [343] of the simple form

$$\dot{p} = \xi p \tag{1.2}$$

with ξ a growth parameter. If the initial tumor volume at time $t = 0$ is given by p_0, then the tumor population evolves as

$$p(t) = e^{\xi t} p_0$$

and the tumor growth rate ξ relates to the tumor doubling time T as

$$\xi = \frac{\ln 2}{T}.$$

This is a commonly used model for tumor growth during avascular and early vascular growth, but it is not adequate over long time periods since generally the net proliferation rate $F = F(p)$ decreases as a function of p with the growth of the population. The rationale behind this assertion simply is that with limited amounts of oxygen and nutrients available and increased competition for these resources, the proliferation rate π decreases as a function of the population size while the death rate μ increases. If there exists a point q where these two rates agree, $\pi(q) = \mu(q)$, then q becomes an equilibrium point for the dynamics (1.1) and, since the initial population is small, this value q provides an upper limit for the population size. This value q is called the *carrying capacity* of the population and represents its theoretically maximal sustainable size. Unfortunately, in the vast majority of cases for tumors, this value q well exceeds values compatible with the life of the host. Initially, for a small tumor size, $p \ll q$, higher-order terms in an expansion of F can be neglected, and thus an exponential growth law is appropriate and mathematically it simply represents a local linearization of the true underlying system. However, as the tumor grows, the neglected terms matter and the model needs to be adjusted. Commonly used models then are the so-called logistic and Gompertzian growth functions.

1.2.2 Gompertzian Growth

Because of its experimental support in data for breast cancer [244, 245, 247], the Gompertzian growth law, introduced in 1825 as a demographic model for mortality by Benjamin Gompertz, and although controversial in some of its aspects, is one of the most commonly used equations to describe tumor growth in its latter stages [343]. The net proliferation rate is modeled in the form

$$F(p) = a - b\ln(p), \qquad a > b > 0, \tag{1.3}$$

with the parameter a representing a baseline proliferation rate (summarizing the effects of mutual inhibition between cells and competition for nutrients) and the coefficient b a growth retardation factor that impedes the growth for large tumor volume. Normalizing the initial tumor volume to $p(0) = 1$, the resulting differential

equation for the tumor volume becomes

$$\dot{p} = p\,(a - b\ln(p))\,.$$

This is a linear differential equation in the variable $y = \ln(p)$,

$$\dot{y} = a - by, \qquad y(0) = 0,$$

with solution given by

$$y(t) = \frac{a}{b}\left(1 - e^{-bt}\right).$$

Thus the tumor volume is given by

$$p(t) = \exp\left(\frac{a}{b}\left(1 - e^{-bt}\right)\right)$$

and has the double exponential structure typical of the Gompertz law. The normalized carrying capacity is $q = \exp\left(\frac{a}{b}\right)$ and it is more convenient and nowadays common to rewrite F in the form

$$F_G(p) = \xi \ln\left(\frac{q}{p}\right) = -\xi \ln\left(\frac{p}{q}\right) \tag{1.4}$$

with the coefficient ξ $(= b)$ the growth parameter that determines the rate of convergence of p to q. An example of the Gompertz growth function F_G is given in Figure 1.2 for $a = 1$ and $b = 5$.

The Gompertzian growth law is reasonable for large tumor volumes that possibly approach the carrying capacity, but it clearly is inadequate for small tumor volumes when its proliferation rate approaches infinity and this is not realistic. Any growth law that has a relative growth rate $\frac{\dot{p}}{p}$ that tends to ∞ as the size p tends to zero is not valid for describing the growth of small aggregate tumors since their doubling time, a quantity related to the complex biological processes in the cell cycle and apoptosis, cannot be arbitrarily small [248, 343].

1.2.3 Logistic and Generalized Logistic Growth

A second classical phenomenological growth model that is based on competition between processes associated with proliferation and death is the ubiquitous generalized logistic law,

$$F_L(p) = \xi\left(1 - \left(\frac{p}{q}\right)^{\nu}\right), \qquad \xi > 0,\ \nu > 0. \tag{1.5}$$

The classical model of logistic growth ($\nu = 1$) was introduced in 1838 by Verhulst in his studies of population growth to describe a self-limiting biological population

under the assumption that the rate of reproduction is proportional to both the existing population and the amount of available resources. The generalized version with an arbitrary exponent $\nu > 0$ goes back to the work of Richards in the 1930s and it allows to differentiate between slowly and fast growing cancers. The higher the exponent ν is, the faster the tumor grows with the exponential growth law the limit as $\nu \to \infty$. The differential equation

$$\dot{p} = \xi p \left(1 - \left(\frac{p}{q}\right)^{\nu}\right), \qquad p(0) = p_0, \tag{1.6}$$

is a Bernoulli equation that can be integrated explicitly (e.g., see [34, 163]) and has, as is easily verified by differentiating, the solution

$$p(t) = p_0 \left[\left(\frac{p_0}{q}\right)^{\nu} + e^{-\nu\xi t}\left(1 - \left(\frac{p_0}{q}\right)^{\nu}\right)\right]^{-\frac{1}{\nu}}.$$

Note that, for small ν, we have the expansion

$$\frac{1-x^{\nu}}{\nu} = \frac{1-\exp(\nu\ln(x)))}{\nu} = \frac{1-(1+\nu\ln(x)+O(\nu^2))}{\nu} \approx -\ln(x) + O(\nu)$$

and thus, if the growth coefficient ξ is made to depend on the parameter ν in the order of $\xi = O(\frac{1}{\nu})$, then the Gompertzian growth function can be recovered in the limit as $\nu \to 0^+$ (from the right). We use the standard Landau notation $O(x^{\alpha})$ to denote functions f of x that have the property that the quotient $\left|\frac{f(x)}{x^{\alpha}}\right|$ is bounded as $x \to 0$. Note that the growth function F is strictly convex, i.e., its second derivative is positive, $F''(p) > 0$, for $\nu < 1$ and strictly concave for $\nu > 1$, $F''(p) < 0$. We illustrate the functions F_L and their corresponding solutions in Figure 1.2 for the values $\nu = \frac{1}{2}, 1$ and 2. A higher exponent causes the system to approach its carrying capacity faster.

1.2.4 Other Growth Models

All of these phenomenological models were obtained through qualitative reasoning and then, for specific cases, validated by means of data fitting with some of them remarkably successful in data-based validation, e.g., [247, 25]. While these are the more commonly used mathematical models for population growth, many other models exist (e.g., see [112, 124, 254]). We only briefly mention the following simple modification of the Gompertzian and logistic models by Wheldon [343] that uses a Gompertzian, respectively logistic growth law above a certain threshold C while retaining a simple exponential growth for smaller tumor sizes, i.e.,

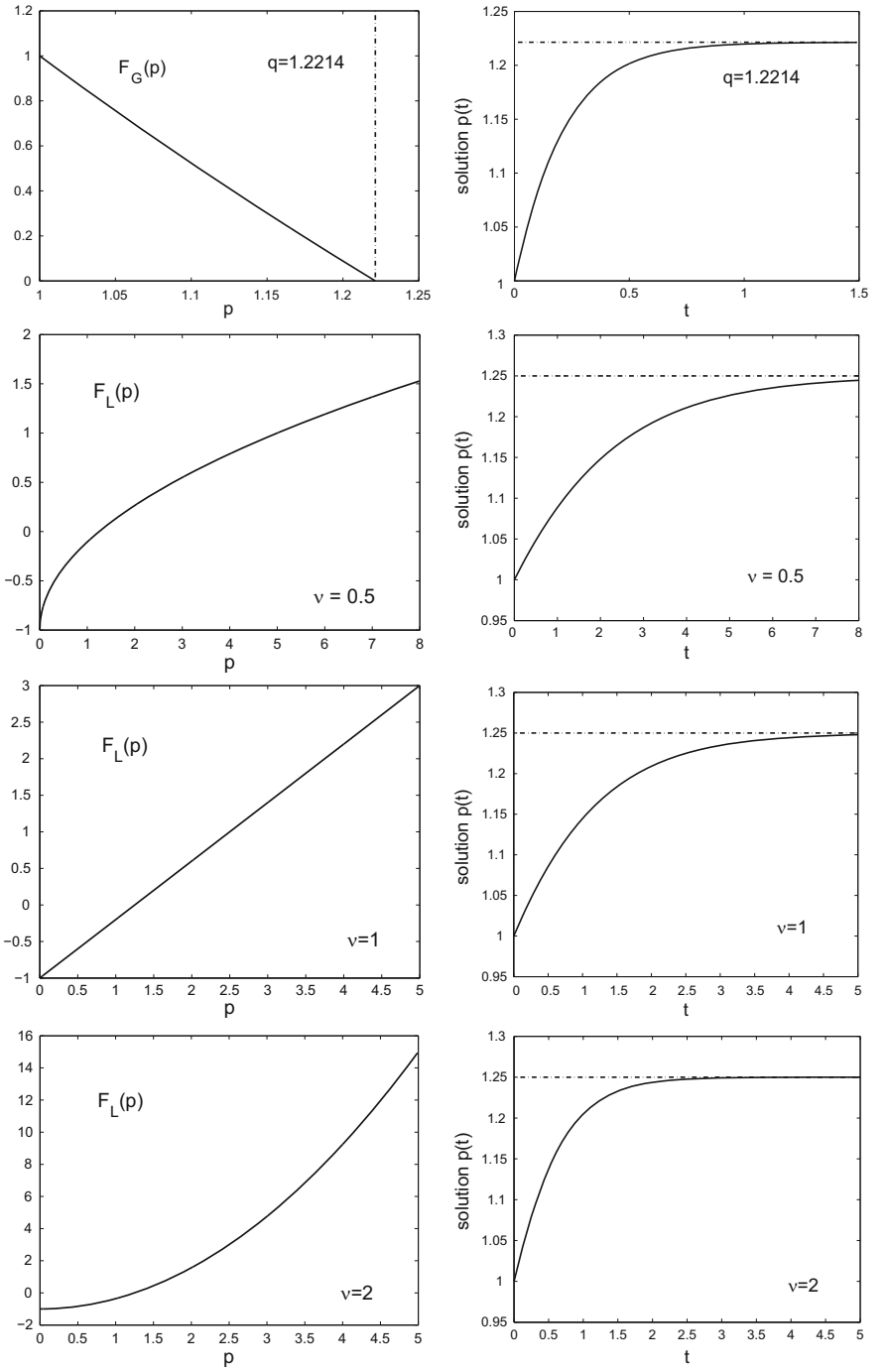

Fig. 1.2 Examples of Gompertzian and generalized logistic growth functions with corresponding responses.

$$\dot{p} = \begin{cases} p(a - b\ln(C)) & \text{for } 0 < p \leq C, \\ p(a - b\ln(p)) & \text{for } C \leq p. \end{cases} \tag{1.7}$$

This automatically stabilizes the ratio $\frac{\dot{p}}{p}$ for small populations regardless of the specific measurement of the tumor size used (e.g., volume, number of cells, etc.), a desired feature.

The argument can be made that all of these models reproduce at a larger degree of approximation finer microscopic details, for example, of intercellular inhibitions. The simple and plausible model in [239], that is based on the realistic hypothesis of long range interactions between cells in a population whose structure is fractal, introduces a mechanistic theory that links macroscopic phenomenological models of this type to microscopic interactions and parameters. This approach allows to make an argument that the various and at times seemingly contradictory *growth models are simply macroscopic different manifestations of a common physical microscopic framework* [254]. In other words, different values of the parameters of the microscopic law result in different analytical laws for $F = F(p)$. Thus, while one of these models may be more appropriate for a specific medical situation (dependent, for example, on the time of development of the tumor or a specific disease), in principle, they all become viable options in the investigation of the development of a tumor under treatment. In this text, various forms of these models will be used.

1.3 Treatment Approaches: An Overview

The main objectives of cancer treatments are two-fold: *curative* and *palliative*. Clearly, if feasible, complete eradication of the tumor is sought and for certain types of cancer this is a realistic and a viable option. For example, in kidney cancer, if the tumor remains encapsulated, removal of the kidney generally eliminates the disease. In other situations, a total cure is unrealistic and then the objective becomes to manage the disease, delay its further progression or maintain it at a tolerable level and alleviate the symptoms. For types of cancer that are still largely not curable, the objective simply becomes to improve the quality of life and survival probabilities by avoiding life threatening toxicity. These are the objectives of palliative care.

But at large, the main objective of cancer treatments is to eradicate the disease. In case of a solid tumor, if possible, the clear first choice of treatment is removal via surgery. The only reason when this will not be pursued is if there would be too much collateral damage. For example, in brain tumors often the risk of lethal damage to vital brain functions becomes limiting. Besides surgery, the main standard treatment approaches to destroy tumors are by means of radiation and drugs. In radiotherapy, guided by medical imaging techniques, it is attempted to destroy the tumor with carefully directed radiation beams. It is estimated that about one half of all cancer patients receive radiotherapy during their course of treatment, either as primary procedure or in conjunction with surgery and chemotherapy [235]. But the most common treatment approach, and in spite of its many negative side effects,

still is chemotherapy. Especially if the cancer has already metastasized, chemotherapy often is the only available option. Various types of drugs are being used whose underlying basic premise simply is to prevent further cell divisions. For example, *spindle poisons* stop the production of new cells by interrupting mitosis at the spindle assembly checkpoint. On the other hand, if the cancer is already progressed far, then such an action may simply not be adequate anymore and it really becomes important to induce apoptosis and kill existing cancer cells like, for example, in metastatic gastrointestinal cancers. However, many commonly used cancer drugs such as paclitaxel do not necessarily induce apoptosis.

Even if the primary tumor can be removed by means of surgery or radiotherapy, microscopic and undetectable metastases may exist which, if left untreated, will grow and may lead to the recurrence of the disease. This may actually happen in an accelerated form, for example, because the removal of the primary tumor may lead to down-regulated activities of the immune system which, before on high alert because of the existing tumor, was able to control small existing metastases. Thus, in order to eradicate remaining microscopic tumors after surgery, and for other reasons, for many types of cancer it becomes necessary to treat a patient with adjuvant (preventive) chemotherapy after surgery. This is commonly done, for example, in cases of breast cancer or colorectal cancers. But chemotherapy has severe side effects and only all too often, in the end it does not work. In the terminal stages of the disease, adverse effects of strong chemotherapy may in fact lead to death. Another all to common scenario is that some cancer cells within the tumor, because of the great genetic variety of tumor cells, are intrinsically resistant to the action mechanisms of cancer drugs or, in the course of time, once again because of their great genetic instability, acquire such resistance as a response to treatment. In these cases, "selection of the fittest" works to our disadvantage. Over time, these partially or fully resistant cell populations grow into the dominant portions of the tumor (as sensitive tumor cells are eradicated by the treatment) leading to failure of chemotherapy. This may possibly only happen after many years of seeming recession of the disease. Indeed, drug resistance has been called the "curse of chemotherapy" [141] and only all too often is the limiting factor in the therapy.

For this reason, modern therapies target not only the cancer cells, but also the various support mechanisms that control tumor growth. Rather than just aiming at destroying the cancerous cell, these multi-target approaches aim at the *tumor microenvironment*. Antiangiogenic treatments disrupt the signaling mechanisms the tumor gives to stimulate the development of its own vasculature or directly inhibit the growth of endothelial cells that form the lining of the vessels and capillaries that support the tumor with oxygen and nutrients. Because they only target the tumor indirectly through the genetically much more stable endothelial cells, these treatments are much less prone to drug resistance and were of great promise for this reason. However, an indirect action alone often seems to be inadequate and thus this promise is still largely unfulfilled. Other approaches, known collectively as immunotherapy, try to recruit the immune system into a stronger reaction against the cancer. New ideas and approaches such as cancer viruses are coming to the forefront of medical research all the time and the search for novel treatment approaches

in cancer is an ongoing activity that will remain with us until significant progress has been made in the elusive "cure of cancer," the holy grail of science.

In this section, we briefly describe the main rationales behind radiotherapy, chemotherapy, antiangiogenic treatments, and immunotherapy and introduce the types of mathematical models that will be used in this text to model and analyze cancer treatment modalities.

1.3.1 Radiotherapy

Radiotherapy is the medical use of ionizing radiation to kill malignant cells. It may be curative if the cancer is well localized to one area of the body, but it is also used in synergy with surgery and chemotherapy to prevent recurrence of the tumor. Ionizing radiation damages the DNA of exposed tissue leading to loss of reproductive functions of the cell. Generally, cells that lose their reproductive capabilities are considered "dead" since they no longer are able to produce a large colony of daughter cells. In radiotherapy, one distinguishes between *brachytherapy*, where a radioactive probe is inserted into the body close to the tumor, and *external beam radiation*, still the more common of the two procedures. To spare normal tissues (such as skin or organs through which radiation must pass in order to treat the tumor), shaped radiation beams are aimed from various angles to intersect at the tumor site giving it a larger absorbed dose than the surrounding, healthy tissue. Naturally, it is necessary to include some margin of normal tissue around the tumor in the treated region simply to allow for uncertainties that may be due to equipment set-up, but also due to unavoidable internal movements of the patient, for example caused by breathing and other bodily functions.

Based on a wealth of experimental data, several mathematical models have been proposed to model cell death and cell survival during radiotherapy. These models describe the fraction of surviving radiated cells as a function of the radiation dose with the so-called *linear-quadratic (LQ) model* [94, 329] having become the standard. It expresses the *probability of cell survival* in the form

$$\exp\left(-\alpha D - \beta D^2\right) \tag{1.8}$$

where D denotes the total radiation dose and α and β are radiosensitive parameters that depend on the tissue that is being treated. Radiation is measured in Gray with 1 Gy being the amount of radiation required to deposit 1 *Joule* of energy in 1 kg of matter. It relates to the historically used unit of *rad* (radiation absorbed dose) by the simple formula that 1 $Gy = 100$ *rad*. The parameters α and β carry units of $[Gy^{-1}]$ and $[Gy^{-2}]$, respectively. The quotient $\frac{\alpha}{\beta}$ is used to differentiate between various types of tissue and often can be determined more accurately than α and β separately. Note that the contributions of the linear term, $e^{-\alpha D}$, and the quadratic term, $e^{-\beta D^2}$, are equal for $D = \frac{\alpha}{\beta}$. Essentially, the parameter $\frac{\alpha}{\beta}$ determines the shape of the single-dose survival curve (see Figure 1.3) with a higher quotient leading to a larger survival fraction. For fast dividing cells, also called the *early responding*

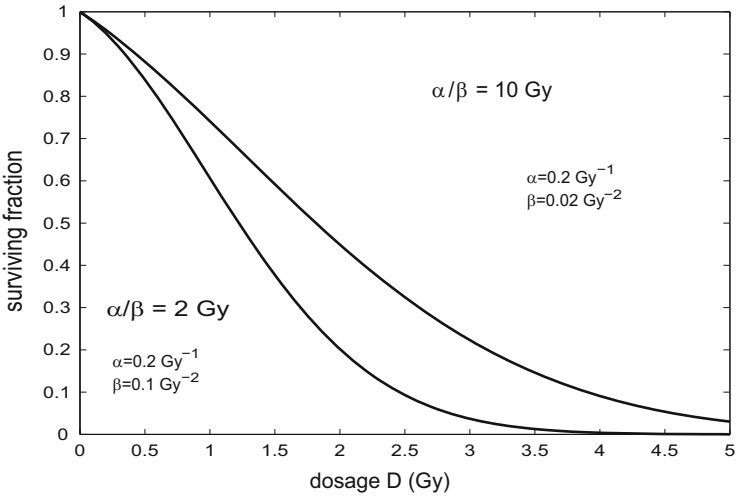

Fig. 1.3 Cell survival probability for the linear-quadratic model under a single dose D.

tissue, this value can be as high as 10 while it is around 3 for most normal tissue, the *late responding tissue*.

There exist numerous theoretical justifications for the linear-quadratic model in the medical literature, among them the classical model by Chadwick and Leenhouts [53]. Radiation causes abnormalities (in medical terms, *lesions*, Latin: *laesio* - injury) that correspond to ruptures of the molecular bonds on the double-stranded DNA. This damage is made up of two components: (i) simultaneous breaks in both DNA strands that are caused by a single particle and (ii) two adjacent (both in location and time) breaks on separate strands. While a double-strand break is assumed to lead to loss of proliferative abilities, a single strand breakage is not considered lethal since DNA has the ability to repair it. Only if a second adjacent break occurs on the other strand before the first one can be repaired, this will lead to loss of proliferation properties. Both scenarios (i) and (ii) are considered lethal in the sense that the cell is no longer able to proliferate. The first situation leads to a linear term in the cell survival model while the second one contributes quadratic terms. We briefly outline the argument.

Consider a single event and let κ denote the fraction of DNA strand breaks that occur per unit dose. These can be either double-strand breaks or only on a single strand. Split these lesions into a fraction q that are double-strand breaks with the remaining fraction $1-q$ generating single-strand breaks. First consider the double-strand breaks and let N_0 denote the initial number of critical molecular bonds that are susceptible to a double-strand break (DSB) under radiation. The number $N = N(D)$ of critical bonds that remain intact after dose D is assumed to follow an exponential law of the form

$$\frac{dN}{dD} = -q\kappa N, \qquad N(0) = N_0,$$

with the number of critical bonds that remain intact at dose D given by $N_0 e^{-\kappa q D}$. Assuming that the proportion of lesions that can be repaired is given by ρ_0, so that $\varphi_0 = 1 - \rho_0$ is the proportion of unrepaired lesions, it follows that the number of double-strand breaks caused in one event is given by

$$N_{DSB} = \varphi_0 \left[1 - \exp(-\kappa q D)\right] N_0. \tag{1.9}$$

Similarly, let N_i, $i = 1,2$ denote the number of critical bonds susceptible to a single-strand break on one of the two strands, labeled 1 and 2. Then, analogously, the number of single-strand breaks on each of the strands is given by

$$N_{SSB,i} = \varphi_i \left[1 - \exp(-\kappa(1-q)D)\right] N_i, \qquad i = 1,2.$$

Assuming statistical independence of these events, the number of double-strand breaks generated by two adjacent single-strand breaks can thus be modeled as

$$N_{adjSSB} = \varepsilon \varphi_0 \varphi_1 \varphi_2 \left[1 - \exp(-\kappa(1-q)D)\right]^2 N_1 N_2 \tag{1.10}$$

where ε denotes a factor that represents the likelihood that two single-strand breaks are sufficiently close to each other (in time and space) for a double-strand breakage to occur and, as in (1.9), φ_0 denotes the fraction of these lesions that are not repaired. Assuming in addition that there is only a proportion p of breaks that are lethal, and combining (1.9) with (1.10), the total number of lethal double-strand breaks is given by

$$N_{lethal} = p\varphi_0 \left(\left[1 - e^{-\kappa q D}\right] N_0 + \varepsilon \varphi_1 \varphi_2 \left[1 - e^{-\kappa(1-q)D}\right]^2 N_1 N_2 \right). \tag{1.11}$$

Typically, the fraction κ is small and using a Taylor expansion we approximately have that

$$N_{lethal} \sim p\varphi_0 \left(q\kappa D N_0 + \varepsilon \varphi_1 \varphi_2 \left((1-q)\kappa D\right)^2 N_1 N_2 \right). \tag{1.12}$$

Finally, assuming that the number of lethal double-strand breaks follows a Poisson random variable X with mean μ, the quantity N_{lethal} is an unbiased estimator for the mean and the *probability of cell survival* is simply given by

$$P(X = 0) = \exp(-\mu) \sim \exp\left(-\alpha D - \beta D^2\right) \tag{1.13}$$

where

$$\alpha \sim p\varphi_0 q \kappa N_0 \qquad \text{and} \qquad \beta \sim p\varepsilon \varphi_0 \varphi_1 \varphi_2 (1-q)^2 \kappa^2 N_1 N_2.$$

There exist several other derivations for the linear-quadratic model based on similar underlying principles, all arriving at the same functional representation. For example, Kellerer and Rossi [139] derive the relation based on a theory of dual radiation action grounded in analyzing clinical data. Tobias et al. [330] use a model of repair and misrepair. For a detailed discussion of cell survival models that are

based on repair/misrepair kinetics and quantify dose-response relations and dose-protraction effects, we refer the reader to the review article by Sachs, Hahnfeldt and Brenner [286]. Although the validity of the linear-quadratic model can be questioned for very low and very high dosages (e.g., see [120, 155]), there are numerous studies that support conclusions derived from the linear-quadratic model [37] and it is widely used to model cell survival in radiotherapy.

In actual treatments with external beam therapy, the total dose D is spread in time and is given in several small, so-called *fractionated doses*. For example, if the total dose D is divided into n equal fractions of treatment of d units, $D = nd$, then, under the assumptions that the biological effects of each fraction are independent of each other and that they are the same for each dose (this assumes complete repair of nonlethal DNA strand ruptures during the time intervals between adjacent administrations of doses), the total probability of cell survival is given by the product,

$$\left[\exp\left(-\alpha d - \beta d^2\right)\right]^n = \exp\left(n\left(-\alpha d - \beta d^2\right)\right).$$

This motivates the definition of the *biologically equivalent dose*, a suitably normalized exponent in this fractionated LQ-survival probability as

$$BED = n \cdot d\left(1 + d\frac{\beta}{\alpha}\right) = D\left(1 + d\frac{\beta}{\alpha}\right) \tag{1.14}$$

with the quantity $1 + d\frac{\beta}{\alpha}$ called the relative effectiveness per fractionated dose. Essentially, the effect of a single fractionated dose is of the form $\exp\left(-\alpha d - \beta d^2\right)$ and these terms are just multiplied which then leads to the exponent given by $-\alpha \cdot BED$. The biologically equivalent dose is an approximation that is generally used in medical practice when comparing different fractionization schemes.

The main reason for fractionation is to improve the effect of radiotherapy. The underlying rationale is based on what are called the *four R's of radiotherapy*: repair, reoxygenation, repopulation, and redistribution. The prolongation of treatment, either by fractionation or decreasing dose-rate, allows a greater time for *repair* between the treatment periods resulting in a reduced cytotoxicity to both tumor and normal tissues. In fact, one of the main rationales behind fractionization schemes is to exploit the differences in the $\frac{\alpha}{\beta}$ values between early and late responding tissues to maximize the damage done to the cancer cells while limiting the side effects. Fractionation allows normal tissue to recover while tumor cells are generally less efficient in repairing radiation damage and thus are more effected by the treatment. A second main reason for fractionization is *reoxygenation*. Tumors generally consist of a mixture of cells some of which have ample supply of oxygen (aerated) while others are deprived of oxygen (hypoxic). Radiation predominantly kills the aerated cells since hypoxic cells are mostly in the quiescent phase in the cell cycle and thus are much less radiosensitive. After radiation treatment, most surviving tumor cells are hypoxic. Fractionation allows for these cells to again become oxygenated and thus once more be radiosensitive. For the same reason, after radiation treatment, tumors tend to go through a phase of increased growth and decreased cell loss called

repopulation. Overall, it therefore becomes advantageous to give repeated doses. *Redistribution*, the possibility of exploiting the dynamics in the cell cycle, seems to be of lesser practical importance since cancer cells often have rather heterogeneous cell-cycle kinetics.

In North America, a typical fractionation schedule for adults is 1.8 to 2 Gy per day, five days a week. If the periods between fractions are too long, the cancer can recover and the beneficial effects of treatment are lessened. For this reason, fractionation schedules are individualized and can vary even between doctors. In fact, medical research is ongoing into various fractionation schemes. In so-called *hyperfractionation*, higher numbers of fractions are used per day near the end of a course of treatment to deprive small tumors that have strong regenerative properties of this option (e.g., head-and-neck tumors). In case of lung cancer, *CHART* (continuous hyperfractionated accelerated radiation therapy) which administers three smaller fractions per day apparently has been quite successful. On the opposite side of the spectrum, *hypofractionation* is a form of radiation treatment in which the total dose of radiation is divided into large doses and treatments are given less than once a day. In this kind of treatment, doses can reach up to $20\,Gy$ per fraction. As these widely differing efforts indicate, mathematical modeling and analysis can be of interest in the scheduling of radiotherapy doses.

We formulate a mathematical model for radiotherapy with cell loss by combining the linear-quadratic model with the phenomenological models introduced in Section 1.2 to describe the loss of tumor size under radiotherapy. However, we do this for an extension of the standard model that takes into account *incomplete repair of DNA damage*. The classical formula (1.8) is adequate under several assumptions, one of which is that DNA repair of sublethal damage is complete by the time the next dosages are administered. Then, indeed, over a reasonable time period that does not allow for the tumor to grow significantly—and radiotherapies are designed like this—a static fractionation policy with the same dose for all the fractions is adequate. In reality, however, these repair processes are imperfect. In addition, as already mentioned above, early and late tissues have very different repair rates ρ. Taking these features into account, and considering an arbitrary, time-varying dose rate $w = w(t) \geq 0$ over an interval $[0, T]$, the surviving fraction of cancer cells under the traditional LQ-model is given by the expression (e.g., see, [340] and [286])

$$\exp\left(-\alpha \int_0^T w(t)dt - 2\beta \int_0^T \int_0^t w(t)w(s)e^{-\rho(t-s)}dsdt\right) \tag{1.15}$$

where, as before, α and β are the constant LQ-parameters corresponding, respectively, to the likelihood of lethal damage through a double-strand break and to the probability that two single-strand breakages occur. But now the probability that two such breaks occurring at times s and t will be lethal is assumed to decay exponentially with the repair rate ρ. Denoting the total dose by $D = \int_0^T w(t)dt$, this expression can be rewritten in the form

$$\exp\left(-\alpha D - \beta G D^2\right) \tag{1.16}$$

with

$$G = \frac{2}{D^2} \int_0^T \int_0^t w(t)w(s)e^{-\rho(t-s)} ds dt, \tag{1.17}$$

the so-called *Lea-Catcheside dose-protraction factor*. This constant represents the fact that a single strand break that is created at time s, if not repaired, will interact with a second single strand break at time t to form a lethal lesion. Note that for a constant dose rate $w(t) = \bar{w} = \text{const}$ and with $D = \bar{w}T$, this term reduces to

$$G = \frac{2\bar{w}^2}{D^2} \left(\frac{e^{-\rho T} - 1 + \rho T}{\rho^2} \right) = 1 + o(\rho T).$$

In particular, if we have $\rho = 0$, then $G = 1$ and this is the classical formula $\exp\left(-\alpha D - \beta D^2\right)$ with $D = \bar{w}T$. More generally, if the irradiation time is short enough, the higher order terms in this expansion can be ignored and G is close to 1. For example, in standard external beam radiotherapy the time duration of a fractionated dose is in the order of seconds compared with a typical repair time constant in the order of an hour. Thus G is effectively 1 and, in case of daily fractionated doses, there is no effective interaction between doses and the standard linear-quadratic formula is adequate. In this case, the effect of fractionated doses is obtained by multiplying the cell survival probabilities for the individual doses and the overall effect thus is described by the biologically equivalent dose as discussed above. But this formula assumes complete cellular repair in between doses. On the other hand, if radiation is given over longer time periods, as is the case in continuous low-dose radiation schedules, then the exponential term $e^{-\rho(t-s)}$ may be significantly smaller than 1 over sizable intervals and in such a case $G < 1$. We therefore choose the more general cell survival probability (1.15) and incorporate it into the phenomenological models for tumor growth.

Note that the integral term

$$r(t) = \int_0^t w(s)e^{-\rho(t-s)} ds$$

is the solution to the first-order linear ODE

$$\dot{r} = -\rho r + w, \qquad r(0) = 0. \tag{1.18}$$

Hence we can formulate the combined model as the following 2-dimensional system with α and β the standard LQ parameters and the equation for r representing the temporal effects of tissue repair with repair rate ρ:

$$\dot{p} = pF(p) - (\alpha + 2\beta r)pw, \qquad p(0) = p_0, \tag{1.19}$$

$$\dot{r} = -\rho r + w, \qquad r(0) = 0. \tag{1.20}$$

The specific parameter values depend on the tissue treated and there will be separate equations modeling the effects on cancerous and healthy tissue. A smaller tumor repair rate implies a larger influence of the integral term in the quadratic component

and thus a greater effectiveness of the therapy on this type of tissue. For a constant dose rate $\bar{w}$, in steady state (i.e., in the limit $\lim_{t\to\infty} r(t) = \bar{r}$), we have that $\bar{r} = \frac{\bar{w}}{\rho}$ and thus the damage term reduces to a standard linear-quadratic expression $-p\left(\alpha\bar{w} + \frac{2\beta}{\rho}\bar{w}^2\right)$. Equation (1.20) better models the transient behavior and, from a mathematical point of view, the structure of the overall model becomes more transparent, and also more manageable, if we replace the integral $\int_0^t w(s)e^{-\rho(t-s)}ds$ with the solution r to this differential equation. For large repair rates, it can be adequate to replace the state r by its steady-state value and then we once more recover the standard LQ-model, basically approximating the case of complete repair.

1.3.2 Chemotherapy

In principle, the term chemotherapy only indicates the use of a chemical to cure a disease, typically in the case of proliferating pathogens such as bacteria or tumor cells. But chemotherapy has such an important role in oncology that nowadays the usage of language commonly refers to cancer chemotherapy. Quite simply, to this day chemotherapy remains the main elective nonsurgical choice for treatment of cancer, both as a stand-alone procedure if a tumor is not operable or as adjuvant therapy to target microscopic metastases after surgery and radiotherapy.

While the specific drug that will be administered depends on the type and stage of the tumor to be treated, the means of action of these drugs often follow similar underlying principles. Broadly one distinguishes between cell-cycle nonspecific and cell-cycle specific drugs. The first class, for example, includes anthracyclines which are among the most effective anticancer treatments ever developed, but unfortunately have high cardiotoxicity that may lead to heart failure. Among cell-cycle specific drugs, one broadly distinguishes between *cytotoxic* or killing agents that kill the neoplastic cell and *cytostatic* or blocking agents that decelerate or block/arrest the tumor cells' proliferation. Typical drug actions cause DNA strand breaks in G_2/M and DNA synthesis inhibition in S. There also exist more specialized mechanisms that play important roles in specific types of cancer. For example, in leukemia, cancer cells spent prolonged periods in the dormant stage of the cell cycle during which time they essentially are not vulnerable. Then they go through a period of cell duplication rather rapidly. Here so-called *recruiting agents* that induce cells to leave the dormant stage and enter the cell cycle are of importance.

Cytotoxic agents interfere with specific processes in the cell-cycle and predominantly act in the G_2/M phase where, during mitosis, the cell walls become thin and porous and thus cells are more vulnerable to an attack. For example, spindle poisons interrupt regulatory proteins that connect the centromere regions of chromosomes, known as spindles, which leads to termination of cell division at the spindle assembly checkpoint (SAC) in mitosis. As in case of radiotherapy, generally an action that prevents the further generation of colonies of daughter cells is considered a killing action, even if it does not induce apoptosis. One of the most typical such

drugs is paclitaxel which is commonly used to treat patients with lung, ovarian, breast, head and neck cancer [58]. Killing agents also include S specific drugs like cyclophosphamide [58] or metatraxate [270] that mainly act in the DNA replication phase. Cytostatic agents, on the other hand, aim to synchronize the transitions of cells through the cell cycle by causing brief and invisible inhibition of DNA synthesis in the synthesis phase S and thus hold cells in the first growth phase G_1 [6, 68, 223]. A recruitment action was demonstrated, for example, for granulocyte colony stimulating factors (G-CSF) and granulocyte macrophage colony stimulating factors (GM-CSF). Generally, cytotoxic and cytostatic drugs are the more important ones and are among the common chemotherapeutic drugs given. But with so many other classifications in medicine, this division is an idealized one and often the mechanisms of actions of the drugs are more varied and mix both features.

We extend the growth model considered in Section 1.2 to include a cytotoxic effect of chemotherapy. These models take a simpler form than in the case of radiotherapy. Generally, for tumor growth, we have a positive net proliferation rate, $R(p) > 0$. Clearly, a negative proliferation rate implies the self-extinction of the neoplasm, a case only of interest for immunogenic tumors. But such a negative net proliferation rate is exactly what chemotherapeutic agents aim at by reducing the proliferation rate π or increasing the death rate μ of the neoplastic cells. When a drug is delivered to a human or an animal host, two fundamental processes take place called pharmacokinetics (PK) and pharmacodynamics (PD): *pharmacokinetics* determines the concentration of the drug in the blood and tissue, i.e., "what the body does to the drug," and *pharmacodynamics* models the effects the drugs have, i.e., "what the drug does to the body." According to the law of mass action, the speed of a chemical reaction is proportional to the product of the active masses (concentrations) of the reactants. If a drug is administered, in an ideal situation it has been postulated by Skipper et al. in 1960 [298] that cell death under cancer drugs follows first order kinetics [343], i.e., the decrease in the number of cancer cells per unit of time is proportional to the number of cancer cells with the rate depending on the concentration of the anti-cancer drug. Thus, if we assume the density profile of the chemotherapeutic agent in the blood stream is described by a time-varying function $c = c(t)$, then the cell loss caused by this concentration is proportional to $c(t)p(t)$, i.e., the pharmacodynamic model is linear in both the concentration c and p. This hypothesis is called the linear *log-kill hypothesis* and incorporating it into the growth law (1.1) results in the following growth model under chemotherapy,

$$\dot{p} = pR(p) - \varphi cp \tag{1.21}$$

with φ some positive constant that describes the effectiveness of the agent.

We briefly discuss the main effects that chemotherapy has on tumor volume using equation (1.21). In medical practice, typical chemotherapy schedules administer drugs in maximum dose therapy sessions with rest periods in between. The concept of the *maximum tolerated dose (MTD)* refers to the highest dose of a radiological or pharmacological treatment that can be given without unacceptably high toxicity. It is determined in clinical trials by simply increasing doses until unacceptable limiting

side effects are found. In order to speed up testing, *drugs generally are given in a single bolus dose*, i.e., concentrated at some time instant. Over a short time-period, it is realistic to assume that growth is exponential, i.e.,

$$\dot{p} = \xi p - \varphi c p, \qquad p(0) = p_0, \tag{1.22}$$

with the time of application normalized to $t_0 = 0$. Also, drug clearance rates often are fast—half-lives tend to be in the order of minutes to hours—while cell-cycle times are in the order of hours to days and even longer for some cell lines. Thus, over a short period, in a first approximation it is reasonable to neglect pharmacokinetic effects. For simplicity, let us also assume that the concentration is constant, $c(t) \equiv \bar{c}$, over a small interval $[0, \Delta t]$. Then the solution to (1.22) is given by

$$p(t) = p_0 \exp\left((\xi - \varphi \bar{c})\,\Delta t\right) = p_0 e^{\xi \Delta t} \cdot \exp\left(-\varphi \bar{c} \Delta t\right). \tag{1.23}$$

Without treatment, the tumor grows to $p_0 e^{\xi \Delta t}$ and thus the second factor determines the reduction due to treatment. The total dose D administered is the product of the concentration and time, $D = \bar{c}\Delta t$. A bolus administration of dose D corresponds to an impulse and is the mathematical limit when this dose is given over decreasingly smaller intervals with higher concentrations in the limit as $\Delta t \to 0$. Since the reduction term only depends on the total dose, the tumor reduction achieved by a bolus injection of dose D is approximately given by

$$r = \exp\left(-\varphi D\right)$$

with φ a positive constant dependent upon the effectiveness of the drug. In particular, note that *a given bolus dose of anti-cancer drugs eliminates a specific proportion of cancer cells regardless of the size of the tumor, not a specific number of cancer cells*. However, this treatment also kills all other strongly proliferating cells as well (especially in the bone marrow) and thus it needs to be followed by a significant rest period that allows the damaged healthy cells to recover. A typical length T for the time between doses in the US is three weeks. During this time the cancer will regrow and, still using the simple exponential growth model, the total effect over a therapy interval of length T is thus given by

$$\exp\left(-\varphi D\right) \cdot \exp\left(\xi T\right).$$

Only if this quantity is less than 1, therapy can in principle be successful.

Figure 1.4 depicts some typical response curves to bolus type chemotherapy with restperiods that result from this reasoning and are common in medical presentations and publications on this topic. We plot the number of cancer cells on a logarithmic scale vertically and time in weeks horizontally. In Figure 1.4(a) the initial condition corresponds to 10^9 cells, probably the smallest size of tumor clinically detectable, and just for sake of numerical illustration it is assumed that 99% of the cancer cells are eliminated by the treatment with the remaining cells then regrowing slowly during the restperiod. Clearly, overall this is a very favorable scenario and this is a

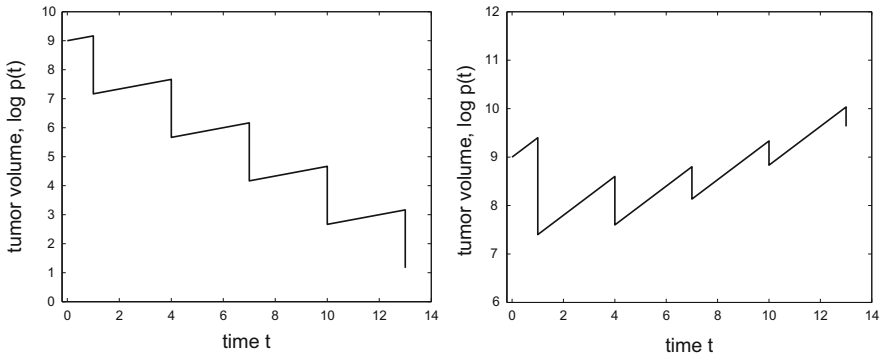

Fig. 1.4 Schematic representation of the evolution of tumor volume under bolus injection at times $t = 1, 4, 7, 10, 13$ weeks: (a, left) if cancer cells are sensitive and (b, right) if cancer cells contain a high portion of resistant cells. In case (a), therapy will be successful while it fails in case (b).

model for a successful chemotherapy. In reality, however, often only a much smaller ratio of cells is sensitive to the therapy and, in the course of time, as these resistant cells are killed, the proportion of the resistant population of cancer cells increases and, unfortunately, healthy cells do not develop similar resistance properties. Thus, over time, chemotherapy becomes less and less effective and eventually may fail. A simple example of such a scenario is shown in Figure 1.4(b).

Although this reasoning is oversimplified in many aspects, it is the staple of much of the praxis of drug scheduling in chemotherapy. For example, this argument does not consider the dynamics of the cell cycle when in reality only cycling cells can be killed. These effects are simply subsumed in the coefficient φ that determines the cancer cell kill fraction. For some types of tumors, especially in leukemia, this fraction may represent only a small percentage, possibly less than 1%, of the total number of cancer cells. For this, and also other reasons, chemotherapy given in an MTD fashion has proven less effective or even ineffective on slowly growing cancers that have a small proportion of cycling cells. Generally, the effectiveness of a specific treatment schedule depends on the type of tumor. Acute myeloid leukemia (AML) is a cancer of the myeloid line of blood cells, characterized by rapid growth of abnormal white blood cells that accumulate in the bone marrow and interfere with the production of normal red blood cells. For this disease, MTD chemotherapy has been very successful in achieving remission by reducing the number of leukemic cells to an undetectable level. On the other hand, acute lymphoblastic leukemia (ALL) is another form of leukemia where an MTD regimen is not that appropriate. This disease is characterized by excess lymphoblasts (immature cells that differentiate to form lymphocytes) and also causes damage and death by crowding out normal cells in the bone marrow. ALL is most common in childhood and it has an overall cure rate of about 80% that is achieved through prolonged low-dose treatment protocols that stretch from 2 to 3 years [332]. There also exist other types of cancer where a so-called *metronomic scheduling of chemotherapy* has been proven successful [118, 162, 272]. In this form of therapy, essentially, drugs are administered

in a continuous low-dose way to avoid toxic side effects, possibly with small interruptions to increase the efficacy of the drugs. As is obvious from equation (1.23), if it is possible to give chemotherapy at lower doses over prolonged time intervals (e.g., if toxic side effects were absent), then the overall effect may be improved because of the greatly extended time horizon in the term $\exp(-\varphi\bar{c}\Delta t)$ than what can be achieved with repeated MTD doses [341]. The optimization of treatment schedules to this day remains an active area of medical research and, in the context of mathematical models, is one of the main topics of our text.

Generally, both in MTD schedules and even more so in a metronomic setting, several drugs are combined to achieve synergistic effects. Figure 1.5 depicts the evolution of the tumor volume under continuous infusion chemotherapy for two drugs labeled drug 1 and drug 2 and a synergistic effect of combinations. This is merely meant to illustrate the features and, for simplicity, we again assume that tumor growth is exponential and that the continuous administrations of the drugs reduce the growth factor ξ of the tumor by death rates μ_1 and μ_2 related to the concentrations $\bar{c}$ and the effectiveness φ of the drug, i.e.,

$$\dot{p} = (\xi - \mu_1)\, p, \qquad \text{and} \qquad \dot{p} = (\xi - \mu_2)\, p,$$

respectively. The combination of the two drugs is said to be *synergistic* if the death rate $\Phi(\mu_1, \mu_2)$ attained by giving both drugs is greater than the sum of the individual death rates, $\Phi(\mu_1, \mu_2) > \mu_1 + \mu_2$, and it is called *antagonistic* if it is smaller, $\Phi(\mu_1, \mu_2) < \mu_1 + \mu_2$. In general, two G_2/M specific cytotoxic agents are expected to be antagonistic, while there is hope that cytotoxic agents that act in different phases of the cell cycle may be synergistic. But the specifics are clearly drug dependent and are largely determined by the interplay of the specific activation mechanisms of the drugs involved and their biochemical properties. In Figure 1.5 we give some typical dose-response curves for tumor growth under continuous infusions for two drugs under a simple linear pharmacokinetic model of the form $\dot{c} = -\rho c + u$. Treatment is initiated at time $t = 1$.

High dose chemotherapy is designed to be as toxic as possible to the cancerous cells and thus naturally has severe side effects. The paradigm simply is that cancer cells need to killed and that they need to be killed now and in large quantities. The underlying rationale for this so-called *induction chemotherapy* is that the patient was only diagnosed in a late stage and that the disease has progressed to a state where immediate action is required, only an all too common scenario with a disease that is widely symptomless in its early stages. (Among all types of tumors, pancreatic cancer has one of the worst survival rates since it generally is only detected in very late stages of the disease.) But most anticancer drugs are not selective to tumor cells and equally kill a large number of proliferating healthy cells. Especially in these first stages of modern chemotherapy that aim at remission of the disease, drugs target all or at minimum large classes of proliferating cells, often with severe effects on a wide range of physiologically proliferating cells important for life like the bone marrow. Anti-cancer drugs interfere with one or more biochemical pathways important in cell duplication. Naturally, the more the targeted pathway is specific to cancer cells,

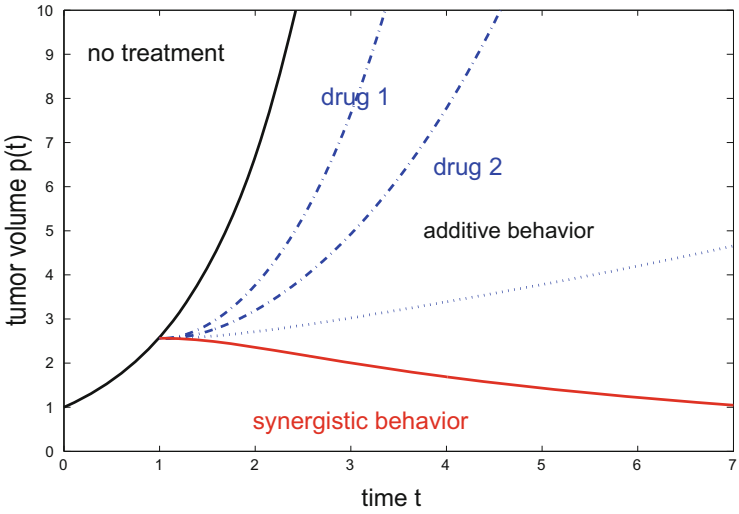

Fig. 1.5 Evolution of tumor volume under continuous time infusions starting at $t = 1$ for two drugs and a synergistic combination.

the less severe side effects are. But since its first use, it has been plain that because of the scarce selectivity of chemotherapeutic agents serious side effects are related to the use of cytotoxic chemicals to cure tumors. If these side effects become too strong, chemotherapy fails.

The main reason for the high number of these failures is *drug resistance*. Cancer cells typically are genetically unstable and coupled with high proliferation rates this leads to significantly higher mutation rates than in healthy cells [107]. If a mutated cell exhibits a biochemical structure that invalidates the mechanism of attack of the chemotherapeutic agent, these cells have become drug resistant (*acquired resistance*). Indeed, the response of tumor cells to chemotherapy is characterized by a considerable evolutionary ability to enhance cell survival in an environment that is becoming hostile. Malignant cancer cell populations are highly heterogeneous—the number of genetic errors present within one cancer cell can lie in the thousands [220]—and fast duplications combined with genetic instabilities provide just one of several mechanisms which allow for quickly developing acquired resistance to anti-cancer drugs. Moreover, because of this tremendous heterogeneity of cancer cells, small sub-populations of cells may exist that are intrinsically not sensitive to the treatment from the beginning (ab initio, *intrinsic resistance*). In this case, after the sensitive cells have been killed by the treatment, a tiny fraction of resistant tumor cells remains that then can grow to become a dominant population leading to the failure of therapy, possibly only after many years of seeming remission of the cancer. Drug resistance has been called the curse of chemotherapy and if it becomes an issue, generally the realistic aim no longer becomes to cure the disease, but to prolong the patient's life expectancy.

Considerable research efforts have been made and still are ongoing to overcome drug resistance [95]. Rather than just killing the cancerous cells, modern treatments take a more holistic approach and also target the tumor's microenvironment [310], especially the tumor vasculature and the immune system. As it was already outlined above, a solid tumor cannot grow beyond a small size without developing its vasculature and for this recruitment of endothelial cells is necessary. Cells of the immune system have both stimulatory and inhibitory effects that are being used in immunotherapies. We still briefly describe these two treatment modalities.

1.3.3 Antiangiogenic Therapy

Chemotherapy targets the main characteristic of tumor cells, their proliferative derangement. But tumor cells also take part in a vast array of microscopic and macroscopic interactions with other cellular populations and this opens the door to alternative treatment approaches that can enhance traditional options. Antiangiogenic therapy falls into this class of treatments. It was already in the early 1970s that J. Folkman observed the importance of the development of a tumor's vasculature for the full development of a solid tumor and proposed antiangiogenic treatment as a possible strategy to combat cancer [85, 86, 87]. But it only became a medical reality with the discovery of inhibitory mechanisms of the tumor in the 1990s [161]. Indeed, the tumor both stimulates and inhibits the growth of the endothelial cells that form the linings of the blood vessels and capillaries that define its vasculature. As a whole, it is now understood that tumor angiogenesis is a tightly regulated process with complex bidirectional signaling that provides a balance between stimulatory and inhibitory mechanisms. Proangiogenic factors are released as the tumor cells lack a full level of nutrients to stimulate the process and antiangiogenic chemicals modulate the growth of the vessel network, deploying a sophisticated strategy to control the tumor's growth. Folkman suggested that inhibiting the development of the tumoral vessel network could be a powerful way to control the neoplastic growth by means of reducing the supply of nutrients. He termed this new kind of therapy *antiangiogenic therapy*. Rather than fighting the fast duplicating, genetically unstable and continuously mutating tumor cells, this indirect treatment approach targets the genetically much more stable endothelial cells that form the walls of blood vessels. These cell lines are far less prone to developing drug resistance [28] and still to this date no limiting clonal resistance to angiogenic inhibitors has been observed in experimental cancer. For this reason, tumor antiangiogenesis has been called a new hope for the treatment of tumors [141, 142]. But antiangiogenic therapy only limits the tumor's support mechanism without actually killing the cancer cells and thus far these high hopes have only been realized in mouse models. As any mathematical model and numerous medical studies confirm, the tumor will grow back once treatment is halted. Thus tumor antiangiogenesis is not efficient as a stand-alone or monotherapy treatment, but in combination with other traditional treatments that kill cancer cells such as chemotherapy or radiotherapy [77], it can

enhance their effect and lead to synergistic benefits. For example, there is strong interest and active research on tumor antiangiogenesis as a method that regularizes the vasculature [131, 132] and thus, when combined with chemotherapy, enhances the delivery of the drugs and thus the efficacy of the procedure.

There exists a large number of antiangiogenic agents with over 60 of them in clinical trials in the US since 2006. Angiogenic inhibitors are commonly classified as *direct inhibitors* which act on the endothelial cells and inhibit their proliferation and migration or induce their apoptosis, or as *indirect inhibitors* that block the production of angiogenic factors by malignant cells [143]; mixed agents target both endothelial and malignant cells. Some direct inhibitors have a cytotoxic action that induces a rapid destruction of existing blood vessels. Several antiangiogenic drugs have undergone clinical development in recent years, and some of them have led to improvement in overall survival or disease-free survival in various clinical scenarios. This way of controlling the tumor burden appears intriguing and there is evidence from experimental work that inhibiting angiogenesis may induce tumor regression and sometimes cure [266]. Also, there exists mounting medical evidence that several cytotoxic drugs have antiangiogenic effects when given at reduced dose rates [118, 162, 272].

Modeling the interplay between tumor growth and the development of its vascular network, as well as the action of angiogenic inhibitors, is an important step that can help in planing effective antiangiogenic therapies. Tumor angiogenesis is a spatial consumption-diffusion process and to date a number of mathematical models have already been proposed. Among these, one can broadly distinguish between *cell-based models* and *population-based models*. Cell-based models, such as they are developed, for example, in [8, 13, 54, 55], aim to fully reflect the complex biological processes that underlie tumor angiogenesis. Population based models try to aggregate these features into dynamical systems with a minimal number of variables and parameters. While being a less accurate approximation of the medical reality, they generally allow for mathematical analysis beyond the large scale simulations of cell based models [236]. With their inherent reliance on specific parameter values, the conclusions drawn from such simulations tend to be less systemic while, as we shall show in Chapter 5, the analysis of population based models leads to robust results and interpretations. Furthermore, medical treatment does operate on a highly aggregated level: once the type of cancer and the stage of progression of the disease have been identified, therapy schedules are determined based on established guidelines and the experience of the physicians without complete knowledge of the intricate details of the specific situation. Therefore, low-dimensional dynamical systems that are *minimally parameterized* allow for a mathematical analysis (using tools from various branches in mathematics, not just optimal control as it is applied in our text) and can provide robust results that are valid over a large range of parameters [263, 264, 201]. Such results then lead to sound qualitative conclusions. It are these kind of results that we shall focus on in this text.

Folkman and his coworkers formulated a simple, but largely influential mathematical model of this type—a minimally parameterized and low-dimensional dynamical system—in [116] that describes the vascular phase of tumor growth.

The appreciation of the role of angiogenesis in tumor development has led Hahnfeldt et al. to introduce the important concept of a *varying carrying capacity*, $q(t)$, defined as the tumor size potentially sustainable by the existing vascular network at a given time [116]. This carrying capacity is an idealized quantity for the tumor's support mechanisms through its microenvironment and, to a large extent, it depends on the tumor vasculature. Introducing such a variable into the phenomenological growth function F in equation (1.1), and simply postulating a dynamics for q determined as a balance of stimulatory (S) and inhibitory (I) effects, results in the following dynamical system:

$$\dot{p} = pF\left(\frac{p}{q}\right), \tag{1.24}$$

$$\dot{q} = S(p,q) - I(p,q). \tag{1.25}$$

In their paper [116], Hahnfeldt, Panigrahy, Folkman, and Hlatky derive specific functional forms for I and S using an asymptotic spatial analysis of the underlying consumption-diffusion process for the concentrations of stimulators and inhibitors under a series of simplifying assumptions that include spherical symmetry of the tumor, a fast degradation of proangiogenic factors and a slow degradation of inhibitory factors. Their model was biologically validated by fitting experimental data on the growth and response to different antiangiogenic drugs for Lewis lung carcinomas implanted in mice. Various extensions and modifications of this model have been proposed and analyzed in the literature and we shall discuss these, along with the precise underlying modeling aspects, in Chapter 5.

Equations (1.24) and (1.25) provide a general framework to portray the effects of antiangiogenic therapies on the tumor, either alone or in combination with traditional therapies. For example, if we denote the concentrations of antiangiogenic and chemotherapeutic agents by u and v, respectively, then, and making the log-kill hypothesis, we obtain a system of the form

$$\dot{p} = pF\left(\frac{p}{q}\right) - \varphi v p, \tag{1.26}$$

$$\dot{q} = S(p,q) - I(p,q) - \gamma u q - \eta v q \tag{1.27}$$

with the coefficient γ describing the effect of an angiogenic inhibitor on the vasculature and the coefficients φ and η describing the effects of a cytotoxic agent on the tumor and its vasculature, respectively. Obviously, this model can be made more realistic by allowing that these quantities depend on the variables p and q with functions of the quotient $\frac{q}{p}$, sometimes called the endothelial density, most intriguing medically (see [259]). Various further extensions of the model, such as, for example, the inclusion of pharmacokinetic equations for the therapeutic agents or models for combination therapies of antiangiogenic agents with chemo- and radiotherapy can be formulated and these are some of the topics considered in Chapters 6 and 7.

1.3.4 Tumor Immune System Interactions

A tumor's microenvironment also contains various types of cells of the immune system with both beneficial and detrimental effects. The purpose of the immune system is to protect the organism from disease. In order to fulfill this function, it needs to be able to detect a wide variety of agents, from viruses to bacteria to parasites, but also must be able to distinguish these from the organism's own healthy tissue. There exist various autoimmune diseases such as diabetes or asthma when the immune system fails to make these distinctions and attacks important functional cells in the body. Tremendous progress in understanding the workings of the immune system has been made in connection with research on HIV and this new knowledge also finds applications in cancer research. Since the immune system's first response to its environment is on the basis of a discrimination between "own" and "foreign" objects, some types of tumor cells may be tolerated by the patient's own immune system if, essentially, they are classified as "own" cells [271]. However, tumor cells generally exhibit a large number of abnormalities (such as mutated proteins, under- or over-expressed normal proteins and many more) that lead to the appearance of specific antigens some of which will be classified as "foreign" and thus do trigger reactions by both the innate and adaptive immune system [144, 309]. In fact, the empirical hypothesis of *immunosurveillance*, i.e., that the immune system may act to eliminate tumors, is well established in the medical community and has recently been confirmed experimentally and epidemiologically [72].

The competitive interaction between tumor cells and the immune system is complex and involves an immense number of events with the kinetics of the interplay strongly nonlinear. Moreover, to fully describe the immuno-oncologic dynamics, one has to take into account a range of spatial phenomena since this interplay is strongly shaped by the mobility of both tumor cells and the effector cells of the immune system [232]. Thus the possible outcome of this interplay is not only constituted by either tumor suppression or tumor outbreak, but by various intermediate scenarios. For example, it has been hypothesized that in case of a fully developed and metastatic tumor, upregulation of the immune system caused by the tumor may be responsible for controlling small metastases. Also, there exist several theoretical immuno-oncologic studies that were largely inferred from clinical data and come to the conclusion that in some cases the immune system may be able to keep the tumor in a dynamic equilibrium that corresponds to a microscopic (undetectable) dormant state [248, 250, 232], so-called *tumor dormancy*. This theoretical prediction was confirmed by Koebel and coworkers [164], who were able to experimentally show, through an ad hoc mouse model, that adaptive immunity can maintain occult cancer in an equilibrium state.

There exists a substantial amount of research literature on the mathematical description of tumor-immune system interaction. This field has seen a strong resurgence due to the increased understanding of the mechanisms of the immune system in connection with AIDS (acquired immune deficiency syndrome) research, e.g., [17, 18, 158, 280, 252], to mention just a small sample of some more recent publications on this topic. Historically, one of the earliest references on this topic is the

1980 paper by Stepanova [303] where a by now classical mathematical model of two ordinary differential equations is proposed that aggregates the interactions between cancer cell growth and the activities of the immune system during the development of cancer. Precisely because of its simplicity, a few parameters incorporate many medically important features, the underlying equations have been widely accepted as a basic model. In that model, the main features of tumor immune system interactions are aggregated into just two variables, the tumor volume, p, and the immunocompetent cell densities, r, a non-dimensional, order of magnitude quantity related to various types of immune cells (T-cells) activated during the immune reaction. Stepanova's model takes the following form:

$$\dot{p} = \xi p F(p) - \theta p r, \tag{1.28}$$

$$\dot{r} = \alpha (1 - \beta p) p r + \gamma - \delta r, \tag{1.29}$$

with all Greek letters denoting constant coefficients. Note that, if we define $\hat{r} = \lambda r$ and rescale the parameters γ and θ as $\hat{\gamma} = \lambda \gamma$ and $\hat{\theta} = \frac{\theta}{\lambda}$, then the solutions to these differential equations are unchanged. This 1-parameter group of scaling symmetries can be used to normalize the set point value for r.

Equation (1.29) summarizes the main interactions of the tumor with the immune system. Various organs such as the spleen, thymus, lymph nodes, and bone marrow, each contribute to the development of immune cells in the body and the parameter γ models a combined rate of influx of T-cells generated through these primary organs; δ is simply the rate of natural death of the T-cells. The first term in this equation models the proliferation of lymphocytes. For small tumors, it is stimulated by tumor antigen and this effect here is taken to be proportional to the tumor volume p. It is argued in [303] that large tumors suppress the activity of the immune system. The reasons lie in an inadequate stimulation of the immune forces as well as a general suppression of immune lymphocytes by the tumor (see [303] and the references therein). This feature is expressed in the model through the inclusion of the term $-\beta p^2$. Thus $1/\beta$ corresponds to a threshold beyond which the immunological system becomes depressed by the growing tumor. The coefficients α and β are used to calibrate these interactions and collectively describe a state-dependent influence of the cancer cells on the stimulation of the immune system. The first equation, (1.28), models tumor growth with ξ a tumor growth coefficient. This parameter could have been subsumed in the functional parameter F, but we prefer to leave the definition of F to account only for the qualitatively different structures that specify various growth models for the cancer cells. In Stepanova's original research an exponential model was used, $F_E(p) \equiv 1$, while Kuznetsov, Makalkin, Taylor, and Perelson [171] use a classical logistic model $F_L(p) = 1 - \left(\frac{p}{p_\infty}\right)$. A Gompertzian model, $F_G(p) = -\ln\left(\frac{p}{p_\infty}\right)$, has been used in the work by de Vladar and Gonzalez [334] and also generalized logistic models of the form $F_L(p) = 1 - \left(\frac{p}{p_\infty}\right)^\nu$, $\nu > 0$, are of interest. The second term, $-\theta p r$, models the beneficial effects of the immune

system reaction on the cancer volume and θ denotes the rate at which cancer cells are eliminated through the activity of T-cells.

Depending on the values of the parameters, the dynamical system (1.28)–(1.29) exhibits a wide range of behaviors that encompass a variety of medically realistic scenarios. These range from cases when tumor-immune system interactions are able to completely eradicate the tumor in the sense that all trajectories converge to the tumor free equilibrium point $(0, \frac{\gamma}{\delta})$ (immuno-surveillance) to situations when *tumor dormancy* is induced (a unique, globally asymptotically stable benign equilibrium point with small positive tumor volume exists) to multi-stable situations that have both persistent benign and malignant behaviors to situations when tumor growth simply is dominant and overcomes the immune system. Despite its simplicity, with just a few parameters, this model rather accurately reflects the main qualitative aspects of tumor-immune interactions: the immune system can be effective in the control of small cancer volumes, but for large volumes the cancer dynamics suppresses the immune system and the two systems effectively become separated. For this reason, the underlying equations have been widely accepted as a basic model.

There exist several modifications and extensions of Stepanova's model, most notably the already mentioned paper by Kuznetsov, Makalkin, Taylor, and Perelson [171] who employed a classical logistic model for cancer growth ($F_L(p) = 1 - \frac{p}{p_\infty}$ with a finite carrying capacity p_∞) and biologically validated the model based on in vivo data of B-lymphoma BCL_1 in the spleen of mice. De Vladar and Gonzalez [334] have carried out a complete bifurcation analysis for the model given here with a Gompertzian growth function. More recently, d'Onofrio formulated and investigated a general class of models [248, 249] that incorporates all of these dynamical models and whose analysis confirms the earlier mathematical findings.

The qualitative dynamical properties described above are not effected by the choice of the growth model (e.g., see [187]). Figure 1.6 shows four phase portraits of the system (1.28)–(1.29) for (a) a Gompertzian growth model, $F_G(p) = -\log\left(\frac{p}{p_\infty}\right)$, (b) a classical logistic model, $F_L(p) \equiv 1 - \frac{p}{p_\infty}$, (c) a generalized logistic model with $\nu = 2$, $F_{GL}(p) = 1 - \left(\frac{p}{p_\infty}\right)^2$, and (d) an exponential growth function, $F_E(p) \equiv 1$. The parameter values that were used to generate these figures are summarized in Table 1.1 and are taken from the paper by Kuznetsov et al. [171] with some modifications to account for Gompertzian growth. These values are non-dimensional on an order of magnitude scale with the tumor volume p expressed in terms of multiples of 10^6 cells and r a dimensionless quantity that describes the immuno-competent cell density as an order of magnitude relative to some base value. The time scale is taken relative to the tumor cell cycle in mice and is in terms of 0.11 days [171].

For the specified parameter values, the dynamics is multi-stable and the system has both locally asymptotically stable microscopic and macroscopic equilibrium points as well as an unstable saddle point. The values for these equilibria are given in Table 1.2. At the microscopic equilibrium point the tumor volumes are small and the immuno-competent cell densities are upregulated. This corresponds to a situation when the immune system is controlling the tumor. We denote the corresponding equilibrium point by (p_b, r_b) and call it *benign*. The macroscopic

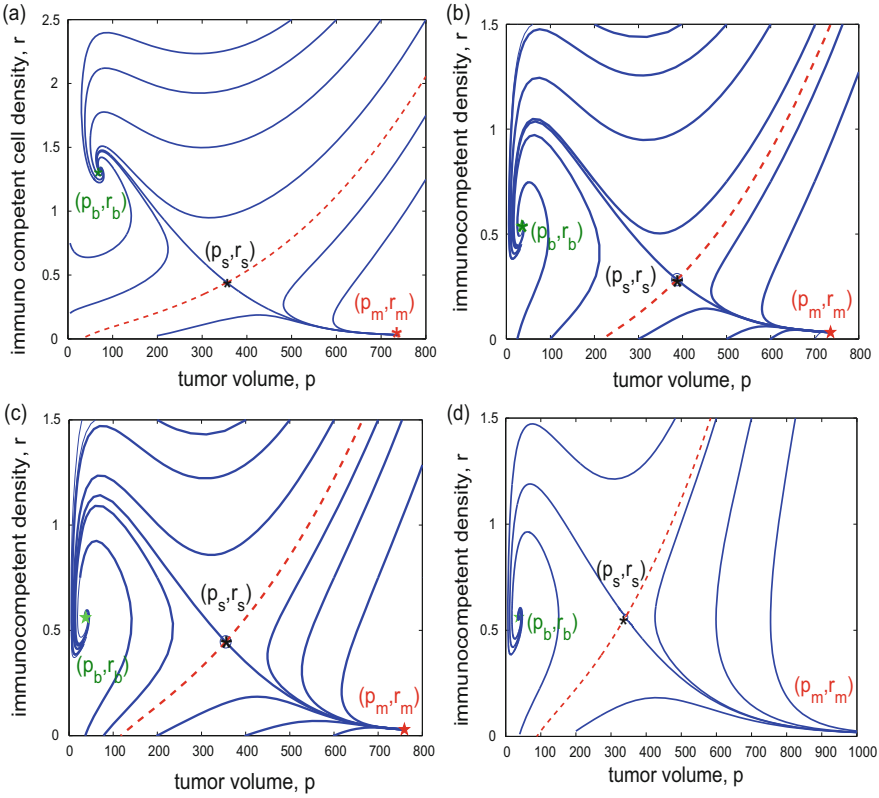

Fig. 1.6 Phase portraits for the system (1.28)–(1.29) with (a) Gompertzian, (b) logistic, (c) generalized logistic, and (d) exponential growth functions for the parameter values given in Table 1.1.

Table 1.1 Variables and parameters used for the phase portraits shown in Figure 1.6.

Variable parameters	Interpretation	Numerical value	Reference
p	Tumor volume		[303]
p_∞	Fixed tumor carrying capacity	780	
r	Immuno-competent cell density		[303]
α	Tumor stimulated proliferation rate	0.00484	
β	Inverse threshold for tumor suppression	0.00264	[171]
γ	Rate of influx of T-cells	0.1181	[171]
δ	Death rate	0.37451	[171]
θ	Tumor-immune interaction rate	1	[171]
ξ	Tumor growth parameter	0.5618	

equilibrium point is characterized by more than tenfold higher tumor volumes and depressed immunocompetent cell densities. In these solutions, the tumor has suppressed the immune system and almost reached its carrying capacity. We denote the

Table 1.2 Equilibria for the phase portraits shown in Figure 1.6.

Growth model	Benign equilibrium (p_b, r_b)	Saddle point (p_s, r_s)	Malignant equilibrium (p_m, r_m)
Gompertz $F_G(p) = -\log\left(\frac{p}{p_\infty}\right)$	(73.155, 1.330)	(355.136, 0.442)	(737.536, 0.031)
Logistic $F_L(p) = 1 - \frac{p}{p_\infty}$	(35.158, 0.537)	(387.527, 0.283)	(736.102, 0.032)
Generalized logistic $F_{GL}(p) = 1 - \left(\frac{p}{p_\infty}\right)^2$	(37.570, 0.560)	(354.617, 0.446)	(759.592, 0.029)
Exponential $F_E(p) \equiv 1$	(37.696, 0.562)	(341.092, 0.562)	$(\infty, 0)$

corresponding equilibrium point by (p_m, r_m) and call it *malignant*. Both of these equilibria are locally asymptotically stable, (p_b, y_b) a stable focus and (p_m, r_m) a stable node. For a dynamical system $\dot{x} = f(x)$ with a locally asymptotically stable equilibrium point x_*, its *region of attraction* [111] is defined as the set of all initial conditions x_0 for which the corresponding solution $x(t; x_0)$ of the initial value problem $\dot{x} = f(x)$, $x(0) = x_0$, exists for all times $t \geq 0$ and converges to x_* as $t \to \infty$. This set is always open and connected. We call the regions of attraction of the benign and malignant equilibria the benign and malignant regions, respectively. More generally, if the equilibrium point x_* is hyperbolic (i.e., the matrix of the partial derivatives of the dynamics at the equilibrium point, $A = DF(x_*)$, does not have any eigenvalues on the imaginary axis), then the stable, respectively unstable sets are manifolds called the *stable*, respectively *unstable manifold* of the equilibrium point x_* [111]. The tangent space to the stable manifold at x_* is given by the stable subspace of the matrix $A = DF(x_*)$, i.e., the linear span of all eigenvectors and generalized eigenvectors corresponding to all eigenvalues λ with negative real parts. As can be seen in all the phase portraits in Figure 1.6, the benign and malignant regions are separated by the stable manifold of the saddle (shown as a dashed red curve in each diagram) which forms the common boundary of these regions. This is a general property of so-called Morse-Smale systems [111]. For the model with an exponential growth function, the tumor size is not limited and in this case no malignant equilibrium exists, but the malignant region is characterized by the fact that the p-component of the trajectories diverges to ∞ while the r-component converges to 0.

In the model, the benign region consists of all initial conditions from which the immune system is able to control the tumor while the malignant region corresponds to initial conditions for which tumor growth is able to evade the actions of the immune system and tumor dormancy and eventually, unless other treatment options will be pursued, becomes lethal. In the first case, so-called *immunosurveillance*, what medically would be considered cancer never develops; in the latter one, only a therapeutic effect on the cancer (e.g., chemotherapy, radiotherapy, ...) needs to

be analyzed. But the phase portraits represent a stationary situation (i.e., constant parameters) that may be valid for a short time duration, but not over prolonged time periods. It is quite intuitive that a benign equilibrium solution can be disrupted by sudden events affecting the immune system (that are not included in the mathematical modeling) leading to a transition of the state into the malignant region. How likely this is relates to the size of the region of attraction of this equilibrium: if the benign region is small, even minor events may bring up the disease while the immune system may well be able to control the disease if this region is large. Indeed, if disease related impairments of innate and adaptive immune systems or *immunosuppressive treatments* preceding organ transplantations occur, then the tumor may restart developing. This has experimentally been shown both by mouse models and through epidemiologic studies [72, 304]. Thus, while there exist good reasons to believe that the immune system is able to control some tumors initially, over a longer period of time, the neoplasm will develop various strategies to evade the actions of the immune system and this allows the tumor to recommence growing [250, 72] into clinically apparent tumors [164] and eventually reach its carrying capacity [250]. These adaptive processes are called *immuno-editing* [72].

We can see from the phase portraits that the malignant region is larger for faster growing tumors corresponding to generalized logistic growth function with high exponents and exponential models. In fact, for a generalized logistic growth model $F_{GL}(p) = 1 - \left(\frac{p}{p_\infty}\right)^\nu$ with $\nu > 0$, and for the parameter values from Table 1.1, for small enough ν there only exists one globally asymptotically stable equilibrium which corresponds to a microscopic and thus benign equilibrium point. In this sense, for slowly growing tumors, the immune system is able to control the disease. However, as ν increases, an unstable saddle and a stable macroscopic (malignant) equilibrium are born in a saddle-node bifurcation and the benign region decreases at the expense of the malignant regions as the parameter ν increases. The malignant region increases in size with increasing parameter ν converging to the malignant region for the model with exponential growth in the limit $\nu \to \infty$ reflecting the fact that the immune system becomes increasingly overwhelmed by a fast growing tumor [187].

Overall, tumor-immune system interactions thus exhibit a multitude of dynamic properties that include multi-stability, i.e., persistence of both benign and malignant scenarios. From a practical point of view, the question how to move an initial condition that lies in the malignant region into the benign region can thus be posed. This requires therapy and can naturally be formulated and analyzed as an optimal control problem. We shall take up this question in Chapter 8. In these efforts, immunotherapy is another treatment modality that broadly comprises therapeutic interventions that are made to stimulate the body's immune system in order to attack, better fight, and hopefully eradicate the cancer cells. There are various methods in which the patient's immune system can be trained to recognize tumor cells (and only those) as targets to be destroyed and thus to coax up an otherwise nonexisting or only minor immune system reaction. One example is dendritic cell transfusion. In this approach, dendritic cells, which are antigen presenting cells of the immune system, are stimulated to activate a cytotoxic response toward specific antigens expressed on

the surface of the tumor. Essentially, in all these approaches, *immune effector cells* such as lymphocytes, macrophages, dendritic cells, natural killer cells, cytotoxic T lymphocytes, etc., are trained to recognize abnormal antigens produced by the cancer and are activated to fight the cancer cells. The basic idea of immunotherapy is simple and promising; however, the results obtained in medical investigations are controversial, even if in recent years there has been evident progress [1, 137].

1.3.5 Summary: Tumor Growth Kinetics and Treatment Modalities

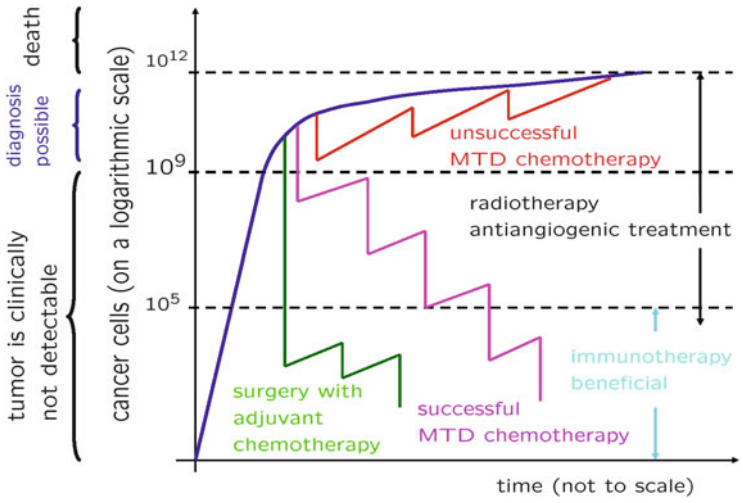

Fig. 1.7 Tumor growth and treatment modalities

We summarize the main treatment options discussed above in the diagram shown in Figure 1.7. Until a growing tumor reaches a size of about 10^9 cells, generally, in lieu of a lack of symptoms, it is considered clinically undetectable. During this phase, its growth probably has been exponential with often a high growth fraction, i.e., a large number of cells that is undergoing cell division, and consequently short doubling times of the tumor. First symptoms typically can be seen with tumors of sizes of 10^9–10^{11} cells when tumor growth slows down. Above these sizes, typically the disease becomes incapacitating and, generally, tumors of sizes of 10^{12}–10^{13} are considered lethal. For tumors that are diagnosed in a range of more than 10^5 cells, treatment commences typically in the forms of (i) surgery with adjuvant chemotherapy to control possible metastases, (ii) multiple, intense chemotherapy regimens or (iii) radiation treatment as well as combinations of any of these treatments with antiangiogenic therapy. In the ideal situation, these treatment approaches are able

to eradicate the tumor or bring it down to clinically undetectable sizes. For tumors below a size of 10^5 cells, immunotherapy also is considered of benefit and may be given as additional treatment option. If treatment fails, the tumor will keep growing, typically with a lower growth fraction, but eventually it will reach an unsustainable plateau and be terminal.

1.4 Treatment as an Optimal Control Problem—An Outlook

Because of limited resources and/or potential side effects of any kind of treatment, the problem of how to administer therapeutic agents to achieve the "best possible" effect is a natural one. Especially with cancer, the underlying biological mechanisms of novel therapy approaches may not be fully understood and guidelines on how to schedule these therapies may need to be established. In clinical trials, because of the great complexity of the underlying medical problem, the scheduling of agents is generally done in exhaustive, medically guided, expensive trial-and-error approaches. More complicated structures are rarely, if ever pursued. But even with all the medical research on this topic, these difficult scheduling questions are far from being settled and there exists an opportunity for *in silico* mathematical modeling and analysis to be useful here.

Optimal control problems deal with the minimization of some performance criterion imposed on an underlying dynamical system subject to constraints. Figure 1.8 gives a sketch of the main components involved in such a problem: *controls* are functions in time that describe allowable outside influences on the system which, when applied, induce a *system response*. Based on this response, an objective function is evaluated which is taken as a *performance measure* for the behavior of the system. It generally includes terms related to the running cost during the interval as well as possibly penalty terms at the end of therapy designed to induce a desired system performance. Optimal control theory addresses the question of *optimizing* this objective function. Naturally, the true response of the system will also be influenced by outside disturbances and unmodeled dynamics that are not included in the mathematical description and thus it may be different from the one computed within the model. Hence questions about robustness of the solutions and various other kind of stability properties are of great importance.

The scheduling of cancer treatments has all the features of such a problem: *treatments are scheduled over time and their interactions with the tumor growth dynamics determine success or failure of the therapy*. At the same time, *constraints on the toxicity of the treatment need to be taken into account*. In essence, important questions that should be answered are of the following type: What are the best dose rates and total amounts of therapeutic agents that need to be administered in order to achieve desired effects? How can a priori specified amounts of therapeutic agents be administered to have the best possible effect? Does the sequencing of therapies make a difference? and many, many more. We do not mean to suggest that the scheduling of the therapies could ultimately decide between success and failure, but there may

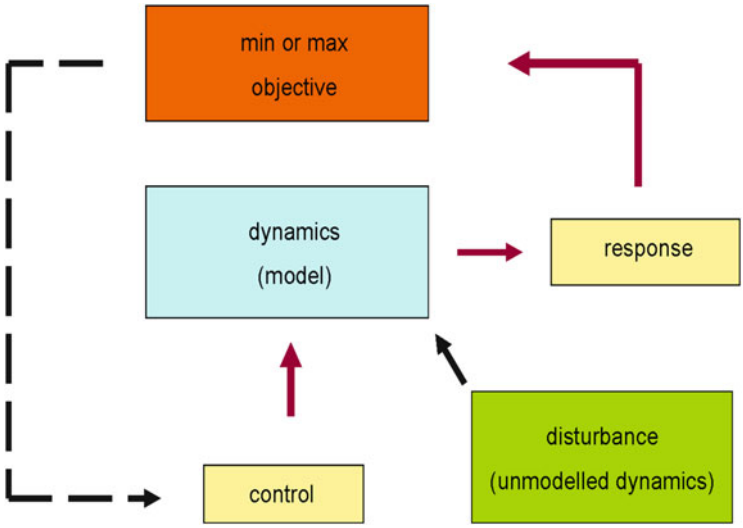

Fig. 1.8 Schematic representation of the structural elements of an optimal control problem.

be ways to achieve the same effects with less severe side effects, at lesser cost, or with other tangible benefits. Methods from optimal control, and in particular those that aim at *constructing full solutions for the underlying problems*, provide an adequate framework to analyze such scheduling questions for cancer treatments. These are the topics that will be pursued in this text.

Optimal control has a long and successful history of applications in engineering and science. Rooted in the methods of Lagrangian and Hamiltonian mechanics in physics, in a certain sense the field was reborn in the 1950s and 1960s with the efforts of space exploration when it was largely influential in putting the first satellite into orbit. Here the problem was to place an object into a sustained geostationary orbit and approaching the problem by imposing some criterion to be maximized led to mathematical conditions that then were used in the computations for the actual flight path. Other well known applications of optimal control techniques include autopilots on commercial aircraft and automated processes in manufacturing, especially in the field of robotics. Encouraged by its success in this field, economists—very much interested in maximizing profits or minimizing cost—took up the techniques in the 1970s with similar success. Merton's investment-consumption model and the Black and Scholes formula in option pricing not only earned their authors a Nobel prize, but have become the foundation of modern finance and are still largely influential nowadays. However, there is a significant difference between these fields and medicine. In science, and also in economics, the underlying dynamics for the problem generally is based on simple *first principle interactions* and as a result, typically is well understood leading to reliable models. In engineering problems, the dynamics more or less follow from the laws of physics or chemistry and some simple design or synthesis principles. In fact, it is a virtue to keep designs as simple

as possible in order to understand the composite structures. While it is a tremendous engineering achievement to send a satellite into outer space, guide it correctly to the outer planets and its moons, and send back images to earth, the dynamics still is based on Newton's laws of motion and gravitational pull, essentially just second-order differential equations. Even in economic applications, the underlying dynamics is generally simple and broadly accepted. It simply is not very complex to describe the effects of a trade, even if commissions are taken into account. Of course, this is not be confused with the complex interactions that arise because of the multitude of market participants. Thus, generally in these problems, the dynamics is well understood and reasonably simple. As our exposition in this introductory chapter already indicated, this is far from the truth for biomedical systems. Here the underlying processes are not determined by simple biological principles (if they are, we simply do not know them yet), but are the outcomes of millions of years of evolution that include many random effects. Hence mathematical models for biomedical processes are formulated at various degrees of abstraction based on *experimental evidence*. Modern biological research has the tendency to make these models as comprehensive as possible, but should be aware of the pitfalls of Borges's cartographers guild [33]. In our view, it is the smallest model that still rather accurately describes a phenomenon that is the best. In this text, our emphasis therefore is on *minimally parameterized models* for biomedical phenomenon with the hope of arriving at *robust qualitative conclusions*.

1.5 Comments on Related Literature on Optimal Control in Cancer Treatment

In this text, we shall focus on a few selected topics where methods from optimal control theory will be applied to biomedical problems arising in cancer treatments. There exists a vast literature in which, more generally, optimal control methods are applied to biological problems. We make no attempt to survey this area, but only would like to highlight some references that specifically deal with problems related to cancer treatments and apply methods generally from the realm of techniques that will be used here.

The early literature on applications of optimal control theory to cancer treatment is almost exclusively on cancer chemotherapy (e.g., [74, 150, 307, 308, 242, 243]). Martin Eisen's fundamental monograph [74], especially Chapter VIII "Towards Mathematical Chemotherapy" and the references in this chapter, provides an excellent overview of these contributions that even nowadays still makes for worthwhile reading. Much of this work is on cell-cycle nonspecific mathematical models, often 1-dimensional, and focussing on different growth models [242]. The later monograph [230] by Martin and Teo from 1994 is entirely devoted to such models, but including increasingly more comprehensive medical conditions such as single and multi-drug resistance. Eisen also gives some introductory discussion of cell-cycle

specific chemotherapy and compartmental models (distinguishing between proliferating and quiescent cells), but mostly in the context of pharmacokinetics and clearly the emphasis is more on modeling than on analysis. Starting in the 1980s, a greater emphasis in research has been put on cell-cycle specific models. Dibrov et al. specifically consider phase-specific administration of cytotoxic agents to increase the selectivity of therapy [67] and A. Swierniak models the proliferation cycle of leukemia [311]. These efforts have seen a strong second effort in the 1990s in the research by Swierniak, Kimmel, and co-workers (e.g., see [313, 318, 323, 324]) with the further development and analysis of compartmental models which describe and analyze the actions of drugs in specific compartments from a control theory point of view. (These will be the topic of Chapter 2.) In these models, the emphasis is on the cancerous cells and side effects are only measured indirectly through the total dose of drugs administered. Fister and Panetta [83] analyze a compartmental model formulated by Eisen and Schiller [75] that takes the reverse point of view and makes the side effects of cancer chemotherapy on the bone marrow the central topic. The papers by F. Billy, J. Clairambault, and O. Fercoq [26] or by H. Sbeity and R. Younes [289] are two more recent surveys about optimization methods in the planning of cancer chemotherapy that also contain a wealth of information about alternative modeling approaches to the topic which more generally lead to the use of numerical optimization procedures, not necessarily methods from optimal control. These topics, however, lie well outside the realm that we shall pursue here.

There exists a vast literature on optimal administration of chemotherapeutical drugs in the presence of drug resistance and some of this will be considered in Chapter 3. This topic also forms an integral component of the monograph by Martin and Teo [230]. As a small sample, we only mention the papers by A. Coldman and J. Goldie [60, 61, 105], M. Costa and J. Baldrini [63, 64], T. Jackson and H. Byrne [130], A. Swierniak et al. [153, 324, 325], or our own [198, 199]. As will be seen, this is also from the mathematical side quite a challenging topic.

In the 2000s there has been an especially strong resurgence of the use of optimal control as a methodology in response to mathematical models for novel cancer treatments that have been proposed in the medical literature. We shall extensively discuss these efforts in connection with antiangiogenic treatments in Chapters 5–7 and will not repeat this here. But a second such topic is immunotherapy and this will be less in the focus of our text. Optimal control of tumor immune interactions will be considered in Chapter 8 in the context of Stepanova's model, but there exists a wide range of literature on this topic also for more general models. De Pillis and Radunskaya consider an optimal control approach to drug therapy with immune resistance [279] that is based on a validated mathematical model of cell-mediated immune response to tumor growth [280]. Some of the mathematical models used in this research are based on an earlier paper by D. Kirschner and J.C. Panetta that models immunotherapy of tumor-immune interaction [158]. An optimal control approach to immunotherapy has been taken in the papers by Burden, Ernstberger, and Fister [42] and by Fister and Hughes Donnelly [82] who also build upon this model by Kirschner and Panetta. In the context of modeling the activities of the immune system, it is also worthwhile to at least mention a wealth of research that has been

conducted in the context of HIV, also with an optimal control angle to it, such as the paper by Kirschner, Lenhart, and Serbin [157]. But immunotherapy reaches well beyond tumor immune-system interactions. For example, the optimal bolus type scheduling of dendritic cell transfection is considered by Castiglione and Piccoli in [49] and N. Komorova and D. Wodarz study oncolytic viruses [167, 168].

Without even attempting to be complete, we merely mention these references as a snapshot for the renewed interest in methods of optimal control for biomedical models. Some of these works and results are summarized as books, even in the form of textbooks with student exercises like S. Lenhart and J. Workman [216] and by S. Anita, V. Arnăutu and V. Capasso [12]. But these texts do not have cancer treatments as the main focus.

Chapter 2
Cell Cycle Specific Cancer Chemotherapy for Homogeneous Tumors

In this chapter, we analyze a class of cell cycle specific compartmental models for cancer chemotherapy. Besides drug resistance, cell cycle specificity of drugs is viewed as one of the major obstacles against successful chemotherapy [83, 52]. By considering the phases of the cell cycle separately, it is possible to appropriately model the different actions of various drugs involved. A first such model was introduced for leukemia in the work of Kimmel and Swierniak [150] and later has been expanded greatly in the work by Swierniak and his co-workers (e.g., see [313, 321, 322, 323, 324] and many more). A common characteristic of all the models analyzed in this section is that it is implicitly assumed that the cancer population is homogeneous and consists of cells that are sensitive to the chemotherapy applied. If we then minimize a weighted average of the tumor population and the total dose of chemotherapy given over a fixed therapy interval, it will be seen that in this scenario it indeed is optimal to give chemotherapy in one full dose session upfront at the beginning of the therapy interval. These results are fully consistent with and confirm as optimal the classical MTD (maximum tolerated dose) regimen. Essentially, the *underlying scenario* in these models is one where *cancer is growing rapidly at a critical level, but sensitive to chemotherapeutic agents*. The intuitive *optimal solution* then is to *hit it as hard as possible, as soon as possible*.

We begin in Section 2.1 with the analysis of the most rudimentary version of these models, a 2-compartment model for chemotherapy for the action of a single G_2/M-specific cytotoxic agent (such as paclitaxel). This model is also used as a vehicle to introduce and describe the tools and techniques of optimal control. These range from an analysis of the first-order necessary conditions for optimality of the Pontryagin maximum principle to the elimination of singular controls from optimality through the Legendre-Clebsch condition (a high-order necessary condition for optimality) to establishing the optimality of bang-bang controls by means of the construction of a field of extremals. From the practical point of view, singular controls correspond to lower-dose, time-varying dosing regimes, while bang-bang controls represent full dose therapy sessions with rest periods. We give a detailed

H. Schättler, U. Ledzewicz, *Optimal Control for Mathematical Models of Cancer Therapies*, Interdisciplinary Applied Mathematics 42,
DOI 10.1007/978-1-4939-2972-6_2

analysis of this particular model to *illustrate the full set of techniques that generally are required to come to a complete solution*. A brief survey of the main theoretical results and procedures from optimal control theory that are used is provided in Appendix A, but the text is written in a self-contained manner that can be read on its own. We only relegate the construction of an optimal field of extremals to a separate appendix, Appendix B, where we carry out the more technical aspects of this argument in detail. In Section 2.2, analogous MTD based structures are confirmed as optimal for two examples of 3-compartment models when a G_2/M-specific cytotoxic agent is combined with a cytostatic and recruiting agent, respectively. Also, as an initial simplification, we ignore the pharmacokinetics of the drugs and identify their dose rates with their concentrations in the blood stream. In Section 2.3, we give a brief introduction to pharmacokinetics (PK) and pharmacodynamics (PD) of drugs and show that the structure of solutions—maximum dose sessions with rest periods—is retained when linear pharmacokinetic models (and these are the standard of the industry) are included in the modeling while only minute quantitative changes in the actual solutions occur.

2.1 A 2-Compartment Model with a Cytotoxic Agent

We begin with a simple model that allows us to introduce and describe the tools of optimal control with minimal mathematical complexity necessary. The same reasoning and analogous computations apply to the more detailed and complex models considered later on. In this sense, this section sets the stage for the rest of the book.

2.1.1 Mathematical Modeling

We consider the problem of administering a single cytotoxic agent that is active in the G_2/M phase of the cell cycle such as, for example, paclitaxel. Taking into account the phase sensitivity of the drug, the cell cycle is therefore broken up into two compartments with one combining the second growth phase G_2 and mitosis M and the other compartment simply made up of the remaining phases of the cell cycle. The state N of the system can then be described by a 2-dimensional vector with $N_1(t)$ denoting the average number of cancer cells in the first compartment at time t (comprised of the phases G_0, G_1 and S) and $N_2(t)$ the average number of cancer cells in the second compartment at time t (comprised of G_2 and M).

Cell division is a stochastic process with individual cells determining the sample paths while the transit times between the various stages follow some empirical distribution. Various probabilistic models have been proposed and can be used to describe these transit times with the Weibull distribution probably the most natural choice. Of these, the simplest structure is provided by an exponential distribution and this is the model that will be used here. Consider a specific compartment, and

suppose the transit times of cells are modeled by an exponential random variable T with mean θ. That is, the probability that a particular cell remains in the compartment after time t is given by

$$P(T \geq t) = \int_t^\infty \frac{1}{\theta} \exp\left(-\frac{s}{\theta}\right) ds = \exp\left(-\frac{t}{\theta}\right).$$

Taking the average over all cells, the outflow from the compartment therefore is simply governed by the linear ordinary differential equation $\dot{M} = -\frac{1}{\theta} M$ with the coefficient the inverse average transit time through the compartment. Applying this to the 2-compartment model, and for the moment assuming that no external stimuli are present, the balance equation for the second compartment takes the form

$$\dot{N}_2(t) = -a_2 N_2(t) + a_1 N_1(t) \tag{2.1}$$

with $a_i > 0$ the inverse mean transit time through the ith compartment. Here we also use that the outflow of the first compartment equals the inflow into the second compartment. For the second compartment this no longer is the case because of cell division. While the outflow is still given by $a_2 N_2(t)$, the inflow into the first compartment doubles and becomes $2a_2 N_2(t)$ giving

$$\dot{N}_1(t) = -a_1 N_1(t) + 2a_2 N_2(t). \tag{2.2}$$

The transit times of cells through the G_2 and M phases are notably shorter than the combined transit times through the remaining phases. Most cells spend 50–80% of the their growth time in the G_1 phase and the shortest time in G_2/M (less than 10% in some cell lines). It is not uncommon to have a cell line with a doubling time of 20 hours to spent 14 hours in G_1 and the G_2/M phase only takes 4 hours. For healthy, rapidly proliferating human cells, rough estimates are for the cell cycle to last for about 24 hours with about 11 hours in G_1, 8 hours in S, 4 hours in G_2 and one hour in M. We therefore generally have that $a_1 < a_2$. However, except for numerical simulations, we do not use specific parameter values, and develop the theory in general.

We write the linear dynamics given by equations (2.1) and (2.2) in matrix form as $\dot{N} = AN$ with $N = (N_1, N_2)^T$ and $A \in \mathbb{R}^{2\times 2}$ given by

$$A = \begin{pmatrix} -a_1 & 2a_2 \\ a_1 & -a_2 \end{pmatrix}. \tag{2.3}$$

The solution to this differential equation is given by the matrix exponential,

$$N(t) = \exp(At) N(0) = \left(\sum_{n=0}^{\infty} \frac{A^n}{n!} t^n \right) N(0).$$

Since the differential equations are linear, quotients of the variables obey Riccati differential equations and it follows that in steady state, i.e., in the "long" run, fixed proportions of the cells will lie in the respective compartments. Let

$$x = \frac{N_1}{N_1 + N_2} \qquad \text{and} \qquad y = \frac{N_2}{N_1 + N_2} \tag{2.4}$$

denote the average proportions of cells in the two compartments, $x, y > 0, x + y = 1$. It then follows that

$$\dot{y} = \frac{d}{dt}\left(\frac{N_2}{N_1 + N_2}\right) = \frac{a_1 N_1 - a_2 N_2}{N_1 + N_2} - \frac{a_2 N_2^2}{(N_1 + N_2)^2} = a_1 x - a_2 y - a_2 y^2,$$

so that y satisfies the Riccati equation

$$\dot{y} = a_1 - (a_1 + a_2)y - a_2 y^2. \tag{2.5}$$

Note that for $y = 0$ we have $\dot{y}_{|y=0} = a_1 > 0$ and for $y = 1$ we have that $\dot{y}_{|y=1} = -2a_2 < 0$. Hence it follows that solutions to this differential equation cannot escape from the interval $[0, 1]$ forward in time.

Definition 2.1.1 (Invariant Regions). A region R is said to be positively invariant for a differential equation $\dot{x} = f(x)$ if whenever x_0 is a point in R, then the solution $x(t; x_0)$ of the initial value problem $\dot{x} = f(x)$, $x(0) = x_0$, exists for all times $t \geq 0$ and lies in R, $x(t; x_0) \in R$ for all $t \geq 0$. Analogously, R is said to be negatively invariant for a differential equation $\dot{x} = f(x)$ if whenever x_0 is a point in R, then the solution $x(t; x_0)$ of the initial value problem $\dot{x} = f(x)$, $x(0) = x_0$, exists for all times $t \leq 0$ and lies in R, $x(t; x_0) \in R$ for all $t \leq 0$. A region R is said to be invariant if it is both positively and negatively invariant.

It is easy to see that (2.5) has a unique, globally asymptotically stable equilibrium point y_* in the open interval $(0, 1)$ given by

$$y_* = \frac{1}{2}\left(\sqrt{\left(1 + \frac{a_1}{a_2}\right)^2 + 4\frac{a_1}{a_2}} - \left(1 + \frac{a_1}{a_2}\right)\right) \tag{2.6}$$

and all solutions approach this value as $t \to \infty$. This limit only depends on the quotient $\frac{a_1}{a_2}$ and this quotient can be recovered from measurements of the steady-state proportion x_* and y_* as

$$\frac{a_1}{a_2} = y_* \frac{1 + y_*}{1 - y_*} = \frac{y_* + y_*^2}{x_*}. \tag{2.7}$$

For example, if we use the rough approximate inverse transit times $a_1 = \frac{24}{19} = 1.263$ [days] and $a_2 = \frac{24}{5} = 4.8$ [days] based on the typical cell cycle transit times quoted above, then at a specific time only about 20% of cells are in the G_2/M compartment where they can be killed ($y_* = 0.1821$). Figure 2.1 illustrates the quick convergence of the proportions to their steady-state values. The graph on the left with initial condition $y(0) = 0$ shows how quickly the cells redistribute after a bolus type MTD injection that would have killed all the cells in the G_2/M compartment.

If we write $C(t) = N_1(t) + N_2(t)$ for the average total number of cancer cells, then the differential equations imply that

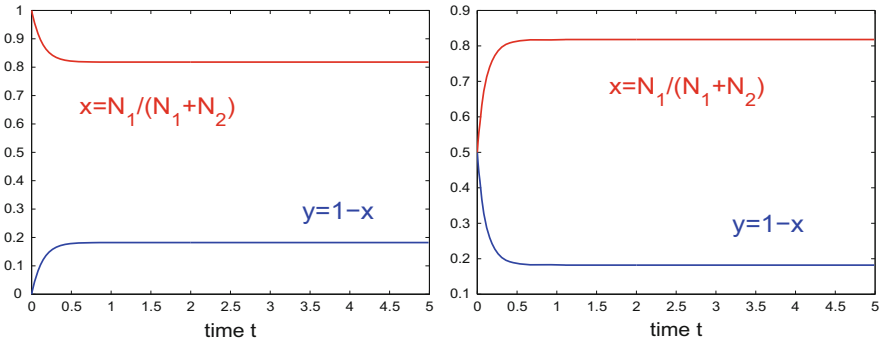

Fig. 2.1 Trajectories for the average fractions x and y of cells in the compartments $G_0/G_1/S$ and G_2/M.

$$\dot{C}(t) = a_2 N_2(t) = a_2 y(t) C(t) \approx a_2 y_* C(t). \tag{2.8}$$

Thus, in steady state, the total tumor population grows approximately exponentially at rate $a_2 y_*$. If T denotes the tumor doubling time, then we have the simple relation $2 = \exp(a_2 y_* T)$, i.e.,

$$T = \frac{\ln 2}{a_2 y_*}. \tag{2.9}$$

The steady-state proportion y_* of cells in the G_2/M phase and the tumor doubling time T are quantities that can be determined experimentally and equations (2.7) and (2.9) can be used to determine the cell cycle parameters a_1 and a_2 used in this model. We summarize these formulas in the next Proposition.

Proposition 2.1.1. *With T denoting the tumor doubling time and x_* and y_* the steady-state proportions of cells in the $G_0/G_1 + S$ and G_2/M phases of the cell cycle, respectively, we have that*

$$a_1 = (1 + y_*)\frac{\ln 2}{T x_*} \qquad \text{and} \qquad a_2 = \frac{\ln 2}{T y_*}.$$

There exist large differences between the transit times through the cell cycle for different types of tumors and even from patient to patient for the same tumor. For example, in clinical evaluations, for pancreatic carcinoma, tumor doubling times have been observed that range from 68 to 255 days and for other carcinomas even wider spreads occurred [237]. Many doubling times listed in that article have ranges that differ by hundreds of days with the range for sarcoma, metastasized lung cancer, the most extreme ranging form 7 to 1172 days. Great progress has been made in estimating cell cycle parameters of tumor cells *in vivo*. The stathmokinetic or "metaphase arrest" technique consists of blocking cell division by an external agent (usually a drug such as vincristine or colchicine). The cells gradually accumulate in mitosis, emptying the postmitotic phase G_1 and with time also the S phases. Flow cytometry allows precise measurements of the fractions of cells residing in different cell cycle phases. The pattern of cell accumulation in mitosis M depends on the

kinetic parameters of the cell cycle and is used for estimation of these parameters. Exit dynamics from G_1 and transit dynamics through S and G_2 and their subcompartments can be used to characterize very precisely both unperturbed and perturbed cell cycle parameters. Thus cell cycle flow cytometry is readily able to assess the proportions of cells that are in the G_0/G_1, S and G_2/M phases of the cell cycle on an individual basis (e.g., see, [73]) and from these proportions, cell cycle transit times can be inferred.

Drug treatment influences the cell cycle in many ways and here only the most fundamental aspect is considered, cell killing by a cytotoxic agent in the G_2/M phase. In this first model, we assume all cells are drug sensitive and do not yet include a pharmacokinetic model on the drug. Thus, for the moment, the *control* variable *u represents the drug concentration in the blood stream* or, for simplicity, we identify the drug's dose rate with its concentration. In accordance with the log-kill hypothesis, we assume that the drug concentration $u(t)$ kills a fraction of the outflow $a_2N_2(t)$ of cells from the G_2/M compartment and thus the number of cells killed is given by $\varphi u(t)a_2N_2(t)$ with φ a constant chemotherapeutic killing parameter. The control set is a compact interval $[0,u_{\max}]$ with $u_{\max}$ denoting the maximum dose rate/concentration. In the model, the control u always appears in conjunction with the constant φ and thus, in order to keep the number of free parameters to a minimum, we combine it with the maximum dose rate into one quantity that we still denote with $u_{\max}$ under the assumption that $u_{\max} \leq 1$. If the concentration is high enough, then indeed $u_{\max} = 1$ is realistic: almost all the cancer cells in that compartment can be killed. Cells which are killed in G_2/M leave this compartment, i.e., are counted as outflows from the second compartment, but they no longer enter the first compartment. In this sense, *the prevention of further cohorts is considered killing* the cell even if no apoptosis is induced. The remaining fraction $(1-u)a_2N_2$ undergoes cell division and thus the controlled mathematical model becomes

$$\dot{N}_1 = -a_1N_1 + 2(1-u)a_2N_2, \qquad N_1(0) = N_{10}, \tag{2.10}$$

$$\dot{N}_2 = a_1N_1 - a_2N_2, \qquad N_2(0) = N_{20}, \tag{2.11}$$

with all initial conditions positive. A system of this type is called a *bilinear control system* [76] since it is linear both in the state N and the control u. Note, however, that there exist quadratic terms uN so that overall this is a nonlinear control system. In matrix form we get

$$\Sigma: \qquad \dot{N}(t) = (A + uB)N(t), \quad N(0) = N_0, \tag{2.12}$$

with A and B given below,

$$A = \begin{pmatrix} -a_1 & 2a_2 \\ a_1 & -a_2 \end{pmatrix}, \qquad \text{and} \qquad B = \begin{pmatrix} 0 & -2a_2 \\ 0 & 0 \end{pmatrix}. \tag{2.13}$$

We illustrate the structure of the model in Figure 2.2.

Clearly, the states of this system correspond to positive numbers and we briefly verify that the model is consistent in this aspect. It is therefore not necessary to add

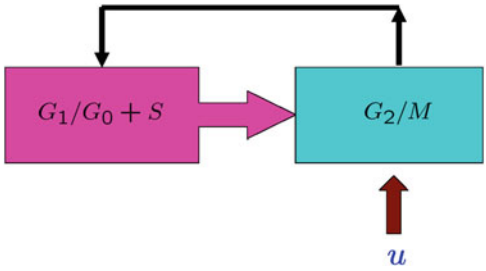

Fig. 2.2 A 2-compartment model with G_2/M-specific cytotoxic agent.

nonnegativity of the states as an explicit state-space constraint. We generally denote by $\mathbb{P}$ the positive orthant in $\mathbb{R}^n$, so that for this model we set $\mathbb{P} = \mathbb{R}^2_+ = \{N \in \mathbb{R}^2 : N_i > 0 \text{ for } i = 1,2\}$.

Definition 2.1.2 (Positively Invariant Control System). A subset P of the state-space M is said to be positively invariant for a control system Σ if, whenever x_0 is an initial condition that lies in P, $x_0 \in P$, and u is an arbitrary admissible control defined on some interval $I \subset [0,\infty)$, then the corresponding trajectory x exists over the full interval I and lies in P, $x(t) \in P$ for all $t \in I$.

Proposition 2.1.2. *The positive orthant $\mathbb{P}$ is positively invariant for the control system (2.12).*

Proof. For this proof, we already anticipate the argument needed for a more general system Σ in Section 2.2. For any admissible control defined over an interval $[0,T]$, the norm of the matrix $A + uB$ is bounded over $[0,T]$ and thus the right-hand side of the differential equation (2.12) is linearly bounded. It therefore follows from well-known results about ordinary differential equations (e.g., see [292, Corollary B.1.3]) that the corresponding trajectory exists on all of $[0,T]$. Positive invariance follows from the fact that the dynamics $\dot{N}$ has the following structure

$$\dot{N}_i(t) = -\beta_{ii}(t)N_i(t) + \beta_{ij}(t)N_j(t), \qquad i \neq j,$$

where, regardless of the admissible control used, the functions β_{ij}, $i \neq j$, are non-negative and the diagonal elements β_{ii} are strictly positive. Proceeding with a proof by contradiction, suppose $\tau = \min\{t \geq t_0 : N_i(t) = 0 \text{ for some index } i\} \leq T$. Since the N_i are continuous functions, the minimum is well defined and for some index i_0 we have that $N_{i_0}(\tau) = 0$. On the interval $[0,\tau)$ it then follows that

$$\dot{N}_{i_0}(t) = -\beta_{i_0 i_0}(t)N_{i_0}(t) + \alpha(t)$$

where $\beta_{i_0 i_0}(t) > 0$ and $\alpha(t) = \beta_{i_0 j}(t)N_j(t) \geq 0$. Thus

$$N_{i_0}(\tau) = \exp\left(-\int_{t_0}^{\tau} \beta_{i_0 i_0}(s)ds\right)\left(N_{i_0}(t_0) + \int_{t_0}^{\tau} \exp\left(-\int_{t_0}^{s} \beta_{i_0 i_0}(r)dr\right)\alpha(s)ds\right) > 0.$$

Contradiction. □

2.1.2 Formulation of the Optimal Control Problem

In all models, within various degrees of approximation, the dynamics represents the underlying biology of the problem. On the other hand, the *objective* in an optimal control problem is artificially imposed from the outside and thus generally there exist options with possibly not necessarily a clear "best" choice. In fact, in engineering problems, it is quite common to vary the forms of the objective and eventually pick one that induces a satisfactory system response, possibly because it shows good properties (like stability, robustness, etc.) with respect to other design criteria that were not included in the modeling. In other fields, like economics, this may be less appropriate as the objective is clearly specified, for example, if the aim is to minimize the cost of some production process. For biomedical problems, the truth often lies somewhere in between these two extremes.

Clearly, the aim is to cure the patient. There are many ways to translate this into a mathematical objective and, one way or the other, it will include the minimization of the overall number of cancer cells. In addition, there is the important constraint of the *toxicity of the treatment*. There are two principal ways of including this into the model, either directly as additional constraint, or indirectly, by including a measure for the side effects of the treatment as a penalty term in the objective.

In a *direct* approach, parts of the states in the model may be related to the side effects. For example, bone marrow cells generally also divide rapidly and thus are especially harmed by chemotherapy. Thus, one possible way of including side effects in the model is to simply make the bone marrow one of the compartments and then to impose a restriction that the bone marrow levels stay above a certain level. This constitutes a so-called state-space constraint, a common feature in some optimal control problems. However, it generally is rather difficult to ascertain when such thresholds are reached. It is therefore practically more convenient to limit the overall amount of drugs to be given a priori (based on medical experience) and then to ask the question how the drugs could best be used. Such a requirement can mathematically be modeled as a terminal constraint and we shall extensively use this approach in Chapter 5. Analyzing the solutions for various a priori specified amounts of therapeutic agents, a comprehensive analysis of the overall problem can be undertaken that will allow to balance the benefits of the treatment with the side effects.

In *indirect* approaches, this is done in one step. Minimizing an objective that includes measures for the quantities of tumor cells and the total amount of drugs given forces a balance between these two conflicting terms: in order to minimize the cancer cells, one needs to give drugs, but these are being penalized. Obviously, the solution depends on the specific parameters and more so on the specific functional forms chosen in the objective. For example, in the literature the penalty term on the drugs often is taken in one of the following two forms known as L_1-, respectively L_2-objectives:

$$\int_0^T u(t)dt \qquad \text{or} \qquad \int_0^T u(t)^2 dt.$$

The quadratic structure offers distinct mathematical advantages (due to the convexity properties that it imposes on the optimal control problem), but is rather difficult to justify biologically. The linear term, on the other hand, has a clear interpretation as the overall amount of drug given and with a log-kill model of cell death under chemotherapy, this term also stands in direct relation to the healthy cells killed by the treatment. Hence *the linear term has a clear biological meaning*, but the mathematics becomes more difficult. We shall consider both formulations, but our emphasis in this text will be on the biologically more appropriate L_1-objective.

Here we chose the performance index or objective in the form

$$J = rN(T) + \int_0^T qN(t) + su(t)dt \to \min \tag{2.14}$$

where T is an a priori specified therapy horizon, $r = (r_1, r_2)$ is a row vector of positive weights and $q = (q_1, q_2)$ is a row vector of nonnegative weights. The penalty term $rN(T) = r_1N_1(T) + r_2N_2(T)$ thus represents a weighted average of the total number of cancer cells at the end of an assumed fixed therapy interval $[0, T]$ and the term $qN(t) = q_1N_1(t) + q_2N_2(t)$ is a running cost that measures the tumor volume during treatment. Side effects of the treatment are only included in the model indirectly through minimization of the total dose, $\int_0^T u(t)dt$. The positive coefficient s at this integral is actually redundant since it could be absorbed into the other weights. But we also want to consider the dependence of the solutions on various coefficients, and especially on this term, and it thus becomes more convenient to retain this coefficient. Recall that the number of cancer cells that do not undergo cell division at time t and are considered "killed" is given by $u(t)a_2N_2(t)$, i.e., $u(t)$ is proportional to the fraction of ineffective cell divisions. Since the drug kills healthy cells at a similar rate, the integral $\int_0^T u(t)dt$ represents the cumulative negative effects of the treatment on the normal tissue or its toxicity. Overall, we thus arrive at the following optimal control problem:

[CC2] for a fixed final time $T > 0$, minimize the objective

$$J(u) = rN(T) + \int_0^T qN(t) + su(t)dt \to \min \tag{2.15}$$

over all Lebesgue-measurable (respectively, piecewise continuous) functions $u : [0, T] \to [0, u_{\max}]$, subject to the dynamics

$$\dot{N}(t) = (A + uB)N(t), \qquad N(0) = N_0, \tag{2.16}$$

with A and B given by the matrices (2.13).

We note that the class of *Lebesgue measurable functions* consists of all pointwise limits of piecewise continuous (in fact, even piecewise constant) functions. We formally employ it in our formulations of the optimal control problems considered in this text since it provides appropriate closure properties that allow the application of standard results in optimal control theory that guarantee the existence of an optimal

solution. Even for the mathematical models considered in this text, optimal controls need not be piecewise continuous, but may only be Lebesgue measurable functions (c.f., Section 6.3). However, familiarity with this concept is not needed to follow our reasoning. In order to make the text more accessible to the non-mathematician, and also since this is more than adequate from a practical point of view, we typically work with piecewise continuous controls. For the same reason we do not discuss the existence of optimal solutions in our text. In fact, optimal solutions exist for all the problems considered in this text (but see Section 8.2) and we refer the interested reader to the corresponding literature (e.g., [51]).

2.1.3 *Necessary Conditions for Optimality: Switching Functions, Bang-Bang and Singular Controls*

The fundamental first-order necessary conditions for optimality for problem [CC2] are given by the Pontryagin maximum principle [282] (Theorem A.2.1 in Appendix A). From an application oriented point of view, this result is a multiplier rule with a constant multiplier $\lambda_0 \geq 0$ associated with the objective and a time-varying multiplier λ associated with the dynamics. The main necessary condition for optimality is the statement that optimal controls minimize (respectively, maximize, as it was in the historical formulation) the so-called Hamiltonian function

$$H = H(\lambda_0, \lambda, N, u) = \lambda_0(qN + su) + \lambda(A + uB)N \tag{2.17}$$

over the control set $[0, u_{\max}]$ pointwise along the optimal controlled trajectory (N_*, u_*) and the multipliers (λ_0, λ). Specifically for the optimal control problem [CC2], the conditions of the Pontryagin maximum principle reduce to the following statement (see, Theorem A.3.1 in Appendix A):

Theorem 2.1.1 (Maximum Principle for Problem [CC2]). *If u_* is an optimal control with corresponding trajectory N_*, then there exist a constant $\lambda_0 \geq 0$ and an absolutely continuous function λ, which we write as row-vector, $\lambda : [0,T] \to (\mathbb{R}^2)^*$, called the adjoint or co-vector, such that the following conditions are satisfied:*

1. nontriviality*: $(\lambda_0, \lambda(t)) \neq (0,0)$ for all $t \in [0,T]$,*
2. adjoint equation and transversality condition*:the multiplier λ is a solution to the terminal value problem*

$$\dot{\lambda} = -\frac{\partial H}{\partial N}(\lambda_0, \lambda, N_*, u_*) = -\lambda_0 q - \lambda(A + u_* B), \qquad \lambda(T) = \lambda_0 r, \tag{2.18}$$

i.e.,

$$\begin{aligned} \dot{\lambda}_1 &= -\lambda_0 q_1 + \lambda_1 a_1 - \lambda_2 a_1, & \lambda_1(T) &= \lambda_0 r_1, \\ \dot{\lambda}_2 &= -\lambda_0 q_2 - 2(1-u_*)\lambda_1 a_2 + \lambda_2 a_2, & \lambda_2(T) &= \lambda_0 r_2, \end{aligned}$$

3. minimum condition*: the optimal control minimizes the Hamiltonian H pointwise over the control set* $[0,u_{\max}]$ *along the optimal controlled trajectory and the multipliers* $(\lambda_0,\lambda(t))$*, i.e.,*

$$H(\lambda_0,\lambda(t),N_*(t),u_*(t)) = \min_{u\in[0,u_{\max}]} H(\lambda_0,\lambda(t),N_*(t),u) \tag{2.19}$$

and the minimum value is constant over the interval $[0,T]$*,*

$$H(\lambda_0,\lambda(t),N_*(t),u_*(t)) = \text{const.} \tag{2.20}$$

We note that the multiplier λ is piecewise continuously differentiable if the control u_* is piecewise continuous and this will be the case for all problems considered in this chapter. These conditions form a highly interwoven system of equations from which the optimal controlled trajectory needs to be determined. Together with the dynamics of the system, the adjoint equation forms a two-point boundary value problem that is linked with the optimal control through the minimization condition. This system may have multiple solutions and, in principle, we need to find them all to determine the globally optimal control.

The following terminology is standard in optimal control theory: A *controlled trajectory* (N,u) for which there exist multipliers λ_0 and λ such that these conditions are satisfied, is called an *extremal* (pair) and the triple $(N,u,(\lambda_0,\lambda))$ is an extremal lift. If the multiplier $\lambda_0 = 0$, the extremal is called *abnormal* while it is called *normal* if $\lambda_0 > 0$. In the latter case, by dividing by λ_0, it is always possible to normalize $\lambda_0 = 1$. It is easily seen that for our case all extremals are normal. For, if $\lambda_0 = 0$, then the terminal condition in (2.18) becomes $\lambda(T) = 0$ and thus λ vanishes identically as solution to a homogeneous linear differential equation. But this contradicts the nontriviality condition on the multipliers. We henceforth normalize $\lambda_0 = 1$ and drop λ_0 in our notation.

The same structure of the equations which gave positive invariance of the positive orthant $\mathbb{P}$ in the state-space for the flow of controlled trajectories also implies negative invariance of the first quadrant in the dual space, $\mathbb{P}^* = \{\lambda \in \left(\mathbb{R}^2\right)^* : \lambda_i > 0 \text{ for } i = 1,2\}$, under the adjoint flow (2.18). This simply is a consequence of the reversal of direction in the two differential equations.

Proposition 2.1.3. *The positive orthant* $\mathbb{P}^*$ *is negatively invariant for the adjoint equation (2.18), i.e., if* $\lambda(T) \in \mathbb{P}^*$*, then the multipliers* $\lambda_1(t)$ *and* $\lambda_2(t)$ *are positive over the interval* $[0,T]$*.*

Proof. Inspection shows that the adjoint equations have the structure

$$\dot{\lambda}_i(t) = \gamma_{ii}\lambda_i(t) - \gamma_{ij}(t)\lambda_j(t), \qquad i \neq j,$$

where the γ_{ii} are positive numbers and, regardless of which admissible control is used, the functions γ_{ij}, $i \neq j$, are nonnegative. Let

$$\tau = \max\{0 \le t \le T : \lambda_i(t) = 0 \text{ for some index } i\}$$

and denote an index for which the minimum is achieved by i_0. Then, on $(\tau, T]$ we have that

$$\dot{\lambda}_{i_0}(t) = \gamma_{i_0 i_0}\lambda_k(t) - \alpha(t)$$

where $\gamma_{i_0 i_0} > 0$ and $\alpha(t) = \gamma_{i_0 j}(t)\lambda_j(t) \geq 0$. Thus

$$\lambda_{i_0}(\tau) = \exp\left(\gamma_{i_0 i_0}(\tau - T)\right)\left(r_{i_0} + \int_\tau^T \exp\left(-\gamma_{i_0 i_0}(s-T)\right)\alpha(s)ds\right) > 0.$$

Contradiction. □

Hence, since $N_0 \in \mathbb{P}$ and $r \in \mathbb{P}^*$, it follows that

Corollary 2.1.1. *For the optimal control problem [CC2], all states N_i and costates λ_i, $i = 1,2$, of an extremal are positive over $[0,T]$.*

Before we go into the discussion of how the conditions of the maximum principle actually will be used to gain information about the structure of optimal controls, we would like to insert one quite **important remark** about the choice of the weights q and r in the objective (2.14). These are *variables of choice* and it would seem obvious—and this is correct—that optimal controls will be identically $u \equiv u_{\max}$ if total disregard of the side effects is built into the model by choosing a small coefficient s and similarly optimal controls will be given by $u \equiv 0$ if these side effects are made far too important by choosing s too high. Once we normalize s, say $s = 1$, then, since the objective has a linear structure, these features are still there if we would choose q or r too small or too high. Since we are not interested in these extreme situations, but into the relevant class of problems that lie in the middle, the question about a proper scaling of these coefficients arises. If we include q and r with the state N and costate λ into one vector, then indeed there exists a one-parameter group of scaling symmetries (i.e., one degree of freedom) that allows us an informed choice. Note that, if κ is a positive constant, then the rescaling

$$(r,q,N,\lambda) \mapsto \mathscr{S}_\kappa = \left(\frac{r}{\kappa}, \frac{q}{\kappa}, \kappa N, \frac{\lambda}{\kappa}\right) \tag{2.21}$$

leaves the extremals and the value of the objective function invariant. For, it follows from the linearity of the dynamics and adjoint equation that under this transformation the states change from N to κN and the costates from λ to $\frac{1}{\kappa}\lambda$. In particular,

$$\begin{aligned} J(u) &= rN(T) + \int_0^T qN(t) + su(t)dt \\ &\to \left(\frac{r}{\kappa}\right)(\kappa N(T)) + \int_0^T \left(\frac{q}{\kappa}\right)(\kappa N(t)) + su(t)dt = J(u) \end{aligned}$$

and

$$H = qN + su + \lambda(A + uB)N \quad \to \quad \frac{q}{\kappa}\kappa N + su + \frac{\lambda}{\kappa}(A + uB)\kappa N = H.$$

The controls are expressed as percentages and once we choose s near 1, then it makes sense—and in our numerical computations this generally has given rise to the nontrivial structures desired—to choose the coefficients r and q proportional to $\frac{1}{N_0}$ with N_0 the initial condition for the tumor volume. Equivalently, without loss of generality we normalize $N_0 = 1$. We shall not make any use of this structure in our theoretical derivations below, but use it in the numerical illustrations that we give.

We return to evaluating the conditions of the maximum principle. The condition that gave this result its name is the third one which, in the original version of the result, was formulated for a maximization problem. This is the most important of the conditions in that it relates the solution of the optimal control problem, a minimization problem on an infinite-dimensional function space defined by a class admissible controls $u(\cdot)$, to a finite-dimensional minimization problem for the control at time t, $u_*(t)$, over the control set $[0, u_{\max}]$. For problem [CC2], after deleting terms that do not depend on the control u, this condition reduces to

$$(s + \lambda(t)BN_*(t))\, u_*(t) = \min_{0 \le v \le u_{\max}} (s + \lambda(t)BN_*(t))\, v. \tag{2.22}$$

But this simply is the problem of minimizing a linear function of the form $a(t)v$ over the compact interval $[0, u_{\max}]$ for some time-varying function a. If we define the function Φ by

$$\Phi(t) = s + \lambda(t)BN_*(t), \tag{2.23}$$

then, whenever this function does not vanish, the optimal controls are simply given by

$$u_*(x) = \begin{cases} u_{\max} & \text{if } \Phi(t) < 0, \\ 0 & \text{if } \Phi(t) > 0. \end{cases} \tag{2.24}$$

A priori, however, the minimum condition does not provide us with any information about $u_*(t)$ if $\Phi(t) = 0$. In this case, every control value $v \in [0, u_{\max}]$ satisfies (2.22). Note that the function Φ is differentiable—both λ and N are solutions of differential equations—and thus, for example, if $\Phi(\tau) = 0$, but the derivative $\dot{\Phi}(\tau)$ does not vanish, then the time τ is an isolated point of the zero set $\mathscr{Z}_\Phi = \{t \in [0,T] : \Phi(t) = 0\}$. In this case, the function Φ changes sign at time τ and the optimal control switches between the values 0 and $u_{\max}$: from 0 to $u_{\max}$ if $\dot{\Phi}(\tau) < 0$ and from $u_{\max}$ to 0 if $\dot{\Phi}(\tau) > 0$. A junction of this type is called a bang-bang switch and the constant controls that take on the extreme values 0 and $u_{\max}$ are called *bang* controls. Because of this behavior, the function Φ is called the *switching function* of the optimal control problem [CC2] and the structure of optimal controls is determined by the zero set $\mathscr{Z}$.

Unfortunately, in general this set $\mathscr{Z}$ can be extremely complicated. In fact, the zero set of a differentiable function can be any closed subset of the domain (e.g., see [292, Proposition 2.8.1]). There is one special case, however, in which the situation simplifies considerably. It arises when the switching function vanishes over an open interval I. For, in this case also all the derivatives of Φ on the interval I vanish as well, and with the exception of degenerate situations, the corresponding

formulas determine the control on this interval. Degenerate situations arise when differentiation of the switching function never leads to a term that explicitly depends on the control. Then all controls that otherwise satisfy the constraints of the problem become optimal. But such structures are almost always related to somewhat ill-posed problem formulations. An example of this situation for problems related to chemotherapy is given in [317]. Generally, extremal controls for which the switching function vanishes identically over an open interval I are called *singular*. Note that, whether a control is singular or not is not just a property of the control, but it depends on the full extremal lift (N_*, u_*, λ) since both the multiplier λ and the optimal trajectory N_* enter into the definition of the switching function.

Definition 2.1.3 (Singular Controls and Extremals). Let (N_*, u_*) be an extremal controlled trajectory with corresponding adjoint vector λ. The extremal lift (N_*, u_*, λ) is said to be singular on an open interval $I \subset [0,T]$ if the switching function Φ vanishes identically on I. We say the control u_* is singular on I and call the corresponding portion of the controlled trajectory a singular arc.

This classical terminology is somewhat unfortunate in that it would seem to indicate that this type of controls are an aberration while nothing could be further from the truth. It has its historical origin in the simple observation that the switching function can be expressed as

$$\Phi(t) = \frac{\partial H}{\partial u}(\lambda(t), N_*(t), u_*(t))$$

and thus, formally, the condition $\Phi(t) = 0$ is the first-order necessary condition for the Hamiltonian to have a minimum in the interior of the corresponding control interval. For a general, possibly multi-input optimal control problem, extremal lifts are called singular, respectively nonsingular, over an open interval I if the first-order necessary condition

$$\Phi(t) = \frac{\partial H}{\partial u}(\lambda(t), N_*(t), u_*(t)) \equiv 0 \tag{2.25}$$

is satisfied for $t \in I$ and if the matrix of the second-order partial derivatives,

$$\frac{\partial^2 H}{\partial u^2}(\lambda(t), N_*(t), u_*(t)),$$

is singular, respectively nonsingular, on I. For control-affine problems (i.e., the dynamics and objective are affine functions of the control) such as [CC2], this quantity is identically zero and thus any portions of an optimal control that take values in the interior of the control set are automatically singular. While the terminology is a bit misleading, *singular controls* nevertheless *are natural candidates for optimality*. They provide what sometimes also has been called *turnpikes* for the control problem with switchings between bang controls making the transitions to and from these structures or simply arising only when singular controls are inadmissible or simply do not exist. We refer the interested reader to Appendix A and, more generally to our textbook [292], for a more complete discussion of these concepts (also see Section 2.1.4).

For many (but not all) practical problems, optimal controls turn out to be finite concatenations of bang and singular controls. The precise concatenation sequences need to be determined through an analysis of the switching function. As the model considered in Chapter 5 will demonstrate, this can become a highly nontrivial task. However, for the compartmental problems for cancer chemotherapy considered in this chapter, the situation is considerably simpler because, as we shall show now, optimal controls do not contain intervals where the control is singular. This is a consequence of necessary conditions for optimality of singular controls that we briefly summarize (also, see Appendix A). As noted above in equation (2.25), the switching function Φ is the partial derivative of the Hamiltonian with respect to the control variable u. The standard procedure of computing singular controls consists in differentiating the switching function until the control explicitly appears in these formulas for the first time and then solve the resulting equation $\Phi^{(r)}(t) \equiv 0$ for the control u. In order to be admissible, the resulting solution also needs to take values in the control set. It is quite possible that this procedure works, but determines a control that takes values outside the admissible range and thus is not allowed.

In order to determine the structure of the optimal controls, we need to analyze the switching function and its derivatives. The following lemma, which is central to the computations, allows us to calculate these derivatives of the switching function in an efficient and organized manner by calculating commutators of matrices. Anticipating further models, we formulate it for a general n-dimensional system.

Proposition 2.1.4. *Let $M \in \mathbb{R}^{n\times n}$ be a constant matrix and define $\Psi(t) = \lambda(t)MN(t)$, where N is a solution to the system equation $\dot{N} = (A+uB)N$ for the control u and λ is a solution of the corresponding adjoint equation $\dot{\lambda} = -q - \lambda(A+uB)$. Then Ψ is differentiable with derivative given by*

$$\dot{\Psi}(t) = \lambda(t)[A+uB, M]N(t) - qMN(t), \tag{2.26}$$

where, for two $n \times n$ matrices X and Y, the bracket $[X,Y]$ denotes the commutator of the matrices X and Y defined as

$$[X,Y] = YX - XY. \tag{2.27}$$

More generally, a similar result holds for single-input control affine systems of the form $\dot{z} = f(z) + ug(z)$ (c.f., Proposition A.3.1 in Appendix A) with the commutator replaced with the Lie-bracket of the vector fields f and g. For the linear vector fields $f(z) = Xz$ and $g(z) = Yz$ this reduces to

$$[f,g](z) = Dg(z)f(z) - Df(z)g(z) = YXz - XYz = [X,Y]z.$$

and we have chosen the order in the commutator to be consistent with this definition of the Lie bracket. We refer the reader to Section A.3.2 in Appendix A for a brief discussion of Lie derivatives and the Lie bracket.

Proof. This is a straightforward verification. Dropping the argument t, along the solutions of the dynamics and adjoint equation, we have that

$$\begin{aligned}\dot{\Psi} &= \dot{\lambda}MN + \lambda M\dot{N}\\ &= (-q - \lambda(A+uB))MN + \lambda M(A+uB)N\\ &= \lambda[A+uB, M]N - qMN\end{aligned}$$

verifying (2.26). □

Thus, for the switching function $\Phi(t) = s + \lambda(t)BN_*(t)$ it follows that

$$\dot{\Phi}(t) = \lambda(t)[A,B]N_*(t) - qBN_*(t). \tag{2.28}$$

In particular, the control does not appear in the first derivative—this also is a general property for single-input control affine systems—and Φ is at least twice continuously differentiable. Applying Proposition 2.1.4 once more to the first derivative then gives

$$\begin{aligned}\ddot{\Phi}(t) &= \lambda(t)[A+u(t)B,[A,B]]N_*(t) - q[A,B]N_*(t) - qB(A+uB)N_*(t)\\ &= \{\lambda(t)[A,[A,B]] - q[A,B] - qBA\}N_*(t)\\ &\quad + u(t)\left\{\lambda(t)[B,[A,B]] - qB^2\right\}N_*(t)\end{aligned} \tag{2.29}$$

with the control u multiplying the term $\left\{\lambda(t)[B,[A,B]] - qB^2\right\}N_*(t)$. If this quantity does not vanish over an interval I, then the control u is said to be singular of order 1 and can formally be computed as

$$u_{\text{sing}}(t) = -\frac{\{\lambda(t)[A,[A,B]] - q[A,B] - qBA\}N_*(t)}{\{\lambda(t)[B,[A,B]] - qB^2\}N_*(t)}. \tag{2.30}$$

Note that this formula only defines the singular control as a function of the state N_* and the multiplier λ (i.e., as a function in the cotangent bundle), not as a feedback function that only depends on the state N.

For the problem [CC2], direct computations verify the following relations for products and commutators of the matrices A and B:

$$\begin{aligned}BA &= 2a_2\begin{pmatrix}-a_1 & a_2\\ 0 & 0\end{pmatrix}, \qquad B^2 \equiv 0,\\ [A,B] &= 2a_2\begin{pmatrix}-a_1 & a_2-a_1\\ 0 & a_1\end{pmatrix} = 2a_1a_2\begin{pmatrix}-1 & 0\\ 0 & 1\end{pmatrix} + (a_1-a_2)B,\end{aligned} \tag{2.31}$$

$$\begin{aligned}[A,[A,B]] &= 2a_2\begin{pmatrix}a_1(a_2-a_1) & -(a_1+a_2)^2\\ 2a_1^2 & -a_1(a_2-a_1)\end{pmatrix}\\ &= (a_1-a_2)[A,B] + 4a_1a_2B + 4a_1^2a_2\begin{pmatrix}0 & 0\\ 1 & 0\end{pmatrix},\end{aligned} \tag{2.32}$$

and

$$[B,[A,B]] = 8a_1a_2^2 \begin{pmatrix} 0 & 1 \\ 0 & 0 \end{pmatrix} = -4a_1a_2B. \tag{2.33}$$

If the control u is singular on an open interval I, then $\Phi(t) \equiv 0$ implies that $\lambda(t)BN_*(t) \equiv -s$ and thus

$$\lambda(t)[B,[A,B]]N_*(t) = -4a_1a_2s\lambda(t)BN_*(t) = 4a_1a_2s > 0. \tag{2.34}$$

Along with the fact that $B^2 \equiv 0$, this implies that singular controls are of order 1.

It is not difficult to compute an explicit formula for the singular control using equation (2.30): Since we also have $\dot{\Phi}(t) \equiv 0$ on the interval I, it follows that

$$\lambda(t)[A,B]N_*(t) \equiv qBN_*(t) = -2a_2q_1N_2(t)$$

and thus

$$\begin{aligned} \lambda(t)[A,[A,B]]N_*(t) &= -2a_2(a_1-a_2)q_1N_2(t) - 4a_1a_2 + 4a_1^2a_2\lambda_2(t)N_1(t) \\ &= -2a_2(a_1-a_2)q_1N_2(t) - 4a_1a_2\left(1 - a_1\lambda_2(t)N_1(t)\right). \end{aligned}$$

But

$$-s \equiv \lambda(t)BN_*(t) = (\lambda_1(t),\lambda_2(t)) \begin{pmatrix} 0 & -2a_2 \\ 0 & 0 \end{pmatrix} \begin{pmatrix} N_1(t) \\ N_2(t) \end{pmatrix} = -2a_2\lambda_2(t)N_1(t)$$

gives us that

$$\lambda_2(t)N_1(t) = \frac{s}{2a_2}$$

and thus

$$\lambda(t)[A,[A,B]]N_*(t) \equiv -2a_2(a_1-a_2)q_1N_2(t) - 4a_1a_2\left(1 - \frac{a_1s}{2a_2}\right)$$

Furthermore,

$$\begin{aligned} q[A,B]N_*(t) &= (q_1,q_2)\,2a_2 \begin{pmatrix} -a_1 & a_2-a_1 \\ 0 & a_1 \end{pmatrix} N_*(t) \\ &= 2a_1a_2\left(q_2N_2(t) - q_1N_1(t)\right) + 2a_2(a_2-a_1)q_1N_2(t), \end{aligned}$$

and

$$qBAN_*(t) = (q_1,q_2)\,2a_2 \begin{pmatrix} -a_1 & a_2 \\ 0 & 0 \end{pmatrix} \begin{pmatrix} N_1(t) \\ N_2(t) \end{pmatrix} = -2a_2q_1(a_1N_1(t) - a_2N_2(t)).$$

Hence, overall the singular control is given by

$$\begin{aligned} u_{\text{sing}}(t) &= \frac{a_1 - a_2}{2a_1} q_1 N_2(t) + 1 - \frac{a_1 s}{2a_2} + \frac{1}{2}\left(q_2 N_2(t) - q_1 N_1(t)\right) + \frac{a_2 - a_1}{2a_1} q_1 N_2(t) \\ &\quad - \frac{1}{2a_1} q_1 \left(a_1 N_1(t) - a_2 N_2(t)\right) \\ &= 1 - \frac{a_1 s}{2a_2} + \frac{1}{2}\left(q_2 N_2(t) - q_1 N_1(t)\right) - \frac{1}{2} q_1 N_1(t) + \frac{a_2}{2a_1} q_1 N_2(t) \\ &= 1 - \frac{a_1 s}{2a_2} - q_1 N_1(t) + \frac{1}{2a_1}\left(a_1 q_2 + a_2 q_1\right) N_2(t). \end{aligned}$$

Note that, and different from (2.30), we now have obtained a feedback formula that only depends on the current state $N_*(t)$ of the system and the data, but not on the multiplier, a merely auxiliary object. In order to be admissible, this control defined by $u_{\text{sing}}(t)$ also needs to take values in the control set $[0, u_{\max}]$.

However, singular controls are not necessarily minimizing, but they can also be maximizing. In this case, they would be the worst possible option to pursue for the problem under consideration. The Legendre-Clebsch condition, a high-order necessary condition for optimality of singular controls (see Theorem A.3.2 in Appendix A), allows us to distinguish between these two classes. If a minimizing control u is singular of order 1 on an open interval I, then the Legendre-Clebsch condition states that

$$\frac{\partial}{\partial u}\frac{d^2}{dt^2}\frac{\partial H}{\partial u}(\lambda(t), N_*(t), u_*(t)) \leq 0 \qquad \text{for all } t \in I. \tag{2.35}$$

As we mentioned above, $\frac{\partial H}{\partial u} = \Phi$, and thus this expression is given by the coefficient that multiplies the control u in the second derivative of the switching function, i.e., here

$$\frac{\partial}{\partial u}\frac{d^2}{dt^2}\frac{\partial H}{\partial u}(\lambda(t), N_*(t), u_*(t)) = \left\{\lambda(t)[B,[A,B]] - qB^2\right\} N_*(t) = 4a_1 a_2 s > 0.$$

Hence the Legendre-Clebsch condition for minimality of a singular control is violated. In fact, singular controls are locally maximizing for the problem [CC2]. We therefore have proven the following result about optimal controls:

Theorem 2.1.2. *If (N_*, u_*) is an optimal controlled trajectory for problem [CC2], then there does not exist an interval on which the control u_* is singular.*

Consequently, the zero set of the switching function for an optimal controlled trajectory does not contain intervals. If the optimal control were to be merely Lebesgue measurable, this could still be a highly complicated set of positive measure. For example, even in this text we shall come across solutions given by chattering controls that have an infinite number of switchings on a finite interval. But if the control is piecewise continuous, then this simply is a bang-bang control with a finite number of switchings and these become the prime candidates for optimality.

2.1.4 An Informal Discussion of Optimal Bang-Bang and Singular Controls

Before proceeding with the details of this specific problem, this seems to be as good a place as any to give an informal discussion of some general properties of the structure of solutions to optimal control problems encountered consistently throughout this text. In a typical situation (ignoring trivial structures of extremals and degenerate scenarios when singular controls are of higher order etc.), the local types of solutions to single-input control-affine optimal control problems can be classified into the following three main scenarios: (i) singular extremals simply do not exist, (ii) singular extremals exist and are locally minimizing (the strengthened Legendre-Clebsch condition is satisfied, $\frac{\partial}{\partial u}\frac{d^2}{dt^2}\frac{\partial H}{\partial u} < 0$), and (iii) singular extremals exist, but are locally maximizing (the Legendre-Clebsch condition is violated, $\frac{\partial}{\partial u}\frac{d^2}{dt^2}\frac{\partial H}{\partial u} > 0$) [292, 31]. In the work of Bonnard and Kupka, because of associated geometric properties of the switching function of the corresponding extremals that are illustrated in Figure 2.3, these three cases are called parabolic, hyperbolic, and elliptic, respectively. Case (i), the parabolic situation, generally is simple and optimal controls are bang-bang with a small number of switchings that can easily be established. Essentially, (more precisely, after some normalizations on the multipliers have been made that resolve simple structures) convexity properties of the switching function along one of the bang controls prevent switchings: either the switching function is convex when it is positive or concave when it is negative, and this limits the overall number of switchings. In case (ii), the hyperbolic case, in fact for both controls the convexity properties prevent switchings: the switching function is convex when it is positive and concave when it is negative. In this case, bang-bang controls with a larger number of switchings are not optimal, but optimal bang arcs typically exist and generally connections are made through 'fast' singular arcs. This, as an example, will be the determining feature for problems of antiangiogenic therapy considered in Chapter 5. In case (iii), the elliptic case, the convexity properties of the switching function induce a potentially very large number of switchings: the switching function is strictly concave when it is positive and strictly convex when it is negative. This, by far is the most difficult of the three scenarios. And it is this one that we have for the cell cycle specific models for cancer chemotherapy. The convexity properties of the switching function entices switchings and there exist extremals with a large number of switchings. But, and very much analogous to the time-optimal control problems analyzed in [292], such controls are not optimal. Heuristically, the singular arc is the limit of bang-bang trajectories with an increasing number of switchings as this number goes to infinity. In case of a fast arc, more switchings do better, but in the limit the singular arc is best and this corresponds to scenario (ii). In case of a slow singular arc, more switchings do not improve the criterion and thus typically then solutions are bang-bang with a small number of switchings. And that is exactly what we shall see for the problems considered in this chapter.

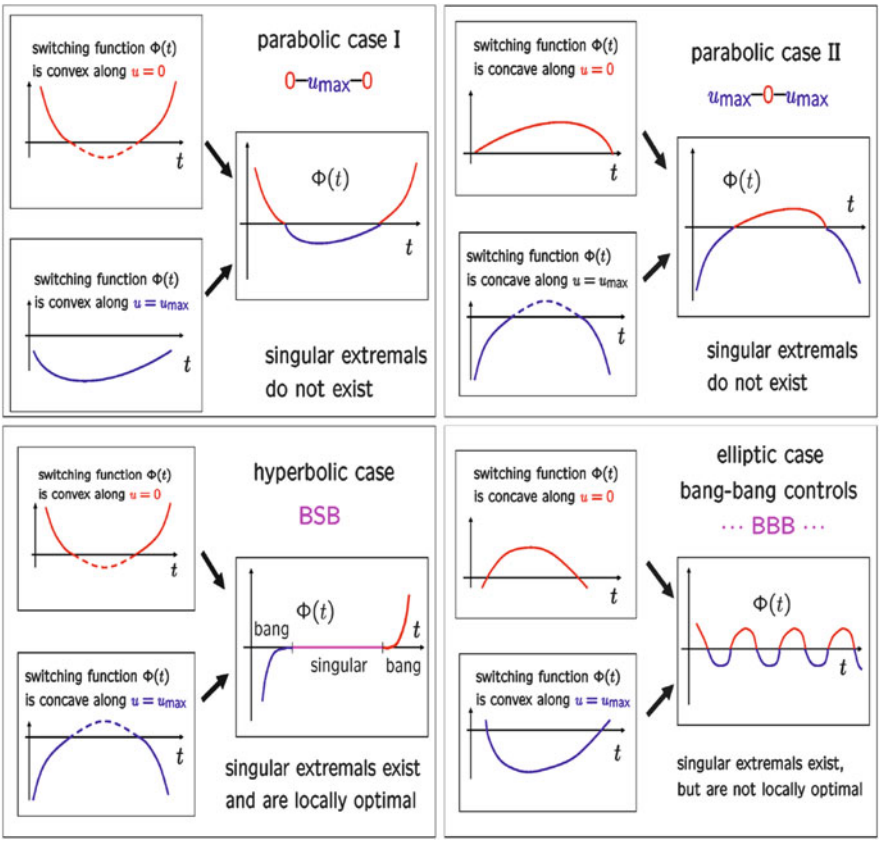

Fig. 2.3 This diagram visualizes the typical **local behavior** of optimal controls (after some normalizations have been made that exclude simpler structures [31, 292]). In the parabolic cases, the switching function is either convex (a, top left) or concave (b, top right) along all extremals. Because of these geometric properties, singular controls are not possible and extremal controls are bang-bang with at most two switchings. In the hyperbolic case (c, bottom left), the switching function is convex along $u = u_{\max}$ (when it is positive) and concave along $u = 0$ (when it is negative). This precludes more than one bang-bang junction and leads to optimal controls of the type *BSB* which are concatenations of a bang control (either $u = 0$ or $u_{\max}$) followed by a singular control and another bang control. In the elliptic case, these convexity properties are reversed and thus extremals whose controls are bang-bang with a large number of switchings exist.

2.1.5 Numerical Computation of Bang-Bang Extremals

The existence of optimal singular controls is a serious obstacle in the numerical computation of optimal controls. The reason is that, as we shall see in Chapter 5, when singular controls are optimal for a system in small dimension, the

corresponding trajectories often lie in a lower dimensional set, e.g., on a surface in 3-dimensional space, that generally is extremely difficult to determine numerically without any a priori theoretical knowledge. Numerical schemes that compute optimal controls through optimization without any a priori knowledge about their structure often are ineffective and fail in these situations. Having eliminated singular controls from optimality for the problem [CC2], allows us to use quite simple procedures to compute bang-bang extremals. In this subsection, we briefly describe a *gradient approach* due to Duda [70, 71] and use it to give some examples of extremals.

Arbitrarily select a bang-bang control with a reasonably large number of switchings k, say $0 = t_0 < t_1 < \cdots < t_k < t_{k+1} = T$. We denote the value of the control on the interval $[t_i, t_{i+1}]$, $i = 0, \ldots, k$, by u_i. The controls alternate between the values $u = 0$ and $u = u_{\max}$ at the times t_i, $i = 1, \ldots, k$, and thus the value of the control on the first interval $[0, t_1]$ determines the sequence. For sake of specificity, we take $u = 0$ as the first value so that u vanishes on the intervals $[0, t_1]$, $[t_2, t_3]$, and so on. Starting from the initial condition $N(t_0)$, then the corresponding trajectory is computed forward in time. Since the controls are constant, the values of the state N at the switching times are simply given by

$$N(t_{i+1}) = \exp(A + u_i B) N(t_i), \qquad i = 0, \ldots, k, \qquad N(t_0) \text{ given.}$$

The transversality condition on the multiplier requires that $\lambda(T) = r$ and thus given this controlled trajectory, the adjoint λ can be computed through backward integration of the adjoint equation. Once more, this only requires to solve linear differential equations, but now these are inhomogeneous and depend on the state N of the system. Having states and costates available, the switching function Φ (and also its derivative $\dot{\Phi}$) are easily evaluated at the switching times t_i using equations (2.23) and (2.28). Naturally, for an arbitrarily selected control u, the zeroes of the switching function will not agree with the switching times t_i of the control. The control will thus be updated recursively until the switching times t_i agree with the zeroes of the computed switching function Φ and an extremal has been found.

In a *gradient based method*, these updates are done by means of small changes in the switching times t_i determined by the values $\Phi(t_i)$ of the switching function. To justify this, we give a brief formal derivation of the first variation δJ (or an infinitesimal increment) of the objective J for this problem when a control u is perturbed by δu,

$$\delta J = J(u + \delta u) - J(u).$$

Adjoining the dynamics to the objective with the multiplier λ, we have that

$$\begin{aligned} J(u) &= rN(T) + \int_0^T qN(t) + su(t) + \lambda(t)\left\{(A + uB)N(t) - \dot{N}(t)\right\} dt \\ &= rN(T) + \int_0^T H(\lambda(t), N(t), u(t)) - \lambda(t)\dot{N}(t) dt. \end{aligned}$$

We denote the response of the system to the control $u+\delta u$ by $N+\delta N$ and rewrite the differential in the form

$$\delta J = r\delta N(T) + \int_0^T \{H(\lambda(t),N(t)+\delta N(t),u(t)+\delta u(t)) \\ -H(\lambda(t),N(t),u(t)) - \lambda(t)\delta\dot{N}(t)\}\,dt$$

with $\delta\dot{N}$ defined by the difference of the differential equations for $N+\delta N$ and N. Integrating $\lambda\delta\dot{N}$ by parts, and noting that $\delta N(0)=0$ (the comparison trajectory obeys the same initial condition) gives

$$\int_0^T \lambda(t)\delta\dot{N}(t)dt = \lambda(t)\delta N(t)|_{t=0}^{t=T} - \int_0^T \dot{\lambda}(t)\delta N(t)dt \\ = \lambda(T)\delta N(T) - \int_0^T \dot{\lambda}(t)\delta N(t)dt.$$

Formally expanding the Hamiltonian H around the controlled trajectory (N,u) and ignoring higher-order terms gives

$$H(\lambda(t),N(t)+\delta N(t),u(t)+\delta u(t)) - H(\lambda(t),N(t),u(t)) \\ = \frac{\partial H}{\partial N}(\lambda(t),N(t),u(t))\delta N(t) + \frac{\partial H}{\partial u}(\lambda(t),N(t),u(t))\delta u(t) + \cdots$$

and putting all these terms together, we obtain that

$$\delta J(u) = (r-\lambda(T))\,\delta N(T) + \int_0^T \left\{\frac{\partial H}{\partial N}(\lambda(t),N(t),u(t)) + \dot{\lambda}(t)\right\}\delta N(t)dt \\ + \int_0^T \frac{\partial H}{\partial u}(\lambda(t),N(t),u(t))\delta u(t)dt + \cdots.$$

But along an extremal we have that

$$\dot{\lambda}(t) = -\frac{\partial H}{\partial N}(\lambda(t),N(t),u(t)), \qquad \lambda(T)=r,$$

and thus the first variation reduces to

$$\delta J = \int_0^T \frac{\partial H}{\partial u}(\lambda(t),N(t),u(t))\delta u(t)dt + \cdots \tag{2.36}$$

Hence the derivative with respect to changes δu in the control is determined by the switching function $\Phi(t) = \frac{\partial H}{\partial u}(\lambda(t),N(t),u(t))$ and any gradient method is based on this quantity.

The procedure itself therefore becomes quite simple: depending on the control used and the value of the switching function at the switching time t_i, simply increase or decrease the lengths of the intervals. If the control is given by $u=0$ on the interval $[t_{i-1},t_i]$ and $\Phi(t_i)>0$, then the optimality condition of the maximum principle is satisfied at time t_i and we increase the switching time by an increment δt_i while

we decrease it if $\Phi(t_i) < 0$ when the optimality condition is violated. Similarly, if $u = u_{\max}$ on the interval $[t_{i-1}, t_i]$ and $\Phi(t_i) > 0$, then the optimality condition is violated and we decrease the switching time while we increase it if $\Phi(t_i) < 0$ when the optimality condition is satisfied. Defining an index ind_i for the interval $[t_{i-1}, t_i]$ as

$$\text{ind}_i = \begin{cases} +1 & \text{if } u = u_{\max} \text{ on } [t_{i-1}, t_i], \\ -1 & \text{if } u = 0 \text{ on } [t_{i-1}, t_i], \end{cases}$$

then, in a gradient method, the increment is simply taken as

$$\delta t_i = -\kappa \text{ind}_i \Phi(t_i) \tag{2.37}$$

where κ denotes some appropriate, possibly adaptive step-size parameter that ensures overall convergence of the procedure [305]. During the iterations, the switching times change and potentially cross. This corresponds to a situation when an intermediate interval gets eliminated and the two adjacent intervals coalesce leading to trajectories with a smaller number of switchings. More generally, if the difference between the switching times t_i and t_{i+1} falls below a prescribed tolerance ε (and this includes being negative), $t_{i+1} - t_i < \varepsilon$, these switching times are eliminated and the controls collapse (with obvious adjustments at the ends of the interval). For example, if the optimal control starts with a full dose interval, but our initialization of the algorithm was with a no dose interval, then at one step in the iterative algorithm the first switching becomes eliminated. Overall, as a gradient method, standard local convergence properties apply (e.g., see [305]).

We include some examples of extremal bang-bang controls that have been computed using this procedure. For the cell cycle parameters we have chosen the values $a_1 = 0.197$ and $a_2 = 0.356$ that were used in [313, 323] and in all computations the initial condition is taken as the steady-state proportions defined by equation (2.6), normalizing the total number of initial cancer cells to 1, i.e., $N_1(0) = 0.7012$ and $N_2(0) = 0.2988$. In view of our earlier remark about the scaling of the coefficients in the objective, these results easily scale to the general case. This situation would be representative of conditions where the cancer has been growing exponentially for some time without treatment. Even if chemotherapy has been given earlier, in the rest periods the cells redistributed over the compartments and once more their proportions are given by these values. The control limit is taken as $u_{\max} = 0.9$, but this is just meant for illustrative purposes. Figure 2.4 shows three examples of controls and corresponding trajectories when the coefficients in the objective have been chosen as $r = (3,3)$, $q = (0.1, 0.1)$ and $s = \frac{1}{2}$. The time horizon has been varied and the examples shown are for $T = 7$, $T = 21$ and $T = 60$ [days]. In all cases, extremals are bang-bang trajectories with exactly one switching from $u = u_{\max}$ to $u = 0$. For shorter time horizons, this switching occurs close to the terminal time (for $T \leq 5.69$ the optimal control is constant given by $u_{\max}$) while the rest periods at the end become longer as T increases. The total reductions in cancer cells at the end of the therapy horizon for $T = 7$, 21 and 60 [days] are given by $N_1(T) + N_2(T) = 0.5660$, 0.5297 and 0.4799, respectively. We summarize the numerical values used in our calculations in Table 2.1.

Table 2.1 Numerical values for the coefficients and parameters used in numerical computations for the optimal control problem [CC2].

Coefficient	Interpretation	Numerical value	Reference
a_1	Inverse transit time through G_0/G_1+S	0.197	[313]
a_2	inverse transit time through G_2/M	0.356	[313]
x_* $N_1(0)=x_*$	Steady-state proportion in compartment G_0/G_1+S, initial condition for N_1	0.2988 0.2988	Eq. (2.6)
y_* $N_2(0)=y_*$	Steady-state proportion in compartment G_2/M, initial condition for N_2	0.7012 0.7012	Eq. (2.6)
$u_{\max}$	Maximum dose rate/concentration effectiveness of the drug	0.90	
s	Penalty/weight for the total dose of cytotoxic agent	0.50	
q_1	Penalty/weight in the objective for the average number of cancer cells in G_0/G_1+S during therapy	0.10	
q_2	Penalty/weight in the objective for the average number of cancer cells in G_2/M during therapy	0.10	
r_1	Penalty/weight in the objective for the average number of cancer cells in G_0/G_1+S at the end of therapy	3	
r_2	Penalty/weight in the objective for the average number of cancer cells in G_2/M at the end of therapy	3	
T	Therapy horizon	$T=7,21,60$	Illustration only

In Table 2.2, we give some numerical results when we vary the coefficient s at the integral of the dosage. We retain the other parameter values, $r=(3,3)$, $q=(0.1.0.1)$, $u_{\max}=0.9$, and the therapy horizon is $T=21$ [days]. As long as $s>0$ optimal controls are bang-bang with exactly one switching from $u=u_{\max}$ to $u=0$. For $s=0$, i.e., when no penalty is imposed on the use of drugs, then naturally the optimal control is given by a constant full dose treatment, $u\equiv u_{\max}$. In this case, the total number of cancer cells at the endpoint is given by $N_1(T)+N_2(T)=0.0703$ and this is the best possible reduction within the model. As s increases, this number increases and the interval when the drug is given diminishes. For $s=1.0$ we have reached a scenario when the total number of cancer cells at the end of therapy in fact exceeds 1 and thus the side effects are deemed worse than the cancer volume. For any other administration of cytotoxic agents, the value of the objective will be larger.

Also, it is the inclusion of the term qN in the Lagrangian that makes optimal controls start with a full dose as it penalizes prolonged high tumor volumes. If this term is very small or nonexistent, then naturally all the efforts will only be put on minimizing the values of N at the terminal time and in this case chemotherapy will be given not at the beginning, but at the end. For several obvious reasons this is a poor choice of strategy and objective. As an illustration, Figure 2.5 shows an

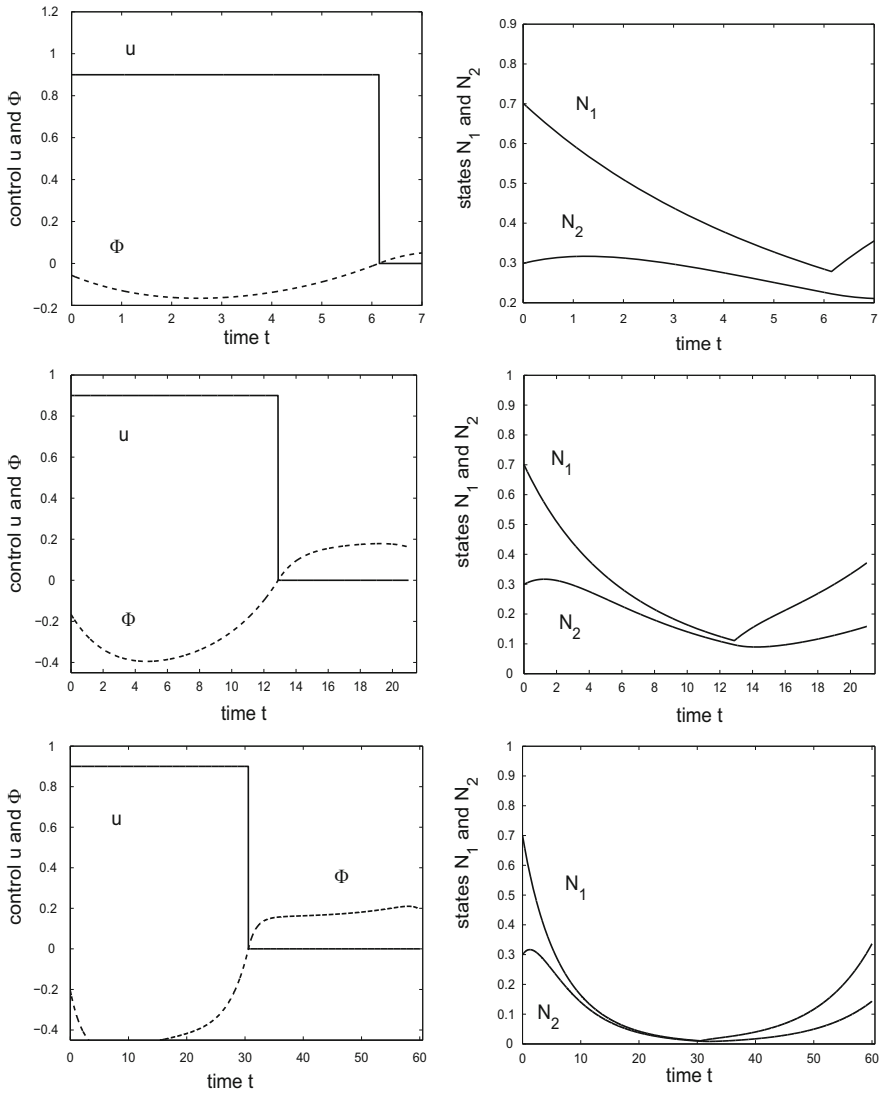

Fig. 2.4 Examples of locally optimal controls (left) and their corresponding trajectories (right) for $T = 7$ (top), $T = 21$ (middle) and $T = 60$ (bottom) from the steady-state solution (2.6) for the parameter values given in Table 2.1.

example of such a control and trajectory for the same parameters as above and $T = 21$ if we set $q = 0$. Clearly, the intermediate rise of cancer volume is undesirable and an objective with q makes much more sense.

In the next subsection we shall show that all extremals computed here are indeed *strong local minima*; that is, there exists a neighborhood W of the graph of the corresponding trajectory in $[0, T] \times \mathbb{P}$ such that the controls are optimal with respect

Table 2.2 Numerical results for the switching times τ and total reductions in tumor volume, $N_1(T)+N_2(T)$. The initial condition is from the steady-state solution (2.6) of the uncontrolled system, the parameter values are given in Table 2.1, and the therapy horizon of $T = 21$ (days).

s	Switching time τ	$N_1(T)+N_2(T)$
0	21.0000	0.0703
0.1	19.3550	0.1104
0.2	16.5051	0.2223
0.3	14.9350	0.3251
0.4	13.7950	0.4272
0.5	12.8949	0.5297
0.6	12.1450	0.6320
0.7	11.5250	0.7344
0.8	10.9849	0.8351
0.9	10.4948	0.9381
1.0	10.0551	1.0388

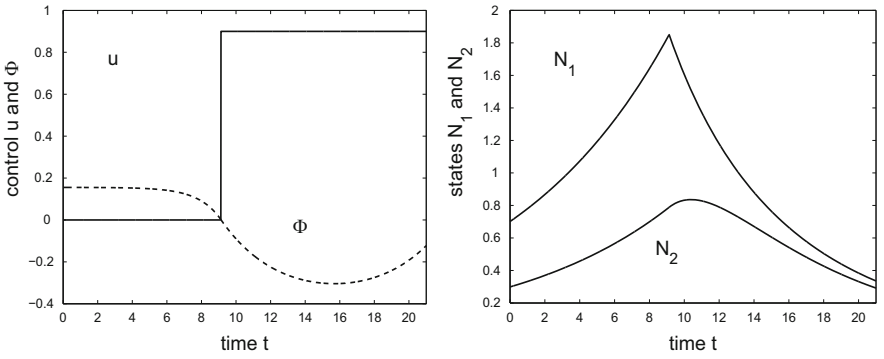

Fig. 2.5 Example of a locally optimal control (left) and its corresponding trajectory (right) from the steady-state solution (2.6) of the uncontrolled system for parameter values $a_1 = 0.197$ and $a_2 = 0.356$, time horizon $T = 21$ (days) and coefficients in the objective given by $r = (3,3)$, $q = (0,0)$ and $s = \frac{1}{2}$.

to any other control u for which the graph of its corresponding trajectory N lies in W. In fact, for this 2-compartment model we have consistently seen that extremal bang-bang trajectories that have more than one switching are not optimal and it is quite likely that all examples shown are indeed globally optimal. This simply means that we can take the neighborhood W as the full space $[0,T] \times \mathbb{P}$.

Given the framework of the model, chemotherapeutic agents are given at the beginning of therapy and in a dose as high as possible. These results are consistent with the medical point of view that *for a homogeneous, therapeutically sensitive tumor, chemotherapy should be given in an MTD scheme upfront*. Also, toxic side effects of chemotherapy are only indirectly modeled in the system and for this reason the problem formulation considered here corresponds to just one chemotherapy session, i.e., it does not take into account the required rest periods between sessions. Different chemotherapy session with the medically required rest periods imposed

simply reduce to repetitions of the structure obtained above. Since the steady-state proportions of cells in the respective compartments stabilize very quickly, indeed the solutions reduce to repetitions of the same scenario if the initial condition is normalized.

2.1.6 *Sufficient Conditions for Strong Local Optimality of Bang-Bang Extremals*

The bang-bang controls and corresponding controlled trajectories computed above were found through a numerical procedure based on the conditions of the Pontryagin maximum principle. These conditions only comprise first order necessary conditions for optimality and a priori there is no guarantee that such an extremal is optimal. This especially is the case in the situation that we have here when singular controls are locally maximizing (which was called "elliptic" earlier) when generally there exist many nonoptimal bang-bang extremals with a large number of switchings as well. It is therefore necessary to follow up on computations like the ones we just described with theoretical arguments that prove at least some kind of local optimality. We give a brief overview of these results and corresponding optimality statements for the problem [CC2]. The theoretical background consists in the construction of a field of extremals or, equivalently, in the construction of a solution to the Hamilton-Jacobi-Bellman equation by means of dynamic programming. The general procedure is outlined in Appendix A and a fully self-contained construction for the 2-compartment model [CC2] is given in Appendix B.1. We relegate the argument to this appendix for the simple reason that these constructions, albeit intuitive and natural, are more on the technical side. Here we merely give the main steps and results.

Let (N_*, u_*) be an extremal controlled trajectory, the *reference extremal*, such that u_* is a bang-bang control with switchings at times t_i, $i = 1, \dots, k$, $0 = t_0 < t_1 < \cdots < t_k < t_{k+1} = T$, and denote the corresponding adjoint variable by λ_*. We *assume* that the derivative of the switching function at time t_i does not vanish at all switchings,

$$\dot{\Phi}_*(t_i) = \{\lambda_*(t_i)[A,B] - qB\}N_*(t_i) \neq 0. \tag{2.38}$$

A bang-bang junction for which the derivative of the switching function does not vanish is called strict and we call the triple $\Gamma = (N_*, u_*, \lambda_*)$ a *strictly bang-bang extremal lift*.

In a first step, it becomes necessary[1] to embed this reference extremal into a *parameterized family of extremals* (see Appendix A). This simply is a collection

[1] Even if we just consider the problem of minimizing a function f, it is not possible to determine the local optimality of a critical point x_* (i.e., $f'(x_*) = 0$) from just the knowledge of the critical point itself, but we need to understand the behavior of the function f over a neighborhood of x_*, as, for example, it can be gained from the fact that the second derivative $f''(x_*)$ does not vanish. The construction of a family of extremals serves this purpose.

of controlled trajectories and associated multipliers that satisfy the conditions of the maximum principle, contain the reference extremal as a member, and in some reasonable sense depend "nicely" on the parameters. For an optimal control problem over a fixed finite interval $[0,T]$ that does not have any terminal constraints like problem [CC2], such a family can be obtained by integrating the dynamics and adjoint equation backward from the terminal time while choosing the control to maintain the minimum condition. Specifically, set $p_* = N_*(T)$ and for p in some neighborhood P of p_*, let $N(t,p)$ and $\lambda(t,p)$, $(t,p) \in [0,T] \times P$, denote the solutions to the terminal value problem for the system and adjoint equations given by

$$\dot{N}(t,p) = (A + u(t,p)B)N(t,p), \qquad x(T,p) = p, \tag{2.39}$$

$$\dot{\lambda}(t,p) = -\lambda(t,p)(A + u(t,p)B) - q, \qquad \lambda(T,p) = r, \tag{2.40}$$

while the control is chosen so that with

$$\Phi(t,p) = s + \lambda(t,p)BN(t,p) \tag{2.41}$$

we have that

$$\Phi(t,p)u(t,p) = \min_{v \in [0,u_{\max}]} \Phi(t,p)v. \tag{2.42}$$

In particular, for $p = p_*$, the control $u(\cdot,p_*)$ reduces to the reference control u_* and $N(\cdot,p_*)$ and $\lambda(\cdot,p_*)$ are the reference trajectory and corresponding multiplier,

$$N(t,p_*) = N_*(t), \qquad u(t,p_*) = u_*(t), \qquad \lambda(t,p_*) = \lambda_*(t).$$

Proposition 2.1.5. *Let $\Gamma = (N_*, u_*, \lambda_*)$ be a strictly bang-bang extremal lift with switching times t_i, $i = 1,\dots,k$, $0 = t_0 < t_1 < \cdots < t_k < t_{k+1} = T$. Then there exists a neighborhood P of $p_* = N_*(T)$ in $\mathbb{P}$ and real-analytic functions τ_i defined on P, $i = 1,\dots,k$, such that for $p \in P$ the controls $u(\cdot,p)$, which are defined as the bang-bang controls that have switchings at the times $0 < \tau_1(p) < \cdots < \tau_k(p) < T$ in the same order as the reference control, satisfy the conditions of the maximum principle. If $N(\cdot,p)$ and $\lambda(\cdot,p)$ denote the corresponding state and costate defined as solutions to equations (2.39) and (2.40), then the triples $\Gamma_p = (N(\cdot,p), u(\cdot,p), \lambda(\cdot,p))$ for $p \in P$ are strictly bang-bang extremal lifts and the family $\mathscr{E} = \{\Gamma_p : p \in P\}$ is a real-analytic parameterized family of broken extremals over the domain $D = \{(t,p) : 0 \le t \le T,\ p \in P\}$.*

We define the associated flow F of controlled trajectories by means of the graphs of the controlled trajectories as

$$\begin{aligned} F : D = [0,T] \times P &\to [0,T] \times \mathbb{P}, \\ (t,p) &\mapsto F(t,p) = (t, N(t,p)). \end{aligned} \tag{2.43}$$

Intuitively, since the optimal control problem is defined on a fixed therapy horizon, the time t, or equivalently, the time until the end of the treatment period matters, and it thus needs to be included in this formulation. Our aim is to determine if a

reference controlled trajectory is locally optimal. This is related to the geometric property whether or not this flow F defines an injective mapping. Essentially, since the controls are constant on the subdomains

$$D_i = \{(t,p) : \tau_{i-1}(p) \le t \le \tau_i(p), p \in P\}, \qquad i = 1,\dots,k,k+1,$$

(where $\tau_0(p) \equiv 0$ and $\tau_{k+1}(p) \equiv T$), the restrictions $F_i = F \restriction D_i$ of the flow map F to these subdomains are diffeomorphisms (this follows from classical results on solutions to ordinary differential equations) and extend as continuously differentiable mappings $\tilde{F}_i$ onto open neighborhoods $\tilde{D}_i$ of D_i. The boundary pieces

$$\mathscr{T}_i = \{(t,p) : t = \tau_i(p),\ p \in P\}$$

are hypersurfaces (n-dimensional embedded submanifolds in $(0,T) \times P$) and their images under the flow are the *switching surfaces* $\mathscr{S}_i$,

$$\mathscr{S}_i = F(\mathscr{T}_i) = \{t,N) :\ t = \tau_i(p),\ N = N(\tau_i(p),p),\ p \in P\}, \qquad i = 1,\dots,k.$$

We recall that a differentiable mapping $F : \mathbb{R}^m \to \mathbb{R}^m$ is said to be *regular* at a point x if the derivative $DF : \mathbb{R}^m \to \mathbb{R}^m$ is nonsingular at x. If the flow map $\tilde{F}_i$ is regular at $(t_i, p_*) = (\tau_i(p_*), p_*)$, then, for a sufficiently small neighborhood P of p_*, the switching surface $\mathscr{S}_i$ is an embedded hypersurface of $(0,T) \times \mathbb{P}$ and the flow $\tilde{F}_i$ is transversal to $\mathscr{S}_i$, i.e., the tangent vectors to the graphs of the trajectories, $(1, \dot{N}(\tau_i(p),p))$, do not lie in the tangent space to $\mathscr{S}_i$ at $F(\tau_i(p),p)$. Equivalently, the graphs of the controlled trajectories cross the switching surface at a nonzero angle.

Definition 2.1.4 (Transversal Crossings and Folds). We say the parameterized family $\mathscr{E} = \{\Gamma_p : p \in P\}$ of broken extremals has a regular junction (or switching point) at $\mathscr{T}_i$ if both flow maps $\tilde{F}_i$ and $\tilde{F}_{i+1}$ are regular at $(\tau_i(p),p)$ for all $p \in P$. In this case the graphs of both the trajectories before and after the switching cross the switching surface $\mathscr{S}_i$ transversally. We call such a regular switching point a transversal crossing if the graphs of the trajectories $t \mapsto N(t,p)$ cross the switching surface $\mathscr{S}_i$ in the same direction and a transversal fold if they cross it in opposite directions.

Figure 2.6 depicts the geometry of a flow of broken extremals near a transversal crossing and fold. While the overall mapping remains injective in the case of a transversal crossing, trajectories overlap and there exist multiple extremals for initial data near a transversal fold. Intuitively, such a structure should no longer be optimal and this indeed is the case: *for a flow of bang-bang trajectories, optimality is preserved between switching surfaces and at transversal crossings, but lost at transversal folds*.

Theorem 2.1.3. *Let $\Gamma = (N_*, u_*, \lambda_*)$ be a strictly bang-bang extremal lift with switching times t_i, $i = 1,\dots,k$, $0 = t_0 < t_1 < \cdots < t_k < t_{k+1} = T$, and let $\mathscr{E} = \{\Gamma_p = (N(\cdot,p), u(\cdot,p), \lambda(\cdot,p)) : p \in P\}$ be the real-analytic parameterized family*

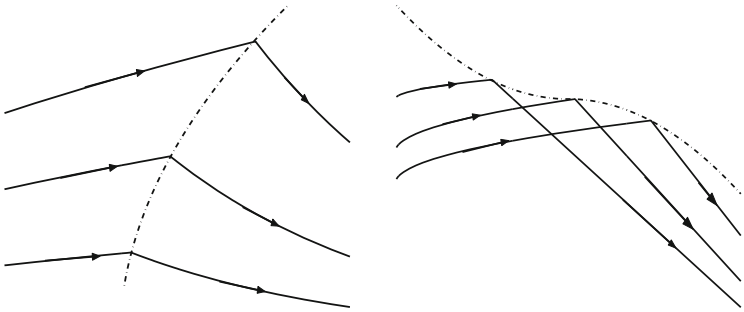

Fig. 2.6 The flow of a parameterized family of broken extremals near a transversal crossing (left) and a transversal fold (right).

of broken extremals constructed in Proposition 2.1.5. If all the switchings (t_i, p_*) *are transversal crossings, then there exists a neighborhood* P *of* $p_* = N_*(t)$ *such that the flow* F *restricted to* $[0,T] \times P$ *is injective and defines a field of broken extremals. The reference control* u_* *is optimal when compared with any other control* u *whose trajectory* N *lies in the region* R *covered by the flow* F, $R = F([0,T] \times P)$.

Theorem 2.1.4. *Let* $\Gamma = (N_*, u_*, \lambda_*)$ *be a strictly bang-bang extremal lift with switching times* t_i, $i = 1, \ldots, k$, $0 = t_0 < t_1 < \cdots < t_k < t_{k+1} = T$, *and let* $\mathscr{E} = \{\Gamma_p = (N(\cdot,p), u(\cdot,p), \lambda(\cdot,p)) : p \in P\}$ *be the real-analytic parameterized family of broken extremals constructed in Proposition 2.1.5. Suppose all the junctions are regular, but there exists a switching* (t_i, p_*) *that is a transversal fold. Then the reference control* u_* *is not locally optimal.*

The proofs of Theorems 2.1.3 and 2.1.4 are given in Appendix B. These two results decisively summarize the geometric properties that determine local optimality of a strictly bang-bang controlled trajectory: *if all switchings are transversal crossings, the associated control is locally optimal while it is not if there exists a switching which is a transversal fold.*

In the theorem below, we still formulate an algorithmic procedure that easily and efficiently allows us to verify these geometric properties for problem [CC2]. This algorithm also is developed in Appendix B. While the states and costates remain continuous at the switching surface, their partial derivatives generally are discontinuous and in the algorithm we update and propagate these derivatives.

Theorem 2.1.5. *Let* $\Gamma = (N_*, u_*, \lambda_*)$ *be a strictly bang-bang extremal lift for problem [CC2] with switching function* $\Phi_*(t) = s + \lambda_*(t)BN_*(t)$. *Suppose the switching times of the control* u_* *are given by* t_i, $0 = t_0 < t_1 < \cdots < t_k < t_{k+1} = T$ *and let* u_i *be the value of the control on the interval* (t_i, t_{i+1}). *Set* $S^-_{k+1} = 0$ *and for* $i = k, k-1, \ldots, 1$, *define*

$$S_i^+ = \exp\left((A+u_iB)^T(t_{i+1}-t_i)\right) S_{i+1}^- \exp\left((A+u_iB)(t_{i+1}-t_i)\right), \tag{2.44}$$

$$G_i = -\frac{u_{\max}}{\left|\dot{\Phi}_*(t_i)\right|}\left(\lambda_*(t_i)B + N_*^T(t_i)B^T S_i^+\right), \tag{2.45}$$

$$S_i^- = \left(B^T\lambda_*^T(t_i)G_i + S_i^+\right)\left(Id + \frac{BN_*(t_i)G_i}{1-G_iBN_*(t_i)}\right). \tag{2.46}$$

If, for $i = k, k-1, \ldots, 1$, we have that

$$\left|\dot{\Phi}_*(t_i)\right| + u_{\max}N_*^T(t_i)B^T S_i^+ BN_*(t_i) > 0, \tag{2.47}$$

then this algorithm is well defined, every switching is a transversal crossing, and u_* is a strong local minimum for the optimal control problem [CC2]. If there exists an index i such that

$$\left|\dot{\Phi}_*(t_i)\right| + u_{\max}N_*^T(t_i)B^T S_i^+ BN_*(t_i) < 0, \tag{2.48}$$

then the ith switching is a transversal fold and the reference controlled trajectory is not locally optimal.

Corollary 2.1.2. *Every extremal strictly bang-bang controlled trajectory with at most one switching is a strong local minimum.*

Proof. The algorithm gives $S_k^+ = 0$ and thus (2.47) is satisfied. □

This concludes our analysis of the 2-compartment model. Except for the fact that we use that $B^2 = 0$ in the formulas above, this algorithm is general and will be used for other problems as well.

2.2 Compartmental Models for Multi-Drug Chemotherapy

We generalize the above results to multi-drug treatment protocols that combine the actions of a G_2/M specific cytotoxic agent with a second chemotherapeutic agent that targets a different mechanism in the cell cycle. As examples, we consider the combined actions of a killing and a recruiting agent and of a killing and a blocking agent. The first model is of importance since dormant cells generally do not respond to chemotherapy and recruiting the resting cells back into active cell division makes them sensitive to the cytotoxic agents. This is of special importance in various types of leukemia that have a large fraction of quiescent cells. Various types of growth factors (colony-stimulating factors, CSFs) have been shown to increase the growth fraction in acute myeloblastic leukemia (AML) by recruiting leukemic cells into the cycle from the resting compartment [219]. The possibility of increasing the fraction of cycling cells in AML populations thus represents a way to render them more sensitive to cytostatic agents. More generally, significant advantages can be obtained by recruiting resting cells into the drug-sensitive cell cycle if drug ineffectiveness is because of large dormant populations [172, 233]. Adding a blocking or cytostatic

agent in the second model aims at synchronizing cells in a drug-sensitive phase of the cell cycle. By then applying the cytotoxic agent when a large fraction of the cancer cells are in this phase, in principle more effective treatments are possible. However, these results very much depend on the underlying assumption of a homogeneous cancer cell population.

2.2.1 General Mathematical Structure and Results

We formulate a mathematical model that has an arbitrary number of compartments. Both the examples just mentioned and other compartmental models that will be considered later, like the models involving cell populations of different chemotherapeutical sensitivities or resistance levels in Chapter 3, fit this general structure. Analyzing the general structure has the obvious advantage that the mathematical arguments that are common to all these models only need to be carried out once.

The state space is the first orthant $\mathbb{P}$ in $\mathbb{R}^n$ and $N = (N_1, \ldots, N_n)^T$ denotes the state with N_i the average number of cancer cells in the ith compartment, $i = 1, \ldots, n$. The control is a vector $u = (u_1, \ldots, u_m)^T$ with u_i denoting various drug concentrations in the blood stream. We still identify the drug dose rates with these concentrations. The control set U is a compact m-dimensional interval of the form $U = [0, u_1^{\max}] \times \cdots \times [0, u_m^{\max}]$ with each $u_j^{\max}$ representing the maximum dose rate/concentration and the lower limit 0 representing that no drugs are administered. Admissible controls are Lebesgue-measurable (respectively, piecewise continuous) functions u that take values in the control set, $u : [0, T] \to U$. The dynamics consists of balance equations that describe the inflows and outflows between the various compartments and takes the form

$$\dot{N}(t) = \left(A + \sum_{j=1}^{m} u_j B_j \right) N(t), \qquad N(0) = N_0, \tag{2.49}$$

where the A and B_j, $j = 1, \ldots, m$, are constant $n \times n$ matrices, $A, B_j \in \mathbb{R}^{n \times n}$. As for the 2-compartment model considered above, the matrix A describes the transitions between the various compartments when no treatment is given and the matrices B_j represent the effects of the jth drug on the system. An equation of the form (2.49) is a multi-input bilinear control system. The dynamics represents in- and outflows of the various compartments and for this reason, no matter what the control is, all diagonal entries of the matrix $A + \sum_{j=1}^{m} u_j B_j$ are negative (there always is a positive outflow from each compartment) and all the off-diagonal entries (which model the inflows) are nonnegative. Zero values may occur when there are no connections between some of the compartments, but every row will have at least one positive entry. In mathematics, matrices with these properties are called M-matrices (named so in honor of Minkowski) and their structure implies the positive invariance properties required for the model to be consistent. We therefore make the following assumption:

(M) For all $u \in U$ the matrices $A + \sum_{j=1}^{m} u_j B_j$ have negative diagonal entries and nonnegative off-diagonal entries,

$$A + \sum_{j=1}^{m} u_j B_j \in \mathscr{M}.$$

Under assumption (M), the state space $\mathbb{P}$ is positively invariant. The reasoning is exactly the same as in the proof of Lemma 2.1.2 and will not be repeated.

Proposition 2.2.1. *Under assumption (M), the positive orthant $\mathbb{P}$ is positively invariant for the control system (2.12).*

Let $r = (r_1, \ldots, r_n)$ and $q = (q_1, \ldots, q_n)$ be n-dimensional row-vectors of positive numbers and let $s = (s_1, \ldots, s_m)$ be a nonzero m-dimensional row-vector of nonnegative numbers. We denote the space of row-vectors by $(\mathbb{R}^n)^*$—mathematically we consider these as linear functionals acting on $\mathbb{R}^n$—so that $q, r \in (\mathbb{R}^n)^*$ and $s \in (\mathbb{R}^m)^*$. The vectors q, r and s represent subjective weights, i.e., variables of choice, which define the objective as

$$\begin{aligned} J &= rN(T) + \int_0^T \{qN(t) + su(t)\}\, dt \\ &= \sum_{i=1}^{n} r_i N_i(T) + \int_0^T \left\{ \sum_{i=1}^{n} q_i N_i(t) + \sum_{j=1}^{m} s_j u_j(t) \right\} dt \to \min \end{aligned} \tag{2.50}$$

Analogously as in the 2-compartment model considered in Section 2.1, the term $su = \sum_{i=j}^{m} s_j u_j$ in the integral is a weighted average of the amounts of the various drugs given and the coefficients s_j represent the degrees of toxicity of the drugs. Side effects generally depend on the specific cytotoxic agent used and may be more severe than those of a cytostatic or recruiting agent. This would be reflected in the choice of these weights. Similarly, the second integral term $qN = \sum_{i=1}^{n} q_i N_i$ represents a weighted average of the number of cancer cells in the respective compartments during treatment and the penalty term $rN(T) = \sum_{i=1}^{n} r_i N_i(T)$ represents a weighted average of the number of cancer cells in the respective compartments at the end of treatment. As before, the inclusion of the term qN in the Lagrangian is important since otherwise optimization will lead to protocols that put all the emphasis on the end of the therapy interval ignoring the behavior in between. While relevant biological information should be taken into account when selecting the parameters, it generally is also useful to modulate these parameters within specified ranges to obtain otherwise desired features of the optimal solutions. As for the 2-compartment model, also the general model has a 1-dimensional group of scaling symmetries that can be used to normalize these weights. We then consider the following optimal control problem:

[CC] for a fixed therapy horizon $[0, T]$, minimize the objective (2.50) over all Lebesgue-measurable (respectively, piecewise continuous) functions $u : [0, T] \to U = [0, u_1^{\max}] \times \cdots \times [0, u_m^{\max}]$, subject to the dynamics (2.49).

First order necessary conditions for optimality again follow from the Pontryagin maximum principle (see Theorem A.3.1). As for the 2-compartment model considered above, all extremals are normal and we already anticipate this in our formulation now and set $\lambda_0 = 1$. Thus the Hamiltonian function is given by

$$H = qN + su + \lambda \left(A + \sum_{j=1}^{m} u_j B_j \right) N. \tag{2.51}$$

Theorem 2.2.1 (Maximum Principle for Problem [CC]). *If $u_* = (u_1^*, \ldots, u_m^*)$ is an optimal control with corresponding trajectory N_*, then there exists an absolutely continuous function λ, which we write as row-vector, $\lambda : [0,T] \to (\mathbb{R}^n)^*$, called the adjoint or co-vector, such that the following conditions are satisfied:*

1. adjoint equation and transversality condition*: the multiplier λ is a solution to the terminal value problem*

$$\dot{\lambda} = -\frac{\partial H}{\partial N}(\lambda, N_*, u_*) = -q - \lambda \left(A + \sum_{j=1}^{m} u_j B_j \right), \qquad \lambda(T) = r, \tag{2.52}$$

2. minimum condition*: the optimal control minimizes the Hamiltonian H pointwise over the control set $U = [0, u_1^{\max}] \times \cdots \times [0, u_m^{\max}]$ along the optimal controlled trajectory and the multiplier $\lambda(t)$, i.e.,*

$$H(\lambda(t), N_*(t), u_*(t)) = \min_{v \in U} H(\lambda(t), N_*(t), v), \tag{2.53}$$

and the minimum value is constant over the interval $[0,T]$,

$$H(\lambda(t), N_*(t), u_*(t)) = \text{const.}$$

Like for the 2-compartment model, it follows from assumption (M) that the positive orthant $\mathbb{P}^* = \{\lambda \in (\mathbb{R}^n)^* : \lambda_i > 0 \text{ for } i = 1, \ldots, n\}$ is negatively invariant.

Proposition 2.2.2. *Under assumption (M), the positive orthant $\mathbb{P}^*$ is negatively invariant for the adjoint equation (2.52), i.e., if $\lambda(T) \in \mathbb{P}^*$, then all the multipliers $\lambda_i(t)$, $i = 1, \ldots, n$, remain positive over the interval $[0,T]$.*

Corollary 2.2.1. *Under assumption (M), all states N_i and costates λ_i are positive over $[0,T]$.*

This is an important relation in evaluating the signs of various expressions that arise in the analysis of optimal controls. As for the 2-compartment model, the Hamiltonian H is linear in the controls u_j and since the control set $U = [0, u_1^{\max}] \times \cdots \times [0, u_m^{\max}]$ is an m-dimensional interval, this minimization problem splits into m separate 1-dimensional minimization problems of minimizing a linear function over an interval. As before, typically the minimum is attained at the boundary points (bang controls) and intermediate values (singular controls) can only be

optimal if the function multiplying the control vanishes. This leads to the definition of the *m switching functions* as

$$\Phi_j(t) = s_j + \lambda(t)B_jN(t), \tag{2.54}$$

and optimal controls satisfy

$$u_j^*(t) = \begin{cases} 0 & \text{if } \Phi_j(t) > 0, \\ u_j^{\max} & \text{if } \Phi_j(t) < 0, \end{cases} \tag{2.55}$$

with singular controls possible if the corresponding switching function vanishes over an open interval. Once again, we thus need to analyze the derivatives of these switching functions. These are computed using the system and adjoint equations and the formula below, which is verified by the same direct computation that was made in Proposition 2.1.4, gives the essential relation.

Proposition 2.2.3. *Suppose M is a constant matrix and let $\Psi(t) = \lambda(t)MN(t)$ with N a solution to the system equation (2.49) corresponding to the control u and λ a solution to the corresponding adjoint equation (2.52). Then*

$$\dot{\Psi}(t) = \lambda(t)\left[A + \sum_{j=1}^{m} u_j(t)B_j, M\right]N(t) - qMN(t), \tag{2.56}$$

with $[X,Y] = YX - XY$ the commutator of the matrices X and Y.

As before, the main term is the commutator of the dynamics of the system with the matrix M that defines the bilinear form in N and λ; the second term is generated by the inhomogeneous term in the adjoint equation (2.52). While further differentiation of the first term leads to additional high-order bracket terms, differentiation of the inhomogeneous term through the dynamics will bring up product terms of the matrices. Also, the multi-control aspect of the problem matters when higher order derivatives need to be computed since it may not be clear a priori that the controls are differentiable functions. This, of course, is trivially true for the constant bang controls.

Whether or not optimal controls can be singular depends on the properties of the matrices A and B_j and needs to be evaluated on a case-by-case basis. In the models that we shall analyze in this chapter, singular controls (along with the partial dose rates they represent) are not optimal for the cytotoxic agent. But again, this is under the implicit assumption that the entire tumor population is chemotherapeutically sensitive. In particular, for the two models that will be considered in this section, bang-bang controls will again be optimal. Their local optimality can then be asserted with the same construction as for the 2-compartment model, but some minor modifications need to be made to account for having more than one control. We still briefly formalize the construction of a field of broken extremals for this scenario, but only giving the relevant formulas and results.

Let (N_*, u_*) be a reference controlled extremal where all the components of u_* are bang-bang controls with switchings at times t_i, $i = 1,\ldots,k$, $0 = t_0 < t_1 < \cdots <$

$t_k < t_{k+1} = T$, and denote the corresponding adjoint variable by λ_*. Essentially, the constructions outlined in Section 2.1.6 for the 2-compartment model (see Appendix B) carry over verbatim to the multi-input situation if we make the following assumptions:

(A1) At every switching t_i only one of the components of the control has a switching.

This is the generic situation. Simultaneous switchings arise as two separate switching surfaces intersect and mathematically they are related to bifurcation scenarios. The underlying geometry is much more complicated and we shall not go into these structures in this text. While possible, simultaneous switchings are rare and can easily be avoided from a practical point of view. Modulo this extra condition, the theory developed in Section 2.1.6 carries over verbatim if the necessary formal changes to adjust for the multi-input dynamics are made. Also, under assumption (A1), all the switching functions are absolutely continuous functions with derivatives given by

$$\dot{\Phi}_j(t) = \lambda(t)\left[A + \sum_{i\neq j} u_i(t)B_i, B_j\right]N(t) - qB_jN(t).$$

In particular, the derivative $\dot{\Phi}_j = \frac{d}{dt}\Phi_j$ is continuous at t_i if the jth control switches at time t_i and all the other controls are continuous at t_i.

(A2) For each switching time t_i, the derivative of the switching function Φ_j of the control that switches, $j = j(i)$, does not vanish, $\dot{\Phi}_j(t_i) = \frac{d}{dt}\Phi_j(t_i) \neq 0$.

We call a triple $\Gamma = (N_*, u_*, \lambda_*)$ along which conditions (A1) and (A2) are satisfied a *strictly bang-bang extremal lift with simple switchings*. Under these assumptions, a parameterized family of strictly bang-bang extremal lifts with simple switchings that contains Γ can be constructed exactly as in Proposition 2.1.5 by integrating the dynamics and the adjoint equation backward from the terminal time T with the terminal condition $N(T,p) = p$ and p varying in a sufficiently small neighborhood of $p_* = N_*(T)$. We have the identical results that local optimality is preserved at transversal crossings and that it ceases at transversal folds. However, the formulas in the algorithm that computes whether switchings are transversal crossings or folds need to be adjusted to the multi-input setting and we here simply give these formulas summarizing the results. Note that for the 2-compartment model we also had that $B^2 \equiv 0$ and this somewhat simplified the formulas. We now no longer have this and thus the formulas take the more general form below.

Theorem 2.2.2. *Let $\Gamma = (N_*, u_*, \lambda_*)$ be a strictly bang-bang extremal lift for problem [CC] with simple switchings and let $\Phi_j^*(t) = s_j + \lambda_*(t)B_jN_*(t)$ be the switching function associated with the control u_j, $j = 1,\ldots,m$. Denote the successive switching times in the controls by t_i, $i = 1,\ldots,k$, $0 = t_0 < t_1 < \cdots < t_k < t_{k+1} = T$ and suppose assumptions (A1) and (A2) are satisfied at the junctions. For the ith switching, let $J = J(i)$ be the indicator of the control that switches and denote the*

absolute value of the jump in the control by θ_J, i.e., $\theta_J = u_j^{\max}$ if $J(i) = j$. Let u_j^i denote the constant value of the controls on the interval (t_i, t_{i+1}). Set $S_{k+1}^- \equiv 0$ and for $i = k, k-1, \ldots, 1$, define

$$S_i^+ = \exp\left(\left(A + \sum_{j=1}^{m} u_j^i B_j\right)^T (t_{i+1} - t_i)\right) S_{i+1}^- \exp\left(\left(A + \sum_{j=1}^{m} u_j^i B_j\right)(t_{i+1} - t_i)\right), \tag{2.57}$$

$$G_i = -\frac{\theta_J}{\left|\dot{\Phi}_J^*(t_i)\right|}\left(\lambda_*(t_i)B_J + N_*^T(t_i)B_J^T S_i^+\right), \tag{2.58}$$

$$S_i^- = \left(B_J^T \lambda_*^T(t_i)G_i + S_i^+\right)\left(Id + \frac{B_J N_*(t_i) G_i}{1 - G_i B_J N_*(t_i)}\right) \tag{2.59}$$

If, for $i = k, k-1, \ldots, 1$, we have that

$$\left|\dot{\Phi}_J^*(t_i)\right| + \theta_J\left\{\lambda_*(t_i)B_J + N_*^T(t_i)B_J^T S_i^+\right\} B_J N_*(t_i) > 0, \tag{2.60}$$

then this algorithm is well defined, every switching is a transversal crossing, and u_* is a strong local minimum for the optimal control problem [CC]. If there exists an index i such that

$$\left|\dot{\Phi}_J^*(t_i)\right| + \theta_J\left\{\lambda_*(t_i)B_J + N_*^T(t_i)B_J^T S_i^+\right\} B_J N_*(t_i) < 0, \tag{2.61}$$

then the ith switching is a transversal fold and the reference controlled trajectory is not locally optimal.

2.2.2 A 3-Compartment Model with a Killing and Recruiting Agent

We now consider a 3-compartment model originally formulated by Swierniak et al. [323] where a cytotoxic agent (that can be active in either the S or the G_2/M phase), is combined with another chemotherapeutic agent that entices dormant cells in the compartment G_0 to reenter the active cell cycle, a so-called recruiting agent. A large residuum of dormant G_0 cells that are not sensitive to most cytotoxic agents is one of the major problems in chemotherapy of some leukemias [52, 128, 224]. Similar findings for breast and ovarian cancers were reported, e.g., in [58, 83]. Experiments indicated that if Ara-C (arabinofuranosyl cytidine) was injected twice during one cell cycle or if it was combined with Andriamycin or anthracyclines, a significant reduction of leukemic burden was achieved without an evident increase of side effect on normal tissues [62]. This therapeutic gain was attributed to the specific recruitment inducing effect of Ara-C on leukemic cells in the dormant phase. Other agents that have a demonstrated effect to recruit quiescent cells into the cycle are cytokines (stimulating factors that play a role in the regulation of normal hemopoiesis) like G-CSF (granulocyte-colony stimulating factor), GM-CSF (gran-

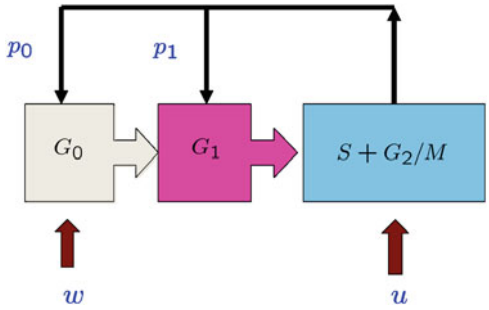

Fig. 2.7 A 3-compartment model with cytotoxic and recruiting agent.

ulocyte macrophage-colony stimulating factor), and especially interleukin-3 combined with SCF (Skp, Cullin, F-box containing complex) [326, 10]. Then a cytotoxic agent may be used to kill the cycling cells.

In the modeling, since one wants to analyze the alteration of the transit time through G_0 due to the feedback mechanism that recruits the cells into the cycle when chemotherapy is applied, now the dormant stage G_0 should be a separate compartment. Cytotoxic agents can be active both in S and G_2/M and thus here these phases of the cell cycle are combined into one compartment. This leads to the following three compartments: G_0, G_1, and $S+G_2/M$. The state space is thus the first orthant in $\mathbb{R}^3$. Because of the association of the compartments with those specific phases of the cell cycle and their established biological nomenclature, here we find it more convenient to label the states N_0, N_1 and N_2. Newly born cells start the cell division process, but then may become dormant and remain in the quiescent stage G_0. Let p_0 and p_1 be positive numbers, $p_0 + p_1 = 1$, that represent the probabilities that the daughter cells pass through the first growth phase unimpeded (p_1) or undergo cell arrest and become quiescent (p_0). A recruiting agent is applied to reduce the average transit time through the compartment G_0 resulting in a higher outflow from G_0. If w (the second control u_2 in the general framework of problem [CC]) denotes the concentration of the recruiting agent, we assume that the outflow is increased by a factor of $1+w$, $0 \le w \le w_{\max}$, with the control $w = 0$ corresponding to no drug being present and $w = w_{\max}$ occurring with a full dose treatment. As before, we do not yet incorporate pharmacokinetic equations into the model. A cytotoxic agent u, $0 \le u \le u_{\max}$, is applied in the third compartment with $u_{\max}$ corresponding to the maximum dose. (This would be our first control u_1 in the framework of problem [CC]). We illustrate the structure of the model in Figure 2.7.

Combining these drugs with the standard features of cell division and cell killing (and again under the log-kill hypothesis) results in a bilinear control system of the form (2.49) with $n = 3$ and $m = 2$ and the following matrices

$$A = \begin{pmatrix} -a_0 & 0 & 2p_0a_2 \\ a_0 & -a_1 & 2p_1a_2 \\ 0 & a_1 & -a_2 \end{pmatrix}, \tag{2.62}$$

$$B_1 = \begin{pmatrix} 0 & 0 & -2p_0a_2 \\ 0 & 0 & -2p_1a_2 \\ 0 & 0 & 0 \end{pmatrix} \qquad \text{and} \qquad B_2 = \begin{pmatrix} -a_0 & 0 & 0 \\ a_0 & 0 & 0 \\ 0 & 0 & 0 \end{pmatrix}. \tag{2.63}$$

As in the 2-compartment model considered earlier, the a_i are positive coefficients related to the inverse transit times for cancer cells through the compartments. It is easily verified that condition (M) holds for all admissible controls,

$$A + uB_1 + wB_2 = \begin{pmatrix} -(1+w)a_0 & 0 & 2p_0(1-u)a_2 \\ (1+w)a_0 & -a_1 & 2p_1(1-u)a_2 \\ 0 & a_1 & -a_2 \end{pmatrix} \in \mathscr{M},$$

and thus the state space $\mathbb{P} = \mathbb{R}^3_+$ is positively invariant.

As for the 2-compartment model, the proportions of cells that are in these compartments obey Riccati differential equations. Again, let $C(t) = N_0(t) + N_1(t) + N_2(t)$ denote the average total number of cancer cells and let x, y and z denote the proportions of cells in these three compartments,

$$x(t) = \frac{N_0(t)}{C(t)}, \qquad y(t) = \frac{N_1(t)}{C(t)} \qquad \text{and} \qquad x(t) = \frac{N_2(t)}{C(t)}.$$

Then we have for the uncontrolled system (with $u \equiv 0$ and $w \equiv 0$) that

$$\dot{x} = -a_0x + 2p_0a_2z - a_2xz, \tag{2.64}$$

$$\dot{y} = a_0x - a_1y + 2p_1a_2z - a_2yz, \tag{2.65}$$

$$\dot{z} = a_1y - a_2z - a_2z^2. \tag{2.66}$$

Regardless of the initial condition, the proportions quickly converge to a unique steady state that gives the average proportions of cancer cells in the three compartments. However, this result is not clear a priori and a proof is required. Note that one of the three equations is redundant because of the trivial relation $x(t) + y(t) + z(t) \equiv 1$ and we use it to eliminate the variable y from the system. We then are left with the following planar system,

$$\dot{x} = -a_0x + 2p_0a_2z - a_2xz, \tag{2.67}$$

$$\dot{z} = a_1(1 - x - z) - a_2z - a_2z^2. \tag{2.68}$$

Theorem 2.2.3. *The unit simplex $\Sigma = \{(x,y,z) : 0 \le x,\ 0 \le y,\ 0 \le z,\ x+y+z = 1\}$ is positively invariant for the dynamical system given by equations (2.64)–(2.66) and has a unique, asymptotically stable equilibrium point (x_*, y_*, z_*) inside of Σ that contains the entire simplex Σ in its region of attraction. That is, given an arbitrary initial condition $(x_0, y_0, z_0) \in \Sigma$, the solution of equations (2.64)–(2.66) exists for all times $t \ge 0$, lies in Σ and converges to (x_*, y_*, z_*) as $t \to \infty$.*

Proof. Because of the relation $x(t) + y(t) + z(t) \equiv 1$, we can identify Σ with the planar set $\tilde{\Sigma} = \{(x,z) : 0 \le x,\ 0 \le z,\ x + z \le 1\}$ and we denote the corresponding vector field by F,

$$F(x,z) = \begin{pmatrix} -a_0 x + 2p_0 a_2 z - a_2 xz \\ a_1 (1-x-z) - a_2 z - a_2 z^2 \end{pmatrix}.$$

In order to show that $\tilde{\Sigma}$ is positively invariant, it suffices to verify that for every initial point (x_0, z_0) in the boundary of $\tilde{\Sigma}$, $(x_0, z_0) \in \partial\tilde{\Sigma}$, the local solution $(x(t;x_0,z_0), z(t;x_0,z_0))$ of the corresponding initial value problem enters the interior of $\tilde{\Sigma}$. (By the uniqueness of solutions to ordinary differential equations, trajectories thus cannot leave $\tilde{\Sigma}$ and it is then a standard argument from the theory of ODEs using the local existence of solutions to show that solutions exist over all of $[0,\infty)$).

We consider the three boundary segments separately and start with $x = 0$ and $0 \leq z \leq 1$. For $x = 0$ and $z \in (0,1)$ we have that $\dot{x} = 2p_0 a_2 z > 0$ and thus the vector field F points inside of $\tilde{\Sigma}$. This also holds at the vertex $(0,1)$ since $F(0,1) = 2a_2 \begin{pmatrix} p_0 \\ -1 \end{pmatrix}$ and $p_0 \in (0,1)$. At the origin, $F(0,0) = \begin{pmatrix} 0 \\ a_1 \end{pmatrix}$ is tangent to the vertical boundary segment of $\tilde{\Sigma}$ and we here need to compute a second order approximation of the solution. By the implicit function theorem, we can express the solution curve starting at the origin as a function of the form $x = h(z)$ and the derivative $h'(z)$ is given by

$$h'(z) = \frac{dx}{dz} = \frac{\dot{x}}{\dot{z}} = \frac{-a_0 x + 2p_0 a_2 z - a_2 xz}{a_1 (1-x-z) - a_2 z - a_2 z^2}.$$

Differentiating the relation $\dot{x} = h'(z)\dot{z}$ once more with respect to t gives that

$$\ddot{x} = h''(z)\dot{z}^2 + h'(z)\ddot{z}$$

and evaluating this expression at the origin, while using $h'(0) = 0$, gives

$$h''(0) = \frac{\ddot{x}}{\dot{z}^2} = \frac{2p_0 a_2 a_1}{a_1^2} = 2p_0 \frac{a_2}{a_1} > 0.$$

Hence the curve $x = h(z)$ has a local minimum at $z = 0$ with contact of order 1 (i.e., the second derivative is nonzero) and lies inside the region $\tilde{\Sigma}$ for small positive times. This verifies that solutions starting at points in the vertical boundary segment of $\tilde{\Sigma}$ enter the interior of $\tilde{\Sigma}$ forward in time.

On the horizontal boundary segment, $0 \leq x \leq 1$ and $z = 0$, we have for $x < 1$ that $\dot{z} = a_1 (1-x) > 0$ and thus $F(x,0)$ points inside $\tilde{\Sigma}$ at those points. At the vertex $(1,0)$, we have $F(1,0) = \begin{pmatrix} -a_0 \\ 0 \end{pmatrix}$ and the trajectory is tangent to the horizontal boundary segment. In this case we can describe the trajectory as a function of x, say $z = k(x)$, and a computation analogous to the one just carried out at the origin verifies that this function also has a local minimum with contact of order 1. Hence, again the trajectory enters the interior of $\tilde{\Sigma}$. Finally, along the line $x + z = 1$, we have that

$$(x+z)^{\cdot} = -2a_2(1-p_0)z - a_0 x < 0$$

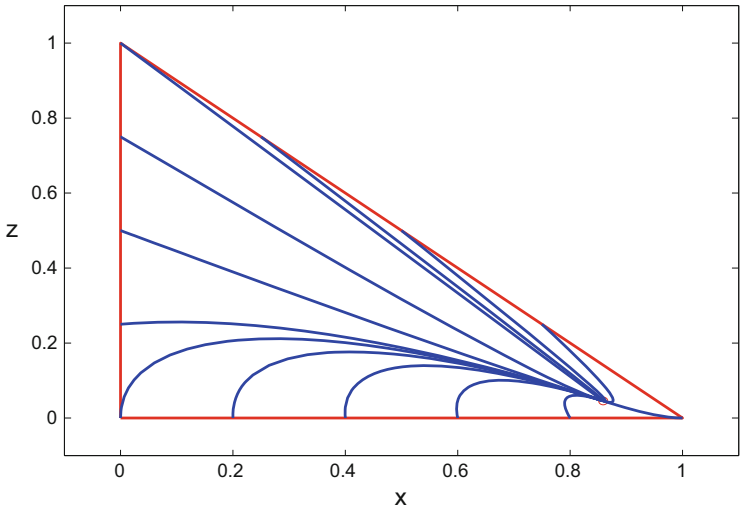

Fig. 2.8 Positive invariance of the unit simplex Σ under the flow for the proportions.

and thus all trajectories starting on this line enter the interior of Σ. This verifies that the simplex $\tilde{\Sigma}$ is positive invariant for the system (2.67) and (2.68). Figure 2.8 illustrates the phase portrait in the (x,z)-plane.

The system has a unique equilibrium point (x_*,z_*) in $\tilde{\Sigma}$: solving the equation $\dot{z}=0$ for x gives

$$x_* = 1 - \left(1+\frac{a_2}{a_1}\right) z_* - \frac{a_2}{a_1} z_*^2$$

and substituting this relation into the equation $\dot{x}=0$ leads to the following cubic polynomial in z whose solutions define the equilibria (x_*,z_*):

$$a_2^2 z^3 + (a_0+a_1+a_2)\, a_2 z^2 + ((a_1+a_2)\, a_0 + (2p_0-1)\, a_1 a_2)\, z - a_0 a_1 = 0.$$

Dividing by a_2^2 and setting $\alpha_0 = \frac{a_0}{a_2}$ and $\alpha_1 = \frac{a_1}{a_2}$ we obtain the simpler expression

$$Q(y) = z^3 + (1+\alpha_1+\alpha_2)\, z^2 + ((1+\alpha_1)\, \alpha_0 + (2p_0-1)\, \alpha_1)\, z - \alpha_0 \alpha_1 = 0.$$

Since $Q''(y)$ is positive for $y \geq 0$, this polynomial Q is strictly convex on $[0,\infty)$. It thus follows from $Q(0) = -\alpha_0\alpha_1 < 0$ and $Q(1) = 2\,(1+a_0+p_0\alpha_1) > 0$ that there exists exactly one positive root that lies in the open interval $(0,1)$. Hence

$$x_* + z_* = 1 - \frac{1}{\alpha_1} z_* (1+z_*) < 1$$

and from $\dot{x} = 0$ we obtain that

$$x_* = \frac{2p_0 z_*}{\alpha_0 + z_*} > 0.$$

Thus there exists a unique equilibrium point (x_*, z_*) in $\tilde{\Sigma}$ and it lies in the interior.

The rest of the argument is an application of Poincaré-Bendixson theory for planar systems (e.g., see [145]): Since $\tilde{\Sigma}$ is compact and positive invariant, every trajectory $(x(t;x_0,z_0),z(t;x_0,z_0))$ with initial condition $(x_0,z_0) \in \tilde{\Sigma}$ has a nonempty ω-limit set.[2] The divergence of the vector field F is negative on the first orthant,

$$\text{div } F = \frac{\partial F_1}{\partial x}(x,z) + \frac{\partial F_2}{\partial z}(x,z) = -a_0 - a_2 z - a_1 - a_2 - 2a_2 z < 0,$$

and thus it follows from Bendixson's theorem that there do not exist periodic orbits for the system (2.67) and (2.68) in $\tilde{\Sigma}$. Hence these ω-limit sets all consist of a unique equilibrium point. Since there is only one such point and ω-limit sets are attractive, all trajectories converge to (x_*, z_*). □

This is an important result in that it says that independently of the size of the tumor, by the time chemotherapy treatment starts, the system has settled down to have specific fractions of cycling cells in the respective compartments. These fractions are only determined by the coefficients that define the cell cycle kinetics. It is possible to give explicit formulas for the equilibrium point (x_*, y_*, z_*) in terms of the coefficients a_i and p_0 using Cardano's formula for the roots of a cubic polynomial, but these expressions are unwieldy and not informative. On the other hand, it is easy to compute these fractions numerically. More interesting, like for the 2-compartment model, the cell cycle parameters a_i, $i = 0,1,2$ can be determined from these steady-state proportions and the tumor doubling time. For the total number of cancer cells, analogously as before, we have that

$$\dot{C}(t) = a_2 N_2(t) = a_2 z(t) C(t) \approx a_2 z_* C(t)$$

approximating $z(t)$ with its steady-state value z_*. Thus the tumor approximately grows exponentially at rate $a_2 z_*$. If T denotes the tumor doubling time, then we again have the simple relation

$$a_2 z_* = \frac{\ln 2}{T}.$$

The other kinetic parameters a_0 and a_1 directly follow from the equilibrium relations and we summarize the relations below:

Proposition 2.2.4. *If T denotes the tumor doubling time and x_*, y_* and z_* are the steady-state proportions of cells in the cell cycle compartments G_0, G_1 and $S + G_2/M$, respectively, then we have that*

[2] The ω-limit set of a positive semi-trajectory $(x(t;x_0,z_0),z(t;x_0,z_0))$ is the set of all accumulation points of this trajectory as $t \to \infty$.

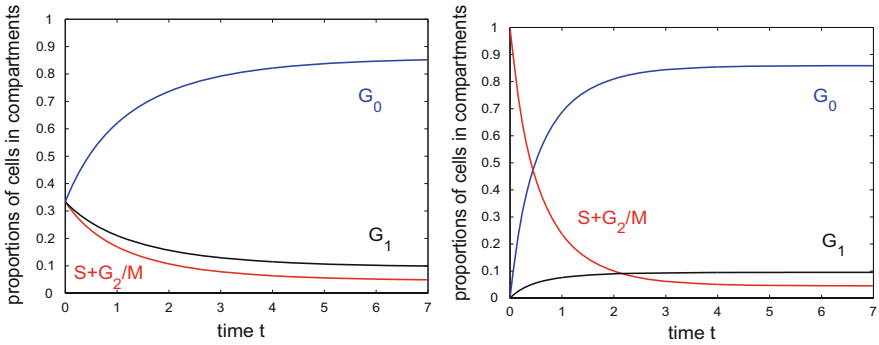

Fig. 2.9 Trajectories for the average fractions of cells in the compartments G_0, G_1 and $S+G_2/M$.

$$a_0 = \frac{\ln 2}{x_* T}\left(p_0 - p_1 + y_* + z_*\right), \qquad a_1 = (1+z_*)\frac{\ln 2}{y_* T} \qquad \text{and} \qquad a_2 = \frac{\ln 2}{z_* T}.$$

Figure 2.9 illustrates the speed of convergence of the fractions to their equilibrium point solution for $a_0 = 0.05$, $a_1 = 0.5$, $a_2 = 1$ and $p_0 = 0.9$. In this case, the limiting proportions are 85% in the dormant compartment G_0, 10% in the first growth phase G_1, and only 5% in the cycling compartment $S+G_2/M$ where killing agents act. The graph on the right in Figure 2.9 shows how quickly a proportion of cycling cells distributes into these fractions. In the graph on the right side of the figure, the initial condition is set to 1 for the proportion of cycling cells and to 0 for the other compartments, an extreme case to illustrate this fact.

We now consider the optimal control problem of administering a killing and a recruiting agent. The objective is taken in the form

$$J = rN(T) + \int_0^T qN(t) + s_1 u(t) + s_2 w(t)dt, \tag{2.69}$$

where $r = (r_0, r_1, r_2) \in \left(\mathbb{R}^3\right)^*$ and $q = (q_0, q_1, q_2) \in \left(\mathbb{R}^3\right)^*$ are row vectors of positive coefficients. The weight s_1 at the cytotoxic agent u is a positive number and the weight s_2 for the recruiting agent is nonnegative. In fact, here $s_2 = 0$ or s_2 a much smaller positive weight than s_1 is a biologically reasonable choice and we want to allow this case. However, this brings in a degenerate scenario which arises if $u_{\max} = \frac{1}{2}$. In this case, for $u \equiv u_{\max} = \frac{1}{2}$, the dynamics is given by

$$\dot{N} = \begin{pmatrix} -(1+w)a_0 & 0 & p_0 a_2 \\ (1+w)a_0 & -a_1 & p_1 a_2 \\ 0 & a_1 & -a_2 \end{pmatrix} N$$

and we have that $\dot{C}(t) \equiv 0$. Hence the total cancer volume is constant along such a trajectory, regardless of the control w used. In the case $s_2 = 0$ there is no penalty on the use of the control w and thus all controls w are equal in their effect and optimal on any interval where $u \equiv u_{\max} = \frac{1}{2}$ since w has no effect on the objective.

This prevents us from making any conclusive statements about w, simply because the effects of all controls are the same and thus any one will do fine. But this is not an important restriction in the sense that in a practical situation $u_{\max}$ will have to be much larger than $\frac{1}{2}$, in fact, typically close to 1 in an MTD style application. If $u_{\max} = \frac{1}{2}$, then, to begin with, it is impossible to reduce the cancer volume. Thus, realistically $u_{\max} \gg \frac{1}{2}$. We therefore consider the following optimal control problem:

[CC3r] for a fixed therapy horizon $[0,T]$, minimize the objective

$$J = rN(T) + \int_0^T qN(t) + s_1u(t) + s_2w(t)dt \to \min$$

over all Lebesgue-measurable (respectively, piecewise continuous) functions $(u,w) : [0,T] \to [0,u_{\max}] \times [0,w_{\max}]$, $u_{\max} \neq \frac{1}{2}$, subject to the dynamics

$$\dot{N}(t) = \begin{pmatrix} -(1+w)a_0 & 0 & 2p_0(1-u)a_2 \\ (1+w)a_0 & -a_1 & 2p_1(1-u)a_2 \\ 0 & a_1 & -a_2 \end{pmatrix} N(t), \qquad N(0) = N_0.$$

For the reader's convenience, we write out the fundamental necessary conditions for optimality for this system. The adjoint equation is given by

$$\dot{\lambda} = -\lambda\,(A + uB_1 + wB_2) - q, \qquad \lambda(T) = r,$$

which, in terms of its components, reads

$$\begin{aligned} \dot{\lambda}_0 &= (1+w)a_0\,(\lambda_0 - \lambda_1) - q_0, & \lambda_0(T) &= r_0, \\ \dot{\lambda}_1 &= a_1\,(\lambda_1 - \lambda_2) - q_1, & \lambda_1(T) &= r_1, \\ \dot{\lambda}_2 &= -2a_2(1-u)\,(p_0\lambda_0 + p_1\lambda_1) + a_2\lambda_2 - q_2, & \lambda_2(T) &= r_2. \end{aligned}$$

The switching functions for the controls u and w are given by

$$\Phi_1(t) = s_1 + \lambda(t)B_1N(t) = s_1 - 2a_2\{p_0\lambda_0(t) + p_1\lambda_1(t)\}N_2(t) \tag{2.70}$$

and

$$\Phi_2(t) = s_2 + \lambda(t)B_2N(t) = s_2 - a_0\{\lambda_0(t) - \lambda_1(t)\}N_0(t), \tag{2.71}$$

respectively. We first show that an optimal control for the cytotoxic agent u cannot be singular.

Theorem 2.2.4. *Suppose (N_*, u_*, w_*) is an optimal controlled trajectory for problem [CC3r]. Then there does not exist an interval on which the control u_* is singular, i.e., the cytotoxic agent is not given at partial dose rates/concentrations.*

Proof. Suppose the control u_* is singular over a nonempty open interval I so that the switching function Φ_1 vanishes identically. It then follows from Proposition 2.2.3 that also

$$\dot{\Phi}_1(t) = \lambda(t)\,[A + w_*(t)B_2, B_1]N_*(t) - qB_1N_*(t) \equiv 0. \tag{2.72}$$

Direct matrix computations verify that

$$[B_2, B_1] = 2p_0 a_0 a_2 \begin{pmatrix} 0 & 0 & -1 \\ 0 & 0 & 1 \\ 0 & 0 & 0 \end{pmatrix} \tag{2.73}$$

and therefore $\dot{\Phi}_1(t)$ depends on the second control w_*. A priori, we have no information about w_* and thus need to consider all possible cases. The switching function Φ_2 is continuous and let us first assume that there exists a time $t \in I$ where Φ_2 does not vanish. Then, by continuity, Φ_2 does not vanish on an open subinterval $J \subset I$ that contains t and on this interval the control w is constant, say $w(t) \equiv w_*$ on J. Differentiating $\dot{\Phi}_1(t)$ once more on J, it follows that

$$\begin{aligned} \ddot{\Phi}_1(t) = \lambda(t)\,[A + u(t)B_1 + w_* B_2, [A + w_* B_2, B_1]]\, N_*(t) \\ - q\,[A + w_* B_2, B_1]\, N_*(t) - qB_1\,(A + u(t)B_1 + w_* B_2)\, N_*(t). \end{aligned}$$

The Legendre-Clebsch condition for local optimality of the singular control u (see Theorem A.3.2 in Appendix A and equation (2.35)) requires that

$$\frac{\partial}{\partial u}\frac{d^2}{dt^2}\frac{\partial H}{\partial u}(\lambda(t), N_*(t), u_*(t), w_*) \le 0 \qquad \text{for all } t \in J.$$

For the model [CC3r], this expression is given by

$$\frac{\partial}{\partial u}\frac{d^2}{dt^2}\frac{\partial H}{\partial u}(\lambda(t), N_*(t), u_*(t), w_*) = \left\{\lambda(t)[B_1, [A + w_* B_2, B_1]] - qB_1^2\right\} N_*(t).$$

We have that $B_1^2 \equiv 0$ and also the second-order Lie bracket $[B_1, [B_2, B_1]]$ vanishes, $[B_1, [B_2, B_1]] \equiv 0$, while

$$[A, B_1] = 2a_2 \begin{pmatrix} 0 & -p_0 a_1 & p_0(a_2 - a_0) \\ 0 & -p_1 a_1 & p_0 a_0 + p_1(a_2 - a_1) \\ 0 & 0 & p_1 a_1 \end{pmatrix}$$

and

$$[B_1, [A, B_1]] = 8p_1 a_1 a_2^2 \begin{pmatrix} 0 & 0 & p_0 \\ 0 & 0 & p_1 \\ 0 & 0 & 0 \end{pmatrix} = -4p_1 a_1 a_2 B_1.$$

Therefore the Legendre-Clebsch condition reduces to

$$\begin{aligned} \frac{\partial}{\partial u}\frac{d^2}{dt^2}\frac{\partial H}{\partial u}(\lambda(t), N_*(t), u_*(t), w_*) &= \lambda(t)[B_1, [A, B_1]] N_*(t) \\ &= -4p_1 a_1 a_2 \lambda(t) B_1 N_*(t). \end{aligned}$$

But it follows from $\frac{d}{dt}\Phi_1(t) \equiv 0$ that $\lambda(t)B_1N_*(t) \equiv -s_1$ and thus overall for $t \in J$ we obtain that

$$\frac{\partial}{\partial u}\frac{d^2}{dt^2}\frac{\partial H}{\partial u}(\lambda(t), N_*(t), u_*(t), w_*) \equiv 4p_1a_1a_2s_1 > 0 \tag{2.74}$$

violating the Legendre-Clebsch condition. Hence singular controls u are locally maximizing on intervals J where the recruiting agent w is constant.

It remains to consider the possibility that also w_* is singular over I. In this case both controls are simultaneously singular over I and there is an additional necessary condition for optimality for this situation, the so-called *Goh-condition* (see Theorem A.3.3 in Appendix A). It requires that

$$\frac{\partial}{\partial w}\frac{d}{dt}\frac{\partial H}{\partial u}(\lambda(t), N_*(t), u_*(t), w_*(t)) \equiv 0 \qquad \text{for all } t \in I.$$

Since $\frac{d}{dt}\frac{\partial H}{\partial u} = \dot{\Phi}_1$, it follows from equations (2.72) and (2.73) that for all $t \in I$ we then must have that

$$0 \equiv \lambda(t)[B_2, B_1]N_*(t) = 2p_0a_0a_2\{-\lambda_0(t) + \lambda_1(t)\}N_2(t) \equiv 0.$$

Since N_2 is positive, it follows that $\lambda_0(t) \equiv \lambda_1(t)$ for all $t \in I$. But the condition $\Phi_2(t) \equiv 0$ reads $s_2 - a_0(\lambda_0(t) - \lambda_1(t))N_0(t) \equiv 0$ and thus this is not possible if $s_2 > 0$.

The scenario $s_2 = 0$ is realistic for this model and requires a separate argument. If $s_2 = 0$, the Goh condition is satisfied, but $\lambda_0(t) \equiv \lambda_1(t)$ is a very restrictive relation and we can exclude the optimality of such a scenario going back to the Legendre-Clebsch condition for the control u_*. For, in this case we actually have that the row-vector $\lambda(t)[B_2, B_1]$ vanishes identically and thus the control w_* drops out of the formula (2.72) for the derivative of the switching function Φ_1 for the control u_*, i.e., we have that

$$\dot{\Phi}_1(t) = \{\lambda(t)[A, B_1] - qB_1\}N_*(t) \equiv 0.$$

Differentiating this equation once more and computing the Legendre-Clebsch condition for the control u gives the same condition (2.74) as in the case when the control w_* is constant and thus the Legendre-Clebsch condition is violated. This concludes the proof. □

Theorem 2.2.5. *Let (N_*, u_*, w_*) be an optimal controlled trajectory for problem [CC3r]. If the weight s_2 in the Lagrangian for the recruiting agent w is zero, $s_2 = 0$, then there does not exist an interval on which the control w_* is singular. However, if this coefficient is positive, $s_2 > 0$, then the Legendre-Clebsch condition for optimality of a singular control w is satisfied.*

Proof. Suppose that the control w_* is singular on a nonempty open interval I. By the previous result, the control u cannot be singular on I and, without loss of generality we therefore assume that u is constant on I, given by either $u = 0$ or $u = u_{\max}$.

First we consider the case $s_2 = 0$. As above, the fact that the switching function $\Phi_2(t) = a_0\{\lambda_0(t) - \lambda_1(t)\}N_1(t)$ vanishes identically on I implies that $\lambda_0(t) \equiv \lambda_1(t)$ for all $t \in I$. Using the adjoint equations for the derivatives of these multipliers gives us that

$$-q_0 = \dot{\lambda}_0(t) = \dot{\lambda}_1(t) = a_1\{\lambda_1(t) - \lambda_2(t)\} - q_1$$

and thus

$$\lambda_1(t) - \lambda_2(t) = \frac{q_1 - q_0}{a_1} = \text{const.}$$

Hence we actually have that $\dot{\lambda}_0(t) \equiv \dot{\lambda}_1(t) \equiv \dot{\lambda}_2(t)$. But then also

$$-q_0 = \dot{\lambda}_0(t) = \dot{\lambda}_2(t) = -2a_2(1-u)\lambda_0(t) + a_2\lambda_2(t) - q_2$$

and thus

$$\frac{q_2 - q_0}{a_2} = -2(1-u)\lambda_0(t) + \lambda_2(t) = -2(1-u)\lambda_0(t) + \lambda_1(t) - \frac{q_1 - q_0}{a_1}.$$

Since $\lambda_0(t) \equiv \lambda_1(t)$, this relation implies that

$$\frac{q_2 - q_0}{a_2} + \frac{q_1 - q_0}{a_1} = \lambda_0(t)(2u - 1).$$

But the control u is given by 0 or $u_{\max}$, and, since $u_{\max} \neq \frac{1}{2}$, this relation implies that $\lambda_0(t)$ is constant. But $\dot{\lambda}_0(t) = -q_0 < 0$. Contradiction. (It is only in this step that we make use of the assumption that $u_{\max} \neq \frac{1}{2}$).

The existence of the degenerate scenario for the case $u_{\max} = \frac{1}{2}$ for $s_2 = 0$ indicates a bifurcation structure. Indeed, for $s_2 > 0$ the Legendre-Clebsch condition is satisfied. Recall that u is constant and thus by Proposition 2.2.3 the first and second derivatives of the switching function Φ_2 are given by

$$\dot{\Phi}_2(t) = \{\lambda(t)[A + uB_1, B_2] - qB_2\}N_*(t)$$

and

$$\begin{aligned}\ddot{\Phi}_2(t) = {} & \lambda(t)[A + uB_1 + w_*(t)B_2, [A + uB_1, B_2]]N_*(t) \\ & - q[A + uB_1, B_2]N_*(t) - qB_2(A + uB_1 + w_*(t)B_2)N_*(t).\end{aligned}$$

Hence

$$\frac{\partial}{\partial w}\frac{d^2}{dt^2}\frac{\partial H}{\partial w}(\lambda(t), N_*(t), u, w_*(t)) = \left\{\lambda(t)[B_2, [A + uB_1, B_2]] - qB_2^2\right\}N_*(t). \quad (2.75)$$

A direct computation verifies that $B_2^2 = -a_0 B_2$ and using that $\dot{\Phi}_2(t) \equiv 0$, we can rewrite equation (2.75) as

$$\begin{aligned}&\frac{\partial}{\partial w}\frac{d^2}{dt^2}\frac{\partial H}{\partial w}(\lambda(t), N_*(t), u, w_*(t)) \\ &\quad = \lambda(t)\{[B_2, [A + uB_1, B_2]] + a_0[A + uB_1, B_2]\}N_*(t).\end{aligned}$$

These brackets are given by

$$[A+uB_1,B_2]=a_0\begin{pmatrix}0 & 0 & -2p_0(1-u)a_2\\ a_1 & 0 & 2p_0(1-u)a_2\\ -a_1 & 0 & 0\end{pmatrix}$$

and

$$[B_2,[A+uB_1,B_2]]=a_0^2\begin{pmatrix}0 & 0 & -2p_0(1-u)a_2\\ -a_1 & 0 & 2p_0(1-u)a_2\\ a_1 & 0 & 0\end{pmatrix},$$

so that

$$[B_2,[A+uB_1,B_2]]+a_0\,[A+uB_1,B_2]=4p_0a_0^2a_2(1-u)\begin{pmatrix}0\,0 & -1\\ 0\,0 & 1\\ 0\,0 & 0\end{pmatrix}.$$

Hence

$$\begin{aligned}&\frac{\partial}{\partial w}\frac{d^2}{dt^2}\frac{\partial H}{\partial w}(\lambda(t),N_*(t),u,w_*(t))\\ &\quad=\lambda(t)\left\{[B_2,[A+uB_1,B_2]]+a_0\,[A+uB_1,B_2]\right\}N_*(t)\\ &\quad=4p_0a_0^2a_2(1-u)\left\{\lambda_1(t)-\lambda_0(t)\right\}N_2(t).\end{aligned}$$

But $\Phi_2(t)\equiv 0$ implies that $a_0\left\{\lambda_0(t)-\lambda_1(t)\right\}N_0(t)\equiv s_2>0$ and thus now we have that $\lambda_0(t)>\lambda_1(t)$ along a singular control w. Hence

$$\frac{\partial}{\partial w}\frac{d^2}{dt^2}\frac{\partial H}{\partial w}(\lambda(t),N_*(t),u_*(t),w_*(t))\le 0$$

and the Legendre-Clebsch condition is satisfied. Note that the strengthened Legendre-Clebsch condition holds if $u\neq 1$ and this will always be the case if $u_{\max}<1$. □

The calculations carried out in the proof also show that a singular control w_{sing} can be expressed in the form

$$w_{\text{sing}}(t)=-\frac{\left\{\lambda(t)\,[A+uB_1,[A+uB_1,B_2]]-q\,[A+uB_1,B_2]-qB_2\,(A+uB_1)\right\}N_*(t)}{\lambda(t)\left\{[B_2,[A+uB_1,B_2]]+a_0\,[A+uB_1,B_2]\right\}N_*(t)}$$

and this expression can be evaluated similar as it was done for the 2-compartment model. The result is messy with complicated algebraic expressions in the a_i and weights q. In addition, the control defined by this equation needs to lie within the control limits and this is not guaranteed a priori. We shall not pursue this further here, but instead give some numerical examples that show that singular controls typically do not arise in optimal solutions.

For small positive weights s_2, and this is the important case for this model, bang-bang controls are optimal. Figure 2.10 shows the graphs of such controls u and w and their corresponding trajectories when the weight s_2 in the Lagrangian is chosen

as $s_2 = 0$ (on the left) and $s_2 = 0.1$ (on the right) for parameter values specified in Table 2.3. All switching surfaces are transversal folds and the computed controlled trajectories are strong local minima. Table 2.4 gives the transversality conditions for these two trajectories computed using Theorem 2.2.2. In both cases, as for the 2-compartment model considered earlier, the cytotoxic agent is given upfront in one maximum dose session at the beginning of therapy. The effectiveness of this agent is enhanced by the recruiting agent that also is given at maximum dose from the beginning. The recruiting agent is withdrawn a short time before the cytotoxic agent is stopped. Clearly, once the cells that were recruited into the cell cycle have gone through the third compartment, the phases $S + G_2/M$, the benefit from killing the small fraction of cancer cells in the third compartment is outweighed by the side effects as measured by the integral of the control u and thus at the right time administration of the cytotoxic agent ceases. However, there is a difference in the administration of the recruiting agent in these two scenarios. In the objective, we have put three times the weight on cancer cells in the dormant stage G_0 than in the other stages of the cell cycle and thus the optimal controls will want to recruit these cells, at a minimum to get them into a phase of the cell cycle that is less "costly" in terms of the objective functional. When the administration of the recruiting agent is "free," i.e., for $s_2 = 0$, then it is simply advantageous (in the sense of minimizing the objective, not necessarily from a medical point of view) to move the cells from the quiescent state into the active phases of the cell cycle and thus in this case there still exists a large interval toward the end of therapy when the recruiting agent is at full dose. From a practical point, this is not desired since these cells then will undergo cell division and the tumor will grow stronger than otherwise would have been the case. Thus, even if there are possibly no side effects to the recruiting agent, it clearly is more prudent to have a small positive weight s_2. As the figures on the right in Figure 2.10 illustrate, when the administration of the recruiting agent is made "costly," the incentive to move cancer cells into the cycling phase of the cell cycle needs to be balanced with its "cost" and in this case the second interval where $w = w_{\max}$ is forgone for longer first segments. Thus, this example also illustrates how the choice of the weights leads to different protocols and that the weights can be—and should be—adjusted to generate medically relevant and satisfactory protocols. For example, these computations raise the specter of making the weight q time-varying: take higher weights q_0 at the beginning of the therapy period in order to induce the controls to recruit dormant cells into the cell cycle and then proceed to equal weights for all compartments in order not to entice recruiting of the cells toward the end of therapy. Changes of this type could be incorporated into the model at the expense of changes in the higher-order derivatives of the switching function. The reasoning can easily be adjusted to this more general setting.

Table 2.3 Numerical values for the coefficients and parameters used in computations for the optimal control problem [CC3r] with cytotoxic and recruitment agent.

Coefficient	Interpretation	Numerical value	Reference
a_0	Inverse transit time through G_0	0.05	
a_1	Inverse transit time through G_1	0.5	
a_2	Inverse transit time through $S+G_2/M$	1	
p_0 $p_1 = 1 - p_0$	Probability that cells enter G_0 Probability that cells enter G_1	0.9 0.1	
x_* $N_0(0)$	Steady-state proportion in G_0 Initial condition for N_0	0.8589 0.8589	Eq. (2.64)
y_* $N_1(0)$	Steady-state proportion in G_1 Initial condition for N_2	0.0954 0.0954	Eq. (2.65)
z_* $N_2(0)$	Steady-state proportion in $S+G_2/M$ Initial condition for N_2	0.0456 0.0456	Eq. (2.66)
$u_{\max}$	Maximum dose rate/concentration effectiveness	0.95	
s	Penalty/weight at the cytotoxic agent	1	
q_0	Penalty/weight in the objective for the average number of cancer cells in G_0 during therapy	3	
q_1	Penalty/weight in the objective for the average number of cancer cells in G_1 during therapy	1	
q_2	Penalty/weight in the objective for the average number of cancer cells in $S+G_2/M$ during therapy	1	
r_0	Penalty/weight in the objective for the average number of cancer cells in G_0 at the end of therapy	3	
r_1	Penalty/weight in the objective for the average number of cancer cells in G_1 at the end of therapy	1	
r_2	Penalty/weight in the objective for the average number of cancer cells in $S+G_2/M$ at the end of therapy	1	
T	Therapy horizon	21	Illustration only

Table 2.4 Numerical values of the transversality conditions at the bang-bang junctions for the extremals in Figure 2.10.

Weight s_2	Control that switches	Switching time	Value of the transversality condition (2.60)
0	w	11.415	0.0125
	u	12.945	0.5144
	w	17.777	0.0062
0.1	w	7.9349	0.0474
	u	12.188	0.4778

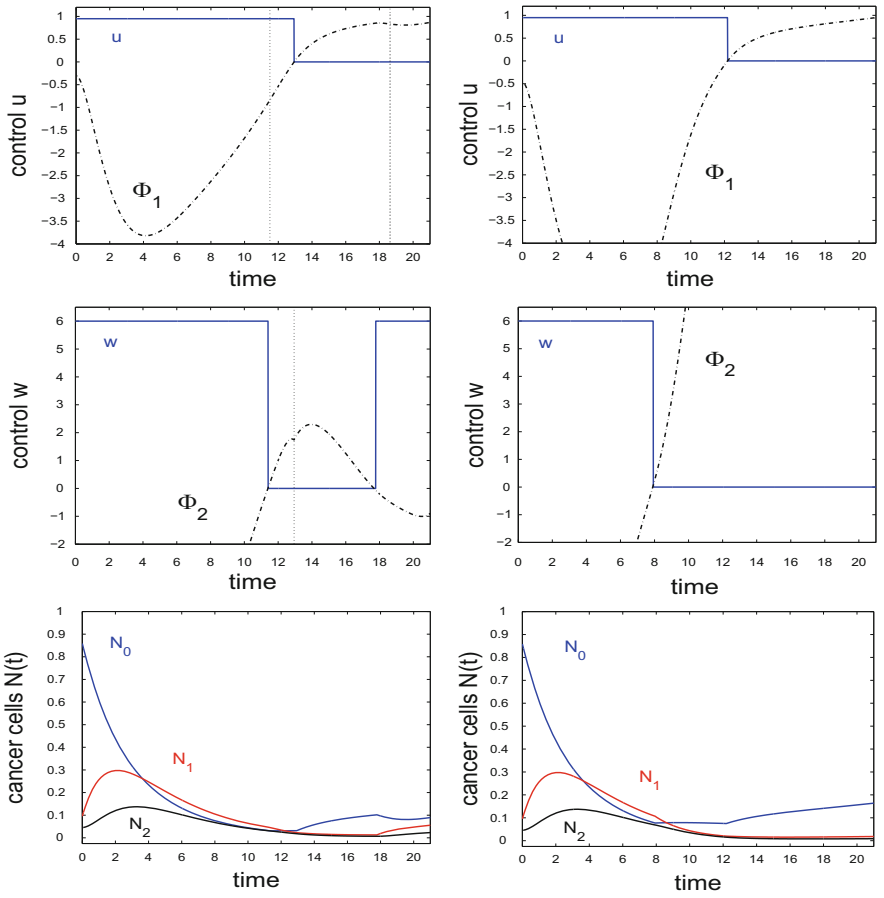

Fig. 2.10 Examples of locally optimal controls u (cytotoxic agent, top), w (recruiting agent, middle) and their corresponding trajectories (bottom) for weights $s_2 = 0$ (left) and $s_2 = 0.1$ (right). The initial condition is the steady-state solution of the proportions (see Theorem 2.2.3) with the total tumor volume normalized to 1. The parameter values are given in Table 2.3.

2.2.3 A 3-Compartment Model with a Killing and Blocking Agent

We also analyze a different type of drug interaction that arises when a G_2/M-specific cytotoxic (killing) agent is combined with a cytostatic (blocking) drug that is used to synchronize the transitions of cells through the cell cycle [169]. Drugs of this type include, for example, anthracycline antibiotics like adriamycin [6] or antineoplastic agents like hydroxyurea (HU) [223, 68] that inhibit DNA and RNA synthesis in S and thus hold cells in the first growth phase G_1. The fractions of cells in the individual phases of the cell cycle vary, especially in tumors, but a rough approximate value when cells are randomly distributed within the cell cycle, is that about 60% of the cells will be in G_1, 20% will be in the S phase and 20% will be G_2/M. The purpose

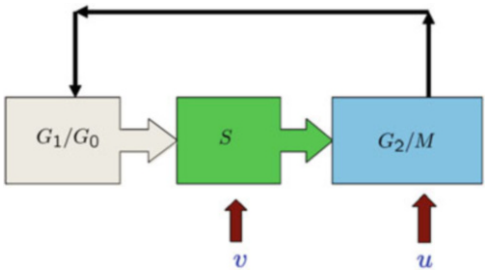

Fig. 2.11 A 3-compartment model with cytostatic agent v and cytotoxic agent u.

of applying a cytostatic drug is to temporarily arrest cancer cells in the cell cycle and then release them when a killing agent is at full potential in the G_2/M phase hoping to maximize the overall fraction of tumor cells killed while also somewhat minimizing the killing effects on normal cells if these are not synchronized.

Cytostatic drugs slow down the growth of malignant cells in the sense that they prevent cells from reaching the phase where cell division occurs. In the model here, cell arrest in phase S is considered. We again use a 3-compartment model, but now the compartments are the first growth phase G_1 (which is lumped with the dormant cells), synthesis S, and the second growth phase and mitosis, G_2/M. The state space thus once more is the first orthant $\mathbb{P}$ in $\mathbb{R}^3$, but here we retain the notation N_1, N_2 and N_3 for the states. A cytostatic blocking agent is applied to slow down the transit times of cancer cells during the synthesis phase S and as a result, the flow of cancer cells from the second into the third compartment is reduced by a factor of $v(t)$ percent from its original flow of $a_2N_2(t)$ to $(1-v(t))a_2N_2(t)$, $0 \le v(t) \le v_{\max} < 1$. This factor v represents a second control in the model with $v(t) \equiv 0$ corresponding to the case when no drug is administered and $v_{\max}$ giving the maximum reductions with full dose. As before, the main control u represents the concentration in the bloodstream of a cytotoxic agent with $u \equiv 0$ corresponding to no treatment and $u = u_{\max}$ corresponding to a maximum dose. We illustrate the general structure of the model in Figure 2.11.

Retaining all the previous assumptions about the model of cell kill (the tumor consists of a homogeneous population of drug sensitive cells and the log-kill hypothesis), the corresponding mathematical model again is a bilinear system of the form (2.49) with $n = 3$ and $m = 2$. Here the matrices are given by

$$A = \begin{pmatrix} -a_1 & 0 & 2a_3 \\ a_1 & -a_2 & 0 \\ 0 & a_2 & -a_3 \end{pmatrix}, \tag{2.76}$$

$$B_1 = \begin{pmatrix} 0\,0 & -2a_3 \\ 0\,0 & 0 \\ 0\,0 & 0 \end{pmatrix} \quad \text{and} \quad B_2 = \begin{pmatrix} 0 & 0 & 0 \\ 0 & a_2 & 0 \\ 0 & -a_2 & 0 \end{pmatrix}. \tag{2.77}$$

Once more it is easily verified that the controlled dynamics is described by M-matrices,

$$A+uB_1+vB_2=\begin{pmatrix}-a_1 & 0 & 2(1-u)a_3\\ a_1 & -(1-v)a_2 & 0\\ 0 & (1-v)a_2 & -a_3\end{pmatrix}\in\mathscr{M},$$

and thus the state space $\mathbb{P}$ is positively invariant.

Again there exists a well-defined steady state for the proportions of cells in the individual compartments. As above, let $C(t)=N_1(t)+N_2(t)+N_3(t)$ denote the total number of cancer cells and define the proportions of cancer cells in these compartments as x, y and z,

$$x(t)=\frac{N_1(t)}{C(t)},\qquad y(t)=\frac{N_2(t)}{C(t)}\qquad\text{and}\qquad x(t)=\frac{N_3(t)}{C(t)}.$$

so that with $u\equiv 0$ and $w\equiv 0$ we have that

$$\dot{x}=-a_1x+2a_3z-a_3xz, \tag{2.78}$$

$$\dot{y}=a_1x-a_2y-a_3yz, \tag{2.79}$$

$$\dot{z}=a_2y-a_3z-a_3z^2. \tag{2.80}$$

Because of the trivial relation $C(t)=N_1(t)+N_2(t)+N_3(t)\equiv 1$, one of the three equations is redundant and again we eliminate the variable y from the system. We then are left with the following planar system,

$$\dot{x}=-a_1x+2a_3z-a_3xz,$$
$$\dot{z}=a_2(1-x-z)-a_3z-a_3z^2.$$

If we identify the respective cell cycle parameters and take $p_0=1$, then these are the same equations as in (2.64)–(2.66). The only difference in the dynamics which this change causes is that the trajectory starting at the vertex $(x,z)=(0,1)$ now is also tangent to the boundary of the unit simplex $\tilde{\Sigma}=\{(x,z):\ 0\le x,\ 0\le z,\ x+z\le 1\}$, but as for the other two vertices, the order of contact of this trajectory with the line $x+z=1$ is 1 and the trajectory enters the interior of $\tilde{\Sigma}$ forward in time. Thus $\tilde{\Sigma}$ remains positively invariant. Theorem 2.2.3 thus immediately gives the following result:

Theorem 2.2.6. *The unit simplex $\Sigma=\{(x,y,z):\ 0\le x,\ 0\le y,\ 0\le z,\ x+y+z=1\}$ is positively invariant under the dynamical system given by equations (2.78)–(2.80) and has a unique, asymptotically stable equilibrium point (x_*,y_*,z_*) inside of Σ that contains the entire simplex Σ in its region of attraction. Given an arbitrary initial condition $(x_0,y_0,z_0)\in\Sigma$, the solution of equations (2.78)–(2.80) exists for all times $t\ge 0$, lies in Σ and converges to (x_*,y_*,z_*) as $t\to\infty$.*

Figure 2.12 illustrates the corresponding phase portrait.

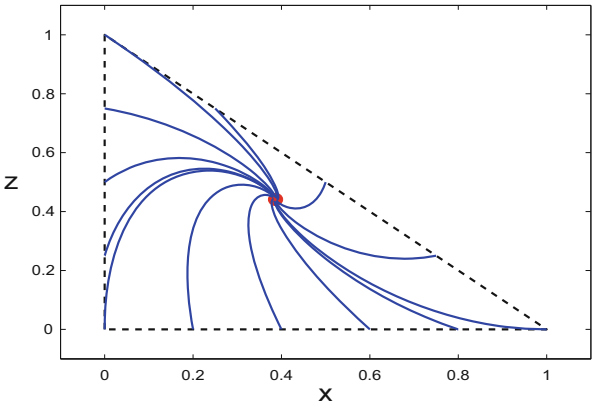

Fig. 2.12 Positive invariance of the unit simplex Σ under the flow for the proportions.

As in the other models, for the average total number of cancer cells $C(t) = N_1(t) + N_2(t) + N_3(t)$ we have that

$$\dot{C}(t) = a_3 N_3(t) = a_3 z(t) C(t) \approx a_3 z_* C(t)$$

so that cancer growth is approximately exponential with rate $a_3 z_*$. Thus we obtain the same relation between the inverse transit time a_3 through the G_2/N compartment and the average fraction z_* of cancer cells in this compartment as before, and, more generally, from the dynamics we have the following relations between the parameters.

Proposition 2.2.5. *If T denotes the tumor doubling time and x_*, y_* and z_* are the steady-state proportions of cells in the cell cycle compartments G_0/G_1, S and G_2/M, respectively, then we have that*

$$a_1 = (1 + y_* + z_*)\frac{\ln 2}{x_* T}, \qquad a_2 = (1 + z_*)\frac{\ln 2}{y_* T} \qquad \text{and} \qquad a_3 = \frac{\ln 2}{z_* T}.$$

We consider the problem to administer a cytotoxic and a cytostatic agent with the objective taken in the same form as before,

$$J = rN(T) + \int_0^T qN(t) + s_1 u(t) + s_2 v(t) dt \to \min,$$

where $r = (r_1, r_2, r_3) \in \left(\mathbb{R}^3\right)^*$ and $q = (q_1, q_2, q_3) \in \left(\mathbb{R}^3\right)^*$ are row vectors of positive coefficients and the weights s_1 and s_2 at the drugs are positive numbers. We thus have the following optimal control problem:

[CC3b] For a fixed therapy horizon $[0, T]$, minimize the objective

$$J = rN(T) + \int_0^T qN(t) + s_1 u(t) + s_2 v(t) dt \to \min$$

over all Lebesgue-measurable (respectively, piecewise continuous) functions $(u,v):[0,T]\to[0,u_{\max}]\times[0,v_{\max}]$, subject to the dynamics

$$\dot{N}(t)=\begin{pmatrix}-a_1 & 0 & 2(1-u)a_3\\ a_1 & -(1-v)a_2 & 0\\ 0 & (1-v)a_2 & -a_3\end{pmatrix}N(t),\qquad N(0)=N_0.$$

For the reader's convenience, we again write out the fundamental necessary conditions for optimality for this system. The adjoint equation is formally unchanged,

$$\dot{\lambda}=-\lambda\,(A+uB_1+wB_2)-q,\qquad \lambda(T)=r,$$

but now, in terms of its components, reads

$$\begin{aligned}\dot{\lambda}_1&=a_1(\lambda_1-\lambda_2)-q_1, & \lambda_1(T)&=r_1,\\ \dot{\lambda}_2&=(1-v)a_2(\lambda_2-\lambda_3)-q_2, & \lambda_2(T)&=r_2,\\ \dot{\lambda}_3&=a_3(\lambda_3-2(1-u)\lambda_1)-q_3, & \lambda_3(T)&=r_3,\end{aligned}$$

and the switching functions for the controls u and v are given by

$$\Phi_1(t)=s_1+\lambda(t)B_1N(t)=s_1-2a_3\lambda_1(t)N_3(t)$$

and

$$\Phi_2(t)=s_2+\lambda(t)B_2N(t)=s_2+a_2\{\lambda_2(t)-\lambda_3(t)\}N_2(t),$$

respectively. We again analyze the optimality properties of singular controls, but start with the cytostatic agent whose analysis is simpler.

Theorem 2.2.7. *If (N_*,u_*,v_*) is an optimal controlled trajectory for problem [CC3b], then there does not exist an interval on which the control v_* is singular.*

Proof. Suppose v is singular on an open interval I, i.e., $\Phi_2(t)\equiv 0$ on I. By Proposition 2.2.3, the derivative of the switching function Φ_2 is given by

$$\dot{\Phi}_2(t)=\{\lambda(t)\,[A+u_*(t)B_1,B_2]-qB_2\}N_*(t)\equiv 0. \tag{2.81}$$

A direct computation verifies that

$$[B_1,B_2]=2a_2a_3\begin{pmatrix}0&-1&0\\0&0&0\\0&0&0\end{pmatrix}$$

and thus equation (2.81) depends on the second control u_*. As for model [CC3r], we have no a priori information about u_* and thus need to consider cases. But the structure of this matrix allows us to exclude that both controls are singular simultaneously. For, if u_* also is singular on an open subinterval $J\subset I$, then it again is a necessary condition for optimality, the Goh-condition (see Theorem A.3.3 in Appendix A), that

$$\frac{\partial}{\partial u}\frac{d}{dt}\frac{\partial H}{\partial v}(\lambda(t),N_*(t),u_*(t),v_*(t)) = \lambda(t)[B_1,B_2]N_*(t) \equiv 0 \qquad \text{for all } t \in J.$$

Here this condition is violated:

$$\lambda(t)[B_1,B_2]N_*(t) = -2a_2a_3\lambda_1(t)N_2(t) < 0.$$

Thus the control u_* must be constant over some subinterval $J \subset I$ given by either 0 or $u_{\max}$. Differentiating (2.81) once more on J, the Legendre-Clebsch condition for the control v takes the form

$$\frac{\partial}{\partial v}\frac{d^2}{dt^2}\frac{\partial H}{\partial v}(\lambda(t),N_*(t),u_*,v_*(t)) = \left\{\lambda(t)[B_2,[A+u_*B_1,B_2]] - qB_2^2\right\}N_*(t). \tag{2.82}$$

These commutators are given by

$$\begin{aligned}[A+u_*B_1,B_2] &= B_2(A+u_*B_1) - (A+u_*B_1)B_2 \\ &= a_2\begin{pmatrix} 0 & 2(1-u_*)a_3 & 0 \\ a_1 & 0 & 0 \\ -a_1 & -a_3 & 0 \end{pmatrix}\end{aligned}$$

and

$$\begin{aligned}[B_2,[A+u_*B_1,B_2]] &= [A+u_*B_1,B_2]B_2 - B_2[A+u_*B_1,B_2] \\ &= a_2^2\begin{pmatrix} 0 & 2(1-u_*)a_3 & 0 \\ -a_1 & 0 & 0 \\ a_1 & -a_3 & 0 \end{pmatrix}.\end{aligned}$$

In particular, this implies that

$$[B_2,[A+u_*B_1,B_2]] = a_2[A+u_*B_1,B_2] - 2a_1a_2^2\begin{pmatrix} 0 & 0 & 0 \\ 1 & 0 & 0 \\ -1 & 0 & 0 \end{pmatrix}. \tag{2.83}$$

Furthermore, $B_2^2 = a_2B_2$, and since the derivative (2.81) of the switching function Φ_2 vanishes identically, we have that

$$\lambda(t)[A+u_*B_1,B_2]N_*(t) \equiv qB_2N_*(t).$$

Hence

$$a_2\lambda(t)[A+u_*B_1,B_2]N_*(t) = qB_2^2N_*(t)$$

and thus, altogether, we obtain

$$\frac{\partial}{\partial v}\frac{d^2}{dt^2}\frac{\partial H}{\partial v}(\lambda(t),N_*(t),u_*,v_*(t)) = \lambda(t)[B_2,[A+u_*B_1,B_2]]N_*(t) - qB_2^2N_*(t)$$
$$= -2a_1a_2^2\lambda(t)\begin{pmatrix} 0 & 0 & 0 \\ 1 & 0 & 0 \\ -1 & 0 & 0 \end{pmatrix} N_*(t)$$
$$= -2a_1a_2^2\{\lambda_2(t)-\lambda_3(t)\}N_1(t).$$

But $\Phi_2(t) = s_2 + a_2\{\lambda_2(t)-\lambda_3(t)\}N_2(t) \equiv 0$ gives that

$$\lambda_2(t)-\lambda_3(t) = -\frac{s_2}{a_2N_2(t)}$$

and thus

$$\frac{\partial}{\partial v}\frac{d^2}{dt^2}\frac{\partial H}{\partial v}(\lambda(t),N_*(t),u_*,v_*(t)) = 2s_2a_1a_2\frac{N_1(t)}{N_2(t)} > 0.$$

Hence singular controls violate the Legendre-Clebsch condition and are not optimal. □

For this model we can no longer assert in general that the cytotoxic agent u cannot be singular, but need to impose an inequality relation on the inverse transit times in the cell cycle and the maximum reduction $v_{\max}$ that the cytostatic agent can achieve.

Theorem 2.2.8. *Suppose that*

$$a_1 + a_2(1-v_{\max}) - 2a_3 \geq 0. \tag{2.84}$$

If (N_*,u_*,v_*) is an optimal controlled trajectory for problem [CC3b], there also does not exist an interval on which the control u_* is singular.

The proof of this result is a more technical calculation than the ones done so far since the singular control cannot be determined from the second derivative of the switching function. In the terminology from Definition A.3.5 in Appendix A, the order of the singular control u is at least 2. This is a somewhat degenerate situation and we relegate this computation to Section B.2 in Appendix B.

We close with some numerical examples of locally optimal controls for problem [CC3b]. The parameter values are given in Table 2.5 and condition (2.84) is satisfied. Figure 2.13 shows two different scenarios. In the graphs on the left, the weights at the cancer cells are all taken to be equal, $r = (1,1,1)$ and $q = (1,1,1)$, and in this case the optimal control u starts with a segment along which we have $u \equiv u_{\max}$. It would make no sense to block the flow of cells while a cytotoxic agent is active and accordingly the cytostatic agent is inactive at the beginning. It only becomes activated between the switching times $t_1 = 10.115$ and $t_3 = 19.835$; the cytotoxic agent is stopped at time $t_2 = 11.054$. It is thus only turned on shortly before the killing agent is withdrawn which corresponds to the timing effects in the cell cycle. After the cytotoxic agent is withdrawn, then the cytostatic agents is activated for most of the time and this simply is an alternative mechanism to slow down the growth of the tumor. If one views the whole therapy interval as one coherent unit

Table 2.5 Numerical values for the coefficients and parameters used in computations for the optimal control problem [CC3b] with cytostatic and cytotoxic agents.

Coefficient	Interpretation	Numerical value	Reference
a_1	Inverse transit time through G_1/G_0	0.197	[313]
a_2	Inverse transit time through S	0.395	[313]
a_3	Inverse transit time through G_2/M	0.107	[313]
x_* $N_0(0)$	Steady-state proportion in G_1/G_0 Initial condition for N_0	0.3866 0.3866	Eq. (2.78)
y_* $N_1(0)$	Steady-state proportion in S Initial condition for N_2	0.1722 0.1722	Eq. (2.79)
z_* $N_2(0)$	Steady-state proportion in G_2/M Initial condition for N_2	0.4412 0.4412	Eq. (2.80)
$u_{\max}$ $v_{\max}$	Maximum dosage/concentration/ effectiveness of cytotoxic agent Maximum blocking effect of cytostatic agent	0.95 0.30	
s_1	Penalty/weight at the cytotoxic agent	1	
s_2	Penalty/weight at the cytostatic agent	0.01	
q_1	Penalty/weight in the objective for the average number of cancer cells in G_1/G_0 during therapy	1, resp. 0.1	
q_2	Penalty/weight in the objective for the average number of cancer cells in S during therapy	1, resp. 0.1	
q_3	Penalty/weight in the objective for the average number of cancer cells in G_2/M during therapy	1, resp. 0.1	
r_1	Penalty/weight in the objective for the average number of cancer cells in G_1/G_0 at the end of therapy	1, resp. 8.25	
r_2	Penalty/weight in the objective for the average number of cancer cells in S at the end of therapy	1, resp. 8.25	
r_3	Penalty/weight in the objective for the average number of cancer cells in G_2/M at the end of therapy	1, resp. 8.25	
T	Therapy horizon	21	Illustration only

and only looks at the total number of cancer cells, $C(t) = N_1(t) + N_2(t) + N_3(t)$, then C decreases from $C(0) = 1$ to $C(21) = 0.868$. In the second example, the weights are skewed to make it more important to minimize the value of the cancer cells at the final time, $r = (8.25, 8.25, 8.25)$, but we relaxed the weight on the intermediate size of the tumor, $q = (0.1, 0.1, 0.1)$. This leads to a shift of the interval where the cytotoxic agent is active toward the end and accordingly then the cytostatic agent is active at the beginning. In fact, and according with the dynamics of the cell cycle, it is withdrawn shortly before the cytotoxic agent becomes active. Nevertheless, for these weights we only see a reduction of the total tumor numbers from $C(0) = 1$ to

$C(21) = 0.978$, basically just a maintenance of the current tumor volume. Clearly, these numbers can be reduced by making chemotherapy less toxic, i.e., by using a lower value for s_1, and the numbers used here only serve to illustrate the general mechanisms Table 2.6 still gives the values of the transversality conditions at the switching times verifying the local optimality of the numerically computed solution.

Table 2.6 Numerical values of the transversality conditions at the bang-bang junctions for the extremals in Figure 2.13.

Weights r and q	Control that switches	Switching time	Transversality condition (2.60)
$r = (1,1,1,)$	v	10.115	0.0097
$q = (1,1,1,)$	u	11.054	0.1765
	v	19.835	0.0332
$r = (8.25, 8.25, 8.25)$	v	10.835	0.1339
$q = (1,1,1,)$	u	11.835	0.0839

2.2.4 Concluding Remarks

The main implicit assumption underlying all these models is that *the tumor consists of a homogeneous collection of drug sensitive cells*. Under this condition our results point to optimal treatment protocols that are bang-bang controls with a small number of switchings. In fact, the cytotoxic agent is always given in one full dose session upfront, i.e., the results agree with the common paradigm of full dose chemotherapy sessions with rest periods. These theoretical results do not dependent of specific parameter values and the numerical illustrations that were given are only meant to illustrate general principles. As always, applications of mathematical models to a practical situation is contingent upon the ability to estimate the respective parameters. These will vary on a case-by-case basis, but in principle, having a small number of parameters is a plus and, as the results about the steady-state proportions of the uncontrolled dynamics show, the parameters that are needed to set up these models are well within the realm of practical medical possibilities.

2.3 Pharmacokinetics and Pharmacodynamics

In view of the tremendous complexity of the medical problem that is cancer treatment, it is a reasonable strategy to start with the analysis of simplified models and then add increasingly more complex and medically more realistic features into the model and to analyze to what extent these structures change the solutions. A commonly used simplification that we also have made so far is to identify the drug dose rates with the drug concentrations and even more, with the effects that these concentrations have. In reality, these clearly are different phenomena and their relations are

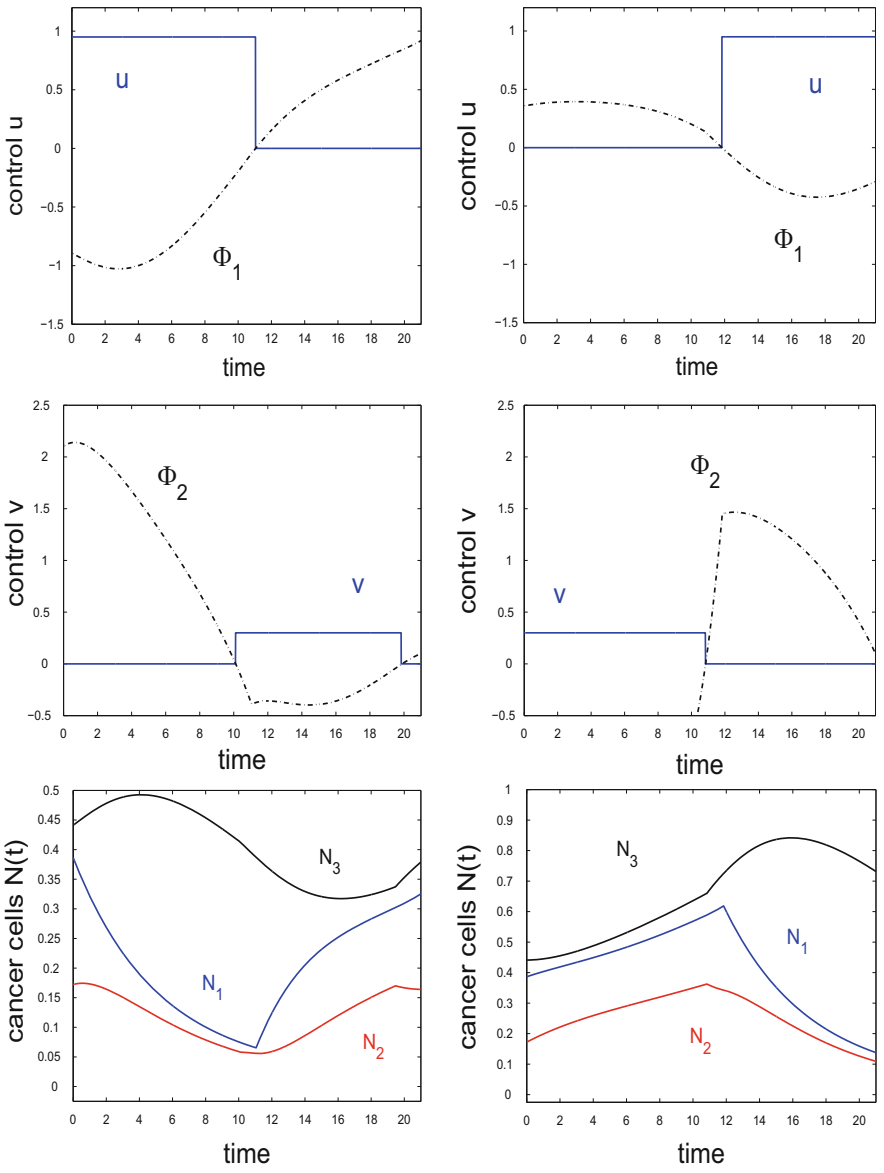

Fig. 2.13 Examples of locally optimal controls u (cytotoxic agent) (top), v (cytostatic agent) (middle) and their corresponding trajectories (bottom) for different weights $r = (1,1,1)$ and $q = (1,1,1)$ on the left and $r = (8.25, 8.25, 8.25)$ and $q = (0.1, 0.1, 0.1)$ on the right. The initial condition is the steady-state solution (see Theorem 2.2.6) with total tumor size normalized to 1. The parameter values are given in Table 2.5.

studied under the names of *pharmacokinetics (PK)* and *pharmacodynamics (PD)*. In the formulations considered so far, the controls represented the drugs' concentrations in the blood stream and only in our language we have identified the drugs' dose rates with their concentrations; the effects were modeled making the linear log-kill hypothesis. In this section, we make these compartmental models more realistic by augmenting them with pharmacokinetic equations. The main question is whether, and if so, to what extent, this more accurate modeling changes the previous analysis about optimal protocols. Indeed, as we shall show, the addition of a standard linear pharmacokinetic model for the drugs' concentrations does not alter the structure of optimal solutions. Singular controls, which are not optimal in the simplified models without a linear pharmacokinetic model, still remain nonoptimal after adding these equations, and, in fact, this is a general feature of the mathematical structure of PK, not just for these compartmental bilinear models. Thus, for the models considered here *optimal controls remain bang-bang and indeed there are only minute quantitative changes in the switching times* that depend on the specific pharmacokinetic parameters. Clearly, the relations between drug dose rates and drug concentrations need to be taken into account in the scheduling of the drugs, but they are rather unrelated to the question about the structures of optimal protocols. These can be determined solely based upon the concentrations of the drugs. This therefore justifies and enables a modular approach to the optimal treatment problems with respect to pharmacokinetics. Mathematically, the reason for this lies in the fact that standard pharmacokinetic models are described by linear differential equations. On the level of pharmacodynamics, the same holds for linear models (e.g., the log-kill hypothesis), but as nonlinearities come into play, qualitative changes arise.

In this section, we briefly describe the basics of commonly used mathematical models for PK and PD in the context of continuous infusions and then analyze the compartmental model [CC] when it is augmented with pharmacokinetic and pharmacodynamic equations.

2.3.1 Mathematical Models for PK and PD

Pharmacokinetic equations model the time evolution of a drug's concentration in the blood plasma, i.e., "what the body does to the drug." If a drug is given at a time-varying dose rate $u = u(t)$, let $c = c(t)$ be its concentration in the plasma that builds up in response. The standard model that describes this concentration c is one of exponential growth and decay,

$$\dot{c} = -\gamma c + u, \qquad c(0) = 0,$$

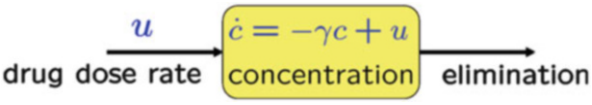

Fig. 2.14 Schematic representation of a 1-compartment pharmacokinetic model.

with γ the so-called *clearance rate* of the drug, a constant. If the drug dose rate is bounded by $u_{\max}$, then the maximum achievable drug concentration $c_{\max}$ in a continuous infusion is given by

$$c_{\max} = \frac{u_{\max}}{\gamma}$$

and generally this saturation level is reached rather quickly, of course, depending on the numerical value of γ. Once no more drugs are administered, $u \equiv 0$, this concentration dissipates at an exponential rate determined by the body's abilities to clear the drug. Clearance quantifies elimination of the drug from the body and is defined as the volume of plasma cleared of the drug per unit time. It usually is expressed in terms of units such as liters per hour or milliliters per minute. The clearance rate γ and the half-life T of the drug, the time it takes for the concentration to fall to half of its previous value, are related by the usual formula, $\gamma T = \ln 2$. These are the simplest, 1-compartment PK models in which the drug dose u is related to the drug's concentration and its elimination is in one part of the body, e.g., the blood plasma or at an absorption side (see Figure 2.14).

More generally, in 2-compartmental models for PK, the drug's concentration and its elimination are considered at a central and a peripheral compartment with their interactions (see Figure 2.15). In such a case, the drug concentrations are modeled by a 2-dimensional vector $c(t) = (c_1(t), c_2(t))^T$ with the components describing the concentrations in the central ($i = 1$) and peripheral compartments ($i = 2$). The model still is one of exponential growth and decay described by a linear system $\dot{c}(t) = Ac(t) + bu(t)$ of the form

$$\dot{c}(t) = \begin{pmatrix} -\gamma - \alpha & \beta \\ \alpha & -\beta \end{pmatrix} c + \begin{pmatrix} b_1 \\ b_2 \end{pmatrix} u(t)$$

where γ again denotes the clearance rate, α and β are positive rates that describe the interactions between the central and peripheral compartments and the coefficients b_i ($b_i \geq 0$, $b_1 + b_2 = 1$) describe the relative influx of the drug into the compartments. Note that the eigenvalues of the matrix A are the roots of the equation

$$t^2 + (\alpha + \beta + \gamma)t + \beta\gamma = 0$$

and thus are given by

$$\frac{1}{2}\left(-(\alpha + \beta + \gamma) \pm \sqrt{(\alpha + \beta + \gamma)^2 - 4\beta\gamma}\right).$$

In particular, both are negative reals and the general solution thus has the form

$$c_1(t) = ae^{-\lambda_1 t} + be^{-\lambda_2 t}$$

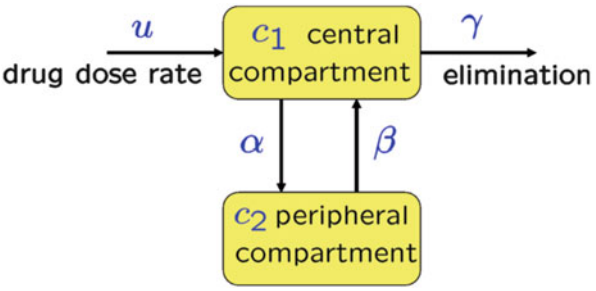

Fig. 2.15 Schematic representation of a 2-compartment pharmacokinetic model.

with $0 < \lambda_1 < \lambda_2$ the negatives of the eigenvalues. Figure 2.16 illustrates the typical two phase behavior shown on a logarithmic scale. The initial phase is called the distribution phase while the second phase, which essentially is only determined by the smaller eigenvalue (in absolute value) is called the elimination phase. Another typical modeling here is when a first compartment describes the concentration in the plasma and the second compartment describes the concentration in the tissue. Depending on the specific situation, the vector b often is given by $b = (1,0)^T$ or $b = (0,1)^T$.

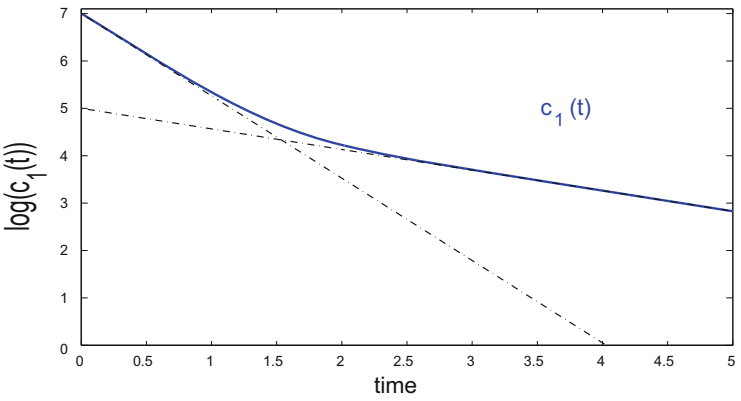

Fig. 2.16 The typical behavior of the concentration in the central compartment for a 2-compartment pharmacokinetic model on a logarithmic scale.

Higher dimensional compartmental models are used less often, but arise, for example, if the peripheral compartment is divided further into a 'shallow' and 'deep' compartment. For example, a 3-compartmental model is commonly used to describe the clearance of insulin in diabetes, but generally one and two compartmental models are the norm for PK of cancer drugs.

Pharmacodynamic models describe the effects that the drug concentrations have on the tumor cells, i.e., "what the drug does to the body." Generally, these effects

can be described in the form $s(c)N$ where s is a function of the concentration c. The linear log-kill hypothesis is the most commonly used model and in this case the function s simply is linear, $s(c) = \sigma c$ with σ a constant that represents the effectiveness of the drug. This model, which was used in the compartmental problems [CC] above, is generally applicable over a reasonably wide range of concentrations, but often is not a valid model for low or high concentrations. In fact, generally drugs show very little and, in fact, often no effect if the concentrations are too low and their effectiveness saturates at high concentrations. For example, paclitaxel is one of the most cytotoxic drugs at high concentrations, but shows no killing effects at low concentrations when indeed its effects can be classified as cytostatic. Thus, generally, the effect of a single chemotherapeutic agent can be modeled by a function s defined on the interval $[0,\infty)$ with values in some interval $[0,E_{\max}]$,

$$\sigma : [0,\infty) \to [0,E_{\max}], \qquad c \mapsto \sigma(c),$$

with $E_{\max}$ denoting the maximum effect. Commonly used forms are the $E_{\max}$ model that more accurately describes the intensity of the effect for high concentrations and sigmoidal functions that capture the behavior at both lower and higher concentrations. The $E_{\max}$ model is described by a standard *Michaelis-Menten* type equation of the form

$$\sigma(c) = \frac{E_{\max} c}{EC_{50} + c} \tag{2.85}$$

and an example of sigmoidal models that are used in pharmacology is of the form

$$\sigma(c) = \frac{E_{\max} c^n}{(EC_{50})^n + c^n} \tag{2.86}$$

with $n > 1$ a positive integer. In these equations, $E_{\max}$ denotes the maximum effect that is achievable and EC_{50} denotes the concentration at which half of this maximum effect is realized. These are commonly used parameters in pharmacology. The $E_{\max}$ model is reasonable for fast acting drugs that quickly reach their saturation levels while the sigmoidal models more accurately approximate the effectiveness at both lower and higher concentrations. Figure 2.17 shows the qualitative behavior of these two models.

Considering the graph of the sigmoidal function s for PD, it is clear that a linear model well represents the important middle segment of the model. For low concentrations, the drug effect simply is negligible and at high concentrations, when the effect has saturated, we can simply assume the concentration is constant. In either of these ranges, it is not necessary to include a detailed pharmacodynamic equation in the model. Similarly, the same effect arises under the $E_{\max}$ model once the concentration saturates. Thus, while these models are more realistic overall, in the most relevant segments of the curves, a linear approximation is valid and for this reason, the linear log-kill hypothesis stands as the most important of these pharmacodynamic models. In the next section, we briefly explore the changes that arise for a general model. We assume that the function s that defines the pharmacodynamic model satisfies the following monotonicity condition:

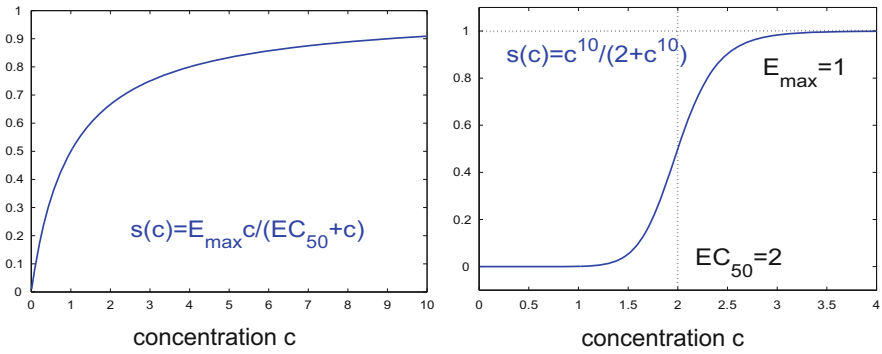

Fig. 2.17 $E_{\max}$ and sigmoidal pharmacodynamic models for the intensity of the effect as a function of the drug concentration.

(PD) the function $\sigma : [0, c_{\max}) \to [0, E_{\max})$, $c \mapsto \sigma(c)$, satisfies $\sigma(0) = 0$, is *strictly increasing* and *twice continuously differentiable*.

Here $c_{\max}$ and $E_{\max}$ are limits for the maximum concentrations and their effects that, in principle, are allowed to be infinity, but generally are finite numbers. In the next section we analyze the changes that may (or, more importantly, may not) arise when the compartmental model [CC] is augmented with these pharmacokinetic and pharmacodynamic models. For simplicity of presentation, we restrict the analysis to a 1-compartment pharmacokinetic model, but analogous results hold for multi-compartmental PK models (e.g., see [215]).

2.3.2 The Effect of PK and PD on the Structure of Optimal Controls

We consider a multi-drug treatment protocols, but assume that the drugs have different mechanisms of actions. For cytotoxic drugs that have similar mechanisms synergistic or antagonistic properties come into play and their combined effectiveness does not just depend on their combined concentrations. Assessing these interactions is a generally difficult and drug specific question that even for the more common drugs is not always fully understood. Therefore, in mathematical models, similarly acting drugs are bundled together and represented by one control. Thus, in the model below it is assumed that the *controls correspond to qualitatively different drugs which act in different compartments in the model* (e.g., a G_2/M-specific cytotoxic agent and a cytostatic agent active in the synthesis phase S). Then the overall dynamics can be described as

$$\dot{N} = \left(A + \sum_{j=1}^{m} \sigma_j(c_j) B_j \right) N, \qquad N(0) = N_0,$$
$$\dot{c}_j = -\gamma_j c_j + u_j, \qquad c_j(0) = 0.$$

In the objective, there are two options to gauge the cost or side effects of the treatment. Recall that, within the compartmental models, side effects of treatment are measured by ineffective cell divisions and these are determined by the pharmacodynamic model of the drugs. Thus this leads to the minimization of an objective of the form

$$J = rN(T) + \int_0^T \left(qN(t) + \sum_{j=1}^{m} s_j(c_j(t)) \right) dt \to \min$$

where, as before $r = (r_1, \ldots, r_n)$ and $q = (q_1, \ldots, q_n)$ are row-vectors of positive numbers and $s = (s_1, \ldots, s_m)$ is a row vector of nonnegative functions of the concentrations that represent the side effects of treatment. If we make the log-kill hypothesis, then these are proportional to the concentrations of the drugs and these functions are simply given by $s_j(c_j) = s_j c_j$ for some constants s_j as before. In this case, comparing this objective with the original one considered for problem [CC], it should be clear that if we disconnect the concentrations c_j from the drug dose rates u_j and simply optimize over the concentrations, this reduces to the original problem. Thus this problem has already been solved, at least under the log-kill hypothesis. The question then simply becomes how the concentrations c_* computed as optimal in the original model can be realized within the pharmacokinetic model. But this is a standard and not very difficult issue in pharmacology not related to the issue of optimizing treatment schedules. For example, for a continuous time infusion, it is simply possible to adjust the dose rate to $u_j^* \equiv \frac{c_*}{\gamma_j}$ to maintain a constant concentration c_* once it has been reached. Figure 2.18 shows how more traditionally such a constant concentration c_* is approximated in pharmacological procedures based on the 1-dimensional pharmacokinetic model by repeated oral or intravenous bolus injections at specifically computed frequencies and doses. But within the task of minimizing J, the optimal schedules can essentially be determined based on the concentrations. Clearly, we can investigate the problem as posed here, and this leads to slightly different models as considered before if different pharmacodynamic models are utilized, but the solutions are not affected by the pharmacokinetic models.

An alternative objective is to consider

$$\hat{J} = rN(T) + \int_0^T qN(s) + su(t)dt \to \min \tag{2.87}$$

where the drug dose rates are used as penalty term to measure both the side effects and other tangible costs associated with treatment. While this may appear to be somewhat inconsistent in view of measuring side effects by ineffective cell divisions, there are other reasons why this might be the preferred objective to use. If we only include the concentrations in the penalty term, but do not penalize the dose

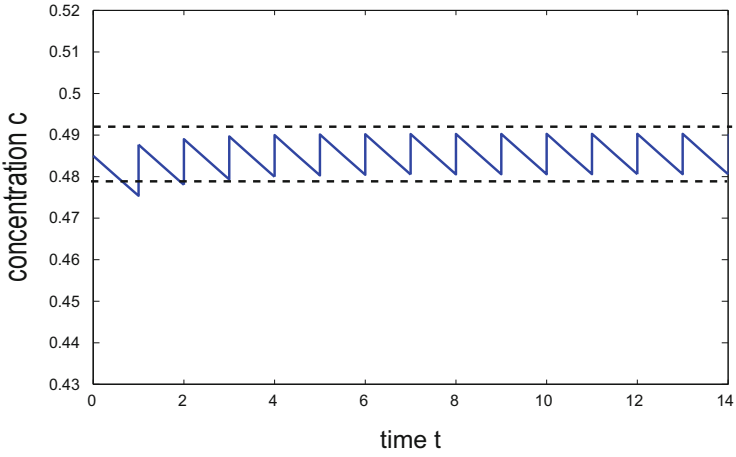

Fig. 2.18 Approximation of a desired drug concentration through bolus injections

rates, then in view of the saturation of the concentrations, there is no mechanism that would prevent the dose rates to go as high as possible if this would still have even a tiny beneficial effect. Such a behavior is not realistic. Clearly, side effects of drugs are manifold and administering too high a dose is undesired practically simply since it is not clear what kind of unforeseen side effects could arise, not to mention the fact that this term is directly related to the cost of the medication. Drastically put, if it is possible to kill one more cancer cell for \$1000, then the optimal control will do so if we minimize the number of cancer cells and cost is not included in the objective. It thus seems imperative, and a far better model, to include the total doses of the drugs given, $\int_0^T u_j(t)dt$, as penalty. Intuitively, the total dose $\int_0^T u_j(t)dt$ and the "area under the curve" (AUC) of the concentrations, $\int_0^T c_j(t)dt$, which so often is used as a measure for the effectiveness of treatment in pharmacological studies, are related by the linear pharmacokinetic model (e.g., if the dose rate is constant, then one is a multiple of the other with the constant only depending on the therapy horizon T and the clearance rate γ) and therefore often one is taken as a surrogate for the other. But overall, *the total dosages* given, $\int_0^T u_j(t)dt$, *seem to be a more adequate measure for the total adverse effects of chemotherapy treatment* if also cost is considered. We therefore take this as our objective and consider the following optimal control problem:

[CCwPK&PD] for a fixed therapy horizon $[0,T]$, minimize the objective (2.87) over all Lebesgue-measurable (respectively, piecewise continuous) functions $u : [0,T] \to U = [0,u_1^{\max}] \times \cdots \times [0,u_m^{\max}]$, subject to the dynamics

$$\dot{N} = \left(A + \sum_{j=1}^{m} \sigma_j(c_j)B_j\right)N, \qquad N(0) = N_0, \tag{2.88}$$

$$\dot{c}_j = -\gamma_j c_j + u_j, \qquad c_j(0) = 0. \tag{2.89}$$

Given the differential equations (2.89), the concentrations c_j always lie in the intervals $[0, c_j^{\max})$ where $c_j^{\max} = \frac{u_j^{\max}}{\gamma_j}$ and the functions σ_j take values in corresponding intervals $[0, E_j^{\max})$. It follows from Proposition 2.2.1 in Section 2.2.1 that the dynamics for the states N is positive invariant if all the matrices $A + \sum_{j=1}^m \sigma_j B_j$, $\sigma_j \in [0, E_j^{\max})$, have negative diagonal and nonnegative off-diagonal entries. We make this assumption:

(M-PK) all the matrices $A + \sum_{j=1}^m \sigma_j B_j$, $\sigma_j \in [0, E_j^{\max})$, have negative diagonal and nonnegative off-diagonal entries.

First-order necessary conditions for optimality are once more given by the Pontryagin maximum principle (Theorem A.2.1 in Appendix A). *We are interested in comparing the structure of optimal solutions to this problem with those of the simplified model [CC]* from Section 2.2.1. In order to distinguish the multipliers and Hamiltonian functions for this problem from those of the original model, we retain the notation λ for the multiplier and H for the Hamiltonian of the original problem [CC] and denote the multipliers and Hamiltonian for the new problem by a hat, $\hat{\ }$. As for problem [CC], it is easily seen that extremals are normal and thus the Hamiltonian for problem [CCwPK&PD] can be defined as

$$\hat{H}(\hat{\lambda}, \hat{\mu}, N, c, u) = qN + \sum_{j=1}^m s_j u_j + \hat{\lambda}\left(A + \sum_{j=1}^m \sigma_j(c_j) B_j\right) N + \sum_{j=1}^m \hat{\mu}_j(-\gamma_j c_j + u_j). \tag{2.90}$$

The necessary conditions for optimality then reduce to the following statement:

Theorem 2.3.1. *If u_* is an optimal control with corresponding trajectory (N_*, c_*), then there exist absolutely continuous functions $\hat{\lambda}$ and $\hat{\mu}$ which we write as row-vectors, $\hat{\lambda} : [0,T] \to (\mathbb{R}^n)^*$, $\hat{\mu} : [0,T] \to (\mathbb{R}^m)^*$, satisfying the adjoint equations with transversality condition,*

$$\dot{\hat{\lambda}}(t) = -\frac{\partial \hat{H}}{\partial N} = -\hat{\lambda}(t)\left(A + \sum_{j=1}^m \sigma_j(c_j^*(t)) B_j\right) - q, \qquad \hat{\lambda}(T) = r, \tag{2.91}$$

$$\dot{\hat{\mu}}_j(t) = -\frac{\partial \hat{H}}{\partial c_j} = \hat{\mu}_j(t)\gamma_j - \sigma_j'(c_j^*(t))\hat{\lambda}(t) B_j N_*(t), \qquad \hat{\mu}_j(T) = 0, \tag{2.92}$$

such the optimal control u_* minimizes the Hamiltonian $\hat{H}$ over the control set $U = [0, u_1^{\max}] \times \cdots \times [0, u_m^{\max}]$ along $(\hat{\lambda}(t), \hat{\mu}(t), N_*(t), c_*(t))$ and the Hamiltonian $\hat{H}$ is constant,

$$\hat{H}(\hat{\lambda}(t), \hat{\mu}(t), N_*(t), c_*(t), u_*(t)) = \max_{u \in U} \hat{H}(\hat{\lambda}(t), \hat{\mu}(t), N_*(t), c_*(t), u) = \text{const.}$$

The Hamiltonian $\hat{H}$ still is affine in the controls, $\hat{H} = \hat{\Phi}_0 + \sum_{j=1}^m u_j \hat{\Phi}_j$, with the switching functions $\hat{\Phi}_j$ given by

$$\hat{\Phi}_j(t) = s_j + \hat{\mu}_j(t) \qquad \text{for } j = 1, \ldots, m,$$

and we also set

$$\hat{\Phi}_0(t) = qN_*(t) + \hat{\lambda}(t)\left(A + \sum_{j=1}^{m} \sigma_j(c_j^*(t))B_j\right)N_*(t) - \sum_{j=1}^{m} \hat{\mu}_j(t)\gamma_j c_j^*(t).$$

As before, the control set is an m-dimensional interval $U = [0, u_1^{\max}] \times \cdots \times [0, u_m^{\max}]$, the minimization condition is equivalent to m scalar minimization problems for each control u_j and we have that

$$u_j^*(t) = \begin{cases} 0 & \text{if } \hat{\Phi}_j(t) > 0, \\ u_j^{\max} & \text{if } \hat{\Phi}_j(t) < 0. \end{cases}$$

Note that $\hat{\Phi}_j(T) = s_j > 0$ for all j and thus optimal controls will always end with an interval where $u_j(t) \equiv 0$. Intuitively this is clear since the addition of a pharmacokinetic model generates a delay in the effectiveness of the control and thus, since side effects are still measured instantaneously in the model in terms of penalizing the drug dose rates, it is not optimal to give drugs until the very end of therapy.

As for the original problem [CC], all states and multipliers $\hat{\lambda}$ are positive, but the signs of the multipliers $\hat{\mu}$ can vary. However, we still have the following simple partial result that applies to cytotoxic agents.

Proposition 2.3.1. *Under assumptions (M-PK), all states N_i and costates $\hat{\lambda}_i$, $i = 1, \ldots, n$, are positive over the interval $[0, T]$. If all entries of the matrix B_j are nonpositive, then the multiplier $\hat{\mu}_j$ is negative on $[0, T)$.*

Proof. For the states N_i and costates $\hat{\lambda}_i$, $i = 1, \ldots, n$, this directly follows from Propositions 2.2.1 and 2.2.2. Assumption (M-PK) ensures that these propositions apply. If all entries of the matrix B_j are nonpositive, then, since $B_j \neq 0$, at least one entry must be negative and thus $\hat{\lambda}(t)B_jN(t) < 0$ for all $t \in [0, T]$. If τ is a zero of $\hat{\mu}_j$, then by the adjoint equation

$$\frac{d}{dt}\hat{\mu}_j(\tau) = -\sigma_j'(c_j(\tau))\hat{\lambda}(\tau)B_jN(\tau).$$

But σ_j is strictly increasing and thus we have that $\dot{\hat{\mu}}_j(\tau) > 0$ whenever $\hat{\mu}_j(\tau) = 0$. Hence the multiplier $\hat{\mu}_j$ can only change sign from negative to positive. Since $\hat{\mu}_j(T) = 0$, it follows that $\hat{\mu}_j$ is negative for $t < T$. □

We want to show that *the optimality status of singular controls is not affected by the augmentation of the model with a linear pharmacokinetic model*. For this purpose, suppose the control u_j^* is singular on a nonempty open interval I. As before, we need to analyze the switching function and its derivatives. In this case, the multiplier $\hat{\mu}_j$ is constant on I given by $\hat{\mu}_j(t) \equiv -s_j < 0$ and

$$\dot{\hat{\Phi}}_j(t) = \dot{\hat{\mu}}_j(t) = -s_j\gamma_j - \sigma_j'(c_j^*(t))\hat{\lambda}(t)B_jN_*(t) \equiv 0. \tag{2.93}$$

For example, if the entries of B_j are nonpositive, then $\hat{\lambda}(t)B_jN_*(t) < 0$ and we always have a difference of negative terms which allows for the possibility of singular arcs. We thus need to differentiate the switching functions further. The analogue of Proposition 2.2.3 now reads as follows:

Proposition 2.3.2. *For any $n \times n$ matrix M, the derivative of $\Psi(t) = \hat{\lambda}(t)MN(t)$ along solutions N of (2.88) and $\hat{\lambda}$ of (2.91) is given by*

$$\dot{\Psi}(t) = \hat{\lambda}(t)\left[A + \sum_{j=1}^{m} \sigma_j(c_j(t))B_i, M\right] N(t) - qMN(t).$$

Differentiating (2.93) once more, we find that

$$\begin{aligned}\frac{d^2}{dt^2}\hat{\Phi}_j(t) = &-\sigma_j''(c_j^*(t))\left(-\gamma_j c_j^*(t) + u_j(t)\right)\hat{\lambda}(t)B_jN_*(t)\\ &-\sigma_j'(c_j^*(t))\left\{\hat{\lambda}(t)[A + \sum_{i\neq j}\sigma_j(c_j^*(t))B_i, B_j] - qB_j\right\}N_*(t).\end{aligned}$$

In particular,

$$-\frac{\partial}{\partial u_j}\frac{d^2}{dt^2}\frac{\partial \hat{H}}{\partial u_j}(\hat{\lambda}(t), \hat{\mu}(t), N_*(t), c_*(t), u_*(t)) = \sigma_j''(c_j^*(t))\hat{\lambda}(t)B_jN_*(t)$$

and thus, whether this expression is negative, i.e., whether or not the Legendre-Clebsch condition is satisfied, depends on convexity properties of the function σ_j and the sign of the expression $\hat{\lambda}(t)B_jN_*(t)$. For example, we immediately have the following result:

Proposition 2.3.3. *If all entries of B_j are nonpositive, then a singular control u_j^* is of order 1 and satisfies the Legendre-Clebsch condition for minimality in regions where the function σ_j is strictly concave ($\sigma_j''(c_j) < 0$) and the Legendre-Clebsch condition is violated in regions where σ_j is strictly convex ($\sigma_j''(c_j) > 0$).*

The function

$$\sigma(c) = \frac{E_{\max}c}{EC_{50} + c}$$

describing the $E_{\max}$ model is strictly concave everywhere and for sigmoidal models this holds for high concentrations. Thus, for fast acting cytotoxic drugs (which are described by the $E_{\max}$ model) or, more generally, at high concentrations, optimal controls could follow singular protocols while singular controls are not optimal for regions where σ is strictly convex (or at low concentrations). This suggests a structure of optimal controls that provide a quick initial boost in terms of bang-bang controls and then regulate the concentration through slowly varying infusions. Intuitively, once the drug's concentration is built up, only the injection of smaller time-varying doses is needed to make up for the clearance of the drug (also, see Figure 2.18).

For the standard log-kill pharmacodynamic model, $\sigma(c) = \sigma_j c$, and thus

$$\frac{\partial}{\partial u_j}\frac{d^2}{dt^2}\frac{\partial \hat{H}}{\partial u_j}(\hat{\lambda}(t), \hat{\mu}(t), N_*(t), c_*(t), u_*(t)) \equiv 0$$

so that singular controls will always be of higher order. But we shall show now that the optimality status of singular controls is not effected by the addition of the pharmacokinetic model. Nevertheless, this case is more involved since interactions between drugs and their concentrations come into play. We compare the structure of optimal solutions to this problem with those of the simplified model [CC] from Section 2.2.1 and follow our original notation for that problem denoting the multiplier by λ and the Hamiltonian by H, i.e.,

$$H = qN + su + \lambda\left(A + \sum_{j=1}^{m} u_j B_j\right) N.$$

Under the log-kill hypothesis the switching function $\hat{\Phi}_j$ and its first two derivatives on the interval I are given by

$$\begin{aligned}
&\hat{\Phi}_j(t) = s_j + \hat{\mu}_j(t) \equiv 0,\\
&\dot{\hat{\Phi}}_j(t) = \dot{\hat{\mu}}_j(t) = -\gamma_j s_j - \sigma_j \hat{\lambda}(t) B_j N_*(t) \equiv 0,\\
&\ddot{\hat{\Phi}}_j(t) = -\sigma_j\left(\hat{\lambda}(t)\left[A + \sum_{i\neq j} \sigma_i c_i^*(t) B_i, B_j\right] - qB_j\right) N_*(t) \equiv 0.
\end{aligned}$$

Since the second derivative does not explicitly depend on the control u_j, the singular arc is at least of intrinsic order 2 (c.f., Definition A.3.5 in Appendix A). What simplifies the computation is the fact that this derivative also does not depend on the concentration c_j^* of the drug dose u_j^* that is singular. Differentiating once more gives

$$\begin{aligned}
\hat{\Phi}_j^{(3)}(t) = -\sigma_j \Bigg(&\hat{\lambda}(t)\left[A + \sum_{k=1}^{m} \sigma_k c_k^*(t) B_k, \left[A + \sum_{i\neq j} \sigma_i c_i^*(t) B_i, B_j\right]\right] N_*(t)\\
&- q\left[A + \sum_{i\neq j} \sigma_i c_i^*(t) B_i, B_j\right] N_*(t)\\
&+ \sum_{i\neq j} \sigma_i \{-\gamma_i c_i^*(t) + u_i^*(t)\}\, \hat{\lambda}(t)[B_i, B_j] N_*(t)\\
&- qB_j\left(A + \sum_{i=1}^{m} \sigma_i c_i(t) B_i\right) N_*(t)\Bigg).
\end{aligned} \tag{2.94}$$

In the fourth derivative, also derivatives of the other controls u_i, $i \neq j$, arise. If the control u_i is singular as well, then the Goh condition implies that $\hat{\lambda}(t)[B_i, B_j] N_*(t) \equiv$

0 and thus the term with the control u_i^* drops out while there is no issue with differentiability if the control is constant. In either case, we can treat the derivatives of these controls as zero. In order to evaluate the generalized Legendre-Clebsch condition, we then need to determine the term that multiplies the control $u_j^*(t)$ in the fourth derivative. But this control only comes up in the dynamics for the derivative of its concentration c_j^*. Other terms do not contribute to the coefficient at the control u_j^* and, overall, we therefore get the following necessary condition for optimality of the singular arc:

$$(-1)^2 \frac{\partial}{\partial u_j} \frac{d^4}{dt^4} \frac{\partial \hat{H}}{\partial u_j} (\hat{\lambda}(t), \hat{\mu}(t), N_*(t), c_*(t), u_*(t))$$
$$= \frac{\partial}{\partial u_j} \hat{\Phi}_j^{(4)}(t) = -\sigma_j^2 \left(\hat{\lambda}(t) \left[B_j, \left[A + \sum_{i \neq j} \sigma_i c_i^*(t) B_i, B_j \right] \right] - q B_j^2 \right) N_*(t) \geq 0.$$

For a single-input system, this reduces to

$$\frac{\partial}{\partial u} \hat{\Phi}^{(4)}(t) = -\sigma^2 \left\{ \hat{\lambda}(t) [B, [A, B]] - q B^2 \right\} N_*(t) \geq 0. \tag{2.95}$$

For example, for the 2-compartment model considered in Section 2.1, using (2.34) we have that

$$\frac{\partial}{\partial u} \hat{\Phi}^{(4)}(t) = 4\sigma^2 a_1 a_2 \hat{\lambda}(t) B N_*(t) = -4\sigma a_1 a_2 \gamma s < 0$$

and the generalized Legendre-Clebsch condition is violated. In fact, more generally, we have the following relation between the Hamiltonian H of original system [CC] and the Hamiltonian $\hat{H}$ of the system augmented with a linear pharmacokinetic model:

$$(-1)^2 \frac{\partial}{\partial u_j} \frac{d^4}{dt^4} \frac{\partial \hat{H}}{\partial u_j} (\hat{\lambda}(t), \hat{\mu}(t), N_*(t), c_*(t), u_*(t))$$
$$= (-1) \frac{\partial}{\partial u_j} \frac{d^2}{dt^2} \frac{\partial H}{\partial u_j} (\lambda(t), N_*(t), u_*(t)).$$

The extra minus sign is generated by the fact that the switching function for problem [CC] is given by $\Phi_j(t) = s_j + \lambda(t) B N_*(t)$ while the derivative of the switching function $\hat{\Phi}_j(t) = s_j + \hat{\mu}_j(t)$ gives us $\dot{\hat{\Phi}}_j(t) = -\gamma_j \hat{\mu}_j(t) - \sigma_j \hat{\lambda}(t) B_j N_*(t)$. This change in sign is exactly what is required in the generalized Legendre-Clebsch condition to preserve the status of optimality or nonoptimality. These computations generalize to singular controls of higher order as well and we have the following useful result that we state without proof.

Theorem 2.3.2. *If the compartmental model [CC] is augmented with a linear pharmacokinetic model for the concentrations of the drugs in the plasma and the log-kill hypothesis is made, then the optimality, respectively nonoptimality properties of*

singular controls are the same for both models, i.e., are as they are for the model without the pharmacokinetic model.

Figure 2.19 compares a locally optimal bang-bang control for the 2-compartment model [CC2] considered in Section 2.1 with the corresponding solution for the model [CCwPK&PD]. The cell cycle parameters and initial conditions for the runs are the same as given in Table 2.1, but obvious adjustments in the control data and the objective need to be made for the runs to be compatible. In the original model, we only used one parameter $u_{\max} = 0.90$ that combined all the pharmacokinetic and pharmacodynamic parameters into one quantity. In the model [CCwPK&PD], we have the effectiveness σ of the cytotoxic drug, its clearance rate γ, and $u_{\max}$ now denotes the true maximum dose rate at which the drug is being given intravenously. The value 0.90 in the model [CC2] thus represents the factor $\sigma c_{\max} = \sigma \frac{u_{\max}}{\gamma}$ in the new model and, in order to have a valid comparison, we need to choose parameters that multiply to the same value 0.90. In the example shown in Figure 2.19 we have used $\sigma = 0.30$, $\gamma = 1$ and $u_{\max} = 3$. Since the maximum dose rate has been changed, we also need to adjust the weight s at the control in the objective to have the same optimal control problem. We changed s so that the product $su_{\max}$ was equal for both formulations, i.e., we chose $s = \frac{3}{20}$. The graph (a) on the left in Figure 2.19 depicts the control u and switching function Φ for the original formulation without a pharmacokinetic model and the graph (b) on the right shows the optimal control u and the switching function $\hat{\Phi}$ for the corresponding model [CCwPK&PD] for these parameter values. As before, optimal controls still are bang-bang with one switching from $u = u_{\max}$ to $u = 0$, i.e., there are no qualitative changes in the structure of optimal controls. The switchings for problem [CCwPK&PD] occur slightly earlier which is caused by the delay effect that the addition of the pharmacokinetic models brings into the problem. These differences depend on the clearance rate γ and in Table 2.7, as an example, we give some of the quantitative changes depending on γ when we chose $\sigma = 0.30\gamma$ to maintain the overall product $\sigma c_{\max} = 0.90$. As these results show, the switching times are earlier for higher clearance rates (and higher effectiveness) and later for lower clearance rates (and lower effectiveness). But overall, the changes in the switching time are minor and this shows that, at least on the level of this model, the relevant pharmacokinetic and pharmacodynamic parameters can succinctly be summarized in the one quantity $\frac{\sigma}{\gamma} u_{\max}$. Computations for the simplified model are more than adequate to obtain results that are very close to the optimal solutions for the more general model [CCwPK&PD].

Table 2.7 Optimal switching times in the model [CCwPK&PD] depending on the clearance rate γ with $\sigma = 0.30\gamma$ and $u_{\max} = 3$.

γ	0.33	0.50	1	2	3
Switching time	31.155	30.776	30.466	30.359	30. 326

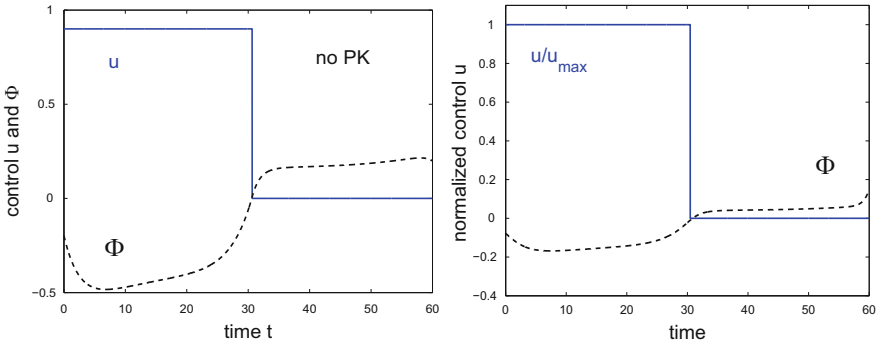

Fig. 2.19 A comparison of optimal controls for the models [CC2] and [CCwPK&PD].

Chapter 3
Cancer Chemotherapy for Heterogeneous Tumor Cell Populations and Drug Resistance

The results of the previous chapter are consistent with the classical MTD paradigm in medicine: give as much of the drug as possible immediately. This makes perfect sense in many situations: cancer is a widely symptomless disease which, once finally detected, often is in an advanced stage where immediate action is required. Then the aim simply is to be as toxic as possible to the cancerous cells. However, this presumes that cells can be killed, i.e., that the tumor population consists of chemotherapeutically sensitive cells. Malignant cancer cell populations on the other hand are often highly genetically unstable and coupled with fast proliferation rates; this leads to a great variety in the structure of the cells within one tumor—the number of genetic errors present within one cancer cell can lie in the thousands [220]. Consequently, many tumors consist of heterogeneous agglomerations of subpopulations of cells that show widely varying sensitivities toward the actions of a particular chemotherapeutic agent [104, 107]. Coupled with the fact that growing tumors also exhibit considerable evolutionary ability to enhance cell survival in an environment that is becoming hostile, this leads to multi-drug resistance of some strains of the cells. Naturally, it makes sense to combine drugs with different activation mechanisms to reach a larger population of the tumor cells—and this is what is being done—but the sad fact remains that some cells develop multi-drug resistance to a wide variety of even structurally unrelated drugs. There may even exist subpopulations of cells that are not sensitive to the treatment from the beginning (ab initio, *intrinsic resistance*). For certain types of cancer cells, there are simply no effective agents known.

The *Norton-Simon hypothesis* [244, 245, 246] postulates that tumors typically consist of faster growing cells that are sensitive to chemotherapy and slower growing populations of cells that have lower sensitivities or even are resistant to the chemotherapeutic agent. Given such a scenario, over time, as the drugs kill sensitive tumor cells, the resistant subpopulation of cancer cells may become the dominant one and eventually an MTD-style therapy may cause more harm to the healthy cells

H. Schättler, U. Ledzewicz, *Optimal Control for Mathematical Models of Cancer Therapies*, Interdisciplinary Applied Mathematics 42,
DOI 10.1007/978-1-4939-2972-6_3

than that it has beneficial effects [198, 215, 325]. Even if initially the fraction of intrinsically resistant tumor cells is tiny, after the sensitive cells have been killed by the treatment, it will grow and may turn into a fully developed tumor of chemotherapeutically resistant cells leading to the eventual failure of therapy, possibly only after many years of apparent remission of the disease.

Tumor heterogeneity thus is an important aspect in chemotherapy and in this chapter we consider the effects it has on the structure of optimal protocols. There exist a great many mathematical models for acquired drug resistance with stochastic models ranging from Markov process models of point mutations [60, 61, 105, 106, 107, 229] to branching processes based on gene amplifications [7, 122, 123, 148, 296] the more common ones. But there also exist various continuum based models using ordinary (e.g., [130]) or partial differential equations (e.g., [331]). Here, in Section 3.1 we briefly discuss a model initially proposed by Lorz et al. [221] and then expanded by Greene, Lavi, Gottesman, and Levy [110, 173] that gives a mathematical framework for multi-drug resistance based on cell density and mutations. The model consists of integro-differential equations parameterized by a continuum of resistance levels x, $x \in [0, 1]$, and it shows that as response to cell densities (different division and death rates) and mutations over time a specific finite number traits or resistance levels emerge to become dominant.

We then return to the topic of optimal administration of chemotherapeutic agents, but take tumor heterogeneity into account. Other aspects of the tumor microenvironment (such as the tumor vasculature and tumor-immune system interactions) will be considered in Chapters 5 and 8. Mathematically, the models have the same bilinear structure as those considered in Chapter 2. The models considered here are not cell-cycle specific, but such effects could easily be incorporated at the expense of higher dimensions [153, 324, 325]. In Section 3.2 we consider a 2-compartment model that only distinguishes between 'sensitive' and 'resistant' subpopulations with the possibility of sensitive cells becoming resistant (by means of gene amplification or some other molecular mechanism, e.g., see [64, 104, 107]). Once more, we consider the problem of administrating chemotherapy in a continuous-time formulation and explore the structure of optimal protocols that minimize the tumor burden as measured by an average of the cancer cell population over an a priori prescribed therapy interval and the total dosage of drugs given. It turns out that it matters whether resistant cells can resensitize or not. If this is not the case, then indeed optimal controls still give all the drugs at maximum dose rate in one session upfront. Essentially, since there is no chance of killing the resistant cells, it still is the 'best' policy (in terms of minimizing this particular objective) to eliminate the sensitive cell population as fast as possible. Clearly, this limits the overall growth of the tumor the most and it also prevents a further supply of resistant cells through transitions from sensitive cells. Naturally, this does not cure the disease, but it still seems to be the "best" of many inadequate choices. However, this changes as resensitizations are brought into the picture. In such a case, as treatment progresses and the fraction of 'resistant' cells becomes large, now there still is some benefit to be gained from chemother-

apy, but the damage caused by chemotherapy to healthy cells must be balanced with the benefits of killing the cancer cells by using lower dose rates. These still provide benefits at reduced side effects and singular controls (defining specific time-varying administration schedules at less than maximum dose) become viable options. More generally, in Section 3.3 we consider a mathematical model that considers three levels of sensitivity. Interestingly, in such a case singular controls and the reduced dose rates they represent become an option for optimal protocols from the very beginning if only three distinct subpopulations are distinguished. As in the cell-cycle specific models considered in Section 2, there always exist well-defined steady states for the proportions of cells that lie in these subpopulations. We close this chapter with some comments on "adaptive therapy," a concept championed by Gatenby [102] in which it is argued that maintenance of the cancer might be a preferable strategy over killing the tumor. The underlying idea is that, and assuming the sensitive cell population is the faster growing one, by preserving a proportion of the sensitive population, this subpopulation will "outcompete" the resistant one through evolutionary mechanisms (simply through crowding). This will limit the growth of the more dangerous resistant subpopulation and thus prevent the development of a malignant tumor in the future. Hence a continuous maintenance type strategy might be preferable over an MTD killing approach. The hope simply is to thus make cancer a managable chronic disease.

3.1 A Mathematical Model for the Emergence of Traits (Resistance Levels) Under Chemotherapy

There exist numerous theories about developing drug resistance, but mutations play a central role in all of them. It is not our intention to get into a discussion of these models here, but we just mention gene amplification as one possible mechanism of acquired drug resistance [123, 148]. In this process, the number of copies of a particular gene is increased causing cells to become increasingly more resistant to drugs. Also, and this phenomenon is well-documented in the medical literature [296], it is possible that resistant cells lose extra copies of the gene in a drug free medium and mutate back to become more sensitive. This, however, is just one of several molecular mechanisms that would explain the emergence of various levels of drug resistance within a tumor. Rather than presenting such a model, here we show that even when the system possibly has a continuum of traits or resistance levels initially, as a response to different net growth rates in the evolutionary dynamics under treatment specific traits emerge to become dominant. The mathematical model, initially formulated in the work by Lorz et al. [221, 222] and then expanded upon by Greene, Lavi, Gottesman, and Levy [110], explains the roles that increasing cell densities and mutations play in the emergence of these traits.

3.1.1 System Response to Variation in Rates for Growth and Apoptosis

In the model, a continuum of possible traits/resistance levels x, $x \in [0,1]$, is considered with $x = 0$ denoting cells that show no resistance to a particular chemotherapeutic agent and $x = 1$ denoting fully resistant cells. If we denote the population density of cells with trait x at time t by $n(t,x)$, then the total number $N(t)$ of cancer cells at time t is

$$N(t) = \int_0^1 n(t,x)dx.$$

It is assumed that the division rate r and the natural death rate μ of cancer cells depend on the specific trait and thus are functions of x, $r = r(x)$ and $\mu = \mu(x)$. Similarly, the effects of chemotherapy depend on the trait of the cell and we denote the cytotoxic killing parameter under the linear log-kill hypothesis by $c = c(x)$. Essentially, this coefficient is related to the drug concentration and trait of the subpopulation. For simplicity, all these rates are assumed to be continuous functions on $[0,1]$. We also assume that the natural death rate μ does not vanish and thus it is bounded away from zero. In the analysis here, only the case of a constant drug administration is considered and its effects are subsumed in the definition of c. Thus the underlying model of trait based growth is simply one of exponential growth dependent on the trait x,

$$\frac{\partial n}{\partial t}(t,x) = (r(x) - \mu(x) - c(x))n(t,x) \tag{3.1}$$

with the initial distribution $n(0,x)$ a continuous positive function. (Without loss of generality, here we assume that all traits are represented. Otherwise, since we do not yet include mutations, at this point of modeling, there is no need to consider these traits.) Clearly, if chemotherapy is strong enough to make all the net growth rates $\Delta(x) = r(x) - \mu(x) - c(x)$ negative, then all subpopulations will go extinct and the therapy will be successful. On the other hand, if there exist traits for which this net growth rate remains positive, these traits will grow exponentially and the fastest growing traits will be become dominant. More precisely, the following result holds:

Proposition 3.1.1. [110, 221] *Suppose the function $\Delta(x) = r(x) - \mu(x) - c(x)$ attains its positive maximum M in a finite number of points x_i, $i = 1,\ldots,k$. Then the total number of cells $N(t)$ grows exponentially while the relative proportions of traits,*

$$\rho(t,x) = \frac{n(t,x)}{N(t)},$$

also called the occupation measure, has a well-defined steady state given by a weighted average of the traits with the fastest net growth rates:

$$\lim_{t\to\infty} \rho(t,x) = \sum_{i=1}^{k} a_i \delta(x - x_i)$$

where $\delta(x-x_i)$ denotes the Dirac-δ-distribution centered at x_i and

$$a_i = \frac{n(0,x_i)}{\sum_{j=1}^{k} n(0,x_j)}.$$

Proof. Note that $n(t,x)$ is positive for all times t and traits x since the initial density $n(0,x)$ is positive. Given $i \in \{1,\dots,k\}$, let x be a point that is not a maximizer of Δ. Since Δ is continuous , there exist positive numbers ε, η and λ so that $\eta < \alpha < M$, $\Delta(y) \geq \alpha$ for all $y \in [x_i-\varepsilon, x_i+\varepsilon]$ and $\Delta(y) \leq \eta$ for all $y \in [x-\varepsilon, x+\varepsilon]$. Defining

$$A(t) = \int_{x_i-\varepsilon}^{x_i+\varepsilon} n(t,x)dx,$$

it follows that

$$\frac{d}{dt}A(t) = \int_{x_i-\varepsilon}^{x_i+\varepsilon} \frac{\partial n}{\partial t}(t,x)dx = \int_{x_i-\varepsilon}^{x_i+\varepsilon} \Delta(x)n(t,x)dx \geq \alpha \int_{x_i-\varepsilon}^{x_i+\varepsilon} n(t,x)dx = \alpha A(t)$$

and $A(0)$ is positive by the continuity of $n(0,x)$. Hence $N(t) \geq A(t) = A(0)e^{\alpha t}$. In particular, $\lim_{t\to\infty} N(t) = \infty$. Furthermore,

$$\frac{n(t,x)}{N(t)} = \frac{n(0,x)e^{\Delta(x)t}}{N(t)} \leq \frac{n(0,x)e^{\eta t}}{A(0)e^{\alpha t}} = \frac{n(0,x)}{A(0)}e^{(\eta-\alpha)t} \to 0 \qquad \text{as } t \to \infty.$$

At the same time

$$\frac{n(t,x_i)}{N(t)} = \frac{n(0,x_i)e^{\Delta(x_i)t}}{N(t)} \leq \frac{n(0,x_i)e^{Mt}}{A(0)e^{\alpha t}} = \frac{n(0,x_i)}{A(0)}e^{(M-\alpha)t} \to \infty \qquad \text{as } t \to \infty.$$

Thus the relative proportions $\rho(t,x)$ satisfy

$$\lim_{t\to\infty} \rho(t,x) = \begin{cases} 0 & \text{if} \quad \Delta(x) < M, \\ \infty & \text{if} \quad \Delta(x) = M. \end{cases}$$

The invariance condition $\int_0^1 \rho(t,x)dx = 1$ implies that the limiting distribution is a finite number of Dirac-δ-distributions at the points where Δ attains its maximum. Since there are no interactions between the different traits in this model (yet), the weights are the same as the relative weights at the initial time. □

3.1.2 System Response to Increasing Cell Densities

Equation (3.1) represents a model of exponential growth generating unbounded total populations. Incorporating some logistic type structure into the model will give finite carrying capacities. Such effects are caused by increasing cell densities.

In reality, the rates for cell division and apoptosis depend on the cell density which is closely related to the total tumor mass N [109]. Thus, more realistically, these equations take the form

$$\frac{\partial n}{\partial t}(t,x) = \{f(N(t))\,(r(x) - c(x)) - g(N(t))\mu(x)\}\,n(t,x) \tag{3.2}$$

with $f = f(N)$ and $g = g(N)$ tumor size dependent functions that model the rates for cell division and apoptosis. As in the models in Chapter 2, cells 'killed' by the chemotherapeutic agent simply signifies that cells no longer divide and thus here these terms are subtracted to lower the reproduction rate r. If the chemotherapeutic agent truly kills the cells, this would lead to increased rates for apoptosis and could also be incorporated within the function μ. But most cytotoxic agents merely prevent further divisions and thus here we follow the earlier and more common approach. Following [110], equation (3.2) can be simplified by rescaling time according to

$$\tau(t) = \int_0^t f(N(s))ds$$

and in the new time-scale we have that

$$\frac{\partial n}{\partial \tau}(\tau,x) = \{r(x) - c(x) - G(N(\tau))\mu(x)\}\,n(\tau,x) \tag{3.3}$$

with

$$G(N) = \frac{g(N)}{f(N)}.$$

Thus in the new time-scale only the apoptosis rates are changed. The model now is nonlinear with the right-hand exhibiting similar features as a logistic term of the form $(a - bN)N$. If one assumes that the growth rate f decays more rapidly than the apoptosis rate g as the tumor size increases—and this is a reasonable assumption—then the scaling factor G increases. Once this term offsets the balance between growth and apoptosis, the population will stabilize.

Proposition 3.1.2. *Let*

$$G_* = \max_{0\le x\le 1}\left\{\frac{r(x) - c(x)}{\mu(x)}\right\}$$

and suppose the function $G : (0,\infty) \to (0,\infty)$, $N \mapsto G(N)$, is strictly increasing with finite limit $G_\infty > G_*$. Then there exists a unique population level N_* such that $G(N_*) = G_*$ and the total tumor population N stabilizes at this level in the sense that

$$\limsup_{\tau\to\infty} N(\tau) = N_*.$$

Proof. Since the functions r, c and μ are continuous, and since μ is bounded away from zero, G_* is well-defined and finite. Defining

$$\gamma(G) = \max_{0\le x\le 1}\{r(x) - c(x) - G\mu(x)\},$$

it then follows that $\gamma(G_*) = 0$ while $\gamma(G) > 0$ for $G < G_*$ and $\gamma(G) < 0$ for $G > G_*$. Since the total tumor population $N(\tau) = \int_0^1 n(\tau,x)dx$ evolves according to

$$\frac{dN}{d\tau}(\tau) = \int_0^1 \frac{\partial n}{\partial \tau}(\tau,x)dx = \int_0^1 \{r(x) - c(x) - G(N(\tau))\mu(x)\}\, n(\tau,x)dx, \qquad (3.4)$$

it follows that,

$$\frac{dN}{d\tau}(\tau) \le \gamma(G(N(\tau)))N(\tau).$$

Whenever the tumor population $N(\tau)$ exceeds N_*, then this derivative is negative and thus the overall tumor population cannot increase beyond level N_*.

Suppose that $\limsup_{\tau\to\infty} N(\tau) = \hat{N} < N_*$. Given $\tilde{N} \in (\hat{N}, N_*)$, there exists a time $\tilde{T}$ so that $N(\tau) < \tilde{N}$ for $\tau > \tilde{T}$. If $\tilde{G} = G(\tilde{N})$, then we have for all $\tau > \tilde{T}$ that $G(N(\tau)) \le G(\tilde{N}) = \tilde{G} < G_*$. Furthermore, it follows from the definition of G_* that $\gamma\left(\tilde{G}\right) > 0$. Let $\tilde{x}$ be a maximizer for the function $r(x) - c(x) - \tilde{G}\mu(x)$ and choose $\alpha > 0$ and an ε-neighborhood of $\tilde{x}$ such that

$$r(x) - c(x) - \tilde{G}\mu(x) \ge \alpha > 0 \qquad \text{for all } x \in [\tilde{x} - \varepsilon, \tilde{x} + \varepsilon].$$

As above, if we define

$$A(\tau) = \int_{\tilde{x}-\varepsilon}^{\tilde{x}+\varepsilon} n(\tau,x)dx,$$

it then follows for $\tau > \tilde{T}$ that

$$\begin{aligned}\frac{dA}{d\tau}(\tau) &= \int_{\tilde{x}-\varepsilon}^{\tilde{x}+\varepsilon} \{r(x) - c(x) - G(N(\tau))\mu(x)\}\, n(\tau,x)dx \\ &\ge \int_{\tilde{x}-\varepsilon}^{\tilde{x}+\varepsilon} \left\{r(x) - c(x) - G(\tilde{N})\mu(x)\right\} n(\tau,x)dx \ge \alpha A(\tau).\end{aligned}$$

Hence $A(\tau) \ge A(\tilde{T})e^{\alpha\tau}$ for $\tau > \tilde{T}$. Once again, since we are assuming that all traits are originally represented, it follows that $A(\tilde{T}) > 0$ and thus this portion grows exponentially. But then also

$$N(\tau) = \int_0^1 n(\tau,x)dx \ge A(\tau) \ge A(\tilde{T})e^{\alpha\tau} \to \infty \qquad \text{as } \tau \to \infty.$$

This contradicts the fact that $N(\tau)$ cannot exceed N_*. □

While this argument does not establish the existence of a limit, if a limit exists, it must be N_*. In principle, it is possible that the total tumor volumes might fluctuate at levels below N_*, but then, again and again the total tumor values get closer and closer to N_*. For all practical intents and purposes, this has the same implications. If the limit exists, we have the same steady-state behavior as described in Proposition 3.1.1: if there exist a finite number of points x_i^*, $i = 1,\ldots,k$, such that

$$r(x_i^*) - c(x_i^*) - G_*\mu(x_i^*) = 0,$$

then the occupation measure of traits,

$$\rho(\tau,x) = \frac{n(\tau,x)}{N(\tau)},$$

has a well-defined steady state:

$$\lim_{\tau\to\infty} \rho(\tau,x) = \sum_{i=1}^{k} a_i^* \delta(x - x_i^*) \qquad \text{where} \qquad a_i^* = \frac{n(0,x_i^*)}{\sum_{j=1}^{k} n(0,x_j^*)}$$

and $\delta(x - x_i^*)$ again is the Dirac-δ-distribution centered at x_i^*.

3.1.3 System Response to Mutations

Mutations are described through transition probabilities from one trait to another. For $x, y \in [0,1]$, let $p(x|y)$ denote the transition density of a change from trait y into trait x. Thus for every $y \in [0,1]$, $p(\cdot|y)$ is a nonnegative function that integrates to 1. For example, if one wants to capture the effect that small mutations are more likely, a modified Gaussian kernel of the form

$$p(x|y) = k(y) \exp\left(-\frac{1}{2}\left(\frac{x-y}{\sigma}\right)^2\right)$$

with the constant $k(y)$ chosen so that

$$\int_0^1 p(x|y)dx = 1$$

is appropriate. If, for simplicity, it is assumed that a fixed fraction θ, $\theta \in (0,1)$, of cells mutate, then this reduces the reproduction rate r by θ and the total flow of all mutating cells is given by

$$\int_0^1 p(x|y)r(y)\theta n(\tau,y)dy.$$

Hence the dynamics (3.3) will be modified to become

$$\frac{\partial n}{\partial \tau}(\tau,x) = \{r(x)(1-\theta) - c(x) - G(N(\tau))\mu(x)\}n(\tau,x) + \theta \int_0^1 p(x|y)r(y)n(\tau,y)dy. \tag{3.5}$$

The net effect of the mutations on the growth of the total population is zero and thus this growth is still described by the same differential equation (3.4):

$$\begin{aligned}\frac{dN}{d\tau}(\tau) &= \int_0^1 \frac{\partial n}{\partial \tau}(\tau,x)dx \\ &= \int_0^1 \{r(x)(1-\theta)-c(x)-G(N(\tau))\mu(x)\}n(\tau,x)dx \\ &\qquad + \int_0^1 \left(\theta \int_0^1 p(x|y)r(y)n(\tau,y)dy\right)dx \\ &= \int_0^1 \{r(x)(1-\theta)-c(x)-G(N(\tau))\mu(x)\}n(\tau,x)dx \\ &\qquad + \theta \int_0^1 \left(\int_0^1 p(x|y)dx\right) r(y)n(\tau,y)dy \\ &= \int_0^1 \{r(x)(1-\theta)-c(x)-G(N(\tau))\mu(x)\}n(\tau,x)dx + \theta \int_0^1 r(y)n(\tau,y)dy \\ &= \int_0^1 \{r(x)-c(x)-G(N(\tau))\mu(x)\}n(\tau,x)dx.\end{aligned}$$

In particular, the total tumor population remains bounded by N_*. However, the behavior of the occupation measure as $t \to \infty$ becomes more complex. An important consequence of the inclusion of the mutating fraction θ into the model is that it allows for the net growth rate $r(x)-c(x)-G(N(\tau))\mu(x)$ to be positive. For, in a reasoning analogous to the one given in the proof of Proposition 3.1.2, we now only have the lower bound

$$\begin{aligned}\frac{dA}{d\tau}(\tau) &= \int_{\tilde{x}-\varepsilon}^{\tilde{x}+\varepsilon} \{r(x)(1-\theta)-c(x)-G(N(\tau))\mu(x)\}n(\tau,x)dx \\ &\qquad + \theta \int_{\tilde{x}-\varepsilon}^{\tilde{x}+\varepsilon} \left(\int_0^1 p(x|y)r(y)n(\tau,y)dy\right)dx \\ &\geq \int_{\tilde{x}-\varepsilon}^{\tilde{x}+\varepsilon} \left\{r(x)(1-\theta)-c(x)-G(\tilde{N})\mu(x)\right\}n(\tau,x)dx.\end{aligned}$$

Therefore, exponential growth of a specific trait $\tilde{x}$ only happens if for some $\alpha > 0$ we actually have that $r(x)(1-\theta)-c(x)-G\mu(x) > \alpha$ in a neighborhood of $\tilde{x}$. While this is precluded by the fact that the population stabilizes, it is perfectly possible that the maximal net growth rate without mutations is positive,

$$r(\tilde{x})-c(\tilde{x})-G_*\mu(\tilde{x}) > 0.$$

For, this growth can be continuously off-set by the mutation rates to other traits that will die out. Hence, and this is confirmed by the simulations given in [110], the proportions no longer converge to Dirac δ's at the maximizers, but the limiting behavior consists of distributions around these maximizers with small variances. There still exists a clear dominance of specific traits in the steady state that are

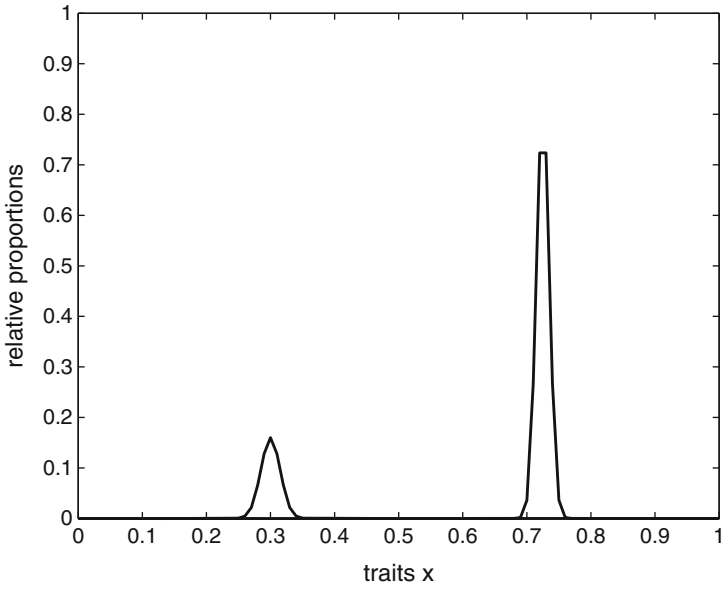

Fig. 3.1 Distribution of traits around the dominant steady states.

close to the maximizers of the function $r(x) - c(x) - G_*\mu(x)$, but now the limits are distributions with positive variance and thus small variations of these traits persist as well (see Figure 3.1).

Summarizing, as an evolutionary response to different rates for growth and apoptosis, increasing cell densities and mutations, in the long run (steady state), specific traits emerge and become dominant, possibly with small variations. In the presence of mutations, this occurs regardless of whether these traits were present originally or not. In the remainder of this chapter we consider two such models from an optimal therapy point of view.

3.2 Cancer Chemotherapy in the Presence of a Resistant Subpopulation

We first consider a model in which only drug resistant (acquired or intrinsic) and drug sensitive subpopulations are distinguished. Mathematically, this situation can be described by a 2-compartment bilinear model similar to the one analyzed in Section 2.1. It would seem intuitive that in this case, as the sensitive population becomes depleted—and different from the results for the models considered in Chapter 2—singular controls and the generally lower dose rates they represent become viable candidates for optimal controls. Interestingly, this is only the case if resensitizations of the resistant subpopulation are allowed. Otherwise, optimal protocols that aim to minimize the cancer volume still follow MTD protocols.

3.2.1 A 2-compartment Model with Sensitive and Resistant Subpopulations

We consider two compartments consisting of drug sensitive and resistant cells and denote the numbers of cells in the sensitive and resistant compartments by S and R, respectively. The dynamical equations describing the growth and interactions of cells in these compartments are classical (e.g., see [74, Section 2.4]) and take the following form:

$$\dot{S} = (\alpha_1 - \gamma_1 - \varphi u)S + \gamma_2 R, \qquad S(0) = S_0, \tag{3.6}$$

$$\dot{R} = \gamma_1 S + (\alpha_1 - \gamma_2)R, \qquad R(0) = R_0. \tag{3.7}$$

Here α_1 and α_2 are the growth rates of the respective populations and γ_1 and γ_2 describe possible exchanges between the two subpopulations. The parameter γ_1 is positive and models the transitions of sensitive cells to become resistant through mutations while γ_2 is nonnegative modeling resensitization of resistant cells. We allow for the possibility that the resistant population is intrinsically resistant, $\gamma_2 = 0$. As before, cell kill is expressed using the standard linear log-kill hypothesis with the coefficient φ modeling the effectiveness of the drug (pharmacodynamics). We do not include a pharmacokinetic model and consider u to be the concentration of the chemotherapeutic agent, but in our language identify it with the dose rates which are bounded by $u_{\max}$. We assume that the initial condition S_0 is positive and R_0 is nonnegative and again denote the state of the system by $N = (S,R)^T$. The dynamics thus is a bilinear system of the form $\dot{N} = (A + uB)N$ with the matrices given by

$$A = \begin{pmatrix} \alpha_1 - \gamma_1 & \gamma_2 \\ \gamma_1 & \alpha_2 - \gamma_2 \end{pmatrix} \qquad \text{and} \qquad B = \begin{pmatrix} -\varphi & 0 \\ 0 & 0 \end{pmatrix}.$$

The matrix describing the dynamics no longer is an M-matrix, but positive invariance of the control system is easily established.

Proposition 3.2.1. *For any admissible control u, $u : [0,T] \to [0,u_{\max}]$, $t \mapsto u(t)$, the solution to the dynamical system (3.6)–(3.7) exists on the full interval $[0,T]$ and the states R and S are positive on $(0,T]$.*

Proof. Existence and uniqueness of solutions on $[0,T]$ for bilinear systems follows from standard results on linearly bounded ODEs. The differential equations for R and S are homogeneous and thus R and S cannot vanish simultaneously. If $R_0 = 0$, then $\dot{R}(0) = \gamma_1 S_0 > 0$ and thus R immediately becomes positive. But none of S or R can vanish on $(0,T]$. If $\gamma_2 = 0$, it is clear that S is positive on $[0,T]$ and thus, whenever $R(\tau) = 0$, we have that $\dot{R}(\tau) = \gamma_1 S(\tau) > 0$. Hence R cannot vanish neither. Similarly, if $\gamma_2 > 0$, then whenever one of the variables vanishes at a time τ, the derivative of the other one will be positive. Hence both R and S remain positive. □

If C again denotes the total number of cancer cells, $C = S + R$, and x and y are the proportions of the cancer cells in the respective compartments,

$$x = \frac{S}{C} = \frac{S}{S+R} \qquad \text{and} \qquad y = \frac{R}{C} = \frac{R}{S+R} = 1 - x,$$

then for the uncontrolled system ($u \equiv 0$) x obeys the ODE

$$\dot{x} = \frac{\dot{S}C - \dot{C}S}{C^2} = (\alpha_2 - \alpha_1)x^2 - (\alpha_2 - \alpha_1 + \gamma_1 + \gamma_2)x + \gamma_2.$$

This equation always has a well-defined steady state.

If we allow for resensitization, $\gamma_2 > 0$, then it follows from $\dot{x}_{|x=0} = \gamma_2 > 0$ and $\dot{x}_{|x=1} = -\gamma_1 < 0$ that the interval $[0,1]$ is positively invariant. Regardless of the parameter values, the polynomial

$$P(x) = (\alpha_2 - \alpha_1)x^2 - (\alpha_2 - \alpha_1 + \gamma_1 + \gamma_2)x + \gamma_2$$

always has a unique root $\bar{x}$ in the open interval: if $\alpha_1 = \alpha_2$, we simply have $\bar{x} = \frac{\gamma_2}{\gamma_1+\gamma_2}$ while P is strictly concave with one negative root and one root in $(0,1)$ if $\alpha_1 > \alpha_2$ and is strictly convex with one root in $(0,1)$ and the second root greater than 1 if $\alpha_1 < \alpha_2$. In any case, there exist well-defined steady states $\bar{x}$ and $\bar{y}$ for the proportions of the uncontrolled system, $\bar{x} + \bar{y} = 1$, given by the unique root of the quadratic polynomial P that lies in the interval $(0,1)$. For example, if $\alpha_1 = 3.5$, $\alpha_2 = 1$, $\gamma_1 = 0.15$ and $\gamma_2 = 0.02$, we have that $\bar{x} = 0.9405$. Such parameter values correspond to a significantly faster growing sensitive population with a substantially higher probability that sensitive cells becoming resistant than that resistant cells resensitize. If the growth rates are equal, the steady-state value is determined by the exchange between the two populations, $\bar{x} = \frac{\gamma_2}{\gamma_1+\gamma_2}$, and in this case the balance would shift to the more resistant population since the transitions from sensitive to resistant are assumed to be higher.

In the case $\gamma_2 = 0$ these relations simplify. If $\alpha_1 - \gamma_1 \leq \alpha_2$, i.e., the net growth rate of the sensitive population is smaller than the growth rate of the resistant population, then the steady state is simply $\bar{x} = 0$: the sensitive cells die out and the entire population turns into resistant cells. If $\alpha_1 - \gamma_1 > \alpha_2$, then the steady state establishes in the balance $\bar{x} = \frac{\alpha_1 - \gamma_1 - \alpha_2}{\alpha_1 - \alpha_2} \in (0,1)$.

3.2.2 Chemotherapy as Optimal Control Problem and Singular Controls

Using the same notation as before, we again consider the following optimal control problem:

[Chet2] For a fixed therapy horizon $[0,T]$, minimize the objective

$$\begin{aligned} J &= rN(T) + \int_0^T (qN(t) + u(t))\,dt \\ &= r_1 S(T) + r_2 R(T) + \int_0^T (q_1 S(t) + q_2 R(t) + u(t))\,dt \to \min \end{aligned} \tag{3.8}$$

over all Lebesgue-measurable (respectively, piecewise continuous) functions $u : [0,T] \to [0,u_{\max}]$ subject to the dynamics (3.6)–(3.7).

We have normalized the coefficient at the penalty term to 1. As it was discussed in Section 2.1.3, it is reasonable to choose the weights for the cancer cells S and R so that the terms $q_1 S$ and $q_2 R$ are compatible with the coefficient at the control since otherwise not enough or too much emphasis is put on the side effects. In this respect, weights in the order $q_1 = \frac{1}{S_0}$ and $q_2 = \frac{1}{R_0}$ or $q_1 = q_2 = \frac{1}{C_0}$ make sense since this will keep the expressions $q_1 S(t)$ and $q_2 R(t)$ reasonably close to 1.

For this problem, singular controls start to come into play. Formally, the mathematical structure is the same as for the 2-compartment model analyzed in Section 2.1 and we briefly recall the relevant formulas. Since there are no constraints at the terminal time, the multiplier at the Lagrangian cannot vanish and thus we define the Hamiltonian function as

$$H = H(\lambda, N, u) = qN + u + \lambda\,(A + uB)N. \tag{3.9}$$

If $u_* : [0,T] \to [0,u_{\max}]$ is an optimal control with corresponding trajectory N_*, then there exists a solution $\lambda = (\lambda_1, \lambda_2) : [0,T] \to \left(\mathbb{R}^2\right)^*$ to the adjoint equation

$$\dot{\lambda} = -\frac{\partial H}{\partial N} = -q - \lambda\,(A + u_* B)\,, \qquad \lambda(T) = r, \tag{3.10}$$

such that $u_*(t)$ minimizes the Hamiltonian H pointwise over the control set $[0,u_{\max}]$ along $(\lambda(t), N_*(t))$. In coordinates, the adjoint equations read

$$\begin{aligned} \dot{\lambda}_1 &= -q_1 - \lambda_1\,(\alpha_1 - \gamma_1 - \varphi u) - \lambda_2 \gamma_1\,, & \lambda_1(T) &= r_1\,, \\ \dot{\lambda}_2 &= -q_2 - \lambda_1 \gamma_2 - \lambda_2\,(\alpha_2 - \gamma_2)\,, & \lambda_2(T) &= r_2\,, \end{aligned}$$

and, as in Proposition 2.1.3, it can be seen that all multipliers remain positive.

Proposition 3.2.2. *The multipliers λ_1 and λ_2 are positive over the interval $[0,T]$.*

The switching function is given by

$$\Phi(t) = 1 + \lambda(t) B N_*(t) = 1 - \varphi \lambda_1(t) S(t) \tag{3.11}$$

and optimal controls satisfy

$$u_*(t) = \begin{cases} 0 & \text{if } \Phi(t) > 0, \\ u_{\max} & \text{if } \Phi(t) < 0. \end{cases}$$

The derivatives of the switching function can be computed using Proposition 2.1.4 and are given by

$$\dot{\Phi}(t) = \{\lambda(t)\,[A,B] - qB\}\,N_*(t)$$

and

$$\ddot{\Phi}(t) = \{\lambda(t)[A,[A,B]] - q[A,B] - qBA\}N_*(t) + u_*(t)\left\{\lambda(t)[B,[A,B]] - qB^2)\right\}N_*(t).$$

Hence the singular control becomes (c.f., equation (2.30))

$$u_{\text{sing}}(t) = -\frac{\{\lambda(t)[A,[A,B]] - q[A,B] - qBA\}N_*(t)}{\{\lambda(t)[B,[A,B]] - qB^2\}N_*(t)}. \tag{3.12}$$

The iterated brackets and products are easily computed. We have

$$[A,B] = \varphi\begin{pmatrix} 0 & -\gamma_2 \\ \gamma_1 & 0 \end{pmatrix}, \qquad BA = -\varphi\begin{pmatrix} \alpha_1-\gamma_1 & \gamma_2 \\ 0 & 0 \end{pmatrix}, \qquad B^2 = \varphi^2\begin{pmatrix} 1 & 0 \\ 0 & 0 \end{pmatrix}$$

and setting $\Delta = (\alpha_1 - \gamma_1) - (\alpha_2 - \gamma_2)$, the difference of the net proliferation rates, the second-order brackets are given by

$$[A,[A,B]] = \varphi\begin{pmatrix} -2\gamma_1\gamma_2 & \Delta\gamma_2 \\ \Delta\gamma_1 & 2\gamma_1\gamma_2 \end{pmatrix} \qquad \text{and} \qquad [B,[A,B]] = \varphi^2\begin{pmatrix} 0 & -\gamma_2 \\ -\gamma_1 & 0 \end{pmatrix}.$$

For this model, the Legendre-Clebsch condition takes the form

$$\begin{aligned}\frac{\partial}{\partial u}\frac{d^2}{dt^2}\frac{\partial H}{\partial u} &= \left\{\lambda(t)[B,[A,B]] - qB^2\right\}N_*(t) \\ &= -\varphi^2(\lambda_1(t)\gamma_2 R(t) + \lambda_2(t)\gamma_1 S(t) + q_1 S(t)).\end{aligned} \tag{3.13}$$

Since states and multipliers are positive, this quantity is negative. Hence singular controls are of order 1 and the strengthened Legendre-Clebsch condition is satisfied.

Proposition 3.2.3. *Singular controls are of order* 1 *and the Legendre-Clebsch condition for minimality is satisfied.*

The multipliers λ_1 and λ_2 along a singular control are uniquely determined as functions of the states S and R by the equations $\Phi = 0$ and $\dot{\Phi} = 0$,

$$\lambda(t)\begin{pmatrix} -\varphi S(t) & -\varphi\gamma_2 R(t) \\ 0 & \varphi\gamma_1 S(t) \end{pmatrix} = \left(-1, -\varphi q_1 S(t)\right),$$

with the solution given by

$$\left(\lambda_1(t)\ \lambda_2(t)\right) = \frac{1}{\varphi S(t)}\left(1, \tfrac{\gamma_2}{\gamma_1}\tfrac{R(t)}{S(t)} - \varphi\tfrac{q_1}{\gamma_1}S(t)\right). \tag{3.14}$$

The multiplier $\lambda_1(t)$ is always positive, while $\lambda_2(t)$ is positive if and only if the states S and R lie in the region

$$D = \left\{(S,R) : \gamma_2 R(t) > \varphi q_1 S(t)^2\right\}.$$

If the weight q_1 is chosen so that $q_1 S_0 \simeq 1$, then the product $q_1 S(t)$ is of order 1 and this therefore can be thought of as representing approximately a linear relation between sensitive and resistant subpopulations. Singular controls are only possible if the corresponding trajectory lies in this region D. This implies the following result:

Proposition 3.2.4. *Optimal controls whose trajectories lie in the region*

$$MTD = \left\{(S,R) : \gamma_2 R(t) \leq \varphi q_1 S(t)^2\right\}, \tag{3.15}$$

are bang-bang with at most one switching from $u = u_{\max}$ to $u = 0$.

Proof. Suppose the switching function Φ has a zero at time τ. If the junction lies in the region MTD, then we have that

$$\begin{aligned}\dot{\Phi}(\tau) &= \{\lambda(t)[A,B] - qB\}N_*(t)\\ &= \varphi\{-\lambda_1(\tau)\gamma_2 R(\tau) + \lambda_2(\tau)\gamma_1 S(\tau) + q_1 S(\tau)\}\end{aligned}$$

$$\begin{aligned}&\geq \varphi\left\{-\frac{1}{\varphi S(\tau)}\varphi q_1 S(\tau)^2 + \lambda_2(\tau)\gamma_1 S(\tau) + q_1 S(\tau)\right\}\\ &= \varphi\lambda_2(\tau)\gamma_1 S(\tau) > 0\end{aligned}$$

and thus the switching function changes from negative to positive values. Hence the corresponding control changes from $u = u_{\max}$ to $u = 0$. In particular, there can only be one switching while the trajectory lies in the region MTD. □

For $\gamma_2 = 0$ the region MTD is the entire state-space and thus optimal controls give as much of the drug as possible upfront, i.e., are in agreement with the MTD paradigm. Thus, if there is no possibility of resensitization for the resistant tumor population, this model still confirms an MTD approach as optimal if the aim is to minimize the cancer volume. Intuitively, since there is no chance of eliminating the resistant cells, it is still the 'best' policy to get to the sensitive cells as quickly as possible. Clearly, this limits the tumor growth to the growth rate of the resistant population and prevents the further supply of resistant cells through transitions from sensitive cells. Naturally, this does not cure the cancer, but it still is the 'best' way of minimizing the cancer volume. Note that we are still operating under the assumption of exponential growth for the total tumor population. In particular, no interactions between the sensitive and resistant populations as response to environmental crowding are incorporated into the model as it is formulated here. This requires a growth model with a limited carrying capacity.

Singular controls, i.e., reduced dose rates, can only be optimal if the number of sensitive cancer cells becomes small. Once trajectories enter the region D, singular controls become viable options as the fact that the Legendre-Clebsch condition is

satisfied indicates. Based on the formulas above, singular controls are easily computed. Using the formulas for the multipliers, the Legendre-Clebsch condition simplifies to

$$\left\{\lambda(t)\,[B,[A,B]] - qB^2\right\} N_*(t) = -2\varphi\gamma_2 \frac{R(t)}{S(t)},$$

while the numerator is more involved and does not simplify. Yet these formulas uniquely determine a singular flow through every point (S,R) in the state space. It needs to be verified that the singular control computed in this way is admissible, i.e., takes values between 0 and $u_{\max}$. In view of the fact that it is the total dose, i.e., the integral $\int_0^T u(t)dt$, that matters and that such a dose often is administered as a bolus rate, the upper limit $u_{\max}$ actually is less significant, but clearly negative dose rates are not possible and in such cases the computed singular controls are not admissible.

For a typical choice of parameter values and a high initial tumor burden C_0, the fraction $\bar{x}$ will be high (above 90%) and if one chooses the weights q on a scale commensurate with the initial tumor burden, say $q_1 = q_2$ and $q_1 C_0 = 1$, then the initial condition will lie in the set MTD and optimal controls will start with a period of maximum dose therapy, i.e., follow an MTD strategy. This simply represents the case of a high tumor burden when immediate action becomes necessary. As the sensitive cells become depleted and the region D is reached, singular controls become an option.

3.3 A Mathematical Model for a Heterogeneous Tumor Cell Population with Resensitization

In view of the emergence of specific traits (or resistance levels) as a response to cell density and mutations, it is of interest to consider mathematical models in which distinct levels of sensitivity are taken into account. We consider such a model with three subpopulations and transitions possible between all subpopulations. The model can be considered a continuous-time dynamical systems analogue of a discrete-time probabilistic model of an ergodic Markov chain. For such a model there exists a unique stationary distribution with the probabilities to be in a particular state all positive. In the model here the dynamics describes the evolution of the average number of cells in the compartments and there exists a well-defined steady-state distribution for the percentages. Interestingly, as there are more levels of sensitivity with resensitizations, in the optimal control problem lower time-varying dose rates given by singular controls always become candidates for optimality. This only is the case once a significant residuum of resistant cells had been created in the simpler 2-compartment model considered above.

3.3.1 A 3-Compartment Markov Chain Based Model for Tumor Heterogeneity

We consider a 3-compartment model for tumor heterogeneity labeling the compartments 'sensitive', 'partially sensitive', and 'resistant'. However, the terminology is only meant to indicate that these populations have distinctly different sensitivities toward a chemotherapeutic agent with the sensitive population having the highest and the resistant one the lowest. The underlying mathematical model again is a stochastic process (more specifically, an ergodic homogeneous continuous time Markov chain with transitions possible between all the states) and the states N_i, $i = 1,2,3$ denote the average number of cells in the sensitive, partially sensitive and resistant compartments, respectively. We assume that these populations grow at growth rates α_1, α_2 and α_3, respectively. In the absence of therapy, an ordering $\alpha_1 \geq \alpha_2 \geq \alpha_3$ would be consistent with the Norton-Simon hypothesis that a tumor consists of faster-growing populations of chemotherapeutically sensitive cells and slower-growing populations of increasingly more resistant cells [244, 245, 246]. Our analysis below equally applies to continuous constant (low-dose) therapies and in such a case the subpopulation with the strongest net growth rate actually may be the resistant one while other populations may experience negative growth rates as result of the treatment. We thus do not make any assumptions about the ordering of the growth rates.

One important aspect in the model is that transitions between the compartments are allowed. This includes the typical effects that sensitive cells can become increasingly more resistant, but also resensitizations are possible that make cells less resistant to the chemotherapeutic agent [115, 296]. We denote the transition rate from the ith into the jth compartment by ρ_{ij} and assume that all these rates are positive constants. This creates an ergodic structure in which all compartments are repeatedly visited by cells. Cell kill by a chemotherapeutic agent is expressed by the standard linear log-kill hypothesis: if we denote the concentration of the drug in the bloodstream by u, then the rate of cells eliminated is given by $\varphi_i u$, $i = 1,2,3$, with the coefficients φ_1, φ_2 and φ_3 representing the effectiveness of the drug on the sensitive, partially sensitive and resistant subpopulations, respectively. In view of the taken nomenclature we thus have that $\varphi_1 > \varphi_2 > \varphi_3 \geq 0$ and the case $\varphi_3 = 0$ corresponds to the situation of a fully resistant subpopulation R. Again we do not include the standard pharmacokinetic model on the agent here and treat u as the control of the system with maximum concentration given by $u_{\max}$. The controlled dynamics is then simply determined by the inflows and outflows from the various compartments and is given by the following 3-dimensional bilinear system:

$$\dot{N}_i = N_i \left(\alpha_i - \sum_{j \neq i} \rho_{ij} - \varphi_i u \right) + \sum_{j \neq i} N_j \rho_{ji}, \qquad N_i(0) = N_{i,0}, \qquad i = 1,2,3. \quad (3.16)$$

The initial conditions $N_{i,0}$, $i = 1,2,3$ are nonnegative, but not all zero. Admissible controls are Lebesgue measurable (respectively piecewise continuous) functions with values in a compact interval $[0,u_{\max}]$, $u : [0,T] \to [0,u_{\max}]$, $t \mapsto u(t)$.

Proposition 3.3.1. *The associated control system is positively invariant: for any admissible control u, the solution to equations (3.16) exists on the full interval* $[0,T]$ *and all components are positive for* $t \in (0,T]$.

Proof. The system (3.16) is a homogeneous linear system whose matrix has entries that are bounded Lebesgue measurable functions; thus solutions exist over the full interval $[0,T]$. Because of the ergodic nature of the underlying Markov chain, the solutions immediately become positive for $t > 0$: since not all initial conditions are zero, we have that $\dot{N}_i(0) > 0$ whenever $N_i(0) = 0$. Hence there exists an interval $(0,\varepsilon)$, $\varepsilon > 0$, so that all states are positive. Suppose there exists a component that would become zero at a positive time and let $\tau \geq \varepsilon$ denote the minimum of all times when one of the components N_i is zero. Since the solution cannot be identically zero, at least one of the remaining states must be positive. Hence $\dot{N}_i(\tau) = \sum_{j \neq i} N_j\,(\tau)\rho_{ji} > 0$. Contradiction. □

3.3.2 Steady-State Behavior of the Relative Proportions

The discrete-time analogue of the model formulated above is a homogeneous Markov chain with states S, P, and R and positive transition probabilities between each pair of states. Such a chain is ergodic and has a well-defined limiting stationary distribution for which all probabilities to be in a particular state are positive [135, 108]. The dynamical systems version has the same steady-state behavior: the proportions of cells in the respective compartments converge to a positive limit. Thus the dynamical system (3.16) again has a well-defined steady-state distribution for the proportions of cells in the compartments.

Let C denote the total number of cancer cells, $C = N_1 + N_2 + N_3$. We then have that

$$\dot{C} = (\alpha_1 - \varphi_1 u)N_1 + (\alpha_2 - \varphi_2 u)N_2 + (\alpha_3 - \varphi_3 u)N_3.$$

More generally, we consider a continuous administration of some chemotherapeutic agent at a constant low dose $u \equiv \text{const}$. Mathematically, the analysis reduces to considering the uncontrolled system by setting $\hat{\alpha}_i = \alpha_i - \varphi_i u$ and thus, without loss of generality, we consider the case $u \equiv 0$. Let x, y and z denote the proportions of the respective populations, i.e.,

$$x = \frac{N_1}{C}, \quad y = \frac{N_2}{C}, \quad \text{and} \quad z = \frac{N_3}{C}.$$

Since the system (3.16) is linear, the quotients x, y, and z obey Riccati equations and direct computations verify that

$$\dot{x} = x(\alpha_1 - \rho_{12} - \rho_{13}) + y\rho_{21} + z\rho_{31} - x(\alpha_1 x + \alpha_2 y + \alpha_3 z), \tag{3.17}$$
$$\dot{y} = x\rho_{12} + y(\alpha_2 - \rho_{21} - \rho_{23}) + z\rho_{32} - y(\alpha_1 x + \alpha_2 y + \alpha_3 z), \tag{3.18}$$
$$\dot{z} = x\rho_{13} + y\rho_{23} + z(\alpha_3 - \rho_{32} - \rho_{33}) - z(\alpha_1 x + \alpha_2 y + \alpha_3 z). \tag{3.19}$$

Let Σ denote the unit simplex in $\mathbb{R}^3$, i.e.,

$$\Sigma = \{(x,y,z) : x \geq 0, y \geq 0, z \geq 0, x+y+z = 1\}.$$

Theorem 3.3.1. *The unit simplex Σ is positively invariant for the dynamics (3.17)–(3.19) and there exists a unique equilibrium point (x_*, y_*, z_*) in Σ that is globally asymptotically stable, i.e., contains the entire simplex Σ in its region of attraction.*

This result establishes that there exists a well-defined steady state for the system of proportions. Its proof is a more involved technical application of Poincaré-Bendixson theory and is given in Section B.3 in Appendix B.

Corollary 3.3.1. *Suppose a chemotherapeutic agent is administered at a constant concentration u and let $(x_*, y_*, z_*) = (x_*(u), y_*(u), z_*(u))$ denote the corresponding steady state of the proportions. Asymptotically the total tumor population grows approximately exponentially at rate*

$$(\alpha_1 - \varphi_1 u)x_*(u) + (\alpha_2 - \varphi_2 u)y_*(u) + (\alpha_3 - \varphi_3 u)z_*(u).$$

Proof. It follows from the dynamics (3.16) that

$$\begin{aligned}\dot{C} &= (\alpha_1 - \varphi_1 u)N_1 + (\alpha_2 - \varphi_2 u)N_2 + (\alpha_3 - \varphi_3 u)N_3 \\ &= [(\alpha_1 - \varphi_1 u)x + (\alpha_2 - \varphi_2 u)y + (\alpha_3 - \varphi_3 u)z]C \\ &\simeq [(\alpha_1 - \varphi_1 u)x_*(u) + (\alpha_2 - \varphi_2 u)y_*(u) + (\alpha_3 - \varphi_3 u)z_*(u)]C.\end{aligned}$$

Hence the result follows. □

In principle, this growth rate can be made negative in the limit $u \to \infty$ if $\varphi_3 > 0$, but this may require unacceptably high doses. However, in case of an intrinsically resistant subpopulation, $\varphi_3 = 0$, this growth rate converges to $\alpha_3 > 0$ (see Figure 3.2). For, once the net growth rates $\alpha_1 - \varphi_1 u$ and $\alpha_2 - \varphi_2 u$ become negative, these populations die out and as $u \to \infty$ it follows that $x_*(u) \to 0$, $y_*(u) \to 0$ and $z_*(u) \to 1$.

We illustrate the dynamic behavior of the dynamical system (3.17)–(3.18) in Figure 3.3. In all four diagrams we have chosen the same transit rates given by $\rho_{12} = 4$, $\rho_{13} = 2$, $\rho_{21} = 1$, $\rho_{23} = 2$, $\rho_{13} = 0.5$ and $\rho_{12} = 0.25$. In diagram (a) (top, left), the growth rates for the respective compartments are $\alpha_1 = 10$, $\alpha_2 = 5$ and $\alpha_3 = 2$ while these rates are $\alpha_1 = -3$, $\alpha_2 = -1$ and $\alpha_3 = 2$ in diagram (b) (top, right). While these numbers are only for illustrative purposes, scenario (a) corresponds to an uncontrolled system with the sensitive cells the most strongly proliferating ones and the resistant population the slowest growing subpopulation. Diagram (b) then would be typical for a system under constant rate chemotherapy $u(t) = \text{const}$ that kills sensitive and partially sensitive cells—and in effect generates

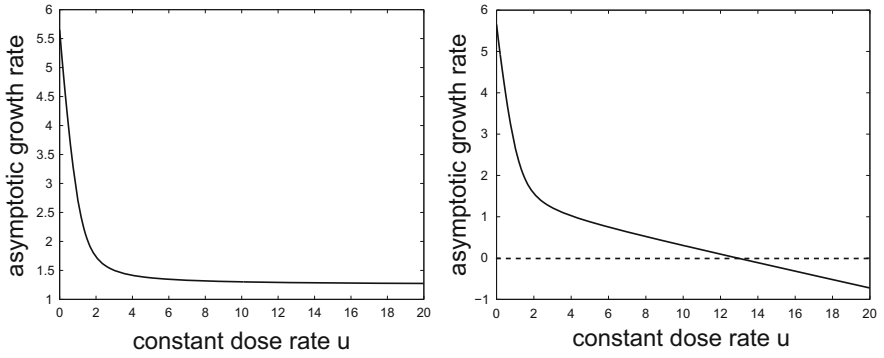

Fig. 3.2 Asymptotic growth rates as function of a constant concentration u for $\varphi_3 = 0$ (left) and $\varphi_3 > 0$ (right).

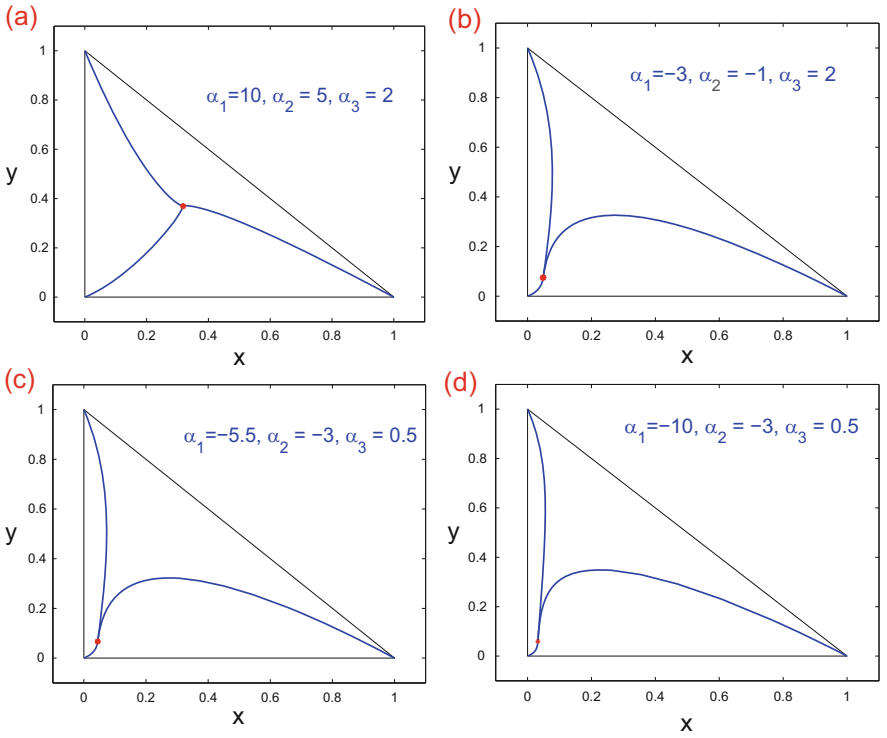

Fig. 3.3 Equilibrium point (x_*, y_*) of the system (3.17)–(3.18) and trajectories from the vertices of the unit simplex Σ. The growth rates are shown in the diagrams; the transit rates are the same in each case and are given by $\rho_{12} = 4$, $\rho_{13} = 2$, $\rho_{21} = 1$, $\rho_{23} = 2$, $\rho_{13} = 0.5$ and $\rho_{12} = 0.25$.

negative growth rates for these subpopulations—while it is assumed that the resistant subpopulation R is fully resistant. Observe how the equilibrium point shifts toward the origin which implies a strong dominance of the resistant subpopulation R. The approximate growth rates $\hat{\alpha}_1 x_* + \hat{\alpha}_2 y_* + \hat{\alpha}_3 z_*$ for the two cases are given by 5.6525 for scenario (a) and by 1.5320 for scenario (b). Thus, while such a chemotherapy dosing is able to reduce the growth, it cannot eliminate it. The reason is that we have $z_* = 0.8765$ in case (b) and coupled with $\hat{\alpha}_3 = 2$, this positive growth rate cannot be overcome by the decline in the other populations. It is only when one assumes that the agent can also reduce the growth rate of the resistant population that one sees lower overall growth rates. Yet, since $z_* \to 1$ as the effectiveness of the drug on the sensitive and partially resistant population becomes very high ($x_* \to 0$ and $y_* \to 0$), it is clear that the net growth rate $\hat{\alpha}_3$ of the resistant subpopulation becomes the determining factor. It is only when this rate becomes so small that it can be overcome by the decrease in the sensitive and resistant populations that the overall growth rate can be made negative. For example, this happens for $\alpha_1 = -10$, $\alpha_2 = -3$ and $\alpha_3 = 0.5$ in which case $(x_*, y_*, z_*) = (0.0322, 0.0598, 0.9080)$ and the overall growth rate is -0.0472. The corresponding diagram is shown in scenario (d) (bottom, right). Scenario (c) (bottom, left) shows another intermediate case for $\alpha_1 = -5.5$, $\alpha_2 = -3$ and $\alpha_3 = 0.5$ characterized by the fact that the overall growth rate of the total population is zero, i.e., the status quo is maintained.

3.3.3 *Chemotherapy as Optimal Control Problem and Singular Controls*

With the presence of a resistant subpopulation, eradication of the cancer by means of a particular chemotherapeutic agent generally is no longer possible. Nevertheless, the problem of how to schedule the chemotherapeutic agent to optimize its benefits remains. As before, we consider the following optimal control problem:

[Chet3] For a fixed therapy horizon $[0, T]$, minimize the objective

$$J(u) = rN(T) + \int_0^T qN(t) + u(t)dt \to \min \tag{3.20}$$

over all Lebesgue-measurable (respectively piecewise continuous) functions $u : [0, T] \to [0, u_{\max}]$ subject to the dynamics (3.16).

As before, we write the dynamics more compactly in matrix form as $\dot{N} = (A + uB)N$ with the matrices A and B given by

$$A = \begin{pmatrix} \alpha_1 - \rho_{12} - \rho_{13} & \rho_{21} & \rho_{31} \\ \rho_{12} & \alpha_2 - \rho_{21} - \rho_{23} & \rho_{32} \\ \rho_{13} & \rho_{23} & \alpha_3 - \rho_{31} - \rho_{32} \end{pmatrix}$$

and

$$B = \begin{pmatrix} -\varphi_1 & 0 & 0 \\ 0 & -\varphi_2 & 0 \\ 0 & 0 & -\varphi_3 \end{pmatrix}.$$

Formally, the necessary conditions for optimality are the same as for the 2-compartment model [Chet2]. If $u_* : [0,T] \to [0,u_{\max}]$ is an optimal control with corresponding trajectory N_*, then there exists a solution $\lambda = (\lambda_1, \lambda_2, \lambda_3) : [0,T] \to \left(\mathbb{R}^3\right)^*$ of the adjoint equation $\dot{\lambda} = -\lambda\,(A + u_* B) - q$, $\lambda(T) = r$ such that $u_*(t)$ minimizes the Hamiltonian

$$H = qN + u + \lambda\,(A + uB)N,$$

pointwise over the control set $[0,u_{\max}]$ along $(\lambda(t), N_*(t))$. In coordinates, the adjoint equations read

$$\begin{aligned}
\dot{\lambda}_1 &= -\frac{\partial H}{\partial N_1} = -q_1 - \lambda_1\,(\alpha_1 - \rho_{12} - \rho_{13} - \varphi_1 u) - \lambda_2 \rho_{21} - \lambda_3 \rho_{13}, \qquad \lambda_1(T) = r_1, \\
\dot{\lambda}_2 &= -\frac{\partial H}{\partial N_2} = -q_2 - \lambda_1 \rho_{12} - \lambda_2\,(\alpha_2 - \rho_{21} - \rho_{23} - \varphi_2 u) - \lambda_3 \rho_{23}, \qquad \lambda_2(T) = r_2, \\
\dot{\lambda}_3 &= -\frac{\partial H}{\partial N_3} = -q_3 - \lambda_1 \rho_{13} - \lambda_2 \rho_{23} - \lambda_3\,(\alpha_3 - \rho_{31} - \rho_{32} - \varphi_3 u), \qquad \lambda_3(T) = r_3.
\end{aligned}$$

and, as before, it follows that all multipliers remain positive.

Proposition 3.3.2. *The multipliers λ_i, $i = 1,2,3$ are positive over the interval $[0,T]$.*

The switching function Φ and its derivatives are as in Section 3.2.2 with the formula for the singular control given by (3.12):

$$u_{\text{sing}}(t) = -\frac{\{\lambda(t)[A,[A,B]] - q[A,B] - qBA\}N_*(t)}{\{\lambda(t)[B,[A,B]] - qB^2\}N_*(t)}.$$

Now we have the following formulas for the matrix products and commutators: B^2 is a diagonal matrix with entries φ_1^2 ,φ_2^2 and φ_3^2 and

$$BA = -\begin{pmatrix} \varphi_1(\alpha_1 - \rho_{12} - \rho_{13}) & \varphi_1\rho_{21} & \varphi_1\rho_{31} \\ \varphi_2\rho_{12} & \varphi_2(\alpha_2 - \rho_{21} - \rho_{23}) & \varphi_2\rho_{32} \\ \varphi_3\rho_{13} & \varphi_3\rho_{23} & \varphi_3(\alpha_3 - \rho_{31} - \rho_{32}) \end{pmatrix},$$

$$[A,B] = \begin{pmatrix} 0 & (\varphi_2 - \varphi_1)\rho_{21} & (\varphi_3 - \varphi_1)\rho_{31} \\ (\varphi_1 - \varphi_2)\rho_{12} & 0 & (\varphi_3 - \varphi_2)\rho_{32} \\ (\varphi_1 - \varphi_3)\rho_{13} & (\varphi_2 - \varphi_3)\rho_{23} & 0 \end{pmatrix},$$

$$[B,[A,B]] = -\begin{pmatrix} 0 & (\varphi_2 - \varphi_1)^2\rho_{21} & (\varphi_3 - \varphi_1)^2\rho_{31} \\ (\varphi_1 - \varphi_2)^2\rho_{12} & 0 & (\varphi_3 - \varphi_2)^2\rho_{32} \\ (\varphi_1 - \varphi_3)^2\rho_{13} & (\varphi_2 - \varphi_3)^2\rho_{23} & 0 \end{pmatrix},$$

and $[A,[A,B]]$ is a 3×3-matrix with full and complex entries. The diagonal terms of $[A,B]$ and $[B,[A,B]]$ vanish since B is a diagonal matrix which commutes with the diagonal part of whatever matrix the bracket is taken with. As before, the coefficient multiplying the control u in the second derivative of the switching function is given by

$$\frac{\partial}{\partial u}\frac{d^2}{dt^2}\frac{\partial H}{\partial u}(\lambda(t),N_*(t),u_*(t)) = \left\{\lambda(t)\,[B,[A,B]] - qB^2\right\}N_*(t).$$

The matrix $[B,[A,B]]$ has all nonpositive entries and since states N_* and multiplier λ are positive, we have that $\lambda(t)[B,[A,B]]N_*(t)\leq 0$. Furthermore,

$$qB^2N_*(t) = q_1\varphi_1^2N_1^*(t) + q_2\varphi_2^2N_2^*(t) + q_3\varphi_3^2N_3^*(t) > 0$$

and thus for this model the strengthened Legendre-Clebsch condition is always satisfied:

$$-\frac{\partial}{\partial u}\frac{d^2}{dt^2}\frac{\partial H}{\partial u}(\lambda(t),N_*(t),u_*(t)) > 0.$$

Proposition 3.3.3. *Singular controls are of order* 1 *and the strengthened Legendre-Clebsch condition for minimality is always satisfied.*

This result, coupled with some general results from optimal control in dimension 3 [103], implies that singular controls will be locally minimizing provided they (i) are admissible, i.e., that its values lie in the control set $[0,u_{\max}]$, and (ii) the corresponding multipliers λ_1, λ_2 and λ_3 are positive. While the upper limit $u_{\max}$ would be less restrictive on the level of dose rates (given the practically important bolus administrations or injections), in the model here the control really stands for the concentration of the agent and thus clearly there is saturation at some maximal feasible limit. In numerical computations, it is not difficult to verify admissibility of the singular control. Regarding (ii), the facts that the switching function and its derivative vanish along a singular arc, $\Phi(t) = 1+\lambda(t)BN_*(t)\equiv 0$ and $\dot{\Phi}(t) = \{\lambda(t)[A,B]-qB\}N_*(t)\equiv 0$, determine the multiplier λ modulo one degree of freedom. Since all components need to be positive, we can parameterize the solutions through $\lambda_3(t)>0$ and solve for $\lambda_1(t)$ and $\lambda_2(t)$. If one of these variables comes out negative, the positivity condition is violated and no singular arc exists through the given point $N_*(t)$. Otherwise, this solution determines the singular control.

Overall, possible concatenations between bang and singular controls need to be analyzed. In general, this becomes difficult for this model (mainly because of the great variety of parameters and possible sign relations between them) and this analysis has not yet been carried out. However, we can illustrate the structure of singular controls and corresponding trajectories with some numerical samples. In Figure 3.4 we give an example of an extremal controlled trajectory (i.e., a trajectory that satisfies the necessary conditions for optimality of the Pontryagin maximum principle) for which the control is given by the maximum dose rate for an initial interval $[0,\tau_b]$ and then by an admissible singular control over the remaining period $[\tau_b,T]$. Ignoring the terminal value, we simply determine a value for $\lambda(\tau_b)$ so that

$\Phi(\tau_b) = \dot{\Phi}(\tau_b) = 0$ and then integrate the combined flow of the system dynamics and adjoint equation corresponding to the singular control forward in time until time T. As long as the multipliers $\lambda_i(t)$, $i = 1,2,3$ remain positive for $t \in [0,T]$, this generates an extremal for the optimal control problem [Chet3] with penalty terms $r_i = \lambda_i(T)$. But this construction is only meant to illustrate the singular control and its flow. In the medical literature, similar control structures are also known as chemo-switch protocols [16, 277].

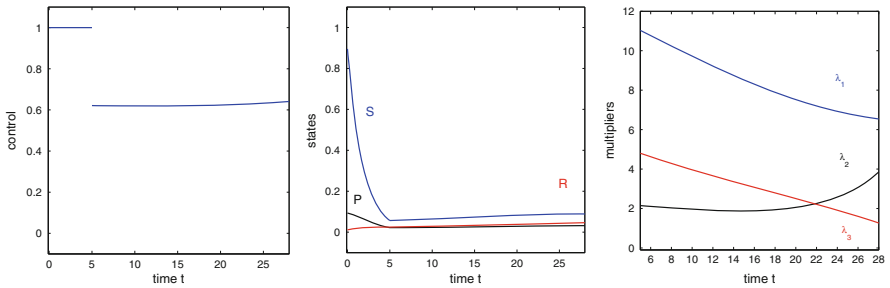

Fig. 3.4 Control, states, and multipliers for a bang-singular controlled extremal.

Figure 3.4 illustrates the structure of a chemo-switch type protocol for the growth rates $\alpha_1 = 1$, $\alpha_2 = 0.5$ and $\alpha_3 = 0.1$, transition rates $\rho_{12} = 0.05$, $\rho_{13} = 0.01$, $\rho_{12} = 0.03$, $\rho_{23} = 0.01$, $\rho_{31} = 0.01$ and $\rho_{32} = 0.03$, and pharmacodynamic coefficients $\varphi_1 = 1.5$, $\varphi_2 = 1$ and $\varphi_3 = 0.1$; the maximum concentration was normalized to $u_{\max} = 1$ and all the weights q_i in the objective were chosen equal to 0.01. The initial interval with maximum dose has length $\tau_b = 5$ and the therapy horizon is $T = 28$. We also normalized the total cancer volume at the initial time to be $C(0) = 1$ and took as initial condition the corresponding steady state of the proportions for the uncontrolled dynamics, i.e., $S_0 = x_* = 0.8954$, $P_0 = y_* = 0.0933$ and $R_0 = z_* = 0.0112$. Figure 3.4(a) (top, left) shows the graph of the corresponding control and 3.4(b) (top, left) shows the graphs of the corresponding states. The value of the singular control $u_{\text{sing}}(t)$ is almost constant at about 60% of the maximum, but it increases slightly over the interval $[5,28]$. The multipliers over the singular interval are shown in part (c) (bottom) and remain positive. It then follows from Proposition 3.3.2 that they are positive on the initial interval as well.

3.3.4 Concluding Remarks

These calculations, although clearly incomplete, nevertheless point to an increased likelihood that singular controls, i.e., time-varying concentrations and dose rates at less than the maximum rate, become increasingly more important when tumor heterogeneity is incorporated into the mathematical model for administration of chemotherapy. This would seem to be intuitive from a cost-benefit type analysis, but

interestingly this is not supported by the results if only drug sensitive and resistant populations are considered and the resistant cell population does not have a mechanism of resensitization. In this case, optimal protocols still follow an MTD schedule. However, as the degree of heterogeneity is increased, the interplay between the various subpopulations makes singular controls and the lower dose administration schedules they represent a viable option. There is an interesting approach to chemotherapy called *adaptive therapy* due to Gatenby et al. [102] that is based on the competitive balance between various tumor subpopulations and also aims to strike a balance between killing the drug sensitive and generally faster growing populations with using them to control the more dangerous resistant, but generally slower growing populations. This is an intriguing idea that also would seem to call for alternative properly calibrated lower dose rates other than MTD administrations that kill as many of the sensitive cells as possible.

Chapter 4
Optimal Control for Problems with a Quadratic Cost Functional on the Therapeutic Agents

In this chapter, we give optimal solutions for systems with a control-affine dynamics (c.f., Section A.3 in Appendix A) when the dependence on the control in the objective is taken as a positive definite quadratic function. The mathematical advantages of such a formulation are obvious: the Hamiltonian H for the optimal control problem becomes strictly convex in the control u and thus has a unique minimizer, albeit only in the state-multiplier space (cotangent bundle). While this does not guarantee that controls found by an analysis of these necessary conditions are necessarily optimal, it considerably simplifies the analysis. However, as already mentioned, a quadratic functional form often is somewhat questionable and may be difficult to justify for biomedical problems. The prevalence of such models has its origin in an abundance of classical problems related to mechanical or electro-dynamical systems when such a term has a clear and justified connection with the kinetic energy of the system. If such a connection is not there—as it is lacking in the case of drug treatments—usually other, and often arbitrary "systemic" cost arguments are put forward to justify the choice. But such reasoning rarely is based on the underlying biology of the problem. Yet, the choice of the objective functional is crucial for the structure of optimal controls and indeed many properties of the optimal solutions are preordained by making this particular choice. For example, it is easily seen that optimal controls are continuous in this L_2-type framework. Thus, overall care needs to be exercised when interpreting the results. Despite these modeling shortcomings, there exists an abundance of literature on optimal control problems for biomedical problems that employ quadratic terms in the controls. We therefore include a brief analysis of such models, but use a more general form for the dynamics that applies to a multitude of systems.

The analysis of the necessary conditions for optimality of the maximum principle is straightforward and an explicit formula for the control as a function of the states and multipliers can be written down. There exist ample numerical methods that will compute an extremal controlled trajectory by solving the resulting two-point boundary problem on states and multipliers, most of them based on some kind of shooting

H. Schättler, U. Ledzewicz, *Optimal Control for Mathematical Models of Cancer Therapies*, Interdisciplinary Applied Mathematics 42,
DOI 10.1007/978-1-4939-2972-6_4

algorithms. But it is often overlooked that despite the quadratic and strictly convex structure in the control variable, in general a solution to these conditions need not be optimal, not even locally.[1] Unfortunately, this is a fact ignored in many publications on applications to biologically motivated problems. In this section, we provide a framework that allows to verify sufficient conditions for local optimality for such problems. We use a general control-affine nonlinear dynamics in the state, simply since there is no significant mathematical difference when compared to the bilinear models considered so far, and since there exist many models that fall into this more general category. For example, this includes models for cancer chemotherapy when more complicated expressions for pharmacodynamics than the typical log-kill framework are used. Similarly, kinetic models using a Michaelis-Menten structure in the dynamics are typical in models for the treatment of HIV infections (e.g., see [157, 159, 300]) or in epidemiological models (e.g., see [35, 101, 125]). Despite the widely differing underlying areas of application, the mathematical structure is uniform and this is what will be presented here. In the last section of this chapter, as an additional example, we present an alternative model for cancer chemotherapy due to Fister and Panetta [83] that puts the side effects of treatment center stage by focussing on the bone marrow dynamics. It perfectly fits into the class of models analyzed so far and we use it to compare the optimal solutions corresponding to L_1 and L_2-type objectives.

4.1 Optimal Control with an L_2-type Cost Functional on the Controls

4.1.1 Problem Formulation

We consider a general control affine, time-invariant dynamical system of the form

$$\dot{x} = f(x) + \sum_{j=1}^{m} u_j g_j(x), \qquad x(0) = x_0, \tag{4.1}$$

over a fixed finite interval $[0, T]$, the therapy horizon. We assume that the state $x \in \mathbb{R}^n$ takes values in some open subset $\mathbb{P} \subset \mathbb{R}^n$ which represents the admissible states for the problem (e.g., points with positive coordinates) and that $\mathbb{P}$ is positively invariant for the control system. This property will need to be verified for the specific model under consideration, but generally amounts to no more than a rudimentary first question of proper modeling. Admissible controls $u = (u_1, \ldots, u_m)$ are Lebesgue measurable (respectively piecewise continuous) functions whose components take values

[1] We refer the interested reader to the discussions of conjugate points and singularities in the value function of an optimal control problem in Chapter 5 of our monograph [292]. Essentially, if the flow of extremals has a singularity, local optimality ceases. Simple mathematical examples to this effect are given in [292].

in a compact interval $[0,u_j^{\max}] \subset \mathbb{R}$, $u_j : [0,T] \to [0,u_j^{\max}]$ and we again denote the full control set by U, $U = [0,u_1^{\max}] \times \ldots \times [0,u_m^{\max}] \subset \mathbb{R}^m$. This control set is an interval in $\mathbb{R}^m$ and we acknowledge that this fact simplifies the technical aspects of the mathematical analysis. However, at the expense of more technical formulations, the results developed in this chapter can be generalized to control sets that are compact convex polyhedra. For the problems that interest us here, control sets which are intervals are the most natural formulation and thus we use this simpler structure. If the solution x to the initial value problem (4.1) corresponding to an admissible control u exists over the full interval $[0,T]$, we associate to the controlled trajectory (x,u) the objective

$$J(u) = \int_0^T \left(L(x(t)) + \frac{1}{2} \sum_{j=1}^{m} \theta_j u_j^2(t) \right) dt + \varphi(x(T)). \tag{4.2}$$

with the coefficients θ_j positive weights. The quadratic term has the form $\frac{1}{2} u^T R u$ with R the *diagonal* matrix $R = \operatorname{diag}(\theta_1, \ldots, \theta_n)$. This also leads to a simplification of the technical argument which, more generally, could be carried out for a positive definite matrix R. These procedures are well known in automatic control (e.g., see [41, 292]), but our interest here is to keep technicalities at a minimum. The drift vector field f, $f : \mathbb{P} \to \mathbb{R}^n$, the control vector fields g_j, $g_j : \mathbb{P} \to \mathbb{R}^n$, $j = 1, \ldots, m$, the Lagrangian L, $L : \mathbb{P} \to \mathbb{R}$, and the penalty function φ, $\varphi : \mathbb{P} \to \mathbb{R}$, all are assumed to be twice continuously differentiable functions on $\mathbb{P}$. No constraints are imposed at the terminal times. We then simply phrase the corresponding optimal control problem in the following form:

[Q] minimize the objective $J(u)$ over all admissible controlled trajectory pairs $(x,u) : [0,T] \to \mathbb{P} \times U$.

4.1.2 Necessary Conditions for Optimality

Once more, necessary conditions for optimality for problem [Q] are given by the Pontryagin maximum principle (Theorem A.2.1 in Appendix A). It is easily seen that extremals are normal and therefore, without loss of generality, we normalize the multiplier at the objective to $\lambda_0 = 1$. Thus, if $u_* = (u_1^*, \ldots, u_m^*)^T$ is an optimal control with corresponding trajectory x_*, then it follows that there exists an absolutely continuous function λ, again written as a row-vector, $\lambda : [0,T] \to (\mathbb{R}^n)^*$, that satisfies the adjoint equation

$$\dot{\lambda}(t) = -\frac{\partial L}{\partial x}(x_*(t)) - \lambda(t) \left(\frac{\partial f}{\partial x}(x_*(t)) + \sum_{j=1}^{m} u_j^*(t) \frac{\partial g_j}{\partial x}(x_*(t)) \right) \tag{4.3}$$

with terminal condition

$$\lambda(T) = \frac{\partial \varphi}{\partial x}(x_*(T)), \tag{4.4}$$

such that the optimal controls u_j^* minimize the Hamiltonian

$$H = H(\lambda, x, u) = L(x) + \lambda f(x) + \sum_{j=1}^{m} \left(\frac{1}{2}\theta_j u_j^2 + \lambda u_j g_j(x) \right) \tag{4.5}$$

pointwise over the control set $U = [0, u_1^{\max}] \times \ldots \times [0, u_m^{\max}]$ along $(\lambda(t), x_*(t))$. We recall that $\frac{\partial f}{\partial x}$ denotes the $n \times n$ matrix with (i, j) entry given by $\frac{\partial f_i}{\partial x_j}$, i.e., the ith row is given by the gradient of the ith entry of the vector field f. Similarly, $\frac{\partial L}{\partial x}$ is the gradient of the function L written as a row vector.

The essential difference of this formulation to the ones considered previously is that the Hamiltonian function H, when considered as a function of the control vector u, has a positive definite Hessian matrix,

$$\frac{\partial^2 H}{\partial u^2}(\lambda, x, u) = \begin{pmatrix} \theta_1 & 0 & \cdots & 0 & 0 \\ 0 & \theta_2 & \cdots & 0 & 0 \\ \vdots & \vdots & \ddots & \vdots & \vdots \\ 0 & 0 & \cdots & \theta_{m-1} & 0 \\ 0 & 0 & \cdots & 0 & \theta_m \end{pmatrix} = \operatorname{diag}(\theta_1, \ldots, \theta_m) > 0.$$

This property implies that every stationary point in u is a strict local minimizer of the Hamiltonian H in the control. In the engineering literature on optimal controls such extremals are called nonsingular [41]. The terminology singular in the context of singular controls considered in Chapters 2 and 3 has its historical origin precisely in the fact that for those problems this matrix is singular; in fact, for an L_1-type formulation with a linear term in the control, the matrix $\frac{\partial^2 H}{\partial u^2}(\lambda, x, u)$ becomes identically zero and it is this fact that makes the mathematical analysis far more challenging. But for the problem under consideration here, the Hamiltonian H is strictly convex over $\mathbb{R}^m$ and has a unique minimum that is attained at the stationary point,

$$0 = \frac{\partial H}{\partial u}(\lambda, x, u) = (\theta_1 u_1 + \lambda g_1(x), \ldots, \theta_m u_m + \lambda g_m(x)).$$

Since the control set U is a product of m intervals, $U = [0, u_1^{\max}] \times \ldots \times [0, u_m^{\max}]$, this minimization problem can be solved componentwise and the minimum for the jth component over $\mathbb{R}$ is attained at

$$\psi_j(t) = -\frac{1}{\theta_j}\lambda(t) g_j(x_*(t)). \tag{4.6}$$

If this value lies in the control interval $[0, u_j^{\max}]$, it is admissible and then this formula defines the global minimum. If $\psi_j(t)$ is negative, then the Hamiltonian is strictly increasing for positive values u_j and the minimum over the interval $[0, u_j^{\max}]$ is attained for $u_j^* = 0$ while the Hamiltonian is strictly decreasing over this interval if $\psi_j(t) > u_j^{\max}$ and in this case the minimal value is attained for $u_j^{\max}$. Hence, an evaluation of the minimum condition leads to the following relations:

$$u_j^*(t) = \begin{cases} 0 & \text{if } \psi_j(t) \le 0, \\ \psi_j(t) & \text{if } 0 \le \psi_j(t) \le u_j^{\max}, \\ u_j^{\max} & \text{if } u_j^{\max} \le \psi_j(t). \end{cases} \tag{4.7}$$

Defining the saturation function sat_j as

$$\mathrm{sat}_j(u) = \min\left\{u_j^{\max}, \max\{0,u\}\right\} = \begin{cases} 0 & \text{if } u \le 0, \\ u & \text{if } 0 \le u \le u_j^{\max}, \\ u_j^{\max} & \text{if } u \ge u_j^{\max}, \end{cases}$$

we can formally express the optimal controls u_j^* in the compact form

$$u_j^*(t) = \mathrm{sat}_j\left(\psi_j(t)\right). \tag{4.8}$$

Optimal controls thus change continuously between the constant values 0 and $u_j^{\max}$ at the boundary of the control interval and differentiable functions which take values in the interior of the control set. We call a time when one of the controls changes from an interior value to a boundary value a *junction*. The functions ψ_j, similar to the switching functions for an L_1-type objective, determine the optimal control and we call them the *indicator functions* for the controls. Like the derivatives of the switching functions in the case of an L_1-type objective, the derivative of ψ_j is computed using the dynamics and adjoint equation and is given by

$$\dot{\psi}_j(t) = -\frac{1}{\theta_j}\left\{\lambda_*(t)\left([f,g_j]\left(x_*(t)\right) + \sum_{i\neq j} u_i(t)\left[g_i,g_j\right]\left(x_*(t)\right)\right) - \frac{\partial L}{\partial x}L(x_*(t))g_j\left(x_*(t)\right)\right\} \tag{4.9}$$

with

$$[f,g](x) = Dg(x)f(x) - Df(x)g(x)$$

denoting the Lie bracket of two vector fields f and g (c.f., Definition A.3.3 in Appendix A). Since the controls remain continuous at junction points, it follows that ψ_j is continuously differentiable. Between junction points, ψ_j can be differentiated further to whatever order the smoothness properties of the dynamics and Lagrangian L allow, but higher order derivatives generally have different left and right limits at junction points. Because of the quadratic nature of the objective, it therefore follows that bang-bang controls are no longer optimal. We summarize these comments in the theorem below.

Theorem 4.1.1 (Maximum Principle for Problem [Q]). *Suppose $u_* = (u_1^*,\ldots,u_m^*)$ is an optimal control for problem $[Q]$ with corresponding trajectory x_*. Then there exists an absolutely continuous function λ, $\lambda : [0,T] \to (\mathbb{R}^n)^*$, that satisfies the adjoint equation*

$$\dot{\lambda}(t) = -\frac{\partial L}{\partial x}(x_*(t)) - \lambda(t)\left(\frac{\partial f}{\partial x}(x_*(t)) + \sum_{j=1}^{m} u_j^*(t)\frac{\partial g_j}{\partial x}(x_*(t))\right),$$

with terminal value $\lambda(T) = \frac{\partial \varphi}{\partial x}(x_*(T))$ *so that the optimal controls satisfy*

$$u_j^*(t) = \mathrm{sat}_j(\psi_j(t)) = \mathrm{sat}_j\left(-\frac{1}{\theta_j}\lambda(t)g_j(x_*(t))\right).$$

The Hamiltonian H is constant over the interval $[0,T]$, $H(\lambda(t), x_*(t), u_*(t)) = \mathrm{const.}$

4.1.3 *Sufficient Conditions for Strong Minima: Construction of a Field of Broken Extremals with Regular Simple Junctions*

The advantage of the quadratic model is that it provides a unique minimizer for the Hamiltonian function. But this only gives an expression for the control that depends on the multiplier λ and does not determine the control completely since there may exist more than one solution to the two point boundary value problem consisting of the dynamics (4.1) and adjoint equation (4.3) coupled by the minimum condition (4.8). Hence there is no a priori guarantee that a numerically computed solution that satisfies the conditions of Theorem 4.1.1 is even locally optimal (e.g., see [292, Sections 5.4 and 5.5]). In this section, we formalize sufficient conditions for strong local optimality of an extremal controlled reference trajectory for the problem [Q]. The constructions are similar to those for the 2-compartment model of Section 2.1.6 that are carried out in Section B.1. A more detailed exposition of the theoretical background is given in Appendix A.

Definition 4.1.1 (Regular Simple Junction). Let (x_*, u_*) be a reference extremal for problem [Q] and denote the corresponding adjoint variable by λ_*. A time $\tau \in (0,T)$ is called a junction time if a component of the control changes between a boundary value (given by 0 or $u_j^{\max}$) and the interior control ψ_j. A junction time is said to be simple if exactly one component of the control vector changes. A simple junction τ is said to be regular if the derivative of the associated indicator function ψ_j for the control that switches, $j = j(\tau)$, does not vanish, $\dot{\psi}_j(\tau) \neq 0$.

Regular simple junction times are the typical (in the sense of most common) scenario and we do not consider the more intricate case of simultaneous junctions. We call an extremal triple $\Gamma = (x_*, u_*, \lambda_*)$ for problem [Q] an extremal lift with *regular simple junctions* if it only has a finite number of junction times and if each junction is simple and regular. Under these conditions, it is rather straightforward to construct a parameterized family of broken extremals $(x(\cdot,p), u(t\cdot,p), \lambda(\cdot,p))$ with regular simple junctions that contains the reference extremal Γ: for values p in a sufficiently small neighborhood P of $p_* = x_*(T)$, integrate the dynamics and

the adjoint equation backward from the terminal time T with terminal conditions $x(T,p) = p$ and $\lambda(T,p) = \frac{\partial \varphi}{\partial x}(p)$ while choosing the control $u(t,p)$ to satisfy (4.8). Specifically,

$$\dot{x}(t,p) = f(x(t,p)) + \sum_{j=1}^{m} u_j(t,p) g_j(x(t,p)), \tag{4.10}$$

$$\dot{\lambda}(t,p) = -\frac{\partial L}{\partial x}(x(t,p)) - \lambda(t,p)\left(\frac{\partial f}{\partial x}(x(t,p)) + \sum_{j=1}^{m} u_j(t,p)\frac{\partial g_j}{\partial x}(x(t,p))\right), \tag{4.11}$$

$$u_j(t,p) = \mathrm{sat}_j\left(-\frac{1}{\theta_j}\lambda(t,p) g_j(x(t,p))\right) \tag{4.12}$$

with terminal values

$$x(T,p) = p \qquad \text{and} \qquad \lambda(T,p) = \frac{\partial \varphi}{\partial x}(p). \tag{4.13}$$

Proposition 4.1.1. *Let $\Gamma_* = (x(\cdot,p_*), u(\cdot,p_*), \lambda(\cdot,p_*))$ be an extremal lift with simple regular junctions at times t_i, $i = 1,\dots,k$, $0 = t_0 < t_1 < \cdots < t_k < t_{k+1} = T$. Then there exists a neighborhood P of p_* and continuously differentiable functions τ_i defined on P, $i = 1,\dots,k$, such that for $p \in P$ the control $u(\cdot,p)$ has regular simple junctions at the times $0 < \tau_1(p) < \cdots < \tau_k(p) < T$ of the same type as the reference control u_*. The corresponding family $\Gamma_p = (x(\cdot,p), u(\cdot,p), \lambda(\cdot,p))$ for $p \in P$ is a parameterized family of broken extremals with regular simple junctions.*

Proof. We inductively define the controls $u = u(t,p)$, trajectories $x = x(t,p)$ and multipliers $\lambda = \lambda(t,p)$ backward from the terminal time. For all p in some open neighborhood P of p_* and $t \le T$, let $x(t,p)$ and $\lambda(t,p)$ denote the solutions to equations (4.10) and (4.11) with terminal conditions (4.13) when the control $u = u(t,p)$ is given by the same structure as the reference control $u(t,p_*)$ on the last interval $[t_k, T]$. That is, for $j = 1,\dots,m$, we choose $u_j(t,p)$ constant and with the same value as $u_j^*(t)$ if the jth component of $u_j^*(t)$ is constant and we define

$$u_j(t,p) = -\frac{1}{\theta_j}\lambda(t,p) g_j(x(t,p)) = \psi_j(t,p)$$

if $u_j^*(t)$ is given by the interior value $\psi_j(t,p_*)$. For values p close enough to $p_* = x_*(T)$, by the continuous dependence of solutions on initial data and parameters, these solutions exist on an interval $[t_k - \varepsilon, T]$ for some $\varepsilon > 0$. Let $j = j(k)$ denote the component of the reference control that has a junction at time t_k. Then, again by keeping the neighborhood P of p_* small enough, we can guarantee that none of the controls $u_i(t,p)$ for $i \neq j$ has a junction over the interval $[t_k - \varepsilon, T]$ and thus the only change in the control occurs in the jth component. For sake of specificity, suppose the jth control changes from an interior value to $u_j^{\max}$. Since $\dot{\psi}_j(t_k,p_*) \neq 0$, by the implicit function theorem the equation $\psi_j(t,p)) = u_j^{\max}$ can be solved for t by a

continuously differentiable function $\tau_k = \tau_k(p)$ near p_* and, because of continuity, this function defines a regular junction for the jth component while no switchings in the other components occur. Thus we adjust the jth component at this hypersurface as for the reference control and then simply iterate the construction. □

The triples $\Gamma_p = (x(\cdot,p), u(\cdot,p), \lambda(\cdot,p))$ define a parameterized family of broken extremals (c.f., Definitions A.4.6 and A.4.8 in Appendix A), that is, they satisfy all the necessary conditions for optimality of the maximum principle and are differentiable functions of the parameter between the junction times. The associated flow map for the controlled trajectories is defined as

$$F : (t,p) \mapsto F(t,p) = (t, x(t,p)), \tag{4.14}$$

and we need to determine whether F is locally a diffeomorphism along the reference trajectory $t \mapsto x_*(t) = x(t,p_*)$. Since we are considering an optimal control problem with a fixed terminal time T—in the terminology from [292] the problem is time-dependent—in this flow map the graphs of the controlled trajectories need to be considered. Essentially, the question of local optimality reduces to the question whether this flow map F is locally a diffeomorphism along the reference trajectory $t \mapsto x_*(t) = x(t,p_*)$. For, it is shown in a more general setting in [292] (also see Section A.4.2) that the reference trajectory Γ_* provides a strong local minimum if *(i) the flow map F is a diffeomorphism on the segments between the junction times t_i* and if *(ii) all junction surfaces are transversal crossings*. For problem [Q], one simplification that occurs is that because controls remain continuous at junction times, all junction surfaces indeed are transversal crossings and thus condition (ii) is always satisfied. If the flows between the junction surfaces are diffeomorphisms, then a continuously differentiable solution to the Hamilton-Jacobi-Bellman equation can be constructed on the region covered by the flow F of extremals in the family by taking the cost along the extremals. From this the desired optimality statements follow by classical results (Theorem A.4.3 and Corollary A.4.2 in Appendix A). Thus it only remains to check inductively whether the flows between the switching surfaces are diffeomorphisms. In the special case when all the controls are constant, (i.e., none of the controls takes values in the interior of the control interval), this simply is a consequence of the uniqueness of solutions to the dynamical system (4.10) and (4.11). However, if one or more of the controls take values that lie in the interior of the interval associated with these controls, then this forms a true requirement. We briefly develop the necessary theory.

The mapping $F : (t,p) \mapsto F(t,p) = (t, x(t,p))$ is a local diffeomorphism along the reference trajectory $t \mapsto x(t,p_*)$ on the interval $[t_i, t_{i+1}]$ if and only if the matrix $\frac{\partial x}{\partial p}(t,p_*)$ is nonsingular on the interval $[t_i, t_{i+1}]$. This is equivalent to the statement that the matrix

$$S_*(t) = \frac{\partial \lambda^T}{\partial p}(t,p_*) \left(\frac{\partial x}{\partial p}(t,p_*) \right)^{-1} \tag{4.15}$$

is well defined on $[t_i, t_{i+1}]$. Recall that, $\frac{\partial x}{\partial p}$ denotes the $n \times n$ matrix with (i,j) entry given by $\frac{\partial x_i}{\partial p_j}$, i.e., the ith row is given by the gradient of x_i. Similarly, the ith row

of $\frac{\partial \lambda^T}{\partial p}$ is given by the gradient of λ_i and the transpose is taken since λ is a row vector. The partial derivatives $\frac{\partial x}{\partial p}(t,p)$ and $\frac{\partial \lambda^T}{\partial p}(t,p)$ are solutions of the *variational equations* of (4.10) and (4.11). Formally, these equations are obtained by differentiating equations (4.10) and (4.11) with respect to p and interchanging the partial derivatives [145]. We briefly derive these equations. For this calculation it is more convenient to write the adjoint equation in terms of the column vector λ^T since this leads to a uniform structure for the second derivatives. We therefore express equations (4.10) and (4.11) in the form

$$\dot{x}(t,p) = \left(\frac{\partial H}{\partial \lambda^T}(\lambda^T(t,p), x(t,p), u(t,p)) \right)^T$$

and

$$\dot{\lambda}^T(t,p) = \left(-\frac{\partial H}{\partial x}(\lambda^T(t,p), x(t,p), u(t,p)) \right)^T,$$

with each differential equation written in column form. We consistently write gradients with respect to column vectors as row vectors and therefore need to include the transposes on the right. Equivalently, we could write gradients with respect to row vectors (such as λ) as column vectors. This is the same as differentiating with respect to the column vector λ^T and then taking the transpose, i.e., the column vector $\frac{\partial H}{\partial \lambda}$ is given by $\frac{\partial H}{\partial \lambda} = \left(\frac{\partial H}{\partial \lambda^T} \right)^T$,

$$\frac{\partial H}{\partial \lambda} = f(x) + \sum_{j=1}^{m} u_j g_j(x).$$

When differentiating the Hamiltonian H twice with respect to column vectors (x, u, or λ^T), we write the corresponding matrices of second derivatives with the components of the first vector as row indices and the components of the second vector as column indices. Thus, the (i,j) entry of $\frac{\partial^2 H}{\partial x \partial u}$ is given by $\frac{\partial^2 H}{\partial x_i \partial u_j}$. In other words, differentiating the n-dimensional column vector $H_x^T = \left(\frac{\partial H}{\partial x} \right)^T$ with respect to u, we get the $n \times m$ matrix whose row vectors are the u-gradients of the components of the column vector H_x^T. We denote this matrix by H_{xu}. In particular, under our general differentiability assumptions the mixed partial derivatives are equal and we have that $H_{xu} = H_{ux}^T$. If one of the derivatives is taken with respect to the row vector λ, we follow this convention for the column vector λ^T. Thus $H_{\lambda^T x}$ is the matrix whose (i,j) entry is given by $\frac{\partial^2 H}{\partial \lambda_i \partial x_j}$ while $H_{x\lambda^T}$ is the matrix with (i,j) entry $\frac{\partial^2 H}{\partial x_i \partial \lambda_j}$, so that $H_{\lambda^T x} = (H_{x\lambda^T})^T$. Hence $H_{\lambda^T x}$ is the matrix whose rows are given by the gradients with respect to x of the column vector $H_\lambda = \left(\frac{\partial H}{\partial \lambda^T} \right)^T$, i.e.,

$$H_{\lambda^T x} = \frac{\partial H_\lambda}{\partial x} = \frac{\partial f}{\partial x}(x) + \sum_{j=1}^{m} u_j \frac{\partial g_j}{\partial x}(x) \tag{4.16}$$

and

$$\begin{aligned} H_{x\lambda^T} &= \left(\frac{\partial}{\partial \lambda^T}\left(H_x^T\right)\right) \\ &= \frac{\partial}{\partial \lambda^T}\left[\lambda\left(\frac{\partial f}{\partial x}(x)+\sum_{j=1}^{m} u_j \frac{\partial g_j}{\partial x}(x)\right)+\frac{\partial L}{\partial x}(x)\right]^T \\ &= \left(\frac{\partial f}{\partial x}(x)+\sum_{j=1}^{m} u_j \frac{\partial g_j}{\partial x}(x)\right)^T = (H_{\lambda^T x})^T . \end{aligned} \tag{4.17}$$

Analogously we have that

$$H_{\lambda^T u} = \frac{\partial H_\lambda}{\partial u} = (g_1(x),\ldots,g_m(x)) \tag{4.18}$$

and

$$\begin{aligned} H_{xu} &= \left(\frac{\partial}{\partial u}\left(H_x^T\right)\right) \\ &= \frac{\partial}{\partial u}\left[\left(\frac{\partial L}{\partial x}(x)\right)^T+\left(\frac{\partial f}{\partial x}(x)+\sum_{j=1}^{m} u_j \frac{\partial g_j}{\partial x}(x)\right)^T \lambda^T\right] \\ &= \left(\left(\frac{\partial g_1}{\partial x}(x)\right)^T \lambda^T,\ldots,\left(\frac{\partial g_m}{\partial x}(x)\right)^T \lambda^T\right). \end{aligned} \tag{4.19}$$

In the subsequent computations x, u, λ and their partial derivatives are evaluated at (t,p), partial derivatives of f and the g_i are evaluated along the controlled trajectories of the family, $(x(t,p),u(t,p))$, and all partial derivatives of H are evaluated along the full extremals, $(\lambda(t,p),x(t,p),\, u(t,p))$. For notational clarity, however, we drop these arguments. The matrix $\frac{\partial x}{\partial p}(t,p)$ of the partial derivatives with respect to the parameter p is the solution of the variational equation of the dynamics, i.e., formally

$$\begin{aligned} \frac{d}{dt}\left(\frac{\partial x}{\partial p}\right) &= \frac{\partial^2 x}{\partial t \partial p} = \frac{\partial}{\partial p}\left(\frac{dx}{dt}\right) \\ &= \frac{\partial}{\partial p}\left(\frac{\partial H}{\partial \lambda^T}(\lambda^T(t,p),x(t,p),u(t,p))\right)^T \\ &= H_{\lambda^T x}\frac{\partial x}{\partial p}+H_{\lambda^T u}\frac{\partial u}{\partial p}, \end{aligned} \tag{4.20}$$

(Since H is linear in λ, it follows that $H_{\lambda^T \lambda^T} \equiv 0$.) The equation for the partial derivative $\frac{\partial \lambda^T}{\partial p}$ follows by differentiating the adjoint equation:

$$\begin{aligned}\frac{d}{dt}\left(\frac{\partial\lambda^T}{\partial p}\right) &= \frac{\partial^2\lambda^T}{\partial t\partial p} = \frac{\partial}{\partial p}\left(\dot{\lambda}^T\right)\\ &= \frac{\partial}{\partial p}\left\{\left(-\frac{\partial H}{\partial x}(\lambda^T(t,p),x(t,p),u(t,p))\right)^T\right\}\\ &= -H_{x\lambda^T}\frac{\partial\lambda^T}{\partial p} - H_{xx}\frac{\partial x}{\partial p} - H_{xu}\frac{\partial u}{\partial p}. \end{aligned} \tag{4.21}$$

Over a fixed interval $[t_i(p),t_{i+1}(p)]$, the entries in the index set J that describes which controls take values in the interior of the respective control intervals do not change along the reference extremal: if the jth control u_j is constant over the interval of consideration, then $\frac{\partial u_j}{\partial p}\equiv 0$ and if the control u_j takes values in the interior of the control set, then, by the maximum principle we have that

$$\frac{\partial H}{\partial u_j}(\lambda^T(t,p),x(t,p),u_1(t,p),\ldots,u_m(t,p))\equiv 0.$$

Differentiating in p, it follows that

$$H_{u_j\lambda^T}\frac{\partial\lambda^T}{\partial p} + H_{u_jx}\frac{\partial x}{\partial p} + \sum_{i=1}^{m} H_{u_ju_i}\frac{\partial u_i}{\partial p}\equiv 0.$$

For the model [Q] all mixed second partial derivatives $H_{u_iu_j}$ for $i\neq j$ are identically zero and $H_{u_ju_j}=\theta_j>0$ so that

$$\frac{\partial u_j}{\partial p} = -\frac{1}{\theta_j}\left(H_{u_jx}\frac{\partial x}{\partial p} + H_{u_j\lambda^T}\frac{\partial\lambda^T}{\partial p}\right). \tag{4.22}$$

We can express the term with the partial derivatives of the controls in a more compact notation by defining a matrix $H_{uu}^{-J}(\lambda,x,u)$ as the diagonal matrix whose entry is 0 if $j\notin J$ and is equal to $\frac{1}{\theta_j}$ if $j\in J$. With this notation, we simply have that

$$\frac{\partial u}{\partial p} = -H_{uu}^{-J}\left(H_{ux}\frac{\partial x}{\partial p} + H_{u\lambda^T}\frac{\partial\lambda^T}{\partial p}\right). \tag{4.23}$$

Substituting this expression into the variational equations gives the following homogeneous matrix linear differential equation:

$$\begin{pmatrix} \frac{d}{dt}\left(\frac{\partial x}{\partial p}\right)\\ \\ \frac{d}{dt}\left(\frac{\partial\lambda^T}{\partial p}\right)\end{pmatrix} = \begin{pmatrix} H_{\lambda^T x} - H_{\lambda^T u}H_{uu}^{-J}H_{ux} & -H_{\lambda^T u}H_{uu}^{-J}H_{u\lambda^T}\\ \\ -H_{xx}+H_{xu}H_{uu}^{-J}H_{ux} & -\left(H_{x\lambda^T}-H_{xu}H_{uu}^{-J}H_{u\lambda^T}\right)\end{pmatrix}\begin{pmatrix}\frac{\partial x}{\partial p}\\ \\ \frac{\partial\lambda^T}{\partial p}\end{pmatrix}.$$

Note that

$$H_{x\lambda^T} - H_{xu}H_{uu}^{-J}H_{u\lambda^T} = \left(H_{\lambda^T x} - H_{\lambda^T u}H_{uu}^{-J}H_{ux}\right)^T.$$

Let $X(t) = \frac{\partial x}{\partial p}(t, p_*)$ and $Y(t) = \frac{\partial \lambda^T}{\partial p}(t, p_*)$ be the solutions of the variational equation along the reference extremal Γ_*. The variational equations are linear matrix differential equations with time-varying coefficients given by continuous functions and thus these solutions always exist on the full interval. It is a classical result in control theory, going back to Legendre and the calculus of variations, that if a pair of $n \times n$ matrices (X, Y) is a solution to a linear matrix differential equation of the form

$$\begin{pmatrix} \dot{X} \\ \dot{Y} \end{pmatrix} = \begin{pmatrix} A & R \\ -M & -A^T \end{pmatrix} \begin{pmatrix} X \\ Y \end{pmatrix}$$

where A, R, and M are matrices whose entries are continuous functions over $[t_i, t_{i+1}]$ and $X(t_{i+1})$ nonsingular, then the matrix $X(t)$ is nonsingular over the interval $[t_i, t_{i+1}]$ if and only if there exists a solution to the Riccati differential equation

$$\dot{S} + SA(t) + A^T(t)S + SR(t)S + M(t) \equiv 0, \qquad S(t_{i+1}) = Y(t_{i+1})X(t_{i+1})^{-1}$$

over the full interval $[t_i, t_{i+1}]$ while the matrix $X(\tau)$ is singular if this Riccati differential equation has a finite escape time $\tau \geq t_i$. (For example, a proof is given in [292, Proposition 2.4.1]). We thus have the following result:

Proposition 4.1.2. *Suppose the matrix $X(t_{i+1}) = \frac{\partial x}{\partial p}(t_{i+1}, p_*)$ is nonsingular. Then $X(t) = \frac{\partial x}{\partial p}(t, p_*)$ is nonsingular on the full interval $[t_i, t_{i+1}]$ if and only if there exists a solution S_* to the matrix Riccati differential equation*

$$\begin{aligned} \dot{S} + S\left(H_{\lambda^T x} - H_{\lambda^T u} H_{uu}^{-J} H_{ux}\right) + \left(H_{\lambda^T x} - H_{\lambda^T u} H_{uu}^{-J} H_{ux}\right)^T S \\ - S H_{\lambda^T u} H_{uu}^{-J} H_{u\lambda^T} S + \left(H_{xx} - H_{xu} H_{uu}^{-J} H_{ux}\right) \equiv 0 \end{aligned} \tag{4.24}$$

with terminal condition $S_*(t_{i+1}) = Y(t_{i+1})X(t_{i+1})^{-1}$ over the full interval $[t_i, t_{i+1}]$. In this case, we have that $S_*(t) = Y(t)X(t)^{-1}$ for all $t \in [t_i, t_{i+1}]$. In equation (4.24) all partial derivatives are evaluated along the reference extremal Γ_* and J denotes the set of indices $j \in \{1, \ldots, m\}$ of controls which take values in the interior of the control set over $[t_i, t_{i+1}]$. If J is empty, then $H_{uu}^{-J} \equiv 0$ and (4.24) reduces to a linear Lyapunov equation for which a solution always exists on the full interval $[t_i, t_{i+1}]$.

If there exists a time $\tau \in [t_i, t_{i+1})$ where the solution to the Riccati differential equation (4.24) ceases to exist, then it can be shown that the associated flow $F : (t, p) \mapsto F(t, p) = (t, x(t, p))$, of the parameterized family of extremals has a singularity at (τ, p_*) and it can be shown that the corresponding trajectory is no longer optimal on intervals $[t, t_{i+1}]$ with $t \leq \tau$ (e.g., this theory is developed in our text [292] with Theorem 5.4.2 applicable to the situation considered here). The time τ is called a *conjugate time* and the point $x(\tau, p_*)$ on the reference extremal is a *conjugate point*. Essentially, near a conjugate point close-by extremals in the parameterized family overlap and this leads to a loss of optimality. This theory is fully developed in [292], but is too lengthy to be even outlined here. On the other hand, the nonexistence of conjugate points along the controlled reference trajectory is a

sufficient condition for strong local optimality—this is the optimal control version of the strengthened Jacobi condition from the calculus of variations—and we shall outline this argument below.

Before doing so, we first simplify the structure of the Riccati differential equation (4.24). The matrices $H_{xx} - H_{xu}H_{uu}^{-J}H_{ux}$ and $H_{\lambda^T u}H_{uu}^{-J}H_{u\lambda^T}$ are symmetric and thus also the solution $S = S(t)$ to (4.24) is a symmetric matrix. The Riccati equation itself can be rewritten in the simpler form

$$\dot{S} + SH_{\lambda^T x} + H_{\lambda^T x}^T S + H_{xx} - (SH_{\lambda^T u} + H_{xu})H_{uu}^{-J}(H_{u\lambda^T}S + H_{ux}) \equiv 0$$

and writing the quadratic term in S componentwise, using the special diagonal form of $H_{uu}^{-J} = JH_{uu}^{-1}J$ with J the diagonal matrix whose entries are 1 for j in the index set J and 0 for j not in the index set J, this term simplifies to

$$\dot{S} + SH_{\lambda^T x} + H_{x\lambda^T}S + H_{xx} - \sum_{j\in J}\frac{1}{\theta_j}\left(SH_{\lambda^T u_j} + H_{xu_j}\right)\left(SH_{\lambda^T u_j} + H_{xu_j}\right)^T \equiv 0$$

with each term in this sum a rank 1 matrix. Thus, over each interval $[t_i, t_{i+1}]$, it just becomes necessary to add or delete the corresponding rank 1 matrix into the sum for the controls that take values in the interior of their respective control intervals. If J is empty, all terms are gone and this reduces to a linear Lyapunov equation. At junction points, the solution is propagated with the right and left limits.

The Riccati differential equation (4.24) does not involve the inverse of the matrix $\frac{\partial x}{\partial p}(t,p)$ and the existence of a solution to (4.24) implies that this matrix is nonsingular. This gives us the desired sufficient condition for local optimality for problem [Q].

Theorem 4.1.2. *Let $\Gamma_* = (x_*(\cdot), u_*(\cdot), \lambda_*(\cdot))$ be an extremal lift with simple regular junctions at times t_i, $i = 1, \ldots, k$, $0 = t_0 < t_1 < \cdots < t_k < t_{k+1} = T$. Suppose there exists a solution S_* to the matrix Riccati differential equation*

$$\dot{S} + SH_{\lambda^T x} + H_{x\lambda^T}S + H_{xx} - \sum_{j\in J(t)}\frac{1}{\theta_j}\left(SH_{\lambda^T u_j} + H_{xu_j}\right)\left(SH_{\lambda^T u_j} + H_{xu_j}\right)^T \equiv 0, \tag{4.25}$$

(all partial derivatives are evaluated along the reference extremal Γ_* and $j \in J(t)$ if and only the jth control u_j takes values in the interior of the control set) with terminal condition

$$S_*(T) = \frac{\partial^2 \varphi}{\partial x^2}(x(T, p_*)) \tag{4.26}$$

over the full interval $[0,T]$. Then there exists a neighborhood P of $x_*(T)$ such that the flow

$$F : [0,T] \times P \to [0,T] \times \mathbb{P}, \quad (t,p) \mapsto (t, x(t,p)),$$

is a local diffeomorphism and the reference control u_* provides a strong local minimum for problem [Q]. Specifically, the reference controlled trajectory (x_*, u_*) is

optimal relative to any other controlled trajectory (x,u) for which the graph of the trajectory x lies in the set $F([0,T]\times P)$ covered by the controlled extremal trajectories in the field.

Proof. It follows from Proposition 4.1.1 that the reference extremal can be embedded into a parameterized family of broken extremals with regular simple junctions defined over some set $[0,T]\times P$ with P a sufficiently small neighborhood of $x_*(T)=p_*$. We show that the existence of the solution S_* over the full interval $[0,T]$ implies that the Jacobian of the flow mapping F is nonsingular for all $t\in[0,T]$ and $p=p_*$, i.e., $\frac{\partial x}{\partial p}(t,p_*)$ is invertible for all $t\in[0,T]$.

We verify this inductively over the intervals $[t_i,t_{i+1}]$, backward from the terminal time T. In the construction of the parameterized family in Proposition 4.1.1, we use the terminal values of the trajectories as parameter, i.e., $p=x(T,p)$. Hence $\frac{\partial x}{\partial p}(T,p_*)=\mathrm{Id}$ is nonsingular. Furthermore, since $\lambda(T,p)\equiv\frac{\partial\varphi}{\partial p}(p)$, we have that

$$S_*(T)=\frac{\partial\lambda^T}{\partial p}(T,p_*)\left(\frac{\partial x}{\partial p}(T,p_*)\right)^{-1}=\frac{\partial^2\varphi}{\partial x^2}(p_*).$$

Since the solution to the Riccati differential equation with index set J determined by the last interval $[t_k,T]$ exists on all of $[t_k,T]$, it follows that $\frac{\partial x}{\partial p}(t,p_*)$ is invertible for $t\in[t_k,T]$. At the junction t_k, the index set J increases or decreases by one element and this leads to discontinuities in the derivatives $\frac{d}{dt}\left(\frac{\partial x}{\partial p}(\cdot,p_*)\right)$ and $\frac{d}{dt}\left(\frac{\partial\lambda^T}{\partial p}(\cdot,p_*)\right)$. But the controls remain continuous and thus the matrices $\frac{\partial x}{\partial p}(\cdot,p_*)$ and $\frac{\partial\lambda^T}{\partial p}(\cdot,p_*)$ remain continuous. This follows from Lemma B.1.1 in Appendix B.1 which implies that

$$\left(\frac{\partial x}{\partial t}(t_k+,p_*),\frac{\partial x}{\partial p}(t_k+,p_*)\right)-\left(\frac{\partial x}{\partial t}(t_k-,p_*),\frac{\partial x}{\partial p}(t_k-,p_*)\right)=\kappa\left(1,-\frac{\partial\tau}{\partial p}(p_*)\right)$$

with the function $t=\tau(p)$ the local solution for t of the equation $\psi_j(t,p)=0$ respectively $\psi_j(t,p)=u_j^{\max}$ that causes the junction at time t_k. This function is well defined and continuously differentiable because the junctions are simple and regular. Since the controls remain continuous at the junction, it follows from the first equation that $\kappa=0$ and thus the gradients of $x(t,p)$ before and after the junction agree. The same applies to the partial derivatives of λ^T. Hence the expression $\frac{\partial\lambda^T}{\partial p}(t,p_*)\left(\frac{\partial x}{\partial p}(t,p_*)\right)^{-1}$ remains continuous at junction points. Thus the existence of the solution $S_*(t)$ on the full interval $[0,T]$ implies that the matrix $\frac{\partial x}{\partial p}(t,p_*)$ is invertible for all $t\in[0,T]$.

For a sufficiently small neighborhood P of $x_*(T)=p_*$ the parameterized family of broken extremals constructed in Proposition 4.1.1 therefore defines a field of broken extremals. The flow F restricted to $[0,T]\times P$ is invertible and it follows from Theorem A.4.3 in Appendix A that the parameterized cost function,

$$C(t,p) = \int_t^T \left(L(x(s,p)) + \frac{1}{2} \sum_{j=1}^{m} \theta_j u_j^2(s,p) \right) ds + \varphi(x(T,p)),$$

gives rise to a continuously differentiable solution $V = C \circ F^{-1}$ of the Hamilton-Jacobi-Bellman equation on the image $G = F([0,T] \times P)$. From this the desired optimality result directly follows from Corollary A.4.2 in Appendix A. □

We only mention that solutions to matrix Riccati differential equations form a staple of automatic control theory in the context of linear-quadratic optimal control and that any numerically computed extremal controlled trajectory for problem [Q] can easily be tested for local optimality by integrating the differential equation (4.25) with terminal condition (4.26).

4.2 Bilinear Models: Special Case and Examples

In this section, we specify the form of the Riccati equation (4.25) further for a general bilinear control systems as it was used in Chapters 2 and 3 and draw some comparisons between the solutions for the L_1 and L_2-type formulations for the 3-compartment model with cytotoxic and cytostatic agents considered in Section 2.2.3.

4.2.1 Problem [Q] for a General Bilinear Model

As in Section 2.2.1 earlier, we take as state space $\mathbb{P}$ the positive orthant in $\mathbb{R}^n$ and denote the states by $N = (N_1, \ldots, N_n)^T$,

$$\mathbb{P} = \mathbb{R}^n_+ = \{N \in \mathbb{R}^n : N_i > 0 \text{ for } i = 1, \ldots, n\}.$$

The dynamics is given by a general bilinear system of the form

$$\dot{N}(t) = \left(A + \sum_{j=1}^{m} u_j B_j \right) N(t), \qquad N(0) = N_0, \tag{4.27}$$

where A and B_j, $j = 1, \ldots, m$, are constant $n \times n$ matrices, $A, B_j \in \mathbb{R}^{n \times n}$. The control $u = (u_1, \ldots, u_m)^T$ represents various drug concentrations in the blood stream and the control set U is a compact m-dimensional interval of the form $U = [0, u_1^{\max}] \times \cdots \times [0, u_m^{\max}]$. We assume that the positive orthant $\mathbb{P}$ is positively invariant. In the objective to be minimized, we retain the linear structure on the state N, but now use a quadratic term on the controls. As before, let $r = (r_1, \ldots, r_n)$ and $q = (q_1, \ldots, q_n)$ be n-dimensional row vectors of positive numbers and let θ_j, $j = 1, \ldots, m$, be positive coefficients representing weights. We then define the objective as to minimize

$$J(u) = rN(T) + \int_0^T \left\{ qN(t) + \frac{1}{2} \sum_{j=1}^{m} \theta_j u_j(t)^2 \right\} dt \to \min \tag{4.28}$$

Contrary to the case of the linear objective used in Section 2.2.1 where the integrals $\int_0^T u_j(t)dt$ are clearly related to the total dose given (if the controls represent dose rates) or the AUC (area under the curve), a standard pharmacological concept, if the controls represent concentrations, here there is no such interpretation for the integrals $\int_0^T u_j(t)^2 dt$. A quadratic objective a priori favors lower concentrations/dose rates: giving one tenth of the maximum dose rate contributes just one hundredth of the cost of the maximum dose rate. One needs to be aware that such a feature in solutions is not coming from the properties of the underlying system, but is artificially imposed from the outside by choice of the objective functional. Thus, generally, we prefer to use an L_1-type criterion on the controls. But here we consider the following L_2-type optimal control problem:

[Qbilin] for a fixed therapy horizon $[0,T]$, minimize the objective (4.28) over all Lebesgue-measurable functions $u : [0,T] \to U = [0,u_1^{\max}] \times \cdots \times [0,u_m^{\max}]$ subject to the dynamics (4.27).

We simplify the results of the previous section to the bilinear model considered here. The Hamiltonian function H is given by

$$H = qN + \frac{1}{2} \sum_{j=1}^{m} \theta_j u_j^2 + \lambda \left(A + \sum_{j=1}^{m} u_j B_j \right) N \tag{4.29}$$

and the adjoint equation and transversality condition read

$$\dot{\lambda} = -q - \lambda(A + uB), \qquad \lambda(T) = r.$$

The indicator functions ψ_j become bilinear expressions of the form

$$\psi_j(t) = -\frac{1}{\theta_j} \lambda(t) B_j N_*(t) \tag{4.30}$$

and the optimal controls u_j^* satisfy

$$u_j^*(t) = \begin{cases} 0 & \text{if } \psi_j(t) \le 0, \\ \psi_j(t) & \text{if } 0 \le \psi_j(t) \le u_j^{\max}, \\ u_j^{\max} & \text{if } u_j^{\max} \le \psi_j(t), \end{cases}$$

or, equivalently,

$$u_j^*(t) = \max\left\{0, \min\left\{u_{\max}, \psi_j(t)\right\}\right\}. \tag{4.31}$$

Furthermore, the minimum value of the Hamiltonian H along the extremal (N_*, u_*, λ) is constant over the interval $[0,T]$.

The dynamics and adjoint equation are the same irrespective of whether an L_1 or L_2-type objective is used for the controls. We thus have the following observation from our results in Chapter 2.

Corollary 4.2.1. *If all the matrices $A+\sum_{j=1}^m u_j B_j$, $0 \le u_j \le u_j^{\max}$ for $j=1,\dots,m$ are $\mathscr{M}$-matrices, then all the states N_i^* and costates λ_i for $i=1,\dots,n$ are positive functions on $[0,T]$.*

The matrix Riccati differential equation (4.25), and replacing the variable x with N, reads

$$\dot{S}+SH_{\lambda^T N}+H_{N\lambda^T}S+H_{NN}-\sum_{j\in J(t)}\frac{1}{\theta_j}\left(SH_{\lambda^T u_j}+H_{Nu_j}\right)\left(SH_{\lambda^T u_j}+H_{Nu_j}\right)^T\equiv 0,$$

and, since for this model we have that $H_{NN}\equiv 0$, it simplifies to the following form:

$$\begin{aligned}\dot{S}+S\left(A+\sum_{j=1}^m u_j B_j\right)+\left(A+\sum_{j=1}^m u_j B_j\right)^T S \\ -\sum_{j\in J(t)}\frac{1}{\theta_j}\left(SB_jN+B_j^T\lambda^T\right)\left(SB_jN+B_j^T\lambda^T\right)^T\equiv 0\end{aligned} \tag{4.32}$$

with terminal condition

$$S(T)=0.$$

Corollary 4.2.2. *The matrix $S=S(t)$ is negative semidefinite.*

Proof. Let $\tilde{A}(t)=A+\sum_{j=1}^m u_j(t)B_j$. If we use the notation $P_1\ge P_2$ to indicate that the matrix P_1-P_2 is positive semidefinite, then equation (4.32) implies that

$$\dot{S}+S\tilde{A}(t)+\tilde{A}(t)^T S\ge 0.$$

Let $\tilde{\Phi}(t,T)$ be the fundamental solution to the equation $\dot{X}=\tilde{A}(t)X$, i.e., $\frac{\partial}{\partial t}\tilde{\Phi}(t,T)=\tilde{A}(t)\tilde{\Phi}(t,T)$ and $\tilde{\Phi}(T,T)=\mathrm{Id}$. The matrix $Q(t)=\tilde{\Phi}(t,T)^T S(t)\tilde{\Phi}(t,T)$ then satisfies

$$\dot{Q}(t)=\tilde{\Phi}(t,T)^T\left\{\tilde{A}(t)^T S(t)+\dot{S}(t)+S(t)\tilde{A}(t)\right\}\tilde{\Phi}(t,T)\ge 0$$

and thus, for any vector $z\in\mathbb{R}^n$, the function $q(t)=z^T Q(t)z$ is nondecreasing. Since $S(T)=0$, all these functions are nonpositive and thus Q is negative semidefinite. Then so is S. □

This property, in conjunction with the fact that the matrix

$$-H_{Nu}H_{uu}^{-J}H_{uN}=-\sum_{j\in J(t)}\frac{1}{\theta_j}B_j^T\lambda(t)^T\lambda(t)B_j$$

which defines the constant term in (4.32) is also negative semidefinite precludes the use of standard results about solutions to Riccati differential equations which

would a priori guarantee the existence of a solution on the interval $[0,T]$ (e.g., see [292]). The existence of solutions over a priori specified intervals therefore needs to be verified on a case by case basis.

4.2.2 *Example: The 3-Compartment Model with Cytotoxic and Cytostatic Agents*

We revisit the mathematical model for cancer chemotherapy from Section 2.2.3 for a quadratic objective. As before, we write the dynamics in the form

$$\dot{N} = (A + uB_1 + vB_2)N$$

with the matrices

$$A = \begin{pmatrix} -a_1 & 0 & 2a_3 \\ a_1 & -a_2 & 0 \\ 0 & a_2 & -a_3 \end{pmatrix},$$

$$B_1 = \begin{pmatrix} 0 & 0 & -2a_3 \\ 0 & 0 & 0 \\ 0 & 0 & 0 \end{pmatrix} \quad \text{and} \quad B_2 = \begin{pmatrix} 0 & 0 & 0 \\ 0 & a_2 & 0 \\ 0 & -a_2 & 0 \end{pmatrix}, \tag{4.33}$$

and with $u \in [0, u_{\max}]$ denoting the concentration of the cytotoxic agent and $v \in [0, v_{\max}]$ representing the reduction in flow from the synthesis phase S to the second growth phase and mitosis, G_2/M. Recall that for any choice of controls the dynamics is described by an $\mathscr{M}$-matrix and thus all states and multipliers are positive functions. We now consider the optimal control problem to minimize the objective

$$J_2 = rN(T) + \int_0^T qN(t) + \frac{1}{2}\theta_1 u(t)^2 + \frac{1}{2}\theta_2 v(t)^2 dt \to \min$$

and will compare its solutions with those of the L_1-type objective

$$J_1 = rN(T) + \int_0^T qN(t) + \frac{1}{2}\theta_1 u(t) + \frac{1}{2}\theta_2 v(t) dt \to \min$$

considered in Section 2.2.3.

The indicator functions ψ_1 for u and ψ_2 for v for the problem [Qbilin] are given by

$$\psi_1 = -\frac{1}{\theta_1}\lambda B_1 N = \frac{2a_3}{\theta_1}\lambda_1 N_3 \qquad \text{and} \qquad \psi_2 = -\frac{1}{\theta_2}\lambda B_2 N = \frac{a_2}{\theta_2}(\lambda_3 - \lambda_2) N_2.$$

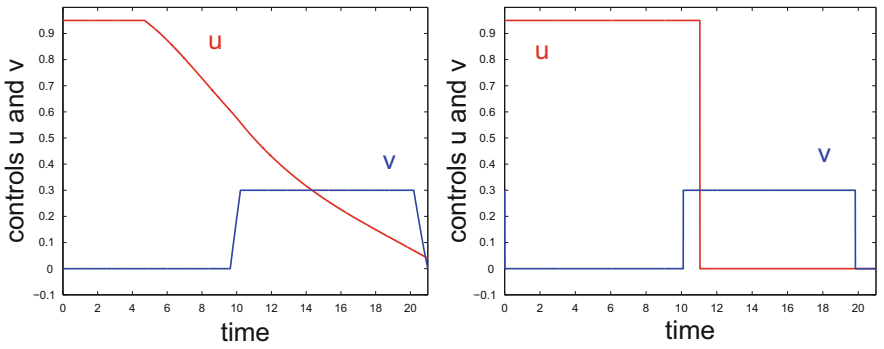

Fig. 4.1 Locally optimal controls (with the cytotoxic agent u shown in red and the cytostatic agent v shown in blue) for the objectives J_2 (left) and J_1 (right)

In particular, ψ_1 is always positive and thus for this problem formulation there are no rest periods; the cytotoxic agent will always be administered:

$$u_*(t) = \begin{cases} u_{\max} & \text{if } \psi_1(t) \geq u_{\max}, \\ \psi_1(t) & \text{if } \psi_1(t) < u_{\max}. \end{cases} \tag{4.34}$$

Analogously,

$$v_*(t) = \begin{cases} 0 & \text{if } \psi_2(t) \leq 0, \\ \psi_2(t) & \text{if } 0 \leq \psi_2(t) \leq v_{\max}, \\ v_{\max} & \text{if } v_{\max} \leq \psi_2(t). \end{cases} \tag{4.35}$$

We compare numerically computed locally optimal controls u_* and v_* for the quadratic objective J_2 and its linear counterpart J_1. The parameters that were used in the controlled dynamics are the same as in Table 2.5, i.e., $a_1 = .197$, $a_2 = .395$, $a_3 = .107$ for the cell cycle coefficients, $u_{\max} = 0.95$ and $v_{\max} = 0.3$ for the control limits, and the weights $r = (1,1,1)$ and $q = (1,1,1)$ in the penalty terms on the states. The coefficients at the controls were taken as $\theta_1 = 2$ and $\theta_2 = 0.02$ to correspond to the values $s_1 = 1$ and $s_2 = 0.01$ used for the L_1-type objective in Section 2.2.3. The therapy horizon again was $T = 21$ [days] and as initial condition we used the steady-state proportions for the uncontrolled system from Section 2.2.3 with the total cancer volume normalized to $C(0) = N_1(0) + N_2(0) + N_3(0) = 1$, i.e.,

$$N_1(0) = 0.3866, \quad N_2(0) = 0.1722 \quad \text{and} \quad N_3(0) = 0.4412.$$

An extremal controlled trajectory for the L_2-type objective J_2 was computed [295] by discretizing the dynamics and the adjoint with 21,000 grid points using an implicit Euler integration method and then using the interior-point solver IPOPT [337] on the resulting optimization problem using the Applied Modeling Programming Language AMPL [93]. The solution to the L_1-type objective J_1 is repeated from Section 2.2.3. Figure 4.1 shows locally optimal controls (cytotoxic agent u

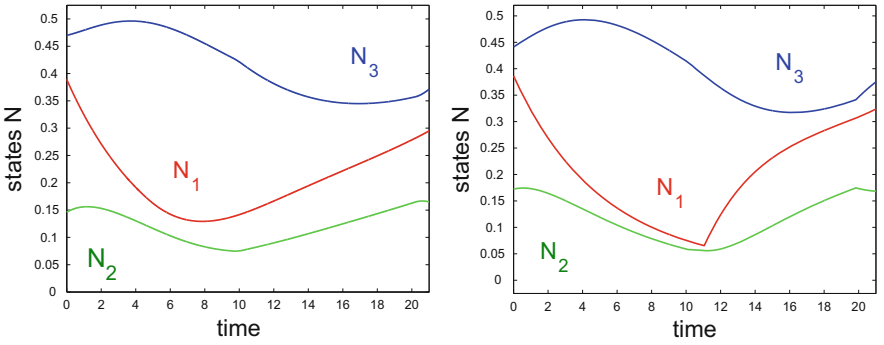

Fig. 4.2 Locally optimal controlled trajectories for the objectives J_2 (left) and J_1 (right)

in red and cytostatic agent v in blue) for the objectives J_2 (on the left) and J_1 (on the right). Since the coefficient θ_2 at the cytostatic agent is small, the L_2-solution closely approximates the L_1-solution for the cytostatic agent with very steep, almost linear connections between the values $v = 0$ and $v = v_{\max}$ approximating the bang-bang switches of the linear solution. For the quadratic case, the time intervals when the dose rate/concentration rises from 0 to $v_{\max}$ respectively decreases from $v_{\max}$ to 0 are given by $[9.637, 10.231]$ and $[20.192, 21]$ with the control v ending with the value $v(T) = 0$ as it is required from the optimality condition since $\psi_2(T) = 0$. For the linear case, the control for the cytotoxic agent switches at times $\sigma_1 = 10.115$ and $\sigma_2 = 19.895$. Since $v_{\max} \ll 1$, squaring the value for v leads to higher amounts of the drug being used with the total values, measured by the integral $\int_0^T v(t)dt$, given by 2.6527 for the linear objective and 3.1959 for the quadratic objective. Similarly, using a quadratic objective, the total amounts of cytotoxic agents used are given by 11.5035 for J_2 and by 9.6089 for J_1. The reduction in the total cancer burden from $C(0) = 1$ to $C(T) = N_1(T) + N_2(T) + N_3(T)$ is given by 0.8673 for minimizing J_1 and by 0.8314 for minimizing J_2. Thus, minimizing the quadratic objective only leads to about a 3% improvement in the reduction of the tumor at the expense of increasing the amounts of both the cytotoxic and cytostatic agents by about 20%. Minimizing J_1 would appear to be the preferred strategy. Figure 4.2 compares the corresponding trajectories and shows that the two solutions lead to very similar behaviors of the controlled systems.

Each controlled trajectory is a strong local minimum for minimizing the corresponding objective. For J_1, these results were developed and given in Section 2.2.3; for J_2, this can be verified by integrating the matrix Riccati differential equation (4.32) along the computed extremal. Figure 4.3 shows the graphs of the entries of the solution S to the matrix Riccati differential equations (4.32).

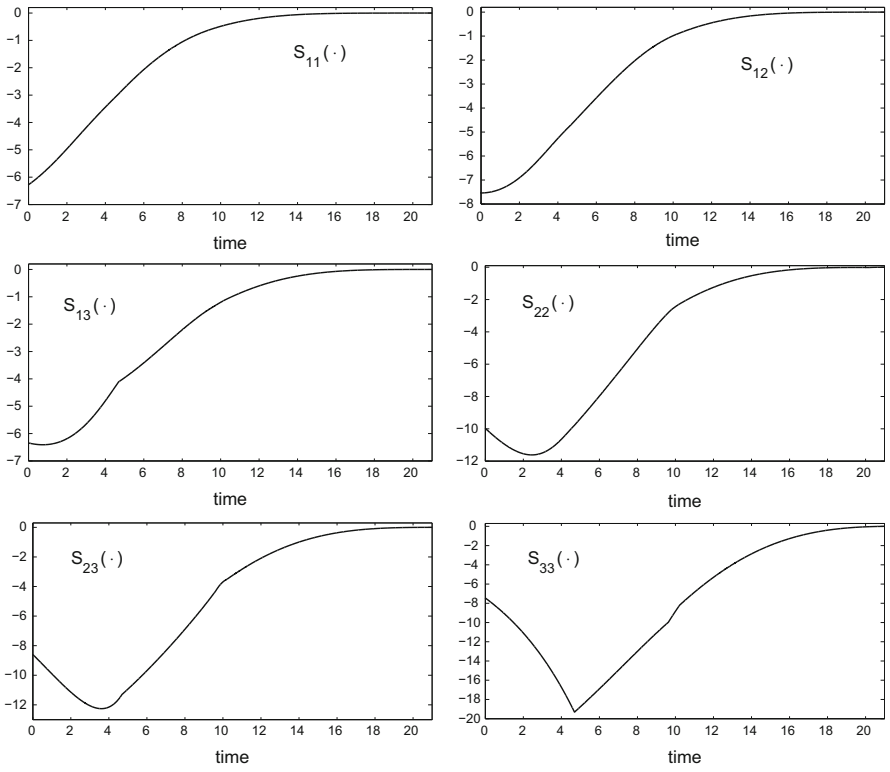

Fig. 4.3 Graphs of the entries of the solution S to the matrix Riccati differential equations (4.32).

4.3 A Mathematical Model with Emphasis on the Side Effects: Bone Marrow Dynamics

We close this chapter by comparing the solutions for L_1- and L_2-type objectives for a mathematical model for cancer chemotherapy originally formulated and analyzed by R. Fister and C. Panetta [83] in which the focus is on the side effects of treatment. In all the models considered so far, side effects were only indirectly taken into account by including in the objective an integral term that measured the total amount of drugs given. In the model considered here, these side effects become central. A typical chemotherapeutic agent acts indiscriminately on rapidly proliferating cells, a feature shown by many lines of cancer cells, but also by certain healthy cells in the body. This, for example, leads to hair loss as a common side effect on chemotherapy. More importantly, it includes bone marrow cells and for this reason often the dosage limiting tissue damage in chemotherapy is hemopoietic (related to blood cell formulation). Mature cells of these renewing tissues are formed through differentiation from the self-renewing stem-cell population in the bone marrow and it is generally accepted that "ideal cancer treatment would aim

to bring about minimal normal stem cell kill" [126]. Toxicity to the bone marrow thus is of tantamount importance in chemotherapy. This directly correlates with the clinical practice of taking a blood cell count of the patient before treatment sessions. If the blood cell count is too low, clinicians will either delay the treatment or give a reduced dose. Thus the blood count is an essential factor in designing the treatment. The particular model considered in this section is based on a standard two-compartment growth model for tissue [74] and focusses on this aspect of treatment. It was formulated by Eisen and Schiller [75] and then analyzed as an optimal control problem by Fister and Panetta in [83] with an L_2 Lagrange-type objective. Mathematically, it fits within the class of bilinear models considered earlier and we use it as one more example to compare L_1 and L_2-type optimal controls.

4.3.1 Model Formulation and Necessary Conditions for Optimality

In the model, only proliferating cells P and quiescent (or dormant) cells Q in the bone marrow are distinguished. The growth rate of the proliferating cells is denoted by γ and the transition rates from proliferating to quiescent cells and vice versa are denoted by α and β, respectively. The rate at which bone marrow enters the blood stream is denoted by ρ and the natural death rate of the proliferating cells is called δ (c.f., Figure 4.4). It is assumed that all these parameters governing the cell cycle remain constant over the time horizon considered. The overall dynamics of the uncontrolled system then becomes a 2-compartment bilinear model of the form

$$\dot{P} = (\gamma - \delta - \alpha)P + \beta Q, \qquad P(0) = P_0, \tag{4.36}$$

$$\dot{Q} = \alpha P - (\rho + \beta)Q, \qquad Q(0) = Q_0, \tag{4.37}$$

with positive initial conditions.

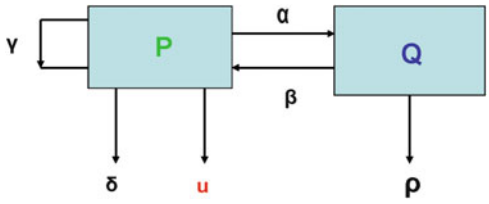

Fig. 4.4 A 2-compartment model of proliferating and quiescent cells in the bone marrow.

As for the 2-compartment model in Section 2.1, there exists a well-defined steady state for the proportions:

$$x = \frac{P}{P+Q} \qquad \text{and} \qquad y = \frac{Q}{P+Q} = 1 - x.$$

For, setting $\omega = \gamma - \delta + \rho$, it follows from equations (4.36) and (4.37) that,

$$\dot{x} = -\omega x^2 + (\omega - \alpha - \beta)x + \beta.$$

The interval $[0,1]$ is positively invariant and has a unique globally asymptotically stable equilibrium point at $\bar{x} \in (0,1)$, the unique positive root of the equation

$$\omega x^2 + (\alpha + \beta - \omega)x - \beta = 0. \tag{4.38}$$

In steady state, the uncontrolled system then approximately grows exponentially at rate ξ given by

$$\xi = \omega \bar{x} - \rho. \tag{4.39}$$

Table 4.1 Numerical values for the coefficients and parameters used in computations for the dynamical system (4.36) and (4.37).

Coefficient	Interpretation	Numerical value	Reference
α	Transition rate from proliferating to quiescent cells	5.643	[83]
β	Transition rate from quiescent to proliferating cells	0.48	[83]
γ	Growth rate of proliferating cells	1.47	[83]
δ	Death rate of proliferating cells	0	
ρ	Rate at which bone marrow enters the blood stream	0.164	[83]
$\bar{x}$	Steady-state proportion of proliferating cells	0.1031	Eq. (4.38)
$\bar{y}$	Steady-state proportion of proliferating cells	0.8869	Eq. (4.38)
ξ	Approximate overall growth rate	0.0044	Eq. (4.39

In our numerical computations below we use the parameter values from [83, 225] that are summarized in Table 4.1. For these data, we have that $\bar{x} = 0.1031$ and $\xi = 0.0044$. In particular, in steady state only about 10% of the bone marrow cells are proliferating and the total bone marrow mass is quite stagnant. Figure 4.5 shows graphs of trajectories of the system for various initial conditions. The percentages of cells in the proliferating compartment are initially set to 10%, 50% and 90%, respectively, with the total bone marrow cells normalized to 1. These simulations illustrate how quickly the steady-state behavior is reached for the percentages. While the total number of bone marrow cells grows slowly as the steady state is reached, note, however, that transient effects due to higher initial numbers of proliferating cells produce significantly higher total numbers of bone marrow cells. The reason

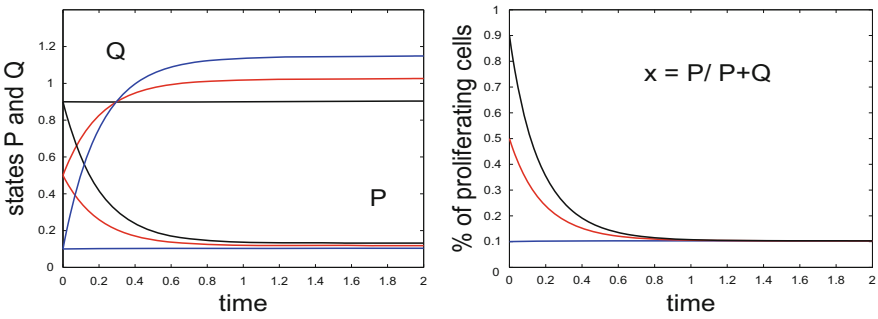

Fig. 4.5 Steady-state behavior of the dynamical system (4.36) and (4.37).

lies in the high transition rate α from proliferating to quiescent cells. Thus, not only the total initial bone marrow cells, but also their distribution as proliferating and dormant cells, i.e., the initial condition of (4.36)–(4.37), determines the total number of bone marrow cells. Such a transient effect, quite common in control theory, would not be captured in a simple scalar exponential growth model.

Once a chemotherapeutic agent is introduced, the controlled dynamics takes the form

$$\dot{P} = (\gamma - \delta - \alpha - \sigma u(t))P + \beta Q, \qquad P(0) = P_0, \tag{4.40}$$

$$\dot{Q} = \alpha P - (\rho + \beta)Q, \qquad Q(0) = Q_0. \tag{4.41}$$

Chemotherapy kills proliferating cells while quiescent cells are not affected by the agent. As in Chapter 2, the log-kill hypothesis is made with parameter σ describing the overall effectiveness of the drug. No pharmacokinetic equations are included in the model. If we set $N = (P, Q)$, this system takes the form of a single-input bilinear system,

$$\dot{N} = (A + uB)N, \quad N(0) = N_0, \tag{4.42}$$

with the matrices given by

$$A = \begin{pmatrix} \gamma - \delta - \alpha & \beta \\ \alpha & -(\rho + \beta) \end{pmatrix} \quad \text{and} \quad B = \begin{pmatrix} -\sigma & 0 \\ 0 & 0 \end{pmatrix}. \tag{4.43}$$

Note that the positive orthant $\mathbb{P} = \mathbb{R}^2_+$ is positively invariant for the control system since, whenever one of the variables P or Q vanishes, then the corresponding derivative is positive.

Different from previous formulations, in this model the side effects are the central aspect of the model and, indeed, cancer cells are not even included. Cancer cells and the effect of chemotherapy on the tumor come into play only implicitly through the total drug dose given. Similarly as for the compartmental models considered in Chapter 2, it is assumed that the total dose stands in a direct relation to the number of cancer cells killed. Thus the objective becomes to give as large as possible a total

dose of drugs—this will kill a proportionally large number of cancer cells—and at the same time keep the bone marrow cells high. Including a parameter $\nu = 1,2$ to model both a linear and a quadratic term on the control, it would, for example, be reasonable to maximize an objective of the following form:

$$\widetilde{J}_\nu(u) = rN(T) + \int_0^T qN(t) + \frac{1}{\nu}u(t)^\nu dt \to \max, \qquad \nu = 1,2. \tag{4.44}$$

As before, $r = (r_1, r_2)$ and $q = (q_1, q_2)$ are vectors of positive weights. This leads to the following optimal control problem:

$[\widetilde{BM\nu}]$ For a fixed therapy horizon $[0,T]$, maximize (4.44) over all Lebesgue measurable functions $u : [0,T] \to [0, u_{\max}]$ subject to the dynamics (4.42).

First-order necessary conditions for optimality again follow from the conditions of the Pontryagin maximum principle (Theorem A.2.1 in Appendix A), with the only difference that the minimization condition of the Hamiltonian function H is replaced by a maximization condition. It follows from Corollary A.2.2 in Appendix A that extremals for either problem are normal and thus we already set $\lambda_0 = 1$ in the definition of the Hamiltonian H,

$$H = qN + \frac{1}{\nu}u^\nu + \lambda(A + uB)N. \tag{4.45}$$

The adjoint equation and transversality condition read the same in both cases:

$$\dot{\lambda} = -\lambda(A + uB) - q, \qquad \lambda(T) = r. \tag{4.46}$$

Again it follows from the structure of the matrices A and B that the positive orthant in the dual space, $\mathbb{P}^* = \left(\mathbb{R}^2_+\right)^*$, is negatively invariant under the adjoint flow and thus, overall, we have the following statement:

Corollary 4.3.1. *For both problems $[\widetilde{BM1}]$ and $[\widetilde{BM2}]$ all states and costates are positive over $[0,T]$.*

In this setting, however, there is not much difference between the two problem formulations. We shall show below that, as expected, optimal controls for the L_1-formulation are bang-bang. But here this also holds for the L_2-formulation. The reason simply is that although the objective is quadratic in u, in the maximum principle we now need to maximize the Hamiltonian H. But this is a strictly *convex* function of the control and thus the maximum will always lie at one of the boundary values $u = 0$ or $u = 1$. In fact, the optimal control u_* for $[\widetilde{BM2}]$ satisfies

$$u_*(t) = \begin{cases} 0 & \text{if } \frac{1}{2} + \lambda(t)BN(t) > 0, \\ \\ 1 & \text{if } \frac{1}{2} + \lambda(t)BN(t) < 0, \end{cases}$$

with $\frac{1}{2}+\lambda BN$ acting as the switching function. In a certain sense, these two problem formulations only differ in the weights in the objective.

Therefore, in order to get the typical L_2-formulation (in which one minimizes a convex or maximizes a concave functional), we rewrite the objective in the same way as it was done in [83] in the form

$$J_\nu(u) = rN(T) + \int_0^T qN(t) - \frac{1}{\nu}(1-u(t))^\nu \, dt \to \max, \qquad \nu = 1,2. \tag{4.47}$$

For the L_1-formulation, the functionals $\tilde{J}_1$ and J_1 are equivalent. We thus consider the following optimal control problems:

[BMν] For a fixed therapy horizon $[0,T]$, maximize (4.47) over all Lebesgue measurable functions $u:[0,T]\to[0,1]$ subject to the dynamics (4.42).

The Hamiltonian H now takes the form

$$H = qN - \frac{1}{\nu}(1-u)^\nu + \lambda(A+uB)N, \tag{4.48}$$

but the adjoint equation and transversality condition are not affected by this change in the functional relation on the control. In particular, Corollary 4.3.1 remains valid and all states and costates are positive. Furthermore, like the models considered previously (e.g., see Section 2), the optimal control problems [BMν] have a 1-dimensional group of scaling symmetries (invariance) that allow us to normalize the initial condition N_0 to $N_0 = 1$. For, if we scale the states as $\varkappa N$ and the coefficients in the objective as $\frac{r}{\varkappa}$ and $\frac{q}{\varkappa}$, then the corresponding solutions to the dynamics and adjoint equation are given by $\varkappa N(t)$ and $\frac{1}{\varkappa}\lambda(t)$. Hence the values of the objective function $J_\nu(u)$, the Hamiltonian H and all associated switching or indicator functions remain invariant. We now distinguish between L_1- and L_2-type objectives.

4.3.2 Analysis with an L_2-type Objective

The maximum of the Hamiltonian H for $u\in\mathbb{R}$ is attained at

$$u = 1+\lambda(t)BN_*(t)$$

and defining the indicator function as

$$\psi(t) = 1+\lambda(t)BN_*(t) = 1-\sigma\lambda_1(t)P_*(t), \tag{4.49}$$

the optimal control u_* therefore satisfies

$$u_*(t) = \begin{cases} 0 & \text{if} \quad \psi(t)\le 0, \\ \psi(t) & \text{if} \quad 0\le\psi(t)\le u_{\max}, \\ u_{\max} & \text{if} \quad u_{\max}\le\psi(t). \end{cases} \tag{4.50}$$

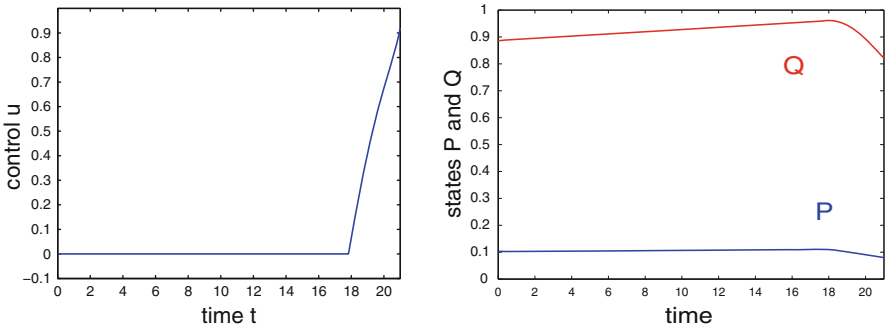

Fig. 4.6 Optimal control and corresponding response of the system for problem [BM2].

Since states and multipliers are positive, it follows that $\psi(t) < 1$. Thus, if $u_{\max} = 1$, then optimal controls will never be at their maximum values. Similarly, if $u_{\max} < 1$ and the penalty term is absent, $r = 0$, then $\psi(T) = 1$ and thus optimal controls will always end with an interval of full dose therapy.

Figure 4.6 shows the optimal control for the parameter values in Table 4.1 from the steady-state initial condition $P_0 = 0.1031$ and $Q_0 = 0.8869$ with the initial tumor volume normalized to $N_0 = 1$ for the coefficients $r = (1,1)$ and $q = (2,2)$ in the objective. The optimal solution is given by $u \equiv 0$ over the interval $[0,\tau]$ with $\tau = 17.82$ and then follows the interior control over the final interval $[\tau,T]$ increasing the dose rate/concentration. Since the emphasis in this model is on side effects and a cumulative measurement of the bone marrow is undertaken by means of the qN term in the Lagrangian in the objective, here administration of chemotherapy is postponed as long as possible and the administration schedule ends with dose intensification toward the end of therapy. This leads to almost the opposite behavior as when the emphasis is put on the tumor cells as it is the case in the cell-cycle specific models in Chapter 2. From a practical side, this may seem somewhat confusing, but it makes perfect sense mathematically. Essentially, in both models chemotherapy kills the proliferating cells, but in the models of Chapter 2 these are tumor cells and optimal controls aim to eradicate them as fast as possible while here these are bone marrow cells that optimal controls want to protect as long as possible. Thus, clearly the different emphasis put into the forms of the objective matters and the analysis of this model offers additional insights into the scheduling of chemotherapeutic agents.

The local optimality of this solution is easily verified using the approach of Section 4.1.3. If we change the control to $v = 1 - u$ and rewrite the maximization problem as a minimization problem, then the objective becomes to minimize

$$\hat{J}(u) = -rN(T) + \int_0^T -qN(t) + \frac{1}{2}v(t)^2 dt \to \min$$

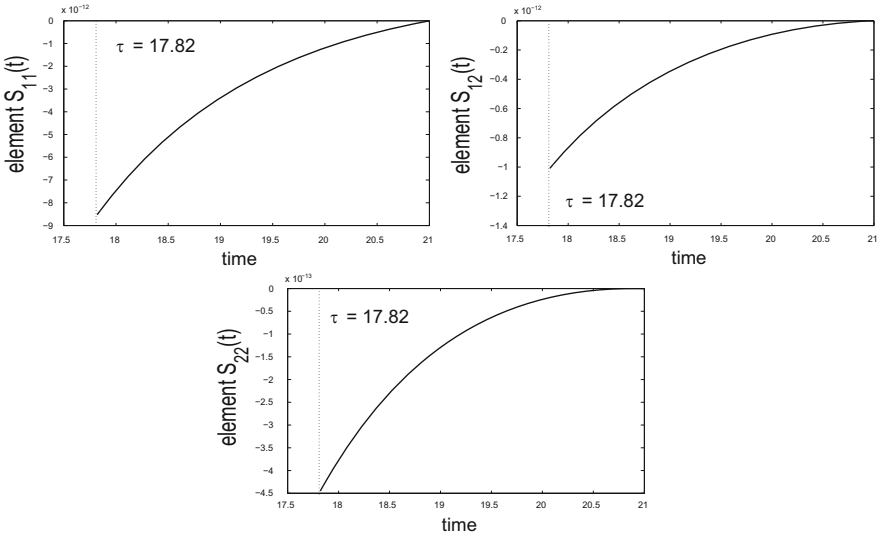

Fig. 4.7 The components of the solution S of the Riccati differential equation (4.51) over the interval $[\tau, T] = [17.82, 21]$.

and is of the form considered in Section 4.2.1 with dynamics

$$\dot{N} = (A + uB)N = (\hat{A} + v\hat{B})N$$

and the matrices $\hat{A}$ and $\hat{B}$ given by

$$\hat{A} = \begin{pmatrix} \gamma - \delta - \alpha - \sigma & \beta \\ \alpha & -(\rho + \beta) \end{pmatrix} \qquad \text{and} \qquad \hat{B} = \begin{pmatrix} \sigma & 0 \\ 0 & 0 \end{pmatrix}.$$

Since the control u is constant over the interval $[0, \tau]$, the Riccati differential equation (4.32) reduces to a linear Lyapunov equation for which a solution always exists. Hence it is only necessary to integrate this equation over the interval $[\tau, T]$ where the control takes values in the interior of the control set. Since $\hat{B} = -B$, equation (4.32) remains valid in the form

$$\begin{aligned} &\dot{S} + S(A + uB) + (A + uB)^T S \\ &\quad - \left(SBN + B^T \lambda^T\right)\left(SBN + B^T \lambda^T\right)^T \equiv 0, \qquad S(T) = 0, \end{aligned} \tag{4.51}$$

and Figure 4.7 shows the components of the solution. The existence of this solution over the interval $[\tau, T]$ then implies the strong local optimality of the control by Theorem 4.1.2.

4.3.3 Analysis with an L_1-type Objective

For the L_1-type objective, as in the other models considered earlier, singular controls are not optimal and optimal controls are bang-bang. For, the switching function for this model is the same as the indicator function for the L_2-formulation, given by

$$\Phi(t) = 1 + \lambda(t)BN_*(t)$$

and thus optimal controls satisfy

$$u_*(t) = \begin{cases} u_{\max} & \text{if } \Phi(t) > 0, \\ 0 & \text{if } \Phi(t) < 0. \end{cases}$$

Regardless of whether a minimization or maximization problem is considered, the adjoint equation remains the same and thus the formulas for the derivative of the switching function derived in Chapter 2 apply. In particular, as in Section 2.1, we have that

$$\frac{\partial}{\partial u}\frac{d^2}{dt^2}\frac{\partial H}{\partial u}(\lambda(t), N_*(t), u_*(t)) = \lambda(t)\left\{[B,[A,B]] - qB^2\right\}N_*(t). \tag{4.52}$$

However, for a maximization problem, the Legendre-Clebsch condition for optimality of a singular control now requires that this expression be nonnegative, i.e., that

$$\frac{\partial}{\partial u}\frac{d^2}{dt^2}\frac{\partial H}{\partial u}(\lambda(t), x(t), u(t)) \geq 0.$$

Since $B^2 = -\sigma B$ and $\dot{\Phi}(t) = \{\lambda(t)[A,B] - qB\}N_*(t) \equiv 0$ along a singular arc, it follows that

$$qB^2N_*(t) = -\sigma qBN_*(t) = -\sigma\lambda(t)[A,B]N_*(t).$$

Hence

$$\frac{\partial}{\partial u}\frac{d^2}{dt^2}\frac{\partial H}{\partial u}(\lambda(t), N_*(t), u_*(t)) = \lambda(t)\{[B,[A,B]] + \sigma[A,B]\}N_*(t).$$

along a singular arc. Direct calculations verify that

$$[A,B] = \sigma\begin{pmatrix} 0 & -\beta \\ \alpha & 0 \end{pmatrix} \qquad \text{and} \qquad [B,[A,B]] = -\sigma^2\begin{pmatrix} 0 & \beta \\ \alpha & 0 \end{pmatrix}$$

so that

$$\frac{\partial}{\partial u}\frac{d^2}{dt^2}\frac{\partial H}{\partial u}(\lambda(t), N_*(t), u_*(t)) = \sigma^2\lambda(t)\begin{pmatrix} 0 & -2\beta \\ 0 & 0 \end{pmatrix}N_*(t) = -2\sigma^2\beta\lambda_1(t)Q_*(t) < 0$$

violating the Legendre-Clebsch condition. Thus all singular arcs locally minimize the objective.

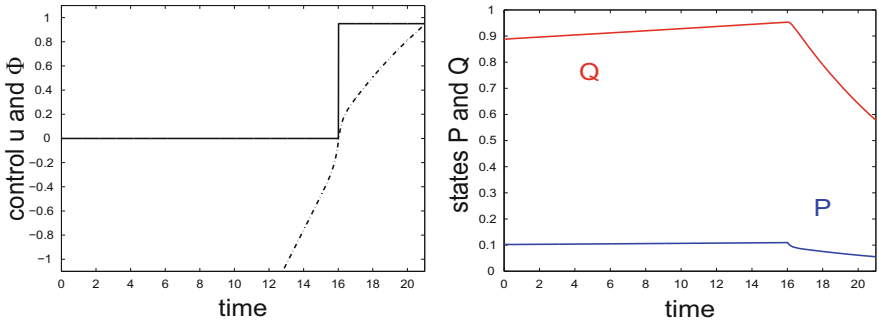

Fig. 4.8 Optimal control and corresponding response of the system for problem [BM1].

Proposition 4.3.1. *If (N_*, u_*) is an optimal controlled trajectory for problem [BM1], then there does not exist an interval on which the control u_* is singular.*

Figure 4.8 shows a locally optimal control and its corresponding trajectory for problem [BM1] and the same parameter values as before. In the objective the same values $r = (1,1)$ and $q = (2,2)$ were used and θ was taken to be $\theta = 1$. The control is bang-bang with one switching from $u = 0$ to $u = u_{\max}$ and it follows that the corresponding controlled trajectory is a strong local minimum (c.f., Corollary 2.1.2). Note that the behavior of the states is very similar for the two models. For the L_1 objective the switching is at time $\tau = 16.04$.

4.3.4 Comments and Interpretations

Different from the solutions in Section 2, for both an L_1- and L_2-type formulation of the objective, the administration of drugs is delayed toward the end of the therapy. The reason lies in the emphasis on the *side effects* in the model. Bone marrow reproduces at a very low rate in steady state ($\xi = 0.0044$ for the parameter values used here) and thus it simply is beneficial in terms of the objective to defer any actions that will deplete it in time. This is just the opposite from when the emphasis is put on minimizing the tumor volume as it was done in the models considered in Chapter 2, but it makes perfect sense from a mathematical optimization point of view. Here simply competing objectives and rationales are employed and finding the proper balance between them is precisely one of the reasons why it is so difficult to find the perfect cancer treatment schedule. In medical practice, often the emphasis first and foremost is on the tumor and this leads to upfront dosing with side effects becoming the limiting aspect of therapy. This would be more in agreement with the models considered in Chapter 2.

Chapter 5
Optimal Control of Mathematical Models for Antiangiogenic Treatments

In the models considered so far, the focus was on the cancerous cells progressing from mathematical models for homogeneous tumor populations of chemotherapeutically sensitive cells to heterogeneous structures of cell populations with varying sensitivities or even resistance. From an optimal control point of view, optimal treatment schedules change from bang-bang solutions with upfront dosing (that correspond to classical MTD approaches in medicine) to administrations that also include singular controls (which correspond to time-varying dosing schedules at less than maximum rates) as heterogeneity of the tumor population becomes more prevalent. In this chapter, we begin to analyze mathematical models that also take into account a tumor's microenvironment.

Arguably the most important component of a tumor's microenvironment is its vasculature. In order to grow beyond a small size, a growing tumor needs to develop its own network of blood vessels and capillaries that will provide it with nutrients and oxygen. This process is called angiogenesis and was already pointed out as a therapeutic target by J. Folkman in the early 1970s [85, 86] (see Section 1.3.3). Antiangiogenenic treatments aim at depriving the tumor of this needed vasculature by either disrupting the signaling process that the tumor uses to recruit surrounding, mature, host blood vessels or by directly inhibiting the growth of endothelial cells that form the lining of the newly developing blood vessels and capillaries. Ideally, without an adequate support network, the tumor shrinks and its further development is halted. Rather than fighting the fast duplicating, genetically unstable, and continuously mutating tumor cells, this indirect treatment approach targets the genetically stable endothelial cells. As a consequence, no clonal resistance to angiogenic inhibitors has been observed in experimental cancer [28] and for this reason, after the discovery of antiangiogenic mechanisms that the tumor uses to control its vasculature in the 1990s [90, 66, 161], antiangiogenic treatments were a new hope in the war on cancer [141], a therapy 'resistant against resistance'. Unfortunately these high hopes have not been fully realized because of the indirect mechanism

H. Schättler, U. Ledzewicz, *Optimal Control for Mathematical Models of Cancer Therapies*, Interdisciplinary Applied Mathematics 42,
DOI 10.1007/978-1-4939-2972-6_5

of targeting cancer cells. Nevertheless, in connection with traditional approaches that directly kill tumor cells like chemo- or radiotherapy, antiangiogenic treatments have become an important part in the overall strategy to combat a tumor. Thus, and especially in combination treatments, the question how to best schedule therapies over time needs to be answered. In clinical trials, because of the great complexity of the medical problem, the scheduling of drugs is pursued in expensive, exhaustive, medically guided trial-and-error approaches (e.g., [39, 69, 160]). But the extent to which treatment schedules can be analyzed in this way are limited and there exists an opportunity for modeling and mathematical analysis—*in silico* procedures—to be useful. As a discipline, optimal control theory is uniquely suited to analyze such scheduling problems and to provide qualitative insights into the structure of optimal protocols. As we shall see, these structures are not at all obvious and relatively difficult, or at least very expensive, to test in a laboratory setting.

We start our analysis of mathematical models for antiangiogenic treatments by considering this treatment modality as a *monotherapy*, that is, as a stand alone procedure. In Chapter 7 we shall consider combinations of antiangiogenic treatments with chemo- and radiotherapy and it will be seen there that the solutions to these multi-input optimal control problems strongly build upon the solutions for the optimal scheduling of antiangiogenic agents developed here. An inductive approach that first analyzes a simplified model and then adds increasingly more realistic features (such as pharmacokinetics and pharmacodynamics and combinations with other treatment modalities) works exceptionally well for the types of models analyzed in this chapter. These models are based on a widely influential population based mathematical model for tumor development under angiogenic signaling that was developed and biologically validated in 1999 by Hahnfeldt, Panigrahy, Folkman, and Hlatky [116] and has become an object of strong interest also in the mathematical literature. For example, its dynamic properties under various types of periodic treatment protocols were analyzed by d'Onofrio and Gandolfi [257] and bifurcation phenomena are considered in the work of Agur, Arakelyan, Daugulis, and Ginosar [4] or Forys, Keifetz, and Kogan [91]. Numerous generalizations and variations of the underlying model have been proposed (e.g., see [77, 251, 259, 281]) and to this date the model is still undergoing vigorous development. It has been analyzed from an optimal control point of view in our work, e.g., [196, 200, 201, 204], and also in the research by Swierniak et al., e.g., [314, 319, 320].

In this chapter, we formulate and analyze as optimal control problem a class of mathematical models for tumor antiangiogenesis that is based on this model by Hahnfeldt et al. [116]. Its principal state variables are the primary tumor volume, p, and the carrying capacity of the vasculature, q. The latter denotes a measure for the tumor volume sustainable by the vascular network. It is predominantly measured by the endothelial cells and we therefore sometimes also refer to it as the endothelial support of the tumor for short. The dynamics describes the interactions between these variables. The tumor volume p changes according to some growth function dependent on the carrying capacity q and the q-dynamics consists of a balance of stimulatory and inhibitory effects. In [116] an asymptotic analysis of the underlying consumption-diffusion model is carried out that leads to the specific form for

these terms proposed by Hahnfeldt et al. However, even within the premises of the approach taken in [116], there exists some freedom in the modeling and the original model has undergone various modifications with the first one given by Ergun, Camphausen, and Wein in [77]. In this paper, the authors also for the first time consider antiangiogenic therapy as an optimal control problem: *given an a priori specified amount of angiogenic inhibitors, how should it be scheduled in time to achieve the best possible effect on minimizing the tumor volume?* It is this formulation that we shall analyze in this chapter. As we shall show, optimal antiangiogenic treatment schedules are strongly determined by a time interval along which controls are singular. Indeed, *optimal controlled trajectories maintain*, as much as this is possible, *a specific relation between tumor volume p and carrying capacity q* that is characterized by an optimal singular arc *along which the destroying capacity of the treatment is maximized*. This is done through a judicious choice of the concentration of the antiangiogenic agent which is expressed by the singular control. These mathematical results show a strong correspondence to the medical idea that normalizing the tumor vasculature through antiangiogenic therapy has beneficial aspects for the delivery of chemotherapeutic agents [131, 132] and this will become even stronger when such combination treatments will be considered in Chapter 7.

Several variations of the model by Hahnfeldt et al. have been proposed in the literature and, more generally, in Section 5.1 we consider a class of systems that includes both the original formulation and the modification by Ergun, Camphausen, and Wein in [77] as well as some systems interpolating between these two models. We also give a detailed derivation of the original model by Hahnfeldt, Panigrahy, Folkman, and Hlatky from an asymptotic analysis of the underlying consumption-diffusion equation. For these models, we derive a complete global solution to the optimal control problem in form of a *regular synthesis* of controlled trajectories. Such a synthesis can be thought of as a GPS-system which, for every possible combination of the tumor volume p, its carrying capacity q and the available amount y of antiangiogenic agents, gives a complete "road map" of how optimal protocols are administered, both qualitatively and quantitatively. This embodies a full *global solution* of the optimal control problem. Since we shall consider several models, in Section 5.2 we give a general formulation of the problem with generic stimulation and inhibition terms, $S = S(p,q)$ and $I = I(p,q)$, in the dynamics for the carrying capacity. We then use this formulation to first develop those aspects and necessary conditions for optimality that are common to all the models considered here. The syntheses of optimal controlled trajectories for the main versions of the system dynamics are then developed in Section 5.3 for the original model by Hahnfeldt et al. and in Section 5.4 for the modification by Ergun et al. As will be seen, although the models differ vastly in some of their modeling premises, their optimal solutions are qualitatively identical. In each case, and this holds for the full class of systems considered here, an *optimal singular arc* is the core structure of these syntheses and optimal controls follow specific concatenations of full- or no-dose treatments with this singular control.

5.1 A Class of Mathematical Models for Tumor Angiogenesis

We formulate a dynamical system for tumor development under angiogenic signaling based on the equations by Hahnfeldt, Panigrahy, Folkman, and Hlatky [116]. In this model, the spatial aspects of the underlying consumption-diffusion process that stimulate and inhibit angiogenesis are incorporated into a nonspatial 2-compartment model with the *primary tumor volume*, p, and the *carrying capacity* of the vasculature, q, as its principal variables. Intuitively, the latter can be thought of as the ideal tumor volume sustainable by the vascular network. It is closely related to the volume of endothelial cells that form the lining of the existing and newly forming capillaries and we sometimes also call it the *endothelial support* of the tumor for short. The dynamics simply consists of two ODEs that describe the evolution of the tumor volume and its carrying capacity. In principle, any of the underlying tumor growth models can be used, but here, and following the original modeling, we shall mostly employ a Gompertzian model of the form

$$\dot{p} = -\xi p \ln\left(\frac{p}{q}\right) \tag{5.1}$$

where ξ is a constant tumor growth parameter. The inverse quotient $\frac{q}{p}$ is sometimes also called the *endothelial density*. Note that the carrying capacity and tumor volume are balanced for $p = q$ and thus $\dot{p} = 0$ in this case while the tumor volume shrinks for inadequate endothelial support ($q < p$) and increases if this support is plentiful ($q > p$). Different from other approaches, the carrying capacity is not considered constant, but becomes a state variable whose evolution is governed by a balance of stimulatory and inhibitory effects. The general structure of this dynamics takes the form

$$\dot{q} = S(p,q) - I(p,q) - \mu q \tag{5.2}$$

where I and S denote endogenous inhibition and stimulation terms and the term μq, $\mu \geq 0$, that has been separated describes the loss to the endothelial cells through natural causes (death, etc.). These effects are small when compared with the stimulation and inhibition exerted by the tumor and μ is often set to 0. The important structures defining the model are the functional forms for the inhibition and stimulation terms, $I(p,q)$ and $S(p,q)$. Clearly, these should reflect the main properties of angiogenesis and important aspects are that *"tumor-derived inhibitors from all sites act more systemically, whereas tumor-derived stimulators act more locally to the individual secreting tumor site"* [116, pg. 4771]. Accordingly, the half lives of endogenous inhibitors greatly exceed those of endogenous stimulators, or, equivalently, their clearance rate is much smaller.

5.1.1 Asymptotic Analysis of a Consumption-Diffusion Model for Angiogenesis

In their paper [116], Hahnfeldt, Panigrahy, Folkman, and Hlatky derive specific functional forms for I and S using an asymptotic spatial analysis of the underlying consumption-diffusion process for the concentrations c of stimulators and inhibitors both inside and outside of the tumor. It is assumed that the tumor is spherically symmetric with radius r_0, that it secrets stimulators at rate s and that these proteins are cleared in the body (i.e., taken up by other proteins) at rate γ. The basic mathematical model therefore is described by the following consumption-diffusion equation

$$\frac{\partial c}{\partial t} = D^2 \Delta c - \gamma c + s \tag{5.3}$$

where D^2 represents a diffusion coefficient, Δc denotes the Laplacian of the concentration as a spatial function in standard coordinates x, y, and z, $c = c(x,y,z)$,

$$\Delta c = \frac{\partial^2 c}{\partial x^2} + \frac{\partial^2 c}{\partial y^2} + \frac{\partial^2 c}{\partial z^2},$$

and s denotes the secretion rate of the stimulators/inhibitors. For simplicity this rate is assumed to be piecewise constant given by $s = s_0$ inside the tumor and by $s = 0$ outside the tumor.

Assuming that the tumor is radially symmetric, the concentration c only depends on the distance r to the center of the tumor, $c = c(r)$. In spherical coordinates, the Laplace operator Δc takes the form

$$\Delta c(r) = \frac{1}{r^2}\frac{\partial}{\partial r}\left(r^2 \frac{\partial c}{\partial r}\right) = c''(r) + \frac{2c'(r)}{r}$$

and in so-called *quasi steady state* it also is assumed that the system has settled down to a temporal stationary scheme, i.e., that $\frac{\partial c}{\partial t} = 0$. Under these assumptions the consumption-diffusion equation (5.3) reduces to the second order ODE

$$c''(r) + \frac{2c'(r)}{r} - \frac{\gamma c(r)}{D^2} + \frac{s}{D^2} = 0$$

or, equivalently,

$$r^2 c''(r) + 2rc'(r) - \gamma \frac{r^2}{D^2}\left[c(r) - \frac{s}{\gamma}\right] = 0.$$

Transforming the dependent variable according to

$$z(r) = \sqrt{r}\left[c(r) - \frac{s}{\gamma}\right], \tag{5.4}$$

a direct calculation verifies that

$$r^2c''(r)+2rc'(r)=\frac{1}{\sqrt{r}}\left(r^2z''(r)+rz'(r)-\frac{1}{4}z\right)$$

and thus

$$r^2z''(r)+rz'(r)-\left(\gamma\frac{r^2}{D^2}+\frac{1}{4}\right)z=0.$$

Rescaling the independent variable as

$$r=\frac{D}{\sqrt{\gamma}}w,$$

we obtain a *modified Bessel equation of order* $\frac{1}{2}$ for the unknown function $z=z(w)$,

$$w^2z''(w)+wz'(w)-\left(w^2+\frac{1}{4}\right)z=0, \tag{5.5}$$

Two linearly independent solutions for this equation can be given in closed form as

$$z_1(w)=\frac{e^w}{\sqrt{w}} \qquad \text{and} \qquad z_2(w)=\frac{e^{-w}}{\sqrt{w}}$$

and thus any solution z of (5.5) is of the form

$$z(w)=\alpha z_1(w)+\beta z_2(w)=\frac{\alpha e^w+\beta e^{-w}}{\sqrt{w}}. \tag{5.6}$$

for some real numbers α and β.

The concentration $c=c(r)$ of stimulators at distance $r=\frac{D}{\sqrt{\gamma}}w$ to the tumor center is a function made up of a solution $n_{\text{in}}(r)$ that describes the concentration inside the tumor, i.e., over the interval $[0,r_0]$, and another solution $n_{\text{out}}(r)$ that describes this concentration outside of the tumor, or, formally, over the interval $[r_0,\infty)$. In the first case, the secretion rate s is set to $s\equiv s_0$ while it is $s\equiv 0$ in the second. The differential equations differ in this constant term. Note that it follows from the transformation (5.4) that

$$n_{\text{in}}(r)=\frac{z_{\text{in}}\left(\frac{\sqrt{\gamma}}{D}r\right)}{\sqrt{r}}+\frac{s_0}{\gamma} \qquad \text{and} \qquad n_{\text{out}}(r)=\frac{z_{\text{out}}\left(\frac{\sqrt{\gamma}}{D}r\right)}{\sqrt{r}}.$$

The concentration inside the tumor cannot have a singularity at $r=0$ and for this reason must be a smooth function of r. This requires that for $z_{\text{in}}(w)$ we have that $\alpha+\beta=0$ in (5.6) and thus necessarily, for some constant a

$$z_{\text{in}}(w)=\frac{a}{2}\left(\frac{e^w}{\sqrt{w}}-\frac{e^{-w}}{\sqrt{w}}\right)=a\frac{\sinh w}{\sqrt{w}}.$$

Similarly, the concentration outside of the tumor decays as $r \to \infty$ and therefore for $z_{\text{out}}(w)$ we must have that $\alpha = 0$. Hence, with some constant b we have that

$$z_{\text{out}}(w) = b\frac{e^{-w}}{\sqrt{w}}.$$

Overall, it is then postulated that the inside and outside concentrations $c_{\text{in}}(r)$ and $c_{\text{out}}(r)$ match in a continuously differentiable way for $r = r_0$. If we set $\tilde{a} = \sqrt{\frac{\sqrt{\gamma}}{D}}a$, $\tilde{b} = \sqrt{\frac{\sqrt{\gamma}}{D}}b$ and $w_0 = \frac{\sqrt{\gamma}}{D}r_0$, then continuity of the concentration at the tumor radius r_0 is equivalent to

$$c_{\text{in}}(r_0) = \frac{s_0}{\gamma} + \tilde{a}\frac{\sinh(w_0)}{w_0} = \tilde{b}\frac{e^{-w_0}}{w_0} = c_{\text{out}}(r_0). \tag{5.7}$$

Similarly, for the derivatives we have that

$$\begin{aligned}\frac{d}{dr}(c_{\text{in}}(r)) &= \tilde{a}\frac{d}{dw}\left(\frac{\sinh w}{w}\right)\frac{dw}{dr} = \tilde{a}\left(\frac{\cosh w}{w} - \frac{\sinh w}{w^2}\right)\frac{\sqrt{\gamma}}{D} \\ &= \tilde{a}\frac{\sqrt{\gamma}}{D}\frac{w\cosh w - \sinh w}{w^2}\end{aligned}$$

and

$$\begin{aligned}\frac{d}{dr}(c_{\text{outside}}(r)) &= \tilde{b}\frac{d}{dw}\left(\frac{e^{-w}}{w}\right)\frac{dw}{dr} = \tilde{b}\left(-\frac{e^{-w}}{w} - \frac{e^{-w}}{w^2}\right)\frac{\sqrt{\gamma}}{D} \\ &= -\tilde{b}\frac{\sqrt{\gamma}}{D}\frac{1+w}{w^2}e^{-w}.\end{aligned}$$

The concentrations match continuously differentiable at r_0 if and only if

$$\tilde{a}(w_0\cosh w_0 - \sinh w_0) = -\tilde{b}(1+w_0)e^{-w_0}. \tag{5.8}$$

Substituting (5.7) into (5.8) gives

$$\tilde{a}(w_0\cosh w_0 - \sinh w_0) = -(1+w_0)\left[\frac{s_0}{\gamma} + \tilde{a}\frac{\sinh(w_0)}{w_0}\right]w_0$$

which yields

$$\tilde{a} = -\frac{s_0}{\gamma}[1+w_0]e^{-w_0} \qquad \text{and} \qquad \tilde{b} = \frac{s_0}{\gamma}[w_0\cosh w_0 - \sinh w_0].$$

Summarizing, we have the following formulas:

Proposition 5.1.1. [116] *The inside and outside tumor concentrations of inhibitors/stimulators are given by*

$$c_{\text{in}}(r) = \frac{s_0}{\gamma}\left[1 - \left(1 + \frac{\sqrt{\gamma}}{D}r_0\right)\exp\left(-\frac{\sqrt{\gamma}}{D}r_0\right)\frac{\sinh\left(\frac{\sqrt{\gamma}}{D}r\right)}{\left(\frac{\sqrt{\gamma}}{D}r\right)}\right],$$

and

$$c_{\text{out}}(r) = \frac{s_0}{\gamma}\left[\frac{\sqrt{\gamma}}{D}r_0\cosh\left(\frac{\sqrt{\gamma}}{D}r_0\right) - \sinh\left(\frac{\sqrt{\gamma}}{D}r_0\right)\right]\frac{\exp\left(-\frac{\sqrt{\gamma}}{D}r\right)}{\left(\frac{\sqrt{\gamma}}{D}r\right)}.$$

For the case of **angiogenic inhibitors**, in accordance with their more systemic effects, the clearance rate γ is small against the diffusion coefficient. Assuming that $\gamma \ll \frac{D^2}{r_0^2}$, or, equivalently that $\frac{\sqrt{\gamma}}{D}r_0 \ll 1$, these solutions give rise to the following asymptotic expansions for the concentrations inside and outside of the tumor:

$$\begin{aligned} c_{\text{in}}(r) &= \frac{s_0}{\gamma}\left[1 - \left(1 + \frac{\sqrt{\gamma}}{D}r_0\right)\left(1 - \frac{\sqrt{\gamma}}{D}r_0 + \frac{1}{2}\left(\frac{\sqrt{\gamma}}{D}r_0\right)^2 + \ldots\right)\right. \\ &\qquad \left.\times\left(1 + \frac{1}{6}\left(\frac{\sqrt{\gamma}}{D}r\right)^2 + \ldots\right)\right] \\ &= \frac{s_0}{\gamma}\left[1 - \left(1 - \frac{1}{2}\gamma\frac{r_0^2}{D^2} + \ldots\right)\left(1 + \frac{1}{6}\gamma\frac{r^2}{D^2} + \ldots\right)\right] \\ &= s_0\left[\frac{1}{2}\frac{r_0^2}{D^2} - \frac{1}{6}\frac{r^2}{D^2} + \ldots\right] \approx \frac{s_0}{6D^2}\left[3r_0^2 - r^2\right] \end{aligned}$$

and

$$\begin{aligned} c_{\text{out}}(r) &= \frac{s_0}{\gamma}\left[\frac{\sqrt{\gamma}}{D}r_0\left(1 + \frac{1}{2}\left(\frac{\sqrt{\gamma}}{D}r_0\right)^2 + \ldots\right) - \left(\frac{\sqrt{\gamma}}{D}r_0 + \frac{1}{6}\left(\frac{\sqrt{\gamma}}{D}r_0\right)^3 + \ldots\right)\right] \\ &\qquad \times\frac{\left(1 - \frac{\sqrt{\gamma}}{D}r + \ldots\right)}{\left(\frac{\sqrt{\gamma}}{D}r\right)} \\ &= \frac{s_0}{\gamma}\frac{r_0}{r}\left[\left(1 + \frac{1}{2}\gamma\frac{r_0^2}{D^2} + \ldots\right) - \left(1 + \frac{1}{6}\gamma\frac{r_0^2}{D^2} + \ldots\right)\right](1 + \ldots) \\ &\approx \frac{1}{3}\frac{s_0 r_0^3}{D^2}\frac{1}{r}. \end{aligned}$$

For $r = r_0$, this expression reduces to the term $\frac{1}{3}\frac{s_0}{D^2}r_0^2$ and it follows that inhibitors will impact endothelial cells in a way that grows with the square of the tumor radius, r_0^2, i.e., is proportional to the tumor surface. With p denoting the primary tumor volume and q representing the carrying capacity measured in terms of the volume of endothelial cells, and arguing that the inhibition term $I(p,q)$ is determined by

tumor cells producing inhibitors that impact the vasculature, the functional form of the inhibition term $I(p,q)$ is given by the product of $p^{\frac{2}{3}}$ with q, i.e., takes the form

$$I(p,q) = dp^{\frac{2}{3}}q \tag{5.9}$$

with d a constant, mnemonically labeled as a "death" rate. More intuitively, inhibitors need to be released through the tumor surface and therefore the interaction is not between the volumes p and q, but between $p^{\frac{2}{3}}$ and q.

On the other hand, tumor-derived **stimulators** act locally and this is reflected in a *fast clearing* of the inhibitors. If γ is large, then the exponential terms are small and approximately we get that

$$\begin{aligned} c_{\text{in}}(r) &= \frac{s_0}{\gamma}\left[1-\left(1+\frac{\sqrt{\gamma}}{D}r_0\right)\exp\left(-\frac{\sqrt{\gamma}}{D}r_0\right)\frac{\sinh\left(\frac{\sqrt{\gamma}}{D}r\right)}{\left(\frac{\sqrt{\gamma}}{D}r\right)}\right] \\ &\approx \frac{s_0}{\gamma}\left[1-\left(\frac{rD}{\sqrt{\gamma}}+\frac{r_0}{r}\right)\frac{1}{2}\exp\left(\frac{\sqrt{\gamma}}{D}(r-r_0)\right)\right] \approx \frac{s_0}{\gamma}, \qquad r<r_0, \end{aligned}$$

and

$$\begin{aligned} c_{\text{out}}(r) &= \frac{s_0}{\gamma}\left[\frac{\sqrt{\gamma}}{D}r_0\cosh\left(\frac{\sqrt{\gamma}}{D}r_0\right)-\sinh\left(\frac{\sqrt{\gamma}}{D}r_0\right)\right]\frac{\exp\left(-\frac{\sqrt{\gamma}}{D}r\right)}{\left(\frac{\sqrt{\gamma}}{D}r\right)} \\ &\approx \frac{s_0}{\gamma}\left[\frac{1}{2}\left(\frac{\sqrt{\gamma}}{D}r_0-1\right)\exp\left(\frac{\sqrt{\gamma}}{D}r_0\right)\right]\frac{\exp\left(-\frac{\sqrt{\gamma}}{D}r\right)}{\left(\frac{\sqrt{\gamma}}{D}r\right)} \\ &\approx \frac{s_0}{\gamma}\left[\frac{1}{2}\left(\frac{r_0}{r}-\frac{D}{r\sqrt{\gamma}}\right)\exp\left(\frac{\sqrt{\gamma}}{D}(r_0-r)\right)\right] \approx 0, \qquad r>r_0. \end{aligned}$$

It thus follows that the impact of the stimulators is relatively constant with tumor size.

As the tumor radius r_0 increases, the effect of the inhibitors on endothelial cells thus will become dominant over the one of the stimulators leading to a saturation of tumor growth. Since $c(r_0) \approx \frac{1}{3}\frac{s_0}{D^2}r_0^2$ for angiogenic inhibitors and $c_{\text{in}}(r_0) \approx \frac{s_0}{\gamma}$ for tumor derived stimulators, it can therefore be argued that the inhibitor term $I(p,q)$ grows at a rate of $p^\alpha q^\beta$ faster than the stimulator term $S(p,q)$ where approximately $\alpha+\beta=\frac{2}{3}$,

$$\frac{I(p,q)}{S(p,q)} \simeq p^\alpha q^\beta, \qquad \alpha+\beta=\frac{2}{3}. \tag{5.10}$$

Summarizing, an asymptotic analysis of the underlying consumption-diffusion model establishes the following two principal conclusions about the relations for endogenous inhibition and stimulation between the tumor and its vasculature:

1. *the inhibitor $I(p,q)$ impacts endothelial cells in a way that is proportional to the tumor surface area, i.e., grows like $p^{\frac{2}{3}}$, and*
2. *the inhibitor $I(p,q)$ term tends to grow at a rate of $p^{\alpha}q^{\beta}$ faster than the stimulator term $S(p,q)$ where $\alpha+\beta=\frac{2}{3}$.*

5.1.2 A Cornucopia of Models

Thus, taking into account (5.9), the stimulation term S can be expressed in the form

$$S(p,q) \simeq p^{\left(\frac{2}{3}-\alpha\right)}q^{1-\beta}, \qquad \alpha+\beta=\frac{2}{3}.$$

But there exists freedom in the choice of α and β. For example, choosing $\alpha=-\frac{1}{3}$ and $\beta=1$ gives a stimulation term that is proportional to the tumor volume,

$$S(p,q)=bp, \tag{5.11}$$

with b a constant labeled for "birth." This choice, made in [116], results in a dynamics for the carrying capacity of the form

$$\dot{q}=bp-dp^{\frac{2}{3}}q-\mu q.$$

But also other choices are consistent with the above conclusions and, for example, taking $\alpha=\frac{2}{3}$ and $\beta=0$ results in the equally simple form

$$S(p,q)=bq \tag{5.12}$$

when the stimulation is proportional to the carrying capacity. The latter choice in fact generates a considerably simpler q-dynamics since q will factor,

$$\dot{q}=bq-dp^{\frac{2}{3}}q-\mu q=q\left(b-dp^{\frac{2}{3}}-\mu\right).$$

In quasi steady state, p and q will be closely related and thus both choices may be thought of as similar, but these two systems have different types of optimal controlled trajectories [204].

In the paper [116], the model using (5.11) was biologically validated based on experimental data for Lewis lung carcinoma implanted in male mice. Lewis lung carcinoma is a very fast growing type of cancer and for the parameter values reported in [116] the q-dynamics is fast and the dynamics overall has a strong differential-algebraic character, i.e., the movement is mostly confined to the slow manifold in (p,q)-space defined by the equation $\dot{q}=0$ (see Figure 5.1). It was argued by Ergun, Camphausen and Wein in [77] that indeed the system reaches this steady state too fast and hence in that paper modifications were made that slow down the q-dynamics. Compared with the first conclusion above, in this approach the inhibitor

term is taken proportional to the tumor radius r_0, not the tumor surface r_0^2, i.e., the exponent $\frac{2}{3}$ in the first conclusion of the analysis from [116] is replaced with $\frac{1}{3}$. This leads to an inhibition term of the form $I(p,q) = dp^{\frac{1}{3}}q$. At the same time, the second conclusion of [116], that inhibitors tend to grow faster than stimulators with the powers α and β adding to $\frac{2}{3}$, is retained which then leads to a stimulation term of the form $S(p,q) = bp^{\frac{2}{3}}$. Since the variables p and q tend to be closely related in quasi steady state, it is still argued that p and q can be interchanged in a quasi steady-state analysis and the variable p is replaced with q in the q-dynamics. This leads to the simplified dynamics

$$\dot{q} = bq^{\frac{2}{3}} - dq^{\frac{4}{3}} - \mu q. \tag{5.13}$$

As a justification for this choice of the stimulation term, it could also be argued that the necrotic core of the tumor does not contribute to the stimulation of the vasculature and thus the exponent $2/3$ could be interpreted as scaling down the stimulation effects from the full tumor volume p to a shell like region around the tumor surface, i.e., use $p^{\frac{2}{3}}$ instead of p in the stimulation term to get $S(p,q) = bp^{\frac{2}{3}}$. Then, once again p is replaced with q in the quasi steady-state analysis. The mathematical advantage of this approach lies in a significant simplification, but formally this eliminates a direct link between tumor volume p and endothelial support q and thus decouples the vasculature from the tumor. While here some in a sense radical changes have been made to the original model, we shall see in Section 5.4 that the synthesis of optimal controlled trajectories is in its structure identical for these two models.

But clearly, replacing p with q, although somewhat justified in the end by our analysis to be given in this chapter, is somewhat problematic. We therefore also consider the model that, as in [77] retains the exponent $\frac{1}{3}$ to model the impact of inhibitors on the vasculature, but does not replace p with q. This leads to the following inhibition and stimulation terms

$$I(p,q) = dp^{\frac{1}{3}}q \qquad \text{and} \qquad S(p,q) = bp^{\frac{2}{3}}$$

with $\frac{I}{S} \simeq qp^{-\frac{1}{3}}$ which is consistent with the second premise of [116]. More generally, we shall consider a stimulation term of the form

$$S(p,q) = bp^{\theta}$$

with θ a parameter. The choice $\theta = 1$ corresponds to the term chosen in [116] while $\theta = \frac{2}{3}$ is consistent with the modification made in [77]. Note that for $\theta = 1$ we have $\frac{I}{S} \simeq qp^{-\frac{2}{3}}$ and thus $\alpha + \beta = \frac{1}{3}$ violating the second modeling premise of [116]. Thus these models can be thought of as interpolating between the models of [116] and [77]. We summarize the q-dynamics of all four models in Table 5.1.

Figure 5.1 illustrates the uncontrolled dynamics for the models $[H]$ from [116], $[E]$ from [77] and the two interpolating models $[I_\theta]$ for $\theta = \frac{2}{3}$ and $\theta = 1$ for parameter values based on the data from [116]. Since we eventually will be interested in

Table 5.1 Models for inhibition and stimulation.

Model	Inhibition $I(p,q)$	Stimulation $S(p,q)$	Reference
[H]	$dp^{\frac{2}{3}}q$	bp	[116]
[I]	$dp^{\frac{1}{3}}q$	$bp^{\theta}, \quad \theta = \frac{2}{3}, 1$	[293]
[E]	$dq^{\frac{4}{3}}$	$bq^{\frac{2}{3}}$	[77]

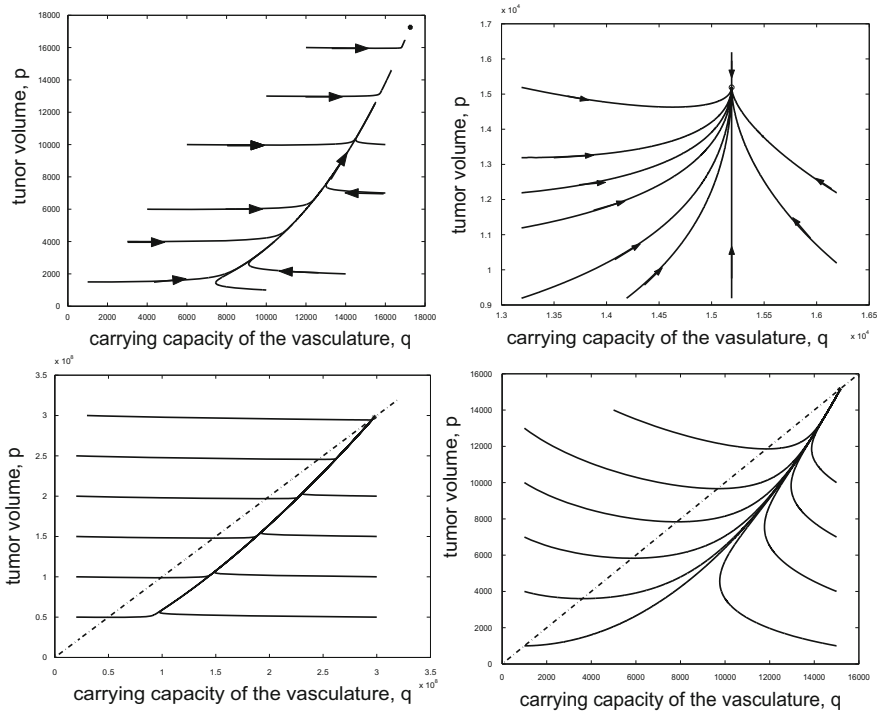

Fig. 5.1 Phase portraits for the dynamical systems $[H]$ (top left), $[E]$ (top right), $[I_1]$ (bottom left), and $[I_{\frac{2}{3}}]$ (bottom right) for the parameter values given in Table 5.2. The diagonal is shown as dash-dotted line.

minimizing the tumor volume, we have elected to plot the tumor volume p vertically and the carrying capacity q horizontally as this better visualizes tumor growth and loss. Note the strong differential-algebraic character that the two models $[H]$ and $[I_1]$ show which have the inhibition term proportional to the tumor surface area; away from the slow manifold the dynamics is almost horizontal. For the systems $[E]$ and $[I_{\frac{2}{3}}]$ when this term is proportional to the tumor radius, this dynamics, although still quite fast, has been modulated. The parameter values that were used to generate these phase portraits are taken from [116] and are summarized in Table 5.2. We shall use these values throughout this chapter in our numerical illustrations, but the theoretical analysis will be done independently of specific parameter values and our results are fully robust.

Table 5.2 Variables and parameter values used in numerical simulations based on the data from [116].

Variable/coefficients	Interpretation	Numerical value	Dimension
p	Tumor volume		mm^3
q	Carrying capacity of the vasculature		mm^3
ξ	Tumor growth parameter	0.084, 0.192	day^{-1}
μ	Natural loss of endothelial support	0, 0.02	day^{-1}
b	Stimulation parameter, 'birth'	5.85	day^{-1}
d	Inhibition parameter, 'death'	0.00873	$mm^{-2}\ day^{-1}$

5.2 Antiangiogenic Treatment as an Optimal Control Problem

We formulate antiangiogenic treatment as an optimal control problem, state the necessary conditions for optimality of the maximum principle (c.f., Theorem A.2.1 in Appendix A), and derive general properties of optimal solutions that will apply to all models considered. We then specialize to the main models separately in later sections.

5.2.1 Formulation as an Optimal Control Problem

We now add treatment in terms of an antiangiogenic agent to the model. As in previous chapters, initially we do not include the standard pharmacokinetic model and identify the agent's dose rate with its concentration in the plasma. The variable u represents this control in the system. Following the log-kill model, a term γqu describes the loss to the vasculature and is subtracted from the dynamics for the carrying capacity; γ is a constant that represents the antiangiogenic killing parameter. In view of subsequent extensions, we prefer not to normalize the control set U, but choose a compact interval $U = [0, u_{\max}]$ with $u_{\max}$ denoting an a priori set maximum dose rate/concentration. Clearly, this interval could be normalized by replacing γ with $\gamma u_{\max}$, but in view of adding a pharmacokinetic model later on we prefer to keep this mathematical redundancy in our formulation.

We consider the problem how an a priori given, fixed amount A of angiogenic inhibitors should be scheduled in time to achieve the smallest possible tumor volume. In this formulation, there is no fixed therapy horizon $[0,T]$, but rather the terminal time T is free, $T \in [0,\infty)$, and it merely represents the time when the minimum tumor volume is being realized. Such a formulation, that also was considered by Ergun, Camphausen, and Wein in [77], is practically of great interest and gives an important alternative to the earlier finite therapy horizon formulations in Chapters 2 and 3. There exist various modifications of the formulation below that could be considered as well and lead to problems that all can be tackled using similar procedures as they will be developed here with only minor modifications in the structure of

the optimal solution (e.g., see [197, 205, 189]). We consider the following optimal control problem for the antiangiogenic monotherapy problem:

[OCA] for a free terminal time T, minimize the terminal value $p(T)$ of the tumor volume subject to the dynamics

$$\begin{aligned} \dot{p} &= -\xi p \ln\left(\frac{p}{q}\right), & p(0) &= p_0, \\ \dot{q} &= S(p,q) - I(p,q) - \mu q - \gamma u q, & q(0) &= q_0, \end{aligned}$$

over all Lebesgue measurable (respectively, piecewise continuous) functions $u : [0,T] \to [0,u_{\max}]$ that satisfy a constraint on the total amount of angiogenic inhibitors to be administered,

$$\int_0^T u(t)dt \leq A. \tag{5.14}$$

The solution to the problem gives the protocol that achieves the smallest tumor volume achievable with the overall available amount A of inhibitors and T is the time when the minimum tumor volume is being realized. Mathematically, it is more convenient to adjoin the isoperimetric constraint (5.14) as a third variable and define the problem in $\mathbb{R}^3_+$. Hence we consider the following equivalent version of formulation [OCA]:

[OCA] For a free terminal time T, minimize the terminal value $p(T)$ of the tumor volume subject to the dynamics

$$\dot{p} = -\xi p \ln\left(\frac{p}{q}\right), \qquad p(0) = p_0, \tag{5.15}$$

$$\dot{q} = S(p,q) - I(p,q) - \mu q - \gamma u q, \qquad q(0) = q_0, \tag{5.16}$$

$$\dot{y} = u, \qquad y(0) = 0, \tag{5.17}$$

over all Lebesgue measurable functions (respectively, piecewise continuous) $u : [0,T] \to [0,u_{\max}]$ for which the corresponding trajectory satisfies $y(T) \leq y_{\max} = A$.

Recall that, for any admissible control $u : [0,T] \to [0,u_{\max}]$, the corresponding trajectory $z = (p,q,y)^T$ is the solution to the initial value problem (5.15)–(5.17) and that we call the pair (z,u) consisting of the control and its corresponding trajectory a *controlled trajectory*. It is clear from the problem formulation that one condition for the system to accurately reflect the underlying biological situation is that the variables p and q remain positive. This holds for each of the models from Table 5.1 and will be established when we take a detailed look at specific systems. We make the following natural assumption on the dynamics:

(A) In quasi steady state, i.e., on the diagonal $p = q$, the upper limit $u_{\max}$ on the control is large enough to overcome the net balance between endogenous stimulatory and inhibitory terms, i.e., for all $q > 0$ we have that

$$S(q,q) - I(q,q) < (\gamma u_{\max} + \mu)\, q.$$

Along intervals on the diagonal where this condition is not satisfied, stimulatory effects are simply too strong and it is not possible to reduce the tumor volume locally with a maximum dose $u_{\max}$. Essentially, we assume that the maximum concentration for the antiangiogenic agent is large enough to overcome the endogenous net-stimulation in equilibrium.

One consequence of using the Gompertzian growth function is that the tumor volume is always decreasing in the region $\mathscr{D}_+ = \{(p,q) : p > q\}$ and increasing in the region $\mathscr{D}_- = \{(p,q) : p < q\}$. This generates some degeneracies in the problem formulation [OCA] that are not very relevant medically and that we want to exclude in our analysis. Essentially, this happens for initial conditions (p_0, q_0) that satisfy $q_0 \gg p_0$ when the overall amount A of angiogenic inhibitors is too small. In such a case, as it is schematically indicated in Figure 5.2, initially the tumor volume will always be increasing until the diagonal $\mathscr{D}_0 = \{(p,q) : p = q\}$ is crossed. Only then the tumor volume can be reduced. But if A is too small, the minimum value that is subsequently realizable will be higher than p_0. In this case, the smallest tumor volume is therefore equal to p_0 and was achieved at $T = 0$. Clearly, the mathematically "optimal" solution for problem [OCA] thus is simply to do nothing and take $T = 0$. It can easily be determined a priori whether this applies to a given initial condition (p_0, q_0, A). In this case, it is still possible to slow down the tumor's growth, for example, by giving the full dose $u = u_{\max}$ until all inhibitors run out (we shall see later on that this need not be the best way of doing this). However, this then becomes a different control problem and, from a practical point of view, we are fighting a lost battle to begin with. We thus make the following definition.

Definition 5.2.1 (Well-Posed Initial Data). We say the initial data (p_0, q_0, A) are *ill-posed* for the optimal control problem [OCA] if for no admissible control it is possible to reach a point (p,q) with $p < p_0$. The optimal solution for the problem $[OCA]$ with ill-posed data is given by $T = 0$. The initial data (p_0, q_0, A) are said to be *well posed* if an objective value better than p_0 is realizable. In this case, the final time T along the optimal control is positive.

Clearly, whether or not given initial data (p_0, q_0, A) are well posed depends on the specific system under consideration (inhibition and stimulation terms, values of the parameters, etc.), but any initial condition (p_0, q_0) that satisfies $p_0 \geq q_0$, i.e., lies in $\mathscr{D}_+ = \{(p,q) : p > q\}$ or on the diagonal $\mathscr{D}_0 = \{(p,q) : p = q\}$, is automatically well posed. The same holds for the majority of initial conditions in $\mathscr{D}_- = \{(p,q) : p < q\}$ with, realistically, only extreme situations ill-posed. Henceforth *we only consider well-posed initial data* (p_0, q_0, A).

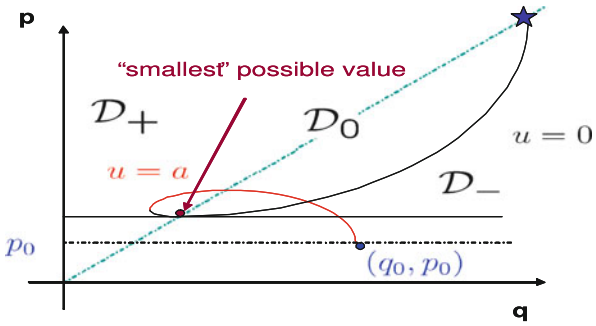

Fig. 5.2 Illustration of the dynamic behavior of the system for an ill-posed initial condition.

5.2.2 Necessary Conditions for Optimality—General Structure

Some arguments about optimality of controlled trajectories apply to all models regardless of the specific terms chosen for the inhibition and stimulation terms and in the rest of this section we develop those general facts before going into the details of the various models. As before, first-order necessary conditions for optimality of a control u are given by the Pontryagin maximum principle (Theorem A.2.1 in Appendix A). With a 3-dimensional row vector $\lambda = (\lambda_1, \lambda_2, \lambda_3) \in (\mathbb{R}^3)^*$, the Hamiltonian function $H = H(\lambda, p, q, u)$ is given by

$$H(\lambda, p, q, u) = -\lambda_1 \xi p \ln\left(\frac{p}{q}\right) + \lambda_2 \left(S(p,q) - I(p,q) - \mu q - \gamma u q\right) + \lambda_3 u. \quad (5.18)$$

Theorem 5.2.1. *If u_* is an optimal control defined over an interval $[0,T]$ with corresponding trajectory (p_*, q_*, y_*), then there exist a constant $\lambda_0 \geq 0$ and an absolutely continuous co-vector, $\lambda : [0,T] \to (\mathbb{R}^3)^*$, such that the following conditions hold:*
(a) *(nontriviality condition) $(\lambda_0, \lambda(t)) \neq (0,0)$ for all $t \in [0,T]$,*
(b) *(adjoint equations) λ_1 and λ_2 satisfy the equations*

$$\dot{\lambda}_1 = -\frac{\partial H}{\partial p} = \lambda_1 \xi \left(\ln\left(\frac{p}{q}\right) + 1\right) - \lambda_2 \left(\frac{\partial S}{\partial p}(p,q) - \frac{\partial I}{\partial p}(p,q)\right), \quad (5.19)$$

$$\dot{\lambda}_2 = -\frac{\partial H}{\partial q} = -\lambda_1 \xi \frac{p}{q} + \lambda_2 \left(\mu - \frac{\partial S}{\partial q}(p,q) + \frac{\partial I}{\partial q}(p,q) + \gamma u\right), \quad (5.20)$$

with terminal conditions

$$\lambda_1(T) = \lambda_0, \qquad \text{and} \qquad \lambda_2(T) = 0; \quad (5.21)$$

λ_3 is constant and satisfies

$$\lambda_3 = \begin{cases} 0 & \text{if } y(T) < y_{\max}, \\ \geq 0 & \text{if } y(T) = y_{\max}. \end{cases} \quad (5.22)$$

(c) *(minimum condition) for almost every time $t \in [0,T]$, the optimal control $u_*(t)$ minimizes the Hamiltonian along $(\lambda(t), p_*(t), q_*(t))$ over the control set $[0, u_{\max}]$ with minimum value given by 0,*

$$H(\lambda(t), p_*(t), q_*(t), u_*(t)) = \min_{0 \le v \le u_{\max}} H(\lambda(t), p_*(t), q_*(t), v) \equiv 0. \tag{5.23}$$

In order to simplify the notation, we write $z = (p,q,y)^T$ for the 3-dimensional state. Also, recall that a pair (z,u) consisting of an admissible control u with corresponding trajectory $z = (p,q,y)^T$ for which there exist multipliers (λ_0, λ) such that the conditions of the Maximum Principle are satisfied is an *extremal* (pair) and the triple $(z,u,(\lambda_0,\lambda))$ is an extremal lift (to the cotangent bundle).

We start with establishing some general properties of optimal controls and extremals. We always assume that the initial conditions are well posed.

Lemma 5.2.1. *Along an optimal trajectory (p_*, q_*, y_*), all available inhibitors are exhausted, $y_*(T) = A$, and at the final time $p_*(T) = q_*(T)$ holds.*

Proof. Since the initial condition is well posed, the optimal final time T is positive. The tumor volume p is growing for $p < q$ and is shrinking for $p > q$. Hence optimal trajectories can only terminate at times where $p_*(T) = q_*(T)$. For, if $p_*(T) < q_*(T)$, then it would simply have been better to stop earlier since p was increasing over some interval $(T-\varepsilon, T]$. On the other hand, if $p_*(T) > q_*(T)$, then we can always add another small interval $(T, T+\varepsilon]$ with the control $u = 0$ without violating any of the constraints and p will decrease along this interval if ε is small enough. Thus, at the final time necessarily $p_*(T) = q_*(T)$. If $y_*(T) < A$, then it is still possible to add a small piece of a trajectory for $u = u_{\max}$ over some interval $[0, \varepsilon]$. Since $p_*(T) = q_*(T)$, it follows from assumption (A) that $\dot{q}_*(T) < 0$ and $\dot{p}_*(T) = 0$. Thus the trajectory enters the region $p > q$ where the tumor volume p is still decreasing further. Hence T was not the optimal time. □

Lemma 5.2.2. *Extremals are normal. The multipliers λ_1 and λ_2 cannot vanish simultaneously and λ_2 has only simple zeroes.*

Proof. The multipliers λ_1 and λ_2 satisfy the homogeneous linear system (5.19) and (5.20) and thus they vanish identically if and only if they both vanish at some time t. This is the case if and only if $\lambda_0 = 0$ and thus in this case the nontriviality of $(\lambda_0, \lambda(t))$ implies that the constant multiplier λ_3 is not zero. Hence it must be positive. The condition (5.23) therefore gives that $u \equiv 0$ and so the initial condition is ill-posed. Contradiction. Without loss of generality, we therefore may assume that $\lambda_0 = 1$ and consequently λ_1 and λ_2 cannot vanish simultaneously. In particular, whenever $\lambda_2(t) = 0$, then the coefficient in (5.20) at $\lambda_1(t)$ does not vanish and thus $\dot{\lambda}_2(t) \neq 0$. Hence λ_2 has only simple zeroes. □

We henceforth normalize $\lambda_0 = 1$. For almost every time t, the Hamiltonian $H(\lambda(t), p_*(t), q_*(t), u)$ is minimized over the interval $[0, u_{\max}]$ as a function of u by the optimal control $u_*(t)$. Since H is linear in u, and defining the *switching function* Φ as

$$\Phi(t) = \lambda_3 - \lambda_2(t)\gamma q_*(t), \tag{5.24}$$

it follows that

$$u_*(t) = \begin{cases} u_{\max} & \text{if } \Phi(t) < 0, \\ 0 & \text{if } \Phi(t) > 0. \end{cases} \tag{5.25}$$

Lemma 5.2.3. *If $\lambda_3 = 0$, then the corresponding optimal control is constant over the interval $[0,T]$ and given by the control $u \equiv u_{\max}$.*

Proof. In this case, the switching function can equivalently be defined by $\lambda_2(t)$ and thus has isolated zeroes by Lemma 5.2.2. Hence the corresponding control is bang-bang. Furthermore, $\lambda_2(T) = 0$ and $\dot{\lambda}_2(T) = -\xi\lambda_1(T)\frac{p_*(T)}{q_*(T)} = -\xi < 0$. Hence λ_2 is positive on some interval $(\tau,T]$ near the terminal time and here the control is given by $u(t) = u_{\max}$. Since $p_*(T) = q_*(T)$, it follows from assumption (A) that the end piece of the trajectory lies in $\mathscr{D}_-$ as long as the control is $u \equiv u_{\max}$. But then λ_2 cannot have another zero τ since otherwise we have $H(\tau) = -\lambda_1(\tau)\xi p_*(\tau)\ln\left(\frac{p_*(\tau)}{q_*(\tau)}\right) \neq 0$ and this contradicts equation (5.23). Thus the control is constant $u \equiv u_{\max}$. □

Except for this degenerate case (the initial condition happens to be such that with giving full dose all the time the diagonal is reached exactly when all inhibitors are exhausted), we can and henceforth will *assume that λ_3 is positive*. In particular, in this case optimal controls always end with an interval $(\tau,T]$ where $u \equiv 0$.

Corollary 5.2.1. *If $\lambda_3 > 0$, then there exists an interval $(\tau,T]$ such that $u_*(t) \equiv 0$ on $(\tau,T]$.*

Proof. By the transversality condition (5.21) we have that $\Phi(T) = \lambda_3 > 0$ and thus optimal controls are 0 near the terminal time. □

Corollary 5.2.2. *If an optimal control is singular over an interval I, then $\lambda_2(t) > 0$ for $t \in I$.*

Proof. This follows from the facts that $\lambda_3 > 0$ and the switching function Φ vanishes identically on I. □

5.2.3 Singular Control and Singular Arcs

Different from the problems considered in Chapter 2, singular controls now are at the heart of the solution for the optimal problem [OCA]. In this section, we give a preliminary analysis of their local structure and optimality under these rather general assumptions. If the control u is singular on some open interval I, the corresponding trajectory $z = (p,q,y)^T$ is called a *singular arc* and the triple (z,u,λ) a singular extremal (see Definition A.3.2 in Appendix A).

Again we need to analyze the switching function and its derivatives and, as already seen earlier, these computations can be expressed concisely within the framework of geometric optimal control theory. We write the dynamics in the form

$$\dot{z} = f(z) + ug(z) \tag{5.26}$$

where

$$f(z) = \begin{pmatrix} -\xi p \ln\left(\frac{p}{q}\right) \\ S(p,q) - I(p,q) - \mu q \\ 0 \end{pmatrix} \quad \text{and} \quad g(z) = \begin{pmatrix} 0 \\ -\gamma q \\ 1 \end{pmatrix}$$

with f the *drift* and g the *control vector field* of the system. With this notation, the Hamiltonian H takes the form

$$H = \langle \lambda, f(z) + ug(z) \rangle, \tag{5.27}$$

the adjoint equation for the multipliers simply reads

$$\dot{\lambda} = -\lambda \left(Df(z(t)) + u(t) Dg(z(t)) \right) \tag{5.28}$$

and the switching function Φ becomes the inner product of the multiplier λ with the control vector field g,

$$\Phi(t) = \lambda_3 - \lambda_2(t)\gamma q(t) = \langle \lambda(t), g(z(t)) \rangle .$$

For nonlinear models, the derivatives of the switching function can elegantly be computed in terms of the Lie-brackets of the drift and control vector fields. Since the Lagrangian L of the general problem formulation [OC] from Section A.3 in Appendix A vanishes for problem [OCA], Proposition A.3.1 takes the following form:

Proposition 5.2.1. *If h is a continuously differentiable vector field h and*

$$\Psi(t) = \langle \lambda(t), h(z(t)) \rangle ,$$

then the derivative of Ψ along a solution to the system equation (5.26) for control u and a solution λ to the corresponding adjoint equation (5.28), is given by

$$\dot{\Psi}(t) = \langle \lambda(t), [f + ug, h](z(t)) \rangle ,$$

with

$$[f,h](z) = Dh(z)f(z) - Df(z)h(z)$$

the Lie bracket of the vector fields f and h.

For the switching function $\Phi(t) = \langle \lambda(t), g(z(t)) \rangle$ we thus obtain that

$$\dot{\Phi}(t) = \lambda(t)[f,g](z(t))$$

and

$$\ddot{\Phi}(t) = \lambda(t)[f+ug,[f,g]](z(t)), \tag{5.29}$$

with the control u once more only appearing in the second derivative. If u is singular on some open interval I, then these derivatives all vanish identically on I and if $\langle \lambda(t), [g,[f,g]](z(t)) \rangle \neq 0$, then the singular control is of order 1 and (5.29) can formally be solved for u as

$$u_{\text{sing}}(t) = -\frac{\langle \lambda(t), [f,[f,g]](z(t)) \rangle}{\langle \lambda(t), [g,[f,g]](z(t)) \rangle}. \tag{5.30}$$

This relation defines the singular control as a function of the state $z(t)$ and the multiplier $\lambda(t)$. For the models considered here, all singular controls are of order 1. The strengthened Legendre-Clebsch condition for optimality of the singular control (c.f., Theorem A.3.2 in Appendix A) thus takes the following form:

$$\langle \lambda(t), [g,[f,g]](z(t)) \rangle < 0 \qquad \text{for all } t \in I. \tag{5.31}$$

The determination of singular controls and the analysis of their local optimality properties therefore reduces to the computation of the Lie brackets $[f,[f,g]]$ and $[g,[f,g]]$ and their inner products with the multiplier λ.

A special situation arises in dimension 3, the setting for the state-space in problem [OCA], if the control vector field g and the Lie brackets $[f,g]$ and $[g,[f,g]]$ are linearly independent. In this case, the Lie bracket $[f,[f,g]]$ can be written as a linear combination of this basis with coefficients that are smooth functions of the state z, say

$$[f,[f,g]](z) = \rho(z)g(z) + \varphi(z)[f,g](z) + \psi(z)[g,[f,g]](z).$$

Along a singular extremal (z,u,λ), the inner products of λ with $g(z(t))$ and $[f,g](z(t))$ vanish identically and thus

$$\langle \lambda(t), [f,[f,g]](z(t)) \rangle = \psi(z(t)) \langle \lambda(t), [g,[f,g]](z(t)) \rangle .$$

If the singular control is of order 1, we therefore simply have that

$$u_{\text{sing}}(t) = -\psi(z(t)). \tag{5.32}$$

In particular, in this case the singular control is given in *feedback* form, i.e., as a function of the state z alone, and no longer depends on the multiplier. Naturally, whether this feedback is admissible, that is, whether it takes values in the control set $[0,u_{\max}]$ needs to be determined for each problem separately and cannot be asserted in general.

Even when admissible, this feedback does not define a singular control everywhere, but only on a thin subset. The reason for this lies in the conditions of the

maximum principle, Theorem 5.2.1, that need to be satisfied. The condition (5.23) that $H \equiv 0$ requires that along a singular arc we also have that

$$\langle \lambda(t), f(z(t)) \rangle \equiv 0 \qquad \text{for all} \quad t \in I.$$

Thus the multiplier $\lambda(t)$ vanishes against the vector fields f, g and $[f,g]$ along a singular trajectory. Since $\lambda(t) \neq 0$ by Corollary 5.2.2, it follows that these vector fields must be linearly dependent along the singular arc and thus (5.32) only defines a singular control on the surface

$$\mathscr{S} = \{z \in \mathbb{R}^3 : \det(f(z), g(z), [f,g](z)) = 0\}$$

with $\det(f(z), g(z), [f,g](z))$ denoting the determinant of the matrix whose ordered columns are formed by the vectors $f(z)$, $g(z)$ and $[f,g](z)$.

We close this section with computing the relevant Lie brackets. If we define Δ as the difference between stimulation and inhibition terms, then direct computations verify that we have that

$$[f,g](z) = \gamma \begin{pmatrix} -\xi p \\ q\frac{\partial \Delta}{\partial q}(p,q) - \Delta(p,q) \\ 0 \end{pmatrix}$$

and

$$[g,[f,g]](z) = \gamma^2 \begin{pmatrix} 0 \\ -q^2\frac{\partial^2 \Delta}{\partial q^2}(p,q) + q\frac{\partial \Delta}{\partial q}(p,q) - \Delta(p,q) \\ 0 \end{pmatrix}.$$

Because of the special form of the control vector field g, the q-coordinates of Lie brackets with g can be expressed in a succinct form: let I denote the interval $(0,\infty)$ and for an infinitely often continuously differentiable function f of a scalar variable (in our case, q), $f \in C^\infty(I)$, denote by $\mathscr{L}$ the linear differential operator

$$\mathscr{L} : C^\infty(I) \to C^\infty(I), \quad f \mapsto \mathscr{L} f, \tag{5.33}$$

defined by

$$(\mathscr{L} f)(q) = q f'(q) - f(q). \tag{5.34}$$

Note that for any $\alpha \in \mathbb{R}$, the powers $f(q) = q^\alpha$ are eigenfunctions of this operator with eigenvalue $\lambda = \alpha - 1$, i.e.,

$$\mathscr{L}(q^\alpha) = (\alpha - 1) q^\alpha. \tag{5.35}$$

This allows for simple and elegant computations of the relevant Lie brackets for the models in Table 5.1, all of which are of such form. With $\mathscr{L}^n$ defined inductively by $\mathscr{L} \circ \mathscr{L}^{n-1}$, these Lie brackets then take the succinct form

$$[f,g](z) = \gamma \begin{pmatrix} -\xi p \\ \mathscr{L}(\Delta)(p,q) \\ 0 \end{pmatrix}, \qquad [g,[f,g]](z) = -\gamma^2 \begin{pmatrix} 0 \\ \mathscr{L}^2(\Delta)(p,q) \\ 0 \end{pmatrix} \tag{5.36}$$

where the operator $\mathscr{L}$ acts on q and all other variables are treated as constants. In particular, we have that

$$\langle \lambda(t), [g,[f,g]](z(t)) \rangle = -\gamma^2 \lambda_2(t) \mathscr{L}^2(\Delta)(p(t),q(t))$$

and using the fact that λ_2 is positive along a singular arc (Corollary 5.2.2), the strengthened Legendre-Clebsch condition (5.31) is satisfied if and only if

$$\mathscr{L}^2(\Delta)(p(t),q(t)) > 0$$

holds along the singular arc. In this case, the vector fields g, $[f,g]$ and $[g,[f,g]]$ are linearly independent and the singular control is given by (5.32). The auxiliary variable y does not appear explicitly in the dynamics of the system. As a result, the Lie bracket $[f,[f,g]]$ has last coordinate 0 and the vector field $[f,[f,g]]$ can be written in the form

$$[f,[f,g]](z) = \varphi(z)[f,g](z) + \psi(z)[g,[f,g]](z). \tag{5.37}$$

For the same reason, the singular surface $\mathscr{S}$ does not depend on y, i.e., is vertical in the y direction defined over the curve in (p,q)-space where the vector fields f and $[f,g]$ are parallel. Naturally, the explicit formulas depend on Δ. Summarizing these general calculations we have the following result:

Theorem 5.2.2. *If a control u is singular on some open interval (α,β), then the strengthened Legendre-Clebsch condition is satisfied on (α,β) if and only if*

$$\mathscr{L}^2(\Delta)(p(t),q(t)) > 0.$$

In this case, the singular control is given as a feedback function of the form

$$u_{\text{sing}}(t) = -\psi(z(t))$$

with ψ defined by the relation (5.37). The corresponding singular trajectory is locally minimizing for problem [OCA] and is located in the vertical surface $\mathscr{S}$ defined over the base locus $\mathscr{S}_0$ of points (p,q) where the vector fields f and $[f,g]$ are linearly dependent, i.e.,

$$\mathscr{S}_0 = \left\{ (p,q,y) : \ \Delta(p,q) + \mathscr{L}(\Delta)(p,q) \ln\left(\frac{p}{q}\right) - \mu q = 0. \right\}$$

The singular curve is admissible at points where the singular control defined by (5.32) takes values in the control interval $[0, u_{\max}]$. ■

The local optimality of the singular arc follows from a classical construction of Gardner-Moyer [103] in dimension 3 (also, see [292, Proposition 2.8.4]). Questions about the global optimality, however, are not resolved. But this local result gives a strong indication that the singular arcs will play an important role in the overall solutions to the problem if the strengthened Legendre-Clebsch condition is satisfied. This indeed is the case as now will be seen.

5.3 Optimal Synthesis for Model [H]

We give a complete solution for the optimal control problem [OCA] in form of a regular synthesis of optimal controlled trajectories when the dynamics for the vasculature is given by $S(p,q) = bp$ and $I(p,q) = dp^{\frac{2}{3}}q$. Thus we consider the following version of the general optimal control problem [OCA]:

[H] For a free terminal time T, minimize the tumor volume at the terminal time, $p(T)$, subject to the dynamics

$$\dot{p} = -\xi p \ln\left(\frac{p}{q}\right), \qquad p(0) = p_0, \tag{5.38}$$

$$\dot{q} = bp - dp^{\frac{2}{3}}q - \mu q - \gamma u q, \qquad q(0) = q_0, \tag{5.39}$$

$$\dot{y} = u, \qquad y(0) = 0, \tag{5.40}$$

over all Lebesgue measurable (respectively, piecewise continuous) functions $u : [0,T] \to [0, u_{\max}]$ for which the corresponding trajectory satisfies $y(T) \leq A$.

5.3.1 The Dynamical System with Constant Controls

For the analysis of the optimal control problem, it is of benefit to first fully understand the dynamic properties of the system for a constant control $u \equiv v$ with v some value in the control set $[0, u_{\max}]$. Note that y is merely an auxiliary variable that tracks the amounts of antiangiogenic agents administered and is immaterial for the dynamic behavior of the system. Thus here we only consider the (p,q)-dynamics. The uncontrolled system ($u \equiv 0$) has a unique equilibrium point at $(\bar{p}, \bar{q})$ given by $\bar{p} = \bar{q} = \left(\frac{b-\mu}{d}\right)^{\frac{3}{2}}$ and this equilibrium point is globally asymptotically stable, i.e.,

as $t \to \infty$ every solution converges to $(\bar{p}, \bar{q})$. (We shall not use this result and therefore refer the interested reader to the paper by d'Onofrio and Gandolfi [257] where these results are proven by means of suitable Lyapunov functions on $\mathbb{R}^2_+$.) However, the dynamic behavior of the system for tumor volumes and carrying capacities that are higher than $\bar{p}$ and $\bar{q}$ is not really medically relevant since this equilibrium point generally corresponds to a situation where life already is not viable. In order to exclude irrelevant discussions about the structure of optimal controls in regions where the model does not represent the underlying medical problem to begin with, we henceforth restrict our discussions to the following square domain $\mathscr{D}$,

$$\mathscr{D} = \{(p,q) : 0 < p < \bar{p},\ 0 < q < \bar{q}\},$$

and we restrict the sets $\mathscr{D}_{\pm,0}$ introduced earlier to this domain, i.e.,

$$\begin{aligned}\mathscr{D}_+ &= \{(p,q) \in \mathscr{D} : p > q\},\\ \mathscr{D}_0 &= \{(p,q) \in \mathscr{D} : p = q\},\\ \mathscr{D}_- &= \{(p,q) \in \mathscr{D} : p < q\}.\end{aligned}$$

Proposition 5.3.1. *$\mathscr{D}$ is positively invariant for the control system, i.e., if $(p_0,q_0) \in \mathscr{D}$ and u is an arbitrary admissible control defined on some interval $[0,T] \subset [0,\infty)$, then the solution $(p(\cdot),q(\cdot))$ to the corresponding dynamics with initial condition $(p(0),q(0)) = (p_0,q_0)$ exists for all $t \in [0,T]$ and lies in $\mathscr{D}$, $(p(t),q(t)) \in \mathscr{D}$.*

Proof. We need to show that, for arbitrary controls u, the corresponding trajectories cannot leave the region $\mathscr{D}$. Recall that we plot tumor volume p along the vertical axis and the carrying capacity q along the horizontal axis.

On the boundary segment $\{(p,q) \in \mathscr{D} : p = \bar{p},\ 0 < q < \bar{q}\}$ we have that $\dot{p} < 0$ and thus the vector field points into $\mathscr{D}$. In order to analyze the vector field on the vertical boundary segment $\{(p,q) \in \mathscr{D} : 0 < p < \bar{p},\ q = \bar{q}\}$, note that the nullclines for $\dot{q} = 0$ for a constant control v are given by

$$q = \Xi_v(p) = \frac{bp}{\mu + \gamma v + dp^{\frac{2}{3}}}$$

and we can rewrite the q-dynamics in the form

$$\dot{q} = bp - dp^{\frac{2}{3}}q - \mu q - \gamma u q = (\Xi_v(p) - q)\left(\mu + \gamma v + dp^{\frac{2}{3}}\right).$$

Thus we have $\dot{q} > 0$ for $q < \Xi_v(p)$ and $\dot{q} < 0$ for $q > \Xi_v(p)$. The functions $\Xi_v = \Xi_v(p)$ satisfy $\Xi_v(0) = 0$, are strictly increasing, and at $\bar{p}$ take the value

$$\Xi_v(\bar{p}) = \frac{b}{b + \gamma v}\bar{p}.$$

Thus, for all p, $0 < p < \bar{p}$, and all $v \in [0, u_{\max}]$ we have that

$$\Xi_v(p) < \Xi_v(\bar{p}) \le \bar{p} = \bar{q}.$$

Hence $\dot{q}$ is negative for trajectories starting at points in $\{(p,q) \in \mathscr{D} : 0 < p < \bar{p},\ q = \bar{q}\}$ and thus these trajectories enter $\mathscr{D}$.

The point $(\bar{p},\bar{q})$ is the equilibrium point for $u = 0$, but for any positive control u, the solution starting at $(\bar{p},\bar{q})$ enters $\mathscr{D}$. On the diagonal, $p = q$, we always have that $\dot{p} = 0$ and the second derivative reduces to $\ddot{p} = \xi\dot{q}$. Thus, at the equilibrium point $(\bar{p},\bar{q})$,

$$\ddot{p} = \xi\bar{p}\left(b - d\bar{p}^{\frac{2}{3}} - \mu - \gamma u\right) = -\xi\bar{p}\gamma u < 0$$

so that all trajectories have a local maximum. For a positive control, we have that $\dot{q} = -\gamma\bar{q}u < 0$ and thus trajectories enter $\mathscr{D}$. Hence, regardless of the value v of the control, trajectories can never leave the region $\mathscr{D}$ through the horizontal or vertical boundary segments for $p = \bar{p}$ or $q = \bar{q}$.

We still need to analyze the segments on the coordinate axes for $p = 0$ and $q = 0$. Here the dynamics has singularities and we therefore consider the lines $p = xq$ for $x > 0$. The dynamics (5.38) and (5.39) induces a motion on the projective variable x and it suffices to show that $\dot{x}$ is positive for small $x > 0$ (near the q-axis) and negative for large x (near the p-axis). We have that

$$\dot{x} = \frac{d}{dt}\left(\frac{p}{q}\right) = -\xi x\ln(x) - x\left(bx - dp^{\frac{2}{3}} - \mu - \gamma u\right) > x\left(-\xi\ln(x) - bx\right)$$

and thus $\dot{x}$ is positive for small $x > 0$. Furthermore, for $x > 1 + \frac{\gamma}{b}u_{\max}$ we have that

$$\dot{x} < x\left(d\bar{p}^{\frac{2}{3}} + \mu + \gamma u_{\max} - bx\right) = bx\left(1 + \frac{\gamma}{b}u_{\max} - x\right) < 0.$$

Hence the region $\mathscr{D}$ is positively invariant for the control system. □

By increasing the value v of the control, the equilibrium point $(\bar{p},\bar{q})$ can be shifted toward the origin along the diagonal and finally be eliminated altogether. As a function of v, the equilibrium is the unique fixed point of the equation $p = \Xi_v(p)$ in $\{p > 0\}$ and is given by

$$\bar{p}(v) = \bar{q}(v) = \left(\frac{b - \mu - \gamma v}{d}\right)^{\frac{3}{2}}$$

provided $b - \mu > \gamma v$; this equilibrium point $(\bar{p}(v),\bar{q}(v))$ remains globally asymptotically stable. As $b - \mu \leq \gamma v$, the system no longer has an equilibrium point and now all trajectories converge to the origin as $t \to \infty$ [257]. Thus, theoretically, eradication of the tumor is possible in this case, albeit only under the unrealistic scenario of constant treatment with unlimited supply of inhibitors.

Figure 5.3 compares the phase portraits of the uncontrolled system on the left with the one for $u \equiv u_{\max}$ on the right. Recall that we show the tumor volume as the vertical axis in our figures since this better visualizes the tumor reduction, respectively increase. For comparison, the diagonal is included in these figures as a dashed line. The dynamics implies that the tumor volume is decreasing in $\mathscr{D}_+$ and increasing in $\mathscr{D}_-$. Note that both the trajectories for the constant controls $u \equiv 0$ and

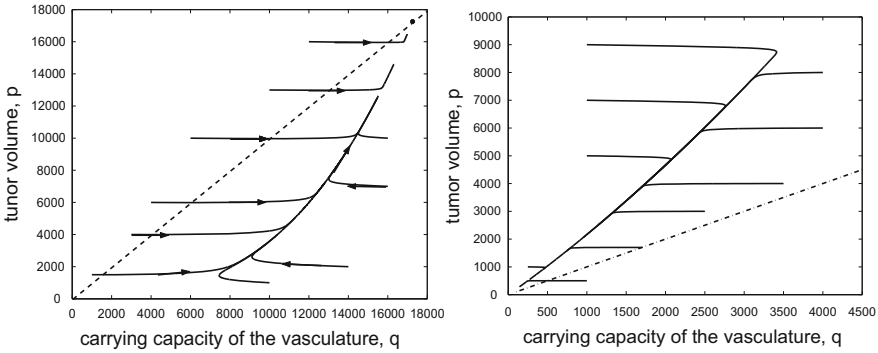

Fig. 5.3 Phase portraits for the dynamics [H] and constant controls $u \equiv 0$ and $u \equiv u_{\max} \equiv 75$.

$u \equiv u_{\max}$ cross the diagonal $\mathscr{D}_0 = \{(p,q) : p = q\}$ transversally: for $u = 0$, trajectories cross from $\mathscr{D}_+$ into $\mathscr{D}_-$ while they cross in opposite direction from $\mathscr{D}_-$ into $\mathscr{D}_+$ for $u = u_{\max}$. Also, trajectories for $u = 0$ approach the stable equilibrium $(\bar{p}, \bar{q})$ from within the region $\mathscr{D}_-$, while trajectories for $u = u_{\max}$ converge to the origin as $t \to \infty$ in the region $\mathscr{D}_+$.

We still note that a portion of the region $\mathscr{D}$ is transient and thus becomes of lower importance. Let

$$\mathscr{N}_0 = \{(p,q) \in \mathscr{D} : bp = (\mu + dp^{\frac{2}{3}})q\}$$

denote the $\dot{q}$-null cline of the uncontrolled system and define

$$\mathscr{N}_- = \{(p,q) \in \mathscr{D} : bp < (\mu + dp^{\frac{2}{3}})q\}$$

and

$$\mathscr{N}_+ = \{(p,q) \in \mathscr{D} : bp > (\mu + dp^{\frac{2}{3}})q\}$$

as the sets below, respectively above this nullcline (see Figure 5.4). We then have the following result:

Lemma 5.3.1. *Controlled trajectories cross $\mathscr{N}_0$ from $\mathscr{N}_-$ into $\mathscr{N}_+$. The region $\mathscr{N}_-$ is transient in the sense that all controlled trajectories leave $\mathscr{N}_-$ and cannot return.*

Proof. For arbitrary control values u, at points in $\mathscr{N}_0$ we have that

$$\dot{p} = -\xi p \ln\left(\frac{p}{q}\right) \qquad \text{and} \qquad \dot{q} = -\gamma u q.$$

In $\mathscr{D}$, i.e., for $0 < p < \bar{p} = \left(\frac{b-\mu}{d}\right)^{\frac{3}{2}}$ it holds that

$$b - \mu - dp^{\frac{2}{3}} = d\left(\frac{b-\mu}{d} - p^{\frac{2}{3}}\right) = d\left(\bar{p}^{\frac{2}{3}} - p^{\frac{2}{3}}\right) > 0$$

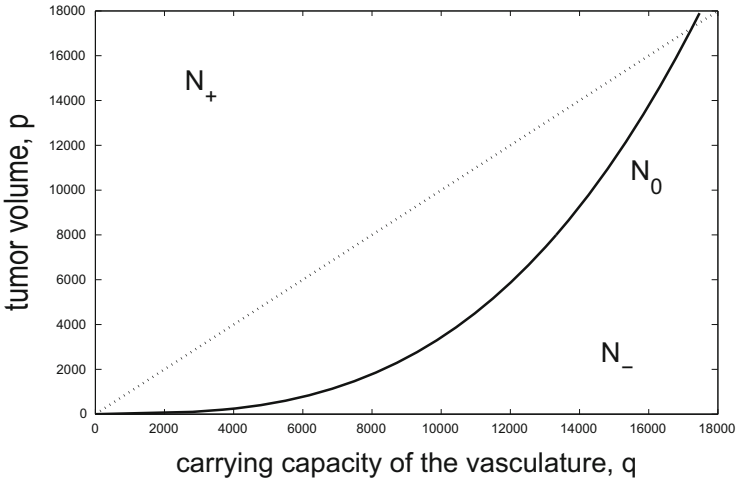

Fig. 5.4 The $\dot{q} = 0$ isocline $\mathscr{N}_0$ for the uncontrolled system, $u \equiv 0$.

and thus for $(p,q) \in \mathscr{N}_0$

$$\frac{p}{q} = \frac{\mu + dp^{\frac{2}{3}}}{b} < 1.$$

Hence $\mathscr{N}_0$ lies in the region $\mathscr{D}_-$. A normal vector to $\mathscr{N}_0$ at (p,q) is given by

$$\mathfrak{n} = \mathfrak{n}(p,q) = \begin{pmatrix} \frac{2}{3} d p^{-\frac{1}{3}} q - b \\ \mu + d p^{\frac{2}{3}} \end{pmatrix}$$

and its inner product with the (p,q)-dynamics is always negative:

$$\begin{aligned} \left\langle \mathfrak{n}, \begin{pmatrix} \dot{p} \\ \dot{q} \end{pmatrix} \right\rangle &= \xi p \ln\left(\frac{p}{q}\right)\left(b - \frac{2}{3} d p^{-\frac{1}{3}} q\right) - \gamma u q \left(\mu + d p^{\frac{2}{3}}\right) \\ &= b\xi p \ln\left(\frac{p}{q}\right)\left(1 - \frac{2}{3}\frac{d p^{\frac{2}{3}}}{\mu + d p^{\frac{2}{3}}}\right) - \gamma u q \left(\mu + d p^{\frac{2}{3}}\right) \\ &= \frac{b}{3}\xi p \ln\left(\frac{p}{q}\right)\left(\frac{3\mu + d p^{\frac{2}{3}}}{\mu + d p^{\frac{2}{3}}}\right) - \gamma u q \left(\mu + d p^{\frac{2}{3}}\right) < 0. \end{aligned}$$

Hence all trajectories of the control system cross $\mathscr{N}_0$ in the same direction. Looking at the control $u = 0$, it is clear that trajectories cross from $\mathscr{N}_-$ into $\mathscr{N}_+$ □

Thus, regardless of which control is used (in particular, for $u = 0$) trajectories leave the region $\mathscr{N}_-$ and states in this region only represent a short lived transient period. In our analysis we therefore restrict our attention to initial conditions (p,q) that lie in the set $\tilde{\mathscr{D}} = \mathscr{D} \cap (\mathscr{N}_+ \cup \mathscr{N}_0)$.

The parameter values for the antiangiogenic killing action that we use in our numerical illustrations are given below in Table 5.3. Our theoretical analysis is independent of these parameter values.

Table 5.3 Parameter values used for the antiangiogenic agent in numerical illustrations for the model [H].

Variable/ coefficient	Interpretation	Numerical value	Dimension
γ	Antiangiogenic killing parameter (for angiostatin)	0.15	conc^{-1} per day
$u_{\max}$	Maximum dose rate/concentration	75	mg per day
A	Total amount of antiangiogenic agents	300	mg

5.3.2 Geometric Analysis of the Singular Arc and Control

We compute explicit formulas for the singular control and corresponding trajectories for this model. The function $\Delta = S - I$ (see Section 5.2.3) is given by

$$\Delta(p,q) = S(p,q) - I(p,q) = bp - dp^{\frac{2}{3}}q.$$

Recall that the operator $\mathscr{L}$ is defined by $(\mathscr{L}f)(q) = qf'(q) - f(q)$ and we thus have that $\mathscr{L}(S) = -S$ and $\mathscr{L}(I) = 0$ which gives

$$\mathscr{L}(\Delta) = \mathscr{L}(S) - \mathscr{L}(I) = -S$$

and

$$\mathscr{L}^2(\Delta) = \mathscr{L}(-S) = S > 0.$$

In particular, by Theorem 5.2.2, singular controls are of order 1 and the strengthened Legendre condition is satisfied. Hence admissible singular arcs are locally optimal.

Recall that the singular surface $\mathscr{S}$ is the vertical surface in (p,q,y)-space defined over the base curve $\mathscr{S}_0$ of points (p,q) where the vector fields f and $[f,g]$ are linearly dependent, i.e.,

$$\Delta(p,q) + \mathscr{L}(\Delta)(p,q)\ln\left(\frac{p}{q}\right) - \mu q = 0.$$

For model [H] this relation reads

$$bp - dp^{\frac{2}{3}}q - bp\ln\left(\frac{p}{q}\right) - \mu q = 0.$$

We desingularize this equation with a blow-up of the form $p = xq$, $x > 0$, and using the projective coordinate x, we have that

$$\mu + dp^{\frac{2}{3}} = bx(1 - \ln x). \tag{5.41}$$

The quotient $\frac{q}{p}$ is proportional to the endothelial density and can be used to replace the carrying capacity of the vasculature as a variable. As it turns out, the singular curve and the corresponding singular control can be expressed solely in terms of the variable x. This fact indicates the importance of this quantity. However, for the overall analysis, and especially in view of a ready interpretation of the results, we prefer to keep the original variables p and q and only use x in the analysis of the singular arc. In these variables, equation (5.41) can be rewritten in the form

$$p^2 + \varphi(x)^3 = 0$$

with

$$\varphi(x) = \frac{1}{d}(x(\ln x - 1) + \mu).$$

The function φ is strictly convex with a minimum at $x = 1$ and minimum value $\frac{\mu - b}{d}$. For $\mu = 0$, the zeroes of φ are given by $x_1^* = 0$ and $x_2^* = e$ and φ is negative on the interval $(0, e)$. For $\mu > 0$ we have $\varphi(0) = \frac{\mu}{d} = \varphi(e)$ and the zeroes x_1^* and x_2^* satisfy $0 < x_1^* < 1 < x_2^* < e$. We thus have the following result:

Proposition 5.3.2. *The base curve $\mathscr{S}_0$ for the singular surface $\mathscr{S}$ entirely lies in the sector $\{(p,q) : x_1^* q < p < x_2^* q\}$ where x_1^* and x_2^* are the unique zeros of the equation $\varphi(x) = 0$ and satisfy $0 \le x_1^* < 1 < x_2^* \le e$. In the variables (p,x) with $x = \frac{p}{q}$, $\mathscr{S}_0$ can be parameterized in the form*

$$\mu + dp^{\frac{2}{3}} = bx(1 - \ln x) \qquad \text{for} \quad x_1^* < x < x_2^*. \tag{5.42}$$

It is important to understand the *geometric properties of the curve $\mathscr{S}_0$* and these are summarized in the result below. These technical considerations are needed in order to determine where the singular control will be admissible.

Proposition 5.3.3. *The singular base curve $\mathscr{S}_0$ traces a loop in (p,q)-space anchored at the origin that consists of the union of the following three segments:*

1. *A curve $\mathscr{S}_0^+$ that is the graph of a differentiable function σ_+ of q,*

$$\sigma_+ : [0, \bar{q}] \to [0, \bar{p}], \quad q \mapsto \sigma_+(q),$$

   that lies in $\mathscr{D}_+$ and connects the origin to the equilibrium point $(\bar{p}, \bar{q})$, i.e., $\sigma_+(0) = 0$ and $\sigma_+(\bar{q}) = \bar{p}$.
2. *A curve $\mathscr{S}_0^{out}$ that is the graph of a differentiable function σ^{out} of p defined over an interval $[\underline{p}, \bar{p}]$,*

$$\sigma^{out} : [\underline{p}, \bar{p}] \to [\bar{q}, \hat{q}], \quad p \mapsto \sigma^{out}(p),$$

   that connects the equilibrium point $(\bar{p}, \bar{q})$ with the point $(\underline{p}, \bar{q})$ and, except for the initial and endpoint, entirely lies in the region $\{(p,q) : p < q, q > \bar{q}\}$ outside of $\mathscr{D}$.

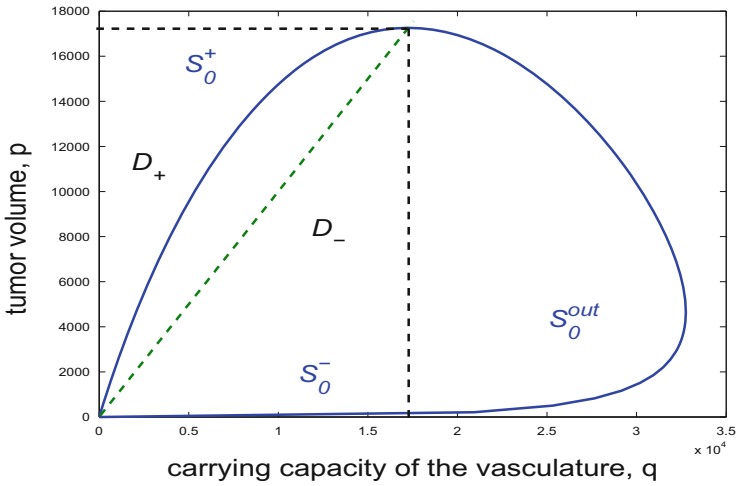

Fig. 5.5 Geometry of the base curve $\mathscr{S}_0$ for the singular surface $\mathscr{S}$.

3. A curve $\mathscr{S}_0^-$ that is the graph of a differentiable function σ_- of q,

$$\sigma_- : [0,\bar{q}] \to [0,\bar{p}], \quad q \mapsto \sigma_-(q),$$

that lies in $\mathscr{D}_-$ and connects the origin to the point $(\underline{p},\bar{q})$, i.e., $\sigma_-(0) = 0$ and $\sigma_-(\bar{q}) = \underline{p}$.

Figure 5.5 illustrates Proposition 5.3.3 for the parameter values given in Tables 5.2 and 5.3. These geometric properties are generally valid under the assumption that $b > \mu \geq 0$ which will always be satisfied for the problems under consideration.

Proof. Implicit differentiation of the relation (5.42) gives

$$\frac{dp}{dx} = -\frac{3}{2}\frac{b}{d}p^{\frac{1}{3}}\ln x.$$

In particular, the values of p along the singular curve $\mathscr{S}_0$ are maximized for $x = 1$ at the equilibrium point $(\bar{p},\bar{q})$ and are smaller than $\bar{p}$ for all $x \neq 1$. Hence all points $(p,q) \in \mathscr{S}_0$ for $x > 1$ lie in the set $\mathscr{D}_+$, i.e., they satisfy $p < \bar{p}$. This segment of $\mathscr{S}_0$ is the curve $\mathscr{S}_0^+$ and since $\frac{dp}{dx}$ does not vanish, it can be described by a function $p = \sigma_+(q)$ of q. This function is well defined near $q = \bar{q}$ and satisfies $\sigma_+(\bar{q}) = \bar{p}$. In the limit $q \to 0+$, because the values of x are bounded above by e, it follows that $\lim_{q\to 0+}\sigma_+(q) = 0$. This proves the first assertion.

For $x < 1$ there exist points on $\mathscr{S}_0$ when the values for the carrying capacity exceed $\bar{q}$ and these portions lie outside of the domain $\mathscr{D}$. In order to see this, fix q and write $p = xq$ so that the equation defining the singular base curve $\mathscr{S}_0$ takes the form

$$bx(1-\ln x) = \mu + dq^{\frac{2}{3}}x^{\frac{2}{3}}. \tag{5.43}$$

The first and second derivatives of the function

$$\varphi_q(x) = bx(1-\ln x) - \mu - dq^{\frac{2}{3}}x^{\frac{2}{3}}$$

are

$$\varphi_q'(x) = -b\ln x - \frac{2}{3}dq^{\frac{2}{3}}x^{-\frac{1}{3}} \quad \text{and} \quad \varphi_q''(x) = -\frac{b}{x} + \frac{2}{9}dq^{\frac{2}{3}}x^{-\frac{4}{3}}.$$

The function $x \mapsto x^{\frac{1}{3}}\ln x$ has a global minimum for $x = e^{-3}$ with minimum value $\varphi\left(e^{-3}\right) = -\frac{3}{e}$. Therefore the equation $\varphi_q'(x) = 0$, $x^{\frac{1}{3}}\ln x = -\frac{2d}{3b}q^{\frac{2}{3}}$, has a unique solution for $\tilde{q} = \left(\frac{9b}{2ed}\right)^{\frac{3}{2}}$, two positive solutions for $q < \tilde{q}$ and no solutions for $q > \tilde{q}$. In the latter case, the function φ_q is strictly decreasing for all $x > 0$ and, since $\varphi_q(0) = -\mu \le 0$, there are no positive solutions to equation (5.43). For $q = \tilde{q}$, the function $\varphi_{\tilde{q}}$ has a global maximum for $x = e^{-3}$ with value $\varphi_{\tilde{q}}(e^{-3}) = -\mu - \frac{1}{2}\frac{b}{e^3} < 0$ and thus there are still no positive solutions to equation (5.43). For values $q < \tilde{q}$, there exist two stationary points $x_a < x_b$. The second derivative φ_q'' has a unique inflection point at

$$\tilde{x}(q) = \left(\frac{2d}{9b}\right)^3 q^2$$

and φ_q is strictly convex for $x < \tilde{x}(q)$ and strictly concave for $x > \tilde{x}(q)$. It therefore follows that x_a is a local minimum and x_b is a local maximum. As long as this maximum is negative, there are no solutions to equation (5.43) and thus there exist no points on the singular base curve $\mathscr{S}_0$ for these q values. If the maximum becomes zero, there exists a unique such solution and once it becomes positive, there are exactly two solutions to equation (5.43).

For $0 < q < \bar{q} = \left(\frac{b-\mu}{d}\right)^{\frac{3}{2}}$ we have that $\varphi_q(1) = b - \mu - dq^{\frac{2}{3}} > b - \mu - d\bar{q}^{\frac{2}{3}} = 0$ and thus in this range there exist exactly two solutions to (5.43), a lower branch for $x < 1$ in $\mathscr{D}_-$ which we denoted by $\mathscr{S}_0^-$ and the upper branch $\mathscr{S}_0^+$ for $x > 1$ in $\mathscr{D}_+$ described above. Note that $\mathscr{S}_0^-$ can also be described by a function $p = \sigma_-(q)$ of q that satisfies $\lim_{q\to 0+}\sigma_-(q) = 0$ and has a well-defined extension near $q = \bar{q}$ with $\sigma_-(\bar{q}) < \bar{p}$. For $q > \bar{q}$, there still exist solutions, but the values lie outside of $\mathscr{D}$ and we denoted this portion of the curve $\mathscr{S}_0$ by $\mathscr{S}_0^{out}$. For later use, we note that the values of q along the singular curve $\mathscr{S}_0$ are maximized at a value $\hat{q}$, the upper limit in the range of the function σ^{out}. There are exactly two solutions to equation (5.43) for $0 < q < \hat{q}$, one solution for $q = \hat{q}$ and none for $q > \hat{q}$. If we denote the associated values for x and p by $\hat{x}$ and $\hat{p}$, then $\hat{q}$ is determined by the equation $\frac{dq}{dx} = 0$. Differentiating $p = xq$ gives

$$\frac{dp}{dx} = q + x\frac{dq}{dx}$$

and thus $\hat{q}$ is a solution to the equation

$$-\frac{3}{2}\frac{b}{d}\hat{p}^{\frac{1}{3}}\ln\hat{x} = \hat{q} = \frac{\hat{p}}{\hat{x}},$$

or, equivalently,

$$d\hat{p}^{\frac{2}{3}} = -\frac{3}{2}b\hat{x}\ln\hat{x}.$$

Substituting into equation (5.43), $\hat{x}$ is a solution to

$$b\hat{x}\left(1+\frac{1}{2}\ln\hat{x}\right) = \mu. \tag{5.44}$$

The function $x \mapsto bx\left(1+\frac{1}{2}\ln x\right) - \mu$ is strictly concave, nonpositive at $x = 0$ and positive for $x = 1$. Hence there exists a unique solution $\hat{x}$ to equation (5.44) in the interval $(0,1)$ which then defines $\hat{p}$ and $\hat{q}$. The portion $\mathscr{S}_0^{out}$ of $\mathscr{S}_0$ that lies outside of the domain $\mathscr{D}$ can be described as the graph of a function $q \to \sigma_{out}(q)$ over an interval $[\underline{p}, \bar{p}]$ with $\underline{p} < \bar{p}$ the second solution of equation (5.43) for $q = \bar{q}$. This verifies the Proposition. The geometric properties are illustrated in Figure 5.5. □

We now compute the singular control. The vector fields f and g introduced in (5.26) and their Lie bracket $[f,g]$ are given by

$$f(z) = \begin{pmatrix} -\xi p \ln\left(\frac{p}{q}\right) \\ bp - \left(\mu + dp^{\frac{2}{3}}\right)q \\ 0 \end{pmatrix}, \quad g(z) = \begin{pmatrix} 0 \\ -\gamma q \\ 1 \end{pmatrix}, \quad [f,g](z) = \gamma p \begin{pmatrix} \xi \\ -b \\ 0 \end{pmatrix} \tag{5.45}$$

and the second order Lie brackets are

$$[g,[f,g]](z) = -\gamma^2 bp \begin{pmatrix} 0 \\ 1 \\ 0 \end{pmatrix} \tag{5.46}$$

and

$$[f,[f,g]](z) = \gamma p \begin{pmatrix} \xi^2 + \xi b\frac{p}{q} \\ \xi b \ln\left(\frac{p}{q}\right) + \xi\left(\frac{2}{3}d\frac{q}{\sqrt[3]{p}} - b\right) - \left(\mu + dp^{\frac{2}{3}}\right)b \\ 0 \end{pmatrix}. \tag{5.47}$$

The vector fields g, $[f,g]$, and $[g,[f,g]]$ are linearly independent everywhere and thus, by Theorem 5.2.2, the singular control is given as

$$u_{\text{sing}}(t) = -\psi(z(t))$$

where the function ψ is the $[g,[f,g]]$-coordinate of the vector field $[f,[f,g]]$, i.e.,

$$[f,[f,g]](z) = \rho(z)g(z) + \varphi(z)[f,g](z) + \psi(z)[g,[f,g]](z).$$

A direct computation verifies that

$$[f,[f,g]](z) = \left(\xi + b\frac{p}{q}\right)[f,g](z) + \psi[g,[f,g]](z) \tag{5.48}$$

with

$$\psi = \psi(p,q) = -\frac{1}{\gamma}\left(\xi \ln\left(\frac{p}{q}\right) + b\frac{p}{q} + \frac{2}{3}\xi\frac{d}{b}\frac{q}{p^{\frac{1}{3}}} - \left(\mu + dp^{\frac{2}{3}}\right)\right).$$

Thus we have the following result:

Proposition 5.3.4. *If the control u is singular on an open interval (α,β) with corresponding trajectory (p,q), then the singular control is given in feedback form as*

$$\begin{aligned} u_{\text{sing}}(t) &= -\psi(p(t),q(t)) \\ &= \frac{1}{\gamma}\left(\xi \ln\left(\frac{p(t)}{q(t)}\right) + b\frac{p(t)}{q(t)} + \frac{2}{3}\xi\frac{d}{b}\frac{q(t)}{p^{\frac{1}{3}}(t)} - \left(\mu + dp^{\frac{2}{3}}(t)\right)\right) \end{aligned} \tag{5.49}$$

The next result gives an equivalent expression for the singular control along the singular arc in terms of the projective variable x alone. This relation is only valid on the singular surface $\mathscr{S}$, but it allows to determine the admissible part of the singular arc, i.e., the portion of $\mathscr{S}$ where the singular control takes values in the interval $[0,u_{\max}]$.

Proposition 5.3.5. *Along the singular arc, the singular control can be expressed as a function of the scalar variable $x = \frac{p}{q}$ in the form*

$$\Psi(x) = \frac{1}{\gamma}\left[\left(\frac{1}{3}\xi + bx\right)\ln x + \frac{2}{3}\xi\left(1 - \frac{\mu}{bx}\right)\right]. \tag{5.50}$$

There exists exactly one connected arc on the singular base curve $\mathscr{S}_0$ along which the control is admissible, i.e., satisfies the bounds $0 \le \Psi \le u_{\max}$. This arc is defined over an interval $[x_\ell^*, x_u^*]$ where x_ℓ^* and x_u^* are the unique solutions to the equations $\Psi(x_\ell^*) = 0$ and $\Psi(x_u^*) = u_{\max}$ and these values satisfy $x_\ell^* < x_u^*$.

Figure 5.6 gives a plot of the petal like singular curve $\mathscr{S}_0$ for the parameter values used before with the admissible portion marked as the solid segment and the inadmissible portion shown as dashed curve. The qualitative structure shown in this figure is always valid with the understanding that the admissible portion shrinks with smaller values $u_{\max}$.

Proof. In the variables p and x, the singular control is given by

$$u_{\text{sing}}(t) = \frac{1}{\gamma}\left(\xi \ln x(t) + bx(t) + \frac{2}{3}\xi\frac{dp(t)^{\frac{2}{3}}}{bx(t)} - \left(\mu + dp(t)^{\frac{2}{3}}\right)\right).$$

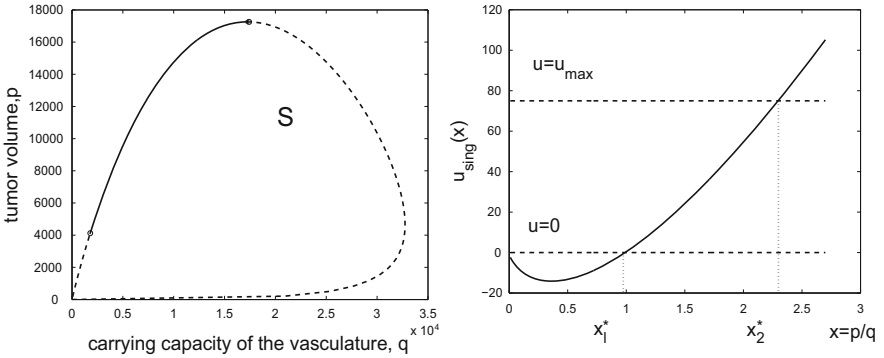

Fig. 5.6 The singular base curve $\mathscr{S}_0$ is plotted in (p,q)-space (left) with the admissible part marked as the solid segment of the curve. Away from this segment the singular control is either negative or exceeds the maximum allowable limit $u_{\max}$. The singular control u_{sing} is plotted as a function of the quotient $x = \frac{p}{q}$ on the right.

Along the singular arc we have that $p^{\frac{2}{3}} = -\varphi(x)$ and thus we obtain the singular control as a feedback function of x alone, $u_{\text{sing}}(t) = \Psi(x(t))$, in the form

$$\begin{aligned}\Psi(x) &= \frac{1}{\gamma}\left(\xi \ln x + bx + \frac{2}{3}\xi\frac{bx(1-\ln x)-\mu}{bx} - bx(1-\ln x)\right)\\ &= \frac{1}{\gamma}\left[\left(\frac{1}{3}\xi + bx\right)\ln x + \frac{2}{3}\xi\left(1-\frac{\mu}{bx}\right)\right].\end{aligned}$$

Note that $\lim_{x\searrow 0}\Psi(x) = -\infty$ and $\lim_{x\to\infty}\Psi(x) = +\infty$. Furthermore,

$$\begin{aligned}\Psi'(x) &= \frac{1}{\gamma}\left[b(\ln x+1) + \frac{1}{3}\xi\left(\frac{1}{x} + 2\frac{\mu}{bx^2}\right)\right],\\ \Psi''(x) &= \frac{1}{\gamma x^3}\left(bx^2 - \frac{1}{3}\xi x - \frac{4}{3}\xi\frac{\mu}{b}\right),\end{aligned}$$

and the second derivative has a unique positive root at

$$x_* = \frac{1}{6}\frac{\xi}{b}\left(1+\sqrt{1+48\frac{\mu}{\xi}}\right).$$

It follows that Ψ is strictly concave for $0 < x < x_*$ and strictly convex for $x > x_*$. If the function Ψ has no stationary points, then Ψ is strictly increasing and thus, as claimed, there exists a unique interval $[x_\ell^*, x_u^*]$ when Ψ takes values in $[0, u_{\max}]$ and the limits are the unique solutions of the equations $\Psi(x) = 0$ and $\Psi(x) = u_{\max}$, respectively. The same holds in the bifurcation scenario when Ψ has a unique stationary point at x_*. Otherwise, it follows from the convexity properties that Ψ has a unique local maximum at $\tilde{x}_1 < x_*$ and a unique local minimum at $\tilde{x}_2 > x_*$. But the values of the function Ψ at these local extrema are negative. For, if $\Psi'(\tilde{x}) = 0$, then

$$-b\ln\tilde{x} = b + \frac{1}{3}\xi\left(\frac{1}{\tilde{x}} + 2\frac{\mu}{b\tilde{x}^2}\right) > 0$$

and thus

$$\begin{aligned}\Psi(\tilde{x}) &= \frac{1}{\gamma}\left[\left(\frac{1}{3}\xi + b\tilde{x}\right)\left(-1 - \frac{1}{3}\frac{\xi}{b}\left(\frac{1}{\tilde{x}} + 2\frac{\mu}{b\tilde{x}^2}\right)\right) + \frac{2}{3}\xi\left(1 - \frac{\mu}{b\tilde{x}}\right)\right] \\ &= -\frac{1}{\gamma}\left[b\tilde{x} + \frac{1}{9}\frac{\xi^2}{b}\left(\frac{1}{\tilde{x}} + 2\frac{\mu}{b\tilde{x}^2}\right) + \frac{4}{3}\frac{\xi\mu}{b\tilde{x}}\right] < 0.\end{aligned}$$

Hence Ψ has a unique positive zero and is strictly increasing when it is positive. This proves the proposition. □

Definition 5.3.1 (Saturation Point). We say the singular control u_{sing} saturates at time τ if its value at time τ is equal to one of the limits of the control set, i.e., if either $u(\tau) = 0$ or $u(\tau) = u_{\max}$.

Note that

$$\Psi(1) = \frac{2}{3}\frac{\xi}{\gamma}\left(1 - \frac{\mu}{b}\right) > 0$$

and thus the lower saturation point occurs for $x_\ell^* < 1$. In principle, it is possible that the singular control already exceeds its admissible value for $x = 1$ and then, since the function $\Psi(x)$ is strictly increasing, the entire portion $\mathscr{S}_0^+$ would be inadmissible. This is the case if $\frac{2}{3}\xi\left(1 - \frac{\mu}{b}\right) \geq \gamma u_{\max}$. For example, for the parameter values from Tables 5.2 and 5.3, this holds if $u_{\max} < 0.374$. Generally $u_{\max}$ will be much higher. If $\Psi(1) \geq u_{\max}$, then, and this follows from our results below, optimal controls are simply given by bang-bang controls with one switching that give all antiangiogenic agents upfront. Henceforth we ignore this simpler case and assume that $\Psi(1) < u_{\max}$.

Corollary 5.3.1. *Suppose that*

$$\frac{2}{3}\xi\left(1 - \frac{\mu}{b}\right) < \gamma u_{\max}$$

and let $\mathscr{S}_{ad}$ denote the restriction of the admissible portion of the singular base curve $\mathscr{S}_0$ to the domain $\mathscr{D}$. Then $\mathscr{S}_{ad}$ is a connected arc that extends from the equilibrium point $(\bar{p},\bar{q})$ in the upper right corner of $\mathscr{D}$ to the unique point $(\tilde{p},\tilde{q})$ on $\mathscr{S}_0$ where the singular control saturates at its upper limit $u_{\max}$; it is a subarc of $\mathscr{S}_0^+$ and entirely lies in $\mathscr{D}_+$. The segment $\mathscr{S}_0^-$ of the singular base curve $\mathscr{S}_0$ that lies in $\mathscr{D}_-$ is inadmissible.

Proof. It follows from the proof of Proposition 5.3.5 that the function $\Psi(x)$ which defines the singular control along $\mathscr{S}_0$ has a unique positive zero x_ℓ^* and is positive for $x > x_\ell^*$ and negative for $x < x_\ell^*$. Since Ψ is strictly increasing for $x > x_\ell^*$, the admissible range is a connected subarc of $\mathscr{S}_0^+$ that extends from the equilibrium point $(\bar{p},\bar{q})$ to the saturation point $(\tilde{p},\tilde{q})$ in $\mathscr{D}_+$ and the control exceeds the upper

control limit $u_{\max}$ for points on $\mathscr{S}_0^+$ beyond $(\tilde{p},\tilde{q})$. It remains to show that the segment $\mathscr{S}_0^-$ of $\mathscr{S}_0$ is inadmissible. It follows from the geometric description of the curve $\mathscr{S}_0$ given earlier that there exists a unique value $\hat{x} \in (0,1)$ where the q-value is maximized over $\mathscr{S}_0$ and that this value is the unique solution of equation (5.44). Hence

$$\begin{aligned}\Psi(\hat{x}) &= \frac{1}{\gamma}\left[\left(\frac{1}{3}\xi + b\hat{x}\right)\ln\hat{x} + \frac{2}{3}\xi\left(1 - \frac{\mu}{b\hat{x}}\right)\right] \\ &= \frac{1}{\gamma}\left[\left(\frac{1}{3}\xi + b\hat{x}\right)\ln\hat{x} + \frac{2}{3}\xi\left(1 - \left(1 + \frac{1}{2}\ln\hat{x}\right)\right)\right] \\ &= \frac{1}{\gamma} b\hat{x}\ln\hat{x} < 0.\end{aligned}$$

Thus the entire portion of the curve $\mathscr{S}_0$ for $x \le \hat{x}$ is inadmissible. This includes the segment $\mathscr{S}_0^-$. □

5.3.3 A Synthesis of Optimal Controlled Trajectories

We thus have explicit analytical formulas for the singular arc, the corresponding singular control that keeps it invariant, and we also have a simple geometric situation that determines the admissible portion. Overall, optimal controls are concatenations of the singular control with bang-bang structures and we need to analyze the possible concatenation sequences. In fact, this is the technical and difficult aspect of the construction. We summarize our results on the structure of optimal controls and trajectories in the following theorem, but relegate the technical and somewhat lengthy details of its proof to Appendix B.4.

Theorem 5.3.1. *Given a well-posed initial condition $(p_0,q_0) \in \tilde{\mathscr{D}}$, optimal controls are* at most *concatenations of 4 segments in the order* $\mathbf{bsu}_{\max}\mathbf{0}$ *where* $\mathbf{0}$ *denotes an arc along the constant control $u = 0$,* $\mathbf{u}_{\max}$ *denotes an arc along the constant control $u = u_{\max}$,* $\mathbf{b}$ *stands for either* $\mathbf{u}_{\max}$ *or* $\mathbf{0}$ *and* $\mathbf{s}$ *denotes an arc in the singular surface $\mathscr{S}$.*

This result provides a in fact sharp upper bound on the number of segments for optimal controls and it significantly limits the structure of possible concatenations of bang and singular arcs. Once this simple maximal concatenation sequence of bang and singular segments has been identified, it becomes relatively straightforward to compute the optimal solutions and this argument also will be carried out in detail in Appendix B.4. It is shown there that for most initial conditions there only exists one extremal of this type (and this then is the optimal solution), but in many cases the concatenation sequence is shorter (i.e., some segments in this sequence are not present). For example, *the medically most important case is for initial conditions (p_0,q_0) that represent a growing tumor with high carrying capacity, $p_0 < q_0$, and ample supply A of inhibitors.* In such a situation, the optimal control is given by

initial full dose therapy, $u \equiv u_{\max}$, until the corresponding trajectory meets the singular surface $\mathscr{S}$. At this point, the optimal control switches to the singular control and then administers agents at these dose rates until all angiogenic inhibitors are exhausted. During that phase, the corresponding trajectory evolves on the singular surface $\mathscr{S}$. Since the singular surface lies in the region $\mathscr{D}_+ = \{(p,q) \in \mathscr{D} : p > q\}$, after termination of therapy, the tumor volume will still be decreasing even if no more agents are administered (because of after effects) as long as the trajectory remains in $\mathscr{D}_+$. The minimum tumor volume will be realized as the trajectory reaches the diagonal $\mathscr{D}_0 = \{(p,q) \in \mathscr{D} : p = q\}$. Thus, for these cases optimal controls follow the concatenation sequence $\mathbf{u}_{\max}\mathbf{s0}$.

This, in fact, is the typical structure of optimal controlled trajectories for medically relevant initial conditions. But it depends on two facts: (i) the overall amount of inhibitors is large enough to reach the singular arc in its admissible range, and (ii) it is not so large that the singular control would saturate along the singular arc. If (i) is violated and trajectories either do not reach $\mathscr{S}$ at all or reach $\mathscr{S}$ in its inadmissible part, then the singular control never becomes an option and in this case optimal controlled trajectories will simply be given by up-front administration of all antiangiogenic agents at full dose rates. Thus, in such a case, optimal controls are bang-bang with exactly one switching from $u = u_{\max}$ to $u = 0$, i.e., of the type $\mathbf{u}_{\max}\mathbf{0}$. This also is the structure of optimal controls if the singular arc is reached at a point where the singular control is inadmissible. If condition (ii) is violated, then optimal concatenation sequences of the forms $\mathbf{0su}_{\max}\mathbf{0}$ and $\mathbf{u}_{\max}\mathbf{su}_{\max}\mathbf{0}$ arise. In such a case, the singular control $u_{\text{sing}}(t)$ reaches the upper limit $u_{\max}$ of the control set and needs to be terminated since it is no longer admissible. In fact, as is shown in Appendix B.4, optimal trajectories need to leave the singular arc with a full dose control $u = u_{\max}$ prior to saturation. Aside from these more complicated cases near saturation where indeed the full concatenation sequences $\mathbf{bsu}_{\max}\mathbf{0}$ will be realized, the optimal synthesis is determined by the singular surface $\mathscr{S}$ and follows a **bs0** pattern. The only difference is that, if the initial condition (p_0, q_0) lies in a region to the "left" of $\mathscr{S}$, the initial segment is given by $u \equiv 0$ while it is given by $u \equiv u_{\max}$ if the initial condition lies to the "right" of $\mathscr{S}$. The region to the left of $\mathscr{S}$ represents lower values for the carrying capacity as they will be realized during therapy, while the region to the right represents the typical scenario of an actively growing tumor. In either case, controls steer the system toward the singular surface $\mathscr{S}$ and, if this surface is encountered, a switch to the singular control occurs and optimal controls remain singular until angiogenic inhibitors run out (see Figure 5.7). The precise structure of optimal controlled trajectories depending on an arbitrary initial condition $(p,q;y)$ will be developed in Appendix B.4.

A *synthesis of optimal controlled trajectories* then consists of a unique covering of the state space $\tilde{\mathscr{D}} \times [0,A] \subset \mathbb{R}^3$ by controlled trajectories with the optimal control $u_{\text{opt}} = u_{\text{opt}}(p,q;y)$ identifying the optimal dose rates as a function of an arbitrary point $(p,q;y)$ of the state (see Section A.4.4 in Appendix A). Intuitively, such a synthesis acts like *a "GPS system" showing for every possible state of the system how optimal protocols are administered*, both qualitatively and quantitatively. Mathematically, a synthesis is defined by a decomposition of the state space into a finite

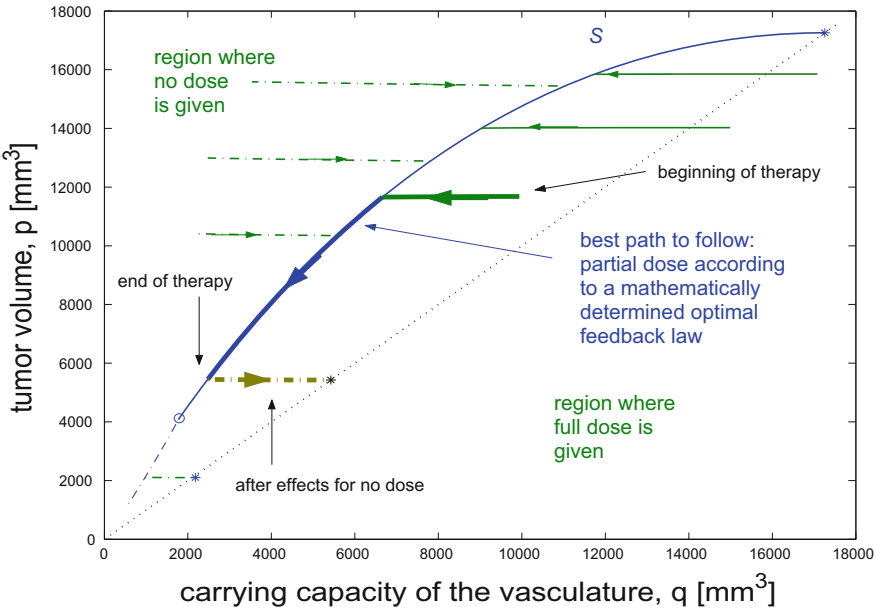

Fig. 5.7 Synthesis of optimal controlled trajectories for the problem [OCA] and model [H].

collection of embedded submanifolds, $\mathscr{M} = \{M_i\}_{i\in\mathbb{N}}$, sometimes also called *strata*, together with (i) a well-defined flow of trajectories corresponding to admissible controls on each stratum and (ii) regular transitions between the strata that generate (iii) a memoryless flow of extremal trajectories, i.e., there exist unique solutions forward in time and the resulting controlled trajectories satisfy the conditions of the Pontryagin maximum principle. The optimal solutions to problem [H] give rise to such a decomposition and the global optimality of all the controlled trajectories that define the synthesis follows from Theorem A.4.4 in Appendix A. Hence this gives *a complete solution to the optimal control problem.*

We illustrate the optimal synthesis geometrically in Figure 5.7. The variable y merely accounts for the amount of inhibitors that already has been used and it is more convenient, and in fact more illustrative, to show the (overlapping) projections of the trajectories into the (p,q)-plane. With only a slight abuse of terminology we do not distinguish in our language between the trajectories in $(p,q;y)$-space and their projections onto the (p,q)-coordinates. Figure 5.7 also identifies one typical optimal controlled trajectory corresponding to an optimal of the form $\mathbf{u}_{\max}\mathbf{s0}$ described above.

In Figure 5.8 we give an example of an optimal controlled trajectory (on the left) and its corresponding control (on the right) of the type $\mathbf{u}_{\max}\mathbf{s0}$. The initial condition is given by $(p_0,q_0) = (12000\ [mm^3], 15000\ [mm^3])$ and the optimal control takes the maximal value $u = u_{\max}$ for the short interval from 0 to $t_1 = 0.0905$ [days] when the trajectory reaches the singular arc. At this point, the control switches to

the time-varying singular control defined by the singular feedback (5.49) until all inhibitors have been exhausted at time $t_2 = 6.5579$ [days]. Then, due to after effects, the minimum value of the tumor volume is realized a short period later at the final time $T = 6.7221$ [days] when the trajectory for $u = 0$ reaches the diagonal. Along the initial segment the tumor volume hardly shrinks. However, the initial carrying capacity of the vasculature is much larger than the initial tumor volume and thus the tumor would vigorously grow (at least in the mathematical model) if left untreated and thus beneficial effects of treatment do show up here as well. Also note the very fast q-dynamics away from the singular arc. Although the almost vertical trajectory segments along the controls $u = 0$ and $u = u_{\max}$ are sizable, the time spent along these pieces is small. Most of the time the control is singular and the trajectory follows the associated singular arc (whose projection in the (p,q)-space is a subset of the base curve S_0), but this dynamics is much slower. The optimal final value is given by $p_*(T) = 8533.4$ $[mm^3]$. The optimal trajectory is shown as a solid curve in Figure 5.8 and the singular curve $\mathscr{S}$ and the diagonal $\mathscr{D}_0$ are indicated as dotted curves.

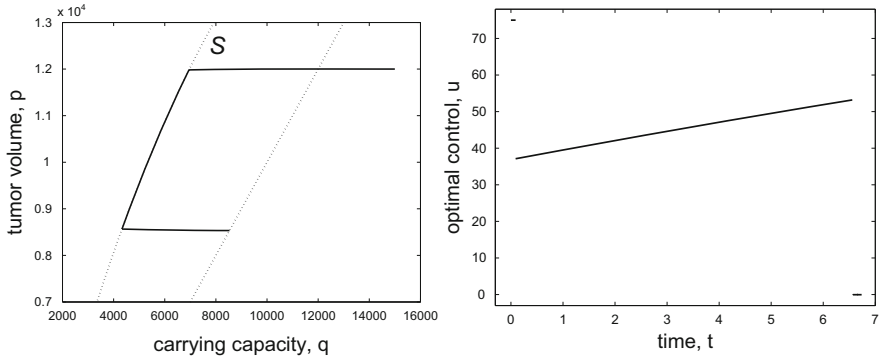

Fig. 5.8 Example of an optimal $\mathbf{u}_{\max}\mathbf{s0}$ controlled trajectory (left) and associated control as function of time (right) for initial data $(p_0, q_0, A) = (12000, 15000, 300)$.

5.4 Optimal Synthesis for Model [E]

One of the main qualitative features of model [H] is the fact that, for the parameter values given in [116], the dynamics of the carrying capacity q is much faster than the dynamics of the tumor volume p. In fact, the system dynamics very much has a differential-algebraic flavor with the system mostly evolving on the $\dot{q}$ nullclines which form the corresponding slow manifolds. In some sense, the singular control shapes this nullcline to achieve optimal tumor reductions. In order to slow down

the q-dynamics, Ergun, Camphausen, and Wein in [77] modified the equations and made the inhibition term in the vasculature proportional to the tumor radius. This, in principle, results in the expression $dp^{\frac{1}{3}}q$. As a further simplification, they still identified p and q in steady state and replaced p with q in the dynamics for the carrying capacity. This gives an inhibition term of the form $dq^{\frac{4}{3}}$. Following the second main conclusion derived in [116]—the inhibition term tends to grow at a rate of $q^{\frac{2}{3}}$ faster than the stimulation term—the dynamics for the vasculature becomes

$$\dot{q} = bq^{\frac{2}{3}} - dq^{\frac{4}{3}} - \mu q - \gamma u q.$$

This is a significant modeling change in that it decouples the dynamics of the carrying capacity from the tumor volume and thus is exposed to obvious criticism. However, as we shall show next, the solution of the associated optimal control problem for this modified dynamics has qualitatively the same structure as the one presented above. One advantage of this formulation is that these same conclusions can be obtained via a much simpler mathematical analysis. In this section, we give the computations for the singular control and singular arc for model [E] and also include the considerably less technical proofs in the construction of the optimal synthesis highlighting the similarities with the one for model [H]. We also would like to point out that the problem formulation considered in this chapter, i.e., the problem to minimize the tumor volume with an a priori given amount of antiangiogenic agents, was originally considered by Ergun, Camphausen, and Wein in their paper [77]. In this section we consider the following version of the general optimal control problem [OCA]:

[E] For a free terminal time T, minimize the tumor volume at the terminal time, $p(T)$, over all Lebesgue measurable (respectively, piecewise continuous) functions $u : [0,T] \to [0,u_{\max}]$ subject to

$$\dot{p} = -\xi p \ln\left(\frac{p}{q}\right), \qquad p(0) = p_0, \tag{5.51}$$

$$\dot{q} = bq^{\frac{2}{3}} - dq^{\frac{4}{3}} - \mu q - \gamma u q, \qquad q(0) = q_0, \tag{5.52}$$

$$\dot{y} = u, \qquad y(0) = 0, \tag{5.53}$$

and terminal condition $y(T) \leq A$.

For our numerical computations we use the same parameter values as before (see Table 5.2 and $\gamma = 0.15$ [conc^{-1}][day^{-1}] for angiostatin), but reduce the maximum dose rate to $u_{\max} = 15$ and the available amount of agents to $A = 45$. Again, our results are general and these values are merely used for numerical illustrations (Table 5.4).

Table 5.4 Parameter values used for the antiangiogenic agent in numerical illustrations for the model [E].

Variable/ coefficient	Interpretation	Numerical value	Dimension
γ	Antiangiogenic killing parameter (for angiostatin)	0.15	conc^{-1} per day
$u_{\max}$	Maximum dose rate/concentration	15	mg per day
A	Total amount of antiangiogenic agents	45	mg

5.4.1 The Dynamical System with Constant Controls and the Biologically Relevant Region

As before, for the analysis of the optimal control problem, it is useful to have an understanding of the dynamic properties of the systems for a constant control $u \equiv v$ with v some value in the control set $[0, u_{\max}]$. Equilibria lie on the diagonal $p = q$ and, setting $x = \sqrt[3]{q}$, satisfy the quadratic equation

$$-dx^2 - (\mu + \gamma v)x + b = 0.$$

It is clear that for each v there exists a unique positive solution. This equilibrium point is a globally asymptotically stable node at

$$p_v = q_v = \left(\frac{-(\mu + \gamma v) + \sqrt{(\mu + \gamma v)^2 + 4db}}{2d} \right)^3.$$

Note that we have the following simple relation which will be used extensively below,

$$\dot{q} = bq^{\frac{2}{3}} - dq^{\frac{4}{3}} - \mu q - \gamma v q = \begin{cases} > 0 & \text{if } q < q_v, \\ < 0 & \text{if } q > q_v. \end{cases} \tag{5.54}$$

Different from model [H], here an equilibrium point exists for all values of v. Naturally, among admissible control values the smallest value for p_v occurs for the full dose rate, $u \equiv u_{\max}$, and the largest value is the uncontrolled equilibrium for $u \equiv 0$. We denote these values by $p_\ell = q_\ell$ and $p_h = q_h$ for low and high, respectively. Figure 5.9 shows the phase portraits of the fully controlled ($u = u_{\max}$) and uncontrolled system ($u = 0$). For the numerical values chosen, the equilibria are at $p_h = 15{,}191$ [mm^3] and $p_\ell = 17$ [mm^3]. The high equilibrium is in the same range as for model [H], but fully controlled trajectories, rather than converging to the origin, now converge to the microscopic stable equilibrium point (p_ℓ, q_ℓ).

The biologically relevant region does not extend beyond the value of the uncontrolled equilibria and henceforth we restrict our analysis to the following square domain $\mathscr{D}$:

$$\mathscr{D} = \{(p,q) : p_\ell < p < p_h,\ q_\ell < q < q_h\}. \tag{5.55}$$

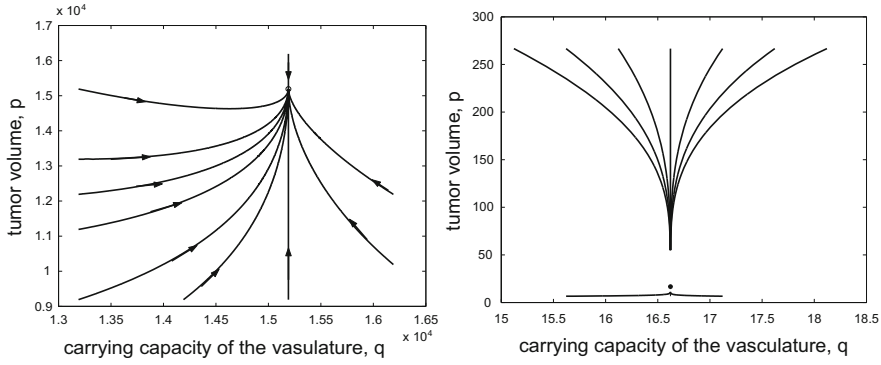

Fig. 5.9 Phase portraits of the uncontrolled ($u \equiv 0$, left) and fully controlled ($u_{\max} = 15$, right) system [E].

If an the initial condition lies outside of the set $\mathscr{D}$ and has small values for p or q, the uncontrolled trajectory eventually will enter the region $\mathscr{D}$ (see Figure 5.9) and then our analysis applies; on the other hand, very large initial conditions that would exceed p_h or q_h simply are not medically realistic. As before, we denote by $\mathscr{D}_+$ and $\mathscr{D}_-$ the subregions of $\mathscr{D}$ that lie above and below the diagonal, $\mathscr{D}_0$, respectively.

Proposition 5.4.1. *The region $\mathscr{D}$ is positively invariant for the flow of the control system, i.e., if $(p_0,q_0) \in \mathscr{D}$, then for any admissible control u defined over the interval $[0,\infty)$ the solution $(p(\cdot),q(\cdot))$ to the corresponding dynamics with initial condition (p_0,q_0) exists for all times $t \geq 0$ and lies in $\mathscr{D}$.*

Proof. We again show that controlled trajectories that start at a point in the boundary of $\mathscr{D}$ enter $\mathscr{D}$. As for model [H], because of the Gompertzian growth model, we have $\dot{p} < 0$ on the boundary segments $\{(p,q) : p_\ell < p \leq p_h,\ q_\ell = q\}$ and $\{(p,q) : p = p_h, q_\ell \leq q < q_h\}$ and $\dot{p} > 0$ on the boundary segments $\{(p,q) : p_\ell = p,\ q_\ell < q \leq q_h\}$ and $\{(p,q) : p_\ell \leq p < p_h, q = q_h\}$. This already implies that trajectories starting in $\{(p,q) : p_\ell = p,\ q_\ell < q < q_h\}$ and in $\{(p,q) : p = p_h,\ q_\ell < q < q_h\}$ enter $\mathscr{D}$. Since q_ℓ is the equilibrium solution for the control $u \equiv u_{\max}$, the line $\{(p,q) : q = q_\ell\}$ is invariant under this control and for $u < u_{\max}$ we have that

$$\dot{q}_\ell = bq_\ell^{\frac{2}{3}} - dq_\ell^{\frac{4}{3}} - \gamma u q_\ell - \mu q_\ell > bq_\ell^{\frac{2}{3}} - dq_\ell^{\frac{4}{3}} - \gamma u_{\max} q_\ell - \mu q_\ell = 0. \tag{5.56}$$

Hence the q-dynamics always points to the right and trajectories starting on the segment $\{(p,q) : p_\ell < p \leq p_h, q_\ell = q\}$ enter $\mathscr{D}$. Similarly, the line $\{(p,q) : q = q_h\}$ is invariant under the control $u = 0$ and for $u > 0$, we have that $\dot{q}_h = -\gamma u q_h < 0$ which implies that trajectories starting on $\{(p,q) : p_\ell \leq p < p_h,\ q = q_h\}$ enter $\mathscr{D}$. Like for model [H], we need to consider the two equilibrium solutions $p_\ell = q_\ell$ and $p_h = q_h$ separately. Recall from the proof of Proposition 5.3.1 that, on the diagonal, $p = q$, we have that $\dot{p} = 0$ and $\ddot{p} = \xi \dot{q}$, and this is irrespective of the q-dynamics. Here we have for the high equilibrium point (p_h,q_h) and any control $u > 0$ that

$\dot{q}_h = -\gamma u q_h < 0$ and thus the trajectory starting at (p_h, q_h) has a local maximum in p and enters $\mathscr{D}$. On the other hand, for the low equilibrium point (p_ℓ, q_ℓ) and any control $u < u_{\max}$ we have $\dot{q}_\ell > 0$ by (5.56) and thus the trajectory starting at (p_ℓ, q_ℓ) has a local minimum in p and enters $\mathscr{D}$ as well. This completes the proof. □

5.4.2 Necessary Conditions for Optimality Revisited

We briefly summarize the first-order necessary conditions for optimality given in Theorem 5.2.1 for problem [E] for well-posed initial data (p_0, q_0). Now the Hamiltonian $H = H(\lambda, p, q, u)$ takes the form

$$H = -\lambda_1 \xi p \ln\left(\frac{p}{q}\right) + \lambda_2 \left(b q^{\frac{2}{3}} - d q^{\frac{4}{3}} - \gamma u q - \mu q\right) + \lambda_3 u,$$

and the adjoint equations with terminal conditions read

$$\dot{\lambda}_1 = -\frac{\partial H}{\partial p} = \lambda_1 \xi \left(\ln\left(\frac{p}{q}\right) + 1\right), \qquad \lambda_1(T) = 1,$$
$$\dot{\lambda}_2 = -\frac{\partial H}{\partial q} = -\lambda_1 \xi \frac{p}{q} + \lambda_2 \left(-\frac{2}{3} b q^{-\frac{1}{3}} + \frac{4}{3} d q^{\frac{1}{3}} + \gamma u + \mu\right), \qquad \lambda_2(T) = 0.$$

The fact that the $\dot{q}$ equation does not depend on p has some immediate consequences for the multipliers λ_1 and λ_2 that will significantly simplify the reasoning.

Lemma 5.4.1. *The multiplier λ_1 is positive on $[0,T]$ and λ_2 is positive on $[0,T)$.*

Proof. The adjoint equation for λ_1 is a homogeneous linear ODE and since $\lambda_1(T) = 1$, the first statement is immediate. The second one follows from the fact that whenever $\lambda_2(\tau) = 0$, then we have that

$$\dot{\lambda}_2(\tau) = -\xi \lambda_1(\tau) \frac{p(\tau)}{q(\tau)} < 0.$$

But then λ_2 can have at most one zero. Since $\lambda_2(T) = 0$, this implies that λ_2 is positive for all times $t < T$. □

All general conclusions from Section 5.2.2 apply: if u_* is an optimal control defined over the interval $[0,T]$ with corresponding trajectory $z_* = (p_*, q_*, y_*)^T$, then optimal controlled trajectories terminate on the diagonal, $p_*(T) = q_*(T)$, and all available agents are used up, $y_*(T) = A$. Furthermore, without loss of generality, we assume that λ_3 is positive. The key properties for the synthesis of optimal controlled trajectories are the same as for model [H], but have significantly easier proofs like the following lemma.

Lemma 5.4.2. *Optimal controlled trajectories cross from* $\mathscr{D}_- = \{(p,q) \in \mathscr{D} : p < q\}$ *into* $\mathscr{D}_+ = \{(p,q) \in \mathscr{D} : p > q\}$ *using the control* $u = u_{\max}$*, but never cross from* $\mathscr{D}_+$ *into* $\mathscr{D}_-$*. If an optimal trajectory reaches the diagonal from within* $\mathscr{D}_+$ *at time* τ*, then* τ *is the terminal time,* $T = \tau$*.*

Proof. Suppose an optimal controlled trajectory is on the diagonal at time τ, $p(\tau) = q(\tau)$. It then follows from the fact that the Hamiltonian H vanishes identically that

$$\lambda_2(\tau)q(\tau)\left(bq(\tau)^{-\frac{1}{3}} - dq(\tau)^{\frac{1}{3}} - \gamma u(\tau) - \mu\right) + \lambda_3 u(\tau) = 0.$$

If $u(\tau) < u_{\max}$, then either $u(\tau) = 0$ or the control is singular. In either case we have that

$$u(\tau)\Phi(\tau) = u(\tau)\left(\lambda_3 - \lambda_2(\tau)\gamma q(\tau)\right) = 0$$

and thus

$$\lambda_2(\tau)q(\tau)\left(bq(\tau)^{-\frac{1}{3}} - dq(\tau)^{\frac{1}{3}} - \mu\right) = 0.$$

Since $q < q_h$, the expression $bq^{\frac{2}{3}} - dq^{\frac{4}{3}} - \mu q$ is positive in the domain $\mathscr{D}$ and thus $\lambda_2(\tau) = 0$. Hence $\tau = T$. On the other hand, if $u = u_{\max}$, then trajectories transversally cross from $\mathscr{D}_-$ into $\mathscr{D}_+$ since $q > q_\ell$ and thus $\dot{q} < 0$ in $\mathscr{D}$. □

5.4.3 Analysis of the Singular Arc and Control

We derive geometric properties of the singular arc and compute the associated singular control. For this model, the function $\Delta = S - I$ is given by

$$\Delta(q) = S(q) - I(q) = bq^{\frac{2}{3}} - dq^{\frac{4}{3}}$$

and thus the operator $\mathscr{L}$, $(\mathscr{L}f)(q) = qf'(q) - f(q)$, gives

$$\mathscr{L}(S) = -\frac{1}{3}S \qquad \text{and} \qquad \mathscr{L}(I) = \frac{1}{3}I.$$

Hence

$$\mathscr{L}(\Delta) = -\frac{1}{3}(S+I) \qquad \text{and} \qquad \mathscr{L}^2(\Delta) = \frac{1}{9}\Delta = \frac{1}{9}q^{\frac{2}{3}}\left(b - dq^{\frac{2}{3}}\right).$$

For $q < q_h$, we have that $bq^{\frac{2}{3}} - dq^{\frac{4}{3}} > \mu q > 0$ and therefore $\mathscr{L}^2(\Delta)$ is positive for trajectories lying in $\mathscr{D}$. Thus it follows from Theorem 5.2.2 that singular controls are of order 1 and that the strengthened Legendre condition is satisfied. Hence, as for model [H], admissible singular arcs are locally optimal. Furthermore, the singular curve $\mathscr{S}$ is the locus of points (p,q) that satisfy the equation

$$\Delta(p,q) + \mathscr{L}(\Delta)(p,q)\ln\left(\frac{p}{q}\right) - \mu q = 0$$

which here is given by

$$bq^{\frac{2}{3}} - dq^{\frac{4}{3}} - \frac{1}{3}\left(bq^{\frac{2}{3}} + dq^{\frac{4}{3}}\right)\ln\left(\frac{p}{q}\right) - \mu q = 0.$$

This equation solves for p as

$$p = q\exp\left(3\frac{b - \mu q^{\frac{1}{3}} - dq^{\frac{2}{3}}}{b + dq^{\frac{2}{3}}}\right).$$

Hence, for this model the singular curve is the graph of a smooth function. Since we have that $b - \mu q^{\frac{1}{3}} - dq^{\frac{2}{3}} > 0$ for all $q < q_h$ with equality for q_h (c.f., (5.54)), it follows that the high equilibrium point (p_h, q_h) lies on $\mathscr{S}$ and otherwise the singular curve again lies in the region $\mathscr{D}_+ = \{(p,q) \in \mathscr{D} : p > q\}$, i.e., above the diagonal. Denote the subregions of $\mathscr{D}_+$ that lie above and below the singular curve by I and II, respectively (see Figure 5.10).

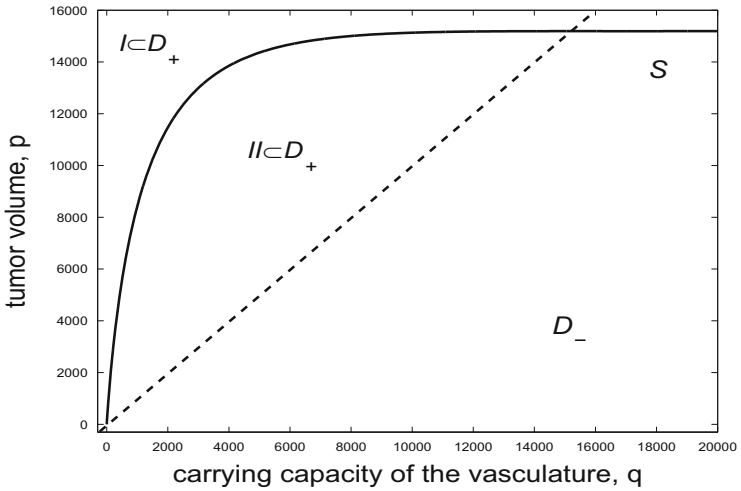

Fig. 5.10 The singular curve $\mathscr{S}$ and the subregions I and II of $\mathscr{D}_+$.

For model [E], the drift and control vector fields f and g are given by

$$f(z) = \begin{pmatrix} -\xi p \ln\left(\frac{p}{q}\right) \\ bq^{\frac{2}{3}} - dq^{\frac{4}{3}} - \mu q \\ 0 \end{pmatrix}, \qquad g(z) = \begin{pmatrix} 0 \\ -\gamma q \\ 1 \end{pmatrix},$$

and their Lie bracket is

$$[f,g](z) = \gamma \begin{pmatrix} \xi p \\ -\frac{1}{3}\left(bq^{\frac{2}{3}} + dq^{\frac{4}{3}}\right) \\ 0 \end{pmatrix}$$

with the higher-order Lie brackets given by

$$[f,[f,g]](z) = \gamma \begin{pmatrix} \xi p\left(\xi + \frac{1}{3}\left(bq^{-\frac{1}{3}} + dq^{\frac{1}{3}}\right)\right) \\ -\frac{4}{9}bdq - \frac{1}{9}\mu\left(bq^{\frac{2}{3}} - dq^{\frac{4}{3}}\right) \\ 0 \end{pmatrix} \tag{5.57}$$

and

$$[g,[f,g]](z) = \gamma^2 \begin{pmatrix} 0 \\ -\frac{1}{9}\left(bq^{\frac{2}{3}} - dq^{\frac{4}{3}}\right) \\ 0 \end{pmatrix}.$$

The vector fields g, $[f,g]$ and $[g,[f,g]]$ are everywhere linearly independent and thus $[f,[f,g]]$ can again be expressed as a linear combination of this basis. This gives us that

$$[f,[f,g]](z) = \left(\xi + \frac{1}{3}\frac{b + dq^{\frac{2}{3}}}{q^{\frac{1}{3}}}\right)[f,g](z) + \psi(z)[g,[f,g]](z) \tag{5.58}$$

with

$$\psi(z) = -\frac{1}{\gamma}\left(\frac{b - dq^{\frac{2}{3}}}{q^{\frac{1}{3}}} + 3\xi\frac{b + dq^{\frac{2}{3}}}{b - dq^{\frac{2}{3}}} - \mu\right).$$

Setting $x = \sqrt[3]{q}$ and defining the function

$$\Psi(x) = \frac{1}{\gamma}\left(\frac{b - dx^2}{x} + 3\xi\frac{b + dx^2}{b - dx^2} - \mu\right),$$

the singular control is then given by

$$u_{\text{sing}}(x) = \Psi(x)$$

and is a smooth feedback control that only depends on $x = \sqrt[3]{q}$.

Note that the function Ψ is well defined on the interval $(0,x_h)$ with $x_h = \sqrt[3]{q_h}$. In fact, x_h is the unique positive root of the quadratic polynomial

$$Q(x) = -dx^2 - \mu x + b$$

and $Q(x)$ is positive on the interval $(0,x_h)$. Since $Q\left(\sqrt{\frac{b}{d}}\right) = -\mu\sqrt{\frac{b}{d}} < 0$, the singularity of the second term, $x = \sqrt{\frac{b}{d}}$, lies to the right of x_h and overall Ψ is positive on $(0,x_h)$. The range where the singular control is admissible is easily determined. The function Ψ is strictly convex with poles at $x = 0$ and $x = \sqrt{\frac{b}{d}}$. For, we have that

$$\Psi'(x) = \frac{1}{\gamma}\left(-\frac{b+dx^2}{x^2} + 12\xi\frac{bdx}{(b-dx^2)^2}\right)$$

and

$$\Psi''(x) = \frac{1}{\gamma}\left(\frac{2b}{x^3} + \frac{12\xi bd}{(b-dx^2)^2}\left[1+\frac{4dx^2}{b-dx^2}\right]\right) > 0$$

in the interval $(0,\sqrt{\frac{b}{d}})$. Hence, for large enough dose rates $u_{\max}$, there exist exactly two values x_ℓ^* and x_h^*, $0 < x_\ell^* < x_h^* < \sqrt{\frac{b}{d}}$, such that the singular control is admissible for $x \in (x_\ell^*, x_h^*)$ and saturates with value $u = u_{\max}$ at both x_ℓ^* and x_h^*; the control is inadmissible for $x \notin [x_\ell^*, x_h^*]$. If the dose rate $u_{\max}$ is too small, then no admissible singular controls may exist and in such a case it will follow from our computations below that optimal solutions are bang-bang with at most two switchings in the order $\mathbf{0u_{\max}0}$. But henceforth we assume that an admissible segment of the singular arc exists. If we set $x_\ell = \sqrt[3]{q_\ell}$, then it holds that $x_\ell < x_\ell^*$. For, at the lower equilibrium we have that $b - dx_\ell^2 - \mu x_\ell = \gamma u_{\max} x_\ell$ and thus the singular control is given by

$$u_{\text{sing}}(x_\ell) = u_{\max} + 3\frac{\xi}{\gamma}\frac{b+dx_\ell^2}{b-dx_\ell^2} > u_{\max}.$$

At the high equilibrium we have that

$$u_{\text{sing}}(x_h) = 3\frac{\xi}{\gamma}\frac{b+dx_h^2}{b-dx_h^2}$$

and thus the location of x_h relative to x_h^* depends on the value for $u_{\max}$. Summarizing, we have the following result:

Proposition 5.4.2. *In the domain $\mathscr{D}$, and defining $x = \sqrt[3]{q}$, the singular curve $\mathscr{S}$ is the graph of a function p_{sing} of x, $p_{\text{sing}} : [x_\ell, x_u] \to [p_\ell, p_h]$, $x \mapsto p_{\text{sing}}(x)$, given by*

$$p_{\text{sing}}(x) = x^3 \exp\left(3\frac{b-\mu x-dx^2}{b+dx}\right). \tag{5.59}$$

The corresponding singular control that keeps $\mathscr{S}$ invariant is given in feedback form by

$$u_{\text{sing}}(x) = \Psi(x) = \frac{1}{\gamma}\left(\frac{b-dx^2}{x} + 3\xi\frac{b+dx^2}{b-dx^2} - \mu\right) \tag{5.60}$$

and it is admissible over an interval $[x_\ell^*, x_u^*]$ with $x_\ell < x_\ell^*$ and the values x_ℓ^* and x_u^* are the unique solutions to the equation $\Psi(x) = u_{\max}$ in $(0, \sqrt{\frac{b}{d}})$.

Figure 5.11 shows the graph of the singular control defined by (5.60) with the horizontal axis representing the variable q. In order to better compare these functions for the various models, we keep the original variable q in the graphs and set $q_\ell^* = \sqrt[3]{x_\ell^*}$ and $q_u^* = \sqrt[3]{x_u^*}$. For the numerical values given earlier, we have that $q_\ell^* = 23.69\ [mm^3]$ and $q_u^* = 12{,}319\ [mm^3]$. For comparison, the equilibrium value is $q_h = 15{,}191\ [mm^3]$ and thus for these parameter values the admissible singular arc $\mathscr{S}_{ad}$ lies strictly between the two equilibria.

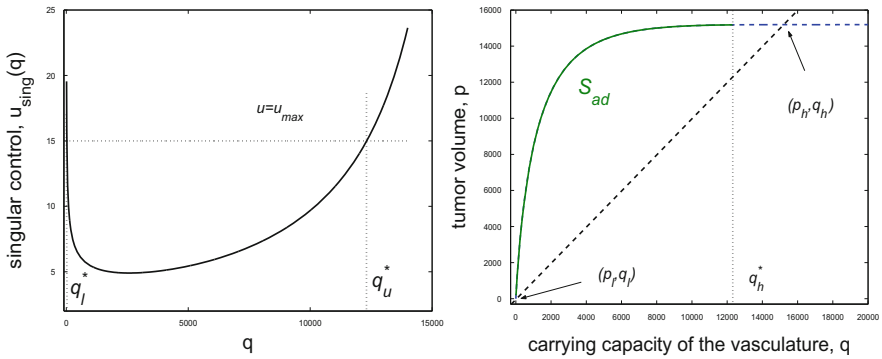

Fig. 5.11 The singular control (left) and singular arc (right) for the model [E] with the admissible part for $u_{\max} = 15$ shown as the solid segment.

5.4.4 Analysis of Junctions Between Bang and Singular Controls

As for model [H], the important step is to limit possible concatenations between optimal bang and singular arcs. Compared with the computations done in Section B.4 in Appendix B, the reasoning is greatly simplified for model [E] and we thus include the details here. Recall that *I* denotes the region in $\mathscr{D}_+$ that lies above the singular curve and *II* denotes the region below it.

Proposition 5.4.3. *Suppose u_* is an optimal control with corresponding trajectory (p_*, q_*). If $(p_*(t), q_*(t))$ lies in region I, then u_* can switch at time t only from $u = 0$ to $u = u_{\max}$; if $(p_*(t), q_*(t))$ lies in region II, then u_* can only switch from $u = u_{\max}$ to $u = 0$. Below the diagonal, only switchings from $u = 0$ to $u = u_{\max}$ are possible.*

Proof. If an optimal control switches at time τ, the multiplier $\lambda(\tau)$ vanishes against $g(z_*(\tau))$ and $f(z_*(\tau))$. Away from the diagonal $\mathscr{D}_0 = \{(p,q) : p = q\}$, the vector fields f, g and the constant coordinate vector field $h = (0,0,1)^T$ are linearly independent and thus the Lie bracket $[f,g]$ can be written as a linear combination of these vector fields in the form

$$[f,g](z) = \rho(z)f(z) + \sigma(z)g(z) + \zeta(z)h,$$

i.e.,

$$\gamma \begin{pmatrix} \xi p \\ -\frac{1}{3}\left(bq^{\frac{2}{3}} + dq^{\frac{4}{3}}\right) \\ 0 \end{pmatrix} = \rho(z) \begin{pmatrix} -\xi p \ln\left(\frac{p}{q}\right) \\ bq^{\frac{2}{3}} - dq^{\frac{4}{3}} - \mu q \\ 0 \end{pmatrix} + \sigma(z) \begin{pmatrix} 0 \\ -\gamma q \\ 1 \end{pmatrix} + \zeta(z) \begin{pmatrix} 0 \\ 0 \\ 1 \end{pmatrix}.$$

This gives $\rho(z) = -\frac{\gamma}{\ln\left(\frac{p}{q}\right)}$ and

$$\sigma(z) = \frac{\frac{1}{3}\left(bq^{\frac{2}{3}} + dq^{\frac{4}{3}}\right)\ln\left(\frac{p}{q}\right) - \left(bq^{\frac{2}{3}} - dq^{\frac{4}{3}} - \mu q\right)}{q\ln\left(\frac{p}{q}\right)} = -\zeta(z).$$

The numerator of σ vanishes where f and the Lie bracket $[f,g]$ are linearly dependent and thus defines the singular curve $\mathscr{S}$. It is positive above $\mathscr{S}$ and negative below $\mathscr{S}$. The denominator is positive in $\mathscr{D}_+$ and negative in $\mathscr{D}_-$. Thus σ is positive in the regions I and $\mathscr{D}_-$ and negative in region II. At a switching time τ we have that

$$\dot{\Phi}(\tau) = -\sigma(z_*(\tau))\lambda_3.$$

Without loss of generality, by Lemma 5.2.3, we may assume that $\lambda_3 > 0$ and thus $\dot{\Phi}(\tau)$ and $\sigma(z_*(\tau))$ have opposite signs. Hence $\dot{\Phi}(\tau)$ is negative in $I \cup \mathscr{D}_-$ and positive in II. Thus, whenever the switching function has a zero and $(p_*(\tau), q_*(\tau))$ lies in $I \cup \mathscr{D}_-$, then the switching function changes sign at time τ from positive to negative values and thus the control switches from $u = 0$ to $u = u_{\max}$. Analogously, whenever the switching function has a zero and $(p_*(\tau), q_*(\tau))$ lies in region II, then the switching function changes sign at time τ from negative to positive values and thus the control switches from $u = u_{\max}$ to $u = 0$. This proves the result. □

Proposition 5.4.4. *An optimal control u_* can take on the value 0 only along an initial interval $[0,\tau]$ or a terminal interval $[\tau,T]$.*

Proof. Suppose there exists an interval $[\alpha,\beta] \subset (0,T)$ such that the switching function Φ vanishes at the endpoints, $\Phi(\alpha) = \Phi(\beta) = 0$, and Φ is positive on (α,β). Then there exists a time $\tau \in (\alpha,\beta)$ where Φ attains its maximum and, with all functions evaluated at τ, we have that

$$0 = \dot{\Phi}(\tau) = \langle \lambda(\tau), [f,g](z(\tau)) \rangle = \lambda_1 \xi \gamma p - \frac{1}{3}\lambda_2 \gamma \left(bq^{\frac{2}{3}} + dq^{\frac{4}{3}} \right).$$

Using this identity in the formula for the second derivative along $u = 0$ at time τ, we get that (c.f., (5.57))

$$\begin{aligned}
\ddot{\Phi}(\tau) &= \langle \lambda(\tau), [f,[f,g]](z(\tau)) \rangle \\
&= \lambda_1 \gamma \xi p \left(\xi + \frac{1}{3} bq^{-\frac{1}{3}} + \frac{1}{3} dq^{\frac{1}{3}} \right) - \frac{1}{9}\lambda_2 \gamma \left(4bdq + b\mu q^{\frac{2}{3}} - d\mu q^{\frac{4}{3}} \right) \\
&= \frac{1}{3}\lambda_2 \gamma \left(bq^{\frac{2}{3}} + dq^{\frac{4}{3}} \right) \left(\xi + \frac{1}{3}(bq^{-\frac{1}{3}} + dq^{\frac{1}{3}}) \right) - \frac{4}{9}\lambda_2 \gamma bdq \\
&\qquad - \frac{1}{9}\lambda_2 \gamma \mu q (bq^{-\frac{1}{3}} - dq^{\frac{1}{3}}) \\
&= \frac{1}{9}\lambda_2 \gamma \left(3\xi \left(bq^{\frac{2}{3}} + dq^{\frac{4}{3}} \right) + \frac{\left(bq^{\frac{2}{3}} - dq^{\frac{4}{3}} \right)^2}{q} - \mu (bq^{\frac{2}{3}} - dq^{\frac{4}{3}}) \right) \\
&= \frac{1}{9}\lambda_2 \gamma \left(3\xi \left(bq^{\frac{2}{3}} + dq^{\frac{4}{3}} \right) + (bq^{\frac{2}{3}} - dq^{\frac{4}{3}}) \frac{bq^{\frac{2}{3}} - \mu q - dq^{\frac{4}{3}}}{q} \right).
\end{aligned}$$

But $bq^{\frac{2}{3}} - \mu q - dq^{\frac{4}{3}}$ is positive in the region $\mathscr{D}$ and thus $\ddot{\Phi}(\tau) > 0$. Contradiction. Hence the switching function is either strictly increasing or strictly decreasing along the control $u \equiv 0$ and trajectories corresponding to $u = 0$ must lie at the beginning or the end of the interval $[0, T]$. □

Proposition 5.4.5. *If u_* is an optimal control, then there exists at most one interval I along which the control is singular.*

Proof. Suppose there exist two consecutive open intervals (α_1, β_1) and (α_2, β_2) where an optimal control is singular and in between the switching function Φ is nonzero. It then follows from the previous Proposition that Φ must be negative and thus there exists a concatenation sequence of the form $\mathbf{su}_{\max}\mathbf{s}$. The singular vector field is given by

$$\begin{pmatrix} -\xi p \ln\left(\frac{p}{q}\right) \\ bq^{\frac{2}{3}} - dq^{\frac{4}{3}} - \mu q \end{pmatrix} + u_{\text{sing}} \begin{pmatrix} 0 \\ -\gamma q \end{pmatrix}$$

and at a point where the control is admissible, we have that $u_{\text{sing}} < u_{\max}$. At any such point the vector field corresponding to the control $u_{\max}$ therefore has a smaller q-component and trajectories for $u_{\max}$ leave the singular arc transversally into the region above (equivalently, to the left of) the singular arc, $p > p_{\text{sing}}(q)$. Along the $u_{\max}$ trajectory, the carrying capacity decreases and it is impossible to once more connect with the singular arc from above as long as the points are admissible. Contradiction. □

Hence, as for model [H], any trajectory for $u = u_{\max}$ that starts on the admissible portion of the singular arc enters the region above the singular curve and can only return to the region below the singular curve through the segment where the control is inadmissible. Propositions 5.4.4 and 5.4.5 immediately imply the following result on concatenation sequences that are optimal.

Corollary 5.4.1. *Given a well-posed initial condition $(p_0, q_0) \in \mathscr{D}$, optimal controls are* at most *concatenations of 5 pieces in the order* $\mathbf{0}\mathbf{u}_{\max}\mathbf{s}\mathbf{u}_{\max}\mathbf{0}$ *with* $\mathbf{0}$ *denoting an arc along the constant control* $u = 0$, $\mathbf{u}_{\max}$ *denoting an arc along the constant control* $u = u_{\max}$, *and* $\mathbf{s}$ *denoting an arc in the singular surface* $\mathscr{S}$.

Different from model [H], here an additional bang-bang junction at the beginning is possible. The reason is that the singular control saturates twice at the upper limit $u_{\max}$ at a low value q_ℓ^* and a high value q_u^*. For model [H], such a saturation was only possible at the exit from the admissible singular arc and it generated the concatenation sequence $\mathbf{s}\mathbf{u}_{\max}\mathbf{0}$. Here this saturation is also possible at the entry into the admissible singular arc and this is what generates the sequence $\mathbf{0}\mathbf{u}_{\max}\mathbf{s}$ at the beginning. But, as for model [H], not all of the intervals in $\mathbf{0}\mathbf{u}_{\max}\mathbf{s}\mathbf{u}_{\max}\mathbf{0}$ need to be present in a particular solution. In fact, for the biologically most relevant situation, again optimal controls typically have the form $\mathbf{bs0}$ where $\mathbf{b}$ stands for an interval along which the optimal control is given by either $u = u_{\max}$ or $u = 0$. The more complex concatenations only arise if the optimal trajectory passes near the saturation points. The reason is that in such a scenario it is not optimal to remain on the singular arc until the saturation point is reached, but optimal trajectories must leave the singular arc prior to this point with the control $u = u_{\max}$.

Proposition 5.4.6. *It is not optimal for a singular control to concatenate with the control $u = u_{\max}$ at saturation points.*

Proof. Suppose τ is a junction time between a singular control and $u = u_{\max}$ where the singular control saturates at $u = u_{\max}$. In general, using (5.58) we have that

$$\begin{aligned}\ddot{\Phi}(t) &= \langle \lambda(t), [f + ug, [f,g]](z(t))\rangle \\ &= \left(\xi + \frac{1}{3}\frac{b + dq(t)^{\frac{2}{3}}}{q(t)^{\frac{1}{3}}}\right)\dot{\Phi}(t) + (u(t) + \psi(p(t),q(t)))\,\langle \lambda(t), [g,[f,g]](z(t))\rangle\,.\end{aligned}$$

Along the singular arc, the derivative of the switching function vanishes, $\dot{\Phi}(t) = 0$, and since $\psi(p(\tau),q(\tau)) = -u_{\max}$ at the saturation point, the second derivative satisfies $\ddot{\Phi}(\tau) = 0$ and is still once more continuously differentiable at τ. Along the control $u = u_{\max}$, we then get that

$$\begin{aligned}\Phi^{(3)}(\tau) &= \left(\frac{d}{dt}_{|t=\tau}\psi(p(t),q(t))\right)\langle \lambda(t), [g,[f,g]](z(t))\rangle \\ &= -\frac{1}{9}\lambda_2(\tau)\gamma^2\left(bq(\tau)^{\frac{2}{3}} - dq(\tau)^{\frac{4}{3}}\right)\left(\frac{d}{dt}_{|t=\tau}\psi(p(t),q(t))\right).\end{aligned}$$

By Lemma 5.4.1, $\lambda_2(\tau)$ is positive and in the region $\mathscr{D}$ we also have that

$$bq(\tau)^{\frac{2}{3}} - dq(\tau)^{\frac{4}{3}} > \mu q(\tau) > 0.$$

In order to compute the derivative of ψ, recall that with $x = \sqrt[3]{q}$ and Ψ defined by (5.60), we have that $\Psi(x(t)) = -\psi(p(t), q(t))$. Hence

$$-\frac{d}{dt}_{|t=\tau}\psi(p(t),q(t)) = \Psi'(\sqrt[3]{q(\tau)})\frac{\dot{q}(\tau)}{3q(\tau)^{\frac{2}{3}}}.$$

Everywhere in the set $\mathscr{D}$ it holds that

$$\dot{q}(\tau) = bq(\tau)^{\frac{2}{3}} - dq(\tau)^{\frac{4}{3}} - \mu q(\tau) - \gamma u_{\max} q(\tau) < 0$$

and thus $\Phi^{(3)}(\tau)$ has the opposite sign as $\Psi'(q(\tau)^{\frac{1}{3}})$. The function Ψ is decreasing at q_ℓ^*, $\Psi'(\sqrt[3]{q_\ell^*}) < 0$, and increasing at q_h^*, $\Psi'(\sqrt[3]{q_h^*}) > 0$. Hence we have $\Phi^{(3)}(\tau) > 0$ if saturation occurs at q_ℓ^* and $\Phi^{(3)}(\tau) < 0$ if saturation occurs at q_h^*. But the singular control moves the system along the singular arc from the high point q_h^* to the low point q_ℓ^* and thus, if saturation occurs at the low value q_ℓ^*, then the singular control terminates at time τ, i.e., the control is singular before time τ and is given by $u = u_{\max}$ after time τ. But Φ is positive for $t > \tau$ near τ and this contradicts the minimization property of the maximum principle. Analogously, if saturation occurs at the high value q_h^*, then the singular control starts at time τ, i.e., the control is given by $u = u_{\max}$ before time τ and becomes singular after time τ. But again the switching function is positive for time $t < \tau$ near τ violating the maximum principle. Thus in either case, it is not optimal to continue with $u = u_{\max}$ if the singular control saturates and optimal controlled trajectories enter and leave the singular arc only along points when the singular control takes values lower than $u_{\max}$. □

5.4.5 *Synthesis of Optimal Controlled Trajectories*

We now have all the building blocks in place to construct a synthesis of optimal controlled trajectories. We only briefly indicate the results, but note that the argument is identical with the one carried out in detail in Appendix B.4 for model [H] and we refer the reader to this section for the precise reasoning.

Medically realistic initial conditions lie below the singular curve, i.e., $(p_0, q_0) \in II \cup \mathscr{D}_0 \cup \mathscr{D}_-$, and in this case optimal controls start with full dose administrations of antiangiogenic agents,

$$u_{\text{opt}}(p,q,y) \equiv u_{\max}, \qquad (p,q) \in II \cup \mathscr{D}_0 \cup \mathscr{D}_-,\ 0 \le y < A.$$

Intuitively, it is rather clear that switchings from $u = 0$ to $u = u_{\max}$ are not optimal in $\mathscr{D}_-$ (although in principle allowed by Proposition 5.4.3). For, if there exists an

initial segment $[0,t_1]$ along which $u \equiv 0$, then we can equivalently take $(p(t_1),q(t_1))$ as initial condition, but the p and q values are higher and given the dynamic properties of the system with a given amount of antiangiogenic agents it is not possible to reach a lower tumor volume than from (p_0,q_0). Thus optimal controlled trajectories start with an initial full dose segment. If the corresponding trajectory does not reach the admissible portion of the singular curve, then the optimal control is of the form $\mathbf{u}_{\max}\mathbf{0}$ given by a full dose rate treatment until all agents have been exhausted followed by a trajectory for $u = 0$ until the diagonal is reached. If the admissible portion of the singular curve is reached, it can be shown that this always happens at points that lie below the high saturation point q_h^*. At this point the control $u = u_{\max}$ remains an option, but also a switch to the singular control is possible. Typically, the latter happens and optimal controlled trajectories follow the singular arc until all antiangiogenic agents have been used up and then end with a segment for $u = 0$ until the diagonal is reached where the minimum tumor volume is realized. Exceptions to this structure exist if at the time when the singular arc is reached enough agents are available so that saturation along the singular would occur. In this case, optimal trajectories leave the singular arc prior to the saturation point with another full dose segment for $u = u_{\max}$ and overall a concatenation sequence of the form $\mathbf{u}_{\max}\mathbf{s}\mathbf{u}_{\max}\mathbf{0}$ arises. The precise reasoning is the same as it is detailed for model [H] in Appendix B.4.

All initial conditions (p_0,q_0) in the region I above the singular curve are automatically well posed, but are medically less important. In such a case, the tumor volume is high while the carrying capacity is low and thus the tumor volume is shrinking. Depending on the location of the initial condition, controls can start with both $u = 0$ and $u = u_{\max}$. In this case, a concatenation sequence in the order $\mathbf{0}\mathbf{u}_{\max}\mathbf{s}\mathbf{u}_{\max}\mathbf{0}$ is possible and indeed is optimal (with all legs present for some initial conditions). We just describe such a case. It arises if ample agents are available so that saturation at both the high and low points becomes involved. For example, a realistic scenario that leads to such a geometric constellation is that the maximum dose rate $u_{\max}$ is relatively small so that the admissible arc of the singular curve becomes rather small (i.e., q_ℓ^* and q_h^* are close). Obviously, one needs that the high saturation value q_h^* lies below the equilibrium value q_h, $q_h^* < q_h$, so that there exists an inadmissible portion of the singular arc. For initial conditions (p_0,q_0) above the singular arc with $q_h^* < q_0 < q_h$ there exist two types of extremals. One is bang-bang of the form $\mathbf{0}\mathbf{u}_{\max}\mathbf{0}$ and gives all agents in a single maximum dose rate session, the other one involves a segment along which the control is singular and is of the form $\mathbf{0}\mathbf{u}_{\max}\mathbf{s}\mathbf{u}_{\max}\mathbf{0}$. Initially, a $u = 0$ trajectory lowers the tumor volume briefly ((p_0,q_0) lies above the diagonal) and then, while still in region I, a switch to $u = u_{\max}$ occurs. The corresponding trajectory then carries the state from region I into region II across the inadmissible segment of the singular arc that lies between q_h^* and q_h. From then on, the analysis for initial points in region II applies and, if saturation occurs along the singular arc, this leads to the full concatenation sequence $\mathbf{0}\mathbf{u}_{\max}\mathbf{s}\mathbf{u}_{\max}\mathbf{0}$. The corresponding value of the objective then needs to be compared with the one for the $\mathbf{0}\mathbf{u}_{\max}\mathbf{0}$ trajectories and the smallest value defines the optimal solution. These adjustments around the saturation points occur only in small neighborhoods of these

points and the sequence with the long period along the singular arc generally does better because of the intermediate reduced dose rates. Such initial data may not always be relevant for the underlying medical problem, but this argument shows that the concatenation structure $\mathbf{0u}_{\max}\mathbf{su}_{\max}\mathbf{0}$ is the mathematically best limit that can be given on the structure of optimal controls.

We illustrate the typical structures of optimal controlled trajectories of the forms **0s0** and $\mathbf{u}_{\max}\mathbf{s}$ in Figure 5.12. Once again, we show projections of the controlled trajectories into (p,q) space with the p-axis taken vertically. The admissible singular arc is shown as a solid blue curve with the inadmissible part shown dotted. Trajectories corresponding to $u \equiv u_{\max}$ are shown as solid green curves whereas trajectories corresponding to $u \equiv 0$ are marked as dash-dotted green curves. The dotted black line in the figure is the diagonal, $p = q$. We also include in Figure 5.13 the synthesis shown in the variables p and $x = \sqrt[3]{q}$ which nicer illustrates the structure for small tumor volumes.

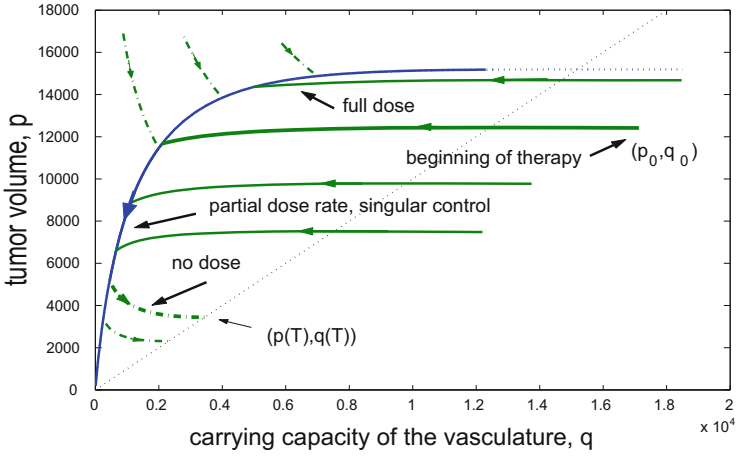

Fig. 5.12 Synthesis of optimal trajectories for model [E] in the variables (p,q).

Figure 5.14 gives an example of the optimal control as a function of time and its corresponding trajectory for the initial condition $p_0 = 12{,}000$ $[mm^3]$, $q_0 = 15{,}000$ $[mm^3]$. The initial condition lies in the region $\mathscr{D}_-$ and thus initially the optimal control is given by the full dose rate $u = u_{\max}$. Note the relatively small shrinkage of the tumor volume p along this interval compared with the changes in the carrying capacity q. Antiangiogenic treatment here prevents the further growth of the tumor that otherwise would have occurred. Once the trajectory corresponding to $u = u_{\max}$ meets the singular arc, the optimal control becomes singular and the optimal trajectory follows the singular arc until all inhibitors are exhausted. It is only on this interval that significant shrinkage of the tumor volume occurs. Since the inhibitors run out in the region $p > q$, the tumor volume still shrinks for $u = 0$ until the trajectory reaches the diagonal $p = q$ at the final time T. For model [E], the intervals

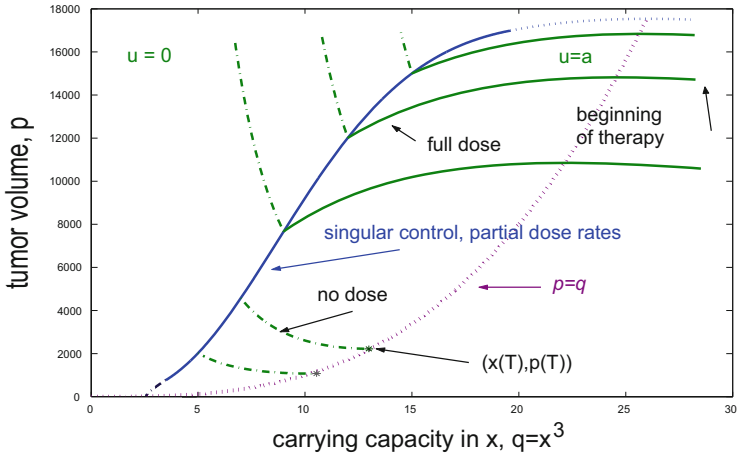

Fig. 5.13 Synthesis of optimal trajectories for model [E] shown in the variables (p,x), $x = \sqrt[3]{q}$.

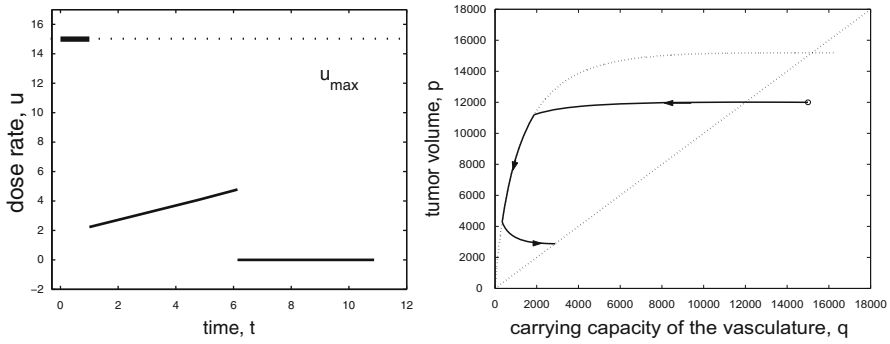

Fig. 5.14 Optimal control (a, left) and corresponding trajectory (b, right) for model [E] for the data from Tables 5.2 and 5.4.

when the optimal control is constant (both for $u = u_{\max}$ and $u = 0$) are much longer when compared with model [H] since the q-dynamics has been slowed down and there still is a sizable shrinkage of the tumor along the final segment for $u = 0$. Note also that, like for model [H], the optimal singular control administers the inhibitors first at lower levels and then the dosage intensifies along the singular arc (*dose intensification*), an observation already made by Ergun et al. in [77].

5.5 Optimal Synthesis for the Models [I_θ]

Modifications involving significant modeling assumptions were made in the change from model [H] to model [E]. Changing the dependence of the inhibitory effects of the tumor on the vasculature from being proportional to the tumor surface in model

[H] to being proportional to the tumor radius in model [E] seems quite reasonable and biological justifications for it can be provided. This also has the beneficial effect of slowing down the dynamics for the vascular support as measured by the carrying capacity. However, the interchange of q with p in quasi steady state is somewhat problematic since it decouples the q-dynamics from the growth of the tumor and thus raises obvious concerns. Nevertheless, as we have just seen, this does not affect the general qualitative form of the solutions to the optimal control problem [OCA] while the analysis of the optimal control problem [E] is considerably simplified. This, in some sense, adds credence to the modeling approach by Ergun et al. At the same time, one reason for making this substitution also was to simplify computations for the combination therapy problem with radiotherapy considered in [77]. For the optimal control problem [OCA], this is not necessary and thus there is an incentive to explore the modeling premises that differentiate these models further. Therefore, in this section we still consider models that interpolate between these two approaches in the sense that *we make the inhibitory effects of the tumor dependent on the tumor radius, but at the same time we retain the tumor volume as variable in the dynamics for the carrying capacity* and thus do not decouple the two dynamics. Thus we take

$$I(p,q) = dp^{\frac{1}{3}}q \tag{5.61}$$

and consider the following models [I_θ] dependent on a parameter θ.

[$\mathbf{I}_\theta$] For a free terminal time T, minimize the tumor volume at the terminal time, $p(T)$, subject to the dynamics

$$\begin{aligned} \dot{p} &= -\xi p \ln\left(\frac{p}{q}\right), & p(0) &= p_0, \\ \dot{q} &= bp^\theta - \left(\mu + dp^{\frac{1}{3}}\right)q - \gamma u q, & q(0) &= q_0, \\ \dot{y} &= u, & y(0) &= 0, \end{aligned}$$

over all Lebesgue measurable (respectively, piecewise continuous) functions $u : [0,T] \to [0,u_{\max}]$ for which the corresponding trajectory satisfies $y(T) \le A$.

The choice $\theta = 1$ gives the same stimulation term as in model [H], but we have $\frac{I}{S} \simeq qp^{-\frac{2}{3}}$ and thus $\alpha + \beta = \frac{1}{3}$ violating the second modeling premise of [116] (see Section 5.1.1) as well. The parameter value $\theta = \frac{2}{3}$ is consistent with this modeling premise. For both models, the same results on the structure of optimal controls are valid as for models [H] and [E] and in this section we only derive the explicit analytic form for the singular control and singular arc, but do not go into the technical details of constructing the synthesis. We merely illustrate the geometry of the singular arc and the structure of the syntheses for some numerical examples.

5.5.1 The Dynamical System with Constant Controls

In order to see the effects that this modeling change has on the dynamics, it is useful to compare the resulting dynamical systems for constant control values. Figure 5.15 gives the phase portraits of the uncontrolled (left) and fully controlled (right) systems [I$_{\frac{2}{3}}$] and [I$_1$] for the parameter values of Table 5.2 and $u_{\max} = 75$. The uncontrolled dynamics very much exhibits the same behavior as for model [H]. For the fully controlled systems, the dynamic behavior of model [I$_{\frac{2}{3}}$] is much closer to the one for model [E] while the dynamic behavior for model [I$_1$] qualitatively is very much identical with the one for model [H]. Note, however, that there is a significant quantitative difference in the values for the parameter values used. For system [I$_1$], the stable equilibrium point of the uncontrolled system is in the unrealistically high range of 10^8. This obviously is caused by changing the term that multiplies q in the inhibition term from $p^{\frac{2}{3}}$ to $p^{\frac{1}{3}}$ which reduces the inhibitory effects of the tumor by one degree of magnitude. Thus the values are no longer realistic. However, as our analysis is completely independent of the specific values that these parameters actually have, we retained them for this illustration. If we counteract these effects by also scaling down the coefficient b that determines the stimulatory effect of the tumor by one order of magnitude, once more similar numerical values arise. As a comparison, in Figure 5.15 we also include as the fourth row the phase portraits for the system [I$_1$] when the parameter b has been chosen as $b = 0.25$.

5.5.2 Analysis of the Singular Arcs and Controls

We briefly discuss the geometry of the singular arc and the corresponding singular controls for the optimal control problems [I$_\theta$]. As before, we write the state of the system as $z = (p,q,y)^T$ and express the dynamics in the form $\dot{z} = f(z) + ug(z)$ where now

$$f(z) = \begin{pmatrix} -\xi p \ln\left(\frac{p}{q}\right) \\ bp^\theta - \left(dp^{\frac{1}{3}} + \mu\right) q \\ 0 \end{pmatrix} \quad \text{and} \quad g(z) = \begin{pmatrix} 0 \\ -\gamma q \\ 1 \end{pmatrix}.$$

The function $\Delta = S - I$ is given by

$$\Delta(p,q) = S(p) - I(p,q) = bp^\theta - dp^{\frac{1}{3}} q.$$

Since the operator $\mathscr{L}$, $(\mathscr{L} f)(q) = qf'(q) - f(q)$, only acts on the variable q, we have the same formulas as for model [H], i.e.,

$$\mathscr{L}(S) = -S \qquad \text{and} \qquad \mathscr{L}(I) = 0.$$

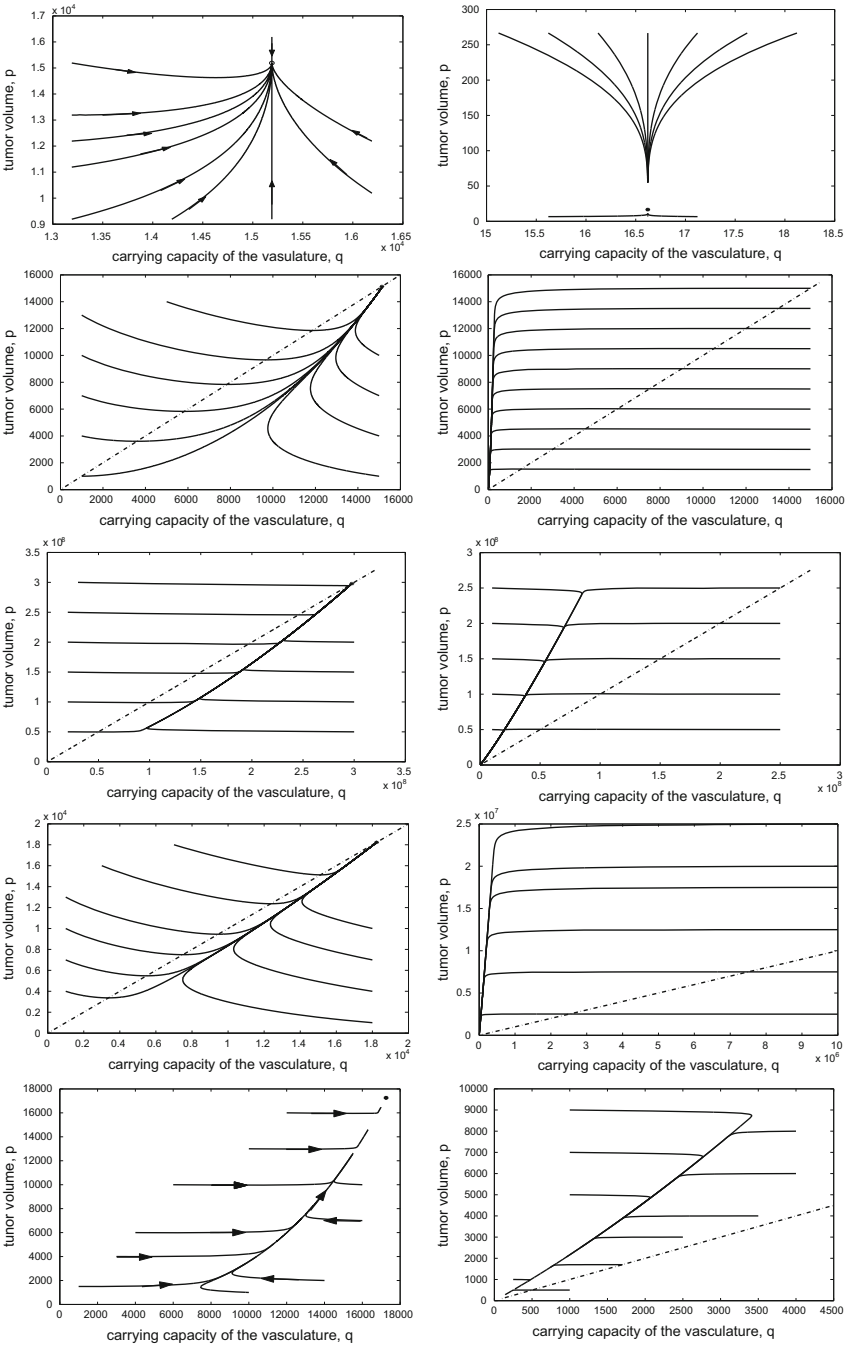

Fig. 5.15 Phase portraits for the uncontrolled (left) and fully controlled (right) systems [E] (top row), $[I_{\frac{2}{3}}]$ (second row), $[I_1]$ for $b = 5.85$ (third row), $[I_1]$ for $b = 0.25$ (fourth row), and [H] (bottom row).

Hence

$$\mathscr{L}(\Delta) = -S \qquad \text{and} \qquad \mathscr{L}^2(\Delta) = S > 0.$$

In particular, $\mathscr{L}^2(\Delta)$ is positive and by Theorem 5.2.2 singular controls are of order 1 and the strengthened Legendre-Clebsch condition is satisfied. Furthermore, the singular curve $\mathscr{S}$ is the locus of points (p,q) that satisfy

$$\Delta(p,q) + \mathscr{L}(\Delta)(p,q)\ln\left(\frac{p}{q}\right) - \mu q = 0$$

which now reads

$$bp^\theta - dp^{\frac{1}{3}}q - bp^\theta \ln\left(\frac{p}{q}\right) - \mu q = 0.$$

Equivalently, and again using the projective coordinate $x = \frac{p}{q}$,

$$bx(1-\ln x) = \left(dp^{\frac{1}{3}} + \mu\right) p^{1-\theta}.$$

The singular control once more is computed as the coefficient at the Lie bracket $[g,[f,g]]$ when we express $[f,[f,g]]$ as a linear combination of the vector fields g, $[f,g]$ and $[g,[f,g]]$. Direct calculations verify that here these brackets are given by

$$[f,g](z) = \gamma \begin{pmatrix} \xi p \\ -bp^\theta \\ 0 \end{pmatrix}, \qquad [g,[f,g]](z) = -\gamma^2 bp^\theta \begin{pmatrix} 0 \\ 1 \\ 0 \end{pmatrix}$$

and

$$[f,[f,g]](z) = \gamma p^\theta \begin{pmatrix} \xi\left(\xi p^{1-\theta} + b\frac{p}{q}\right) \\ \theta\xi b\left(\ln\left(\frac{p}{q}\right) - 1\right) + \frac{1}{3}\xi d p^{\frac{1}{3}-\theta} q - b\left(dp^{\frac{1}{3}} + \mu\right) \\ 0 \end{pmatrix}$$

and thus g, $[f,g]$ and $[g,[f,g]]$ are linearly independent everywhere. As before, expressing $[f,[f,g]](z)$ as a linear combination of this basis as in Section 5.2.3, we obtain the singular control as a feedback function of p and q. Summarizing, we have the following formulas for the singular arc and its corresponding singular control for the interpolating models [I$_\theta$].

Proposition 5.5.1. *For model [I$_\theta$] there exists a locally optimal singular arc defined by the zero set of the equation*

$$bx(1-\ln x) = \left(dp^{\frac{1}{3}} + \mu\right) p^{1-\theta} \tag{5.62}$$

and the singular control that makes this curve invariant is given as

$$u_{\text{sing}}(p,q) = \frac{1}{\gamma}\left[\theta\xi\left(\ln\left(\frac{p}{q}\right)-1\right)+\frac{1}{3}\xi\frac{d}{b}p^{\frac{1}{3}-\theta}q-\left(dp^{\frac{1}{3}}+\mu\right)+b\frac{p^{\theta}}{q}+\xi\right]. \tag{5.63}$$

Recall that the singular curve for the model [H] is given by

$$bx(1-\ln x) = dp^{\frac{2}{3}}+\mu.$$

If we set $\theta = 1$ in (5.62), then the only difference lies in the exponent at the d-term which is $\frac{2}{3}$ if the inhibition term is taken proportional to the surface area and is $\frac{1}{3}$ if it is taken proportional to the tumor radius. Figure 5.16 shows the singular arcs with the admissible portions identified for the models [H], [I_1] and [$I_{\frac{2}{3}}$]. All three have the same geometric shape and the basic structure of the admissible portion of the singular arc is preserved. Note that for both models saturation of the singular control no longer becomes an issue since here the saturation points at upper limits are for very small tumor volumes; negative values again make the portion that lies in $\mathscr{D}_-$ inadmissible. We include graphs of the singular controls as defined by equation (5.63) in Figure 5.17. The singular dose rates become much smaller for these two models.

Based on these formulas and analogous constructions as they were carried out for the systems [H] and [E], a synthesis of optimal controlled trajectories can be constructed and once more the same qualitative structure is verified as optimal for the models [I_θ]. Figure 5.18 gives these optimal syntheses for $\theta = \frac{2}{3}$ and $\theta = 1$, respectively. Comparing these structures with the optimal syntheses for the models [H] and [E], the same features are easily recognizable. In fact, the optimal syntheses for problems [$I_{\frac{2}{3}}$] and [I_1] are virtually identical with the one for model [E] as the geometric shape of the trajectories for $u = 0$ and $u = u_{\max}$ are concerned. Trajectories corresponding to the control $u = 0$ no longer show the fast, almost horizontal dynamics caused by the differential-algebraic structure of the equations for [H], but much closer follow trajectories similar to those for the model [E]. But the shape of the singular arc closely resembles the one for the model [H].

As these figures illustrate, *there exists a uniform and consistent structure to the synthesis of optimal controlled trajectories for all the models* within the class considered in this chapter. These last results also indicate that it would be possible, if so desired, to incorporate more general fractal dependencies on both the inhibitory and stimulatory effects of the tumor on the vasculature (not just through the tumor radius, dimension 1, tumor surface, dimension 2, or tumor volume, dimension 3) into these models without changing the qualitative structure of the optimal solutions. If no limits are imposed on the dose rates of the antiangiogenic agents, the following simple structure of mathematically optimal therapies emerges: *at time $t = 0$ give the properly measured bolus dose that moves the initial condition (p_0, q_0) onto the singular arc and then maintain the relation between p and q defined by the singular arc through singular dose rates.*

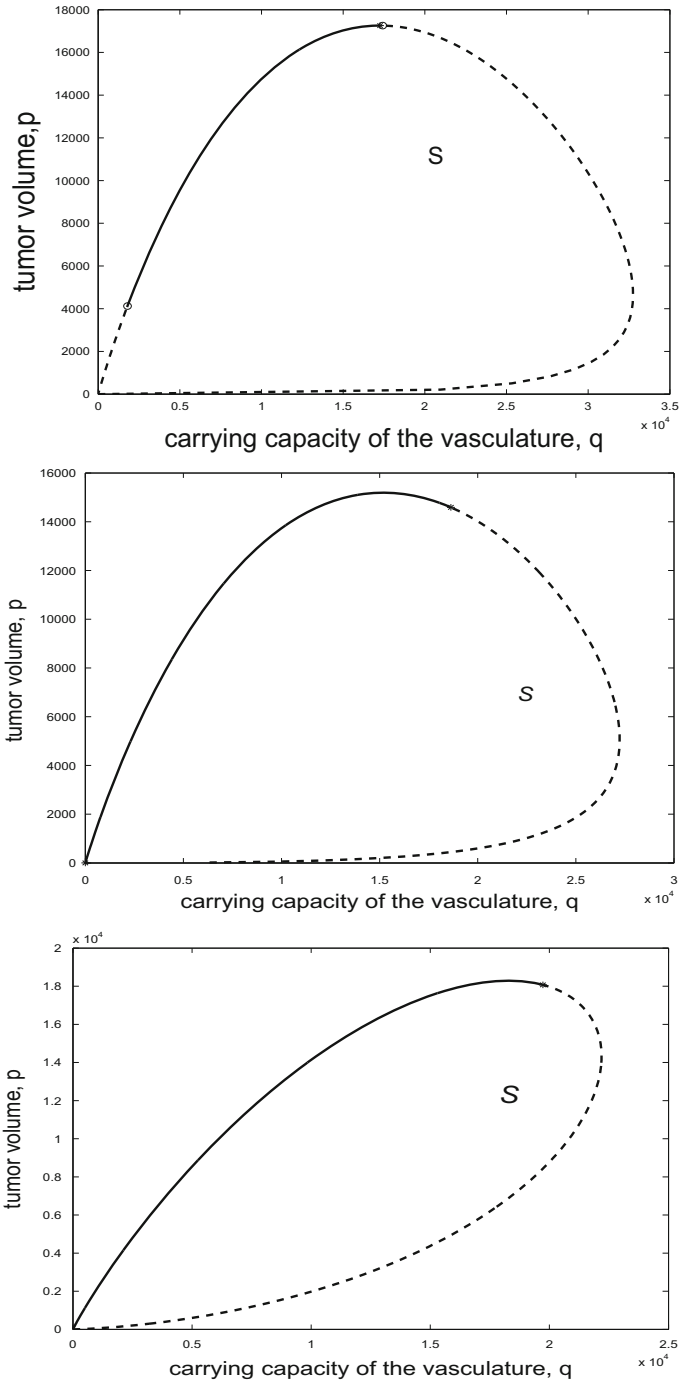

Fig. 5.16 Singular arcs with admissible portions identified for the systems [H] (top), [I$_{\frac{2}{3}}$] (middle) and [I$_1$] (bottom) and parameter values from Table 5.2 ($b = 0.25$ has been used for model $[I_1]$.

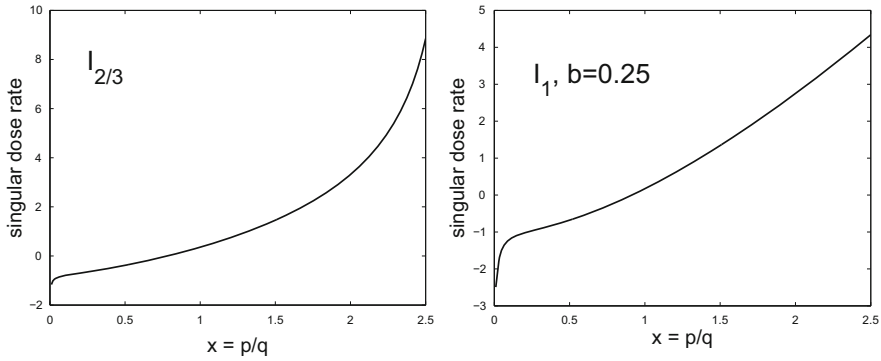

Fig. 5.17 Graphs of the singular control for models $[I_{\frac{2}{3}}]$ (left) and $[I_1]$ (right) for parameter values from Table 5.2 ($b = 0.25$ has been used for model $[I_1]$).

5.6 Medical Interpretations and Modeling Extensions

Summarizing our results, for various mathematical models of antiangiogenic therapy that are based on the research in [116], we presented a complete theoretical solution for the problem of optimally scheduling an a priori given amount of antiangiogenic agents in order to minimize the primary tumor volume. These solutions show *a uniform picture across various modeling assumptions* that is *fully robust with respect to parameter values*. Optimal controls implement the following strategy: give antiangiogenic agents at maximum dose rates until an ideal relation between tumor volume and carrying capacity has been established (defined by the singular arc), then maintain this relation by judiciously chosen lower reduced dose rates (defined by the singular controls). The singular arc and its associated singular controls thus play the central role in the structure of optimal solutions. *"More" is definitely not better as far as the administration of antiangiogenic agents is concerned, but properly designed dose rates are optimal*. Only if the singular surface $\mathscr{S}$ is not reachable in the region where the singular control is admissible, optimal controls will administer agents at full dose rates upfront, but otherwise the partial dose rates along the singular arcs better distribute the antiangiogenic agents over time and lead to lower tumor volumes. If we were to put no limitations on the dose rates, optimal solutions consist of an initial bolus injection to reach the singular arc $\mathscr{S}_0$ and then administer antiangiogenic agents according to the singular control until all agents are exhausted. This simple structure, which can be established rigorously mathematically by letting $u_{\max} \to \infty$ in the optimal solution presented here, is the best possible scenario and represents the essence of the solutions to the problem. These robust structural findings give strong credence to the underlying model as a high-level, minimally parameterized model for antiangiogenic therapy.

An important conclusion from this analysis is that there does exist an *ideal relation between tumor volume and vasculature along which tumor shrinkage is maximized*. For each mathematical model employed here, rather elegant Lie-algebraic

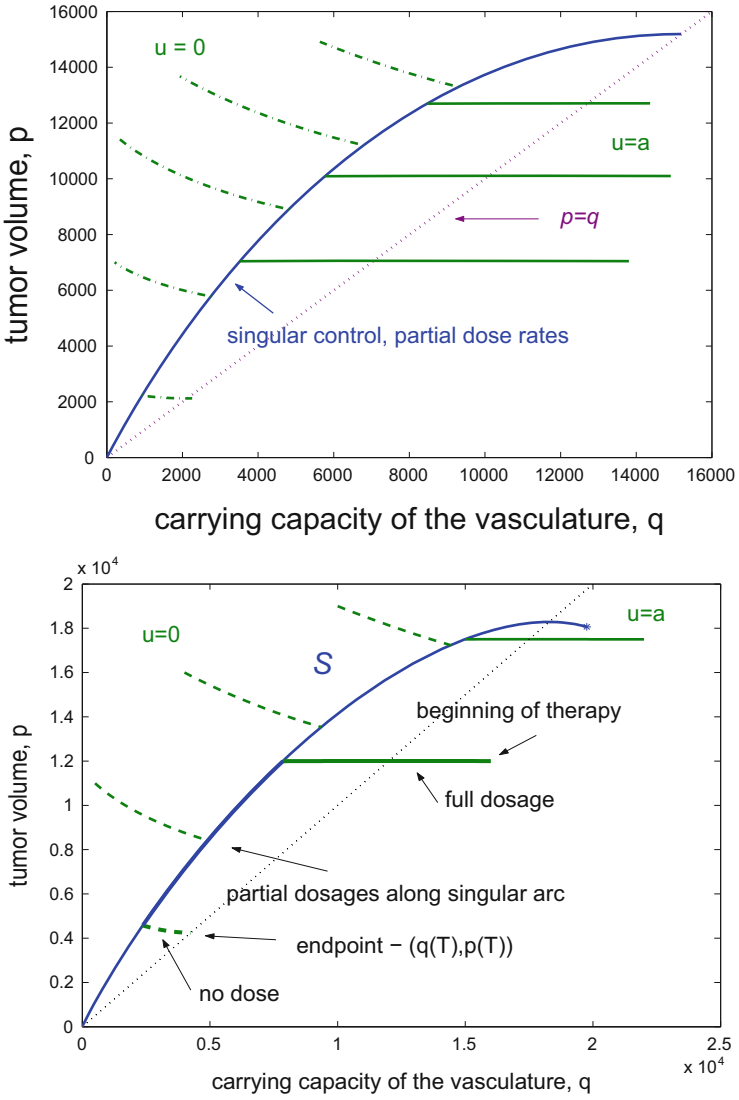

Fig. 5.18 Optimal synthesis for problems $[\mathrm{I}_{\frac{2}{3}}]$ (top) and $[\mathrm{I}_1]$ (bottom) for the parameter values from Table 5.2 ($b = 0.25$ has been used for model $[I_1]$).

computations provide us with explicit formulas for the singular arc and the corresponding singular control that keeps it invariant. The singular surface lies in the region where the tumor volume p is higher than its carrying capacity q, but the carrying capacity q is not pushed to zero too fast. Rather, a specific balance between p and q is maintained along the optimal solution. We shall see in Chapter 7 that this balance is preserved in combinations of antiangiogenic therapy with

chemo- or radiotherapy. Since the vascular network of the tumor is needed to deliver the chemotherapeutic agents, this perfectly makes sense and it is reminiscent of the medical notion of a regularization of the vasculature proposed by Jain et al. [131, 132]. In the models analyzed here, such a possibility is introduced purely from an optimization point of view.

From a more practical point of view, singular controls may not seem realistic with current technologies. But implementing the optimal strategies is not the only reason for solving optimal control problems. In fact, solutions to optimal control problems provide *benchmark values* to which any other strategy can be compared in order to evaluate their efficiency. Naturally, strategies of the type $u_{\max}0$ that give all available inhibitors in one session are the easiest to implement in practice and for some initial conditions these are indeed the optimal ones. This holds for initial conditions for which $u_{\max}$-trajectories do not meet the admissible singular arc, but also for initial conditions when this intersection point is close to the saturation point. Indeed, for model [H] the dynamics for $u \equiv u_{\max}$ very much has a differential-algebraic structure with the q-dynamics fast and the p-dynamics slow. As a result, after a brief transient phase, in steady state the system essentially follows the $\dot{q}$-nullcline. This nullcline is very close to the singular curve near the saturation point (also, see Figure 6.3 in Chapter 6) and thus the differences in the objective are almost unnoticeable near such initial conditions. For initial conditions far away from this point, the singular arc and the $\dot{q}$-nullcline are separated and then the singular control is noticeably better. Of course, only knowing the optimal solution allows to make such an comparison. In Chapter 6, we shall give an exhaustive numerical evaluation of the structure of easily practically realizable, piecewise constant protocols and show that *simple, suboptimal protocols can be designed that come within a few percent of the optimal solutions*. Furthermore, and this also is a consequence of the structure of optimal solutions, these protocols are fully robust with respect to the carrying capacity, a theoretical quantity difficult to measure. Thus these solutions lead to several practically interesting findings.

We close this chapter with a few comments about the modeling premises. It has already been stated that model [H], on which the class of models analyzed in this chapter is based, was formulated by Hahnfeldt, Panigrahy, Folkman, and Hlatky, a group of researchers then at Harvard Medical School, as a model for angiogenic signaling and first published in the journal *Cancer Research* in 1999 [116]. The optimal control problem to minimize the tumor volume with a given amount of antiangiogenic agents was formulated in 2003 by Ergun, Camphausen, and Wein in the paper [77] who studied it in the context of a combination of tumor antiangiogenic treatment with radiotherapy. In order to alleviate somewhat the complicated mathematical structures that arise in the radiotherapy calculations (c.f., also Chapter 7), the simplifications that led to the model [E] were introduced. The results on the structure of optimal controls presented in this chapter are our own and various aspects of it have been published piecemeal in the literature (e.g., see [196, 200, 201, 204, 206]). Other variations of the model exist as well, for example the one by d'Onofrio and Gandolfi where the stimulation term is taken to be $S(p,q) = bq$. For this model, it can be shown that singular arcs do not exist and hence—and still consistent with the

structures derived here—the concatenation structure of optimal controls collapses to become bang-bang with at most two switchings in the order $\mathbf{0u}_{\max}\mathbf{0}$ [204, 314]. In some sense, this situation represents an extreme within the class we considered here. Naturally, all models can be considered with different growth functions [183]. Also if a classical logistic model is used, $F(x) = 1 - x$, singular arcs do not exist and simple bang-bang solutions arise [314, 319]. But, in our view, these are the exceptional cases. Optimal controls are bang-bang not because these are the better structures, but simply because the truly best options, namely those presented by the singular controls, are not available. This very much is a general principle in solutions to optimal control problems with L_1-type objectives. The problem formulation considered in this chapter is what appears to us as the most intriguing formulation from which many medically natural questions can easily be answered, but clearly other options for defining the objective functional exist. These include, for example, fixed therapy horizon formulations similar to the ones considered in Chapter 2. Generally, the same techniques apply and similar results are obtained. We refer the interested reader to the literature on this topic (e.g., see [189, 197, 205, 314, 316, 319]). Finally, numerous other modifications of the underlying model have been proposed in the literature (e.g., see [251, 259, 281]), though generally not in an optimal control setting.

Chapter 6
Robust Suboptimal Treatment Protocols for Antiangiogenic Therapy

As was shown in the previous chapter, singular controls play an essential role in determining the overall structure of optimal controlled trajectories for the class of mathematical models for antiangiogenic treatments based on the model by Hahnfeldt et al. Lie algebraic computations provide an elegant framework in which the singular controls and corresponding arcs can be determined analytically, but the resulting formulas define feedback controls that administer time varying partial doses depending on the current state of the system, that is, on the tumor volume p and its carrying capacity q. Even at the initial time, while a reasonably reliable estimate for the tumor volume p_0 may be available, the carrying capacity of the vasculature, q_0, is a highly idealized quantity and there are no accurate methods to measure it. Thus, indeed there is significant uncertainty about the actual values of the states. Even if it were possible to monitor the states $p(t)$ and $q(t)$, medical devices that would administer such time-varying state-dependent dosages do not exist. The value of the theoretical optimal solution that was derived for problem [OCA], apart from giving important qualitative insights into the underlying system, lies in clarifying what in principle is possible. In fact, for many practical problem, this precisely is the contribution that optimal control methodologies provide. Then, based on the benchmarks that the theoretically optimal solutions provide, it becomes of importance to formulate *simple, easily implementable*, but also *robust strategies* that could be employed even in the face of great uncertainty in the parameters and the state of the system. The models considered in Chapter 5 exhibit strong robustness with respect to parameter values and in this chapter we shall see that this also is valid in their dependence with respect to the values of the carrying capacity q. More generally, the *question* becomes *what kind of responses can be achieved, and how closely can the optimal values be approximated with realistic and medically realizable protocols that are robust with respect to a wide range of parameters and uncertainties*. This will be the topic of this chapter.

H. Schättler, U. Ledzewicz, *Optimal Control for Mathematical Models of Cancer Therapies*, Interdisciplinary Applied Mathematics 42,
DOI 10.1007/978-1-4939-2972-6_6

For both model [H] and [E] we analyze in Sections 6.1 and 6.2 the effectiveness of some simple, practically common therapy protocols. Constant dose therapies can be applied without any information on the initial data, but they are not necessarily a good strategy. Essentially, if the resulting concentration is too low, no positive effect may be achieved while too high a concentration unnecessarily wastes inhibitors that could have been used more effectively at lower dose applications spread out in time. We shall see below that the averaged value of the theoretically optimal control computed in Chapter 5 provides an excellent suboptimal strategy. More generally, we shall analyze the performance of piecewise constant protocols with a small number of segments (constant dose rates, two rate regimens, daily dosages, etc.). The value of knowing the theoretically optimal solutions thus is bifold: it directly gives rise to an excellent simple protocol and it provides benchmark values against which one can judge the quality of simple, heuristically chosen strategies and protocols. Using the knowledge of the theoretically optimal solution, it is indeed possible to design excellent realizable suboptimal protocols for the models of antiangiogenic therapy discussed in Chapter 5. Here a numerical evaluation will be carried out for the models [H] and [E]. These results are based on joint work with John Marriott of the University of Hawaii at Manoa and Helmut Maurer from the Rheinisch Westfälische Wilhelms Universität Münster in Germany and have been reported in various publications (e.g., [178, 179, 203]).

In the models in Chapter 5 dose rates of the agent are identified with concentrations in the blood stream. We here also consider extensions of the models that include a linear pharmacokinetic model for the antiangiogenic agent, i.e., distinguish between these two quantities. We already have seen for the compartmental models considered in Chapter 2 that the optimality status of singular controls was preserved when a linear pharmacokinetic model was added to the reduced model (see Theorem 2.3.2 in Section 2.3.2). The same holds true here and, in fact, in great generality. However, it becomes necessary to adjust the formulas and equations to the new model description. We shall see in Section 6.3 that the analytic equations derived in Chapter 5 for the singular arc as a function of p and q remain valid verbatim except that the expressions which defined the singular control in the reduced models now describe the corresponding concentrations. Thus these explicit computations directly carry over and all essential features of the simplified model are preserved. Once more this gives credence to the approach of inductively adding more medically realistic features into the model. At the same time, however, mathematically under this modeling extension the intrinsic order of the singular arc increases from 1 to 2 and this has significant implications on the structure of optimal concatenations of trajectories with the singular arc. It is no longer optimal to switch from a full or no dose control to the singular control, but now this transition is accomplished by means of chattering controls (see Proposition A.3.3 in Appendix A). Thus, while essential features are preserved verbatim under this modeling extension, the qualitative structure of the optimal synthesis is not the same and indeed optimal solutions become more complicated and even less practically feasible. Thus, once again, the important question becomes how to construct suboptimal realizable protocols that come close to the optimal results. Thus this topic naturally fits into this

chapter. After establishing the theoretical results in Section 6.3, we again describe simple suboptimal protocols that come very close to the optimal solution. As before, information about the structure of the optimal solutions directly suggests excellent suboptimal approximations. From a practical point of view, these provide satisfactory control schemes for treatment protocols for antiangiogenic therapy.

6.1 Realizable Suboptimal Treatment Protocols for Model [H]

We optimize treatment strategies over some simple classes of piecewise constant treatment protocols and evaluate their effectiveness by comparing the results with the optimal values for the model [H]. (Dose rates of the agent are still identified with the concentrations in the bloodstream.) For realistic initial conditions some simple strategies that divide the overall amount of antiangiogenic agents to be given into a small number of intervals with constant values can come within 1% of the theoretically optimal values when the times of administration are included as variables in this optimization problem. We also consider the case when these times are fixed a priori to fit some practically imposed constraints. Naturally, due to the resulting lack of freedom, these strategies perform worse, but they still come reasonably close to the theoretically optimal values. Our main conclusion is that *simple, piecewise constant, and hence realistic protocols can be found that come very close to the theoretically optimal solution*. We note that it is not difficult to compute these solutions numerically, but that it is only the knowledge of the theoretically optimal solution that allows to judge their quality. Unless specified otherwise, throughout this section we use the parameter values from Tables 5.2 and 5.3 for our numerical illustrations, but the principal conclusions are valid for a wide range of initial conditions and are fully robust with respect to changes in the parameters.

6.1.1 Constant Protocols

It is straightforward to compute the *best constant protocol* for a fixed initial condition. As one example, we consider $(p_0, q_0) = (12{,}000\,[mm^3]; 15{,}000\,[mm^3])$. For this initial condition, the optimal concatenation sequence is given by $\mathbf{u}_{\max}\mathbf{s0}$: initially the optimal control administers agents at full dose rate $u_{\max} = 75$ until the singular base curve $\mathscr{S}_0$ is reached at time $t_1 = 0.091$ [days]. Then administration follows the time-varying singular control until the antiangiogenic agents are exhausted at time $t_2 = 6.558$ [days]. Because of after effects, the maximum tumor reduction is realized along a trajectory for control $u = 0$ at the optimal terminal time $T = 6.722$ [days] when the trajectory reaches the diagonal $p = q$. The theoretically optimal minimum value for these data is given by $p_* = p(T) = 8533.38\,[mm^3]$. Figure 6.1 shows the corresponding optimal control and its associated trajectory.

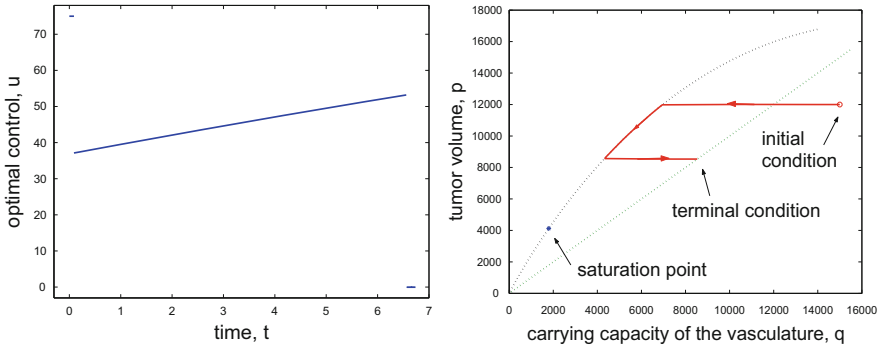

Fig. 6.1 Optimal control (left) and corresponding trajectory (right) for problem [H] and initial conditions $(p_0, q_0) = (12{,}000\,[mm^3]; 15{,}000\,[mm^3])$

One way to compute a good constant dose rate is to simply give the available amount A of anti-angiogenic agents at a constant dose rate u over time $t_u = \frac{A}{u}$ and then to take as the dose rate the value $\hat{u}$ that minimizes the values of the solutions $\hat{p}_u$ at the times t_u,

$$\hat{u} = \arg\min \hat{p}_u(t_u).$$

This is a straightforward one-dimensional numerical minimization problem and for the initial condition $(p_0, q_0) = (12{,}000\,[mm^3]; 15{,}000\,[mm^3])$ the optimal dose rate and the final time are given by

$$\hat{u} = 45.27 \quad \text{and} \quad t_u = A/\hat{u} = 6.626\ [\text{days}].$$

Note, however, that this problem formulation is not consistent with the optimal control problem [H] that was formulated in Chapter 5 since the terminal values of the trajectories, $(\hat{p}_u(t_u), \hat{q}_u(t_u))$, do not lie on the diagonal. For example, for the value $\hat{u} = 45.27$ we have that $(\hat{p}_{\hat{u}}(t_{\hat{u}}), \hat{q}_{\hat{u}}(t_{\hat{u}})) = (8570.0\ [mm^3], 4807.1\ [mm^3])$. Since the carrying capacity is smaller than the tumor volume, there will still be an additional tumor reduction after all agents have been exhausted. The amount of this reduction also depends on the value of the carrying capacity $\hat{q}_u(t_u)$ at the endpoint and minimizing the values that are realized as the trajectories cross the diagonal indeed slightly changes the value of the optimal dose rate. The formulation that is consistent with problem [H] is to give all available antiangiogenic agents at rate u over the interval $[0, \frac{A}{u}]$ and then still concatenate the trajectory at the point $(\hat{p}_u(t_u), \hat{q}_u(t_u))$ when all agents have been exhausted with a trajectory corresponding to the control $u = 0$. The minimum tumor volume then is realized as this trajectory crosses the diagonal at some time T_u. We denote this minimum tumor volume by $\pi_u(T_u)$ and minimizing over u gives the following slightly different optimal constant dose rate,

$$u_* = \arg\min \pi_u(T_u) = 46.34.$$

The minimal tumor volume is $p_* = 8544.15[mm^3]$. Figure 6.2 shows the graph of the function $\pi_u(T_u)$ with a small interval around the optimal value blown up on the right.

For comparison, if one still adds the $u = 0$ segment to the trajectory for $\hat{u} = 45.27$, then the corresponding value on the diagonal is slightly larger given by $\pi_{\hat{u}}(T_{\hat{u}}) = 8544.62\ [mm^3]$ with final time $T = 6.777$ [days]. Clearly, from a practical point of view, there is no difference between these values and both are extraordinarily close to the theoretically optimal value $8533.38\ [mm^3]$.

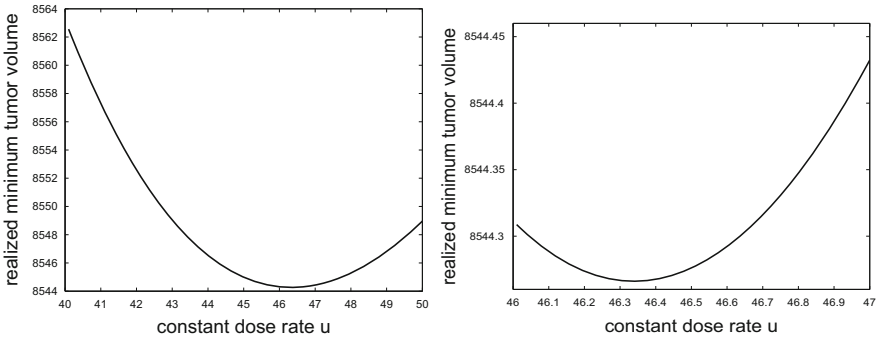

Fig. 6.2 Graph of $\pi_u(T_u)$ over $[40,50]$ (left) and a blow-up over $[46,47]$ (right).

A different type of constant protocol can be obtained by averaging the optimal control over the interval of administration, i.e.,

$$\bar{u} \equiv \frac{1}{T_{\text{opt}}} \int_0^{T_{\text{opt}}} u_{\text{opt}}(t)dt = \frac{A}{T_{\text{opt}}}.$$

In this formula, u_{opt} denotes the optimal control as a function of time, T_{opt} is the time when all antiangiogenic agents have been exhausted and, as before, A denotes the a priori specified overall amount of agents to be given. Since all antiangiogenic agents are used along the optimal control, the integral is simply given by this total amount A. The final interval when the tumor volume still decreases because of after effects is not included in this computation. We call this the *averaged optimal dose rate protocol*. For $(p_0, q_0) = (12{,}000\,[mm^3]; 15{,}000\,[mm^3])$, the averaged optimal dose rate is $\bar{u} = 45.75$ and gives the value $p_{\bar{u}} = 8570.09\ [mm^3]$ at the time when inhibitors run out. Adding the final segment $u = 0$, we obtain as minimum value $8544.30\ [mm^3]$ with final time $T = 6.709$ days. This value only lies slightly above

Table 6.1 Comparison of minimal values for various constant dose rate protocols for problem [H].

Control	Minimal value $[mm^3]$	Terminal time [days]	Switching time [days] to $u = 0$
Optimal	8533.38	6.722	6.558
$\bar{u} = 45.75$	8544.30	6.709	6.558
$\hat{u} = 45.27$	8544.62	6.777	6.626
$u_* = 46.34$	8544.15	6.626	6.474

the best constant dose rate protocol, but does better than when we simply minimize at the time when all agents are used up. Table 6.1 summarizes the numerical results.

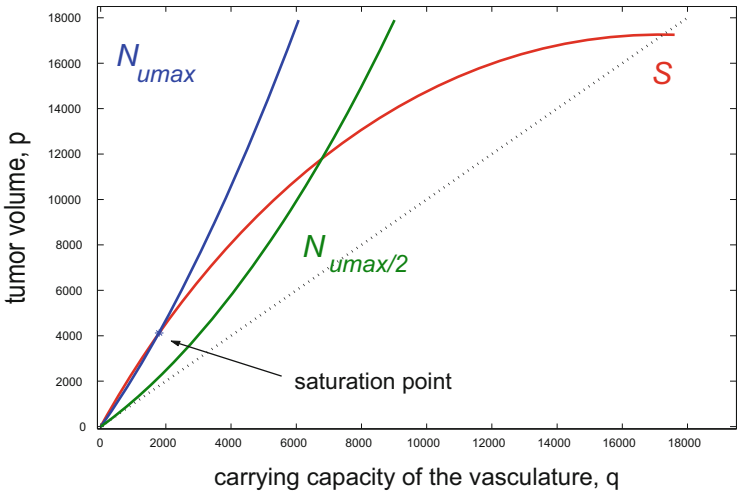

Fig. 6.3 Model [H]: The singular curve $\mathscr{S}$ (shown in red) and the nullclines $\mathscr{N}_{u_{\max}}$ (shown in blue) and $\mathscr{N}_{\frac{1}{2}u_{\max}}$ (shown in green) for the constant dose protocols for $u \equiv u_{\max}$ and $u \equiv \frac{1}{2}u_{\max}$.

Clearly, these optimal values depend on the initial condition (p_0, q_0) and we now investigate the robustness of these values with respect to the initial data. It follows from our theoretical results developed in Chapter 5 that *full dose rate protocols* of the form $\mathbf{u}_{\max}\mathbf{0}$ are optimal if the initial tumor volume p_0 is close to the p-value for the lower saturation point on the singular arc and indeed these strategies are the optimal solutions for all realistic values of the carrying capacity q_0. Naturally, thus an $\mathbf{u}_{\max}\mathbf{0}$-protocol is an *excellent sub-optimal strategy for small tumor volumes* that is almost as good as the optimal solution. However, reduced dose rates do better for initial conditions with higher values p_0. While this may seem counterintuitive, for this problem it is simply the case that agents are less effective (or more wasteful) at higher rates and therefore it is beneficial to administer an a priori given amount of antiangiogenic agents at lower rates. As a simple comparison, in our figures we also include the optimal values that correspond to *half dose rate protocols* that give the full amount of inhibitors at half the maximum dose over twice the time. This is a simple ad-hoc strategy that generally does better than a full dose protocol for high tumor values p_0. The reasons for this can easily be understood mathematically from the synthesis of optimal controlled trajectories: the dynamics for a general constant dose protocol $u \equiv v$ has a strong differential-algebraic character with fast variable q and slow variable p. Essentially, the system follows an almost "horizontal" line until the algebraic constraint manifold determined by the $\dot{q} = 0$ nullcline,

$$q = \frac{bp}{\mu + \gamma v + dp^{\frac{2}{3}}},$$

is reached; then the dynamics evolves along this curve. This nullcline very much plays the same role for constant dose protocols as the singular curve does for the optimal solutions. Figure 6.3 shows both the singular curve (in red) and the $\dot{q} = 0$ nullclines for the full dose $u = u_{\max}$ (in blue) and half dose $u = \frac{1}{2}u_{\max}$ (in green). The $u_{\max}$-nullcline intersects the singular curve in the saturation point and the two curves are almost identical around and below this saturation point. Hence in this area the full dose protocols come very close to the optimal protocols. But for higher values of p and q these curves separate and now the singular curve is better approximated by the $\frac{1}{2}u_{\max}$-nullcline. Hence a half-dose rate protocol does better there. In fact, it seems clear from Figure 6.3 that, as the tumor volumes increase, lower dose rates should still do better.

While the full and half dose rate protocols are mere ad-hoc strategies that do not take into account the initial data, the optimal constant dose and the averaged optimal dose rate protocols are functions of p_0 and q_0. It is therefore of interest how sensitive these dose rates are with respect to the initial data. In Figures 6.4–6.6 we compare the minimum tumor volumes that can be achieved with these constant rate dose protocols with the one for the optimal control for initial tumor volumes for $p_0 = 6{,}000$ $[mm^3]$, $p_0 = 9{,}000$ $[mm^3]$, and $p_0 = 12{,}000$ $[mm^3]$ and values of the carrying capacity q_0 ranging from $q_0 = 2{,}500$ $[mm^3]$ to $q_0 = 12{,}000$ $[mm^3]$. The top row of each figure shows the graphs for the minimum tumor volume realized by the various protocols for a fixed initial condition p_0 and varying initial conditions q_0, i.e., slices through the graph of the associated value function for $p_0 = const$. In all diagrams, the solid red curve gives the theoretically optimal values corresponding to the optimal controls determined in Chapter 5, the dashed blue curve corresponds to the full dose rate $u_{\max}$, the dashed-dotted blue curve to half dose rate $\frac{1}{2}u_{\max}$, the dashed black curve gives the values for the averaged optimal dose rate and the dash-dotted black curve gives the values corresponding to the optimal constant dose rate. The graphs in the bottom row give the optimal constant dose rates (left) and the averaged optimal dose rates (right) for fixed p_0 as a function of q_0. In all cases, *the averaged optimal dose rate protocol* is very close to the optimal constant dose rates and both stay within 0.5% of the theoretically optimal value. These averaged values are easily computed while the computations of the optimal constant dose rates is straightforward, but lengthier. For smaller tumor volumes, there is no discernable difference between the optimal control, the averaged optimal and optimal constant dose rate protocols. Only as the tumor volume becomes high, separation of the corresponding slices of the value function is seen. The curves for the values corresponding to the optimal constant dose rates and the averaged optimal dose rates are almost identical and differences are hardly discernible in the diagrams. We show on the top right portion of each figure blow-ups of the graphs that show that the optimal constant dose rates just lie slightly below the averaged optimal dose rates.

The saturation point for the singular control lies at $p_{sat} = 4{,}122$ $[mm^3]$ and in this range, as the value of the singular control is close to $u_{\max} = 75$, the optimal, averaged, and full dose protocols give almost identical values. The half dose protocol does noticeable worse for these values. In fact, it is so far off that we did not include this curve in the range for Figure 6.4. Naturally, the realizable minimum

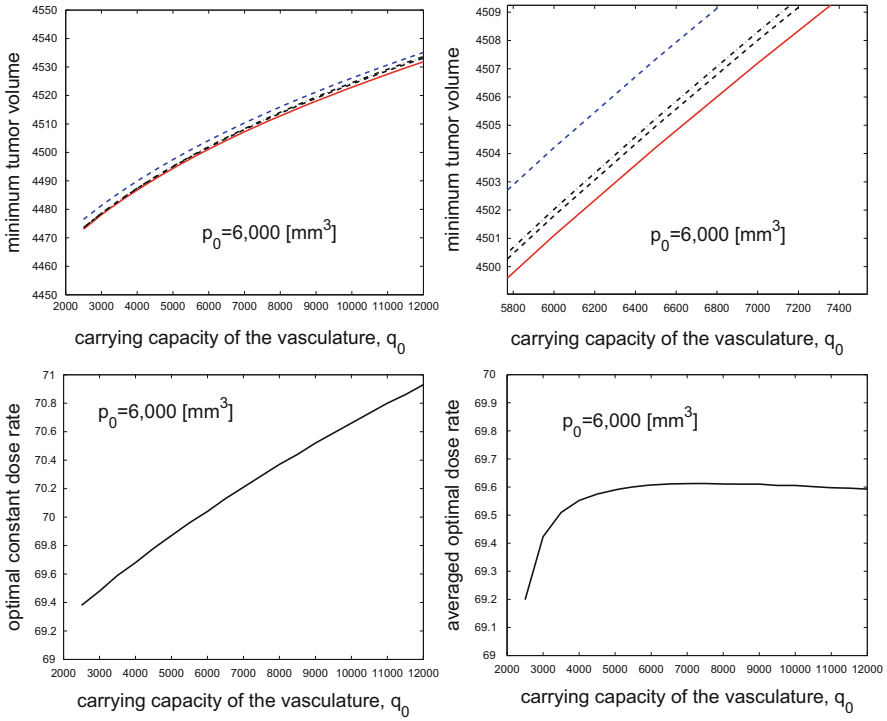

Fig. 6.4 The graphs of the minimum tumor volumes realized by the optimal control (solid red curve), a full dose rate protocol (dashed blue curve), the averaged optimal control protocol (dashed black curve), and the optimal constant dose rate protocol (dash-dotted black curve) for the fixed initial tumor volume $p_0 = 6{,}000\ [mm^3]$ as a function of the initial carrying capacity q_0 (top, left) and a blow-up of the graphs (top, right). The values for the half-dose rate protocol lie outside of the range shown and are not included in this figure. The graphs at the bottom give the optimal constant dose rates (left) and the averaged optimal dose rates (right) as functions of the initial carrying capacity q_0.

values increase with growing initial endothelial support q_0. As the initial tumor volume p_0 increases, the full dose rate protocol starts to perform worse while the half dose rate protocol improves. For $p_0 = 12{,}000\ [mm^3]$ (see Figure 6.6), the full dose protocol does considerably worse while the half dose protocol does markedly better. In all cases, *the averaged optimal dose rate protocol* comes remarkably close to the optimal constant dose rates and both stay within 0.5% of the theoretically optimal value. But even for the full dose rate protocols, the differences to the optimal value barely exceed 2% for high initial values of q_0 if the initial condition (p_0, q_0) lies to the right of the singular curve (see Figure 6.3) since the optimal control starts with $u \equiv u_{\max}$ in this region. If, however, the initial condition lies to the left of the singular curve, then the discrepancies become larger, exceeding the 5% range for the full dose rate protocol. The reason is that in this region it is optimal to first wait (i.e., start with the control $u = 0$) until the level of endothelial support reaches the

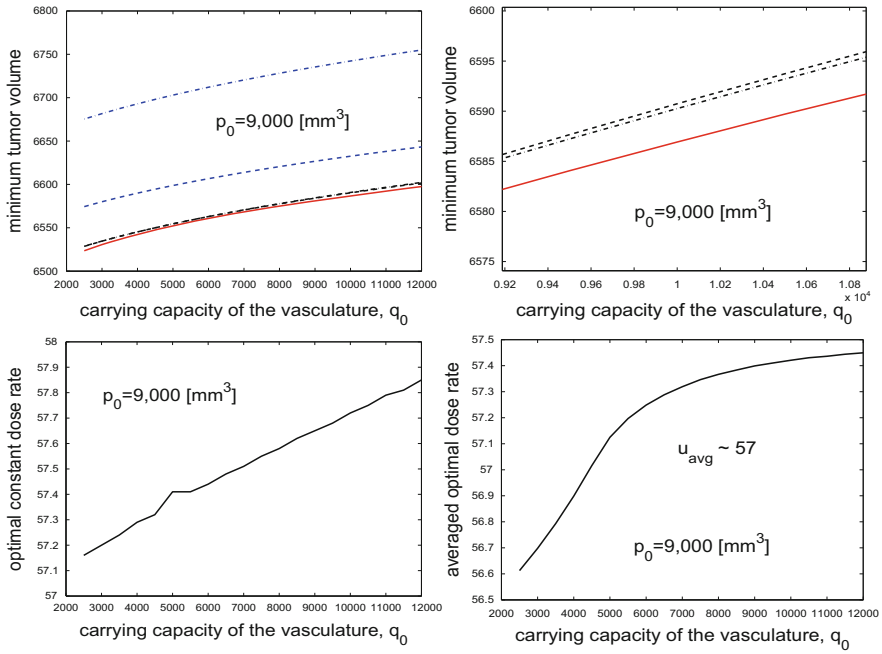

Fig. 6.5 The graphs of the minimum tumor volumes realized by the optimal control (solid red curve), a full dose rate protocol (dashed blue curve), the half-dose rate protocol (dash-dotted blue curve), the averaged optimal control protocol (dashed black curve), and the optimal constant dose rate protocol (dash-dotted black curve) for the fixed initial tumor volume $p_0 = 9{,}000\ [mm^3]$ as a function of the initial carrying capacity q_0 (top, left) and a blow-up of the graphs (top, right). For increasing tumor volumes the effects of the half-dose rate protocols now lie in the range shown here, but are still worse than a full dose rate protocol. The graphs at the bottom give the optimal constant dose rates (left) and the averaged optimal dose rates (right) as functions of the initial carrying capacity q_0.

singular curve upon which treatment ensues. This feature, that the optimal control starts with a segment where $u \equiv 0$ if the initial condition (p_0, q_0) lies to the left of the singular curve, also is responsible for the fact that the optimal constant and averaged optimal dose rates in Figure 6.4 increase for small values of q_0 and then tend to level off. These values tend to increase in q_0 since the initial interval when $u \equiv u_{\max}$ is being used, however brief it is, increases with q_0.

One important qualitative feature of the optimal constant and averaged optimal dose rates is how little the values vary with q_0. For all the cases here (that cover realistic scenarios) these variations are tiny. Consequently, these dosages *are fully robust with respect to the initial condition* q_0, a quantity that generally is not measurable. Hence it is not important to know the value exactly, but even the crudest of approximations will do. However, these three figures clearly show that the dose rates (optimal or averaged) for fixed q_0 *decrease* with increasing initial tumor volume p_0. The reason for this somewhat counterintuitive property lies in the fact that

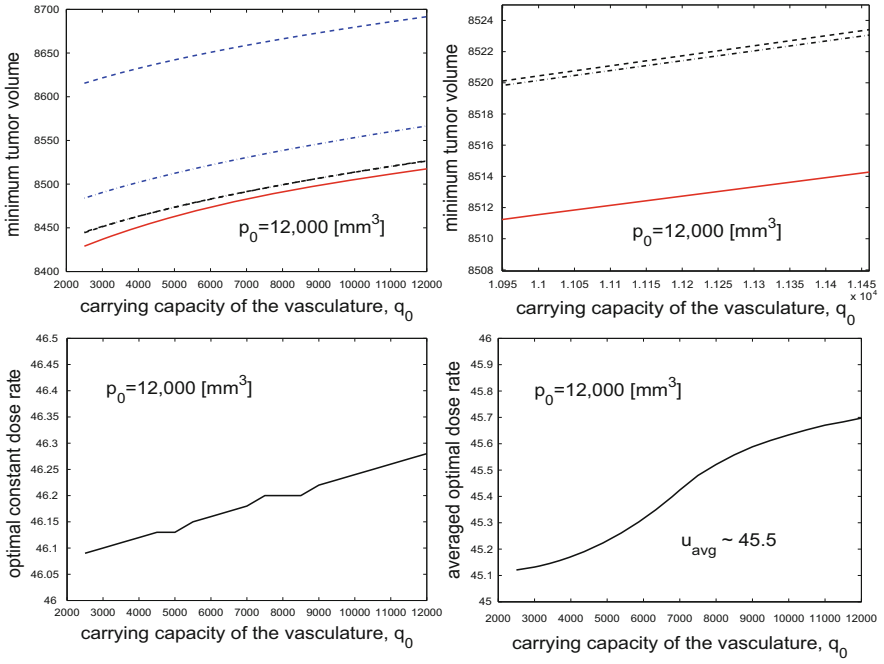

Fig. 6.6 The graphs of the minimum tumor volumes realized by the optimal control (solid red curve), a full dose rate protocol (dashed blue curve), the half-dose rate protocol (dash-dotted blue curve), the averaged optimal control protocol (dashed black curve), and the optimal constant dose rate protocol (dash-dotted black curve) for the fixed initial tumor volume $p_0 = 12{,}000\ [mm^3]$ as a function of the initial carrying capacity q_0 (top, left) and a blow-up of the graphs (top, right). For high tumor volumes the effects of the half-dose rate protocols are better than for a full dose rate protocol. The graphs at the bottom give the optimal constant dose rates (left) and the averaged optimal dose rates (right) as functions of the initial carrying capacity q_0.

the optimal singular control has this property of *dose-intensification* that was already noted for model $[E]$ in [77] - the dosage increases in time as the tumor volume becomes smaller. This feature is inherited by the optimal constant dose rates.

Since antiangiogenic therapy does not kill the tumor directly, but only impedes its growth, another positive effect of the optimal solution over a full dose rate protocol is that it delays the time when this minimum is reached. For the averaged optimal dose rate protocol, the time when all agents are exhausted is the same as for the optimal protocols and thus the times when the minimum tumor reductions are achieved are almost identical. But since the optimal singular arc applies the inhibitors at time-varying lower doses, the time T_{opt} when the minimum is realized along the optimal solution is larger, at times significantly, than the time T_{full} for the full dose rate protocol. In Table 6.2 these times are compared for the optimal control and full dose rate protocols. Given the data, with a full dose rate protocol all inhibitors are exhausted in $4 = \frac{A}{u_{\max}}$ days. For $\mathbf{u}_{\max}\mathbf{0}$-protocols, the minimum tumor volumes are being realized almost immediately afterward and this does not change

much with the initial condition (p_0, q_0) (see Table 6.2, left portion). However, if the initial tumor volume p_0 is high, then antiangiogenic agents are given at a much lower rate initially along the optimal control and this leads to significantly larger times T for which the minimum is realized (see Table 6.2, right portion). For example, if $p_0 = 15{,}000\ [mm^3]$ and $q_0 = 18{,}000\ [mm^3]$, then the time T_{opt} for the optimal control (9.077 [days]) is more than double the time for the straightforward $\mathbf{u}_{\max}\mathbf{0}$-protocol (4.229 [days]). Clearly, this indicates that in these cases it was not a good strategy to give all inhibitors in one session at the beginning and that they might have better been applied at lower dose rates as the singular control does.

Table 6.2 Comparison of the times when the minimum tumor volumes are realized for model [H] for the optimal control (left) and a maximum dose rate protocol (right).

$q_0 \diagdown p_0$	6000	9000	12000	15000
6000	4.446	5.390	6.784	9.138
12000	4.447	5.371	6.729	9.103
18000	4.451	5.369	6.718	9.077

$q_0 \diagdown p_0$	6000	9000	12000	15000
6000	4.139	4.164	4.192	4.228
12000	4.139	4.164	4.193	4.229
18000	4.140	4.165	4.193	4.229

It is clear from these computations that *lower concentrations do better as the tumor volume increases*. This behavior can be understood from the geometry of the trajectories involved. Figure 6.7 shows an example of the relevant trajectories for the initial condition $(p_0, q_0) = (15{,}000\ [mm^3];\ 6{,}000\ [mm^3])$. It is clear that the $\dot{q} = 0$ nullcline for $u \equiv \frac{1}{2}u_{\max}$ is a much better approximation of the optimal singular curve for high initial values of p_0 than is the $\dot{q} = 0$ nullcline for $u \equiv u_{\max}$. Naturally, the half dose rate strategy is then a better sub-optimal control for large tumor volumes than a full dose rate strategy. In fact, if we were to reduce the upper limit $u_{\max}$ defining the control set to $\frac{1}{2}u_{\max}$ in the optimal control problem, the saturation point of the singular arc will be at $p_{\text{sat}} = 11{,}902\ [mm^3]$ and thus for almost all initial conditions considered here the optimal controls will be given by bang-bang controls that give the new "full" dose $\frac{1}{2}u_{\max}$ from the beginning. This explains the superior performance of the half dose rate protocols for this range of initial conditions. Lowering the upper limit of the dose further to $\frac{1}{4}u_{\max}$, no longer improves the value. In fact, these protocols generally do quite worse, since the $\dot{q} = 0$ nullcline for $u = \frac{1}{4}u_{\max}$ now becomes a poor approximation of the singular curve. For the initial condition $(15{,}000\ [mm^3]; 6{,}000\ [mm^3])$, the realized minimal value for the quarter dose strategy is only $p(T) = 12{,}316\ [mm^3]$, almost 20% worse than the value realized with the half dose rate protocol. Thus *the geometric shape of the optimal singular arc very much explains the effects of these simple constant protocols.*

Summarizing, given an a priori specified amount of antiangiogenic agents, the maximum tumor reductions that can be realized with a constant protocol depend on the concentration and *a higher concentration is not necessarily better*. Optimal protocols give guidance on how to choose this value and, for example, the averaged optimal control provides a generally excellent suboptimal concentration level that is quite insensitive to changes in the initial value of the carrying capacity, a highly

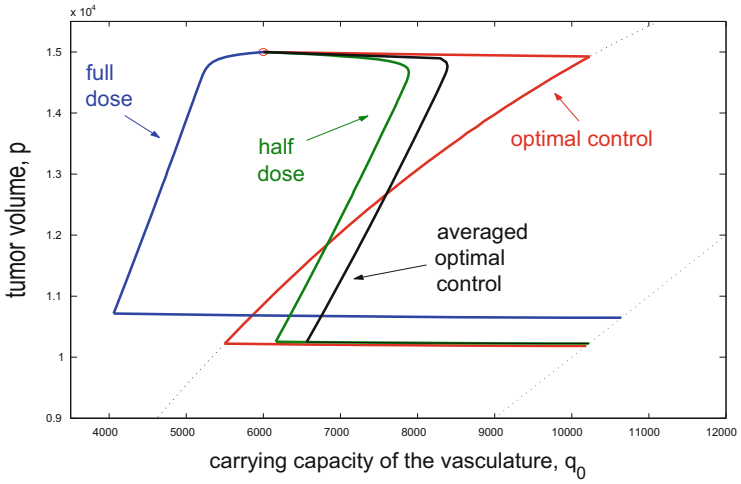

Fig. 6.7 Model [H]: A comparison of the optimal trajectory (red curve) with trajectories for the averaged optimal dose rate protocol (black curve), the full dose rate protocol (blue curve) and half dose rate protocol (green curve) for the initial condition $(p_0, q_0) = (15{,}000\ [mm^3]; 6{,}000\ [mm^3])$.

desirable feature. For model [H], this protocol consistently comes within 1% of the theoretically optimal value. Full dose rate protocols are optimal for low initial tumor volumes p_0, but the optimal dose rates decrease with increasing tumor volumes p_0.

6.1.2 Optimal Two-Stage Protocols

Clearly, these constant protocols already provide excellent approximations to the theoretically optimal control. The value can still be improved by increasing the number of switchings in the control. Since the constant approximations already do so well, we only consider controls that have one switching, i.e., take a constant value u_1 for time t_1 and a second value u_2 for time t_2. The second time is calculated so that all antiangiogenic agents become exhausted, i.e.,

$$u_1 t_1 + u_2 t_2 = A.$$

This is a simple 3-dimensional minimization problem with variables u_1, t_1, and u_2, and we denote this 3-tuple by v, $v = (u_1, t_1; u_2)$. As above, if we denote the point when the agents are exhausted by $(\hat{p}_v(t_v), \hat{q}_v(t_v))$ and the associated point on the diagonal by $\pi_v(T_v)$, then we can define controls $\hat{v}$ and v_* as the corresponding minimizers,

$$\hat{v} = \arg\min \hat{p}_v(t_v) \qquad \text{and} \qquad v_* = \arg\min \pi_v(T_v).$$

The optimal values for the initial condition $(p_0, q_0) = (12{,}000\,[mm^3]; 15{,}000\ [mm^3])$ and the same data used earlier are summarized in Table 6.3. The dosages are close to

each other, but their durations differ by quite a bit. However, this does not effect the minimum tumor volume much, although, overall, of course there is an improvement in the sense that the difference to the optimal value is cut in half. But on an absolute scale this improvement is irrelevant.

Table 6.3 Comparison of minimal values for various 2-stage constant protocols for problem [H]

Control	u_1	t_1 [days]	u_2	t_2[days]	Minimal value [mm^3]	Terminal time [days]
Optimal					8533.38	6.722
v_*	42.47	3.525	49.73	3.022	8539.21	6.736
$\hat{v}$	41.83	2.931	47.20	3.758	8540.20	6.843

Figure 6.8 compares the constant control u_* (in red) with the 2-stage control v_* (in blue). Consistent with dose intensification along the optimal singular control, these dosages increase: $u_2 > u_1$.

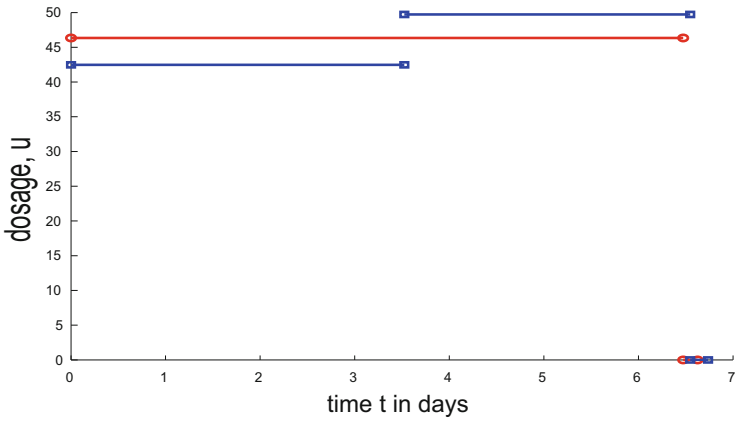

Fig. 6.8 The suboptimal controls u_* and v_* for problem [H](right).

Figures 6.9 and 6.10 show the graphs of the values $\pi_v(T_v)$ when the first and second control, respectively, have been fixed at its optimal values.

6.1.3 Daily Regimes

In the above formulations the durations of administration at the various dose rates are included as optimization variables. It is also of practical interest to specify these durations a priori and consider daily or even semi-daily dosages (e.g., give a dose over 8 or 12 hour periods and include a rest period during the night). Any such strategy significantly reduces the flexibility of possible schedules and it should come as

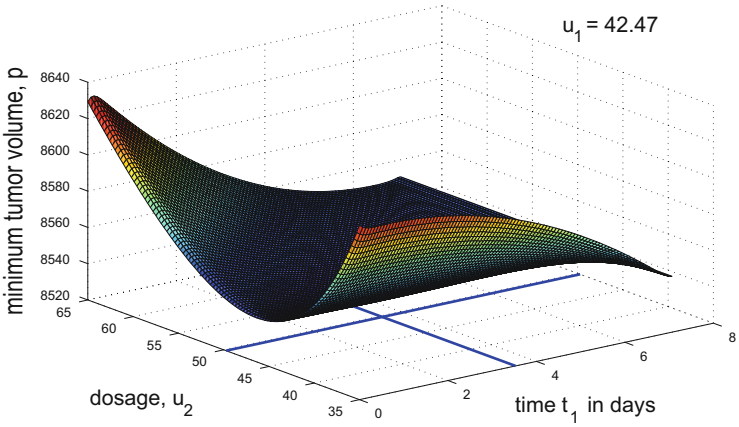

Fig. 6.9 Cross section through the graph of $\pi_v(T_v)$ for $u_1 = 42.47$ $[mm^3]$.

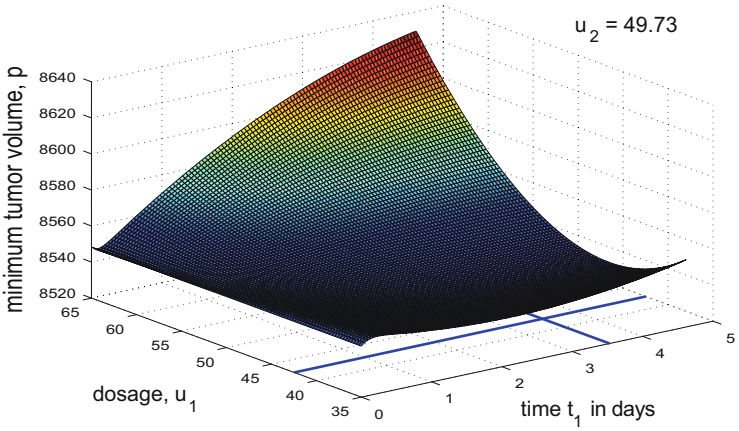

Fig. 6.10 A cross section through the graph of $\pi_v(T_v)$ for $u_2 = 49.73$ $[mm^3]$.

no surprise that with such restrictions the number of segments needs to be increased to obtain a similar degree of approximation. It seems reasonable to give the full amount of anti-angiogenic agents over the same time period as the optimal control does and in this section we still consider this optimization problem for the same data as before.

For the initial condition $(p_0, q_0) = (12{,}000\,[mm^3]; 15{,}000\,[mm^3])$, all antiangiogenic agents are used up at time 6.558 [days] along the optimal solution and we restrict the protocols to give the same total amount in 6 daily doses. The best such solution is given by

$$u_1 = 46.61,\ u_2 = 45.31,\ u_3 = 48.15,\ u_4 = 50.71,\ u_5 = 53.20,\ \text{and}\ u_6 = 56.02.$$

The tumor volume still decreases along the trajectory for $u = 0$ for time $t_7 = 0.169$ days until the diagonal $p = q$ is reached with minimal value $p(T) = 8544.4\ [mm^3]$. These 'daily' dose rates closely mimic the structure of the theoretically optimal control. Note the small dip in the values from the first to the second day and then the values gradually increase over the remaining days. Since the piece along which the optimal control is given by $u_{\max}$ is small, the first daily value is significantly lower than $u_{\max} = 75$, but it still is higher than the value for the second day. Along the optimal singular arc the dose intensifies and this is reflected in the increasing values of the daily doses over the remaining days. Still, specifying the time structure by restricting to daily doses reduces the quality of the approximation. The minimal value of 8544.4 $[mm^3]$ for the 6 day strategy is virtually identical with the optimal constant dose value, but the higher number of pieces does not make up for the loss of freedom by choosing the times in a 2-piece control when the minimal value is 8539.2 $[mm^3]$. Figure 6.11 shows the daily dosages and corresponding trajectory in the (p,q)-space.

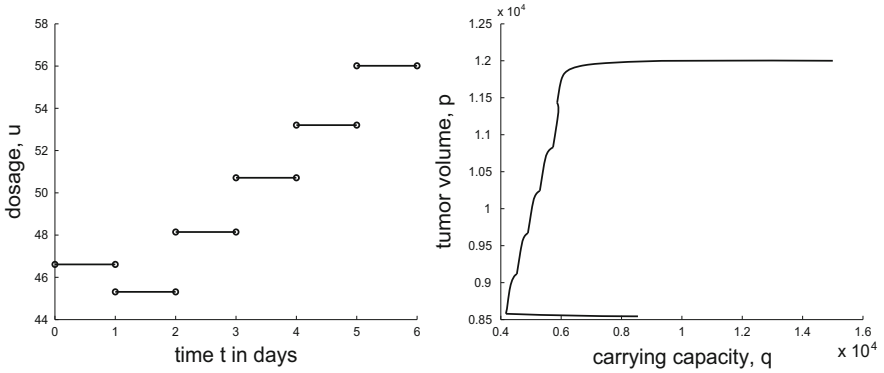

Fig. 6.11 Optimal 'daily' doses (left) and corresponding trajectory (right) for problem [H] and initial conditions $(p_0, q_0) = (12{,}000\,[mm^3]; 15{,}000\,[mm^3])$.

6.1.4 Summary and Medical Interpretation

Optimal solutions for problem [H] contain a in-time substantial segment where the control is given by a time-varying feedback function of the primary tumor volume p and its carrying capacity q. Such a strategy is not realizable with current medical technologies. The numerical results presented in this section show that excellent realizable protocols can easily be obtained from the theoretically optimal solution. For example, for the initial condition $(p_0, q_0) = (12{,}000\,[mm^3]; 15{,}000\,[mm^3])$, these approximations consistently come within 0.5% of the optimal tumor values for the specified data. In fact, in all the cases considered here the corresponding value functions are relatively flat around the optimal solution and thus dose rates that are reasonably close to the optimal values do not give any degradation in

the approximation. This conclusion is valid for a wide range of initial conditions [179, 203]. Furthermore, these approximations are robust with respect to variations in the value q_0 for the carrying capacity. This gives practical relevance to the results obtained. While constant protocols provide very good approximations to the optimal solutions, the choice of the dose rate and resulting concentration makes a difference. Generally, for higher tumor volumes lower dose rates do better as high concentrations waste limited antiangiogenic agents. Hence the computation of optimal, piecewise constant dosages with a small number of switchings, a simple and easily executed numerical procedure, is worthwhile.

6.2 Realizable Suboptimal Treatment Protocols for Problem [E]

We briefly show that similar approximation results are valid for the modification [E] by Ergun, Camphausen, and Wein. We recall that the structure of the synthesis of optimal controlled trajectories is qualitatively identical with the one for [H] and in Figure 6.12 we show the optimal control (left) and its corresponding trajectory (right) for the initial condition $(p_0, q_0) = (8{,}000\,[mm^3];\ 10{,}000\,[mm^3])$. We use the same numerical values for the parameters, but, as before, limit the maximum dose for this model to $u_{\max} = 15$ and the total amount of inhibitors to $A = 45$. The optimal control is at full dose rate until the singular curve $\mathscr{S}$ is reached at $t_1 = 1.341$ [days]. The administration then follows the time-varying singular control for $t_2 = 3.722$ [days] until all anti-angiogenic agents are exhausted after 5.062 [days]. Due to after effects, the maximum tumor reduction is realized along a trajectory for control $u = 0$ at the optimal terminal time $T = 9.378$ [days] when the trajectory reaches the diagonal $p = q$. The theoretically optimal minimum value for these data is given by $p_* = p(T) = 2242.65\ [mm^3]$. We use this particular example since it illustrates the longer time segments along the bang controls $u = u_{\max}$ and $u = 0$ caused by the slower q-dynamics for model [E] and the effect this has on suboptimal protocols. Although the values are not directly comparable because of the different q-dynamics, we shall see that the quality of approximations here is equally excellent. As for model [H], we first analyze constant dose protocols.

6.2.1 Constant Protocols

We only consider the minimization problem that is consistent with the optimal control formulation [OCA] in Section 5.2.1 and minimize over the values of the corresponding trajectories as the diagonal is reached along a final no dose segment. Thus the control corresponding to a constant dose rate u is given by

$$v(t) = \begin{cases} u & \text{for } 0 \le t \le \frac{A}{u}, \\ 0 & \text{for } \frac{A}{u} < t \le T_u, \end{cases}$$

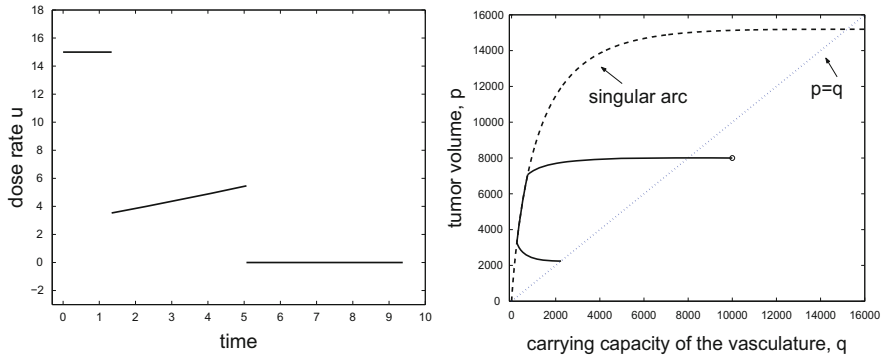

Fig. 6.12 Optimal control for problem [E] (left) and corresponding trajectory (right) for the initial condition $(p_0, q_0) = (8{,}000\,[mm^3]; 10{,}000\,[mm^3])$.

with T_u the time when the diagonal is reached. We again denote the minimum tumor volume reached by such a strategy at time T_u by $\pi_u(T_u)$ and the best solution (for a particular initial condition) is given by

$$u_* = \arg\min \pi_u(T_u).$$

For the initial condition $(p_0, q_0) = (8{,}000\,[mm^3]; 10{,}000\,[mm^3])$, we obtain $u_* = 9.246$ and this rate is given over $t_1 = 4.867$ [days]; then the control is still $u_* = 0$ for $t_2 = 4.735$ [days] until the minimum tumor volume is realized as the trajectory crosses the diagonal at the time $T = 9.602$ [days]. Figure 6.13, on the left, shows the graph of the associated value function $\pi_u(T_u)$ for dose rates lying between $u = 8$ and $u = 11$ around the optimal value u_*. On the right, it gives the corresponding trajectory. The minimal tumor volume realized by this optimal constant dose rate trajectory is $p_* = 2264.22\,[mm^3]$ and has a relative error of about 1% compared with the optimal value. As a comparison, the constant averaged optimal dose is given by $\bar{u} = 8.888$ over the time span of 5.063 [days] and for this strategy the virtually identical value $p_{\bar{u}} = 2264.44\,[mm^3]$ is obtained at $T = 9.732$ [days]. Indeed, for model $[E]$, and notwithstanding the blow-up shown in Figure 6.13, the value $\pi_u(T_u)$ is flat around its minimum value varying only between 2264.5 and 2268.2 for u between $u = 8$ and $u = 11$ and any intermediate dose rate gives excellent approximations.

In Figures 6.14 and 6.15, we compare the minimum tumor volumes that can be realized by the various strategies considered for varying initial carrying capacity q_0 and fixed initial tumor volume p_0 for $p_0 = 8{,}000\,[mm^3]$ and $p_0 = 15{,}000\,[mm^3]$, respectively. As for model [H], in the diagrams, the solid red curve gives the theoretically optimal values corresponding to the optimal controls determined in Section 5.4, the dashed blue curve corresponds to the full dose rate $u_{\max}$, the dashed-dotted blue curve to half dose rate $\frac{1}{2}u_{\max}$, the dashed black curve gives the values for the averaged optimal dose rate, and the dash-dotted black curve gives the values corresponding to the optimal constant dose rate. The graphs in the second row of these figures give the optimal constant dose rates (left) and the averaged optimal

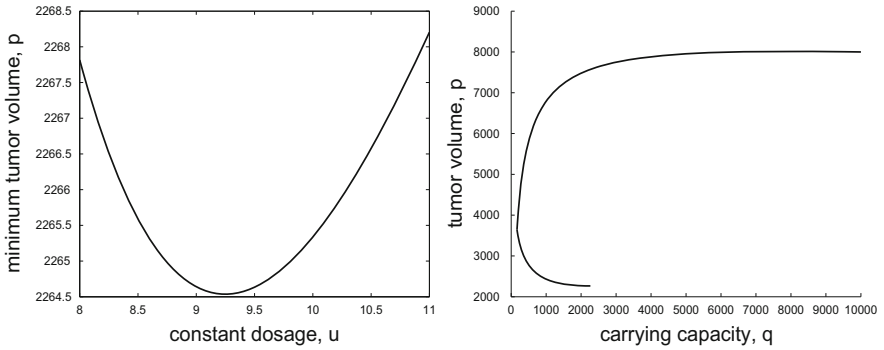

Fig. 6.13 The value of the minimum tumor volumes $\pi_u(T_u)$ for constant dose rates $u \in [8, 11]$ (left) and the trajectory corresponding to the optimal dose rate $u_* = 9.246$ for initial condition $(p_0, q_0) = (8{,}000\,[mm^3]; 10{,}000\,[mm^3])$

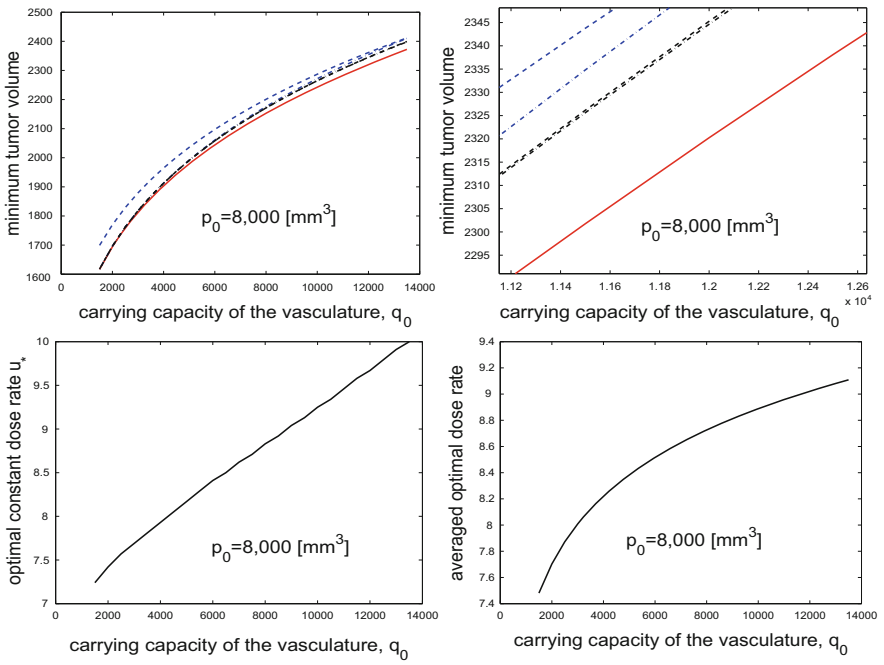

Fig. 6.14 The graphs of the minimum tumor volumes realized by the optimal control (solid red curve), a full dose rate protocol (dashed blue curve), the half-dose rate protocol (dash-dotted blue curve), the averaged optimal control protocol (dashed black curve), and the optimal constant dose rate protocol (dash-dotted black curve) for the fixed initial tumor volume $p_0 = 8{,}000\ [mm^3]$ as a function of the initial carrying capacity q_0 (top, left) and a blow-up of the graphs (top, right). The graphs at the bottom give the optimal constant dose rates (left) and the averaged optimal dose rates (right) as functions of the initial carrying capacity q_0.

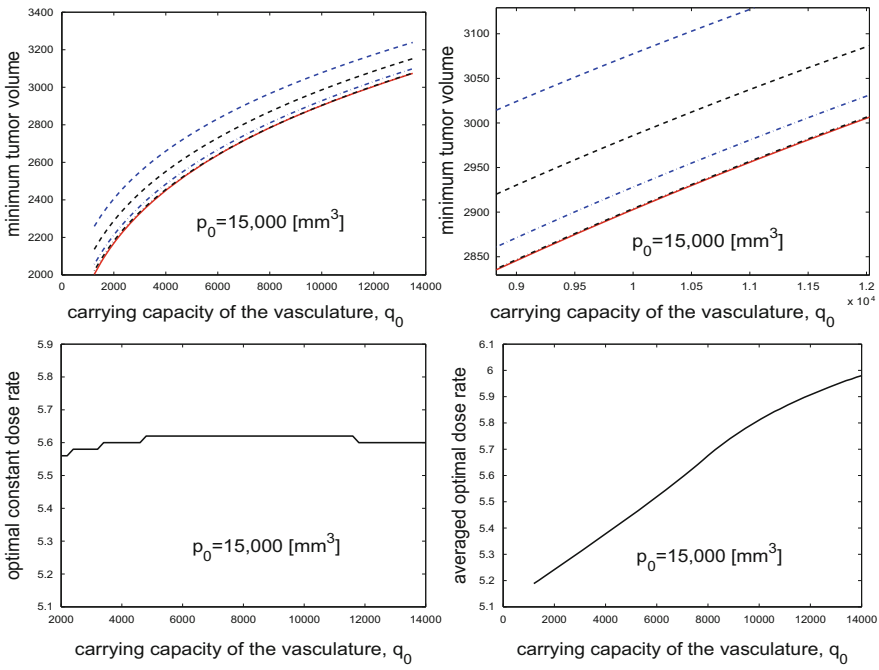

Fig. 6.15 The graphs of the minimum tumor volumes realized by the optimal control (solid red curve), a full dose rate protocol (dashed blue curve), the half-dose rate protocol (dash-dotted blue curve), the averaged optimal control protocol (dashed black curve), and the optimal constant dose rate protocol (dash-dotted black curve) for the fixed initial tumor volume $p_0 = 15{,}000\ [mm^3]$ as a function of the initial carrying capacity q_0 (top, left) and a blow-up of the graphs (top, right). The graphs at the bottom give the optimal constant dose rates (left) and the averaged optimal dose rates (right) as functions of the initial carrying capacity q_0.

dose rates (right) for fixed p_0 as a function of q_0. For both examples, the optimal constant dose rates and the averaged optimal dose rates are very close and there is virtually no difference noticeable in the graphs of the corresponding value functions, not even in the blow-ups in the top right panels of the figures. This again confirms the optimal average dose rate as an excellent sub-optimal approximation that can easily be determined from the theoretically optimal solutions. For $p_0 = 8{,}000\ [mm^3]$ these values are close to the half dose rate for small values of the carrying capacity q_0 and there is no difference visible in the value functions. For higher values of q_0, the optimal constant dose rates increase and there is a small separation from the half dose values, but the optimal constant dose rates and the averaged optimal dose rates remain so close throughout that even in the blow-up there is hardly a difference noticeable in the achieved values. As for model [H], for high values of p_0, like

$p_0 = 15{,}000\ [mm^3]$ shown here, the optimal constant dose rates decrease and now both the curves corresponding to a full dose and half dose rate lie above the curves for the optimal constant and averaged optimal dose rates.

6.2.2 Optimal Two-Stage Protocols

Going to a 2-stage protocol, the approximation of the optimal value can still be improved. Once more, using $(p_0, q_0) = (8{,}000\,[mm^3]; 10{,}000\,[mm^3])$ as initial condition, and following the same scheme and the same notation as in Section 6.1.2, the minimizing controls $v_* = \arg\min \pi_v(T_v)$ are given by $u_1 = 15.00$ for time $t_1 = 1.273$ [days], $u_2 = 6.710$ for $t_2 = 3.861$ [days], and the time along the final $u = 0$ segment is $t_3 = 4.240$ [days]. The diagonal is reached at time $T = 9.374$ [days] when the minimum value is realized. The optimal value decreases to 2242.75 $[mm^3]$ compared with the optimal value of 2242.65 $[mm^3]$ and thus for any practical standard such a protocol duplicates the optimal solution. In this case, the optimal two-stage regimen starts out at maximum dose (like the theoretically optimal control) and then lowers the value to reflect the lower dosages along the singular control. Figures 6.16 and 6.17 give cross sections of the value $\pi_v(T_v)$ when the first control u_1, respectively the time t_1 along the first dose rate, are fixed at their optimal values. We summarize the results for the constant and 2-stage protocols in Table 6.4.

Table 6.4 Comparison of the minimal values for piecewise constant protocols for problem [E]; t_1, t_2, and t_3 denote the times of administration (in days).

Control	u_1	t_1	u_2	t_2	t_3	T	Min. value (mm^3)
Optimal	15.00	1.341	Singular	3.722	4.315	9.378	2242.65
One stage, u_*	9.246	4.867	–	–	4.735	9.602	2264.22
Averaged optimal, $\bar{u}$	8.888	5.063	–	–	4.669	9.732	2264.44
Two stage, v_*	15.00	1.273	6.992	3.861	4.240	9.374	2242.75

6.2.3 Daily and Semi-Daily Regimes

Along the optimal solution for $(p_0, q_0) = (8{,}000\,[mm^3]; 10{,}000\,[mm^3])$, antiangiogenic agents are used up in 5.062 days. Running a minimization over 6 constant daily doses gives the optimal dose for the sixth day as $u = 0$. Minimizing a daily regimen gives the following optimal dose rates,

$$u_1 = 15.00,\ u_2 = 9.73,\ u_3 = 5.45,\ u_4 = 6.88, \quad \text{and} \quad u_5 = 7.94$$

with the minimum value 2243.15 $[mm^3]$. Again, this is the value that the trajectory corresponding to the control $u = 0$ attains as the diagonal $p = q$ is crossed, in this

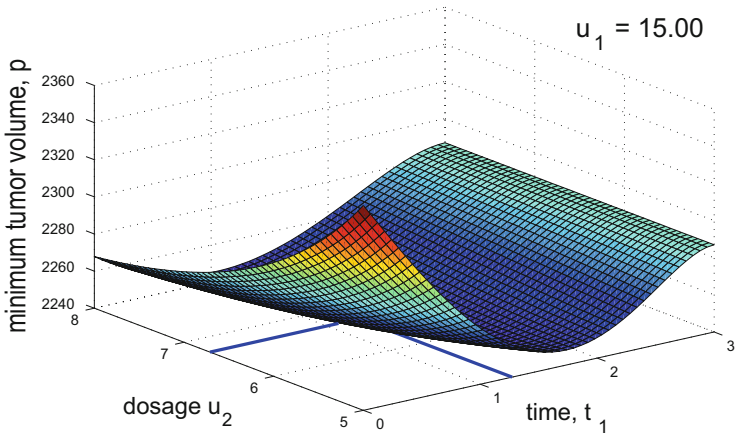

Fig. 6.16 A cross section through the graph of $\pi_v(T_v)$ at $u_1 = 15.00$.

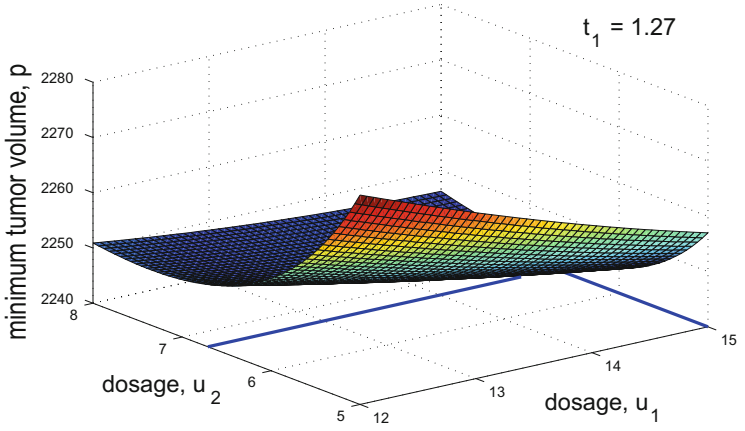

Fig. 6.17 A cross section through the graph of $\pi_v(T_v)$ for $t_1 = 1.27$.

case at time at 9.373 [days]. Here, because of the slower q-dynamics of this modification, the optimal daily strategy is comparable to the optimal 2-stage regimen v_*. Figure 6.18 shows these dosages and the corresponding trajectory.

As for model [H], also here the pattern resembles the structure of the optimal control. During the first day the control is at maximum level and then drops down. The value for the second day is an average of the maximum dose rate with the much lower singular control. In the optimal solution, the dosage is still at maximum for about 8 hours while it then is lowered to the value $u = 3.53$ at the onset of the singular arc. In the dose for the second day, this averages out to a value that still is higher than the third dose when the optimal control is singular for the entire period, and hence much smaller than the maximum. But the dose rate intensifies along the singular arc and thus the values increase. The last daily dosage on the fifth

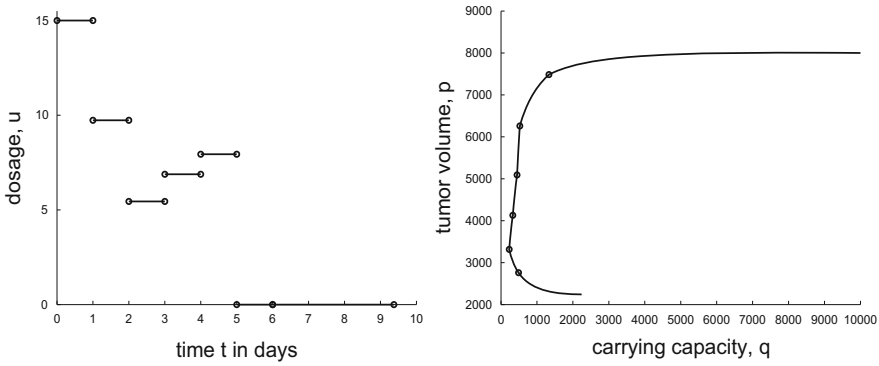

Fig. 6.18 Optimal 'daily' doses (left) and corresponding trajectory (right) for problem $[E]$ and initial conditions $(p_0, q_0) = (8{,}000\,mm^3; 10{,}000\,mm^3)$.

day is determined by the fact that all agents are being used up, but still increases because of dose intensification along the singular arc and the fact that the optimal time exceeds 6 hours and an average over slightly more than one day is taken. Thus, while the structure of dosages resulting from a solution of the finite-dimensional optimization problem might appear erratic, it makes perfect sense if one compares them to the optimal solution found in Chapter 5. *It is the knowledge of the structure of the optimal solution that elucidates the behavior of these numerically computed optimal values and thus gives insights into the problem.*

If one were to include rest periods into each daily regimen, say antiangiogenic agents are given at a constant rate for 8, respectively 12 hours, then the 12 hour scheme would use up the total amount $A = 45$ in exactly 6 daily dosages at the maximum $u = 15$ and, due to the requirement that all agents should be exhausted, no optimization problem arises. Similarly, if we only give antiangiogenic agents for 8 hours, then, in order to use up the full amount, 9 days need to be considered at maximum dosage. The trajectories corresponding to these strategies are shown in Figure 6.19 and, naturally, the quality of approximation decreases. As a reference, in this and the subsequent figures the black curve is the optimal trajectory. For the 12 hour scheme the realized value is given by $p_{12\text{ hr}} = 2262.29$ and for the 8 hour scheme by $p_{8\text{ hr}} = 2335.99$. While the 12 hour value still realizes a value in the range of the optimal constant dosage, degradation starts to occur if the rest-periods become too large. Longer rest periods allow the vascular support to recover and with the 8 hour scheme the relative error is 4.16%, quite large compared to other values.

Figure 6.20, on the left, compares the corresponding optimal strategies when the upper limit $u_{\max}$ in the control set has been doubled to $u_{\max} = 30$. The solid red lines give the optimal 12 hour doses while the solid blue lines give the optimal daily doses when $u_{\max} = 15$. For comparison, the dashed lines are the average values of the 12 hour doses for the full day and these are close to these optimal daily values. The optimal trajectory for the semi-daily doses is shown to the right. In this figure, we also kept the optimal trajectory for $u_{\max} = 15$ as the solid black curve and it is

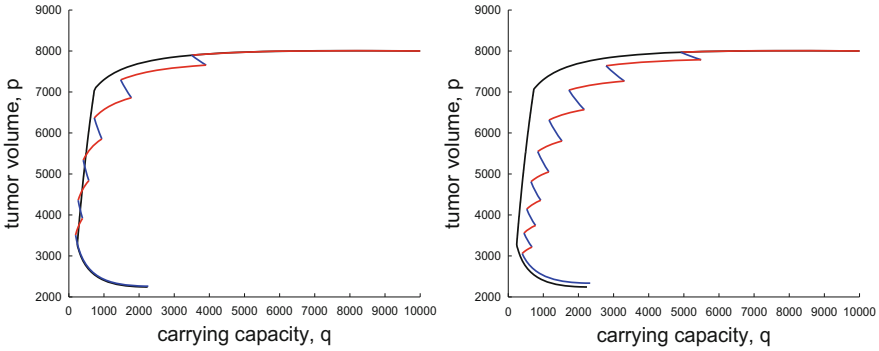

Fig. 6.19 Trajectories corresponding to 12 (left) and 8 hour daily doses (right) for problem [E], respectively.

seen how closely now the semi-daily doses approximate this particular trajectory. But, of course, the optimal control for problem $[E]$ with $u_{\max} = 30$ is different and in this case the maximum tumor reduction possible is given by $p_{**} = 2231.98\ [mm^3]$ compared with $p_* = 2242.65\ [mm^3]$ when $u_{\max} = 15$.

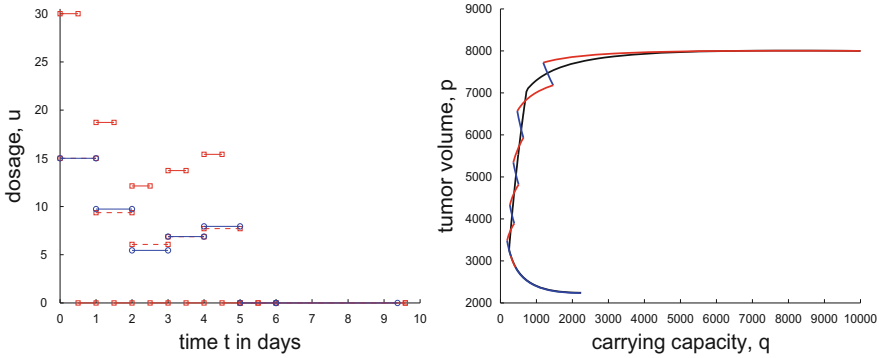

Fig. 6.20 Comparison of the optimal daily doses for $u_{\max} = 15$ with the optimal 12 hour dosages (left) and corresponding trajectory for $u_{\max} = 30$ (right).

It is noteworthy that a higher initial boost which drives the system to the singular arc faster leads to a small decrease in the optimal value. Thus, as already pointed out in Chapter 5, without limitations on the dosage, the optimal overall strategy would be to get to the singular arc as fast as possible with a high dose bolus injection (mathematically, an impulse) and then follow the singular arc with much smaller dosages.

6.3 Mathematical Models with Linear Pharmacokinetic Equations

In most parts of the text we do not include a pharmacokinetic model for the agent, i.e., we identify an agent's dose rates with the concentrations in the blood stream. Naturally, bang-bang controls make sense if we think of the control representing dose rates, but not if these represent concentrations which vary continuously. Yet, if modeling extensions with pharmacokinetic equations do not alter the structure of the solutions significantly, then this simplified modeling is justified. We have already seen in Chapter 2 that augmenting the dynamics with a linear pharmacokinetic model did not change the optimality status of singular controls for compartmental models for cancer chemotherapy (Theorem 2.3.2). This actually holds true in great generality and also for the solutions to the optimal control problem [OCA] of Chapter 5. Thus, for this problem singular controls remain locally optimal. However, the order of the singular control increases (see also Section 2.3.2) and this leads to qualitative changes in the structure of the optimal synthesis as the concatenations with singular arcs are concerned. Now these transitions are accomplished by means of chattering controls that rapidly alternate between the maximum dose rate $u = u_{\max}$ and rest periods for $u = 0$ and, in fact, have an infinite number of switchings on a finite interval. Such controls no longer are piecewise continuous, but only Lebesgue measurable. While this is a significant departure from the structure of optimal controls from a theoretical point of view, on the level of realizable protocols, again simple, piecewise constant suboptimal approximations exist that come close to the optimal values. Thus the main conclusions drawn so far remain valid if the models are made more realistic by including a standard linear pharmacokinetic model (PK) for the antiangiogenic agents.

6.3.1 Augmentation of the Model [OCA] with Linear Pharmacokinetic Equations

Following the models described in Section 2.3, we augment the dynamics with a first-order linear ordinary differential equation that describes the concentration c of the antiangiogenic agent in the blood stream. From a control theoretic point of view, this corresponds to the output injection of a linear system into the original dynamics which generates this concentration as a new state c with the dose rate u as input. The role of the control in the original formulations is then taken over by the state c in the extended model (see Figure 6.21).

We first analyze such an extension in a general framework and show how it effects the defining equations for optimal singular controls and arcs. The models considered in Chapter 5 are 2-dimensional systems with the state $x = (p, q)^T$ to which a third variable y has been added to track the amount of antiangiogenic agents that

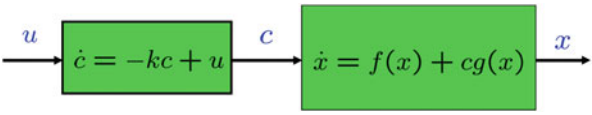

Fig. 6.21 A block diagram representation for the augmentation of the original dynamics with a linear pharmacokinetic model.

is being given. For this reason, here we consider a general 2-dimensional dynamics of the form

$$\Sigma: \qquad \dot{x} = f(x) + cg(x), \qquad x \in \mathbb{X} \subset \mathbb{R}^2, \quad c \geq 0, \tag{6.1}$$

where $\mathbb{X}$ denotes some open subset of $\mathbb{R}^2$ that serves as the state-space of the system and the variable c denotes the concentration of some agent and is defined by the output of a first order linear time-invariant system of the form

$$\dot{c} = -kc + u, \qquad c(0) = 0, \qquad 0 \leq u \leq u_{\max}. \tag{6.2}$$

The parameter k is the clearance rate of the agent. This is the commonly used 1-compartment model of exponential growth/decay that also was included in the original modeling in [116]. We consider the following augmentation of the optimal control problem [OCA]:

[OCAPK] For a free terminal time T, minimize an objective given by $J(u) = \varphi(x(T))$ in Mayer form for some continuously differentiable function $\varphi : \mathbb{X} \to \mathbb{R}$ over all Lebesgue measurable functions $u : [0,T] \to [0,u_{\max}]$ subject to the dynamics

$$\begin{aligned} \dot{x} &= f(x) + cg(x) & x(0) &= x_0, \\ \dot{c} &= -kc + u & c(0) &= 0, \\ \dot{y} &= u, & y(0) &= 0, \end{aligned}$$

and the terminal constraint $y(T) \leq A$.

Compared with the original problem formulation [OCA], the control has been replaced by the concentration c of the agent and the new control u represents the actual dose rate of administration with upper limit $u_{\max}$. This limit determines the supremum for the achievable concentration as $c_{\max} = u_{\max}/k$, but the concentration will always lie below this value and take values in the interval $[0, c_{\max})$. Note that, once agents are administered, the concentration will become positive and remain so for all times.

As before, the model is a single-input control affine system and the main candidates for optimality are the constant bang controls $u = 0$ and $u = u_{\max}$ and singular controls. Since singular controls are inherently defined through nonlinear relationships, a priori it is not clear to what extent their optimality properties, let alone their analytic representations, will be preserved under such a modeling extension. This

indeed is the case for a planar system. *All equations that define an order* 1 *singular control and its optimality status carry over verbatim from the optimal control problem* [OCA] *to the model* [OCAPK]. At the same time, for the first-order linear pharmacokinetic model (6.2), the order of the singular arc increases by 1 (see Definition A.3.5 in Appendix A) and this has significant implications on the concatenation structures of optimal trajectories. Direct concatenations of the optimal singular control with the bang controls $u = 0$ and $u = u_{\max}$ are no longer optimal and now this transition can only be accomplished by means of chattering controls (e.g., see [292, 348]). Thus, while essential features are preserved under the modeling extension considered here, the qualitative structure of the optimal synthesis changes.

6.3.2 Prolongation of the Formulas for Singular Controls and Arcs

We briefly recall from Chapter 5 the relevant facts about the singular controls and arcs needed below. Both in the original and the augmented models, the variable y merely tracks the amount of antiangiogenic agents and has no influence on the singular control and arc; we thus drop it in our analysis. Denote by λ the 2-dimensional adjoint variable corresponding to the state $x \in \mathbb{X}$ and, in order to distinguish it from the control of the augmented model, here denote the control in the original model by v. If this control is singular on an open interval I, then the first and second derivatives of the switching function,

$$\dot{\Phi}(t) = \langle \lambda(t), [f,g](x(t)) \rangle$$

and

$$\ddot{\Phi}(t) = \langle \lambda(t), [f+vg,[f,g]](x(t)) \rangle,$$

vanish identically. For all models considered in Chapter 5, $\langle \lambda(t), [g,[f,g]](x(t)) \rangle$ is negative, singular controls are of order 1 and the strengthened Legendre-Clebsch condition for minimality is satisfied. Furthermore, the Lie bracket $[f,[f,g]]$ can be expressed as a linear combination of the vector fields $[f,g]$ and $[g,[f,g]]$ with coefficients that are smooth functions of the state x,

$$[f,[f,g]](x) = \varphi(x)[f,g](x) + \psi(x)[g,[f,g]](x), \tag{6.3}$$

and the singular control is given in feedback form by

$$u_{\text{sing}}(t) = -\psi(x(t)). \tag{6.4}$$

When admissible, this feedback defines a singular control only on the set

$$\mathscr{S} = \{x \in \mathbb{X} : \Delta(x) = \det(f(x),[f,g](x)) = 0\} \tag{6.5}$$

where the vector fields f and $[f,g]$ are linearly dependent. Furthermore, since the strengthened Legendre-Clebsch condition is satisfied along these arcs, wherever the singular control takes values in the interior of the control set, it can be concatenated with the bang controls $u = u_{\max}$ or $u = 0$ without violating the conditions of the conditions of the maximum principle (see Section A.3.3 in Appendix A). This leads to a local synthesis of extremals around $\mathscr{S}$ by integrating the constant controls $u = u_{\max}$ or $u = 0$ forward and backward from the singular arc.

The formulas that define the singular arc and its control carry over verbatim (albeit with a different interpretation) once equation (6.2) is added to the model. Denote by $z = (x,c)$ the augmented state and write the dynamical equations in the form

$$\dot{z} = F(z) + uG,$$

with

$$F(z) = \begin{pmatrix} f(x) + cg(x) \\ -kc \end{pmatrix} \qquad \text{and} \qquad G = \begin{pmatrix} 0 \\ 1 \end{pmatrix}. \tag{6.6}$$

It is important for the subsequent computations that the new control vector field G is constant. Denote the adjoint variable corresponding to the new state $z = (x,c)$ by $\Lambda = (\hat{\lambda}, \hat{\mu})$ with $\hat{\lambda}$ associated with x and $\hat{\mu}$ associated with c. The Hamiltonian $\hat{H}$ for problem [OCAPK] is

$$\hat{H} = \hat{\lambda}\,(f(x) + cg(x)) + \hat{\mu}(-kc + u) + \hat{\nu}u$$

with $\hat{\nu}$ a constant multiplier associated with the isoperimetric constraint on y. The new adjoint equations and transversality conditions take the form

$$\begin{aligned} \dot{\hat{\lambda}} &= -\hat{\lambda}\,(Df(x) + cDg(x))\,, & \hat{\lambda}(T) &= \frac{\partial \varphi}{\partial x}(x(T)), \\ \dot{\hat{\mu}} &= -\hat{\lambda} g(x) + k\hat{\mu}, & \hat{\mu}(T) &= 0. \end{aligned}$$

The switching function for the augmented problem is thus given by

$$\Psi(t) = \hat{\mu}(t) + \hat{\nu} = \langle \Lambda(t), G(z(t)) \rangle + \hat{\nu},$$

and, as before, we need to calculate its derivatives. The control vector field G is the coordinate vector field that differentiates with respect to the variable c and the Lie bracket is simply given by

$$[F,G](z) = -DF(z)G = -\frac{\partial F}{\partial c}(z) = \begin{pmatrix} -g(x) \\ k \end{pmatrix}. \tag{6.7}$$

It no longer depends on the concentration c and thus all higher order Lie brackets with G vanish identically: if we write $\mathrm{ad}_G^{\mathrm{n}}(F) = \mathrm{ad}_G \circ \mathrm{ad}_G^{\mathrm{n}-1}(F)$ with $\mathrm{ad}_G(F)$ defined by $\mathrm{ad}_G(F) = [G,F]$, then, for $n \geq 2$ we have that

$$\mathrm{ad}_G^{\mathrm{n}}(F)(z) = \frac{\partial^n F}{\partial c^n}(z) \equiv 0.$$

In particular, $[G,[F,G]](z) \equiv 0$, and singular controls for problem [OCAPK] are of higher order. The first three derivatives of the switching function are thus given by

$$\begin{aligned}\dot{\Psi}(t) &= \langle \Lambda(t), [F,G](z(t)) \rangle \equiv 0,\\ \ddot{\Psi}(t) &= \left\langle \Lambda(t), \mathrm{ad}_F^2(G)(z(t)) \right\rangle \equiv 0,\end{aligned} \tag{6.8}$$

and

$$\dddot{\Psi}(t) = \left\langle \Lambda(t), \mathrm{ad}_F^3(G)(z(t)) \right\rangle \equiv 0.$$

In the last equation, we use the fact that the Jacobi condition (cf., (A.18) in Appendix A) implies that

$$[G,[F,[F,G]]] = [F,[G,[F,G]]] = [F,0] = 0.$$

The control u therefore only enters the fourth derivative in the form

$$\Psi^{(4)}(t) = \left\langle \Lambda(t), [F+uG, \mathrm{ad}_F^3(G)](z(t)) \right\rangle \equiv 0. \tag{6.9}$$

We shall compute the quantity $\left\langle \Lambda(t), [G, \mathrm{ad}_F^3(G)](z(t)) \right\rangle$ that multiplies the control below and verify that it is nonzero. Hence the singular control is of *intrinsic order* 2 (see Definition A.3.5 in Appendix A).

If the control u is singular on an open interval I, then Λ vanishes against the vector fields F (since $\hat{H} \equiv 0$), G, and their Lie brackets $[F,G]$, $\mathrm{ad}_F^2(G)$ and $\mathrm{ad}_F^3(G)$. Generically, these are too many conditions to be met simultaneously in low dimensions and for this reason singular controls of higher order are rare. However, because of the special structure of the overall dynamics defined by the linear output injection, for the problem considered here there exist relations between these vector fields that cause all these conditions to be satisfied. Note that

$$F(z) = \begin{pmatrix} f(x) \\ 0 \end{pmatrix} - c[F,G](z)$$

and thus

$$\begin{aligned}\mathrm{ad}_F^2 G(z) &= [F,[F,G]](z) = D([F,G])(z)F(z) - DF(z)[F,G](z)\\ &= \begin{pmatrix} -Dg(x) & 0 \\ 0 & 0 \end{pmatrix} \begin{pmatrix} f(x)+cg(x) \\ -kc \end{pmatrix} - \begin{pmatrix} Df(x)+cDg(x) & g(x) \\ 0 & -k \end{pmatrix} \begin{pmatrix} g(x) \\ k \end{pmatrix}\\ &= \begin{pmatrix} -[f+cg,g](x) - kg(x) \\ k^2 \end{pmatrix}\\ &= -\begin{pmatrix} [f,g](x) \\ 0 \end{pmatrix} + k[F,G](z).\end{aligned} \tag{6.10}$$

Similar computations verify that

$$\mathrm{ad}_F^3 G(z) = -\begin{pmatrix} [f+cg,[f,g]](x) \\ 0 \end{pmatrix} + k\mathrm{ad}_F^2 G(z) \tag{6.11}$$

and

$$[G, \mathrm{ad}_F^3(G)](z) = -\begin{pmatrix} [g,[f,g]](x) \\ 0 \end{pmatrix}. \tag{6.12}$$

For well-posed initial conditions the multiplier Λ is nonzero (otherwise the control is $u \equiv 0$). Hence the condition that Λ vanishes against the vector fields F, $[F,G]$ and $\mathrm{ad}_F^2(G)$ is equivalent to the statement that these vector fields are linearly dependent. Using (6.5), we obtain that

$$\begin{aligned} 0 &= \det\left[\, F(z),\, [F,G](z),\, \mathrm{ad}_F^2(G)(z)\,\right] \\ &= \det\left[\begin{pmatrix} f(x)+cg(x) \\ -kc \end{pmatrix}, \begin{pmatrix} -g(x) \\ k \end{pmatrix}, \begin{pmatrix} -[f,g](x)-kg(x) \\ k^2 \end{pmatrix}\right] \\ &= \det\left[\begin{pmatrix} f(x) \\ 0 \end{pmatrix}, \begin{pmatrix} -g(x) \\ k \end{pmatrix}, \begin{pmatrix} -[f,g](x) \\ 0 \end{pmatrix}\right] = k\Delta(x). \end{aligned} \tag{6.13}$$

Hence this equation reduces to the relation (6.5) that defines the singular arc for the model [OCA]. Now, however, this relation, which does not depend on the third variable c, only defines a vertical surface in (x,c)-space on which singular arcs need to lie. But $\Lambda(t)$ also vanishes against the vector field $\mathrm{ad}_F^3(G)$ and the linear dependence of the vector fields $\mathrm{ad}_F(G)$, $\mathrm{ad}_F^2(G)$ and $\mathrm{ad}_F^3(G)$ determines c:

$$\begin{aligned} 0 &= \det\left[\, [F,G](z),\, \mathrm{ad}_F^2(G)(z),\, \mathrm{ad}_F^3(G)(z)\,\right] \\ &= \det\left[\, [F,G](z),\, \mathrm{ad}_F^2(G)(z),\, -\begin{pmatrix} [f+cg,[f,g]](x) \\ 0 \end{pmatrix} + k\mathrm{ad}_F^2(G)(z)\right] \\ &= -\det\left[\, [F,G](z),\, -\begin{pmatrix} [f,g](x) \\ 0 \end{pmatrix} + k[F,G](z),\, \begin{pmatrix} [f+cg,[f,g]](x) \\ 0 \end{pmatrix}\right] \\ &= \det\left[\begin{pmatrix} -g(x) \\ k \end{pmatrix}, \begin{pmatrix} [f,g](x) \\ 0 \end{pmatrix}, \begin{pmatrix} [f+cg,[f,g]](x) \\ 0 \end{pmatrix}\right] \\ &= k\det\left[\, [f,g](x),\, [f+cg,[f,g]](x)\,\right]. \end{aligned} \tag{6.14}$$

Using the relation (6.3) to express $[f,[f,g]]$ as a linear combination of $[f,g]$ and $[g,[f,g]]$, it thus follows that

$$\begin{aligned} 0 &= \det\left[\, [f,g](x),\, [f+cg,[f,g]](x)\,\right] \\ &= \det\left[\, [f,g](x),\, \varphi(x)[f,g](x) + (\psi(x)+c)[g,[f,g]](x)\,\right] \\ &= (c+\psi(x))^2 \det\left[\, [f,g](x),\, [g,[f,g]](x)\,\right] \end{aligned}$$

and the linear independence of $[f,g]$ and $[g,[f,g]]$ implies that c is given by

$$c = -\psi(x) = -\psi(p,q), \tag{6.15}$$

the very same function that defines the optimal singular control in the model [OCA].

Theorem 6.3.1. *For the models [H], [E], and [I_θ] considered in Chapter 5, the singular arc of the optimal control problem [OCA] in (p,q)-space is preserved as a vertical surface in (p,q,c)-space. The equation that defines the singular control for problem [OCA] now defines the concentration c as a function of p and q, $c = -\psi(p,q)$. The graph of this function intersects the vertical singular surface in a unique curve, the new singular arc $\hat{\mathscr{S}}$. The corresponding singular control that keeps this arc invariant is given as feedback function by*

$$u_{\text{sing}}(p,q,c) = kc - D\psi(p,q)\left(f(p,q) + cg(p,q)\right).$$

The formula for the singular control is easily obtained from (6.2) by implicit differentiation:

$$u_{\text{sing}} = \dot{c} + kc = -D\psi(p,q)\left(f(p,q) + cg(p,q)\right) + kc.$$

Figures 6.22 and 6.23 illustrate the geometry for model [H] when a linear pharmacokinetics is added. Figure 6.22 shows the vertical surface V that is obtained in (p,q,c)-space when the singular base curve $\mathscr{S}_0$ for problem [H] defined by the equation $\left(\mu + dp^{\frac{2}{3}}\right) q = bp\left(1 - \ln\left(\frac{p}{q}\right)\right)$ in the coordinate plane $c = 0$ is plotted as a subset of the first quadrant in 3-space. In Figure 6.22, this surface is then intersected with the graph of the function $c = -\psi(p,q)$ where ψ is the function

$$\psi(p,q) = -\frac{1}{\gamma}\left(\xi \ln\left(\frac{p}{q}\right) + b\frac{p}{q} + \frac{2}{3}\xi\frac{d}{b}\frac{q}{p^{\frac{1}{3}}} - \left(\mu + dp^{\frac{2}{3}}\right)\right)$$

defining the singular control as a feedback. Since the admissible portion of the singular curve lies in the region $p > q$, we only graph this function in that region. The

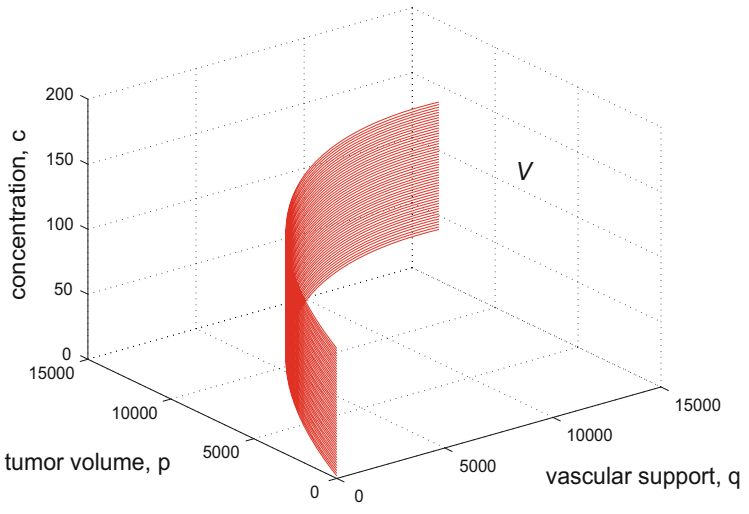

Fig. 6.22 Vertical singular surface in (p,q,c)-space for problem [H].

intersection of these two surfaces defines the new singular arc $\hat{\mathscr{S}}$ for the problem [OCAPK] for model [H].

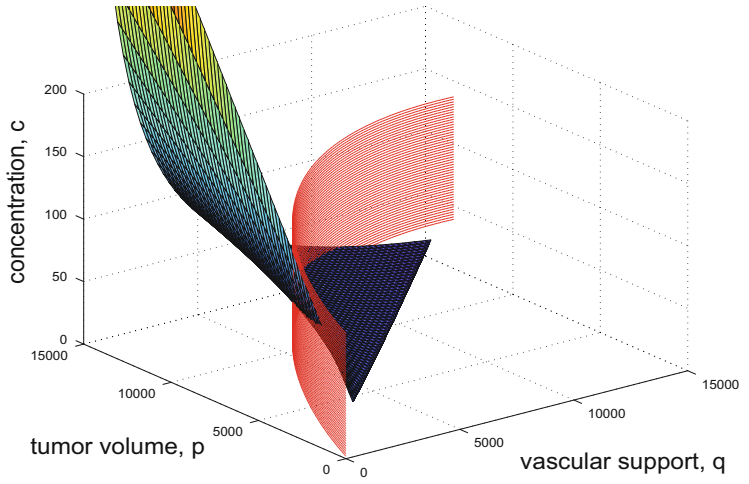

Fig. 6.23 Singular arc in (p,q,c)-space for problem [H] defined by the intersection of the vertical singular surface with the graph of the function $c=-\psi(p,q)$.

6.3.3 The Kelley Condition and Chattering Arcs

Higher order necessary conditions for optimality take the place of the Legendre-Clebsch condition if a singular control is intrinsic of order $k>1$. These generalized Legendre-Clebsch conditions (see Theorem A.3.2 in Appendix A) can succinctly be formulated in terms of the Hamiltonian function H of the optimal control problem and for minimization problems take the following form:

$$(-1)^k \frac{\partial}{\partial u}\frac{d^{2k}}{dt^{2k}}\frac{\partial H}{\partial u} \geq 0. \tag{6.16}$$

For $k=2$ this result is also known as the Kelley condition and for problem [OCAPK] it becomes

$$\frac{\partial}{\partial u}\frac{d^{2k}}{dt^{2k}}\frac{\partial H}{\partial u} = \frac{\partial}{\partial u}\left(\frac{d^4}{dt^4}\Psi(t)\right) = \left\langle \Lambda(t), [G, ad_F^3(G)](z(t))\right\rangle \geq 0.$$

By equation (6.12) this expression reduces to

$$\left\langle \Lambda(t), [G, ad_F^3(G)](z(t))\right\rangle = -\left\langle \hat{\lambda}(t), [g,[f,g]](x(t))\right\rangle. \tag{6.17}$$

Hence, if the multiplier $\hat{\lambda}$ can be identified with the adjoint vector λ of the original optimal control problem [OCA] over an interval I where the control is singular, then *the strengthened Legendre-Clebsch condition for the original problem is equivalent to the strengthened version of the Kelley condition for problem* [OCAPK]. This indeed can be done: since the singular arc $\mathscr{S}$ is preserved and the concentration c is defined by the same feedback function of x, it follows that λ and $\hat{\lambda}$ satisfy the same differential equation on such an interval I. Furthermore, by (6.8) and (6.10) we also have that

$$\left\langle \hat{\lambda}(t), [f,g](x(t)) \right\rangle = 0.$$

The fact that the switching function Φ for problem [OCA] vanishes on I implies that

$$\langle \lambda(t), g(x(t)) \rangle = -\nu$$

while the fact that the switching function Ψ and its derivative vanish for problem [OCAPK] imply that

$$\hat{\mu}(t) \equiv -\hat{\nu} \qquad \text{and} \qquad \left\langle \hat{\lambda}(t), g(x(t)) \right\rangle = k\hat{\mu}(t).$$

We thus have that

$$\left\langle \hat{\lambda}(t), g(x(t)) \right\rangle = -k\hat{\nu}$$

and for the multipliers $\lambda(t) \equiv \hat{\lambda}(t)$ and $\nu = k\hat{\nu}$ all the conditions of the maximum principle for problem [OCA] that the corresponding control is singular on the interval I are satisfied. But these multipliers are uniquely determined by the conditions for an optimal singular arc and thus they are equal. Hence the status of the necessary condition for optimality of a singular control carries over from problem [OCA] to [OCAPK].

Theorem 6.3.2. *For the models [H], [E], and [I_θ] considered in Chapter 5, the Kelley condition for optimality of a singular extremal of order* 2 *is satisfied for problem [OCAPK].*

However, the fact that the Kelley condition carries a positive sign has significant implications on possible concatenations between the singular control and bang controls. If the singular control takes a value in the interior of the control set, $0 < u_{\text{sing}}(z(t)) < u_{\max}$, then, by Proposition A.3.3 in Appendix A, it is no longer optimal to concatenate the singular control at time t with any of the two bang controls $u = 0$ or $u = u_{\max}$. For example, suppose that for some $\varepsilon > 0$ the control is singular on the interval $(\tau - \varepsilon, \tau)$ and is given by $u = 0$ on the interval $(\tau, \tau + \varepsilon)$. Since the fourth derivative of the switching function vanishes on $(\tau - \varepsilon, \tau)$, the Kelley condition gives $\left\langle \Lambda(\tau), ad_F^4(G)(z(t)) \right\rangle < 0$ and thus it follows that

$$\Phi^{(4)}(\tau+) = \left\langle \Lambda(\tau), ad_F^4(G)(z(t)) \right\rangle < 0.$$

Hence the switching function has a local maximum for $t = \tau$, i.e., is negative over the interval $(\tau, \tau + \varepsilon)$. But this contradicts the minimization condition on

the Hamiltonian. An analogous contradiction arises for each of the other types of concatenations. Thus an optimal singular control of order 2 that takes values in the interior of the control set cannot be concatenated with a bang control.

The structure of the optimal syntheses of controlled trajectories therefore differs significantly from the one constructed in Chapter 5 qualitatively. Transitions onto the singular arc now occur by means of so-called *chattering controls* that switch infinitely often between the extremal controls $u = 0$ and $u = u_{\max}$ on any small interval $(\tau, \tau + \varepsilon)$. In particular, optimal controls no longer need to be piecewise continuous, but are only Lebesgue measurable functions. The classical example for such a synthesis is given by the Fuller problem where indeed this structure is optimal (e.g., see [292, Sections 2.11 and 5.2.3]). From a practical point of view, for medical problems chattering controls are not realistic. But, as before, there exist excellent suboptimal approximations with a small number of switchings. It is for this reason that we have included this topic in this chapter.

We only mention that optimal bang-bang controls with an arbitrarily large number of switchings become optimal near such chattering transitions. For example, if for a certain initial condition inhibitors are insufficient for trajectories to approach the singular arc on a chattering spiral, then, at one point controls change from a strategy that is spiraling in to one that is spiraling away from the singular arc. This generates optimal controls with a very large number of switchings. While the overall structure of optimal controls thus is complex, the situation is much simpler on the level of the controlled trajectories and can still be fully understood geometrically. This helps clarify what otherwise, on the level of optimal controls, would appear to be a quagmire of unrelated structures. But this is of a mere theoretical interest and will not be pursued here. From the practical point of view, knowing the structure of optimal solutions again establishes benchmark values to which we can compare other, simple and realizable strategies. For a particular initial condition, this question can satisfactorily be settled numerically. As an example, in the next section we show for model [E] that simple, nonoptimal concatenations with bang controls will provide satisfactory suboptimal approximations.

6.3.4 Suboptimal Approximations for Model [E] with Linear PK

For model $[E]$, incorporating the standard linear pharmacokinetic model (6.2) into the mathematical model results in the following optimal control problem: minimize $p(T)$ subject to

$$\begin{aligned}
\dot{p} &= -\xi p \ln\left(\frac{p}{q}\right), & p(0) &= p_0,\\
\dot{q} &= bq^{\frac{2}{3}} - dq^{\frac{4}{3}} - \mu q - \gamma cq, & q(0) &= q_0,\\
\dot{c} &= -kc + u, & c(0) &= 0,\\
\dot{y} &= u, & y(0) &= 0.
\end{aligned}$$

Recall that the singular curve $\mathscr{S}$ for the optimal control problem [E] is defined in (p,q)-space by the equation

$$p_{\text{sing}}(w) = q\exp\left(3\frac{b-\mu w-dw^2}{b+dw}\right)$$

where $w = \sqrt[3]{q}$ and the corresponding singular control u_{sing} that keeps $\mathscr{S}$ invariant is given in feedback form by as $u_{\text{sing}}(w) = -\psi(w)$ with

$$\psi(w) = -\frac{1}{\gamma}\left(\frac{b-dw^2}{w} + 3\xi\frac{b+dw^2}{b-dw^2} - \mu\right).$$

Figure 6.24 shows the corresponding vertical surface in (p,q,c)-space and Figure 6.25 also shows the graph of the function $c = -\psi(\sqrt[3]{q})$. Note that the concentration only depends on w in this case and therefore the graph of ψ consists of horizontal lines in the p-direction. Again, the singular curve $\mathscr{S}$ lies in the region $p > q$ and we only plot the function ψ in that region. The intersection of these two surfaces defines the new singular arc $\hat{\mathscr{S}}$ for the problem [OCAPK] for model [E].

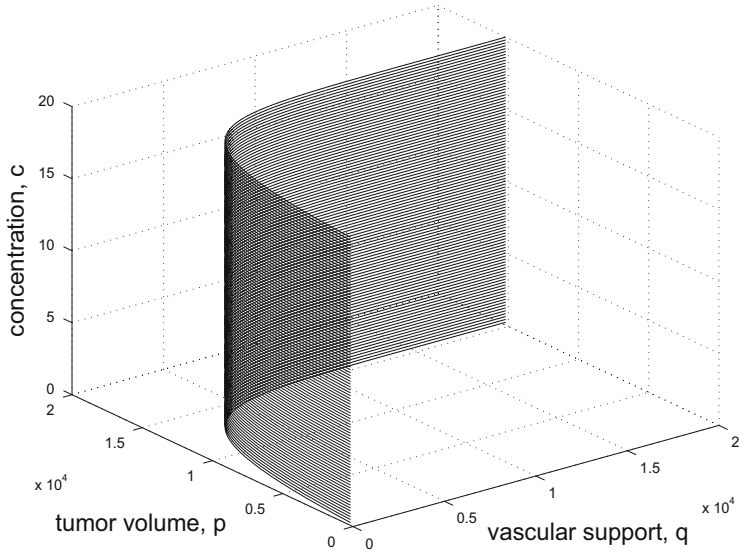

Fig. 6.24 Vertical singular surface in (p,q,c)-space for model $[E]$.

We include some numerical results obtained by H. Maurer [181] which show that simple suboptimal controls achieve a tumor volume which gives an excellent approximation of the optimal value. In the calculations, the values from Tables 5.2 and 5.4 were used with tumor growth parameter $\xi = 0.192$ per day and total amount of inhibitors given by $A = 60$. The half-life k of the agent in equation (6.2) is taken for angiostatin as $k = 0.38$ per day [116]. As always, the variables p and q are volumes measured in $[mm^3]$.

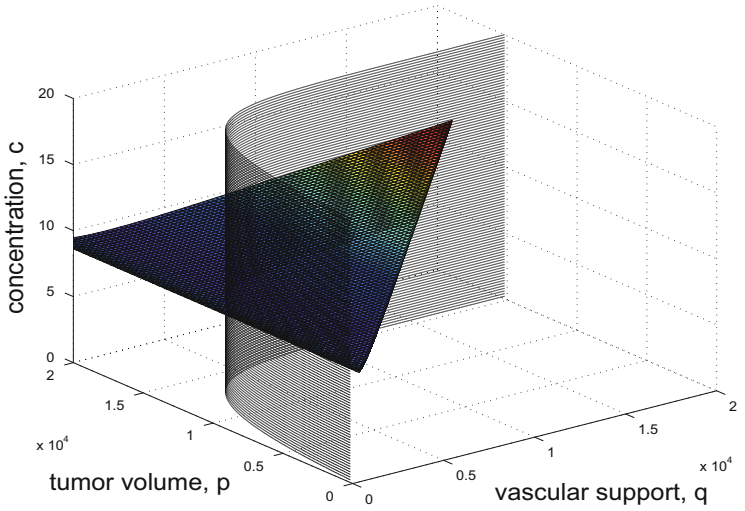

Fig. 6.25 The singular curve for model [E] in (p,q,c)-space is defined by the intersection of the vertical singular surface with the graph of the concentration, $c = -\psi(w)$, $w = \sqrt[3]{q}$.

The computational results are for the initial conditions $p_0 = 8{,}000\ [mm^3]$ and $q_0 = 10{,}000\ [mm^3]$. The optimal control package NUDOCCCS due to Büskens [43] was implemented to compute a solution of the discretized control problem using nonlinear programming methods. A time grid with $N = 400$ points and a high order Runge-Kutta integration method were chosen. Figure 6.26 shows the graph of a numerically computed 'optimal' chattering control (top, left) and its corresponding concentration c (top, right) as well as the graphs of the states and their corresponding trajectory in (p,q)-space (bottom). The highly irregular structure of the numerically computed control is caused by the fact that the theoretically optimal control chatters and has a singular middle segment. Consequently, as the intervals shrink to 0, the actual control values no longer alternate between their upper and lower values ± 1 and thus this control only gives a numerical approximation of the optimal value, as it is unavoidable with any numerical computation of optimal chattering arcs. The value of the objective is within the preset error tolerance and the tumor volume is given by $p(T) = 78.5326\ [mm^3]$ obtained at the final time $T = 11.6406$ [days].

For the same parameter values, Figure 6.27 gives an example of a heuristic sub-optimal control that is computed by taking a control of the following simple bang-bang structure:

$$u(t) = \begin{cases} u_{\max} & \text{for} \quad 0 \le t < t_1, \\ 0 & \text{for} \quad t_1 \le t < t_2, \\ u_{\max} & \text{for} \quad t_3 \le t < t_3, \\ 0 & \text{for} \quad t_4 \le t \le T. \end{cases}$$

Thus, both the chattering and singular arcs are completely eliminated at the expense of two adjacent bang-bang arcs that become larger. The switching times t_1, t_2, t_3 and

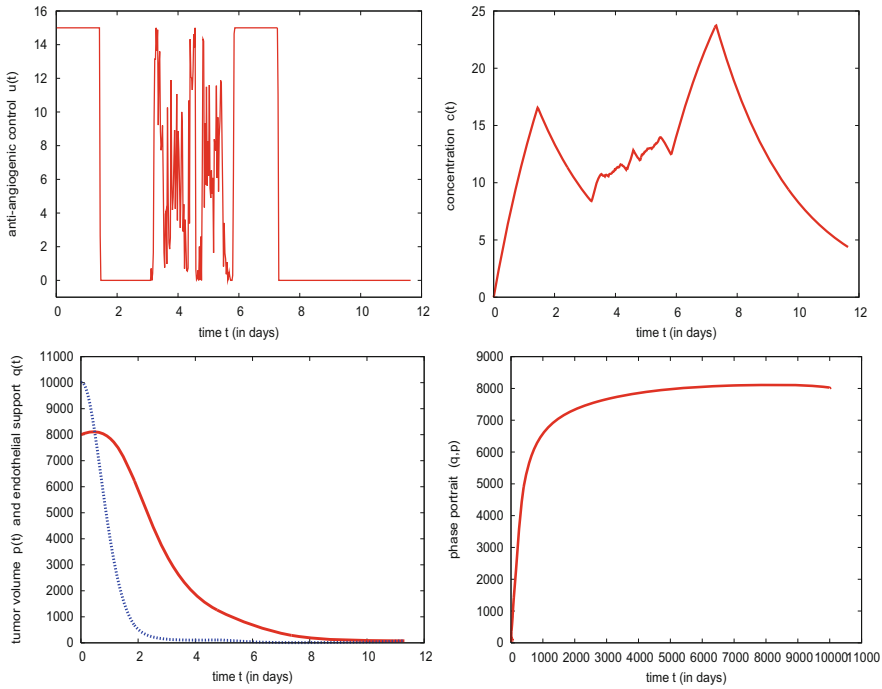

Fig. 6.26 A numerically computed chattering control (top, left) with corresponding concentration c (top, right), states p and q (bottom, left), and corresponding trajectory (bottom, right) for problem [OCAPK] for model [E] with initial conditions $p_0 = 8{,}000\ [mm^3]$ and $q_0 = 10{,}000\ [mm^3]$.

the final time T here are free optimization variables. Using the arc-parametrization method developed in [234] and the code NUDOCCCS [43], the switching times $t_1 = 1.78835$ [days], $t_2 = 4.60461$ [days], $t_3 = 6.86696$ [days], and the final time $T = 11.3101$ [days] were obtained. Surprisingly, this rather crude suboptimal control already gives an excellent approximation with a minimal tumor volume of $p(T) = 78.8853\ [mm^3]$. On the right of Figure 6.27, the corresponding concentration is shown.

Tumor volumes that are virtually identical with the numerically optimal ones can be achieved with a slightly more refined control structure of the form

$$u(t) = \begin{cases} u_{\max} & \text{for} \quad 0 \le t < t_1, \\ 0 & \text{for} \quad t_1 \le t < t_2, \\ v & \text{for} \quad t_2 \le t < t_3, \\ u_{\max} & \text{for} \quad t_3 \le t < t_4, \\ 0 & \text{for} \quad t_4 \le t \le T. \end{cases}$$

Once more the chattering arcs are approximated by a simple bang-bang control that switches once from $u_{\max}$ to 0 and the singular segment is approximated by a constant intermediate control value v over the full singular interval. This particular choice is

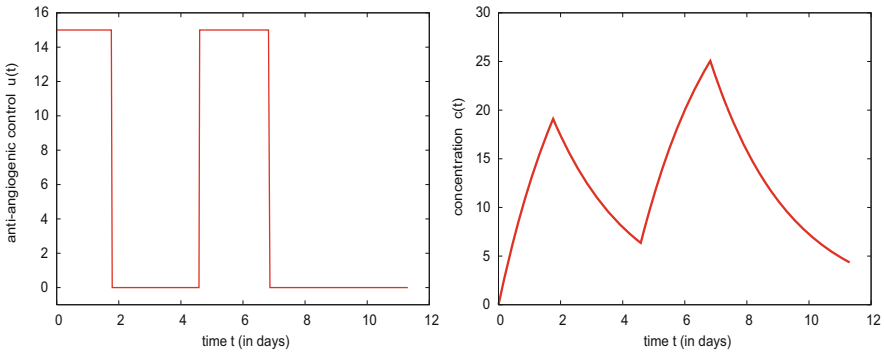

Fig. 6.27 A simple suboptimal bang-bang control with four arcs (left) and corresponding concentration c (right) for model [E].

probably the simplest reasonable approximation to the theoretically optimal control structure: a chattering control followed by a singular control and one more chattering control. The switching times t_i, $i = 1,\ldots,t_4$, the final time T, and the value v of the control are free optimization variables. Again, the arc-parametrization method [234] and the code NUDOCCCS [43] were used to compute the switching times: $t_1 = 1.467$ [days], $t_2 = 3.081$ [days], $t_3 = 5.986$ [days], $t_4 = 7.358$ [days], the final time $T = 11.639$ [days] and the constant control v is given by $v = 6.24784$. These are the optimal values within this restricted class of controls. This generates a tumor volume of $p(T) = 78.5329$ $[mm^3]$ for the suboptimal approximation which is basically identical with the minimal tumor volume $p(T) = 78.5326$ $[mm^3]$ for the chattering control. On the right of Figure 6.28 the corresponding concentration is shown. Overall, the behavior is very similar as in case of the chattering control, but the system has a much smoother and thus for many aspects preferable response. Like in the case of problem [OCA] without PK, the differences in the minimum tumor volumes that can be achieved on the level of suboptimal controls are negligible.

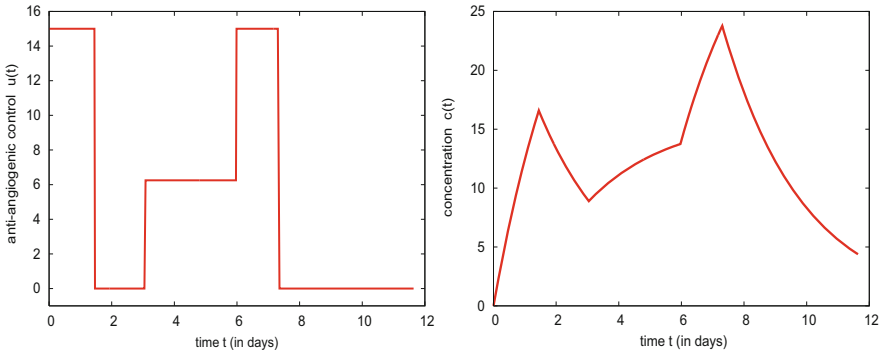

Fig. 6.28 A suboptimal piecewise constant control (left) and corresponding concentration c (right) for model $[E]$.

6.4 Toward the Practical Side

In this chapter, we illustrated the bifold role that optimal solutions have in designing practical protocols for antiangiogenic treatments. Obviously, the theoretically optimal protocols define benchmark values to which other—simple and heuristically chosen, but implementable—protocols can be compared. Optimal solutions thus determine a measure for how good an otherwise given protocol is. Equally important, the structure of theoretically optimal solutions suggests simple realizable suboptimal protocols that generally give excellent approximations. Here we considered some simple piecewise constant suboptimal protocols and evaluated their overall efficiency by comparing the minimum tumor volumes that these protocols achieve with the optimal solution for problem [OCA]. For example, the averaged optimal dose protocol which is easily obtained from the theoretically optimal solution, provides a generally excellent approximation for models [H] and [E].

While the choice of a suboptimal protocol naturally depends on the specific model considered, the initial tumor volume, and the size of the carrying capacity of the vasculature, some general observations can be made that are of interest:

1. Both *optimal and suboptimal protocols are strongly robust with respect to the carrying capacity*. Since generally no reliable data or observations about this quantity are available, this is of practical significance.
2. *For higher initial tumor volumes, protocols that generate lower concentrations perform better*. The reason is that for high dose rates in the models considered here the dynamics for the carrying capacity overshoots the "optimal" path for tumor reduction (that is determined by the optimal singular arc). Hence, in a certain sense, inhibitors are wasted at higher dose rates/concentrations whereas better effects can be achieved if the total available dose is spread out over time.
3. Under the augmentation of the dynamics with a standard linear pharmacokinetic model for the antiangiogenic agent, not only are essential features of the optimal synthesis (e.g., optimal singular controls and arcs) preserved, but the formulas carry over verbatim to the new model formulation, albeit with different interpretation. While there exist both qualitative and quantitative changes in the structure of optimal protocols, again simple, close to optimal suboptimal protocols exist. Like for the simplified model [OCA], the structure of theoretically optimal solutions points to some straightforward simple classes of controls that are parameterized by a small number of parameters and thus can easily be minimized. Overall, this gives credence to a modeling approach that initially neglects the pharmacokinetic model.

Chapter 7
Combination Therapies with Antiangiogenic Treatments

Antiangiogenic treatment discussed in Chapters 5 and 6 is an indirect approach to cancer therapy that aims at limiting a tumor's ability to grow by depriving it of the required vasculature. It initially provided a new hope in cancer treatment since targeting the healthy and genetically stable endothelial cells of the lining for the blood vessels showed no drug resistance, the curse of chemotherapy [141, 142]. However, since the treatment is only limiting the tumor's support mechanism without actually killing the cancer cells, antiangiogenic therapy by itself only achieves a temporary, "pseudo-therapeutic effect" that goes away with time. In some cases, once treatment is halted, the tumor grows back even more vigorously than before. While antiangiogenic monotherapy thus is not considered a viable treatment option, it has become a staple of anticancer treatments in combination with radio- and chemotherapy. In this way, simultaneously two separate mechanisms that support cancer are targeted, the cancerous cells and the vasculature that supports them [283]. The idea simply is that *antiangiogenic therapy can enhance the efficacy of traditional approaches by normalizing a tumor's vasculature*. For example, Jain and Munn argue that a normalization of a tumor's irregular and dysfunctional vasculature [131, 132] through prior antiangiogenic treatment enhances the delivery of chemotherapeutic agents and thus improves the effectiveness of chemotherapy.

In this chapter, in Section 7.1, we consider mathematical models for combinations of antiangiogenic treatments with chemotherapy and, in Section 7.2, with radiotherapy. Combination therapies provide a double challenge, both from the modeling perspective and in the subsequent mathematical analysis of such models. Different from the problems considered in Chapter 2 which all were within the context of chemotherapy (e.g., combining cytotoxic and cytostatic drugs), here fundamentally different mechanisms of operation are merged. When doing so, sometimes even the most fundamental questions do not have obvious answers. For example, if chemotherapy is combined with antiangiogenic treatments, which procedure should come first? The delivery of chemotherapeutic agents takes place by means of the

H. Schättler, U. Ledzewicz, *Optimal Control for Mathematical Models of Cancer Therapies*, Interdisciplinary Applied Mathematics 42,
DOI 10.1007/978-1-4939-2972-6_7

bloodstream and thus requires the tumor's vasculature. But this exactly is the target of antiangiogenic treatments. Thus, should chemotherapy be given first in order not to destroy this vasculature? Or is it be better to normalize this vasculature to enable a more efficient delivery of chemotherapy? We shall see below, that it is the second alternative that optimization of mathematical models suggests. However, this mathematical analysis now becomes more difficult since we need to deal with fully nonlinear models and generally high dimensional multi-input optimal control problems. The optimal solutions for the monotherapy problem computed in Chapter 5 lay the foundation on which the solutions for these multi-input models for the combination therapies can be built. Indeed, as will be seen, both for combinations with chemo- and radiotherapy, these optimal solutions have close connections with the optimal solutions for the combination therapy models. This property also gives credence to the modular approach that we have pursued in this text of building up on simpler models by increasingly incorporating more medically relevant features.

The main conclusion of our results presented in Chapter 5 is that there exists a in a certain way *optimal relation between tumor volume p and its carrying capacity q when tumor kill is maximized*. By no means was this to destroy as much of the vasculature as possible, but to maintain a proper balance between tumor size and vasculature through the administration of antiangiogenic agents according to an optimal singular control. Here we shall see that for all the models of angiogenic signaling considered in Chapter 5, and both for combinations with chemotherapy and with radiotherapy, simple modifications to this relation exist that adjust this relation to account for the additional treatment modalities. And once more explicit Lie algebraic calculations allow to make the necessary modifications. The persistence of an optimal relation between tumor volume and carrying capacity of the vasculature in so many mathematical models gives strong credibility to the belief that indeed an ideal relation between these two variables gives the best tumor reductions that can be achieved. The question how these optimal paths can be characterized and computed is answered, at least in the mathematical models considered here, decisively by the optimal control approach. These paths correspond to so-called *singular arcs* and the concentrations, respectively dose rates, that keep them invariant, are the so-called *singular controls*. Lie derivative based computations provide a powerful means to perform these nonlinear calculations and to arrive at explicit formulas for singular controls and arcs.

7.1 Combination of Antiangiogenic Treatment and Chemotherapy as Multi-Input Optimal Control Problem

We combine the mathematical model [H] for angiogenic signaling with the action of a chemotherapeutic agent. In his concluding remarks in the paper [251], A. d'Onofrio introduces such a model along with fundamental biological inferences. In that model, a simple linear killing term was added to the dynamics of tumor growth. This is a reasonable approximation to describe chemotherapies that are not

cell-cycle specific, or even, as a first crude approximation to model radiotherapy ignoring the quadratic effects. Possible cytotoxic effects of the chemotherapeutic agent on the endothelial cells for the combined model have been considered by A. Swierniak in [315] and in our joint paper [264] with A. d'Onofrio and H. Maurer for combination of a vessel disrupting and a cytotoxic agent. This is the model that we formulate below and analyze as an optimal control problem. Mathematically, the challenge lies in the fact that this is now *a fully nonlinear multi-input optimal control problem* and a much more complex structure of optimal controls is possible. We briefly describe the model in Section 7.1.1 and derive the adjusted formula for the singular control of the antiangiogenic agent in Section 7.1.3. For the administration of the cytotoxic agent optimal controls are bang-bang. In fact, in Section 7.1.4 we give several numerical examples that support the following structure of optimal protocols: administration of the vessel disrupting antiangiogenic agent u follows the same pattern as for the monotherapy problem derived in Chapter 5 (i.e., for a medically typical initial condition, after a full dose segment, antiangiogenic agents are administered following the optimal singular control until they run out at some time τ) and administration of the cytotoxic agent v follows a bang-bang control. In fact, chemotherapy is given in one full dose session that commences at a specific, optimal time σ. In some sense, a regularization of the vasculature has been achieved that maximizes the killing potential of the cytotoxic drugs. Depending on the available amounts of both antiangiogenic and chemotherapeutic agents, the time σ can lie anywhere in the interval. For a typical set of parameters, σ occurs during the interval when the antiangiogenic agent is given by the singular control. Cases when σ would lie before the singular curve has been reached correspond to mathematical scenarios when a very large amount of cytotoxic drugs to be given is assumed and generally are medically unrealistic, while σ will only occur after antiangiogenic inhibitors are exhausted, if this amount of cytotoxic agents is assumed very small. As before, the minimum tumor volume is realized at a later time $T > \tau$ after all the chemotherapeutic drugs have been given.

7.1.1 Model [H] Under Combination with Chemotherapy

We again assume that the total amounts of vessel disruptive antiangiogenic and chemotherapeutic agent have been determined a priori and the question becomes how they can be optimally administered to achieve the best possible effects. Once more, we just consider the minimization of the tumor volume. Thus the optimal control formulation follows the same premises as in Chapter 5 in the sense that we assume the question of limiting side effects has already been determined (by a medical practitioner) in terms of limiting the total dosage. From a mathematical side, once the solution to the problem formulated below is known, by comparing these solutions for various maximum dosages, a desired protocol can be chosen, very much like what is a common procedure in engineering applications of optimal control. Mathematically, we thus consider the following optimal control problem:

[ACh] For a free terminal time T, minimize the objective $J(u) = p(T)$ subject to the dynamics

$$\dot{p} = -\xi p \ln\left(\frac{p}{q}\right) - \varphi p v, \qquad p(0) = p_0, \tag{7.1}$$

$$\dot{q} = bp - \left(\mu + bp^{\frac{2}{3}}\right) q - \gamma q u - \eta q v, \qquad q(0) = q_0, \tag{7.2}$$

$$\dot{y} = u, \qquad y(0) = 0, \tag{7.3}$$

$$\dot{z} = v, \qquad z(0) = 0, \tag{7.4}$$

over all Lebesgue measurable (respectively, piecewise continuous) functions

$$u : [0,T] \to [0,u_{\max}] \quad \text{and} \quad v : [0,T] \to [0,v_{\max}]$$

for which the corresponding trajectory satisfies

$$y(T) \le y_{\max} \qquad \text{and} \qquad z(T) \le z_{\max}.$$

As before, the variables y and z keep track of the total amounts of agents administered. The constants $u_{\max}$and $v_{\max}$ represent the maximum dose rates/concentrations of the antiangiogenic agent u and the cytotoxic agent v, respectively, and the total dosages of each drug are limited by $y_{\max}$ and $z_{\max}$. Like in the previous models, γ is the antiangiogenic killing parameter and φ and η are the pharmacodynamic coefficients for the cytotoxic agent. As usual, we use the linear log-kill hypothesis in these terms.

As in Section 5.3, we only consider the following medically relevant square domain $\mathscr{D}$,

$$\mathscr{D} = \left\{ (p,q) : 0 < p < \bar{p} = \left(\frac{b-\mu}{d}\right)^{\frac{3}{2}}, 0 < q < \bar{q} = \left(\frac{b-\mu}{d}\right)^{\frac{3}{2}} \right\}.$$

The following lemma, whose proof is analogous to the one of Proposition 5.3.1 in the monotherapy case, implies that no state-space constraints need to be imposed on the variables.

Lemma 7.1.1. *For arbitrary positive initial conditions p_0 and q_0 and any admissible controls u and v, the solution (p,q,y,z) to the dynamics (7.1)–(7.4) exists for all times $t > 0$ and both p and q remain positive.*

We summarize the notation for the variables and give the values used in the numerical computations in Table 7.1.

It is convenient to have a single notation for the state vector. Since, as before, the quotient $\frac{p}{q}$ plays an important role in the analysis of the problem and was denoted by x previously, we retain the notation $x = \frac{p}{q}$ and denote the full state vector by χ, $\chi = (p,q,y,z)^T$. The dynamics then takes the form

$$\dot{\chi} = f(\chi) + u g_1(\chi) + v g_2(\chi) \tag{7.5}$$

Table 7.1 Notations for the variables, parameters and controls for the optimal control problem [ACh].

Symbol		Units	Value used in computations	Reference
p	Primary tumor volume	mm^3		
q	Carrying capacity of the vasculature	mm^3		
$x = \frac{p}{q}$	Inverse of the endothelial density			
y	Amount of antiangiogenic agent used	mg		
z	Amount of cytotoxic agent used	mg		
χ	State vector - $(p,q,y,z)^T$			
ξ	Tumor growth parameter	[per day]	0.084	[116]
b	Stimulation parameter	[per day]	5.85	[116]
d	Inhibition parameter	[per day]	0.00873	[116]
μ	Loss of vascular support through natural causes		0.02	
u	Antiangiogenic agent			
$u_{\max}$	Maximum allowable dose rate/concentration of the antiangiogenic agent	$[mg]$	75	
$y_{\max}$	Available total dose of the antiangiogenic agent	$[mg]$	300	
v	Chemotherapeutic agent			
$v_{\max}$	Maximum allowable dose rate/concentration of the chemotherapeutic agent		$1/2$	
$z_{\max}$	Available total dose of the chemotherapeutic agent		$2/10$	
γ	Antiangiogenic elimination parameter	$[\frac{kg}{mg \text{ of dose}}$ per day$]$	0.15	[116]
φ	Cytotoxic killing parameter for the tumor		0.1	
η	Cytotoxic killing parameter for the vasculature		$0-0.1$	

where

$$f(\chi) = \begin{pmatrix} -\xi p \ln\left(\frac{p}{q}\right) \\ bp - \left(\mu + dp^{\frac{2}{3}}\right) q \\ 0 \\ 0 \end{pmatrix}, \tag{7.6}$$

$$g_1(\chi) = \begin{pmatrix} 0 \\ -\gamma q \\ 1 \\ 0 \end{pmatrix}, \qquad \text{and} \qquad g_2(\chi) = \begin{pmatrix} -\varphi p \\ -\eta q \\ 0 \\ 1 \end{pmatrix}. \tag{7.7}$$

We note that the control vector fields g_1 and g_2 commute, i.e., their Lie bracket vanishes identically:

$$\begin{aligned} [g_1, g_2](\chi) &= Dg_2(\chi) g_1(\chi) - Dg_1(\chi) g_2(\chi) \\ &= \begin{pmatrix} -\varphi & 0 & 0 & 0 \\ 0 & -\eta & 0 & 0 \\ 0 & 0 & 0 & 0 \\ 0 & 0 & 0 & 0 \end{pmatrix} \begin{pmatrix} 0 \\ -\gamma q \\ 1 \\ 0 \end{pmatrix} - \begin{pmatrix} 0 & 0 & 0 & 0 \\ 0 & -\gamma & 0 & 0 \\ 0 & 0 & 0 & 0 \\ 0 & 0 & 0 & 0 \end{pmatrix} \begin{pmatrix} -\varphi p \\ -\eta q \\ 0 \\ 1 \end{pmatrix} \equiv 0. \end{aligned}$$

This significantly will simplify the mathematical analysis.

7.1.2 Necessary Conditions for Optimality

Our aim is to characterize and compute optimal controlled trajectories. As in the monotherapy problem analyzed in Chapter 5, there exist sets of data when the mathematically optimal solution degenerates and is given by $T = 0$. Once again this happens when the available amounts of antiangiogenic and cytotoxic agents are too small to achieve a reduction in tumor volume beyond its initial value p_0. For problem [ACh] however, also other, less degenerate situations are possible in which the cytotoxic agents are being used up while antiangiogenic agents are not. This makes it necessary to distinguish various cases in the analysis of optimal solutions. Here we elect not to do so and instead restrict our analysis to the most typical scenario when both angiogenic inhibitors and cytotoxic drugs are fully used up.

Definition 7.1.1 (Well-Posed Initial Condition). We say the initial condition (p_0, q_0) is well posed for the data of the optimal control problem [ACh] if the terminal time T along an optimal solution is positive and if all available therapeutic agents are used up, i.e., $y(T) = y_{\max}$ and $z(T) = z_{\max}$ hold.

Suppose (u_*, v_*) are optimal controls for well-posed initial data defined over the interval $[0, T]$ with corresponding trajectory $\chi_* = (p_*, q_*, y_*, z_*)^T$. Necessary conditions for optimality are given by the Pontryagin maximum principle (cf., Theorem

A.3.1 in Appendix A) and they state that there exist a constant $\lambda_0 \geq 0$ and an absolutely continuous co-vector, $\lambda : [0,T] \to (\mathbb{R}^4)^*$, that do not vanish simultaneously, $(\lambda_0, \lambda(t)) \neq 0$ for all t, such that λ satisfies the adjoint equations (using $x = \frac{p}{q}$)

$$\dot{\lambda}_1(t) = \lambda_1(t)\left(\xi\left(\ln\left(x_*(t)\right)+1\right)+\varphi v_*(t)\right)+\lambda_2\left(\frac{2}{3}d\frac{q_*(t)}{p_*^{\frac{1}{3}}(t)}-b\right), \qquad \lambda_1(T)=\lambda_0, \tag{7.8}$$

$$\dot{\lambda}_2(t) = -\lambda_1(t)\xi x_*(t)+\lambda_2(t)(\mu+dp_*^{\frac{2}{3}}(t)+\gamma u_*(t)+\eta v_*(t)), \qquad \lambda_2(T)=0, \tag{7.9}$$

$$\dot{\lambda}_3(t)=0, \qquad \text{and} \qquad \dot{\lambda}_4(t)=0, \tag{7.10}$$

and such that the optimal controls $u_*(t)$ and $v_*(t)$ minimize the Hamiltonian H,

$$H = -\lambda_1\left(\xi p\ln\left(\frac{p}{q}\right)+\varphi pv\right)+\lambda_2\left(bp-\left(\mu+dp^{\frac{2}{3}}+\gamma u+\eta v\right)q\right)+\lambda_3 u+\lambda_4 v \tag{7.11}$$

along $(\lambda_0, \lambda(t), \chi_*(t))$ over the control set $[0,u_{\max}]\times[0,v_{\max}]$ with minimum value given by 0.

Lemma 7.1.2. *If the initial condition (p_0,q_0) is well posed for the data, then extremals are normal. The multipliers λ_1 and λ_2 do not vanish identically (equivalently, have no common zeros) and are positive on an open interval (τ,T) near the terminal time. The multipliers λ_3 and λ_4 are constant and nonnegative.*

Proof. Suppose $\lambda_0 = 0$. Then, since λ_1 and λ_2 satisfy the homogeneous equations (7.8) and (7.9), they vanish identically. By the nontriviality condition on the multiplier, λ_3 and λ_4 cannot both vanish. Suppose $\lambda_3 \neq 0$. If $\lambda_3 < 0$, then by the minimum condition $u \equiv u_{\max}$ and thus, since $H \equiv 0$, we have that $\lambda_4 v = -\lambda_3 u_{\max} > 0$. But then both λ_4 and v are positive which contradicts the minimum condition on v. Hence λ_3 is positive. But then the minimum condition implies that $u \equiv 0$ and this contradicts the fact that the initial data are well posed. An analogous argument gives a contradiction if $\lambda_4 \neq 0$. Without loss of generality we therefore normalize $\lambda_0 = 1$.

This implies that the multipliers λ_1 and λ_2 are nontrivial. For λ_1 this is clear since $\lambda_1(T) = 1$ and for λ_2 it follows from $\dot{\lambda}_2(T) = -\xi x_*(T) < 0$. In particular, both λ_1 and λ_2 are positive on some open interval (τ,T). The fact that λ_3 and λ_4 are constant follows from the adjoint equations since the right-hand side of the dynamics does not depend on the variables y and z.

The multipliers λ_3 and λ_4 are the partial derivatives of the optimal value with respect to the auxiliary variables y and z at the initial condition (cf., equation (A.30) in Theorem A.4.2 in Appendix A). If we denote the value function of the optimal control problem [ACh] by V, then $\lambda_3 < 0$ means that $\frac{\partial V}{\partial y}(p_0,q_0,0,0) < 0$ and thus $V(p_0,q_0,\varepsilon,0) < V(p_0,q_0,0,0)$ for some sufficiently small $\varepsilon > 0$. The optimal control corresponding to the initial condition $(p_0,q_0,\varepsilon,0)$ only uses a total of $\tilde{y}_{\max} = y_{\max} - \varepsilon$ antiangigenic agents and thus a better effect can be achieved with

less inhibitors. Clearly, this cannot be the case since the optimal solution for the initial point (p_0, q_0) with $\tilde{y}_{\max}$ and $\tilde{z}_{\max} = z_{\max}$ is also an admissible control for the original optimal control problem [ACh]. Hence $\lambda_3 \geq 0$. Analogously it follows that $\lambda_4 \geq 0$. In fact, this reasoning is generally valid and these inequalities are merely complementary slackness conditions. □

Optimal controls satisfy the minimum condition on the Hamiltonian H. Since H is linear in u and v, and since the control sets are compact intervals, their values once more are determined by their respective *switching functions* Φ_1 and Φ_2,

$$\Phi_1(t) = \langle \lambda(t), g_1(\chi_*(t)) \rangle = \lambda_3 - \lambda_2(t)\gamma q_*(t), \tag{7.12}$$

$$\Phi_2(t) = \langle \lambda(t), g_2(\chi_*(t)) \rangle = \lambda_4 - \lambda_1(t)\varphi p_*(t) - \lambda_2(t)\eta q_*(t), \tag{7.13}$$

and we have that

$$u_*(t) = \begin{cases} 0 & \text{if} \quad \Phi_1(t) > 0 \\ u_{\max} & \text{if} \quad \Phi_1(t) < 0, \end{cases} \tag{7.14}$$

and

$$v_*(t) = \begin{cases} 0 & \text{if} \quad \Phi_2(t) > 0 \\ v_{\max} & \text{if} \quad \Phi_2(t) < 0 \end{cases}. \tag{7.15}$$

Singular controls are possible over an open interval I if one or both of the switching functions vanish identically. In the latter case, the controls are called totally singular.

7.1.3 Analysis of Singular Controls

Like for the models considered in Chapter 5, the Lagrangian is independent of the state. The adjoint equations therefore can be written compactly as

$$\dot{\lambda} = -\lambda \left(Df(\chi) + uDg_1(\chi) + vDg_2(\chi) \right). \tag{7.16}$$

This provides us with the following simple formula to compute the derivatives of the switching functions (cf., Proposition A.3.1 in Appendix A):

Proposition 7.1.1. *Let $\chi(\cdot)$ be a solution of the dynamics (7.5) for the controls u and v and let λ be a solution of the corresponding adjoint equation (7.16). For a continuously differentiable vector field h, let*

$$\Psi(t) = \langle \lambda(t), h(\chi(t)) \rangle = \lambda(t) h(\chi(t)). \tag{7.17}$$

Then the derivative of Ψ is then given by

$$\dot{\Psi}(t) = \langle \lambda(t), [f + ug_1 + vg_2, h](\chi(t)) \rangle. \tag{7.18}$$

Proof. Dropping the argument t, along the solutions of the dynamics and adjoint equation, we have that

$$\begin{aligned}\dot{\Psi} &= \dot{\lambda}h(\chi) + \lambda Dh(\chi)\dot{\chi} \\ &= -\lambda\left(Df(\chi) + uDg_1(\chi) + vDg_2(\chi)\right)h(\chi) + \lambda Dh(\chi)\left(f(\chi) + ug_1(\chi) + vg_2(\chi)\right) \\ &= \lambda\left(Dh(\chi)f(\chi) - Df(\chi)h(\chi)\right) + u\lambda\left(Dh(\chi)g_1(\chi) - Dg_1(\chi)h(\chi)\right) \\ &\qquad + v\lambda\left(Dh(\chi)g_2(\chi) - Dg_2(\chi)h(\chi)\right) \\ &= \langle\lambda, [f + ug_1 + vg_2, h](\chi)\rangle\end{aligned}$$

verifying (7.18). □

For any vector field h it holds trivially that $[h,h] \equiv 0$ and the control vector fields g_1 and g_2 for problem [ACh] commute. Thus the first derivatives of the switching functions Φ_1 and Φ_2 are simply given by

$$\dot{\Phi}_1(t) = \langle\lambda(t), [f, g_1](\chi_*(t))\rangle \tag{7.19}$$

and

$$\dot{\Phi}_2(t) = \langle\lambda(t), [f, g_2](\chi_*(t))\rangle\,. \tag{7.20}$$

Direct calculations verify that (also see Section 5.3.2)

$$[f, g_1](\chi) = \gamma p \begin{pmatrix} \xi \\ -b \\ 0 \\ 0 \end{pmatrix} \tag{7.21}$$

and

$$[f, g_2](\chi) = \begin{pmatrix} (\eta - \varphi)\xi p \\ (\varphi - \eta)bp - \frac{2}{3}\varphi d p^{\frac{2}{3}} q \\ 0 \\ 0 \end{pmatrix} = \frac{\eta - \varphi}{\gamma}[f, g_1](\chi) - \frac{2}{3}\varphi d p^{\frac{2}{3}} q \begin{pmatrix} 0 \\ 1 \\ 0 \\ 0 \end{pmatrix}. \tag{7.22}$$

In particular, the vector fields g_1, $[f, g_1]$, g_2, and $[f, g_2]$ are everywhere linearly independent and thus the adjoint variable λ can never vanish against all four vectors.

Proposition 7.1.2. *The controls u and v cannot be singular simultaneously. If one of them is singular over an open interval I, then the other control is bang-bang over I.* ■

Proof. Suppose both Φ_1 and Φ_2 vanish at some time τ. If also $\dot{\Phi}_i(\tau) = 0$, then, by the nontriviality of the multiplier λ, it follows that $\dot{\Phi}_j(\tau) \neq 0$ for $i \neq j$. □

Furthermore, the derivatives of the switching function do not depend on the controls and thus can be differentiated one more time to give

$$\ddot{\Phi}_1(t) = \langle\lambda(t), [f + ug_1 + vg_2, [f, g_1]]\,(\chi(t))\rangle \equiv 0. \tag{7.23}$$

and

$$\ddot{\Phi}_2(t) = \langle \lambda(t), [f + ug_1 + vg_2, [f, g_2]](\chi(t)) \rangle \equiv 0. \tag{7.24}$$

We first consider antiangiogenic dose rates that are singular. These computations mimic the results from Chapter 5 with the appropriate modifications for the presence of the chemotherapeutic agent. Suppose that an optimal control u_* is singular on an open interval $I = (\alpha, \beta)$. Then both $\Phi_1(t)$ and its derivative $\dot{\Phi}_1(t)$ vanish identically on I and we have that

$$\lambda_3 \equiv \lambda_2(t)\gamma q_*(t) \qquad \text{and} \qquad \lambda_1(t)\xi \equiv \lambda_2(t)b. \tag{7.25}$$

These relations imply that all the multipliers $\lambda_1(t)$, $\lambda_2(t)$, and λ_3 are positive on I and that $\beta < T$. A direct computation (see also (5.46)) verifies that

$$[g_1, [f, g_1]](\chi_*(t)) = -\gamma^2 b p_*(t) \begin{pmatrix} 0 \\ 1 \\ 0 \\ 0 \end{pmatrix} = \gamma [f, g_1](\chi_*(t)) - \gamma^2 \xi p_*(t) \begin{pmatrix} 1 \\ 0 \\ 0 \\ 0 \end{pmatrix}.$$

Since $\langle \lambda(t), [f, g_1](\chi(t)) \rangle \equiv 0$ on I, it follows that

$$\langle \lambda(t), [g_1, [f, g_1]](\chi_*(t)) \rangle = -\lambda_1(t)\gamma^2 \xi p_*(t) < 0 \tag{7.26}$$

and thus singular controls u are of order 1 and the strengthened Legendre-Clebsch condition is satisfied.

Proposition 7.1.3. *Suppose (u_*, v_*) is an optimal control. If u_* is singular on $I = (\alpha, \beta)$, then the multipliers λ_1, λ_2 and λ_3 are positive on I. Furthermore, the control u_* ends with an interval (τ, T) where $u \equiv 0$ and v_* is bang-bang on I with at most one switching from $v = 0$ to $v = v_{\max}$.*

Proof. Since $\Phi_1(T) = \lambda_3 > 0$, the minimum condition on the Hamiltonian H implies that $u_* \equiv 0$ near the terminal time T.

By equation (7.22) the derivative of the switching function Φ_2 for v is given by

$$\dot{\Phi}_2(t) = \langle \lambda(t), [f, g_2](\chi_*(t)) \rangle = \frac{\eta - \varphi}{\gamma} \langle \lambda(t), [f, g_1](\chi_*(t)) \rangle - \frac{2}{3} \lambda_2(t) \varphi d p_*(t)^{\frac{2}{3}} q_*(t).$$

Since $\langle \lambda(t), [f, g_1] \rangle (\chi_*(t))$ vanishes on I, it follows that

$$\dot{\Phi}_2(t) = -\frac{2}{3} \lambda_2(t) \varphi d p_*(t)^{\frac{2}{3}} q_*(t) < 0$$

and thus Φ_2 is strictly decreasing on I. Hence v is bang-bang on I with at most one switching from $v = 0$ to $v = v_{\max}$. □

Solving equation (7.23) for u, the singular control is given by

$$u_{\text{sing}}(t) = -\frac{\langle \lambda(t), [f + v_*(t)g_2, [f,g_1]](\chi(t))\rangle}{\langle \lambda(t), [g_1,[f,g_1]](\chi(t))\rangle}.$$

The Lie brackets $[f,[f,g_1]]$ and $[g_1,[f,g_1]]$ were already computed in Chapter 5 (cf., (5.46) and (5.47)) and another computation verifies that

$$[g_2,[f,g_1]](\chi(t)) = (\varphi-\eta)\gamma bp\begin{pmatrix}0\\1\\0\\0\end{pmatrix} = -\frac{\varphi-\eta}{\gamma}[g_1,[f,g_1]](\chi(t)). \tag{7.27}$$

We therefore have that

$$u_{\text{sing}}(t) = -\frac{\langle \lambda(t), [f,[f,g_1]](\chi(t))\rangle}{\langle \lambda(t), [g_1,[f,g_1]](\chi(t))\rangle} + \frac{\varphi-\eta}{\gamma}v_*(t).$$

The first term in this expression is the singular control for the monotherapy case from Proposition 5.3.4 in Chapter 5 and we can simply draw on these results to determine the singular controls. It follows from those calculations that $[f,[f,g_1]]$ lies in the linear span of the vector fields $[f,g_1]$ and $[g_1,[f,g_1]]$,

$$[f,[f,g_1]](\chi) = \left(\xi + b\frac{p}{q}\right)[f,g_1](\chi) - \psi[g_1,[f,g_1]](\chi)$$

with

$$\psi(p,q) = \frac{1}{\gamma}\left(\xi\ln\left(\frac{p}{q}\right) + b\frac{p}{q} + \frac{2}{3}\xi\frac{d}{b}\frac{q}{p^{\frac{1}{3}}} - \left(\mu + dp^{\frac{2}{3}}\right)\right).$$

Overall, we have the following result:

Theorem 7.1.1. *If the optimal control u_* is singular on an open interval I, then*

$$\gamma u_{\text{sing}}(t) + (\eta-\varphi)v_*(t) = \gamma\psi(p_*(t),q_*(t)). \tag{7.28}$$

and v_* is bang-bang on I with at most one switching on I from $v=0$ to $v=v_{\max}$.

Recall that it is the function ψ that determines the optimal singular antiangiogenic dose rates/concentrations. Equation (7.28) corrects these rates in the presence of chemotherapy by adjusting according to the effects of the chemotherapy on the tumor and the vasculature. Indeed, $\gamma u_*(t) + \eta v_*(t)$ is the combined killing rate on the vasculature and $\varphi v_*(t)$ is the killing rate on the tumor volume.

Suppose u_* is singular on an open interval $I=(\alpha,\beta)$. It then follows from Proposition 7.1.3 that the control v_* has at most one switch from $v=0$ to $v=v_{\max}$ on I. While $v=0$, the problem reduces to the monotherapy situation analyzed in Chapter 5. In this case, the fourth coordinate of the vector fields f, g_1 and $[f,g_1]$ is zero and these fields span the (p,q,y)-subspace. The only multiplier that is orthogonal

to all these vectors is $(0,0,0,\lambda_4)$. But along an optimal singular control the multiplier λ_2 must be positive and thus it follows that the vector fields f, g_1 and $[f,g_1]$ must be linearly dependent along the singular arc. Hence, although formulated in $\mathbb{R}^4$, this case reduces to the three-dimensional problem considered earlier and all the formulas given there apply.

Once the control v switches to $v_{\max}$, the condition $H \equiv 0$ of the maximum principle implies that

$$\langle \lambda(t), f(\chi(t)) + v_{\max} g_2(\chi(t)) \rangle \equiv 0$$

and thus $\lambda(t)$ vanishes against the vector fields g_1, $[f,g_1]$ and $f + v_{\max} g_2$,

$$g_1(\chi) = \begin{pmatrix} 0 \\ -\gamma q \\ 1 \\ 0 \end{pmatrix}, \quad [f,g_1](\chi) = \gamma p \begin{pmatrix} \xi \\ -b \\ 0 \\ 0 \end{pmatrix},$$

$$f + v_{\max} g_2(\chi) = \begin{pmatrix} -\xi p \ln\left(\frac{p}{q}\right) - v\varphi p \\ bp - (\mu + d p^{\frac{2}{3}})q - \eta v_{\max} q \\ 0 \\ v_{\max} \end{pmatrix}.$$

These three vector fields are linearly independent and the fourth coordinate in $f + v_{\max} g_2$ is nonzero given by $v_{\max}$. Hence there exists an up to multiples unique multiplier λ that is orthogonal to these three vector fields. It is clear that the solution has multipliers λ_1, λ_2 and λ_3 which have the same sign and we need to choose the direction so that these entries are positive. Therefore, in this case, there are no restrictions on the locus of points where the singular control is admissible and the singular control is a feedback function defined in (p,q)-space that also depends on $v_{\max}$. As always, any such computed singular control u needs to be admissible, i.e., take values in the control set $[0, u_{\max}]$.

In principle, for this problem singular controls are also possible for the *chemotherapeutic agent v*. In the computations below we assume that $\varphi > 3\eta$, a realistic assumption for high dose chemotherapy that has a more prevalent effect on the rapidly duplicating tumor cells than the slowly proliferating endothelial cells. Suppose that an optimal control v_* is singular on an open interval $I = (\alpha, \beta)$. In this case we have that

$$\lambda_4 \equiv \lambda_1(t)\varphi p_*(t) + \lambda_2(t)\eta q_*(t) \tag{7.29}$$

and

$$\lambda_1(t)\xi p_*(t) \equiv \lambda_2(t)\left(bp_*(t) - \frac{2}{3}\frac{\varphi}{\varphi - \eta} d p_*(t)^{\frac{2}{3}} q_*(t)\right). \tag{7.30}$$

Proposition 7.1.4. *Suppose that $\varphi > 3\eta$. If the optimal control v_* is singular on an open interval $I = (\alpha, \beta)$, then λ_1 and λ_2 are positive on I. The corresponding controlled trajectory lies in the region*

$$D_{v,\text{sing}} = \left\{(p,q) : bp > \frac{2}{3}\frac{\varphi}{\varphi - \eta} d p^{\frac{2}{3}} q\right\} = \left\{(p,q) : q < \frac{3}{2}\left(1 - \frac{\eta}{\varphi}\right)\frac{b}{d} p^{\frac{1}{3}}\right\}$$

and the strengthened Legendre-Clebsch condition for minimality is satisfied. Over the interval I, the control u_* can have at most one switching from $u = 0$ to $u = u_{\max}$.

Proof. In a first step, we show that λ_1 and λ_2 cannot change sign on I. It follows from (7.30) that λ_2 cannot change sign on I since λ_1 and λ_2 do not vanish simultaneously. Suppose λ_1 changes sign and we have that $\lambda_1(\tau) = 0$. It then follows from (7.29) that λ_4 is positive ($\lambda_2(\tau)$ would have to vanish as well if $\lambda_4 = 0$) and thus λ_2 is positive on I as well. Hence we have that

$$bp_*(\tau) = \frac{2}{3}\frac{\varphi}{\varphi-\eta} d p_*(\tau)^{\frac{2}{3}} q_*(\tau).$$

Furthermore, the fact that $H \equiv 0$ implies that

$$\begin{aligned} H &= \lambda_2(\tau)\left(bp_*(\tau) - \left(\mu + d p_*^{\frac{2}{3}}(\tau)\right) q_*(\tau)\right) + \Phi_1(\tau) u_*(\tau) \\ &= \lambda_2(\tau)\left(\left(\frac{2}{3}\frac{\varphi}{\varphi-\eta} - 1\right) d p_*(\tau)^{\frac{2}{3}} - \mu\right) q_*(\tau) + \Phi_1(\tau) u_*(\tau) = 0. \end{aligned}$$

For $\varphi > 3\eta$, the first term is negative. However, we always have that $\Phi_1(\tau)u_*(\tau) \le 0$ and thus this is not possible. Hence λ_1 has constant sign on I as well.

This implies that the quantity $\Delta = bp - \frac{2}{3}\frac{\varphi}{\varphi-\eta} d p^{\frac{2}{3}} q$ has constant sign along an extremal controlled trajectory for which the control v is singular. Consider the full relation $H = 0$:

$$H = -\lambda_1 \xi p \ln\left(\frac{p}{q}\right) + \lambda_2\left(bp - \left(\mu + d p^{\frac{2}{3}}\right) q\right) + \Phi_1 u.$$

If Δ is negative, then we have that

$$bp - \left(\mu + d p^{\frac{2}{3}}\right) q < \left[\left(\frac{2}{3}\frac{\varphi}{\varphi-\eta} - 1\right) d p^{\frac{2}{3}} - \mu\right] q < 0$$

and

$$\frac{p}{q} < \frac{2}{3}\frac{\varphi}{\varphi-\eta}\frac{d}{b} p^{\frac{2}{3}} \le \frac{d}{b} p^{\frac{2}{3}} \le \frac{d}{b} \bar{p}^{\frac{2}{3}} = \frac{d}{b}\frac{b-\mu}{d} = 1 - \frac{\mu}{d} \le 1.$$

Furthermore, in this case it follows from (7.30) that λ_1 and λ_2 have opposite signs. If λ_2 is positive, then we have that

$$H = -\lambda_1 \xi p \ln\left(\frac{p}{q}\right) + \lambda_2\left(bp - \left(\mu + d p^{\frac{2}{3}}\right) q\right) + \Phi_1 u < 0$$

contradicting the condition $H = 0$. Similarly, if λ_2 is negative, then the switching function $\Phi_1(t) = \lambda_3 - \lambda_2(t)\gamma q(t)$ is positive and thus $u \equiv 0$. But then in this case

$$H = -\lambda_1 \xi p \ln\left(\frac{p}{q}\right) + \lambda_2\left(bp - \left(\mu + d p^{\frac{2}{3}}\right) q\right) + \Phi_1 u > 0$$

again contradicting the condition $H = 0$. Hence Δ must be positive and extremal controlled trajectories along which v is singular must lie in $D_{v,\text{sing}}$.

In this case, λ_1 and λ_2 have the same sign and it follows from (7.29) that they are positive. The Lie bracket $[g_2,[f,g_2]]$ is given by

$$\begin{aligned}[g_2,[f,g_2]](\chi) &= D([f,g_2])(\chi)g_2(\chi) - Dg_2(\chi)[f,g_2](\chi)\\ &= -(\varphi-\eta)^2\left(bp - \frac{4}{9}\left(\frac{\varphi}{\varphi-\eta}\right)^2 dp^{\frac{2}{3}}q\right)\begin{pmatrix}0\\1\\0\\0\end{pmatrix}\end{aligned}$$

and thus the Legendre Clebsch condition takes the form

$$\langle\lambda(t),[g_2,[f,g_2]](\chi_*(t))\rangle = -\lambda_2(t)(\varphi-\eta)^2\left(bp_*(t) - \frac{4}{9}\left(\frac{\varphi}{\varphi-\eta}\right)^2 dp_*^{\frac{2}{3}}(t)q_*(t)\right).$$

But $0 < \frac{2}{3}\frac{\varphi}{\varphi-\eta} \leq 1$ and thus on $D_{v,\text{sing}}$ we have that

$$bp > \frac{2}{3}\frac{\varphi}{\varphi-\eta}dp^{\frac{2}{3}}q \geq \left(\frac{2}{3}\frac{\varphi}{\varphi-\eta}\right)^2 dp^{\frac{2}{3}}q.$$

Hence $\langle\lambda(t),[g_2,[f,g_2]](\chi_*(t))\rangle$ is negative and the strict Legendre-Clebsch condition for minimality is satisfied.

Furthermore, it follows from (7.30) that the derivative of the switching function Φ_1 for u is given by

$$\dot{\Phi}_1(t) = \gamma p_*(t)[\lambda_1(t)\xi - \lambda_2(t)b] = -\frac{2}{3}\gamma\lambda_2(t)\frac{\varphi}{\varphi-\eta}dp_*(t)^{\frac{2}{3}}q_*(t) < 0$$

and thus Φ_1 is strictly decreasing over I. Hence the control u_* can have at most one switching from $u = 0$ to $u = u_{\max}$. □

Using equation (7.24), a singular control v is given by

$$v_{\text{sing}}(t) = -\frac{\langle\lambda(t),[f+u_*(t)g_1,[f,g_2]](\chi_*(t))\rangle}{\langle\lambda(t),[g_2,[f,g_2]](\chi_*(t))\rangle}.$$

It follows from the Jacobi identity (see equation (A.18) in Appendix A) that

$$[g_1,[f,g_2]] + [f,[g_2,g_1]] + [g_2,[g_1,f]] \equiv 0. \tag{7.31}$$

Since g_1 and g_2 commute, we have that

$$[g_1,[f,g_2]](\chi) = [g_2,[f,g_1]](\chi) = (\varphi-\eta)\gamma bp \begin{pmatrix} 0 \\ 1 \\ 0 \\ 0 \end{pmatrix}$$
$$= -\frac{\gamma}{\varphi-\eta}\frac{bp}{bp-\frac{4}{9}\left(\frac{\varphi}{\varphi-\eta}\right)^2 dp^{\frac{2}{3}}q}[g_2,[f,g_2]](\chi).$$

All the vector fields arising in these computations have zero y and z coordinates and we can therefore write $[f,[f,g_2]]$ in the form

$$[f,[f,g_2]](\chi) = \omega(\chi)[f,g_2](\chi) + \rho(\chi)[g_2,[f,g_2]](\chi).$$

Since the multiplier λ vanishes against $[f,g_2]$, it follows that

$$v_{\text{sing}}(t) = -\rho(\chi_*(t)) + u_*(t)\frac{\gamma}{\varphi-\eta}\frac{bp_*(t)}{bp_*(t)-\frac{4}{9}\left(\frac{\varphi}{\varphi-\eta}\right)^2 dp_*^{\frac{2}{3}}(t)q_*(t)}. \tag{7.32}$$

Equivalently,

$$(\varphi-\eta)\left[bp_*(t)-\frac{4}{9}\left(\frac{\varphi}{\varphi-\eta}\right)^2 dp_*^{\frac{2}{3}}(t)q_*(t)\right]\left(v_{\text{sing}}(t)+\rho(\chi_*(t))\right) = \gamma bp_*(t)u_*(t).$$

Higher order brackets have zero y- and z-coordinates. For simplicity of notation, we delete these components in the following computations, but retain the names of the vector fields. A somewhat lengthier computation verifies that

$$[f,[f,g_2]](\chi) = D([f,g_2])(\chi)f(\chi) - Df(\chi)[f,g_2](\chi)$$
$$= \begin{pmatrix} -(\eta-\varphi)\xi^2 p\ln\left(\frac{p}{q}\right) \\ -\left((\varphi-\eta)b-\frac{4}{9}\varphi dp^{-\frac{1}{3}}q\right)\xi p\ln\left(\frac{p}{q}\right)-\frac{2}{3}\varphi dp^{\frac{2}{3}}\left(bp-\left(\mu+dp^{\frac{2}{3}}\right)q\right) \end{pmatrix}$$
$$- \begin{pmatrix} -(\eta-\varphi)\xi^2 p\left(1+\ln\left(\frac{p}{q}\right)\right)+\xi\frac{p}{q}\left((\varphi-\eta)bp-\frac{2}{3}\varphi dp^{\frac{2}{3}}q\right) \\ \left(bp-\frac{2}{3}dp^{\frac{2}{3}}q\right)(\eta-\varphi)\xi-\left(\mu+dp^{\frac{2}{3}}\right)\left((\varphi-\eta)bp-\frac{2}{3}\varphi dp^{\frac{2}{3}}q\right) \end{pmatrix}$$
$$= (\varphi-\eta)\begin{pmatrix} -\xi^2 p-\xi\frac{p}{q}\left(bp-\frac{2}{3}\frac{\varphi}{\varphi-\eta}dp^{\frac{2}{3}}q\right) \\ \left(-bp+\frac{4}{9}\frac{\varphi}{\varphi-\eta}dp^{\frac{2}{3}}q\right)\xi\ln\left(\frac{p}{q}\right)+\xi\left(bp-\frac{2}{3}dp^{\frac{2}{3}}q\right)+bp\left[\mu+\frac{\frac{1}{3}\varphi-\eta}{\varphi-\eta}dp^{\frac{2}{3}}\right] \end{pmatrix}.$$

Writing

$$\begin{pmatrix} -\xi^2 p - \xi \frac{p}{q}\left(bp - \frac{2}{3}\frac{\varphi}{\varphi-\eta} dp^{\frac{2}{3}} q\right) \\ \left(-bp + \frac{4}{9}\frac{\varphi}{\varphi-\eta} dp^{\frac{2}{3}} q\right)\xi \ln\left(\frac{p}{q}\right) + \xi\left(bp - \frac{2}{3} dp^{\frac{2}{3}} q\right) + bp\left[\left(\mu + dp^{\frac{2}{3}}\right) - \frac{2}{3}\frac{\varphi}{\varphi-\eta} dp^{\frac{2}{3}}\right] \end{pmatrix}$$
$$= \omega(\chi)\begin{pmatrix} -\xi p \\ bp - \frac{2}{3}\frac{\varphi}{\varphi-\eta} dp^{\frac{2}{3}} q \end{pmatrix} - \rho(\chi)(\varphi-\eta)\begin{pmatrix} 0 \\ bp - \frac{4}{9}\left(\frac{\varphi}{\varphi-\eta}\right)^2 dp^{\frac{2}{3}} q \end{pmatrix},$$

it follows that

$$\omega(\chi) = \xi + b\frac{p}{q} - \frac{2}{3}\frac{\varphi}{\varphi-\eta} dp^{\frac{2}{3}}$$

and

$$\begin{aligned} &-\rho(\varphi-\eta)\left[bp - \frac{4}{9}\left(\frac{\varphi}{\varphi-\eta}\right)^2 dp^{\frac{2}{3}} q\right] \\ &= -\xi \ln\left(\frac{p}{q}\right)\left(bp - \frac{4}{9}\frac{\varphi}{\varphi-\eta} dp^{\frac{2}{3}} q\right) + \xi\left(bp - \frac{2}{3} dp^{\frac{2}{3}} q\right) + bp\left(\mu + \frac{\frac{1}{3}\varphi-\eta}{\varphi-\eta} dp^{\frac{2}{3}}\right) \\ &\qquad - \left(\xi + b\frac{p}{q} - \frac{2}{3}\frac{\varphi}{\varphi-\eta} dp^{\frac{2}{3}}\right)\left(bp - \frac{2}{3}\frac{\varphi}{\varphi-\eta} dp^{\frac{2}{3}} q\right) \\ &= -\xi \ln\left(\frac{p}{q}\right)\left(bp - \frac{4}{9}\frac{\varphi}{\varphi-\eta} dp^{\frac{2}{3}} q\right) + \frac{2}{3}\xi\frac{\eta}{\varphi-\eta} dp^{\frac{2}{3}} q \\ &\qquad + bp\left(\mu + \frac{\frac{1}{3}\varphi-\eta}{\varphi-\eta} dp^{\frac{2}{3}}\right) - \left(bp - \frac{2}{3}\frac{\varphi}{\varphi-\eta} dp^{\frac{2}{3}} q\right)^2 \frac{1}{q}. \end{aligned}$$

This relation defines the function ρ and through it the singular control $v_{\text{sing}}(t)$. For example, if $u \equiv 0$, then the singular control is given by

$$\begin{aligned} v_{\text{sing}}(t) &= -\rho(\chi) \\ &= \left\{-\xi \ln(x)\left(bx - \frac{4}{9}\frac{\varphi}{\varphi-\eta} dp^{\frac{2}{3}}\right) + \frac{2}{3}\xi\frac{\eta}{\varphi-\eta} dp^{\frac{2}{3}}\right. \\ &\qquad \left. + bx\left(\mu + \frac{\frac{1}{3}\varphi-\eta}{\varphi-\eta} dp^{\frac{2}{3}}\right) - \left(bx - \frac{2}{3}\frac{\varphi}{\varphi-\eta} dp^{\frac{2}{3}}\right)^2\right\} \\ &\quad /(\varphi-\eta)\left[bx - \frac{4}{9}\left(\frac{\varphi}{\varphi-\eta}\right)^2 dp^{\frac{2}{3}}\right]. \end{aligned}$$

Furthermore, along a v-singular arc, and using the notation $x = \frac{p}{q}$, the condition $H \equiv 0$ implies that

$$
\begin{aligned}
H &= -\lambda_1 \xi p \ln x + \lambda_2 \left(bp - \left(\mu + dp^{\frac{2}{3}} \right) q \right) + \Phi_1 u \\
&= -\lambda_2 \left[bp - \frac{2}{3} \frac{\varphi}{\varphi - \eta} dp^{\frac{2}{3}} q \right] \ln x + \lambda_2 \left(bp - \left(\mu + dp^{\frac{2}{3}} \right) q \right) + \Phi_1 u \\
&= \lambda_2 \left(-\ln x + \frac{bx - (\mu + dp^{\frac{2}{3}})}{bx - \frac{2}{3} \frac{\varphi}{\varphi - \eta} dp^{\frac{2}{3}}} \right) \left[bx - \frac{2}{3} \frac{\varphi}{\varphi - \eta} dp^{\frac{2}{3}} \right] q + \Phi_1 u.
\end{aligned}
$$

Note that we always have that $\Phi_1 u \leq 0$ since Φ_1 is negative if $u = u_{\max}$. It thus follows that

$$
\ln(x) \leq \frac{bx - \left(\mu + dp^{\frac{2}{3}} \right)}{bx - \frac{2}{3} \frac{\varphi}{\varphi - \eta} dp^{\frac{2}{3}}} < 1 \tag{7.33}
$$

with equality if $u = 0$. In particular, in this case

$$
dp^{\frac{2}{3}} = \frac{bx(1 - \ln x) - \mu}{1 - \frac{2}{3} \frac{\varphi}{\varphi - \eta} \ln x}. \tag{7.34}
$$

Figure 7.1 visualizes the singular curve for the control v if $u = 0$ and for the parameter values given in Table 7.1. The loop shown in the figure on the left gives the full solutions to equation (7.34) and the figure on the right shows the values of the singular control $v_{\text{sing}}(t)$ along this loop. The upper branch gives the values of the control as the system traverses the lower portion of the singular curve and the lower branch gives the values along the upper portion of the singular control. In particular, the singular control is admissible (the precise locus depends on the value $u_{\max}$) on the portion that lies in the region $\mathscr{D}_-$ below the diagonal, but is inadmissible in the region $\mathscr{D}_+$ above the diagonal. More generally, it follows from (7.33) that for $u = u_{\max}$ singular arcs are only possible inside the loop shown in Figure 7.1.

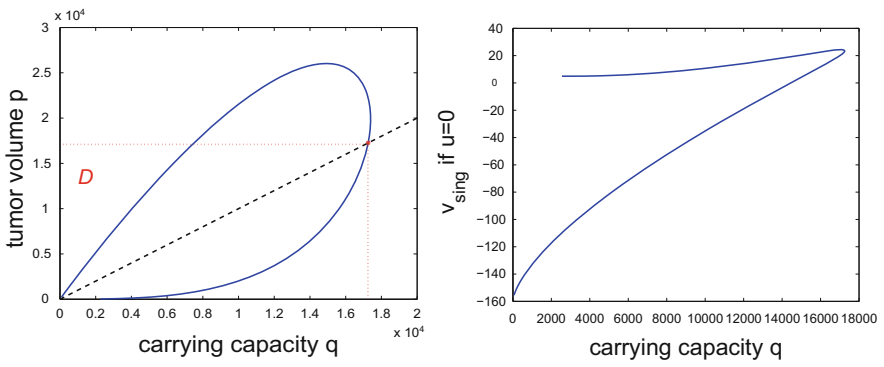

Fig. 7.1 The singular curve for the cytotoxic agent if $u \equiv 0$ (left) and corresponding control values that keep the singular arc invariant (right).

7.1.4 Toward an Optimal Synthesis and Numerical Results

Singular controls thus are also an essential part of the optimal solutions for the optimal control problem [ACh] describing combinations of antiangiogenic treatment with chemotherapy. However, given the much broader range of possibilities for the multi-input optimal control problem, it now is more difficult to develop a full solution from all possible candidates of bang and partially singular segments in form of a regular synthesis. The theoretical computations above point to solutions that have an interval on which one of the two controls is singular, but they are not conclusive in whether this is the antiangiogenic dose rate or the chemotherapy and it is quite likely that from a mathematical point it is the initial condition (p_0, q_0) that becomes the determining factor in this analysis. While all such initial conditions make sense for the mathematical model, there is a much smaller set that would be typical for the medical situation. Clearly, the carrying capacity should exceed the tumor volume since otherwise the system would be shrinking already and thus initial conditions when q_0 is larger are the natural situation while it would not be expected that q_0 exceeds p_0 by orders of magnitude.

In this section, we give several numerical computations when, because of its adverse side effects, *the amount of cytotoxic agents is limited to be much smaller than the amount of antiangiogenic agents*. In this case, and for a realistic range of initial conditions, *optimal combination treatment protocols* all have the following *structure*: initially the vessel disruptive antiangiogenic agent, the optimal control u_*, follows the identical pattern as for the monotherapy problem (of the form $\mathbf{u}_{\max}\mathbf{s0}$) and the chemotherapeutic agent, the optimal control v_* is bang-bang with exactly one switching from $v = 0$ to $v = v_{\max}$. Cytotoxic agents are given in one session at maximum dose. In principle, the activation of the chemotherapeutic agent v is possible anywhere along the optimal monotherapy trajectory, but for a typical set of data, this switching occurs while the control u_* is singular. Only if the total amount of cytotoxic agents is large (respectively small), then the activation can already occur on the first interval where the antiangiogenic dose rate is maximal (respectively, only after all antiangiogenic inhibitors have been used up). In all these cases the minimum value of the tumor volume is realized as the chemotherapeutic drugs run out and this occurs after the angiogenic inhibitors have been used up. Hence treatment ends with an interval where chemotherapy is at maximum dose while antiangiogenic therapy is over.

We present some numerical results for the initial conditions, $(p_0, q_0) = (12{,}000; 15{,}000)$ which corresponds to what may be considered a typical scenario for a strongly growing tumor. In the paper [264], additional examples are given that all support the same structure of optimal protocols. The parameter values for the numerical calculations are given in Table 7.1. The computations, carried out by H. Maurer, proceed in two steps. In a first step, the optimal control problem is discretized on a fixed time grid with $N = 100$ to $N = 500$ time points. The resulting large-scale, nonlinear programming problem is solved by means of a sequential quadratic programming method or by Interior-Point-Methods (cf., e.g., Büskens [43] or Büskens and Maurer [44, 45]). Since singular arcs in an optimal solution often cause numerical

chattering, it is advisable in order to avoid, or at least keep this effect under control numerically, to modify the cost functional by adding a small penalty on the control and thus consider the modified cost functional

$$\min \to J_\varepsilon(u) = p(T) + \varepsilon \int_0^T u(t)^2 dt$$

with a small value of ε, e.g., $\varepsilon = 0.005$. Incorporation of the quadratic term simplifies the numerical computations (see Chapter 4) and for ε small enough the concatenation structure between the bang and interior pieces that is revealed resembles the concatenation structure of optimal controls for the original problem with $\varepsilon = 0$. This step generally only provides a somewhat crude approximation of the singular controls and associated switching times. Hence in a second step the switching times are optimized directly using the arc-parametrization method developed in [234]. The application of this method is made possible by the fact that explicit formulas are available for the controls along each subarc. In all cases considered the cytotoxic agent v was bang-bang with exactly one switching from zero to full dose at a switching time t_v,

$$v_*(t) = \begin{cases} 0 & \text{for} \quad 0 \le t < t_v, \\ v_{\max} & \text{for} \quad t_v \le t < T, \end{cases} \tag{7.35}$$

while the antiangiogenic agent u followed the concatenation sequence $\mathbf{u}_{\max}\mathbf{s0}$ of the monotherapy solution with

$$u_{\text{sing}}(p,q) = \frac{1}{\gamma}\left(\xi \ln\left(\frac{p}{q}\right) + b\frac{p}{q} + \frac{2}{3}\xi\frac{d}{b}\frac{q}{p^{1/3}} - (\mu + p^{2/3})\right) + \frac{\varphi - \eta}{\gamma} v_c$$

where v_c denotes the value of the control v with either $v_c = 0$ or $v_c = v_{\max}$.

Specifically, if we take $\eta = 0$ in the q-dynamics (7.2) and use low upper bounds $v_{\max}$ and $z_{\max}$ for the chemotherapy, then the control structure that results from the discretization procedure is of the following type:

$$(u_*(t), v_*(t)) = \begin{cases} (u_{\max}, 0) & \text{for} \quad 0 \le t < t_1, \\ (u_{\text{sing}}(p(t), q(t)), 0) & \text{for} \quad t_1 \le t < t_2, \\ (u_{\text{sing}}(p(t), q(t)), v_{\max}) & \text{for} \quad t_2 \le t < t_3, \\ (0, v_{\max}) & \text{for} \quad t_3 \le t < T, \end{cases} \tag{7.36}$$

with switching times t_1, t_2 and t_3. Optimizing this structure in the arc-parametrization method, for the upper bounds $v_{\max} = 1$ and $z_{\max} = 2$, the following values were obtained:

$$\begin{aligned} &p(T) = 7019.09, \;\; q(T) = 7365.27, \\ &t_1 = 0.09051, \;\; t_2 = 4.647, \; t_3 = 6.485, \; T = 6.647. \end{aligned}$$

Figure 7.2 shows the corresponding controls and trajectories. The treatment starts with a short period of full dose antiangiogenic therapy and then follows the singular regimen computed above. During this time, the chemotherapy treatment initiates with full dose and continues until the cytotoxic drug is exhausted. Angiogenic inhibitors are fully used up while the chemotherapy is on and before the cytotoxic drugs run out. Local optimality of this control structure with respect to the switching times has been verified through second-order sufficient conditions for the induced switching time optimization problem [234].

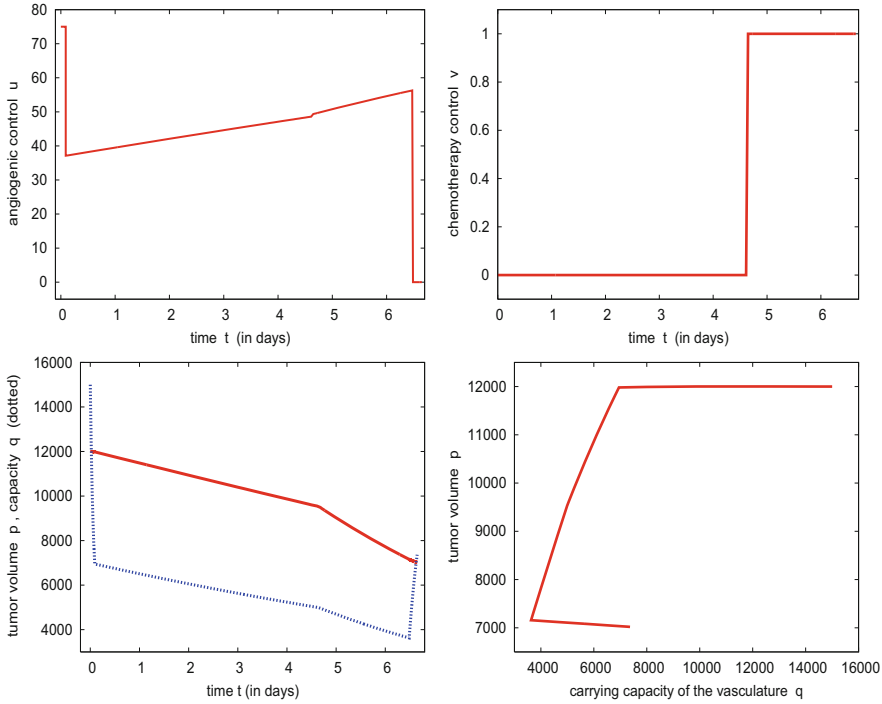

Fig. 7.2 The optimal controls u_* (a, top left) and v_* (b, top right) for initial values $(p_0, q_0) = (12{,}000\,mm^3; 15{,}000\,mm^3)$ with time histories for p and q (c, bottom left) and corresponding trajectory in the (p,q)-plane (d, bottom right) for the case when $v_{\max} = 1$ and $z_{\max} = 2$.

Increasing the bounds on the maximum concentration and available amounts for the cytotoxic agents leads to the same concatenation structure. For the upper limits $v_{\max} = 2$ and $z_{\max} = 10$, a direct optimization of the arc-lengths yields the results given below. The corresponding graphs of the controls and trajectories are shown in Figure 7.3.

$$p(T) = 3285.09,\ \ q(T) = 3993.07,$$
$$t_1 = 0.09051,\ \ t_2 = 1.016,\ t_3 = 5.855,\ T = 6.016.$$

In these calculations we have taken $\eta = 0$ in the dynamics (7.2) for the carrying capacity q, i.e., we assumed that the cytotoxic agent does not effect the vasculature.

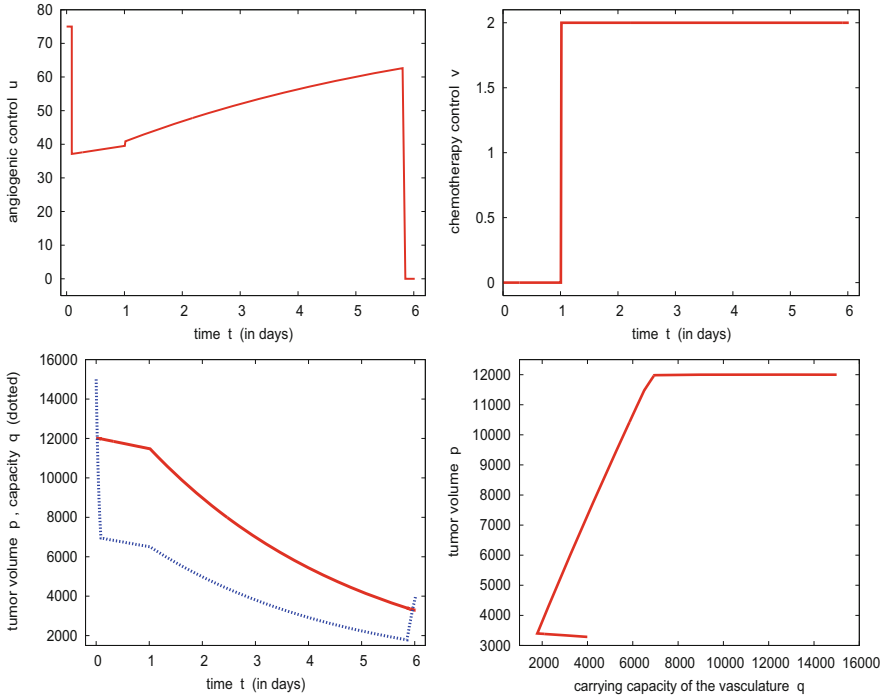

Fig. 7.3 The optimal controls u_* (a, top left) and v_* (b, top right) for initial values $(p_0, q_0) = (12{,}000\,mm^3; 15{,}000\,mm^3)$ with time histories for p and q (c, bottom left) and corresponding trajectory in the (p,q)-plane (d, bottom right) for $v_{\max} = 2$ and $z_{\max} = 10$.

Table 7.2 Terminal values of $p(T)$, $q(T)$ and T for initial condition $(p_0, q_0) = (12{,}000\,mm^3; 15{,}000\,mm^3)$ as η varies from $\eta = 0$ to $\eta = \varphi = 0.1$.

η	$p(T)$	$q(T)$	T
0.0	3285.09	3993.07	6.016
0.01	3282.66	3982.28	6.029
0.02	3280.24	3971.79	6.042
0.05	3272.98	3940.43	6.080
0.1	3260.94	3888.83	6.114

For small positive values of η the value of the performance slightly improves (see Table 7.2), but no qualitative changes occur in the structure of the optimal controls and trajectories. Increasing the parameter η has the effect that the tumor volume $p(T)$ and the carrying capacity $q(T)$ slightly decrease while the final time T slightly increases. Note that for $\eta = \varphi = 0.1$, the second term in the relation (7.28) drops out and in this case the singular control is identical with the one for the monotherapy problem.

Various other calculations support the same structure for the optimal controls, even when extreme sets of initial conditions are considered, like, for example, $(p_0, q_0) = (15{,}000; 1{,}500)$. For very small values, such as $(p_0, q_0) = (625, 200)$ and $(p_0, q_0) = (200, 625)$ the singular control u_{sing} is no longer admissible since its value exceeds the upper bound $u_{\max}$. In these cases the optimal monotherapy is bang-bang of the type $\mathbf{u}_{\max}\mathbf{0}$ and the optimal concatenation structure becomes

$$(u_*(t), v_*(t)) = \begin{cases} (u_{\max}, 0) & \text{for} \quad 0 \le t < t_1, \\ (u_{\max}, v_{\max}) & \text{for} \quad t_1 \le t < t_2, \\ (0, v_{max}) & \text{for} \quad t_2 \le t \le T. \end{cases}$$

Even for these extreme cases, these computations confirm the assertion that the optimal combination therapy follows the optimal monotherapy for u and that chemotherapy is bang-bang with one switching from $v = 0$ to $v = v_{\max}$ which occurs while angiogenic therapy is active; chemotherapy then continues until after angiogenic inhibitors have run out. It follows from Theorem 7.1.1 that chemotherapy cannot be stopped while the antiangiogenic dose rate is singular.

7.1.5 Summary and Medical Discussion

In the optimal control problem [ACh], for a priori determined total doses of antiangiogenic and chemotherapeutic agents, we analyzed the question how to schedule these agents in order to maximize the tumor reduction. Mathematically, this becomes a multi-control problem and the structure of a synthesis of optimal controls is more complex than in the monotherapy case analyzed earlier (Chapter 5). While a theoretical proof of optimality in form of a regular synthesis of optimal controlled trajectories still has not been carried out, once again singular controls along with the partial lower dose rates they determine are the crucial element in the solutions. Numerical results suggest that for a large range of realistic, well-posed initial conditions optimal controls (u_*, v_*) have the following *structure*: the vessel disruptive antiangiogenic agent u_* follows the same pattern as for the monotherapy problem and the cytotoxic agent v_* is bang-bang with one switching from $v = 0$ to $v = v_{\max}$. This switching occurs while the control u_* is singular and the minimum value of the tumor volume is realized as the chemotherapeutic drugs run out. In all cases for which we calculated the optimal solutions numerically, therapy starts with giving angiogenic inhibitors and chemotherapy commences at some optimal time during angiogenic therapy. Chemotherapy then lasts beyond the time when all angiogenic inhibitors are used up and the maximum tumor reduction is achieved as the chemotherapeutic agent became exhausted.

Clearly, this structure is in agreement and supportive of the notion that a regularization of the vasculature is beneficial in order to maximize the effects of

chemotherapy. Naturally, this model is only a first attempt at capturing a very complex situation and more detailed modeling of the response of a tumor to cytotoxic chemotherapy interacting with a vessel-disrupting treatment probably should also take into account that the now perturbed dynamics of the vessels does influence the effectiveness of both those drugs. The drug-induced reduction of the carrying capacity, aside from its influence on the size of the tumor, might decrease the supply of the chemotherapeutic agent and thus, in turn, decrease the beneficial effect of this second therapy. On the other hand, this drug induced reduction, by eliminating small and leaky vessels, makes drug delivery more effective and this precisely is the biomedical rationale of regularizing the tumor vasculature first. In any case, optimal solutions never fully destroy the vasculature, but rather strive to maintain what may be considered an optimal relation between the variable p and q. But, overall, the complex nonlinear interlinking of effects and counter-effects might open interesting perspectives also for the optimal control approach to the problem.

7.2 Combination of Antiangiogenic Treatment and Radiotherapy as Multi-Input Optimal Control Problem

Antiangiogenic treatments have also been combined with radiotherapy in order to achieve a better definition of the target tumor. In fact, this was the motivation for the paper by Ergun, Camphausen, and Wein [77]. Basic models for the effects of radiotherapy have been described in Section 1.3 and combining them with a model for angiogenic signaling again leads to multi-input control systems. Depending on how detailed an approach is taken to model the radiation damage (e.g., to what extent its effects on tumor cells, the vasculature, and healthy cells are distinguished), systems of varying dimensions arise. Once more singular controls arise naturally in the solutions of the corresponding optimal control problems, but their form depends on the available degrees of freedom and these are closely related to the dimension of the state space. In this section, we derive these formulas for a 5-dimensional model where the dynamics for tumor-vascular interactions is given by model [E] and a 6-dimensional model that differentiates radiation damage to the healthy tissue and is based on the model [H].

7.2.1 A General Formulation

We recall the linear-quadratic (LQ) model for radiation damage from Section 1.3.1. Denoting the radiation dose rate by w, the damage of radiation to the tumor can be modeled in the form

$$-p(t)\left(\alpha+\beta\int_0^t w(s)\exp(-\rho(t-s))ds\right)w(t) \tag{7.37}$$

where α, β and ρ are positive constants. The linear component $-\alpha pw$ is equivalent to a log-kill term and represents the damage done by double-strand breaks with α the corresponding probability. The coefficient β in the quadratic term is related to the probability that two single-strand breakages occur and the coefficient ρ in the exponential denotes the tumor repair rate. The probability that two such breaks occurring at times s and t will be lethal is modeled to decay exponentially with repair rate ρ. The parameters α and β are the tumor LQ parameters in the medical literature. The integral term in parenthesis in (7.37) is simply the solution to the first order linear differential equation

$$\dot{r}=-\rho r+w, \qquad r(0)=0, \tag{7.38}$$

and thus the radiation damage can also be written in the form

$$-p(t)\left(\alpha+\beta r(t)\right)w(t). \tag{7.39}$$

For a constant dose rate $\bar{w}$ in steady state we have that $\bar{r}=\frac{\bar{w}}{\rho}$ and thus the damage term becomes the standard linear-quadratic expression $-p\left(\alpha\bar{w}+\frac{\beta}{\rho}\bar{w}^2\right)$. Equation (7.37) better models the transient behavior and the structure of the overall model becomes clearer if we replace the integral with the differential equation (7.38).

A slow tumor repair rate implies a larger influence of the integral term in the quadratic component and thus a greater effectiveness of the therapy. On the other hand, for fast repair rates, the integral may be replaced with its steady-state value. In the combined model with angiogenic signaling we distinguish three different types of tissue: cancer cells, endothelial cells related to the carrying capacity of the vasculature, and healthy cells that endure the side effects of treatments. The parameters that describe the damage of radiotherapy are tissue specific and thus, incorporating a linear-quadratic model into the general dynamical system that describes the tumor-vascular interactions, we arrive at the following five-dimensional system:

$$\begin{aligned}
\dot{p} &= pF\left(\frac{p}{q}\right)-(\alpha+\beta r_p)pw, && p(0)=p_0\\
\dot{q} &= S(p,q)-I(p,q)-\gamma qu-(\eta+\delta r_q)qw, && q(0)=q_0\\
\dot{r}_i &= -\rho_i r_i+w, && i=p,q,z,
\end{aligned}$$

with the parameters α and η accounting for the linear damage caused by radiation to the tumor and the vasculature, respectively, and β and δ the parameters associated with the quadratic part of the damage. The three equations for r_p, r_q and r_z, respectively, represent the effects of tissue repair with the coefficients ρ_p, ρ_q and ρ_z denoting the *repair rates* for the tumor, the vasculature and the healthy cells, accordingly.

An optimal control problem now arises as we limit the available amounts of antiangiogenic agents and the damage done to healthy cells by the radiation ionization. Mathematically, this gives rise to two isoperimetric constraints. As before, we simply limit the total amount of antiangiogenic agents administered, $\int_0^T u(t)dt \le y_{\max}$, and we also limit the total damage caused by the radiation treatment to the healthy tissue expressed in terms of its biologically equivalent dose (BED) as

$$\int_0^T (1+\theta r_z(t))w(t)dt \le z_{\max}. \tag{7.40}$$

In [77], in addition a constraint on the early-responding tissue [340] is considered that is related to the behavior of these tissues between fractionated dosages and takes into account repopulation. Here we only consider a simplified model that does not distinguish between early and late responding tissue and thus the early responding tissue constraint is omitted. In medical practice, the limits $y_{\max}$ and $z_{\max}$ generally are decided upon at the beginning of the therapy period. The question thus becomes how these amounts of therapeutic agents and total radiation dose can best be administered to have an "optimal" effect. Again, we choose as objective to be minimized the tumor volume $p(T)$ and incorporate the constraints into the problem by adding extra states y and z that keep track of the total amounts of antiangiogenic agents given, respectively, the total damage done by radiotherapy. We thus arrive at the following formulation:

[AR-gen] for a free terminal time T, minimize the objective $J(u,w) = p(T)$ subject to the dynamics

$$\dot{p} = pF\left(\frac{p}{q}\right) - (\alpha + \beta r_p)\, pw, \qquad p(0) = p_0, \tag{7.41}$$

$$\dot{q} = S(p,q) - I(p,q) - \gamma q u - (\eta + \delta r_q)\, qw, \qquad q(0) = q_0, \tag{7.42}$$

$$\dot{r}_i = -\rho_i r_i + w, \qquad i = p,q,z \qquad r(0) = 0, \tag{7.43}$$

$$\dot{y} = u, \qquad y(0) = 0, \tag{7.44}$$

$$\dot{z} = (1+\theta r_z)w, \qquad z(0) = 0, \tag{7.45}$$

over all Lebesgue measurable (respectively, piecewise continuous) functions

$$u : [0,T] \to [0,u_{\max}] \quad \text{and} \quad w : [0,T] \to [0,w_{\max}]$$

for which the corresponding trajectory satisfies the end-point constraints

$$y(T) \le y_{\max} \qquad \text{and} \qquad z(T) \le z_{\max}.$$

We only remark that under any assumptions on the general functions F, S and I that define a reasonable model for the tumor-vascular interactions, and for any admissible controls u and w, the solutions p and q to the dynamics will remain positive for all times and there is no need to impose a nonnegativity constraint on p and q. Also, it needs to be pointed out that we consider a fully continuous-time formulation. It is our aim to illustrate that such a model leads to effective and simple

procedures to arrive at formulas for singular treatment schedules. Similarly as it was done for the antiangiogenic monotherapy problem in Chapter 6, from these solutions piecewise continuous approximations that relate to fractionated dosages can be obtained.

7.2.2 Necessary Conditions for Optimality

We write the dynamics (7.41)–(7.45) underlying the optimal control problem [ARgen] in the form

$$\dot{\chi} = f(\chi) + ug_1(\chi) + wg_2(\chi), \tag{7.46}$$

with $\chi = (p, q, r_p, r_q, r_z, y, z)^T$ the 7-dimensional state vector and the vector fields f, g_1 and g_2 describing the dynamics. As in the problems considered earlier, the issue of whether the total amounts of agents suffice to reduce the tumor volume below its initial volume comes up. Throughout this section we assume that this is the case. Specifically, we assume that the initial condition (p_0, q_0) is *well posed* in the sense that the terminal time T along an optimal solution is positive and that all available therapeutic agents are used up. Thus we have that $y_*(T) = y_{\max}$ and $z_*(T) = z_{\max}$ hold along an optimal solution. Then, if u_* and w_* are optimal controls defined over an interval $[0, T]$ with corresponding trajectory χ_*, it follows from the maximum principle (Theorem A.2.1 in Appendix A) that there exist a constant $\lambda_0 \geq 0$ and an absolutely continuous co-vector, $\lambda : [0, T] \to (\mathbb{R}^7)^*$, such that (i) $(\lambda_0, \lambda(t)) \neq (0, 0)$ for all $t \in [0, T]$, (ii) λ satisfies the adjoint equations

$$\dot{\lambda}(t) = -\langle \lambda(t), Df(\chi_*(t)) + u_*(t)Dg_1(\chi_*(t)) + w_*(t)Dg_2(\chi_*(t)) \rangle, \tag{7.47}$$

with terminal condition

$$\lambda(T) = (\lambda_0, 0, 0, 0, 0, \lambda_6, \lambda_7)^T \tag{7.48}$$

where λ_6 and λ_7 are nonnegative constants and (iii) the controls $u_*(t)$ and $w_*(t)$ minimize the Hamiltonian H,

$$H = \langle \lambda, f(\chi) + ug_1(\chi) + wg_2(\chi) \rangle,$$

along $(\lambda(t), \chi_*(t))$ over the control set $[0, y_{\max}] \times [0, z_{\max}]$ with the minimum value given by 0.

We note that the multiplier $\lambda = \lambda(t)$ is always nonzero. For, λ is a solution to a homogenous linear differential equation and if $\lambda(\tau) = 0$ for some time τ, then λ vanishes identically and thus also $\lambda_0 = 0$. This contradicts the nontriviality condition (i) for the multipliers. Also, it follows from the adjoint equation (7.47) that the multipliers λ_6 and λ_7 are constant and the nonnegativity requirements are the same complementary slackness conditions as derived in Lemma 7.1.2 for the case of the optimal control problem [ACh]. As before, we define the switching functions Φ_1 and Φ_2 as,

$$\Phi_1(t) = \langle \lambda(t), g_1(\chi_*(t)) \rangle \qquad \text{and} \qquad \Phi_2(t) = \langle \lambda(t), g_2(\chi_*(t)) \rangle. \tag{7.49}$$

It follows that optimal controls u_* and w_* satisfy

$$u_*(t) = \begin{cases} 0 & \text{if } \Phi_1(t) > 0, \\ u_{\max} & \text{if } \Phi_1(t) < 0, \end{cases} \quad \text{and} \quad w_*(t) = \begin{cases} 0 & \text{if } \Phi_2(t) > 0, \\ w_{\max} & \text{if } \Phi_2(t) < 0. \end{cases}$$

Derivatives of the switching functions are computed using Proposition 7.1.1.

The further analysis of the problem requires to specify the growth function F and the stimulation and inhibition terms, $S(p,q)$ and $I(p,q)$. Below we consider both the underlying dynamics from model [E] and [H] considered in Chapter 5. Furthermore, in order to elucidate the roles of singular controls, we first consider a model where we identify the repair rates for the various types of tissue resulting in a simplified five-dimensional system and then increase the dimension as we differentiate these rates for healthy and tumor cells.

7.2.3 A 5-dimensional Model with Equal Repair Rates

We use a Gompertzian function, $F(x) = -\xi \ln x$, to model tumor growth and employ the terms $S(p,q) = bq^{\frac{2}{3}}$ and $I(p,q) = dq^{\frac{4}{3}}$ of model [E] for the stimulation and inhibition terms in the dynamics for the carrying capacity. Also, in this first model, rather than distinguishing between the repair rates ρ_p, ρ_q and ρ_z for the tumor, vasculature, and healthy cells, we take them all equal and thus instead of having three equations for r_p, r_q and r_z that enter the quadratic effects, we only have one equation, $\dot{r} = -\rho r + w$, reducing the dimension by 2. Thus, we consider the following optimal control problem with five-dimensional state space $\chi = (p,q,r,y,z)^T$ and two controls u and w:

[AR5] for a free terminal time T, minimize the objective $J(u,w) = p(T)$ subject to the dynamics

$$\dot{p} = -\xi p \ln\left(\frac{p}{q}\right) - (\alpha + \beta r)\, pw, \qquad p(0) = p_0, \tag{7.50}$$

$$\dot{q} = bq^{\frac{2}{3}} - dq^{\frac{4}{3}} - \gamma qu - (\eta + \delta r)\, qw, \qquad q(0) = q_0, \tag{7.51}$$

$$\dot{r} = -\rho r + w, \qquad c(0) = 0, \tag{7.52}$$

$$\dot{y} = u, \qquad y(0) = 0, \tag{7.53}$$

$$\dot{z} = (1 + \theta r)w, \qquad z(0) = 0, \tag{7.54}$$

over all Lebesgue measurable (respectively, piecewise continuous) functions

$$u : [0,T] \to [0, u_{\max}] \quad \text{and} \quad w : [0,T] \to [0, w_{\max}]$$

for which the corresponding trajectory satisfies the end-point constraints

$$y(T) \le y_{\max} \qquad \text{and} \qquad z(T) \le z_{\max}.$$

Formally, if we allow the coefficients β, δ and θ to be zero, this model reduces to the mathematical model for combination of antiangiogenic therapy with chemotherapy for model [E] similarly to the one considered for model [H] in Section 7.1. The adjoint equations read as follows:

$$\dot{\lambda}_1(t) = \lambda_1(t)\left(\xi\left(\ln\left(\frac{p_*(t)}{q_*(t)}\right)+1\right)+(\alpha+\beta r_*(t))\,w_*(t)\right), \qquad \lambda_1(T)=\lambda_0, \tag{7.55}$$

$$\dot{\lambda}_2(t) = -\lambda_1(t)\xi\frac{p_*(t)}{q_*(t)} - \lambda_2(t)\left(\frac{2}{3}bq^{-\frac{1}{3}} - \frac{4}{3}dq^{\frac{1}{3}} - \gamma u_*(t) - (\eta+\delta r)\,w_*(t)\right), \qquad \lambda_2(T)=0, \tag{7.56}$$

$$\dot{\lambda}_3(t) = \lambda_1(t)\beta p_*(t)w_*(t) + \lambda_2(t)\delta q_*(t)w_*(t), \qquad \lambda_3(T)=0, \tag{7.57}$$

and λ_4 and λ_5 are nonnegative constants.

The drift vector field f and the control vector fields g_1 and g_2 are given by

$$f(\chi)=\begin{pmatrix} -\xi p\ln\left(\frac{p}{q}\right) \\ bq^{\frac{2}{3}} - dq^{\frac{4}{3}} \\ -\rho r \\ 0 \\ 0 \end{pmatrix}, \quad g_1(\chi)=\begin{pmatrix} 0 \\ -\gamma q \\ 0 \\ 1 \\ 0 \end{pmatrix} \quad \text{and} \quad g_2(\chi)=\begin{pmatrix} -(\alpha+\beta r)\,p \\ -(\eta+\delta r)\,q \\ 1 \\ 0 \\ 1+\theta r \end{pmatrix}. \tag{7.58}$$

The vector fields g_1 and g_2 commute, $[g_1,g_2]=0$, and somewhat longer, but direct and elementary calculations verify the following formulas for the first- and second-order Lie brackets:

$$[f,g_1](\chi) = \gamma\begin{pmatrix} \xi p \\ -\frac{1}{3}\left(bq^{\frac{2}{3}} + dq^{\frac{4}{3}}\right) \\ 0 \\ 0 \\ 0 \end{pmatrix}, \tag{7.59}$$

$$\begin{aligned}[f,g_2](\chi) &= \begin{pmatrix} (\eta+\delta r)\,\xi p - (\alpha+\beta r)\,\xi p + \beta\rho rp \\ -\frac{1}{3}(\eta+\delta r)\left(bq^{\frac{2}{3}} + dq^{\frac{4}{3}}\right) + \delta\rho rq \\ \rho \\ 0 \\ -\rho\theta r \end{pmatrix} \\ &= \frac{\eta+\delta r}{\gamma}[f,g_1](\chi) + \begin{pmatrix} -(\alpha+\beta r)\,\xi p + \beta\rho rp \\ \delta\rho rq \\ \rho \\ 0 \\ -\rho\theta r \end{pmatrix},\end{aligned} \tag{7.60}$$

$$[g_1,[f,g_1]](\chi) = -\frac{1}{9}\gamma^2 \begin{pmatrix} 0 \\ bq^{\frac{2}{3}} - dq^{\frac{4}{3}} \\ 0 \\ 0 \\ 0 \end{pmatrix}, \tag{7.61}$$

$$[g_2,[f,g_1]](\chi) = -\frac{1}{9}\gamma(\eta+\delta r) \begin{pmatrix} 0 \\ bq^{\frac{2}{3}} - dq^{\frac{4}{3}} \\ 0 \\ 0 \\ 0 \end{pmatrix} \tag{7.62}$$

and

$$[g_2,[f,g_2]](\chi) = \begin{pmatrix} (\delta-\beta)\xi p + 2\rho\beta p \\ -\frac{1}{9}(\eta+\delta r)^2\left(bq^{\frac{2}{3}} - dq^{\frac{4}{3}}\right) - \frac{\delta}{3}\left(bq^{\frac{2}{3}} + dq^{\frac{4}{3}}\right) + 2\rho\delta q \\ 0 \\ 0 \\ -2\rho\theta \end{pmatrix}. \tag{7.63}$$

The formulas for the second-order Lie brackets with f, especially, for $[f,[f,g_2]]$, become rather unwieldy and we do not list them.

These brackets collectively determine explicit analytical formulas for singular controls u and w. Since the control vector fields g_1 and g_2 commute, $[g_1,g_2](\chi) \equiv 0$, applying Proposition 7.1.1 to Φ_i gives that

$$\dot{\Phi}_i(t) = \langle \lambda(t), [f+ug_1+wg_2, g_i](\chi(t))\rangle = \langle \lambda(t), [f,g_i](\chi(t))\rangle \tag{7.64}$$

and

$$\ddot{\Phi}_i(t) = \langle \lambda(t), [f+ug_1+wg_2, [f,g_i]](\chi(t))\rangle \equiv 0, \quad i=1,2. \tag{7.65}$$

Formulas for singular controls u can quite simply be computed explicitly and regardless of the structure of the control w. The reason lies in the following relation that is satisfied between second-order Lie brackets. Simple inspection of (7.62) shows that

$$[g_2,[f,g_1]](\chi) = \frac{\eta+\delta r}{\gamma}[g_1,[f,g_1]](\chi). \tag{7.66}$$

This relation allows to eliminate the Lie bracket $[g_2,[f,g_1]]$ from equation (7.65) for $\ddot{\Phi}_1$. In fact,

$$\ddot{\Phi}_1(t) = \langle \lambda(t), [f,[f,g_1]](\chi(t))\rangle + \frac{1}{\gamma}(\gamma u + (\eta+\delta r)w)\langle \lambda(t), [g_1,[f,g_1]](\chi(t))\rangle. \tag{7.67}$$

If we set

$$\tilde{u} = u + \frac{\eta+\delta r}{\gamma}w, \tag{7.68}$$

then equation (7.67) is identical with the formula that defines the singular control in the monotherapy case considered in Section 5.4,

$$\ddot{\Phi}_1(t) = \langle \lambda(t), [f + \tilde{u}g_1, [f, g_1]](x(t)) \rangle \equiv 0.$$

Hence all results directly carry over if we replace u with $\tilde{u}$. More specifically, in the monotherapy case, the effect of the antiangiogenic agent on the carrying capacity q is given by $-\gamma q u$. Replacing u with $\tilde{u}$, this term becomes

$$-\gamma q \tilde{u} = -\gamma q u - (\eta + \delta r) q w$$

and thus for model [AR5] the *combined effect* that an optimal singular control u_{sing} and a radiation dose rate w have on $\dot{q}$ *is identical to the monotherapy case*. Furthermore,

$$\langle \lambda(t), [g_1, [f, g_1]](\chi(t)) \rangle = -\gamma^2 b p \lambda_2(t).$$

The conditions of the maximum principle give that the multipliers λ_4 and λ_5 are constant and nonnegative. Since the switching function vanishes on I, we have that $\lambda_2(t)\gamma q_*(t) \equiv \lambda_4 \geq 0$. If $\lambda_4 = 0$, it follows that λ_2 vanishes identically on I and then the adjoint equations (7.55)–(7.57) imply that also λ_1 and λ_3 vanish identically. But then λ_5 must be positive and $\Phi_2(t) \equiv \lambda_5$ implies that $w_*(t) \equiv 0$ contradicting the fact that the initial condition is well posed for the data. Thusλ_2 is positive on I and the strengthened Legendre-Clebsch condition is satisfied. The following result therefore directly follows from Proposition 5.4.2.

Proposition 7.2.1. *If the optimal control u_* is singular on an open interval I, $u_*(t) = u_{\text{sing}}(t)$, and the radiotherapy schedule given by $w_*(t)$, then $\gamma u_{\text{sing}}(t) + (\eta + \delta r_*(t)) w_*(t)$ is a smooth feedback control that only depends on the carrying capacity $q_*(t)$ in the form*

$$\gamma u_{\text{sing}}(t) + (\eta + \delta r_*(t)) w_*(t) = \Psi\left(\sqrt[3]{q_*(t)}\right), \tag{7.69}$$

where

$$\Psi(x) = \frac{b - dx^2}{x} + 3\xi \frac{b + dx^2}{b - dx^2}. \tag{7.70}$$

If we set β, δ, and θ to be zero, then this formula also gives us the formula for combining antiangiogenic treatment with chemotherapy for model [E]. Thus, like for the model considered in Section 7.1, also in this case there is an immediate and mathematically simple extension of the formula that determines the optimal singular antiangiogenic dose rate to the more structured and more complicated mathematical model that describes the combination treatment with chemo- or radiotherapy.

However, for radiotherapy the structure of the second control is very different. Different from the case of combined antiangiogenic treatment with chemotherapy, the radiation dose rate typically will—if the bounds on the dosages permit—be singular as well. Generally, if all controls of a multi-input control are simultaneously singular, these controls are said to be *totally singular*. Such controls are the defining

structure for the combination of antiangiogenic therapy with radiotherapy. For this, we need a second equation that links u_{sing} with w_{sing}. If w is singular on an open interval I, then also

$$\Phi_2(t) = \langle \lambda(t), g_2(\chi(t)) \rangle \equiv 0, \qquad \dot{\Phi}_2(t) = \langle \lambda(t), [f, g_2](\chi(t)) \rangle \equiv 0$$

and

$$\ddot{\Phi}_2(t) = \langle \lambda(t), [f + ug_1 + wg_2, [f, g_2]](\chi(t)) \rangle = 0. \tag{7.71}$$

Since g_1 and g_2 commute, it follows from the Jacobi-identity that $[g_1, [f, g_2]](\chi) = [g_2, [f, g_1]](\chi)$ (also see (7.31)). The vector fields g_1, g_2, $[f, g_1]$, $[f, g_2]$ and $[g_2, [f, g_2]]$ are linearly independent and form a basis for the state space. The second-order Lie brackets $[f, [f, g_2]]$ and $[g_1, [f, g_2]]$ can therefore be expressed in the form

$$[f, [f, g_2]] = a_1 g_1 + a_2 g_2 + a_3 [f, g_1] + a_4 [f, g_2] + A [g_2, [f, g_2]] \tag{7.72}$$

$$[g_1, [f, g_2]] = b_1 g_1 + b_2 g_2 + b_3 [f, g_1] + b_4 [f, g_2] + B [g_2, [f, g_2]] \tag{7.73}$$

where the vector fields and coefficients a_i, b_i, A, and B all are functions of χ. It is easy to see that, because of the overall structure of the dynamics, the y (or fourth) coordinate of the vector fields g_2, $[f, g_1]$, $[f, g_2]$, $[g_2, [f, g_2]]$, $[g_1, [f, g_2]]$, and $[f, [f, g_2]]$ vanishes and thus the coefficients a_1 and b_1 vanish identically. If desired, it is possible (using Cramer's rule) to give explicit analytical formulas for the remaining coefficients in terms of determinants that only involve the vector fields in the dynamics and some of their iterated Lie brackets. If both controls are singular over an open interval I, then the multiplier $\lambda(t)$ vanishes against the vector fields g_1, g_2, $[f, g_1]$ and $[f, g_2]$ along the trajectory $\chi_*(t)$. We therefore get that

$$\langle \lambda(t), [f, [f, g_2]](\chi_*(t)) \rangle = A(\chi_*(t)) \langle \lambda(t), [g_2, [f, g_2]](\chi_*(t)) \rangle,$$

and

$$\langle \lambda(t), [g_1, [f, g_2]](\chi_*(t)) \rangle = B(\chi_*(t)) \langle \lambda(t), [g_2, [f, g_2]](\chi_*(t)) \rangle.$$

Since the multiplier λ is nontrivial, it cannot vanish against $[g_2, [f, g_2]]$ along χ_* and thus the expression $\langle \lambda(t), [g_2, [f, g_2]](\chi_*(t)) \rangle$ is nonzero. Equation (7.71) therefore reduces to the linear equation

$$0 = A(\chi_*(t)) + u_{\text{sing}}(t) B(\chi_*(t)) + w_{\text{sing}}(t).$$

Thus we have the following result:

Proposition 7.2.2. *If both the optimal antiangiogenic dose rate/concentration u and the radiation dose schedule w follow singular regimens u_{sing} and w_{sing} on an open interval I, then, in addition to equation (7.69), the relation*

$$A(\chi_*(t)) + B(\chi_*(t)) u_{\text{sing}}(t) + w_{\text{sing}}(t) \equiv 0 \tag{7.74}$$

holds along the optimal controlled trajectory χ_* on I; A and B are the smooth functions defined in equations (7.72) and (7.73).

Overall, $(u_{\text{sing}}, w_{\text{sing}})$ thus are the solutions of the 2×2 system of linear equations defined by (7.69) and (7.74) whose coefficients are determined solely by the equations defining the dynamics of the system. As already mentioned, it is possible to give explicit expressions for the functions A and B and thus also for the singular controls. But these formulas depend on the second derivatives of the terms in the dynamics and they are long and unwieldy. On the other hand, given a particular value (p,q) and values of the parameters, it is straightforward to compute these coefficients A and B numerically and then solve for the controls. Figure 7.4 shows two examples of singular controls u_{sing} and w_{sing} computed in this way for the parameter values given in Table 7.3. These values are based on the data in [77] and [116], but are only meant to illustrate the mathematical procedure.

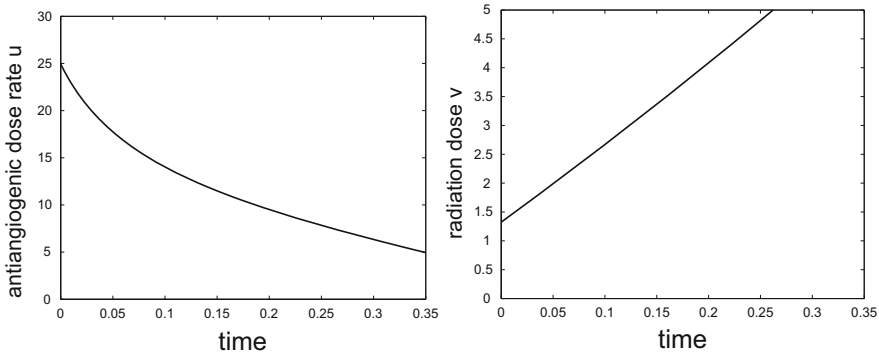

Fig. 7.4 Examples for singular dose rates u_{sing} and w_{sing} for the values in Table 7.3.

If both controls u and w are singular over an interval I, then the multiplier λ vanishes against the vector fields g_1, g_2, $[f,g_1]$ and $[f,g_2]$ along the trajectory χ_*. Furthermore,

$$H = \langle \lambda(t), f(\chi_*(t)) \rangle + u_{\text{sing}}(t)\Phi_1(t) + w_{\text{sing}}(t)\Phi_2(t) \equiv 0,$$

and thus λ also vanishes against the vector field f. Since λ is nontrivial, these five vector fields must be linearly dependent along a singular arc. Hence totally singular controls are only optimal on a singular hyper-surface $\mathscr{S}$ defined by

$$\mathscr{S} = \{\chi : \det(f(\chi), g_1(\chi), g_2(\chi), [f,g_1](\chi), [f,g_2](\chi)) = 0\}, \tag{7.75}$$

where, as before, det denotes the determinant of the matrix whose ordered columns are f, g_1, g_2, $[f,g_1]$ and $[f,g_2]$. The auxiliary variables y and z that keep track of how much inhibitors are still available, respectively, how close to the maximum allowable total BED the radiation damage already is, do not enter into this computation and $\mathscr{S}$ therefore can be visualized as a surface in (p,q,r)-space. The values of the variables y and z only indicate whether it is still allowed to follow trajectories on this surface or not. A somewhat longer computation shows that this surface actually can be described as the graph of a function of q and r in the form

Table 7.3 Notations for the variables, controls, and coefficients for the optimal control problem [AR-5].

Symbol		Units	Value used in computations	Reference
p	Primary tumor volume	$[\text{mm}^3]$		
q	Carrying capacity of the vasculature	$[\text{mm}^3]$		
r	Variable related to quadratic radiation effects (repair)			
y	Amount of antiangiogenic agent used so far	[mg]		
z	Cumulative radiation dose in BED	$[Gy]$		
x	State vector - $(p,q,r,y,z)^T$			
ξ	Tumor growth parameter	$[\text{day}^{-1}]$	0.192	[17]
b	Tumor-induced stimulation parameter	$[\text{day}^{-1}]$	5.85	[17]
d	Tumor-induced inhibition parameter	$[\text{mm}^{-2}\ \text{day}^{-1}]$	0.00873	[17]
μ	Baseline loss of vascular support through natural causes	$[\text{day}^{-1}]$	0 for [AR5] 0.02 for [AR6]	
u	Antiangiogenic agent dose rate	$\left[\frac{mg\,\text{of dose}}{kg}\right]\ \text{day}^{-1}$		
$u_{\max}$	Maximum allowable dose for the antiangiogenic agent	$\left[\frac{mg\,\text{of dose}}{kg}\right]\ \text{day}^{-1}$		
$y_{\max}$	Available total amount for the antiangiogenic agent	$\left[\frac{mg\,\text{of dose}}{kg}\right]$		
w	Radiation dose	$[Gy]\ \text{day}^{-1}$		
$w_{\max}$	Maximum allowable radiation dose	$[Gy]\ \text{day}^{-1}$		
$z_{\max}$	Maximum allowable total BED	$[Gy]$		
γ	Antiangiogenic elimination parameter	$\left[\frac{kg}{mg\,\text{of dose}}\right]\ \text{day}^{-1}$	0.15	[17]
α	Tumor LQ parameter	$[Gy^{-1}]$	0.7	[18]
β	Tumor LQ parameter	$[Gy^{-2}]$	0.140	[18]
η	Endothelial LQ parameter	$[Gy^{-1}]$	0.136	[18]
δ	Endothelial LQ parameter	$[Gy^{-2}]$	0.086	[18]
θ	Healthy tissue parameter	day^{-1}	0.5	[18]
ρ	Tumor/endothelial repair rate	day^{-1}	$\frac{\ln(2)}{0.02}$	[18]
σ	Healthy tissue repair rate	day^{-1}	$\frac{\ln(2)}{0.16}$	[18]

$$\mathscr{S}: \qquad p = q\exp(\zeta(q,r))$$

with ζ given by

$$\zeta(q,r) = 3\frac{b-dq^{\frac{2}{3}}}{b+dq^{\frac{4}{3}}} - \frac{\alpha r + \left[\beta\left(1-\frac{\rho}{\xi}\right)+\theta\alpha\left(1+\frac{\rho}{\xi}\right)\right]r^2+\theta\beta r^3}{1+2\theta r} - 3\rho\left(\eta\theta-\delta\right)\frac{r^2}{1+2\theta r}\frac{q^{\frac{1}{3}}}{b+dq^{\frac{4}{3}}}.$$

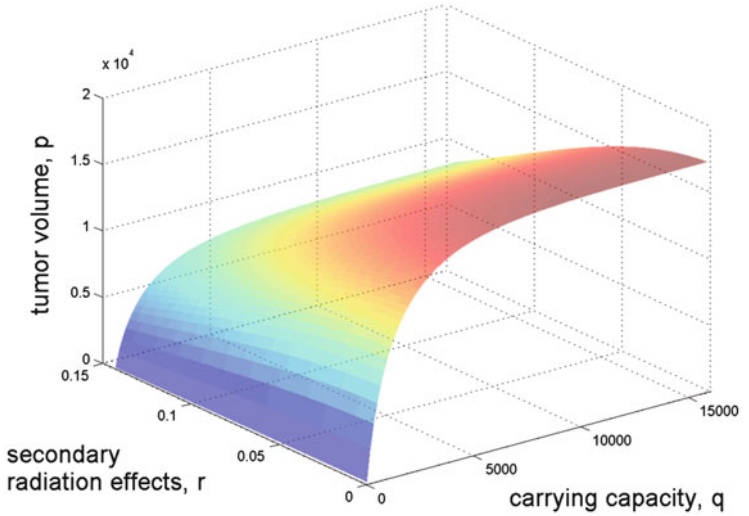

Fig. 7.5 The totally singular surface $\mathscr{S}$ for model [AR5] and parameter values given in Table 7.3.

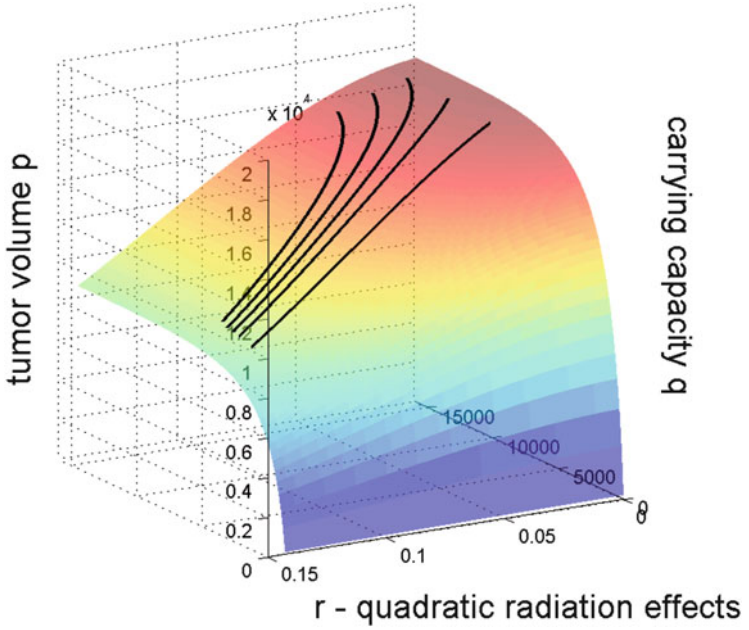

Fig. 7.6 Samples of totally singular controlled trajectories on $\mathscr{S}$ for the parameter values in Table 7.3.

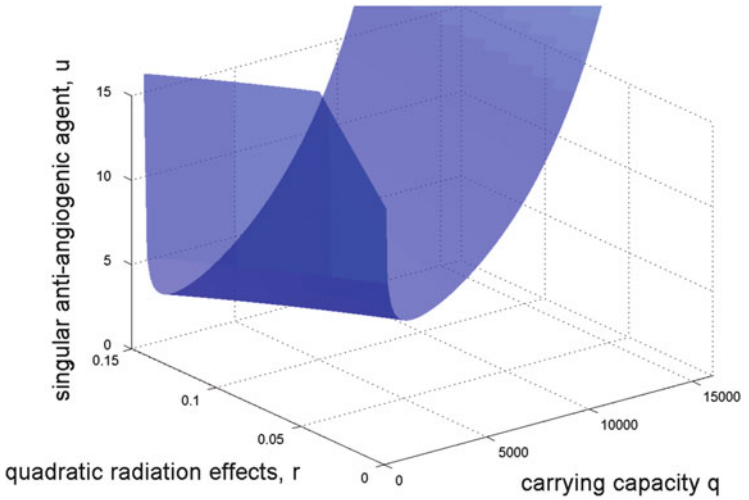

Fig. 7.7 Values of the singular control u_{sing} on the singular surface $\mathscr{S}$ expressed as function of the base values q and r for the parameter values in Table 7.3.

Figure 7.5 shows the surface $\mathscr{S}$ in the three-dimensional (p,q,r)-subspace. For $r = 0$, we obtain the curve representing the optimal singular arc in the case of monotherapy treatment from Section 5.4. We see that, once the variable $r(t)$, which determines the quadratic terms for the radiation damage, increases, both the tumor volume $p(t)$ and the vasculature $q(t)$ decrease. Figure 7.6 shows a different view of the same surface with some of the responses corresponding to the totally singular flow shown on the surface and Figures 7.7 and 7.8 show the values of the singular controls u_{sing} and w_{sing} on the singular surface as functions of the base variables q and r.

7.2.4 A 6-dimensional Model with a Different Repair Rate for the Healthy Tissue

Naturally, the repair rates for tumor cells, endothelial cells, and healthy cells are not the same and thus should be modeled by separate equations (7.52) with different parameters ρ_i. This leads to similar formulations, but in spaces of varying dimensions. Mathematically, this generates different behaviors since the degrees of freedom that come with higher dimensional state-spaces no longer force singular flows to be constrained to lower dimensional submanifolds as this is the case for the 5-dimensional system just considered. In the literature, often the effects of radiation therapy on the tumor cells and its vasculature are modeled by one equation (e.g., see [77], where equal numerical values are used for these repair rates that are based on [36]) and here we take this approach as well. As before, we then include

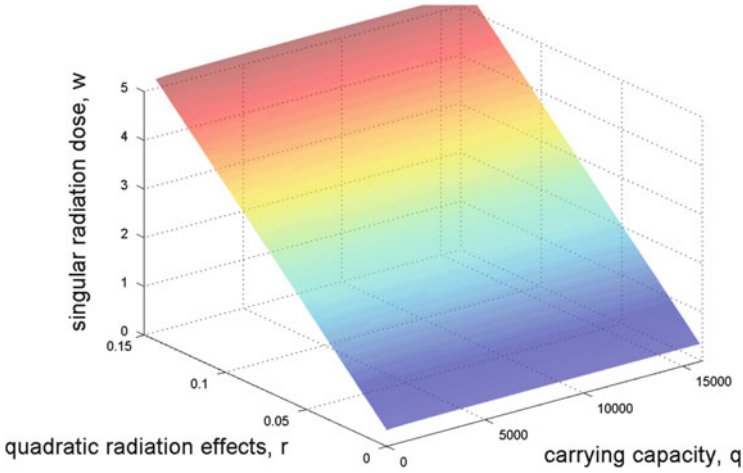

Fig. 7.8 Values of the singular control w_{sing} on the singular surface $\mathscr{S}$ expressed as function of the base values q and r for the parameter values in Table 7.3.

separate states y and z that keep track of the total amounts of antiangiogenic agents given, respectively, the total damage done by radiotherapy measured in terms of its biologically equivalent dose (BED). In this section, we also change back equation (7.52) for the carrying capacity from model [E] to model [H]. We then arrive at the following 6-dimensional optimal control formulation:

[AR6] for a free terminal time T, minimize the objective $J(u,w) = p(T)$ subject to the dynamics

$$\dot{p} = -\xi\, p \ln\left(\frac{p}{q}\right) - (\alpha + \beta r)\, pw, \qquad p(0) = p_0, \tag{7.76}$$

$$\dot{q} = bp - \left(\mu + d p^{\frac{2}{3}}\right) q - \gamma q u - (\eta + \delta r)\, qw, \qquad q(0) = q_0, \tag{7.77}$$

$$\dot{r} = -\rho r + w, \qquad r(0) = 0, \tag{7.78}$$

$$\dot{y} = u, \qquad y(0) = 0, \tag{7.79}$$

$$\dot{z} = (1 + \theta s) w, \qquad z(0) = 0, \tag{7.80}$$

$$\dot{s} = -\sigma s + w, \qquad s(0) = 0, \tag{7.81}$$

over all Lebesgue measurable (respectively, piecewise continuous) functions

$$u : [0,T] \to [0, u_{\max}] \quad \text{and} \quad w : [0,T] \to [0, w_{\max}]$$

for which the corresponding trajectory satisfies the end-point constraints

$$y(T) \le y_{\max} \qquad \text{and} \qquad z(T) \le z_{\max}.$$

The meaning of the parameters is the same as before (see Table 7.3). The only new parameter is a different repair rate σ for healthy tissue in (7.81). We also are

interested to see what implications the changes in the q-dynamics have on the system. The state of the system is now given by $\chi = (p,q,r,y,z,s)^T$ and the drift vector field f and the control vector fields g_1 and g_2 take the form

$$f(\chi) = \begin{pmatrix} -\xi p \ln\left(\frac{p}{q}\right) \\ bp - (\mu + dp^{\frac{2}{3}})q \\ -\rho r \\ 0 \\ 0 \\ -\sigma s \end{pmatrix}, \; g_1(\chi) = \begin{pmatrix} 0 \\ -\gamma q \\ 0 \\ 1 \\ 0 \\ 0 \end{pmatrix}, \; g_2(\chi) = \begin{pmatrix} -(\alpha + \beta r)\, p \\ -(\eta + \delta r)\, q \\ 1 \\ 0 \\ 1 + \theta s \\ 1 \end{pmatrix}.$$

The control vector fields g_1 and g_2 still commute and, like for the five-dimensional model considered above, iterated Lie brackets that involve the vector field g_1 only have nonzero terms in the first two coordinates. If we introduce the notation $\frac{\partial}{\partial p}$ and $\frac{\partial}{\partial q}$ (common in differential geometry) for these first two coordinate fields, respectively, then we can express these vector fields more concisely in the form

$$[f,g_1](\chi) = \gamma p \left(\xi \frac{\partial}{\partial p} - b \frac{\partial}{\partial q}\right), \tag{7.82}$$

$$[g_1,[f,g_1]](\chi) = -\gamma^2 bp \frac{\partial}{\partial q}, \tag{7.83}$$

$$[g_2,[f,g_1]](\chi) = ((\alpha + \beta r) - (\eta + \delta r))\, \gamma bp \frac{\partial}{\partial q}. \tag{7.84}$$

The formulas for the Lie brackets with g_2 generally are full, only having a zero value in the fourth coordinate corresponding to the variable y. For example, we have that

$$[f,g_2](\chi) = \begin{pmatrix} [(\eta + \delta r) - (\alpha + \beta r)]\, \xi p + \beta \rho r p \\ -[(\eta + \delta r) - (\alpha + \beta r)]\, bp - \frac{2}{3} d p^{\frac{2}{3}} q\, (\alpha + \beta r) + \delta \rho r q \\ \rho \\ 0 \\ -\sigma \theta s \\ \sigma \end{pmatrix}$$

$$= \frac{(\eta + \delta r) - (\alpha + \beta r)}{\gamma} [f,g_1](\chi) + \begin{pmatrix} \beta \rho r p \\ -\frac{2}{3} d p^{\frac{2}{3}} q\, (\alpha + \beta r) + \delta \rho r q \\ \rho \\ 0 \\ -\sigma \theta s \\ \sigma \end{pmatrix}.$$

Similar to the five-dimensional model of Section 7.2.3, we have the relation

$$[g_2,[f,g_1]](\chi) = \frac{(\eta + \delta r) - (\alpha + \beta r)}{\gamma} [g_1,[f,g_1]](\chi) \tag{7.85}$$

which again allows us to eliminate the Lie bracket $[g_2,[f,g_1]]$ from the relation for the second derivative of the switching function:

$$\begin{aligned}\ddot{\Phi}_1(t) &= \langle \lambda(t),[f+ug_1+wg_2,[f,g_1]](\chi(t))\rangle \\ &= \langle \lambda(t),[f,[f,g_1]](\chi(t))\rangle \\ &\quad + \left(u+\frac{(\eta+\delta r)-(\alpha+\beta r)}{\gamma}w\right)\langle \lambda(t),[g_1,[f,g_1]](\chi(t))\rangle .\end{aligned}$$

Also, as for model [AR5], we have that

$$\langle \lambda(t),[g_1,[f,g_1]](\chi(t))\rangle = -\gamma^2 bp\lambda_2(t)$$

and $\lambda_2(t)$ is positive along a singular arc since $\gamma q(t)\lambda_2(t)\equiv\lambda_4>0$. Hence the strengthened Legendre-Clebsch condition for local optimality of a singular arc is satisfied. If we now set

$$\tilde{u}=u+\frac{(\eta+\delta r)-(\varphi+\beta r)}{\gamma}w, \tag{7.86}$$

then, once more, we have exactly the monotherapy case considered in Section 5.4 and, as for problem [AR5], all the formulas directly carry over with u replaced by $\tilde{u}$.

Proposition 7.2.3. *If the optimal anti-angiogenic dosage u follows a singular control $u_{\text{sing}}(t)$ on an open interval I and if the radiotherapy schedule is given by w_*, then we have the following relation between the controls u and w:*

$$\gamma u_{\text{sing}}(t)+[(\eta+\delta r)-(\alpha+\beta r)]\,w_*(t)=\Psi(p(t),q(t)) \tag{7.87}$$

with Ψ the function defining the singular feedback control for the optimal anti-angiogenic monotherapy given by

$$\Psi(p,q)=\xi\ln\left(\frac{p}{q}\right)+b\left(\frac{p}{q}\right)-(\mu+dp^{\frac{2}{3}})+\frac{2}{3}\frac{d}{b}\xi p^{-\frac{1}{3}}q. \tag{7.88}$$

Note that, as in the monotherapy case, whenever the antiangiogenic control u follows a singular regimen, then the quotient $\frac{p}{q}$ obeys the simple dynamics

$$\begin{aligned}\frac{d}{dt}\left(\frac{p}{q}\right) &= \frac{\dot{p}q-p\dot{q}}{q^2} \\ &= -\xi\frac{p}{q}\ln\left(\frac{p}{q}\right)-(\alpha+\beta r)\frac{p}{q}w \\ &\quad -\frac{p}{q}\left[b\left(\frac{p}{q}\right)-\left(\mu+dp^{\frac{2}{3}}\right)-\gamma u_{\text{sing}}-(\eta+\delta r)w\right] \\ &= \left(\frac{p}{q}\right)\left[-\Psi(p,q)+\gamma u_{\text{sing}}+[(\eta+\delta r)-(\alpha+\beta r)]w+\frac{2}{3}\frac{d}{b}\xi p^{-\frac{1}{3}}q\right] \\ &= \frac{2}{3}\xi\frac{d}{b}p^{\frac{2}{3}}.\end{aligned} \tag{7.89}$$

For the parameter values used in [116] and [77], and for realistic values for p, this quotient is small and varies little. As a result, the corresponding controlled trajectories follow an almost linear relation between p and q. Also note that for this model, replacing u with $\tilde{u}$, the combined effect of a singular antiangiogenic and radiotherapy treatment is given by

$$-\gamma q u - (\eta + \delta r)\, qw = -\gamma q \tilde{u} - (\alpha + \beta r) qw$$

with the $-(\alpha+\beta r)w$ the same term that determines the damage to the tumor. This once more states that, in a certain way antiangiogenic treatment compensates for radiotherapy in the sense to make the effects of radiotherapy on tumor and vasculature equal.

As for the 5-dimensional problem, we need a second equation to determine totally singular protocols $(u_{\text{sing}}, w_{\text{sing}})$. If w is singular as well, then

$$\Phi_2(t) = \langle \lambda(t), g_2(\chi(t)) \rangle \equiv 0 \qquad \dot{\Phi}_2(t) = \langle \lambda(t), [f, g_2](\chi(t)) \rangle = 0$$

and

$$\ddot{\Phi}_2(t) = \langle \lambda(t), [f + u g_1 + w g_2, [f, g_2]](\chi(t)) \rangle \equiv 0. \tag{7.90}$$

Since the dimension is increased by one, we need one more vector field to represent the second order Lie brackets and thus include f in our basis. Note that it follows from the maximum principle that

$$0 \equiv H = \langle \lambda(t), f(\chi) + u g_1(\chi) + w g_2(\chi) \rangle = \langle \lambda(t), f(\chi) \rangle,$$

so that λ vanishes against the vector fields f, g_1, g_2, $[f, g_1]$ and $[f, g_2]$ along a totally singular trajectory χ. If we now express the second-order brackets in the form

$$[f, [f, g_2]] = a_0 f + a_1 g_1 + a_2 g_2 + a_3 [f, g_1] + a_4 [f, g_2] + A [g_2, [f, g_2]], \tag{7.91}$$
$$[g_1, [f, g_2]] = b_0 f + b_1 g_1 + b_2 g_2 + b_3 [f, g_1] + b_4 [f, g_2] + B [g_2, [f, g_2]], \tag{7.92}$$

with coefficients that are smooth functions of χ (assuming that the vector fields on the right are linearly independent), then, as above, along an optimal controlled trajectory χ_* we get that

$$\langle \lambda(t), [f, [f, g_2]](\chi_*(t)) \rangle = A(\chi_*(t)) \langle \lambda(t), [g_2, [f, g_2]](\chi_*(t)) \rangle$$

and

$$\langle \lambda(t), [g_1, [f, g_2]](\chi_*(t)) \rangle = B(\chi_*(t)) \langle \lambda(t), [g_2, [f, g_1]](\chi_*(t)) \rangle.$$

The nontriviality of the multiplier implies that $\langle \lambda(t), [g_2, [f, g_1]](\chi_*(t)) \rangle$ cannot vanish and thus, as before, we get from (7.90) that

$$A(\chi_*(t)) + B(\chi_*(t)) u_{\text{sing}}(t) + w_{\text{sing}}(t) \equiv 0.$$

Of course, the coefficients A and B are not the same as in model [AR5], but formally we have the identical statement and conclusions.

Proposition 7.2.4. *If the optimal antiangiogenic dosage u and the radiotherapy schedule w both follow singular regimens u_{sing} and w_{sing} on an open interval I, then in addition to equation (7.87) we have that*

$$A(\chi_*(t)) + B(\chi_*(t))u_{\text{sing}}(t) + w_{\text{sing}}(t) \equiv 0 \tag{7.93}$$

holds on I with A and B smooth functions defined by (7.91) and (7.92).

As before, $(u_{\text{sing}}, w_{\text{sing}})$ are the solutions of a 2×2 system of linear equations whose coefficients are determined solely by the equations defining the dynamics of the system. Using Cramer's rule, it is possible to give explicit expressions for the functions A and B and thus also for the totally singular controls. As before, these formulas are long and unhandy, but numerically the controls are easily computed.

Different from the five-dimensional model [AR5], in this case the number of constraints defining totally singular controls matches the degrees of freedom in the model. Along a totally singular controlled trajectory the multiplier $\lambda(t)$ vanishes against the vector fields f, g_1, g_2, $[f, g_1]$ and $[f, g_2]$. Now these conditions uniquely determine the multiplier (up to a positive scalar multiple that is determined by the terminal condition on $\lambda_1(T)$) and thus there exists a well-defined totally singular flow for the system. Rather than only being able to use totally singular controls on a hypersurface, as it is the case for the five-dimensional version of this model, now at every point in the state space totally singular controls computed as solutions to (7.87) and (7.93) are available, provided they do not violate the control limits.

Figure 7.9 gives an example of a totally singular antiangiogenic dose rate u and a radiotherapy schedule w that have been computed in this way for parameter values taken from [77]. Part (a) shows the graph of the radiation schedule if no upper limit on the dosage is imposed. If we set the radiation limit to $w_{\max} = 4$, then this upper bound is initially exceeded and part (b) shows the control that has been computed by saturating this schedule at $w_{\max}$. Since equation (7.87) is valid regardless of the structure of w, the calculations easily adjust. The corresponding graph of the singular control u is given in part (c) and part (d) shows the corresponding trajectory. Note that, in accordance with our earlier observation, since the antiangiogenic dose rate is always singular, this trajectory is almost linear. For this simulation, the right-hand side of (7.89) only varies between 0.03 and 0.09.

The controls given in this figure were not computed to be optimal, but they only illustrate a totally singular control structure for the combined antiangiogenic and radiotherapy model. Based on our theoretical analysis, it is clear that these controls will play an integral part in the structure of optimal protocols. This is seconded by the structure of optimal protocols computed through numerical optimization in [77] where all the solutions are totally singular when no hard limits are imposed on the dose rates. In order to solve the overall optimal control problem [AR6], however, it is necessary to take these constraints into account and to establish the structure of optimal controls before and after the singular segments. Different from the monotherapy problem described earlier, in this case there exists a vector field whose integral curves are the trajectories for totally singular controls everywhere, but it matters which of these trajectories is taken. Research on determining an optimal synthesis is ongoing.

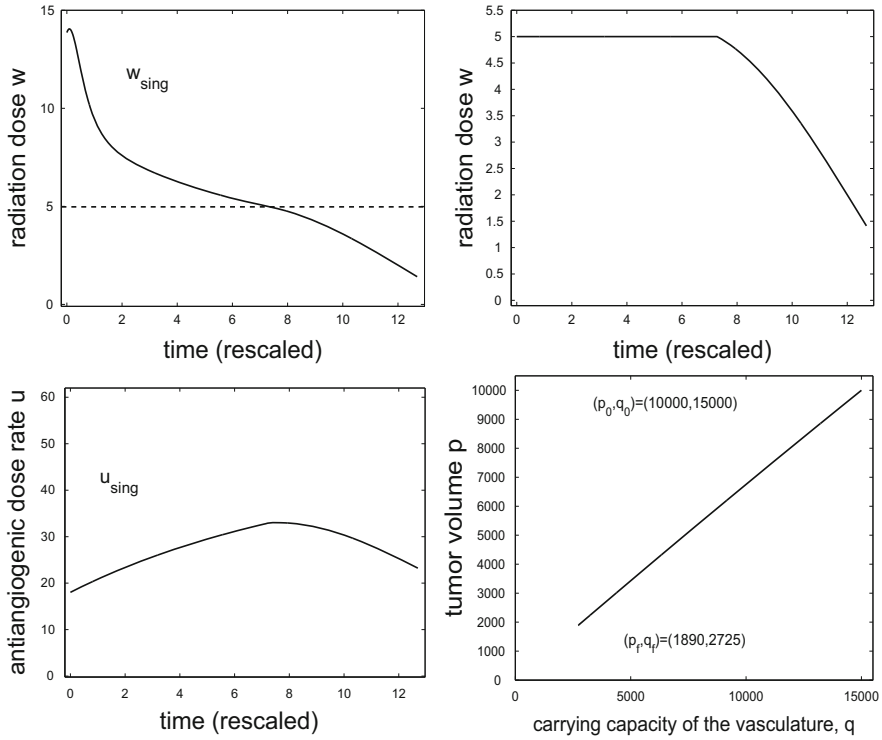

Fig. 7.9 Examples of totally singular controls for initial conditions $(p_0, q_0) = (10000, 15000)$ and values of the parameters in Table 7.3: (a, top left) the unsaturated singular radiation schedule w, (b, top right) the radiation schedule w with upper limit $w_{\max}$ enforced, (c, bottom left) corresponding singular anti-angiogenic agent u, and (d, bottom right) corresponding trajectory (p, q) with p plotted vertically and q horizontally.

7.2.5 Summary and Discussion

We formulated a model for the combination of antiangiogenic treatment with radiotherapy and considered two particular realizations of it, a five-dimensional model when we identified the repair rates for the various tissues and used the model [E] by Ergun et al. [77] to describe the tumor vascular interactions, and a six-dimensional model when we differentiated between the repair rates for the tumor and the healthy tissues and used the model [H] by Hahnfeldt et al. [116]. For the antiangiogenic monotherapy problem considered in Chapter 5 singular controls form the core of the optimal solutions and our computations here verify that the structure of these singular arcs prevails if combinations with chemo- and radiotherapy are considered. In fact, simple extensions of the earlier computations now determine totally singular controls for the optimal control problem when antiangiogenic treatments are combined with radiotherapy. Clearly, the analysis of these problems is not finished, and we do not claim that our computations give the optimal controls. But, based on the

earlier analysis of the related problems, there is a strong expectation that the singular controls computed here will be of importance to the optimal structures. Compared with extensive numerical computations that are the standard in radiotherapy, the computations of these singular regimes is exceedingly simple. However, we have not considered fractionated dosages that give radiation only for a brief instant in time, the standard in medical practice. A continuous-time model has mathematical advantages over a pure optimization procedure in that and one can also obtain some insights into the structure of optimal protocols from explicit formulas. From this it may be possible to come up with suboptimal fractionization schedules that are close to the solutions of the continuous-time models. However, a challenge in doing so is to properly relate the values of the parameters for these two vastly different models.

Chapter 8
Optimal Control for Mathematical Models of Tumor Immune System Interactions

In this chapter, we consider the second major feature of the tumor microenvironment: interactions between the tumor and the immune system. Fundamental principles that have already been outlined in the introduction (see Section 1.3.4) will be expanded upon in this chapter. As a vehicle for the analysis we use the classical model by Stepanova [303] and some of its modifications that have been developed in the literature. This model captures the main features that we want to discuss here—immune surveillance and tumor dormancy—and, at the same time, being low-dimensional and minimally parameterized, has the advantage of allowing us to easily visualize associated geometric features (regions of attractions, stability boundaries, etc.). We formulate an optimal control problem whose objective to be minimized is tailored to the inherent multi-stable structure that these systems have. These problems are considered under chemotherapy and under combinations of chemotherapy with a rudimentary form of an immune boost. Interestingly, after a brief administration of maximum dose chemotherapy, for these models optimal treatment schedules switch to singular controls and significantly lower concentrations. In the medical literature such protocols have been tested and sometimes are referred to as *"chemo-switch" protocols* [16, 277].

In these solutions, the tumor microenvironment plays a major role: an initial MTD style chemotherapy brings the state of the system into a region where the immune system is potent enough to control (not necessarily to eliminate or to eradicate) the tumor and there lower concentrations of chemotherapy are sufficient to maintain the system in a benign state. In fact—but such a structure is not included in the model considered here—higher concentrations of the cytotoxic agent may be harmful in that they might adversely effect the immune system which otherwise would have come to the assistance in combating the tumor. There exists substantial medical evidence that low-dose chemotherapy, while still having a moderate cytotoxic effect on cancerous cells in the absence of significant negative side effects, has both antiangiogenic and immune stimulatory effects (e.g., see [9, 24, 39, 118, 162, 277] as well as the survey article [272] and editorial [273]).

H. Schättler, U. Ledzewicz, *Optimal Control for Mathematical Models of Cancer Therapies*, Interdisciplinary Applied Mathematics 42,
DOI 10.1007/978-1-4939-2972-6_8

Metronomic chemotherapy is a term used in the medical literature for the almost continuous administration of chemotherapeutic agents at significantly lower dose rates than MTD, possibly with small interruptions to increase the efficacy of the drugs. The idea behind such administration schedules is that, in the absence of limiting side effects, it is possible to give chemotherapy over prolonged time intervals so that, because of the greatly extended time horizon, the overall effect may be improved when compared with repeated short MTD doses [136, 341]. Furthermore, while low dose chemotherapy has an immune stimulatory effect, high dose chemotherapy simply suppresses the immune system as well taking out another factor that could be utilized in fighting the tumor.

In this chapter, we explore the structure of optimal administrations of chemotherapeutic agents when such interactions with the tumor immune system and its vasculature are taken into account. In Section 8.1 we formulate a dynamics for tumor-immune system interactions based on Stepanova's model [303] and also describe the needed fundamental concepts from dynamical systems theory such as the region of attraction of a locally asymptotically stable equilibrium point. Depending on the nature of the equilibrium point, we call these the benign and malignant regions. Based on the geometric properties of the dynamical system, in Section 8.2 we formulate treatment as an optimal control problem with the aim to move the state of the system from the malignant into the benign region. We then analyze the case of a strongly targeted chemotherapeutic agent in Section 8.3. We close out this chapter—and our text—by combining the model for tumor-immune system interactions considered here with the model [H] for angiogenic signaling from Chapter 5 to formulate a dynamical system for metronomic chemotherapy that incorporates the main features of the tumor microenvironment. This model exhibits the same multi-stable characteristics as the model for tumor-immune system interactions and its optimization once more suggests chemo-switch type protocols as solutions.

8.1 Multistability and Immune Surveillance

The competitive interaction between tumor cells and the immune system is complex, to say the least, and still is the topic of immense medical research. It involves an excessively large number of events with the kinetics of the interplay strongly nonlinear and characterized by multi-stability, i.e., persistence of both benign and malignant scenarios. The possible outcome of this interplay is not only constituted by tumor suppression or tumor outbreak, but there exist many intermediate scenarios. However, depending on the specific aim of the mathematical analysis, a more detailed and precise model, may not necessarily be the better one to use since it may simply obscure, or even hide the main features.[1] Especially, if the aim is to study treatment protocols—and we are just interested in their general structure rather than a particular case—then low-dimensional mathematical models that capture the essence

[1] The reader may find the short fragment "On Exactitude in Science" by Jorge Luis Borges [33] of interest.

within a few parameters are preferred. For this reason, here we use Stepanova's classical model [303] for tumor interactions along with its various generalizations. It is perfectly adequate to make the main points that no doubt can also be extracted from more complex models, but at considerably more effort with not necessarily more insight.

In her 1980 paper [303], Stepanova formulated a by now classical mathematical model of two ordinary differential equations that aggregate the interactions between tumor cell growth and the activities of the immune system during the development of cancer. Precisely because of its simplicity—a few parameters incorporate the medically most important features—the underlying equations have been widely accepted as a basic model. There exist numerous extensions and generalizations of this model, e.g., [158, 171, 248, 249, 250, 334], that all share in similar qualitative findings: while the immune system can be effective in the control of small cancer volumes, for large volumes the cancer dynamics suppresses the immune dynamics and the two systems effectively become separated [334, appendix B]. In the first case, so-called *immunosurveillance*, what medically would be considered cancer never develops; in the latter case therapeutic action is needed to cure the disease. But, as we shall see, the persistence of both benign and malignant scenarios significantly effects the structure of optimal chemotherapy protocols.

Stepanova's model has been introduced in Section 1.3.4 and here we only briefly recall the equations, but do not repeat the medical motivations:

$$\dot{p} = \xi p F(p) - \theta p r, \tag{8.1}$$

$$\dot{r} = \alpha \left(p - \beta p^2\right) r + \gamma - \delta r. \tag{8.2}$$

As before, the tumor volume is denoted by p while $p_\infty \leq \infty$ is a fixed carrying capacity; r is a nondimensional, order of magnitude variable called the *immunocompetent cell density* and is related to the activities of various types of T-cells activated during the immune reaction. While Stepanova [303] uses an exponential model for the growth of the tumor, we, more generally, include an arbitrary growth rate $F(p)$ depending on the tumor volume p only assuming that F is a positive, nondecreasing, twice continuously differentiable function defined on an interval $(0, p_\infty)$. If the carrying capacity p_∞ is finite, we also assume that $F(p_\infty) = 0$. At various times we shall consider Gompertzian, logistic, or exponential growth models. All Greek letters in these equations denote constant coefficients. Recall that, if we scale r as $\hat{r} = \iota r$, then the solutions are unchanged if we also scale the parameters γ and θ as $\hat{\gamma} = \iota \gamma$ and $\hat{\theta} = \frac{\theta}{\iota}$. This 1-parameter group of symmetries thus can be used to normalize the set point value for r.

In Table 8.1 we list the numerical values that we use for the computations and illustrations shown in this chapter. They almost exclusively are taken from the paper [171] by Kuznetsov, Makalkin, Taylor, and Perelson who estimate these parameters based on in vivo experimental data for B-lymphoma BCL_1 in the spleen of mice. In that paper, a classical logistic growth term is used for cancer growth and we adjusted the growth rates to account for Gompertzian growth using linear data fitting. Also, the functional form $\left(p - \beta p^2\right) r$ used in Stepanova's model in

Table 8.1 Variables and parameter values used in numerical illustrations.

Variable/ parameters	Interpretation	Numerical value	Dimension	Reference
p	Tumor volume		10^6 cells	[303]
p_0	Initial value for p	600	10^6 cells	
p_∞	Carrying capacity	780	10^6 cells	
r	Immuno-competent cell density		Orders of magnitude Non-dimensional	[303]
r_0	Initial value for r	0.10	Non-dimensional	
α	Tumor stimulated proliferation rate	0.00484	Non-dimensional	
β	Inverse threshold for tumor suppression	0.00264	Non-dimensional	[171]
γ	Rate of influx	0.1181	Non-dimensional	[171]
δ	Death rate	0.37451	Non-dimensional	[171]
θ	Interaction rate	1	10^7 cells/day	[171]
ξ	Tumor growth parameter	0.5618	10^7 cells/day	

equation (8.2) is a quadratic expansion of the term used in [171]. Following [171], p is given in multiples of 10^6 cells and r is a dimensionless quantity that describes the immuno-competent cell density on an order of magnitude basis. The time scale is taken relative to the tumor cell cycle and is in terms of 0.11 days [171]. As before, we only use these particular values to illustrate our analytical results.

8.1.1 *Stability Properties of Equilibria, Bifurcations, and Regions of Attraction*

We briefly review some fundamental concepts and results from dynamical systems theory that we shall be using in this chapter. Given a differential equation of the form $\dot{x} = f(x)$ with $f : G \to \mathbb{R}^n$ a continuously differentiable vector field defined on some open set $G \subset \mathbb{R}^n$, it follows from standard results on ordinary differential equations that the initial value problem with initial condition $x(0) = x_0 \in G$ has a unique solution $x = x(t;x_0)$ which is defined on a maximal open interval $I \subset \mathbb{R}$. The solution curves in the state space, $x(\cdot;x_0) : I \to G$, $t \mapsto x(t;x_0)$, are called the *trajectories* of the system and the totality of all solution curves for $x_0 \in G$ is called the *phase portrait* of the dynamical system. If $f(x_*) = 0$, then this solution curve is just the point $x(t;x_*) \equiv x_*$ defined for $I = \mathbb{R}$ and x_* is called an *equilibrium point*.

Definition 8.1.1 (Stable, Asymptotically Stable and Unstable Equilibria). An equilibrium point x_* is said to be stable if for every $\varepsilon > 0$ there exists a $\delta = \delta(\varepsilon) > 0$ such that whenever $\|x_0 - x_*\| < \delta$ then for all $t > 0$ it follows that $\|x(t;x_0) - x_*\| < \varepsilon$; otherwise it is said to be unstable. An equilibrium point x_* is said to be locally

attractive if there exists a neighborhood U of x_* such that for all initial conditions $x_0 \in U$ the solution $x(t;x_0)$ exists for all times $t \geq 0$ and satisfies $\lim_{t\to\infty} x(t;x_0) = x_*$. An equilibrium point that is both stable and locally attractive is said to be locally asymptotically stable.

The simple linear system $\dot{x}_1 = -x_2$ and $\dot{x}_2 = x_1$, the harmonic oscillator, shows that equilibria can be stable without being attractive. (Solutions are given by the circles $x_1^2 + x_2^2 \equiv r^2$.) It is a much less trivial fact that equilibria which are locally attractive need not be stable [114].

If x_* is an equilibrium point, then the linear system $\dot{y} = Ay$ with $A = Df(x_*)$, the Jacobian matrix of f at x_*, is called the linearization around the equilibrium point. The eigenvalues of the matrix A are also called the eigenvalues of f at x_*.

Definition 8.1.2 (Hyperbolic Equilibrium). An equilibrium point x_* of f is said to be hyperbolic if none of its eigenvalues λ lie on the imaginary axis, i.e., $\operatorname{Re}\lambda \neq 0$ for all $\lambda \in \sigma(A)$, the spectrum of A.

Hyperbolic equilibria play an important role in the theory of dynamical systems since important local properties of the system are 'stable' near such a point in the sense that they do not change if small changes in the dynamics (such as in values of parameters that define the vector field f) occur. For example, local stability properties can be determined in terms of its eigenvalues.

Proposition 8.1.1 ([111, 145]). *Let x_* be a hyperbolic equilibrium point for $\dot{x} = f(x)$. If all eigenvalues of $A = Df(x_*)$ have negative real part, then x_* is locally asymptotically stable; if there exists an eigenvalue with positive real part, then x_* is unstable.*

In the plane, $G = \mathbb{R}^2$, an equilibrium point with complex conjugate eigenvalues with $\operatorname{Re}\lambda \neq 0$ is called an asymptotically stable, respectively unstable *focus*. If both eigenvalues are real and nonzero, the equilibrium point is an asymptotically stable/unstable node if the eigenvalues are negative, respectively positive. If it has both a positive and negative real eigenvalue, it is called a saddle.

Proposition 8.1.2 (Hartman-Grobman Theorem [111]). *If x_* is a hyperbolic equilibrium point, then there exist neighborhoods U of x_* and V of 0 and a homeomorphism $\varphi : U \to V$ (i.e., an invertible continuous mapping that has a continuous inverse) such that the trajectories of the nonlinear system $\dot{x} = f(x)$ in U are mapped bijectively onto the trajectories of the linearization $\dot{y} = Ay$ in V.*

This theorem thus states that, essentially, a nonlinear system looks like a linear systems near a hyperbolic equilibrium point.

Definition 8.1.3 (Region of Attraction). Let x_* be a locally asymptotically stable equilibrium point for $\dot{x} = f(x)$. Its region of attraction, $A(x_*)$, consists of all initial conditions x_0 for which the corresponding solution exists for all $t \geq 0$ and converges to x_* as $t \to \infty$,

$$A(x_*) = \left\{ x_0 \in G : x(t;x_0) \text{ exists for all } t > 0 \text{ and } \lim_{t\to\infty} x(t;x_0) = x_* \right\}.$$

It is not difficult to see that the region of attraction of a locally asymptotically stable equilibrium point is an open and connected subset of the state space. For an unstable equilibrium point there still exist points on a lower dimensional set, in fact, lying on a manifold, for which a similar convergence result holds true.

Definition 8.1.4 (Local Stable Manifold). Given any hyperbolic equilibrium point x_* and a sufficiently small neighborhood U of x_*, the local stable manifold of x_* in U is defined as the set of all initial conditions $x_0 \in U$ such that the corresponding solution $x(t;x_0)$ exists for all $t \geq 0$, lies in U, $x(t;x_0) \in U$ for all $t > 0$, and converges to x_* as $t \to \infty$, $\lim_{t\to\infty} x(t;x_0) = x_*$,

$$W^s_{loc}(x_*;U) = \left\{ x_0 \in U : x(t;x_0) \in U \text{ for all } t > 0 \text{ and } \lim_{t\to\infty} x(t;x_0) = x_* \right\}.$$

Theorem 8.1.1 ([111]). *Let x_* be a hyperbolic equilibrium point and let W denote the linear subspace of $\mathbb{R}^n$ generated by all eigenvectors and generalized eigenvectors of the matrix $Df(x_*)$ that correspond to eigenvalues with negative real parts; suppose $\dim W = k$. Then, for U sufficiently small, the local stable manifold of x_* in U is a k-dimensional embedded submanifold and its tangent space at x_* is given by W.*

This is an a bit technical, but not difficult result which, however, requires some familiarity with manifolds. We only remark that *embedded* submanifolds M in $\mathbb{R}^n$ are what typically are curves, surfaces, etc. and that they can be described locally as the zero set of some mapping $\Psi : V \subset \mathbb{R}^n \to \mathbb{R}^\ell$, $M = \{x \in U : \Psi(x) = 0\}$, with the matrix $D\Psi$ of constant rank equal to $n-k$ on M and k the dimension of the manifold. For example, the 2-sphere S^2 in $\mathbb{R}^3$ can even globally be described as $S^2 = \left\{(x,y,z) \in \mathbb{R}^3 : x^2+y^2+z^2 = 1\right\}$ and $\nabla\Psi = (2x, 2y, 2z)$ is nonzero on S^2.

The global stable manifold of x_* is then defined by propagating the solutions that lie in a local stable manifold backward in time. Denote the flow of the differential equation by Φ_t, i.e., we simply have that $\Phi_t(x_0) = x(t;x_0)$ for $t \in I$. Thus we get the following definition:

Definition 8.1.5 (Global Stable Manifold). Given a hyperbolic equilibrium point x_*, for a sufficiently small neighborhood U of x_* let $W^s_{loc}(x_*;U)$ denote the local stable manifold. The global stable manifold of x_* is then defined as

$$W^s(x_*) = \cup_{t\leq 0} \left\{ \Phi_t(x_0) : x_0 \in W^s_{loc}(x_*;U) \right\}.$$

Unfortunately, by propagating trajectories backward, nice geometric properties may be lost and generally global stable manifolds need no longer be embedded submanifolds, but are only what are called immersed submanifolds. In our text, however, we only encounter the more regular structures and therefore do not go into these details.

Corresponding local and global unstable manifolds are defined by reversing the orientation of time.

Definition 8.1.6 (Local Unstable Manifold). Given a hyperbolic equilibrium point x_* and a sufficiently small neighborhood U of x_*, the local unstable manifold of x_* in U is defined as the set of all initial conditions $x_0 \in U$ such that the corresponding solution $x(t;x_0)$ exists for all $t \leq 0$, lies in U, $x(t;x_0) \in U$ for all $t < 0$, and converges to x_* as $t \to -\infty$, $\lim_{t\to-\infty} x(t;x_0) = x_*$,

$$W^u_{loc}(x_*;U) = \left\{ x_0 \in U : x(t;x_0) \in U \text{ for all } t < 0 \text{ and } \lim_{t\to-\infty} x(t;x_0) = x_* \right\}.$$

Theorem 8.1.2 ([111]). *Let x_* be a hyperbolic equilibrium point and let W denote the linear subspace of $\mathbb{R}^n$ generated by all eigenvectors and generalized eigenvectors of the matrix $Df(x_*)$ that correspond to eigenvalues with positive real parts; suppose* $\dim W = k$. *Then, for U sufficiently small, the local unstable manifold of x_* in U is a k-dimensional embedded submanifold and its tangent space x_* is given by W.*

Definition 8.1.7 (Global Unstable Manifold). Given a hyperbolic equilibrium point x_*, for a sufficiently small neighborhood U of x_* let $W^u_{loc}(x_*;U)$ denote the local unstable manifold. The global unstable manifold of x_* is then defined as

$$W^u(x_*) = \cup_{t\geq 0} \{\Phi_t(x_0) : x_0 \in W^u_{loc}(x_*;U)\}.$$

No qualitative changes in the local behavior of a dynamical system occur at hyperbolic equilibria. If we write the vector field f more explicitly in the form $f : G \times \Theta \to \mathbb{R}^n$, $(x,\theta) \mapsto f(x,\theta)$ with $\theta \in \Theta \subset \mathbb{R}^k$ denoting the dependence of the equations on parameters, for a fixed value of the parameters naturally all the concepts defined above apply. For example, if x_* is a hyperbolic equilibrium point at the parameter value θ_*, then in particular the Jacobian matrix $\frac{\partial f}{\partial x}(x_*,\theta_*)$ is nonsingular and therefore by the implicit function theorem there exists a unique solution $x = x(\theta)$ to the equation $f(x,\theta) = 0$ that satisfies $x_* = x(\theta_*)$ in a neighborhood of θ_*. Hence the number of equilibria does not change. Furthermore, since eigenvalues depend continuously on the entries of a matrix, it also follows (if necessary on a smaller neighborhood of θ_*) that the number of eigenvalues that lie in the positive and negative halfplanes in $\mathbb{C}$ remain unchanged and thus also the local stability properties (such as the dimensions of stable and unstable manifolds) do not change as the parameter θ varies in this neighborhood. But such changes do occur as the eigenvalues cross the imaginary axis as parameters vary and are called *bifurcations*. Of these, the simplest one is the so-called saddle-node bifurcation that plays an important role for the models considered here. Intuitively, a *saddle-node bifurcation* occurs as *a single real eigenvalue crosses the imaginary axis* and it leads to the birth, respectively annihilation, of two equilibria.

Definition 8.1.8 (Saddle-Node Bifurcation). Consider the dependence of the dynamics on a single parameter $\theta \in \mathbb{R}$. A point (x_*,θ_*) is a saddle-node bifurcation point if the Jacobian matrix $\frac{\partial f}{\partial x}(x_*,\theta_*)$ has a simple eigenvalue 0, no other eigenvalues on the imaginary axis, and the following transversality conditions are

satisfied: if λ and v are a left- and right-eigenvectors for the eigenvalue 0 of the matrix $\frac{\partial f}{\partial x}(x_*, \theta_*)$, respectively,

$$\lambda \frac{\partial f}{\partial x}(x_*, \theta_*) = 0 \qquad \text{and} \qquad \frac{\partial f}{\partial x}(x_*, \theta_*)v = 0$$

then

$$\lambda \frac{\partial^2 f}{\partial x^2}(x_*, \theta_*)(v, v) \neq 0 \qquad \text{and} \qquad \lambda \frac{\partial f}{\partial \theta}(x_*, \theta_*) \neq 0. \tag{8.3}$$

Then the following saddle-node bifurcation theorem [111, Theorem 3.4.1] holds:

Theorem 8.1.3 (Saddle-Node Bifurcation Theorem [111]). *If (x_*, θ_*) is a saddle-node bifurcation point, then near (x_*, θ_*) there exists a smooth curve of equilibria passing through (x_*, θ_*) that is tangent to the hyperplane $\theta \equiv \theta_*$ such that depending on the signs in equations (8.3) there are no equilibria for $\theta < \theta_*$ (respectively, $\theta > \theta_*$), a unique equilibrium point for $\theta = \theta_*$ and two equilibria for $\theta > \theta_*$ (respectively, $\theta < \theta_*$). The two equilibria near (x_*, θ_*) are hyperbolic and have stable manifolds that differ in their dimensions by one.*

The transversality conditions (8.3) enforce that the real eigenvalue actually crosses the imaginary axis along the smooth curve of equilibria and thus the change in the dimension of the stable manifold by one. It is generically satisfied and prevents more degenerate situations from occurring. In this sense, the saddle-node bifurcation is the most common of the so-called *static* bifurcations that arise as the number of equilibria change. If this number is not affected, but the stability behavior of the equilibrium point changes, one speaks of a *dynamic* bifurcation. Of these the most typical one is the Hopf bifurcation which occurs as a simple pair of complex eigenvalues crosses the imaginary axis. This bifurcation, or the even more general global bifurcations, do not occur in this model. (We refer the interested reader to the text by Guckenheimer and Holmes [111] for this topic.)

We return to our discussion of the system (8.1)–(8.2). There always exists a *disease free equilibrium point* at $(p_f, r_f) = (0, \frac{\gamma}{\delta})$. The Jacobian matrix is given by

$$DF(p_f, r_f) = \begin{pmatrix} \xi F(0) - \theta \frac{\gamma}{\delta} & 0 \\ \alpha \frac{\gamma}{\delta} & -\delta \end{pmatrix}$$

and thus this equilibrium point is a locally asymptotically stable node if $F(0) < \frac{\theta\gamma}{\xi\delta}$ and a saddle point for $F(0) > \frac{\theta\gamma}{\xi\delta}$. The latter case includes the Gompertzian model when $\lim_{p \to 0+} F(p) = +\infty$. Essentially, if the initial tumor growth rate $\xi F(0)$ is small enough, then the beneficial effects of the immune system are able to eliminate the cancerous growth near the tumor free equilibrium point in an extreme form of immunosurveillance. However, if there also exist equilibria with positive p-values (and this is the case if the disease free equilibrium point is unstable), then, even if the disease free equilibrium is locally stable, a strong enough perturbation (unforeseen event or not modeled dynamics) may dislocate the state out of the region of

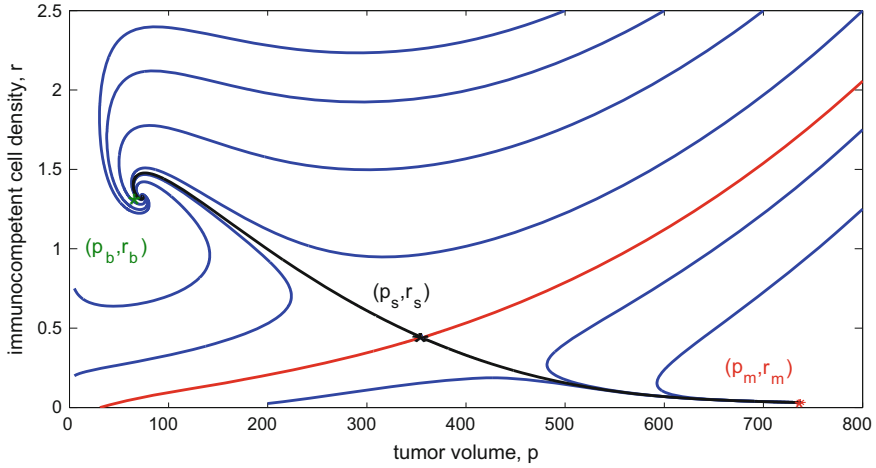

Fig. 8.1 Phase portraits of the system (8.1) and (8.2) for a Gompertzian growth function $F(p) = -\log\left(\frac{p}{p_\infty}\right)$ and parameter values from Table 8.1.

attraction of this equilibrium point. Note that the positive half-line $\{p = 0, r > 0\}$ is invariant and forms the stable manifold of the disease free equilibrium point if $F(0) > \frac{\theta\gamma}{\xi\delta}$.

Typically there exist equilibria with positive tumor volumes and we call such equilibrium points positive equilibria. Figure 8.1 shows the phase portrait of the system (8.1) and (8.2) for a Gompertzian growth rate and the parameters listed in Table 8.1. Here there exist three equilibria with positive tumor volumes: a locally asymptotically stable focus at $(p_b, r_b) = (72.961, 1.327)$ (marked by a green star), a saddle point at $(p_s, r_s) = (356.174, 0.439)$ (marked by a black star) and a second asymptotically stable node at $(p_m, r_m) = (737.278, 0.032)$ (marked by a red star). This indeed is the situation for a wide range of parameters (see also Proposition 8.1.3 below and Proposition 8.4.1 in Section 8.4). In the phase portrait we have also marked the unstable manifold of the saddle as the black curve and its stable manifold as the red curve. Both of these, since the dimension is 2, are differentiable curves. Note that the regions of attraction of the stable equilibria are open and that they are separated by the stable manifold of the saddle. A similar geometric structure is commonly valid for what are called Morse-Smale systems [111] and we shall encounter similar geometric pictures throughout this section.

The tumor volume for the stable equilibrium point (p_m, r_m) is close to the carrying capacity and it is by an order of magnitude larger than for the equilibrium point (p_b, r_b). For a typical set of parameter values, these values might be interpreted as a *microscopic* and a *macroscopic locally asymptotically stable equilibrium point* with the high value indicating that the patient will succumb to the disease.

Definition 8.1.9 (Benign and Malignant Equilibria). We call a locally asymptotically stable positive equilibrium point (p_*, r_*) of the equations (8.1) and (8.2)

malignant if the corresponding tumor volume p_* is close to the carrying capacity of the system; we call it benign if it is by at least an order of magnitude smaller. We call the region of attraction of a malignant, respectively benign equilibrium point the malignant, respectively benign regions.

In case of a microscopic benign equilibrium, this region can be interpreted as the set of all states of the system where the immune system is able to control the cancer and this is one possible way of describing what medically has been called *immunosurveillance*. The region of attraction of the macroscopic equilibrium point, on the other hand, corresponds to conditions when the system has escaped from this immunosurveillance and the disease, if untreated, will become lethal. Obviously, a relevant structure therefore is the boundary between these two behaviors which is formed by the stable manifold of the saddle point. Since reality is far more complicated than accounted for in this or any model, constantly random (and otherwise) events will take place that perturb the state of the system in the state-space and, once such a temporary disturbance has passed, the system will settle down to follow the trajectories in the phase portrait. Thus tumors that have a large malignant regions correspond to more aggressive form since it is more likely for a perturbation to land in this set. Once this happens, the question becomes how (if possible) to move the state back into the benign region. This will be the main topic discussed in this section.

8.1.2 On Immune Surveillance: Benign and Malignant Regions for Stepanova's Model with Generalized Logistic Growth

We explore the dynamics of the system for a generalized logistic growth rate

$$F(p) = 1 - \left(\frac{p}{p_\infty}\right)^\nu, \qquad \nu > 0,$$

and, especially, how the benign and malignant regions change with the parameter ν. This exponent largely determines the rate of tumor growth: for small values of ν, the term $\left(\frac{p}{p_\infty}\right)^\nu$ will be close to 1 and the model reflects a slowly growing tumor while tumor growth accelerates with increasing values of ν reaching unrestricted exponential growth in the limit $\nu \to \infty$. We just remark that if the tumor growth parameter ξ that multiplies the function F is made to depend on the parameter ν in the order of $\xi = O(\frac{1}{\nu})$, then a Gompertzian model is obtained in the limit $\nu \to 0$. Thus, in a certain sense, the generalized logistic rate function F interpolates between Gompertzian and exponential growth models with the parameter ν related to the speed of tumor growth. For the models of the tumor-vasculature dynamics that were considered in Chapter 5 it has been argued by d'Onofrio, Gandolfi, and Rocca [263] that models with $\nu < 1$ more realistically reflect a slowing down process of tumor proliferation as a response to its changing environment. This

also agrees with a mechanistic model for non-immunogenic tumors as discussed by d'Onofrio in [254]. In the context of tumor immune system interactions, which play a major role at the onset of the disease, it would seem that all values of ν are reasonable, simply modeling different rates of tumor growth lying between the extremes of Gompertzian and exponential growth models. Thus we consider the full range $\nu \in (0,\infty)$.

For a generalized logistic growth model, the disease free equilibrium point is locally asymptotically stable if $\xi\delta < \theta\gamma$ and unstable if $\xi\delta > \theta\gamma$. In the first case, we shall see below that if ν is close to 0, then there are no other equilibria and the disease free equilibrium point is globally asymptotically stable, i.e., every solution converges to $(0, \frac{\gamma}{\delta})$. This simply corresponds to a scenario when the immune system indeed is able to control the cancerous growth. Solving the equation $\dot{p} = 0$ for r and substituting into the relation $\dot{r} = 0$, positive equilibria are the solutions of the nonlinear equation

$$\xi\left(1 - \left(\frac{p}{p_\infty}\right)^\nu\right) - \frac{\theta\gamma}{\alpha\beta p^2 - \alpha p + \delta} = 0. \tag{8.4}$$

in the interval $(0, p_\infty)$. Note that no solutions p_* exist where the quadratic polynomial $Q(p) = \alpha\beta p^2 - \alpha p + \delta$ is negative. If $\alpha \geq 4\beta\delta$, then Q has two positive roots $p_- < p_+$ given by

$$p_- = \frac{1}{2\beta}\left(1 - \sqrt{1 - 4\frac{\beta\delta}{\alpha}}\right) \qquad \text{and} \qquad p_+ = \frac{1}{2\beta}\left(1 + \sqrt{1 - 4\frac{\beta\delta}{\alpha}}\right)$$

and all zeros p_* of (8.4) lie in the intervals $(0, p_-)$ or (p_+, p_∞); for $\alpha < 4\beta\delta$ the roots are complex and Q is always positive so that the location of the roots in $(0, p_\infty)$ is not restricted. Also note that, in the case $\nu = 1$ of classical logistic growth, equation (8.4) is equivalent to a cubic polynomial and thus there exist at most three roots. This holds in general.

Proposition 8.1.3. *For a generalized logistic growth rate $F(p) = 1 - \left(\frac{p}{p_\infty}\right)^\nu$ and for all values of $\nu > 0$, there exist at most three positive equilibria for the dynamical system (8.1)–(8.2). Generically, a saddle-node bifurcation occurs if*

$$\frac{\left(\frac{p_*}{p_\infty}\right)^\nu}{1 - \left(\frac{p_*}{p_\infty}\right)^\nu} = \frac{2\alpha\beta p_*^2 - \alpha p_*}{\alpha\beta p_*^2 - \alpha p_* + \delta}. \tag{8.5}$$

In particular, this is only possible in the region $2\beta p_* > 1$. If we order the equilibrium points $(p_*^{(i)}, r_*^{(i)})$ according to their tumor volumes, $p_*^{(1)} < p_*^{(2)} < p_*^{(3)}$, then the low and high equilibrium points $(p_*^{(1)}, r_*^{(1)})$ and $(p_*^{(3)}, r_*^{(3)})$ are locally asymptotically stable while the intermediate equilibrium point $(p_*^{(2)}, r_*^{(2)})$ is unstable.

Proof. We rewrite equation (8.4) in the following form using as variable x and defining functions P_ν and R:

$$P_\nu(x) = 1 - \left(\frac{x}{x_\infty}\right)^\nu = \frac{\theta\gamma}{\xi}\frac{1}{\alpha\beta x^2 - \alpha x + \delta} = R(x).$$

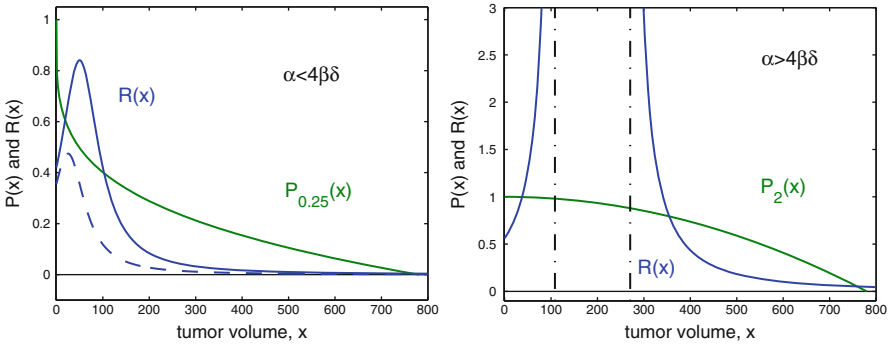

Fig. 8.2 Equilibria for the system (8.1) and (8.2) for a generalized logistic growth function $F(x) = 1 - \left(\frac{x}{x_\infty}\right)^\nu$.

If the roots of Q are complex, then R is positive on $[0,\infty)$ with a global maximum at $\tilde{x} = \frac{1}{2\beta}$. Furthermore, R is strictly increasing on $[0,\tilde{x})$ and strictly decreasing on $(\tilde{x},\infty)$. Since P_ν is a decreasing function, it follows that there exists at most one equilibrium point in the interval $[0,\frac{1}{2\beta}]$, possibly none. In the interval $[\frac{1}{2\beta},\infty)$, the function R has a unique inflection point $\hat{x}$ and is strictly concave over the interval $[\frac{1}{2\beta},\hat{x})$ and strictly convex over $[\hat{x},\infty)$. Coupled with monotonicity and convexity properties of the function F, it follows that there can be no more than two additional zeroes on the interval $[\frac{1}{2\beta},\infty)$ for a maximum of three possible zeros. Note that it is possible that there are no solutions for certain parameter values. If the roots of Q are real, then R has simple poles at $x_- = p_-$ and $x_+ = p_+$ and is positive, strictly monotonically increasing and convex over $(0,x_-)$ and positive, strictly monotonically decreasing and convex over (x_+,x_∞). It immediately follows from these monotonicity properties that there can be at most one zero on $(0,x_-)$ and since $\lim_{x\to x_1-} R(x) = +\infty$, it is clear that there exists a solution in this interval if and only if $\theta\gamma \le \xi\delta$. If $\nu \ge 1$, then F is concave over the interval (x_+,x_∞) and this implies that there can be at most two intersections with the graph of R. If $\nu < 1$, it follows that the difference $R - F$ is strictly increasing after a second intersection and thus also in this case no more equilibria are possible. In either case, this allows for at most two more solutions. The underlying geometric properties are illustrated in Figure 8.2.

Using the relation that

$$\theta r_* = \xi \left(1 - \left(\frac{p_*}{p_\infty}\right)^\nu\right),$$

the Jacobian matrix A at a positive equilibrium point (p_*, r_*) is given by

$$\begin{pmatrix} -\xi\nu\left(\frac{p_*}{p_\infty}\right)^\nu & -\theta p_* \\ \alpha(1-2\beta p_*)r_* & \alpha\left(p_* - \beta p_*^2\right) - \delta \end{pmatrix}$$

and thus its characteristic polynomial

$$\chi_A(t) = \det(t \cdot \mathrm{Id} - A) = t^2 + at + b$$

has coefficients

$$a = \left(\alpha\beta p_*^2 - \alpha p_* + \delta\right) + \xi\nu\left(\frac{p_*}{p_\infty}\right)^\nu$$

and

$$b = \det(A) = \left(\alpha\beta p_*^2 - \alpha p_* + \delta\right)\xi\nu\left(\frac{p_*}{p_\infty}\right)^\nu + \alpha\theta(1-2\beta p_*)p_* r_*. \tag{8.6}$$

At a positive equilibrium point p_*, $Q(p_*) = \alpha\beta p_*^2 - \alpha p_* + \delta$ is positive. For, this always holds if the roots of Q are complex and if the roots are real, then the equilibria lie outside of the interval $[p_-, p_+]$. Hence the coefficient a is positive and A has a positive real eigenvalue if and only if $b = \det(A) < 0$ while all eigenvalues have negative real parts if $b = \det(A) > 0$. Thus the equilibrium point (p_*, r_*) is unstable if $\det(A) < 0$ and locally asymptotically stable if $\det(A) > 0$. If $b = 0$, and this is equivalent to (8.5), A has eigenvalue 0 and a negative eigenvalue and generically a saddle-node bifurcation occurs. This is only possible if $p_* \leq \frac{1}{2\beta}$. Since the benign equilibrium point is always locally asymptotically stable, the remaining stability properties are a consequence of the saddle-node bifurcation theorem. □

Figure 8.3 shows the values of the equilibria as function of ν for the data from Table 8.1. We have $\xi\delta > \theta\gamma$ and thus the disease free equilibrium point $(p_f, r_f) = (0, \frac{\gamma}{\delta})$ is unstable. For small values of ν, $\nu < \nu_* = 0.40355$, there only exists one globally asymptotically stable equilibrium point with small p-value that corresponds to a microscopic benign state. These parameter values medically reflect a situation where the tumor growth is very small and the reaction of the immune system is able to control the tumor. For $\nu_* = 0.40355$ the system undergoes a saddle-node bifurcation and two additional equilibria, one stable (malignant), the other unstable, are created and the system becomes multi-stable for $\nu > \nu_*$ with three equilibria. The benign equilibrium point (p_b, r_b) is a *stable focus* whose values are represented by the green curves in Figure 8.3 and the malignant equilibrium point (p_m, r_m) is a *stable node* whose values are represented by the red curves; the values for the

saddle point (p_s, r_s) are represented by the blue curves. For example, for classical logistic growth ($\nu = 1$) the numerical values are given by $(p_b, r_b) = (35.158, 0.537)$, $(p_s, r_s) = (387.527, 0.283)$ and $(p_m, r_m) = (736.102, 0.032)$.

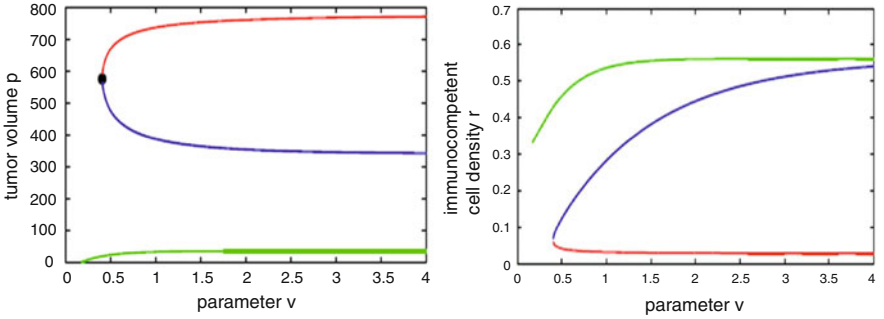

Fig. 8.3 Values of the positive equilibria for the system (8.1) and (8.2) as a function of ν (x-values on the left and y-values on the right). The values for the benign equilibrium point are shown as the green curve, for the saddle as the blue curve and for the malignant equilibrium point as the red curve.

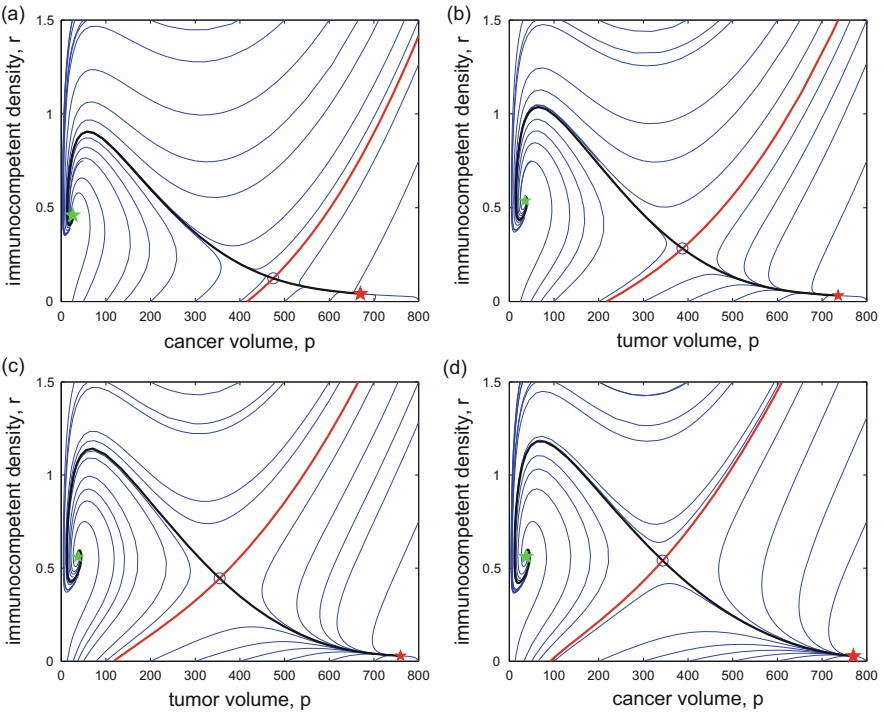

Fig. 8.4 Phase portraits of the system (8.1) and (8.2) for (a) $\nu = \frac{1}{2}$, (b) $\nu = 1$, (c) $\nu = 2$, and (d) $\nu = 4$ and the parameter values from Table 8.1.

Figure 8.4 illustrates the phase-portraits for the values $\nu = \frac{1}{2}, 1, 2$, and 4. In each of the figures, we have highlighted the stable manifold of the saddle (p_s, y_s), which forms the stability boundary for the benign and malignant regions, as a thick solid red line. This curve also is called the separatrix for planar systems. These phase portraits show the decrease of the benign region at the expense of the malignant regions as the parameter ν increases reflecting the fact that the immune system becomes increasingly overwhelmed by a faster growing tumor. In the limit $\nu \to \infty$ we obtain a malignant region similar to the one for exponential growth. The benign equilibrium point (p_b, r_b) converges to the disease free equilibrium point $(0, r_f)$ as $\nu \to \infty$.

These phase portraits reflect a general structure of the dynamics that is multistable and has both an asymptotically stable microscopic (benign) and an asymptotically stable macroscopic (malignant) equilibrium point. The corresponding regions of attraction are separated by the stable manifold of a saddle. Figure 8.5 shows a blow-up of the curve of saddle points for $\nu \in [\frac{1}{2}, 4]$ along with a normalized stable eigenvector. It is always possible to choose this vector so that both coordinates are positive. The figure shows that the direction is quite stable, but that with increasing values of ν the stable manifold moves toward lower p and higher r values. The tumor growth rate directly relates to the sizes of the regions of attraction of the stable equilibria with slower growing tumors having larger benign regions and faster growing tumors having larger malignant regions. From a practical point of view, the question of curing cancer then is related to the mathematical problem of how one can move an initial condition that lies in the malignant region into the benign region through therapy. But first we need to incorporate therapeutic action into the dynamics (8.1) and (8.2).

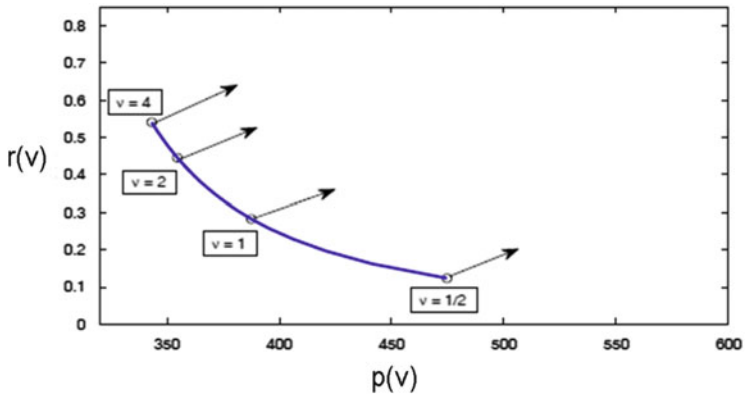

Fig. 8.5 The saddle points for $\nu \in [\frac{1}{2}, 4]$ with a stable eigenvector at the saddle point.

8.2 Formulation of an Optimal Control Problem: Transfer from the Malignant into the Benign Region Through Therapy

We incorporate both a standard chemotherapeutic agent and a rudimentary immunotherapy in the form of an immune boost into the model. As before, we use the log-kill hypothesis to model tumor loss under chemotherapy, i.e., we assume that the elimination of tumor cells is proportional to the tumor volume p and the concentration of the chemotherapeutic agent which we denote by u. The cytotoxic effects of the chemotherapeutic agent on the immune system are complex and are more difficult to assert. The effects on existing cells of the immune system may be modeled as a separate log-kill type term in the equation for $\dot{r}$, but the negative side effects of chemotherapy also include a lower influx of T-cells from the primary organs that are potentially damaged by chemotherapy, especially the bone marrow. These can be incorporated into the model by reducing the factor γ that denotes this influx. But these effects are secondary to the main chemotherapy and initially we assume they are smaller and neglect them. This is a reasonable assumption for so-called *strongly targeted chemotherapeutic drugs*. For simplicity, we also do not include a pharmacokinetic model and identify dose rates with concentrations. Generally, when a standard linear pharmacokinetic model is added to the model, the changes that occur follow the same principles discussed earlier (see Sections 2.3 and 6.3) and thus here we follow this simpler modeling approach. For example, optimal control for this system with PK is considered in [176]. While most of the models in this chapter will focus on chemotherapy, in some we also include a rudimentary immunotherapy in the form of an immune boost which is added as a positive term to equation (8.2). Overall, the controlled equations with treatment take the form

$$\dot{p} = \xi pF(p) - \theta pr - \kappa pu, \tag{8.7}$$

$$\dot{r} = \alpha\left(p - \beta p^2\right) r + \gamma(1 - \zeta u) - \delta r - \eta ru + \rho rv. \tag{8.8}$$

Admissible controls are Lebesgue measurable (respectively, piecewise continuous) functions u and v that take values in the interval $[0,1]$. Since no pharmacokinetic model is included, without loss of generality we normalize the maximum values for the controls to 1 and subsume the maximum dose rates/concentrations in the coefficients for the pharmacodynamic model (κ,ζ,η and ρ). As before, all Greek letters denote constant positive coefficients and in addition we have that $\zeta < 1$. The state space for the problem is given by $\mathbb{M} = \{(p,r) : 0 < p < p_\infty, 0 < r\}$ and we assume that initial conditions lie in $\mathbb{M}$. We also restrict the tumor growth rate F to Gompertzian, logistic or generalized logistic models. For each of these the carrying capacity is finite and we have that $F(p_\infty) = 0$.

Proposition 8.2.1. *The region $\mathbb{P}$ is positively invariant for the control system, i.e., given arbitrary admissible controls $u : [0,T] \to [0,1]$ and $u : [0,T] \to [0,1]$ defined over an interval $[0,T]$, $T \leq \infty$, the solution to the dynamics (8.7) and (8.8) exists on $[0,T]$ and the corresponding trajectory lies in $\mathbb{M}$.*

Proof. Since $\dot{q}_{|q=0} = \gamma(1-\zeta u) > 0$, it follows that the q-coordinate of the solution is always positive. Furthermore, for any control u, $p \equiv 0$ is an equilibrium solution to equation (8.7) and we also have that $\dot{p}_{|p=p_\infty} < 0$. Hence the p-component of the solution cannot leave the finite open interval $(0, p_\infty)$. It follows that the right-hand side of the dynamics is linearly bounded and, by a standard argument of ODEs, this implies that solutions exist on all of $[0,T]$. □

The practical aim of therapy thus becomes to move an initial state (p_0, r_0) of the system that lies in the malignant region of the uncontrolled system into the region of attraction of the stable, benign equilibrium point while keeping side effects tolerable. Here we consider the following optimal control problem:

[CI] For a free terminal time T, minimize the objective

$$J = Ap(T) - Br(T) + \int_0^T (Mu(t) + Nv(t) + S)\,dt, \tag{8.9}$$

over all Lebesgue measurable (respectively, piecewise continuous) functions $u : [0,T] \to [0,1]$ and $v : [0,T] \to [0,1]$ subject to the dynamics (8.7) and (8.8),

$$\begin{aligned} \dot{p} &= \xi pF(p) - \theta pr - \kappa pu, & p(0) &= p_0, \\ \dot{r} &= \alpha\left(p - \beta p^2\right) r + \gamma(1-\zeta u) - \delta r - \eta ru + \rho yv & r(0) &= r_0. \end{aligned}$$

The objective function consists of three separate pieces: (i) the penalty term $Ap(T) - Br(T)$ at the final time is designed to induce the state of the system to move from the malignant into the benign region, (ii) the terms $\int_0^T u(t)dt$ and $\int_0^T v(t)dt$ measure the amounts of drugs given, and (iii) the penalty term ST on the final time makes the mathematical problem well posed. All coefficients are positive. We emphasize that, like in engineering, the coefficients in the objective (8.9) are actually variables of choice that should be calibrated to fine-tune the response of the system. The choice of the weights aims at striking a balance between the benefit at the terminal time T, $Ap(T) - Br(T)$, and the overall side effects measured by the total amount of drugs given, while it guarantees the existence of an optimal solution by also penalizing the free terminal time T. We discuss the rationale behind each term.

(i) The main feature here is to formulate the objective (8.9) in such a way that minimization induces a transfer of the system from the malignant into the benign region of the state space. For this, it may no longer be adequate to just minimize the tumor volume since, as can be seen in the phase-portraits, small tumor volumes are possible that lie in the malignant region if the immune system is depressed. Rather, the geometric shape of the separatrix matters. Ideally, if a functional description of this manifold could be given, one would minimize or maximize the level sets of this function to achieve a transfer into the benign region. But these are generally highly transcendental equations that cannot be solved explicitly. On the other hand, local approximations for the separatrix at the saddle point are easily obtained. It follows from Theorem 8.1.1 that the stable eigenspace at the saddle is the tangent space to the separatrix. This tangent

line is easily computed and its normal vector can serve as a reasonable direction in which we want the system to move. A second natural option would be to take the direction of the unstable eigenvector at the saddle point. For, this is the tangent vector to the path which uncontrolled trajectories in the benign region will follow closely when in the benign region. For sake of specificity, we consider the first approach. Let $\mathfrak{v} = (B,A)^T$ denote a stable eigenvector $\mathfrak{v}$ of the saddle point (p_s, r_s) oriented so that both A and B are positive numbers. It follows from the geometry of the stable manifold that A and B will have the same sign and including in the objective a term of the form $Ap(T) - Br(T)$ gives the correct direction to minimize in the objective. The level sets of this quantity are lines parallel to the tangent space of the stable manifold of the saddle, and minimizing this quantity thus creates an incentive for the system to move into the benign region.

(ii) As for the models considered earlier, we do not include a separate compartment of healthy cells that would describe the side effects of treatment. These are only measured indirectly through the total amounts of drugs given. Therefore, in the objective function to be minimized, we once more include the terms $\int_0^T Mu(t) + Nv(t)dt$ as soft constraints. Clinical data as to the severity of the drugs should be reflected in the choices for C and D. Naturally, the specific type of tumor and stage of cancer will enter into the calibration of these coefficients. In a more advanced stage, higher side effects need to be tolerated and thus smaller values of C would be taken.

(iii) The last term in the objective function, which can be written either under the integral or as a separate penalty term ST, is included to give a mathematically well-posed problem formulation. The reason is that the existence of the asymptotically stable, benign equilibrium point generates controlled trajectories that improve the value $Ap(T) - Br(T)$ of the objective along the trivial controls $u = 0$ and $v = 0$. If no penalty is imposed on the terminal time, then this creates a "free pass" structure in which the value of the objective can be improved without incurring a cost. As a result, in such a situation an optimal solution may not exist. Intuitively, the controls can switch to $(u,v) = (0,0)$ immediately as the separatrix is crossed and then take an increasingly longer time as they pass near the saddle point with the infimum arising in the limit $T \to \infty$ as the control switches to follow $u = 0$ when the controlled trajectory intersects the separatrix, then follows the separatrix for an infinite time to the saddle and then again leaves this saddle point along the unstable manifold, once more taking an infinite time. This indeed would be the "optimal" solution for this problem formulation, but it is not an admissible trajectory in our system. From a practical point of view, of course it would also be unacceptable for the system to move along the boundary between benign and malignant behaviors. In view of imprecise and mathematically not modeled dynamics and other random perturbations, the addition of this term not only makes the optimal control problem well defined, but it also provides desired robustness and stability properties for the underlying real system. Thus it makes perfect sense,

both mathematically and practically, to include a penalty term on the final time in the objective. It creates a well-posed mathematical problem for which the existence of solutions follows from standard theory.

Writing the state of the system as $z = (p,r)^T$, we again express the dynamics in the vector field form

$$\dot{z} = f(z) + ug_1(z) + vg_2(z) \tag{8.10}$$

with drift vector field

$$f(z) = \begin{pmatrix} \xi pF(p) - \theta pr \\ \\ \alpha\left(p - \beta p^2\right) r + \gamma - \delta r \end{pmatrix} \tag{8.11}$$

and control vector fields

$$g_1(z) = -\begin{pmatrix} \kappa p \\ \\ \eta r + \gamma\zeta \end{pmatrix} \qquad \text{and} \qquad g_2(z) = \begin{pmatrix} 0 \\ \\ \rho r \end{pmatrix}. \tag{8.12}$$

8.2.1 Necessary Conditions for Optimality

We briefly state the necessary conditions for optimality of the maximum principle for the general form. Since there are no terminal constraints, extremals for this problem are normal (see Corollary A.2.2 in Appendix A) and, with $\lambda = (\lambda_1, \lambda_2)$, we therefore define the Hamiltonian $H = H(\lambda, p, r, u, v)$ as

$$\begin{aligned} H = {} & Mu + Nv + S + \lambda_1\left(\xi pF(p) - \theta pr - \kappa pu\right) \\ & + \lambda_2\left(\alpha\left(p - \beta p^2\right) r + \gamma(1 - \zeta u) - \delta r - \eta ru + \rho rv\right). \end{aligned} \tag{8.13}$$

Equivalently, in terms of the drift and control vector fields we have that

$$H = S + \langle \lambda, f(z)\rangle + u\left(M + \langle \lambda, g_1(z)\rangle\right) + v\left(N + \langle \lambda, g_2(z)\rangle\right).$$

If (u_*, v_*) is an optimal control defined over an interval $[0,T]$ with corresponding trajectory $z_* = (p_*, r_*)^T$, then it follows from the maximum principle (Theorem A.3.1 in Appendix A) that there exists an absolutely continuous covector $\lambda : [0,T] \to \left(\mathbb{R}^2\right)^*$, that satisfies the adjoint equations

$$\dot{\lambda}_1 = -\frac{\partial H}{\partial p} = -\lambda_1\left(\xi\left(pF'(p) + F(p)\right) - \theta r - \kappa u\right) - \lambda_2\alpha(1 - 2\beta p)r \tag{8.14}$$

$$\dot{\lambda}_2 = -\frac{\partial H}{\partial r} = \lambda_1\theta p - \lambda_2\left(\alpha\left(p - \beta p^2\right) - \delta - \eta u + \rho v\right) \tag{8.15}$$

with terminal conditions $\lambda_1(T) = A$ and $\lambda_2(T) = -B$ such that for almost every time $t \in [0,T]$, the optimal controls $(u_*(t), v_*(t))$ minimize the Hamiltonian H along

$(\lambda(t), p_*(t), r_*(t))$ over the control set $[0,1]\times[0,1]$ and the minimized Hamiltonian is constant equal to 0,

$$H(\lambda_0, \lambda(t), p_*(t), r_*(t), u_*(t), v_*(t)) \equiv 0.$$

Since the Lagrangian in the objective does not depend on the state variables p and r, the adjoint equation again is a homogeneous linear equation of the form

$$\dot{\lambda}(t) = -\lambda(t)\left(Df(z_*(t)) + u_*(t)Dg_1(z_*(t)) + v_*(t)Dg_2(z_*(t))\right). \tag{8.16}$$

Since $\lambda(T) \neq 0$, it follows that the multiplier λ doesn't vanish: $\lambda(t) \neq 0$ for all $t \in [0,T]$.

The minimization of the Hamiltonian H decouples and can be carried out separately. Defining the *switching functions* Φ_1 for u and Φ_2 for v as

$$\Phi_1(t) = M + \langle \lambda(t), g_1(z_*(t))\rangle = M - \lambda_1(t)\kappa p_*(t) - \lambda_2(t)\left(\eta r_*(t) + \gamma\zeta\right), \tag{8.17}$$

and

$$\Phi_2(t) = N + \langle \lambda(t), g_2(z_*(t))\rangle = N + \lambda_2(t)\rho r_*(t), \tag{8.18}$$

it follows that

$$u_*(t) = \begin{cases} 0 & \text{if} \quad \Phi_1(t) > 0, \\ 1 & \text{if} \quad \Phi_1(t) < 0, \end{cases} \qquad \text{and} \qquad v_*(t) = \begin{cases} 0 & \text{if} \quad \Phi_2(t) > 0, \\ 1 & \text{if} \quad \Phi_2(t) < 0. \end{cases} \tag{8.19}$$

The controls will be singular if the respective switching functions vanish over an open interval I and, as before, we need to compute the derivatives of these functions. As for the models considered in Chapter 7, the Lagrangian is independent of the state and thus we have the same result as in Proposition 7.1.1 (cf., Proposition A.3.1 in Appendix A):

Proposition 8.2.2. *Let $z(\cdot)$ be a solution of the dynamics (8.10) for the controls u and v and let λ be a solution of the corresponding adjoint equation (8.16). For a continuously differentiable vector field h, let*

$$\Psi(t) = \langle \lambda(t), h(z(t))\rangle = \lambda(t)h(z(t)). \tag{8.20}$$

The derivative of Ψ is then given by

$$\dot{\Psi}(t) = \langle \lambda(t), [f + ug_1 + vg_2, h](z(t))\rangle. \tag{8.21}$$

The first derivatives of the switching functions Φ_1 and Φ_2 are thus given by

$$\dot{\Phi}_1(t) = \langle \lambda(t), [f + vg_2, g_1](z_*(t))\rangle$$

and

$$\dot{\Phi}_2(t) = \langle \lambda(t), [f + ug_1, g_2](z_*(t)) \rangle .$$

The commutator of the control vector fields is the constant vector field

$$[g_1, g_2](z) = \begin{pmatrix} 0 & 0 \\ 0 & \rho \end{pmatrix} \begin{pmatrix} -\kappa p \\ -\eta r - \alpha\zeta \end{pmatrix} - \begin{pmatrix} -\kappa & 0 \\ 0 & -\eta \end{pmatrix} \begin{pmatrix} 0 \\ \rho r \end{pmatrix} = \begin{pmatrix} 0 \\ \rho\alpha\zeta \end{pmatrix}. \quad (8.22)$$

If $\zeta = 0$, the two control vector fields commute and this at times considerably simplifies the mathematical analysis.

8.3 Cancer Chemotherapy with Strongly Targeted Cytotoxic Drugs

We consider the single-input optimal control problem for chemotherapy with a strongly targeted chemotherapeutic drug. In this case, we assume that the side effects on the immune system are negligible and consider the following simplified form of the dynamics:

$$\begin{aligned} \dot{p} &= \xi p F(p) - \theta p r - \kappa p u, & p(0) &= p_0, \\ \dot{r} &= \alpha \left(p - \beta p^2\right) r + \gamma - \delta r, & r(0) &= r_0. \end{aligned}$$

In this section we shall analyze the structure of optimal controls for both a Gompertzian ($F_G(p) = -\ln\left(\frac{p}{p_\infty}\right)$) and generalized logistic growth model ($F_L(p) = 1 - \left(\frac{p}{p_\infty}\right)^\nu$, $\nu > 0$). It will be seen that the results for the Gompertzian model relate to the limiting behavior of the results for the generalized logistic model as $\nu \to 0$. The drift and control vector fields are

$$f(z) = \begin{pmatrix} \xi p F(p) - \theta p r \\ \\ \alpha \left(p - \beta p^2\right) r + \gamma - \delta r \end{pmatrix} \quad \text{and} \quad g(z) = \begin{pmatrix} -\kappa p \\ \\ 0 \end{pmatrix}.$$

We label the corresponding optimal control problem [CI1].

8.3.1 Singular Controls and Arcs

For this optimal control problem the way in which singular controls and arcs are computed is somewhat different than in Chapters 2 and 3. The procedure is independent of the particular growth function, but the formulas for singular controls and curves will of course depend on this specification.

As before, if an optimal control u_* is singular on an open interval I, then the switching function Φ,

$$\Phi(t) = M + \langle \lambda(t), g(z_*(t)) \rangle = M - \lambda_1(t)\kappa p_*(t),$$

and all its derivatives vanish on I. Furthermore, the Hamiltonian H vanishes identically over $[0,T]$ and thus we also have that

$$H = S + \langle \lambda(t), f(z_*(t)) \rangle + u_*(t)\Phi(t) \equiv 0.$$

Along a singular arc it therefore follows that

$$H = S + \langle \lambda(t), f(z_*(t)) \rangle \equiv 0$$

and combining this relation with $\Phi(t) \equiv 0$, we obtain

$$\langle \lambda(t), Mf(z_*(t)) \rangle \equiv -MS \equiv \langle \lambda(t), Sg(z_*(t)) \rangle$$

so that

$$\langle \lambda(t), Mf(z_*(t)) - Sg(z_*(t)) \rangle \equiv 0.$$

Furthermore, it follows from Proposition 8.2.2 that

$$\dot{\Phi}(t) = \langle \lambda(t), [f,g](z_*(t)) \rangle \equiv 0$$

on I. Since $\lambda \in \left(\mathbb{R}^2\right)^*$ is nontrivial, the vector fields $Mf - Sg$ and $[f,g]$ must be linearly dependent when the optimal control is singular. Hence a singular arc must lie in the zero set of the determinant,

$$\det\left(Mf(z) - Sg(z), [f,g](z)\right) = 0. \tag{8.23}$$

Proposition 8.3.1. *For the optimal control problem [CI1], the singular curve $\mathscr{S}$ is contained in the zero set of a function $W = W(p,r)$ which is quadratic in r with coefficients that are functions of p,*

$$W(p,r) = w_2(p)r^2 + w_1(p)r + w_0(p),$$

given by

$$\begin{aligned}
w_0(p) &= -M\gamma\xi pF'(p),\\
w_1(p) &= [M\xi F(p) + S\kappa]\,\alpha(p - 2\beta p^2) - \xi pF'(p)M\left(\alpha\left(p - \beta p^2\right) - \delta\right),\\
w_2(p) &= -M\theta\alpha\left(p - 2\beta p^2\right).
\end{aligned}$$

Proof. The Lie bracket $[f,g]$ is given by

$$\begin{aligned}[f,g](z) &= Dg(z)f(z) - Df(z)g(z)\\ &= \begin{pmatrix} -\kappa\xi pF(p) + \kappa\theta pr \\ 0 \end{pmatrix} - \begin{pmatrix} -\kappa\xi p\left(F(p) + pF'(p)\right) + \kappa\theta pr \\ -\kappa\alpha\left(1-2\beta p\right)pr \end{pmatrix}\\ &= \kappa p \begin{pmatrix} \xi pF'(p) \\ \alpha(1-2\beta p)r \end{pmatrix}.\end{aligned}$$

Hence

$$\begin{aligned}\det\left(Mf(z) - Sg(z), [f,g](z)\right) &= \kappa p \begin{vmatrix} M\left(\xi pF(p) - \theta pr\right) + S\kappa p & \xi pF'(p) \\ M\left(\alpha\left(p-\beta p^2\right)r + \gamma - \delta r\right) & \alpha(1-2\beta p)r \end{vmatrix}\\ &= \kappa p \cdot W(p,r)\end{aligned}$$

with the function W defined by the determinant on the right-hand side. Multiplying out the terms verifies the functional form and the coefficients specified above. □

Because W is quadratic in r, for every fixed value of p, the singular curve $\mathscr{S}$ contains at most two points in $\mathbb{M}$. For a Gompertzian growth model we have that $pF_G'(p) \equiv -1$ and for the generalized logistic model we get $pF_L'(p) = -\nu\left(\frac{p}{p_\infty}\right)^\nu$. In either case, the coefficient $w_0(p)$ is always positive. The quadratic coefficient $w_2(p)$ does not depend on the growth function and is negative for $p < \frac{1}{2\beta}$ and positive for $p > \frac{1}{2\beta}$. In particular, for $p < \frac{1}{2\beta}$ there exist two real solutions, one positive, one negative. Only the positive one is of interest for the problem and thus the singular curve $\mathscr{S}$ is the graph of a function over the interval $(0, \frac{1}{2\beta})$. Whether solutions exist for $p > \frac{1}{2\beta}$ depends on the actual parameter values. Analytic formulas for r as a function of p can still be written down, but they get unwieldy.

We still compute the Legendre-Clebsch condition for optimality of a singular arc. By Proposition 8.2.2 the second derivative of the switching function is given by

$$\ddot{\Phi}(t) = \langle\lambda(t), [f,[f,g]](z_*(t))\rangle + u(t)\,\langle\lambda(t), [g,[f,g]](z_*(t))\rangle$$

and it is a necessary condition for optimality of a singular control u_* that

$$\langle\lambda(t), [g,[f,g]](z_*(t))\rangle \leq 0.$$

This Lie bracket is given by

$$\begin{aligned}[g,[f,g]](z) &= D([f,g])(z)g(z) - Dg(z)[f,g](z) \\ &= -\kappa p \begin{pmatrix} \kappa\xi\left(2pF'(p)+p^2F''(p)\right) \\ \\ \kappa\alpha(1-4\beta p)r \end{pmatrix} + \kappa p \begin{pmatrix} \kappa\xi pF'(p) \\ \\ 0 \end{pmatrix} \\ &= -\kappa^2 p \begin{pmatrix} \xi\left(pF'(p)+p^2F''(p)\right) \\ \\ \alpha(1-4\beta p)r \end{pmatrix}.\end{aligned}$$

We now need to analyze the different growth functions separately. For the *Gompertzian model*, $F_G(p) = -\ln\left(\frac{p}{p_\infty}\right)$, we have that

$$pF_G'(p) \equiv -1 \qquad \text{and} \qquad pF_G'(p) + p^2F_G''(p) \equiv 0.$$

Hence the Lie brackets are given by

$$[f,g](z) = \kappa p \begin{pmatrix} -\xi \\ \\ \alpha(1-2\beta p)r \end{pmatrix}$$

and

$$[g,[f,g]](z) = -\kappa^2 p \begin{pmatrix} 0 \\ \\ \alpha(1-4\beta p)r \end{pmatrix}.$$

Furthermore, a direct computation verifies that $[f,[f,g]]$ takes the form

$$[f,[f,g]](z) = \kappa p \begin{pmatrix} -\xi^2 + \alpha\theta(p-2\beta p^2)r \\ \\ -\alpha(1-4\beta p)r\left[\xi\ln\left(\frac{p}{p_\infty}\right) + \theta p r^2\right] + (\gamma - \xi r)\alpha(1-2\beta p)r \end{pmatrix}.$$

The vector fields g and $[f,g]$ are linearly independent unless $p = \frac{1}{2\beta}$. For $p = \frac{1}{2\beta}$ there does not exist a point on the singular curve: it follows from $\dot{\Phi}(t) = -\lambda_1(t)\frac{\kappa\xi}{2\beta} = 0$ that $\lambda_1(t) = 0$ and thus $\Phi(t) = M > 0$. For $p \neq \frac{1}{2\beta}$, we can express the second-order brackets $[f,[f,g]]$ and $[g,[f,g]]$ as linear combinations of this basis in the form

$$[f,[f,g]](z) = \varphi_1(z)g(z) + \varphi_2(z)[f,g](z) \tag{8.24}$$

and

$$[g,[f,g]](z) = \psi_1(z)g(z) + \psi_2(z)[f,g](z). \tag{8.25}$$

Along a singular arc $\langle\lambda(t), g(z_*(t))\rangle = -M < 0$ and $\langle\lambda(t), [f,g](z_*(t))\rangle = 0$. Hence

$$\langle\lambda(t), [g,[f,g]](z_*(t))\rangle = -M\psi_1(z_*(t))$$

and thus the Legendre-Clebsch condition is satisfied if and only if $\psi_1(z_*(t))$ is non-negative. Direct computations verify that

$$\psi_1(z) = \kappa\xi\frac{1-4\beta p}{1-2\beta p} \qquad \text{and} \qquad \psi_2(z) = -\kappa\frac{1-4\beta p}{1-2\beta p}. \tag{8.26}$$

Thus the strengthened Legendre-Clebsch condition is satisfied for $0 < p < \frac{1}{4\beta}$ and $\frac{1}{2\beta} < p$ and it is violated for $\frac{1}{4\beta} < p < \frac{1}{2\beta}$.

By solving the equation $\ddot{\Phi}(t) = 0$ for u, the singular control can again formally be expressed as

$$u_{\text{sing}}(t) = -\frac{\langle \lambda(t), [f,[f,g]](z_*(t))\rangle}{\langle \lambda(t), [g,[f,g]](z_*(t))\rangle}.$$

Using the representations for the second order brackets, this simplifies to

$$u_{\text{sing}}(t) = -\frac{\varphi_1(z_*(t))}{\psi_1(z_*(t))}. \tag{8.27}$$

Overall, we therefore get the following result:

Proposition 8.3.2. *For the optimal control problem [CI1] with a Gompertzian growth rate $F_G(p) = -\ln\left(\frac{p}{p_\infty}\right)$, the control that keeps the singular curve $\mathscr{S}$ invariant is given in feedback form as*

$$u_{\text{sing}}(t) = -\frac{\varphi_1(z_*(t))}{\psi_1(z_*(t))}$$

with the coefficients φ_1 and ψ_1 defined through the relations (8.24) and (8.25). This control is admissible if and only if its value lies in the interval $[0,1]$. The strengthened Legendre-Clebsch condition is satisfied for $p < \frac{1}{4\beta}$ and $\frac{1}{2\beta} < p$, and it is violated for $\frac{1}{4\beta} < p < \frac{1}{2\beta}$.

Based on the formulas derived above, the singular arc, the singular control, and their admissible portions can easily be evaluated numerically. Note that, given a point $z_*(t) \in \mathscr{S}$, the equations $\Phi(t) = 0$ and $\dot{\Phi}(t) = 0$ have a unique solution for the multiplier $\lambda(t)$ and if the singular control is admissible, this locally defines a singular arc along which the strengthened Legendre-Clebsch condition is satisfied. In Figure 8.6 we illustrate the structure of the singular curves for the data from Table 8.1 and several parameter values C and S for the objective.

For the generalized logistic growth rate, $F_L(p) = 1 - \left(\frac{p}{p_\infty}\right)^\nu$, $\nu > 0$, we have that

$$pF_L'(p) = -\nu\left(\frac{p}{x_\infty}\right)^\nu \qquad \text{and} \qquad p^2F_L''(p) = -\nu(\nu-1)\left(\frac{p}{p_\infty}\right)^\nu$$

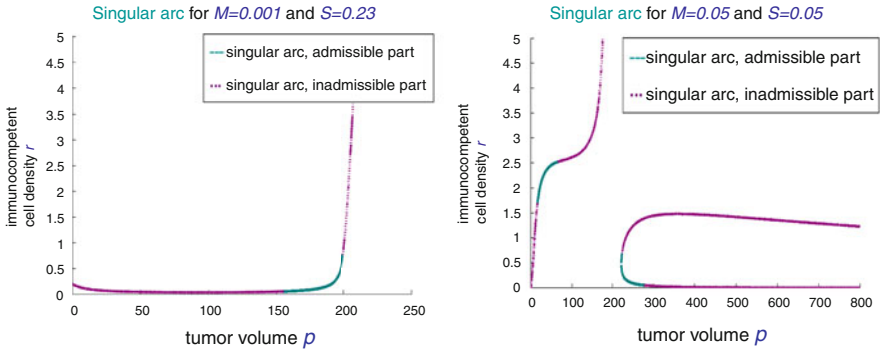

Fig. 8.6 Examples of singular curves for problem [CI1] with a Gompertzian growth function. The admissible portions are identified by the solid segments.

and thus

$$[f,g](z) = \kappa p \begin{pmatrix} -\xi \nu \left(\frac{p}{p_\infty}\right)^\nu \\ \\ \alpha (1-2\beta p) r \end{pmatrix}$$

and

$$[g,[f,g]](z) = -\kappa^2 p \begin{pmatrix} -\xi \nu^2 \left(\frac{p}{p_\infty}\right)^\nu \\ \\ \alpha (1-4\beta p) r \end{pmatrix}.$$

Proposition 8.3.3 ([187]). *For the optimal control problem [CI1] with a generalized logistic growth rate* $F_L(p) = 1 - \left(\frac{p}{p_\infty}\right)^\nu$, $\nu > 0$, *singular controls are of order* 1 *and the strengthened Legendre-Clebsch condition is satisfied if and only if*

$$\nu < \frac{1-4\beta p_*(t)}{1-2\beta p_*(t)}. \tag{8.28}$$

Proof. Suppose the control u_* is singular over an open interval I. Then $\Phi(t) \equiv 0$ on I, i.e., $\lambda_1(t)\kappa p_*(t) \equiv M > 0$, implies that λ_1 is positive along a singular arc. Furthermore, $\dot{\Phi}(t) \equiv 0$ on I gives that

$$\lambda_2(t)\alpha(1-2\beta p_*(t))\, r_*(t) \equiv \lambda_1(t)\xi\nu\left(\frac{p_*(t)}{p_\infty}\right)^\nu > 0.$$

Evaluating the Legendre-Clebsch condition, and using this relation to eliminate the multiplier λ_2, we therefore obtain that

$$\begin{aligned}
&\langle \lambda(t), [g,[f,g]](z_*(t))\rangle \\
&\quad = \kappa^2 \left\{ \lambda_1(t)\xi \left(\frac{p_*(t)}{p_\infty}\right)^\nu \nu^2 p_*(t) + \lambda_2(t)\alpha\left(4\beta p_*^2(t) - p_*(t)\right) r_*(t) \right\} \\
&\quad = \kappa^2 \lambda_1(t) p_*(t) \left\{ \xi \left(\frac{p_*(t)}{p_\infty}\right)^\nu \nu^2 + \frac{\xi\left(\frac{p_*(t)}{p_\infty}\right)^\nu \nu}{1-2\beta p_*(t)} (4\beta p_*(t) - 1) \right\} \\
&\quad = \kappa^2 \lambda_1(t) \xi \left(\frac{p_*(t)}{p_\infty}\right)^\nu \nu p_*(t) \left\{ \nu - \frac{1-4\beta p_*(t)}{1-2\beta p_*(t)} \right\}. \qquad (8.29)
\end{aligned}$$

Since $\lambda_1(t)$ is positive along a singular arc, this implies that the Legendre-Clebsch condition is satisfied if and only if (8.28) is satisfied. □

This determines the following intervals along which an optimal control can be singular dependent on the parameter ν.

Corollary 8.3.1. *Suppose an optimal control u_* for the optimal control problem [CI1] with a generalized logistic growth rate is singular at time t. Then, it follows that*

1. *if $0 < \nu < 1$, we have either $0 \le \beta p_*(t) < \frac{1}{2}\frac{1-\nu}{2-\nu} < \frac{1}{4}$ or $\frac{1}{2} < \beta p_*(t)$,*
2. *if $1 \le \nu \le 2$, then $\frac{1}{2} < \beta p_*(t)$ and*
3. *if $\nu > 2$, then $\frac{1}{2} < \beta p_*(t) < \frac{1}{2}\frac{1-\nu}{2-\nu}$.* □

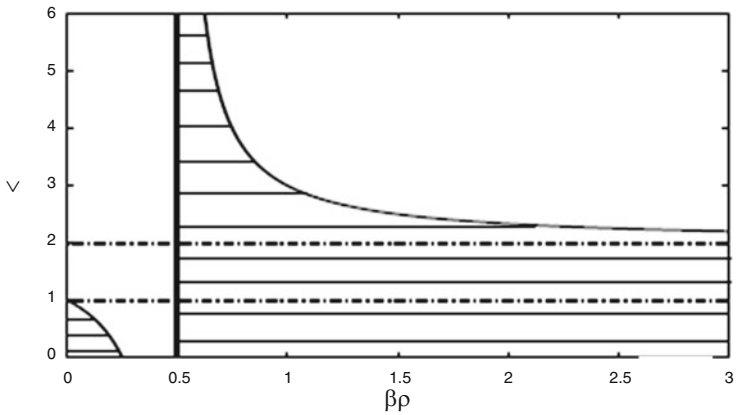

Fig. 8.7 The highlighted region represents the intervals (horizontally, for fixed value of ν and scaled as βp) on which the Legendre-Clebsch condition for minimality of singular arcs is satisfied.

These relations readily follow from condition (8.28) and are illustrated in Figure 8.7. In the limiting case $\nu \to 0$ we obtain that the Legendre-Clebsch condition is satisfied for βp in the intervals $[0, \frac{1}{4}) \cup (\frac{1}{2}, \infty)$ and this agrees with Proposition 8.3.2 for a Gompertzian growth function. As ν increases, these intervals continuously

shrink until, in the limit $\nu \to \infty$, for exponential growth singular controls are no longer optimal. The computation of the singular control is exactly as for the case of a Gompertzian function and the same formula (8.27) is valid, albeit with different functions ψ_1 and φ_1.

8.3.2 Optimal Controlled Trajectories for Gompertzian Growth

Since the Hamiltonian H vanishes identically, it follows from the transversality conditions $\lambda_1(T) = A$ and $\lambda_2(T) = -B$ that the terminal points of optimal controlled trajectories need to lie on specific curves.

Lemma 8.3.1. *If the optimal control ends with a segment where $u = 0$ or the control is singular, $u = u_{\text{sing}}$, then the terminal point $(p_*(T), r_*(T))$ lies on the curve*

$$A\left(-\xi p \ln\left(\frac{p}{x_\infty}\right) - \theta p r\right) - B\left(\alpha\left(p - \beta p^2\right) r + \gamma - \delta r\right) + S = 0; \tag{8.30}$$

if it ends with a segment for $u = 1$, then it lies on the curve

$$A\left(-\xi p \ln\left(\frac{p}{p_\infty}\right) - \theta p r - \kappa p\right) - B\left(\alpha\left(p - \beta p^2\right) r + \gamma - \delta r\right) + M + S = 0. \tag{8.31}$$

Generally, optimal controls need to be synthesized from bang and singular arcs. In this section, we give examples of optimal controlled trajectories for different scenarios that show the typical structures of the solutions. Optimal controls for problem [CI1] are no longer bang-bang and the potential presence of optimal singular arcs makes numerical computations challenging. There exists a large literature on algorithms that solve optimal control problems when the Hamiltonian is quadratic (cf., Chapter 4) or more generally positive definite in the controls, but numerical methods and software for problems that would include optimal singular arcs and, especially, concatenations with bang controls, is relatively scarce. The numerical difficulties lie with the fact that typically, as it is the case for the problem considered here, singular controls are only optimal on lower dimensional submanifolds and without any a priori information about these structures, numerical algorithms just are not able to locate these sets. 'Solutions' often exhibit chattering, i.e., controls that seemingly switch rapidly between various values, not necessarily the extreme points 0 and 1 of the control interval (e.g., see Figure 6.26 in Chapter 6). These are tell-tale signs of optimal singular arcs. For the computations reported in this section[2] we used the classical ε-algorithm approach in which a quadratic penalty term $\varepsilon \int_0^T u^2(t)dt$ is added to the objective and then the optimal controls for the underlying problem are recovered in the limit as $\varepsilon \to 0$ [15]. For the first step in the computations we also

[2] The numerical computations were carried out by our former graduate students Mohammad Naghneian and Mozhdeh Moselman Faraji Sadat.

used GPOPS (*G*eneral *P*seudo-spectral *OP*timal Control *S*oftware), an open-source MATLAB optimal control software that implements the Gauss hp-adaptive pseudospectral methods (`http://www.gpops.org/`, [284]). In these algorithms the state is approximated using a basis of Lagrange polynomials and the dynamics at the Legendre-Gauss nodes is collocated [19, 20, 129]. The continuous-time optimal control problem is then transformed into a finite-dimensional nonlinear programming problem that is being solved using standard algorithms. These type of algorithms are especially effective to find controls that lie in the interior of the control set like the singular controls for our problem, but they have issues when the controls are discontinuous as it is the case here for the concatenations of the singular controls with bang controls. The analytic formulas derived above allow us to verify whether a numerically found solution for interior controls is accurate in the sense that the corresponding controlled trajectories follow the singular curve $\mathscr{S}$ along singular controls. While these computations thus are not able to determine the optimal solutions completely, they are accurate enough to determine optimal finite concatenation structures. Then a subsequent local optimization over the switching times completes the computation of the optimal solutions. This algorithm based on GPOPS generates local minima and, when there were more than one candidate, a simple comparison of the values was done to obtain the best of these solutions that we describe below.

We illustrate the changes in the structure of optimal controls as we vary the coefficients M and S in the objective. The coefficients A and B are chosen according to the stable eigenvector of the saddle point and are kept constant at $A = 0.00192$ and $B = 1$; so is the numerical value chosen for κ, $\kappa = 1$. In our computations, we always use the same initial condition given by $(p_0, r_0) = (600, 0.1)$. The initial tumor volume p_0 denotes a multiple of some reference value and represents a tumor cell count that is 600 times higher than some chosen base value (say 10^6 cells); r_0 is a dimensionless, order-of-magnitude quantity that represents a depletion of the immuno-competent cell densities to 10% of a nominal value. These initial conditions lie well within the malignant region and initially in each scenario considered below the control is given by $u \equiv 1$ for some interval $[0, t_1]$.

Scenario 1: If the penalty on the terminal time T is large relative to the side-effects of treatment, $S \gg M$, this term becomes dominant and the optimal control is simply constant given by a full dose treatment, $u \equiv 1$. Figure 8.8 shows an example for this kind of trajectory with $M = 0.001$ and $S = 0.28$. The initial and terminal points are labeled in the figure as $z_0 = (p_0, r_0)$ and $z_T = (p_T, r_T)$, respectively. It is noticeable that with such a high cost on the terminal time, the optimal trajectory barely crosses into the benign region. A blow-up of the trajectory near the terminal point is given in the small box inserted into the figure. Yet, assuming the dynamics follows the uncontrolled system after the final time T, the state then converges to the benign equilibrium point. The figure also shows the potential singular arc for these coefficients which in this range is the graph of a function with its admissible portion identified by the solid green segment. For these parameter values, the optimal solution terminates exactly at the time when the singular arc is reached, but this is a mere coincidence without significance. This figure, as well as the ones given below, also identifies the two curves defined in equations (8.30) and (8.31) where an

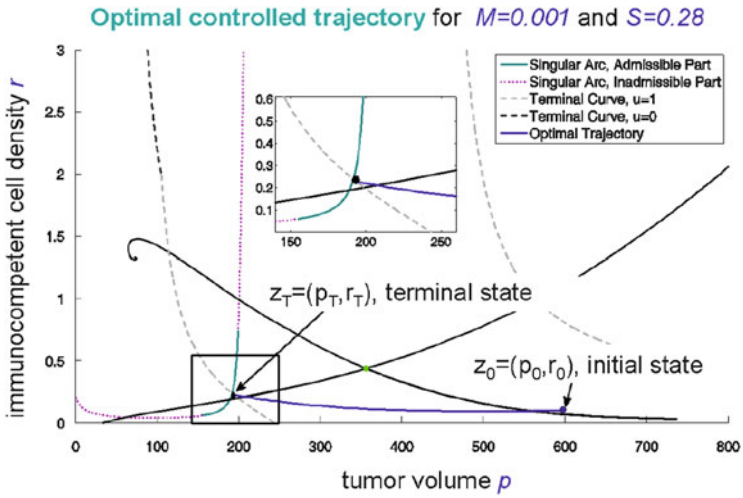

Fig. 8.8 Optimal controlled trajectory for $M = 0.001$ and $S = 0.28$. The corresponding control is constant, $u_*(t) \equiv 1$.

optimal control satisfies the required transversality conditions for ending with $u = 0$ and $u = 1$, respectively. The terminal point needs to lie on this curve according to the final value of the control being used.

Scenario 2: As the penalty S for the time used is decreased, the optimal controlled trajectory starts from $z_0 = (p_0, r_0)$ with an initial maximum dose chemotherapy segment, $u \equiv 1$, until the singular curve $\mathscr{S}$ is reached. At that time, the control changes and becomes singular. Optimal controlled trajectories then follow the singular arc from the malignant into the benign region across the separatrix. In the benign region, at a certain time τ the control switches to $u \equiv 0$ and follows the uncontrolled trajectory toward the benign equilibrium point. In some situations, optimal controls still switch one more time to a short full dose chemotherapy segment toward the end of treatment, possibly after a prolonged period of rest. We use the notation **1s0**, respectively **1s01**, to label such concatenation sequences of the optimal controls. That is, an **1s01**-trajectory starts with an interval $[0, t_1]$ when the control is at maximum dose rate, $u \equiv 1$, followed by an interval $[t_1, \tau]$ where the control is singular and the trajectory follows an admissible singular arc. The optimal behavior then includes a rest period over an interval $[\tau, \sigma]$ when no drugs are given, $u \equiv 0$. For chemotherapeutic agents with low side effects, the overall therapy session ends with another short burst of full dose chemotherapy over a final interval $[\sigma, T]$. This structure can also be used to define a three-dimensional minimization problem over the variables (τ, σ, T) whose numerical solution defines the optimal control. Overall, a concatenation sequence for the control of at most the form **1s01** results.

Figure 8.9 shows three examples of numerically optimal controlled trajectories for $(M, S) = (0.001, 0.23)$, $(M, S) = (0.01, 0.2)$ and $(M, S) = (0.05, 0.2)$. As before, we label the initial and terminal conditions as $z_0 = (p_0, r_0)$ and $z_T = (p_T, r_T)$, respectively, and we mark the consecutive switching points by black dots. In the

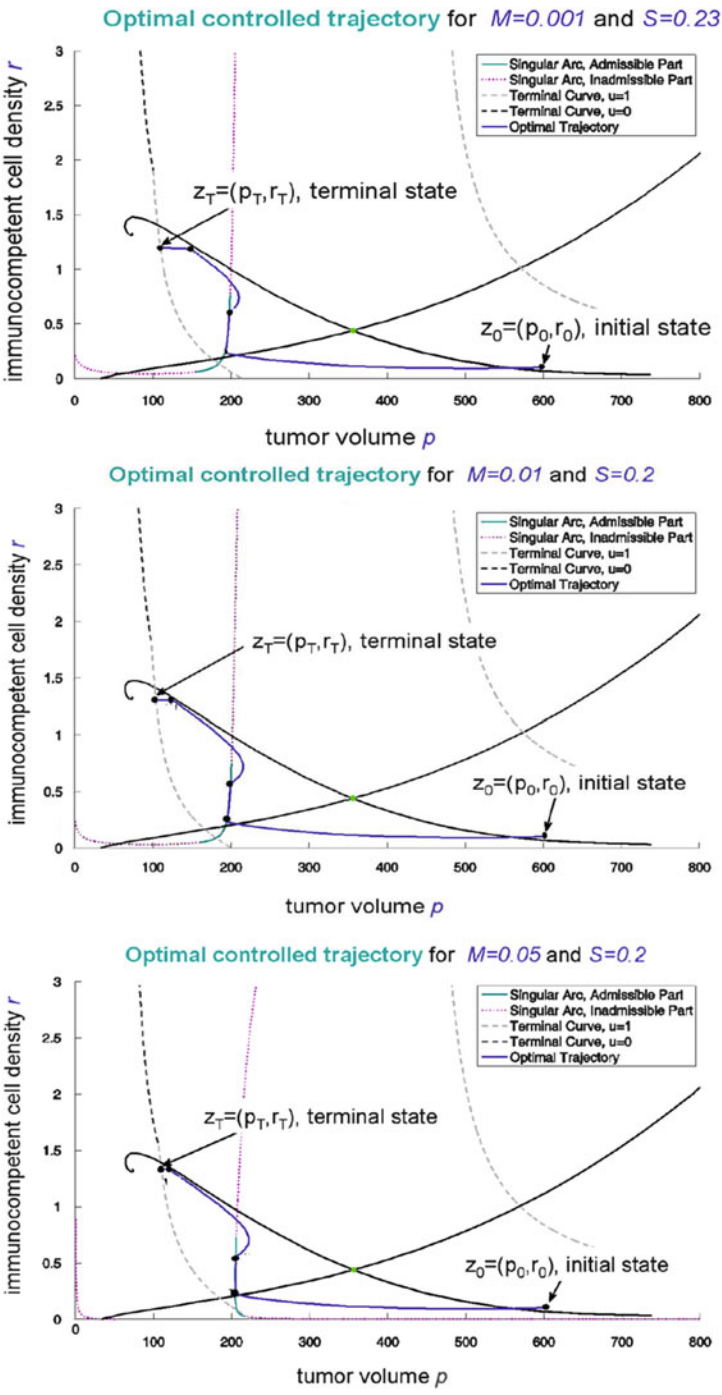

Fig. 8.9 Three examples of numerically computed optimal controlled trajectories whose controls follow the concatenation structure **1s01** for $(M,S) = (0.001, 0.23)$ (top), $(M,S) = (0.01, 0.2)$ (middle), and $(M,S) = (0.05, 0.2)$ (bottom).

range where the singular arc comes into play, it is the graph of a function and the figure also identifies its admissible segment.

Scenario 3: If the penalty on the chemotherapeutic agent is increased further, the last full dose therapy segment disappears and the structure of optimal controlled trajectories reduces to **1s0**. Increasing the parameter M gives a stronger role to the side effects and in this case the optimal trajectory ends on the curve (8.30) that defines the terminal values for the control $u = 0$. This situation is rather typical and we illustrate it for the two cases $(M,S) = (0.05, 0.01)$ and $(M,S) = (0.05, 0.05)$ in Figure 8.10.

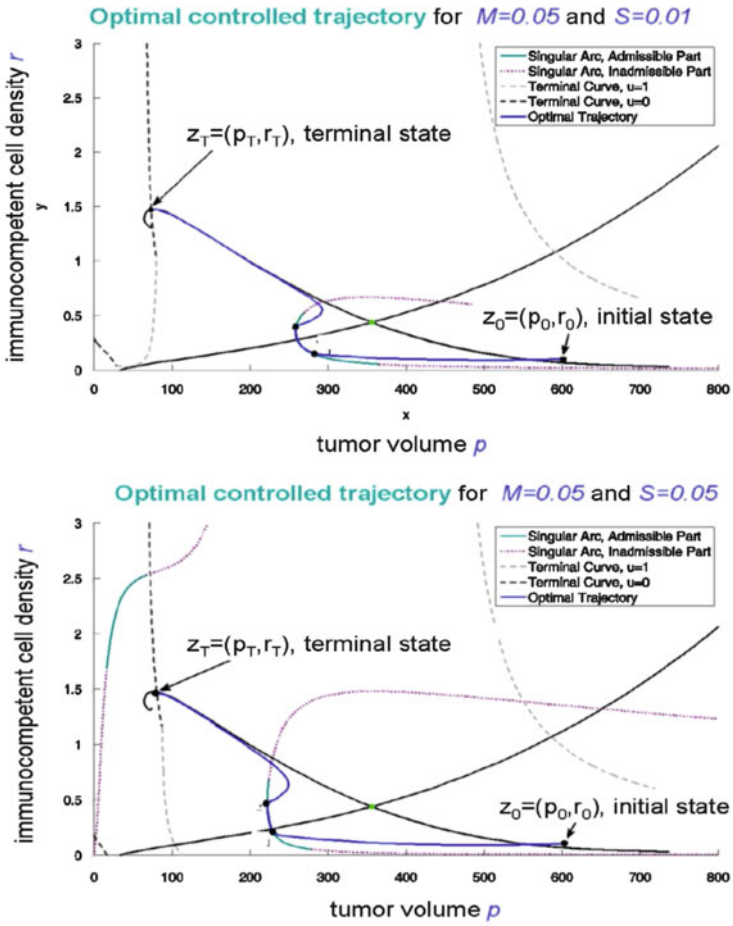

Fig. 8.10 Two examples of numerically computed optimal controlled trajectories whose controls follow the concatenation structure **1s0** for $(M,S) = (0.05, 0.01)$ (top) and $(M,S) = (0.05, 0.05)$ (bottom).

8.3.3 Comments and Interpretation

There are some interesting theoretical insights about optimal therapies in the presence of tumor immune interactions that can be drawn from these numerical computations. Firstly, by including a penalty term on the final time T, we obtain a well-posed formulation for which optimal controls exist. If too much prominence is given to this penalty, optimal controls simply will be constant maximum dose therapies, i.e., *if time is of the essence, give as much as you can as soon as you can*. However, if the time horizon is longer and the coefficient at the terminal time is lowered, optimal responses are concatenations that start with a full dose therapy session, but then are followed by a segment when the dose rates are lowered and given according to a singular control. As some of the examples given above show, during such a period it is even possible that the tumor volume p increases. However, the immunocompetent density r increases as well and this leads to an overall better state that lies in the benign region. Thus, optimal controls no longer aim at eradicating the tumor, but rather are content to move the state of the system into a region where the beneficial actions of the innate immune system are able to control the cancer. These strategies correspond to protocols that initially apply a burst of chemotherapy to reduce the tumor volume and then sustain a smaller volume with reduced dosages. In the medical literature, such protocols have been considered under the terminology of "*chemo-switch*" strategies. The additional, and usually very short burst of full dose chemotherapy that marks the end of some of these therapies also is quite interesting. While this may appear a bit odd at first, there indeed exist practical chemotherapy protocols that, based on the physicians experience, follow such a pattern.

With the prominent role played by the singular arc, these solutions for model [CI1] contrast with the optimal bang-bang controls for cell cycle specific models for cancer chemotherapy considered earlier when tumor-immune system interactions were not taken into account. It is the mitigating influence of the immune system which, for smaller tumor volumes, leads to the abandonment of the strict bang-bang scheme that is seen in the cell cycle specific models. Intuitively, if the system is in a condition where it is able to control the cancer itself, why administer chemotherapy if this might destroy this innate ability of the organism? Thus, despite the model's simplicity, its solutions address the important practical question how to schedule therapies over time and lead to some qualitative structures that give some ideas about designing treatment protocols for more complex models.

8.3.4 Combination Treatment: Targeted Chemotherapy with Immune Boost

We now add rudimentary immunotherapy in the form of an immune boost (e.g., application of a drug based on the interleukin family) to the model. The system thus takes the multi-input form (8.10) with two controls u and v and we label the corresponding optimal control problem [CI2]. Figure 8.11 shows the phase-portraits

for the corresponding system for a Gompertzian growth function when no agents are used (left) and when only an immune boost at constant maximum dose is used (right). As before, the parameters for the dynamics are from Table 8.1 and in the control vector field for the immune boost we choose $\rho = 1$. The uncontrolled system shows the typical bistable behavior which is preserved under the immune boost. The malignant region shrinks with the immune boost, but immunotherapy alone is not able to eliminate it and thus control the tumor. The stable manifold of the saddle at $(p_s, r_s) = (555.1, 0.191)$ still separates a region where the immune system, aided by the immune boost, can eliminate the cancer (here the r-values of the system approach $+\infty$ while p converges to 0 from the right) from a region where the cancer eventually will dominate and trajectories converge to the asymptotically stable malignant equilibrium point $(p_m, r_m) = (715.6, 0.048)$.

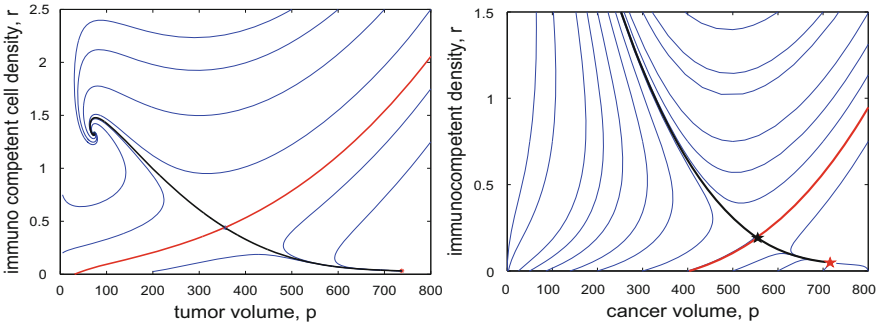

Fig. 8.11 Phase-portraits for a Gompertzian growth function when no agents are used (left) and when only an immune boost at constant maximum dose is used (right).

An important feature of the optimal control problem [CI2] is that the control vector fields g_1 and g_2 commute (see (8.22)). This implies that the derivatives of the switching functions, $\Phi_1(t) = M + \langle \lambda(t), g_1(z_*(t)) \rangle$ for u and $\Phi_2(t) = N + \langle \lambda(t), g_2(z_*(t)) \rangle$ for v, are given by

$$\dot{\Phi}_i(t) = \langle \lambda(t), [f, g_i](z(t)) \rangle, \qquad i = 1, 2. \tag{8.32}$$

In particular, these derivatives do not depend on the controls u or v and thus can be differentiated once more. It follows from Proposition 8.2.2 that

$$\ddot{\Phi}_i(t) = \langle \lambda(t), [f + ug_1 + vg_2, [f, g_i]](z(t)) \rangle, \qquad i = 1, 2.$$

From above, we have that

$$[f, g_1](z) = \kappa p \begin{pmatrix} \xi p F'(p) \\ \\ \alpha(1 - 2\beta p) r \end{pmatrix}$$

and

$$[f,g_2](z) = Dg_2(z)f(z) - Df(z)g_2(z)$$
$$= \begin{pmatrix} 0 \\ \rho\alpha\left(p-\beta p^2\right)r+\gamma-\delta r \end{pmatrix} - \begin{pmatrix} -\rho\theta pr \\ \rho\left(\alpha\left(p-\beta p^2\right)-\delta\right)r \end{pmatrix} = \rho \begin{pmatrix} \theta pr \\ \gamma \end{pmatrix}$$

does not depend on the particular growth model F used. Furthermore,

$$[g_1,[f,g_2]](z) = D\left([f,g_2]\right)(z)g_1(z) - Dg_1(z)[f,g_2](z)$$
$$= \rho \begin{pmatrix} \theta r & \theta p \\ 0 & 0 \end{pmatrix} \begin{pmatrix} -\kappa p \\ 0 \end{pmatrix} - \rho \begin{pmatrix} -\kappa & 0 \\ 0 & 0 \end{pmatrix} \begin{pmatrix} \theta pr \\ \gamma \end{pmatrix} \equiv 0$$

and also

$$[g_2,[f,g_1]](z) = D\left([f,g_1]\right)(z)g_2(z) - Dg_2(z)[f,g_1](z)$$
$$= \begin{pmatrix} 0 \\ \kappa\alpha\left(p-2\beta p^2\right)\rho r \end{pmatrix} - \begin{pmatrix} 0 \\ \rho\kappa\alpha\left(p-2\beta p^2\right)r \end{pmatrix} \equiv 0.$$

Thus, regardless of the tumor growth model used, we have that the second derivatives of the switching functions are given by

$$\ddot{\Phi}_1(t) = \langle \lambda(t), [f+ug_1,[f,g_1]](z_*(t)) \rangle \tag{8.33}$$

and

$$\ddot{\Phi}_2(t) = \langle \lambda(t), [f+vg_2,[f,g_2]](z_*(t)) \rangle . \tag{8.34}$$

The Lie bracket relations of the vector fields therefore decouple the controls u and v in the first two derivatives of the switching functions. In particular, the general formulas derived above for a singular control for the chemotherapeutic agent u remain valid, but with the one change that the equation $H \equiv 0$ now involves the second control v_* and thus reads

$$H = S + \langle \lambda(t), f(z_*(t)) \rangle + v_*(t)\left(N + \langle \lambda(t), g_2(z_*(t)) \rangle\right) \equiv 0.$$

Proposition 8.3.4. *Optimal controls v_* are not singular on any interval.*

Proof. Suppose the control v_* is singular on an open interval I. Regardless of the specific form of the control u_*, by the Legendre-Clebsch condition it is a necessary condition for optimality of v_* that

$$\frac{\partial}{\partial v}\frac{d^2}{dt^2}\frac{\partial H}{\partial v}(\lambda(t), z_*(t), u_*(t), v_*(t)) = \langle \lambda(t), [g_2,[f,g_2]](z(t)) \rangle \leq 0 \qquad \text{on} \quad I.$$

On I we have that

$$\Phi_2(t) = N + \langle \lambda(t), g_2(z_*(t)) \rangle \equiv 0 \qquad \text{and} \qquad \dot{\Phi}_2(t) = \langle \lambda(t), [f,g_2](z_*(t)) \rangle \equiv 0.$$

The vector fields g_2 and $[f,g_2]$ are linearly independent on $\mathbb{M}$ and can therefore be used as a basis for the higher order Lie brackets. We write the second-order Lie bracket $[g_2,[f,g_2]]$ as a linear combination of g_2 and $[f,g_2]$ in the form

$$[g_2,[f,g_2]](z) = \omega_1(z) g_2(z) + \omega_2(z)[f,g_2](z)$$

with smooth functions ω_1 and ω_2. We have that

$$\begin{aligned}[g_2,[f,g_2]](z) &= D([f,g_2])(z) g_2(z) - Dg_2(z)[f,g_2](z) \\ &= \rho \begin{pmatrix} \theta r & \theta p \\ 0 & 0 \end{pmatrix} \begin{pmatrix} 0 \\ \rho r \end{pmatrix} - \rho \begin{pmatrix} 0 & 0 \\ 0 & \rho \end{pmatrix} \begin{pmatrix} \theta pr \\ \gamma \end{pmatrix} = \rho^2 \begin{pmatrix} \theta pr \\ -\gamma \end{pmatrix},\end{aligned}$$

and solving the equations

$$\rho \begin{pmatrix} \theta pr \\ -\gamma \end{pmatrix} = \omega_1(z) \begin{pmatrix} 0 \\ r \end{pmatrix} + \omega_2(z) \begin{pmatrix} \theta pr \\ \gamma \end{pmatrix}$$

yields

$$\omega_1(z) = -\frac{2\rho\gamma}{r} \qquad \text{and} \qquad \omega_2(z) = \rho.$$

Hence it follows along a singular control v_* that

$$\begin{aligned}\langle \lambda(t), [g_2,[f,g_2]](z_*(t)) \rangle &= \omega_1(z_*(t)) \langle \lambda(t), g_2(z_*(t)) \rangle \\ &\qquad + \omega_2(z_*(t)) \langle \lambda(t), [f,g_2](z_*(t)) \rangle \\ &= \omega_1(z_*(t))(-D) + \omega_2(z_*(t)) \cdot 0 \\ &= \frac{2N\rho\gamma}{r_*(t)} > 0\end{aligned}$$

violating the Legendre-Clebsch condition. □

Thus, for a singular control u_*, we only need to consider the cases $v_* = 0$ and $v_* = 1$. If $v = 0$, we have the earlier situation with the same formulas valid verbatim. For $v = 1$ we now get that

$$\det(M(f(z) + g_2(z)) - (N+S) g_1(z), [f,g_1](z)) = 0$$

and this expression is equal to

$$\det(Mf(z) - Sg_1(z), [f,g_1](z)) + M \det(g_2(z), [f,g_1](z)) - N \det(g_1(z), [f,g_1](z)).$$

The first term corresponds to the expression computed earlier and the other terms are given by

$$\det\left(g_2(z),[f,g_1](z)\right)=\kappa\rho pr\begin{vmatrix}0 & \xi pF'(p)\\ 1 & \alpha(1-2\beta p)r\end{vmatrix}=-\kappa\rho\xi p^2F'(p)r$$

and

$$\det\left(g_1(z),[f,g_1](z)\right)=\kappa p\begin{vmatrix}-\kappa p & \xi pF'(p)\\ 0 & \alpha(1-2\beta p)r\end{vmatrix}=-\kappa^2\alpha(p-2\beta p^2)pr.$$

Hence, if we write

$$\begin{aligned}&\det\left(M\left(f(z)+g_2(z)\right)-(N+S)g_1(z),[f,g_1](z)\right)\\&=\kappa p\cdot Q(p,r)=\kappa p\cdot\left(q_2(p)r^2+q_1(p)r+q_0(p)\right),\end{aligned}$$

then Q differs from W only in the linear term which now is given by

$$q_1(p)=\alpha(p-2\beta p^2)\left[M\xi F(p)+(N+S)\kappa\right]-M\xi pF'(p)\left[\alpha(p-\beta p^2)-\delta+\rho\right]$$

with $q_0\equiv w_0$ and $q_2\equiv w_2$.

Based on the formulas derived above, the singular arc, the singular control, and their admissible portions can easily be evaluated numerically. As an illustration, Figure 8.12 shows how the singular curve $\mathscr{S}$ changes from $v\equiv 0$ (blue curve) to $v\equiv 1$ (red curve) for the parameter values from Table 8.1 for the dynamics, $\kappa=2$ and $\rho=1$, and the coefficients $M=0.036$, $N=0.007$ and $S=0.036$ for the objective.

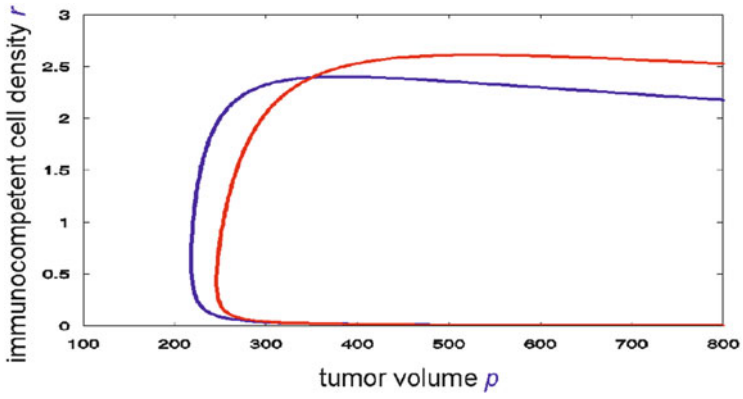

Fig. 8.12 The singular curve $\mathscr{S}$ for the chemotherapeutic agent u with constant controls $v\equiv 0$ (blue curve) and $v\equiv 1$ (red curve).

Scenario 4: Figure 8.13 shows an optimal control (top) and its corresponding trajectory (bottom) for the same parameter values for the dynamics as before and coefficients $\kappa = 2$ and $\rho = 1$ in the control vector fields. Also, the initial condition is the same as before, $(p_0, r_0) = (600, 0.1)$. The objective is defined with $A = 0.00192$ and $B = 1$ (coming from the stable eigenvector of the saddle for the uncontrolled system) and we have chosen the other weights as $M = 0.01, N = 0.025$ and $S = 0.001$. For these weights, both the side effects of chemotherapy and the immune boost are significant. Chemotherapy has overall the better effectiveness and becomes the dominant therapy. Initially, chemotherapy is given at full dose without any immune boost. However, already after a brief time interval, as the state of the system nears the separatrix, chemotherapy is reduced drastically and is only administered at lower dose rates according to the singular control u_{sing}. Once more the "chemo-switch" type behavior of administration of a chemotherapeutic agent is seen as optimal. In the figure on the right the corresponding switching points are indicated on the trajectory by a red asterisk. Once a "safe" distance to the separatrix has been established, chemotherapy is turned off and the system follows the uncontrolled trajectory toward the benign stable equilibrium point. This portion of the trajectory closely follows the unstable manifold of the saddle for the uncontrolled system and is labeled a "free pass" in Figure 8.13. Along this trajectory, only a small penalty for the time is incurred. Toward the end, when the cancer volume is already quite small, it becomes beneficial to give an immune boost with the precise timing depending on the penalty S given to the terminal time. The two green asterisks on the corresponding trajectory mark the beginning and end of the arc generated by the action of the immune boost. Toward the end, as it was the case in scenario 2, another short full dose chemotherapy session starting at the point marked on the trajectory with a red star reduces the cancer volume further. Thus for this choice of weights in the objective, chemotherapy is the dominant portion and overall for the administration of the chemotherapeutic agent we have a concatenation structure for the optimal controls of the form **1s01** with **1** and **0** denoting full dose and no dose segments, respectively, and **s** denoting an interval along which the optimal control u_* is singular. Immunotherapy is only used as an additional tool once the cancer volume has become small so that the tumor-immune interactions become significant and for the immune boost the concatenation structure for the controls is **010**.

8.4 Toward Metronomic Chemotherapy: A Mathematical Model with Antiangiogenic and Immune Stimulatory Effects

There exists medical evidence that low-dose chemotherapy, while it still has moderate cytotoxic effects on cancerous cells in the absence of significant negative side effects, has both antiangiogenic and immune stimulatory effects (e.g., see [9, 24, 39, 118, 162, 277] as well as the survey article [272] and editorial [273]). This has led to the concept of *metronomic chemotherapy*. Essentially, this is the almost continuous administration of chemotherapeutic agents at significantly lower

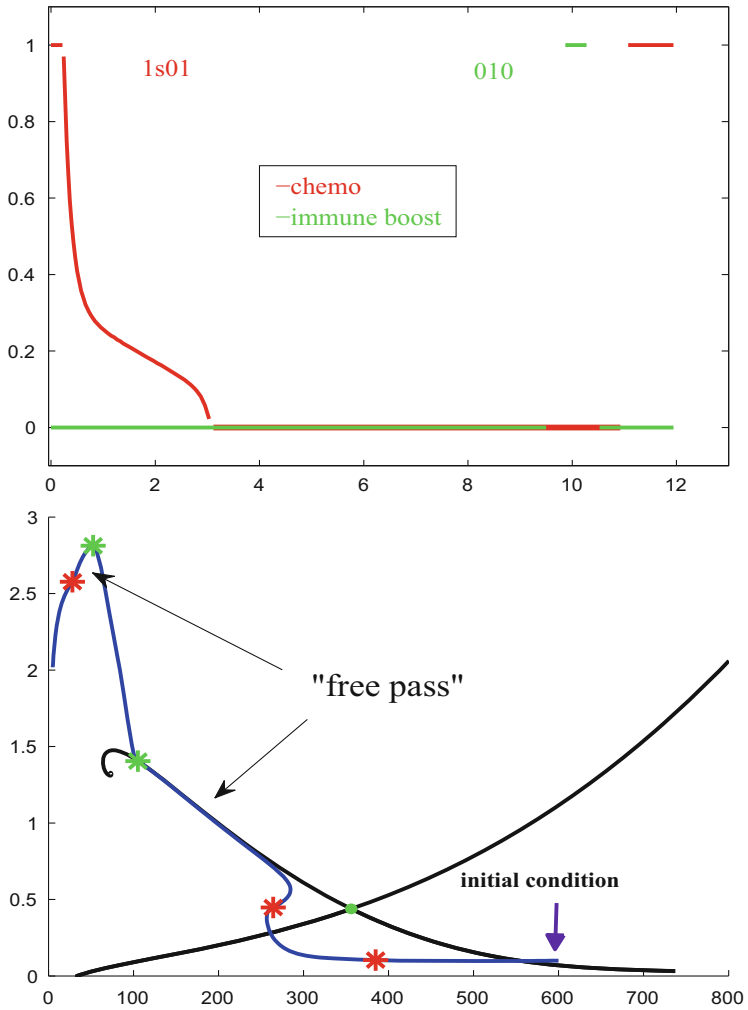

Fig. 8.13 Optimal controls (top) and corresponding trajectory (bottom) for scenario 4. The stars in the panel on the right indicate the points when switchings in the optimal controls occur (red asterisks for switchings in the chemotherapy, green asterisks for switchings in the immunotherapy). The curve gives the response of the system to the optimal controls.

dose rates than MTD, possibly with small interruptions to increase the efficacy of the drugs. The hope is that, in the absence of limiting side effects, it is possible to give chemotherapy over prolonged time intervals so that, because of the greatly extended time horizon, the overall effect may be improved when compared with repeated short MTD doses [136, 341]. Furthermore, while low dose chemotherapy seems to have an immune stimulatory effect, high dose chemotherapy simply suppresses the immune system taking out another factor that could be utilized in fighting the tumor. Higher doses thus may not only be more harmful to the healthy cells,

but they may also adversely effect the immune system which otherwise would have come to the assistance in combating the tumor.

Several mathematical models that explore the efficiency of a metronomic versus an MTD-type administration of chemotherapy have been formulated and analyzed going back to the paper [117] by Hahnfeldt, Folkman and Hlatky. We have already seen in Chapter 3 that, as tumor populations become more heterogeneous, mathematically optimal strategies favor lower concentrations of the agents (e.g., see the review articles [211, 212] and the references quoted therein). More recently, Benzekry et al. [21] and Benzekry and Hahnfeldt [23] also have analyzed the impact of such types of protocols on metastatic spreading of cancers and found that metronomic dosing generally does better. Thus there exists increasing evidence which, under certain conditions, would support a metronomic scheduling of chemotherapeutic drugs.

In this section, we close our analysis with formulating a model for low-dose chemotherapy that combines Stepanova's model for tumor-immune system interactions with Hahnfeldt's model [H] for angiogenic signaling to consider the full antitumor, antiangiogenic and immune stimulatory effects. We carry out a dynamical systems analysis of the equilibria—including regions of attraction of stable equilibria and bifurcation phenomena—and provide a comprehensive overview of the dynamical systems properties of the model for the full range of parameters. We close with a brief discussion of optimal controls for this combined model.

8.4.1 A Minimally Parameterized Mathematical Model for Metronomic Chemotherapy

Combining the mathematical model [H] of tumor growth under angiogenic signaling with the above model for tumor-immune system interactions we obtain the following equations:

$$\begin{aligned}
\dot{p} &= -\xi p \ln\left(\frac{p}{q}\right) - \theta p r,\\
\dot{q} &= p - \left(\mu + d p^{\frac{2}{3}}\right) q,\\
\dot{r} &= \alpha\left(p - \beta p^2\right) r + \gamma - \delta r.
\end{aligned}$$

As before p denotes the primary *tumor volume*, q the *carrying capacity of its vasculature* and r the *immunocompetent cell density*. All other symbols in these equations denote constant coefficients which have the same meaning as in the previous chapters. We now add *constant, low-dose chemotherapy* to this model. In such a case, there is no need to add the standard linear pharmacokinetic model. For, if we denote the dose rate of the chemotherapeutic agent by u and its concentration by c, $\dot{c} = -\omega c + u$, the concentration quickly saturates at the steady-state value $c_*(u) = \frac{u}{\omega}$. It is therefore possible to absorb the coefficient ω in the constant for

the pharmacodynamic model and we thus identify u with c while retaining u as the variable. Using the linear log-kill hypothesis [298, 343], the influence of the chemotherapeutic agent on the tumor volume and its carrying capacity therefore take the form $-\varphi_1 pu$ and $-\varphi_2 qu$, respectively. Accordingly, we also use $\varphi_3 ru$ to model the immune stimulatory effect of chemotherapy. For our theoretical analysis below, we do not make any assumptions on the relations between the parameters φ_i, but for low dose metronomic chemotherapy typically the antiangiogenic effect is dominant while the cytotoxic and pro-immune effects are lower. Overall, the controlled equations take the following form:

$$\dot{p} = -\xi p \ln\left(\frac{p}{q}\right) - \theta pr - \varphi_1 pu, \tag{8.35}$$

$$\dot{q} = bp - \left(\mu + dp^{\frac{2}{3}}\right) q - \varphi_2 qu, \tag{8.36}$$

$$\dot{r} = \alpha\left(p - \beta p^2\right) r + \gamma - \delta r + \varphi_3 ru. \tag{8.37}$$

We shall give a complete analysis of the dynamical systems properties of this model (equilibria, stability, bifurcations). The state-space for the model is the positive octant $\mathbb{P} = \mathbb{R}^3_+ = \{(p,q,r) : p > 0, q > 0, r > 0\}$. It follows from general results of ODEs that the solution $(p(t), q(t), r(t))$ with initial condition $(p_0, q_0, r_0) \in \mathbb{P}$ exists, forward in time, on a maximal interval $[0, \tau)$. The equations imply that the solutions remain positive over the interval of existence, but it is possible that trajectories converge to the tumor free equilibrium point, $(p(t), q(t), r(t)) \to (0, 0, \frac{\gamma + \varphi_3 u}{\delta})$ as $t \to \tau$. This corresponds to the medical situation when the low-dose metronomic chemotherapy is able to eradicate the tumor and its vasculature while upregulating the immune system.

A complete analysis of the dynamical properties of the two separate systems that make up this model has been given before. It follows from the results in Chapter 5 that the model for angiogenic signaling (consisting of equations (8.35) and (8.36) with $\theta = 0$) is well posed in the region $\{p > 0, q > 0\}$ and has a unique globally stable equilibrium point at $(\bar{p}, \bar{q}) = \left(\left(\frac{b-\mu-\varphi_2 u}{d}\right)^{\frac{2}{3}}, \left(\frac{b-\mu-\varphi_2 u}{d}\right)^{\frac{2}{3}}\right)$ if $b > \mu + \varphi_2 u$ while all solutions converge to $(0,0)$ if $b \leq \mu + \varphi_2 u$. For $u = 0$, and, more generally, for low values of u, this corresponds to a malignant situation when the equilibrium point represents death of the patient. In the other extreme, for large values of u, constant chemotherapy (while ignoring side effects) would be able to eradicate the disease. For a Gompertzian tumor growth model, de Vladar and Gonzalez [334] have carried out a complete analysis of the submodel defined by equations (8.35) and (8.37) and for this model, depending on the parameter values, various equilibrium structures are possible that include a multi-stable scenario when both locally asymptotically stable and unstable equilibria persist very much like it was described in Section 8.1. We shall see that these features of the two models combine and for the model (8.35)–(8.37) we have scenarios that range from a unique, asymptotically stable benign equilibrium point (that represents a situation of immune surveillance) to a multi-stable situation with both benign and malignant equilibria to the situation

when only a unique, asymptotically stable malignant equilibrium point (that represents death of the patient) exists like for the uncontrolled model [H].

8.4.2 Static Bifurcations

We begin with the analysis of the static bifurcations, i.e., changes in the number of equilibria. Recall that we call an equilibrium point positive if it has a positive tumor volume p. For any equilibrium point (p_*, q_*, r_*) of the system (8.35)–(8.37) in $\mathbb{P}$ we have that

$$r_* = -\frac{1}{\theta}\left(\xi \ln\left(\frac{p_*}{q_*}\right) + \varphi_1 u\right) \qquad \text{and} \qquad q_* = \frac{b p_*}{\mu + \varphi_2 u + d p_*^{\frac{2}{3}}}. \tag{8.38}$$

Given p_*, these equations define the remaining coordinates of the equilibrium point, $q_* = q_*(p_*)$ and $r_* = r_*(p_*)$. Furthermore,

$$b\frac{p_*}{q_*} = \mu + \varphi_2 u + d p_*^{\frac{2}{3}}, \tag{8.39}$$

a relation that will be used frequently. Substituting these expressions into the equation $\dot{r} = 0$ and rearranging terms results in the following equivalent equation:

$$\xi \ln\left(\frac{\mu + \varphi_2 u + d p_*^{\frac{2}{3}}}{b}\right) + \varphi_1 u = -\frac{\theta\gamma}{\alpha\beta p_*^2 - \alpha p_* + \delta - \varphi_3 u}. \tag{8.40}$$

We have grouped terms so that the expression on the left side only contains parameters that depend on the tumor-vascular interactions while the right-hand side only contains parameters that depend on the tumor-immune system interactions. This, in some sense, allows us to look at these features individually and then only consider the intersections of these two graphs. For $p \geq 0$ define

$$\Phi(p) = \xi \ln\left(\frac{\mu + \varphi_2 u + d p^{\frac{2}{3}}}{b}\right) + \varphi_1 u \tag{8.41}$$

and

$$\Psi(p) = -\frac{\theta\gamma}{\alpha\beta p^2 - \alpha p + \delta - \varphi_3 u}. \tag{8.42}$$

Proposition 8.4.1. *There exist at most three positive equilibria for the dynamical system (8.35)–(8.37).*

Proof. Equilibria correspond to solutions of the equation $\Phi(p) = \Psi(p)$ and between any two solutions there needs to lie a solution of the derivatives, $\Phi'(p) = \Psi'(p)$. We show that the equation for the derivatives can have at most two positive roots and the result follows from this.

The equation for the derivatives takes the form

$$\frac{2}{3}\frac{\xi d p^{-\frac{1}{3}}}{\mu+\varphi_2 u+d p^{\frac{2}{3}}}=\frac{\theta\gamma\alpha\,(2\beta p-1)}{\left(\alpha\beta p^2-\alpha p+\delta-\varphi_3 u\right)^2}. \tag{8.43}$$

The left-hand side is positive and thus solutions can only exist for $p>\frac{1}{2\beta}$. The equation itself is equivalent to

$$\frac{2}{3}\frac{\xi d}{\theta\gamma\alpha}\frac{\left(\alpha\beta p^2-\alpha p+\delta-\varphi_3 u\right)^2}{(2\beta p-1)}=(\mu+\varphi_2 u)\,p^{\frac{1}{3}}+dp.$$

The quadratic polynomial $Q(p)=\alpha\beta p^2-\alpha p+\delta-\varphi_3 u$ has its minimum for $p=\frac{1}{2\beta}$ and completing the square, the left-hand side can be written in the form

$$\frac{1}{3}\frac{\xi d}{\theta\gamma}\frac{\left(\left(p-\frac{1}{2\beta}\right)^2+\Xi\right)^2}{p-\frac{1}{2\beta}}=\frac{1}{3}\frac{\xi d}{\theta\gamma}\left[\left(p-\frac{1}{2\beta}\right)^3+2\Xi\left(p-\frac{1}{2\beta}\right)+\frac{\Xi^2}{p-\frac{1}{2\beta}}\right]$$

with

$$\Xi=\frac{4\beta\,(\delta-\varphi_3 u)-\alpha}{4\alpha\beta^2}.$$

The second derivative of the difference

$$\Delta(p)=\frac{1}{3}\frac{\xi d}{\theta\gamma}\left[\left(p-\frac{1}{2\beta}\right)^3+2\Xi\left(p-\frac{1}{2\beta}\right)+\frac{\Xi^2}{p-\frac{1}{2\beta}}\right]-(\mu+\varphi_2 u)\,p^{\frac{1}{3}}-dp \tag{8.44}$$

is given by

$$\Delta''(p)=\frac{1}{3}\frac{\xi d}{\theta\gamma}\left[6\left(p-\frac{1}{2\beta}\right)+\frac{2\Xi^2}{\left(p-\frac{1}{2\beta}\right)^3}\right]+\frac{2}{9}(\mu+\varphi_2 u)\,p^{-\frac{5}{3}}$$

and is positive for $p>\frac{1}{2\beta}$. Hence Δ is a strictly convex function on this interval and thus can have at most two zeros. This verifies the result. □

The function Φ is strictly increasing and strictly concave over the interval $(0,\infty)$ and takes the value

$$\Phi_0=\xi\ln\left(\frac{\mu+\varphi_2 u}{b}\right)+\varphi_1 u$$

for $p=0$. From a purely mathematical point of view, for high doses u we will have $\Phi(0)>0$ and thus the function Φ is positive. If the quadratic polynomial Q has complex roots, then the function Ψ will always be negative and thus the graphs of Φ and Ψ do not intersect. Hence no positive equilibria exist and in this case all trajectories of the system converge to the tumor free equilibrium point given by

$(0,0,\frac{\gamma+\varphi_3 u}{\delta})$. Intuitively, this simply means that continuous administration of such a dose would be able to eliminate the tumor. However, the model is realistic only for low doses u since high doses no longer stimulate the immune system, but have a detrimental effect. Thus these are academic discussions and we shall not consider the equilibrium analysis for large u. Furthermore, the realistic situation is that the death rate μ is very small, $\mu \approx 0$; in particular, it is much smaller that b, $\mu \ll b$. Thus Φ_0 is negative for low doses; in fact $\Phi_0 \to -\infty$ as $\mu \to 0+$ and $u \to 0+$. Henceforth we *assume* that $u \in [0, u_{\max}]$ with the maximum dose rate $u_{\max}$ so small that for $p = 0$ we have that

$$\Phi_0 = \xi \ln\left(\frac{\mu + \varphi_2 u_{\max}}{b}\right) + \varphi_1 u_{\max} < \Psi_0 = \frac{\theta\gamma}{\varphi_3 u_{\max} - \delta}. \tag{8.45}$$

Here Ψ_0 could be positive. This simply means that the immune stimulatory effect of metronomic chemotherapy is greater than the natural death rate δ. Under assumption (8.45), there always exists at least one equilibrium point (p_*, q_*, r_*) with $p_* > 0$.

We illustrate the typical equilibrium structures for the system (8.35)–(8.37) in $\mathbb{P}$. The number of equilibria depends on the geometric shape of the graph of Ψ and thus ultimately on the roots of the quadratic polynomial $Q(p) = \alpha\beta p^2 - \alpha p + \delta - \varphi_3 u$. These are given by

$$p_\pm = \frac{1}{2\beta}\left(1 \pm \sqrt{1 - 4\frac{\beta}{\alpha}(\delta - \varphi_3 u)}\right) \tag{8.46}$$

and are complex for $4\beta(\delta - \varphi_3 u) > \alpha$ and real for $4\beta(\delta - \varphi_3 u) \le \alpha$. These cases lead to similar, but in their details different bifurcation scenarios.

If the roots are complex, Q is always positive and the function Ψ is negative on $[0,\infty)$ with a global minimum at $p_{\min} = \frac{1}{2\beta}$ and the minimum value is given by

$$\Psi_{\min} = -\left(\frac{\theta\gamma}{\delta - \varphi_3 u - \frac{\alpha}{4\beta}} + \varphi_1 u\right).$$

Figure 8.14 shows the typical scenarios for complex roots on the left. If $\Phi\left(\frac{1}{2\beta}\right) < \Psi_{\min}$, there only exists one intersection for (generally large) $p_*^{(3)} > \frac{1}{2\beta}$ and, as we shall show below, the corresponding equilibrium point (p_*, q_*, r_*) is globally asymptotically stable and corresponds to a malignant scenario. If $\Phi\left(\frac{1}{2\beta}\right) = \Psi_{\min}$, then, since Ψ has a local minimum at $\frac{1}{2\beta}$ and $\Phi'\left(\frac{1}{2\beta}\right) > 0$, the graphs of Φ and Ψ intersect in two points, $p_*^{(1)} = \frac{1}{2\beta}$ and $p_*^{(2)} > \frac{1}{2\beta}$ close to $\frac{1}{2\beta}$. A unique intersection happens as $\Phi\left(\frac{1}{2\beta}\right) \to \Psi_{\min}$ from below and the graphs of Φ and Ψ become tangential. At this point, a second equilibrium point $\left(p_*^{(1)}, q_*^{(1)}, r_*^{(1)}\right) = \left(p_*^{(2)}, q_*^{(2)}, r_*^{(2)}\right)$ is

born in a saddle-node bifurcation (see Theorem 8.4.1 below). Then three equilibria persist, ordered in our notation so that $p_*^{(1)} < p_*^{(2)} < p_*^{(3)}$. We shall show below that the lowest equilibrium point $p_*^{(1)}$ is locally asymptotically stable and can be considered a benign scenario. Also, the highest equilibrium point $p_*^{(3)}$ is always locally asymptotically stable, but it corresponds to a malignant scenario. The intermediate equilibrium point $p_*^{(2)}$ is always unstable with a 2-dimensional stable manifold that separates the regions of attraction of the low and high equilibria.

Similar features exist when the roots of the quadratic polynomial Q are real, $4\beta(\delta - \varphi_3 u) \leq \alpha$. In this case, the function Ψ has two simple poles at the roots $p_\pm$ of Q (respectively a double pole if the roots are equal) and is negative to the left and to the right of these poles and positive in between. The smaller pole p_- is positive if and only if $\varphi_3 u < \delta$, i.e., if the immuno-stimulatory effects of the metronomic chemotherapy cannot overcome the natural death rate of the cells associated with the immunocompetent cell density. Figure 8.14 depicts the typical scenarios for this case on the right. Under assumption (8.45), there always exists an asymptotically stable low (benign) equilibrium point $p_*^{(1)} < \frac{1}{2\beta}$. In the illustration on the top this is the only equilibrium point and it is globally asymptotically stable. Medically this corresponds to a scenario when the low-dose metronomic chemotherapy is able to control the disease. As the parameters are varied, in the middle panel, again a saddle-node bifurcation occurs in which an unstable equilibrium point $p_*^{(2)}$ and a high (malignant) equilibrium point $p_*^{(3)}$ are born. These then persist as the graphs of Φ and Ψ shift to generate two intersections. For the case $\varphi_3 u \geq \delta$, i.e., if the immuno-stimulatory effects of the metronomic chemotherapy overcomes the natural death rate of the cells associated with the immunocompetent cell density, the smaller pole p_- is negative. Essentially, the possible scenarios are the same as shown in Figure 8.14 with the difference that the value $p = 0$ now lies to the right of the pole. In this case, the low (benign) equilibrium point does not exist and its role is taken over by the tumor-free equilibrium point $(0, 0, \frac{\gamma + \varphi_3 u}{\delta})$. When there are no other equilibria, all trajectories converge to this equilibrium. This corresponds to a scenario when metronomic chemotherapy at dose rate u is able to eradicate the tumor.

Figure 8.15 shows one of many bifurcation scenarios. Here only the tumor growth factor ξ is varied while all other parameters are kept constant. The parameter values are chosen to illustrate the full range of the behaviors, but have no specific medical significance. For low tumor growth rates we have that $\Phi_0 > \Psi_0$ and no equilibrium points exist. All trajectories converge to the tumor free equilibrium point, i.e., metronomic chemotherapy is able to eradicate the tumor. As ξ increases, a first saddle-node bifurcation occurs when the graph of Φ becomes tangential to the graph of Ψ at some value $p_*^{(2=3)} > \frac{1}{2\beta}$ and the unstable equilibrium point $p_*^{(2)}$ and the high (malignant) equilibrium point $p_*^{(3)}$ are born. As the tumor growth rate increases further, the value Φ_0 drops below Ψ_0, the tumor free equilibrium becomes unstable and a low (benign) locally asymptotically stable positive equilibrium point $p_*^{(1)} > 0$ is

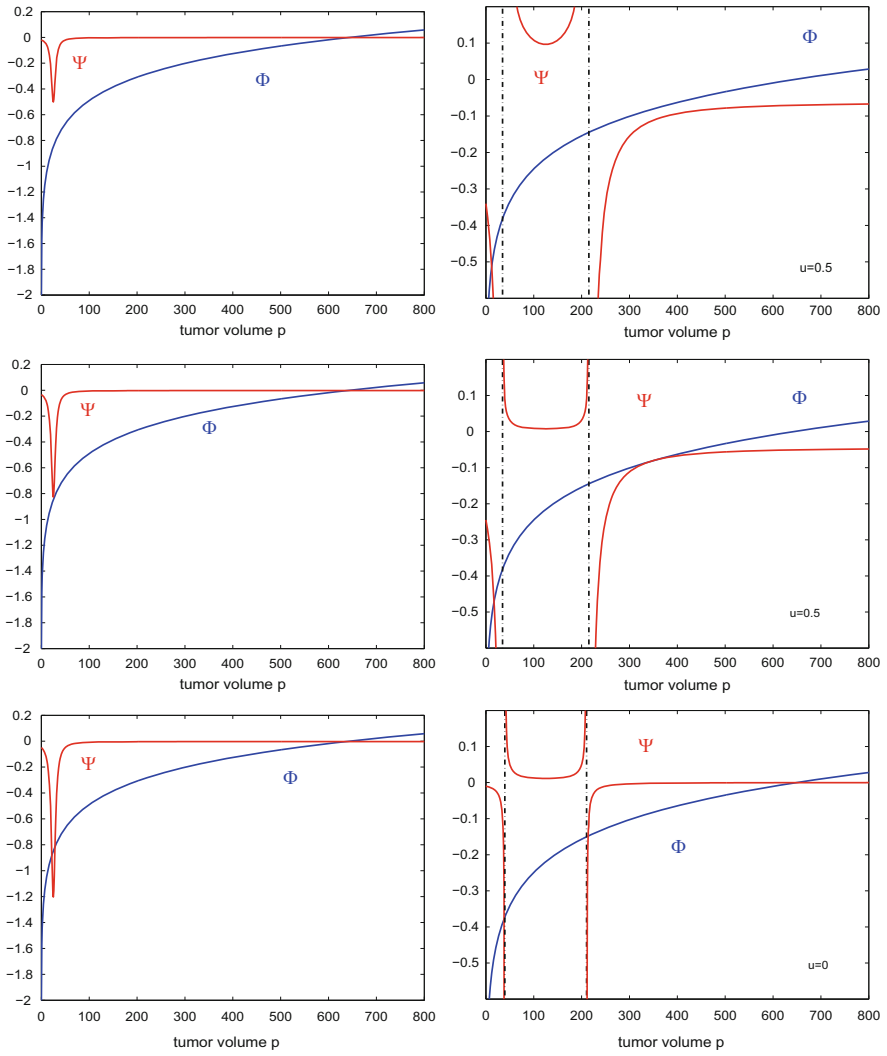

Fig. 8.14 Saddle node bifurcation mechanism in the case of complex (left) and real (right) roots.

born. Now the system has become multi-stable with both a benign region, the region of attraction of the low equilibrium point, and a malignant region, the region of attraction of the high equilibrium point. These are separated by the stable manifold of the unstable equilibrium point $p_*^{(2)}$. As the tumor growth rate ξ increases further, the benign equilibrium point $p_*^{(1)}$ and the unstable equilibrium point $p_*^{(2)}$

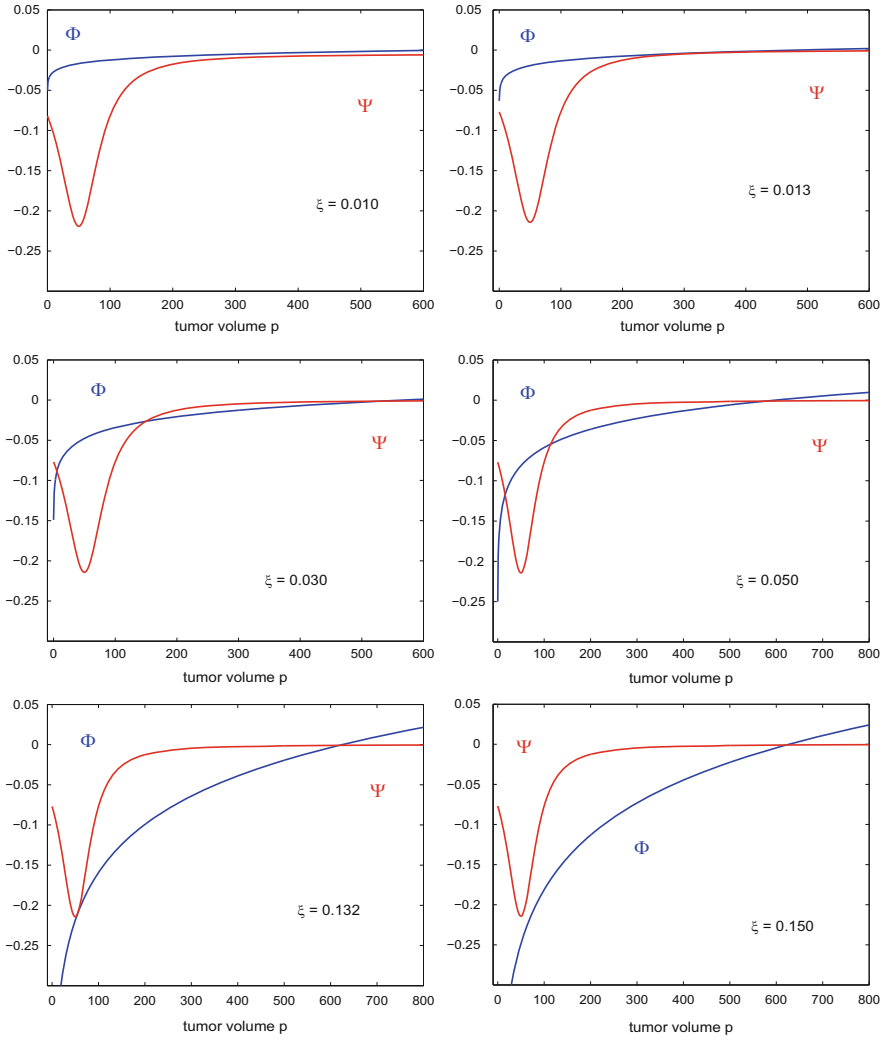

Fig. 8.15 Bifurcations as the tumor growth rate ξ is varied.

move closer to each other and eventually coalesce and disappear in a second saddle node bifurcation which occurs when $\Phi'(p_*) = \Psi'(p_*)$. For higher tumor growth rates only the high (malignant) equilibrium point exists and this simply describes a medical scenario when the tumor growth cannot be overcome by a constant low dose chemotherapy. Figure 8.15 illustrates the corresponding bifurcation scenario and the corresponding bifurcation diagram is shown qualitatively in Figure 8.16.

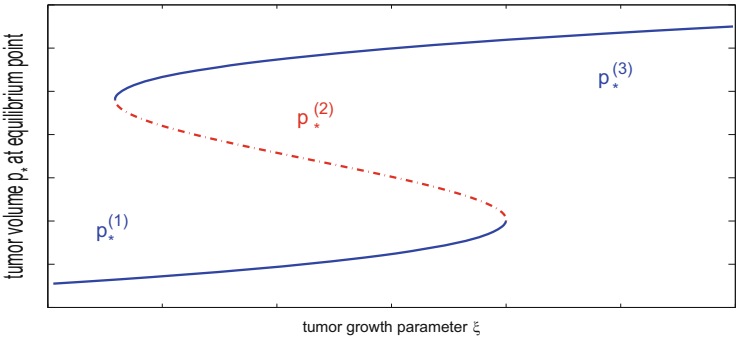

Fig. 8.16 Qualitative illustration of the bifurcation diagram. The stable (benign and malignant) equilibria are shown as a solid curve while the unstable equilibrium point is shown as a dashed curve.

8.4.3 Stability Properties of the Equilibria

We analyze the stability properties of the equilibria and prove that saddle-node bifurcations occur as the graphs of Φ and Ψ intersect tangentially. We use the classical stability criterion by Routh and Hurwitz about zeros of a polynomial. For a normed cubic polynomial, this result is elementary and is given by the following statement:

Proposition 8.4.2. *All roots of a real cubic polynomial* $\chi(t) = t^3 + a_2 t^2 + a_1 t + a_0$ *have negative real part if and only if* $a_0 > 0$, $a_1 > 0$ *and* $a_2 > \frac{a_0}{a_1}$.

Let (p_*, q_*, r_*) be an equilibrium point of the system (8.35)–(8.37) in $\mathbb{P}$. Using (8.38), the Jacobian matrix A of the system at the equilibrium point simplifies as follows:

$$A = \begin{pmatrix} -\xi & \xi \frac{p_*}{q_*} & -\theta p_* \\ b \frac{\mu + \varphi_2 u + \frac{1}{3} d p_*^{\frac{2}{3}}}{\mu + \varphi_2 u + d p_*^{\frac{2}{3}}} & -b \frac{p_*}{q_*} & 0 \\ \alpha(1 - 2\beta p_*) r_* & 0 & \alpha\left(p - \beta p^2\right) - \delta + \varphi_3 u \end{pmatrix}.$$

Let

$$\chi_A(t) = \det(t \cdot \mathrm{Id} - A) = t^3 + a_2 t^2 + a_1 t + a_0$$

denote the characteristic polynomial of the matrix A. We then have that

$$\chi_A(t) = \begin{vmatrix} t+\xi & -\xi\frac{p_*}{q_*} & \theta p_* \\ -b\frac{\mu+\varphi_2 u+\frac{1}{3}dp_*^{\frac{2}{3}}}{\mu+\varphi_2 u+dp_*^{\frac{2}{3}}} & t+b\frac{p_*}{q_*} & 0 \\ -\alpha(1-2\beta p_*)r_* & 0 & t-\alpha\left(p_*-\beta p_*^2\right)+\delta-\varphi_3 u \end{vmatrix}$$

$$= \left[(t+\xi)\left(t+b\frac{p_*}{q_*}\right)-\xi\frac{p_*}{q_*}b\frac{\mu+\varphi_2 u+\frac{1}{3}dp_*^{\frac{2}{3}}}{\mu+\varphi_2 u+dp_*^{\frac{2}{3}}}\right]\left(t-\alpha\left(p_*-\beta p_*^2\right)+\delta-\varphi_3 u\right)$$
$$+\theta p_*\left(t+b\frac{p_*}{q_*}\right)\alpha(1-2\beta p_*)r_*,$$

so that

$$a_0 = b\frac{p_*}{q_*}\left[\xi\left(\frac{\frac{2}{3}dp_*^{\frac{2}{3}}}{\mu+\varphi_2 u+dp_*^{\frac{2}{3}}}\right)\left(\alpha\beta p_*^2-\alpha p_*+\delta-\varphi_3 u\right)+\theta\alpha(1-2\beta p_*)p_* r_*\right],$$

$$a_1 = \xi b\frac{p_*}{q_*}\left(\frac{\frac{2}{3}dp_*^{\frac{2}{3}}}{\mu+\varphi_2 u+dp_*^{\frac{2}{3}}}\right)+\left(\xi+b\frac{p_*}{q_*}\right)\left(\alpha\beta p_*^2-\alpha p_*+\delta-\varphi_3 u\right)$$
$$+\theta\alpha(1-2\beta p_*)p_* r_*,$$

and

$$a_2 = \alpha\beta p_*^2-\alpha p_*+\delta-\varphi_3 u+\xi+b\frac{p_*}{q_*}.$$

Using the relation (8.39), the coefficients a_0 and a_1 simplify to

$$a_0 = \frac{2}{3}\xi dp_*^{\frac{2}{3}}\left(\alpha\beta p_*^2-\alpha p_*+\delta-\varphi_3 u\right)+\left(b\frac{p_*}{q_*}\right)\theta\alpha(1-2\beta p_*)p_* r_*,$$

$$a_1 = \frac{2}{3}\xi dp_*^{\frac{2}{3}}+\left(\xi+b\frac{p_*}{q_*}\right)\left(\alpha\beta p_*^2-\alpha p_*+\delta-\varphi_3 u\right)+\theta\alpha(1-2\beta p_*)p_* r_*.$$

Without loss of generality we make the following positivity assumption at an equilibrium point p_*:

$$\alpha\beta p_*^2-\alpha p_*+\delta-\varphi_3 u>0.$$

For, if the polynomial Q has complex roots, this holds for all p whereas, if the roots are real, for u small enough, i.e., under low dose chemotherapy, this also holds since the roots lie outside of the interval (p_-,p_+) between the two poles. Only with increasing dose rates u it is possible that zeros arise that lie in (p_-,p_+), but we do not consider these cases since the model no longer reflects the medical scenario that is modeled. Thus, in particular, we always have that $a_2>0$.

Proposition 8.4.3. *If a_0 is positive, then the equilibrium point (p_*, q_*, r_*) is locally asymptotically stable.*

Proof. We verify that the conditions of the Routh-Hurwitz criterion are satisfied. More generally, and again using (8.39), $a_0 \geq 0$ implies that

$$\theta\alpha(1-2\beta p_*)p_*r_* \geq -\xi\left(\frac{\frac{2}{3}dp_*^{\frac{2}{3}}}{\mu+\varphi_2 u+dp_*^{\frac{2}{3}}}\right)\left(\alpha\beta p_*^2-\alpha p_*+\delta-\varphi_3 u\right) \quad (8.47)$$

and thus also

$$\begin{aligned} a_1 &> \left(\xi+b\frac{p_*}{q_*}\right)\left(\alpha\beta p_*^2-\alpha p_*+\delta-\varphi_3 u\right)+\theta\alpha(1-2\beta p_*)p_*r_* \\ &\geq \left(b\frac{p_*}{q_*}+\xi\frac{\mu+\varphi_2 u+\frac{1}{3}dp_*^{\frac{2}{3}}}{\mu+\varphi_2 u+dp_*^{\frac{2}{3}}}\right)\left(\alpha\beta p_*^2-\alpha p_*+\delta-\varphi_3 u\right)>0. \end{aligned}$$

Furthermore, we always have that

$$\begin{aligned} a_1a_2-a_0 = {} & \frac{2}{3}\xi dp_*^{\frac{2}{3}}\left[\alpha\beta p_*^2-\alpha p_*+\delta-\varphi_3 u+\left(\xi+b\frac{p_*}{q_*}\right)\right] \\ & +\left(\xi+b\frac{p_*}{q_*}\right)\left(\alpha\beta p_*^2-\alpha p_*+\delta-\varphi_3 u\right)^2 \\ & +\left(\xi+b\frac{p_*}{q_*}\right)^2\left(\alpha\beta p_*^2-\alpha p_*+\delta-\varphi_3 u\right) \\ & +\theta\alpha(1-2\beta p_*)p_*r_*\left[\alpha\beta p_*^2-\alpha p_*+\delta-\varphi_3 u+\left(\xi+b\frac{p_*}{q_*}\right)\right] \\ & -\frac{2}{3}\xi dp_*^{\frac{2}{3}}\left[\alpha\beta p_*^2-\alpha p_*+\delta-\varphi_3 u\right]-\left(b\frac{p_*}{q_*}\right)\theta\alpha(1-2\beta p_*)p_*r_* \end{aligned}$$

$$\begin{aligned} = {} & \frac{2}{3}\xi dp_*^{\frac{2}{3}}\left(\xi+b\frac{p_*}{q_*}\right)+\left(\xi+b\frac{p_*}{q_*}\right)\left(\alpha\beta p_*^2-\alpha p_*+\delta-\varphi_3 u\right)^2 \\ & +\left(\xi+b\frac{p_*}{q_*}\right)^2\left(\alpha\beta p_*^2-\alpha p_*+\delta-\varphi_3 u\right) \\ & +\theta\alpha(1-2\beta p_*)p_*r_*\left(\alpha\beta p_*^2-\alpha p_*+\delta-\varphi_3 u+\xi\right). \end{aligned}$$

Using the lower bound (8.47) and trivial positivity bounds, it follows that

$$\begin{aligned}
a_1a_2 - a_0 &> \left(\xi + b\frac{p_*}{q_*}\right)\left(\alpha\beta p_*^2 - \alpha p_* + \delta - \varphi_3 u\right)^2 \\
&\quad + \left(\xi + b\frac{p_*}{q_*}\right)^2\left(\alpha\beta p_*^2 - \alpha p_* + \delta - \varphi_3 u\right) \\
&\quad - \xi\left(\frac{\frac{2}{3}dp_*^{\frac{2}{3}}}{\mu + \varphi_2 u + dp_*^{\frac{2}{3}}}\right)\left(\alpha\beta p_*^2 - \alpha p_* + \delta - \varphi_3 u\right) \\
&\quad \times \left(\alpha\beta p_*^2 - \alpha p_* + \delta - \varphi_3 u + \xi\right) \\
&> \xi\frac{\mu + \varphi_2 u + \frac{1}{3}dp_*^{\frac{2}{3}}}{\mu + \varphi_2 u + dp_*^{\frac{2}{3}}}\left(\alpha\beta p_*^2 - \alpha p_* + \delta - \varphi_3 u\right)^2 \\
&\quad + \left(\xi + b\frac{p_*}{q_*}\right)^2\left(\alpha\beta p_*^2 - \alpha p_* + \delta - \varphi_3 u\right) \\
&\quad - \xi^2\left(\frac{\frac{2}{3}dp_*^{\frac{2}{3}}}{\mu + \varphi_2 u + dp_*^{\frac{2}{3}}}\right)\left(\alpha\beta p_*^2 - \alpha p_* + \delta - \varphi_3 u\right) \\
&> \xi^2\frac{\mu + \varphi_2 u + \frac{1}{3}dp_*^{\frac{2}{3}}}{\mu + \varphi_2 u + dp_*^{\frac{2}{3}}}\left(\alpha\beta p_*^2 - \alpha p_* + \delta - \varphi_3 u\right) > 0.
\end{aligned}$$

This verifies that all the conditions of the Routh-Hurwitz criterion are satisfied if a_0 is positive and thus the equilibrium point is locally asymptotically stable. □

Corollary 8.4.1. *There exists at most one equilibrium point (p_*, q_*, r_*) in the range $0 < p \leq \frac{1}{2\beta}$ and, if it exists, this equilibrium point is locally asymptotically stable.*

Proof. On the interval $(0, \frac{1}{2\beta}]$ the function Φ is strictly increasing and Ψ is strictly decreasing. Hence there exists at most one point of intersection for the graphs in this range. For $p_* \leq \frac{1}{2\beta}$, the coefficient a_0 is positive and thus the result follows from Proposition 8.4.3. □

Note that, if a_0 is negative, then the equilibrium point (p_*, q_*, r_*) is unstable since A has a positive real eigenvalue. It is clear that $a_0 = -\det A$ needs to vanish at saddle-node bifurcations and if a_0 vanishes, then saddle-node bifurcations arise as long as the transversality conditions in Definition 8.1.8 are satisfied. This is true generically.

Theorem 8.4.1. *If $a_0 = 0$, then generically the system undergoes a saddle-node bifurcation. Geometrically, saddle-node bifurcations correspond to tangential intersections of the graphs of Φ and Ψ and can be characterized as the solutions to the equation $\Delta(p_*) = 0$ with Δ defined in equation (8.44). They are only possible for $p > \frac{1}{2\beta}$.*

Proof. Saddle node bifurcations occur when the Jacobian matrix A has a simple eigenvalue 0 and the transversality conditions related to the corresponding left- and right eigenvectors and the bifurcation parameter in Definition 8.1.8 are satisfied [111]. These conditions are generically met. Since $a_0 = -\det A$, the condition $a_0 = 0$ is equivalent to A having eigenvalue 0. It was shown in the proof of Proposition 8.4.3 that a_1 is positive if a_0 vanishes and thus the eigenvalue 0 is always simple.

For the system considered here, saddle node bifurcations can be characterized geometrically by the fact that the graphs of Φ and Ψ intersect tangentially. This can easily be seen from the formulas for a_0, Φ and Ψ. Using the relations (8.38) and (8.39), we can express the coefficient a_0 at an equilibrium point (p_*, q_*, r_*) as a function of p_* in the form

$$a_0 = \frac{2}{3}\xi d p_*^{\frac{2}{3}}\left(\alpha\beta p_*^2 - \alpha p_* + \delta - \varphi_3 u\right) - \alpha\left(\mu + \varphi_2 u + d p_*^{\frac{2}{3}}\right)\left(p_* - 2\beta p_*^2\right)\left(\xi \ln\left(\frac{\mu + \varphi_2 u + d p_*^{\frac{2}{3}}}{b}\right) + \varphi_1 u\right).$$

Using equation (8.40), we can replace the logarithmic expression to obtain

$$a_0 = \frac{2}{3}\xi d p_*^{\frac{2}{3}}\left(\alpha\beta p_*^2 - \alpha p_* + \delta - \varphi_3 u\right) + \alpha\left(\mu + \varphi_2 u + d p_*^{\frac{2}{3}}\right)\frac{\theta\gamma(p_* - 2\beta p_*^2)}{\alpha\beta p_*^2 - \alpha p_* + \delta - \varphi_3 u}.$$

Note that a_0 vanishes if and only if

$$\frac{2}{3}\frac{\xi d p_*^{-\frac{1}{3}}}{\mu + \varphi_2 u + d p_*^{\frac{2}{3}}} = \frac{\alpha\theta\gamma(2\beta p_* - 1)}{\left(\alpha\beta p_*^2 - \alpha p_* + \delta - \varphi_3 u\right)^2}$$

and this is exactly the relation $\Phi'(p_*) = \Psi'(p_*)$ for the functions Φ and Ψ defined in equations (8.41) and (8.42). Since Φ is strictly increasing and Ψ is strictly decreasing for $p < \frac{1}{2\beta}$, no intersections are possible for $p \le \frac{1}{2\beta}$. For $p > \frac{1}{2\beta}$ we can write

$$a_0 = \frac{\alpha\theta\gamma(2\beta p_* - 1)p_*^{\frac{2}{3}}}{\alpha\beta p_*^2 - \alpha p_* + \delta - \varphi_3 u}\Delta(p_*) \tag{8.48}$$

with

$$\Delta(p) = \frac{1}{3}\frac{\xi d}{\theta\gamma}\left[\left(p - \frac{1}{2\beta}\right)^3 + 2\Xi\left(p - \frac{1}{2\beta}\right) + \frac{\Xi^2}{p - \frac{1}{2\beta}}\right] - (\mu + \varphi_2 u)\, p^{\frac{1}{3}} - dp.$$

This is the function defined by equation (8.44) in the proof of Proposition 8.4.1. Note that no equilibria exist that would correspond to the roots of the quadratic

polynomial $Q(p) = \alpha\beta p^2 - \alpha p + \delta - \varphi_3 u$ and thus the coefficient multiplying Δ is always nonzero and well defined at an equilibrium point p_*. Hence a_0, equivalently $\det A$, vanishes if and only if $\Delta(p_*) = 0$. □

Proposition 8.4.4. *If there exist two equilibria with* $\frac{1}{2\beta} < p_*^{(2)} < p_*^{(3)}$*, then the equilibrium point* $(p_*^{(2)}, q_*^{(2)}, r_*^{(2)})$ *is unstable (with a* 2*-dimensional stable manifold) and the high equilibrium point* $(p_*^{(3)}, q_*^{(3)}, r_*^{(3)})$ *is locally asymptotically stable.*

Proof. We distinguish between the cases when the roots of Q are real and complex. In the case of real roots, the equilibria $p_*^{(2)}$ and $p_*^{(3)}$ lie to the right of the second zero p_+ of Q. The term multiplying Δ in (8.48) is therefore positive. Furthermore,

$$\Delta(p_+) = -(\mu + \varphi_2 u)\, p_+^{\frac{1}{3}} - d p_+ < 0.$$

Since Δ is strictly convex and $\lim_{p\to\infty} \Delta(p) = +\infty$, in this range, if $\Delta(p_*) = 0$, then $\Delta'(p_*) > 0$. Hence Δ and a_0 are negative at the equilibrium point $p_*^{(2)}$ generated in a saddle-node bifurcation and positive at $p_*^{(3)}$. Thus, by Proposition 8.4.3, $p_*^{(3)}$ is locally asymptotically stable and $p_*^{(2)}$ is unstable.

In the case of complex roots, the term multiplying Δ in (8.48) is always positive. The function Δ can have two zeros $\tilde{p}_1 < \tilde{p}_2$ with $\Delta'(\tilde{p}_1) < 0$ and $\Delta'(\tilde{p}_2) > 0$. Accordingly two possibilities exist (see Figure 8.15). The value $\tilde{p}_1$ is close to $\frac{1}{2\beta}$ and in this case the two equilibria $p_*^{(1)} < p_*^{(2)}$ are generated (or merge). The functions Δ and a_0 are positive for $p_*^{(1)}$ and negative for $p_*^{(2)}$ so that $p_*^{(1)}$ is locally asymptotically stable (also, see Corollary 8.4.1) and $p_*^{(2)}$ is unstable. On the other hand, at $\tilde{p}_2$ the equilibria $p_*^{(2)} < p_*^{(3)}$ are generated and in this case the signs of Δ and associated stability properties are reversed so that $p_*^{(2)}$ is unstable and $p_*^{(3)}$ is locally asymptotically stable.

It remains to show that the equilibrium point $p_*^{(2)}$ has a 1-dimensional unstable manifold. Since $a_0 < 0$, there exists a positive real eigenvalue $\lambda > 0$. We therefore can factor the characteristic polynomial $\chi_A(t)$ in the form

$$\chi_A(t) = (t - \lambda)(t^2 + vt + w) = t^3 + (v - \lambda)t^2 + (w - \lambda v)t - \lambda w.$$

Since a_0 is negative, we have $w > 0$ and $a_2 > 0$ implies that $v > \lambda > 0$. Hence the other two roots are negative or have negative real parts. □

Thus the low and high equilibrium points, $(p_*^{(1)}, q_*^{(1)}, r_*^{(1)})$ and $(p_*^{(3)}, q_*^{(3)}, r_*^{(3)})$, are always locally asymptotically stable and have corresponding regions of attraction. The tumor volumes for the low equilibrium point cannot exceed $\frac{1}{2\beta}$ by much and, away from the saddle-node bifurcation points, are smaller. This equilibrium point therefore can be interpreted as the benign equilibrium point and its region of attraction the benign region. This region can be interpreted as the set of all states of the system where a low-dose metronomic chemotherapy is able to control the

cancer to the benign equilibrium point. Situations when this is the only equilibrium point are related to the concepts of *tumor dormancy* and *immunosurveillance*. On the other hand, tumor volumes at the high equilibrium point are by an order of magnitude larger than for the low equilibrium point and these can be interpreted as the malignant equilibrium point and its region of attraction is the malignant region. This region corresponds to conditions where tumor growth overcomes the effects of the low dose chemotherapy, is able to evade the actions of the immune system and tumor dormancy and eventually, unless other treatment options will be pursued, becomes lethal.

Naturally, reality is far more complicated than accounted for in this or any model, and random (and otherwise) events take place that perturb the state of the system in the state-space. In particular, for parameter values for which both benign and malignant regions exist, transitions from one into the other always become a possibility due to unmodeled structures and/or random perturbations that misplace the state of the system. Once such a temporary disturbance has passed, the system will settle down to follow the trajectories in the phase portrait. Tumors that have large malignant regions correspond to more aggressive forms simply since it is more likely for a perturbation to land in this set.

8.4.4 Numerical Illustrations and Choice of the Parameter Values

Biologically validated data are available for the separate models: for the model for angiogenic signaling in the paper by Hahnfeldt et al. [116] for Lewis lung carcinoma and for the mathematical model for tumor-immune system interactions in the paper by Kuznetsov et al. [171] based on in vivo experimental data for B-lymphoma BCL_1 in the spleen of mice. But these data cannot just be combined. The equilibrium of the model for angiogenic signaling from [116] is given by $\left(\frac{b-\mu}{d}\right)^{\frac{3}{2}}$ and is by an order of magnitude larger than the carrying capacity for the model in [171]. We therefore here adjust the values of b and d for the high equilibrium point to be in the same range as the carrying capacity for the tumor-immune system model. Also, the dynamical model for the immunocompetent density in [171] is of the form

$$\dot{r} = \left(\frac{\rho}{\eta + p} - \mu\right) rp + \gamma - \delta r$$

and we approximated the expression $\frac{\rho}{\eta+p} - \mu$ for the parameter values from [171] by the linear term $\alpha(1-\beta p)$ that has the same value for $p = 0$ and the same zero. Table 8.2 below lists the numerical values that we use for the computations and illustrations shown here. Following [171], p and q are given in multiples of 10^6 cells and y is a dimensionless quantity that describes the immuno-competent cell density on a relative order of magnitude basis. The time scale is taken relative to the tumor cell cycle in mice and is in terms of 0.11 days [171].

Table 8.2 Variables and parameter values used in numerical computations.

Variable/ parameters	interpretation	Numerical values used in illustrations	Dimension	Reference
p	Tumor volume		10^6 cells	[303, 171]
q	Carrying capacity		10^6 cells	[116]
r	Immuno-competent cell density		Orders of magnitude Non-dimensional	[303]
u	Concentration of the cytotoxic agent		mg of dose/10^6 cells	
α	Tumor stimulated proliferation rate of immune system	0.0529	Non-dimensional	
β	Inverse threshold of tumor suppression	0.00291	Non-dimensional	[171]
γ	Constant influx into immune system	0.05	10^6 cells/day	[171]
δ	Death rate	0.3743	Non-dimensional	[171]
θ	Tumor immune system interaction rate	1		
ξ	Tumor growth parameter	0.0347		
b	Tumor induced stimulation parameter of vasculature	5	Cells/day	
d	Tumor induced inhibition parameter of vasculature	0.0667	Non-dimensional	
μ	Loss of vascular support through natural causes	0	Cell/day	
φ_1	Cytotoxic killing parameter	0.005	10^6 cells/mg of dose	
φ_2	Antiangiogenic elimination parameter	0.06	10^6 cells/mg of dose	
φ_3	Immune stimulatory parameter	0.02	10^6 cells/mg of dose	

In order to better visualize the structure of the phase portrait, Figure 8.17 shows 2-dimensional projections of the phase portraits into the (p,q) and (p,r) planes. In each figure, the malignant equilibrium point is marked by a blue star and the unstable equilibrium by a red star; the benign equilibrium point is very close to the origin and is not marked on these diagrams. The red curves through the unstable equilibrium point depict the corresponding sections of the stability boundary between benign and malignant behaviors and its 1-dimensional unstable manifold is shown as the

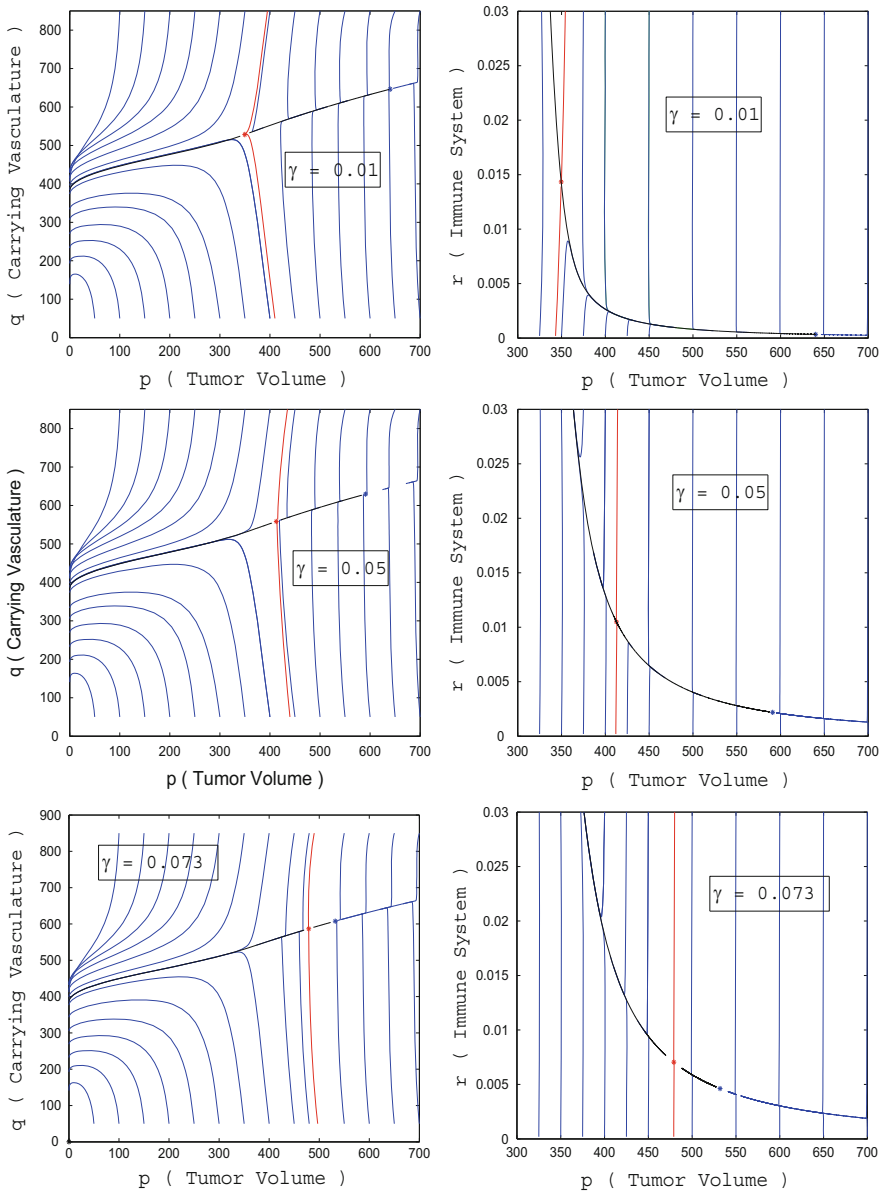

Fig. 8.17 Two-dimensional cross sections of the phase portrait for equations (8.35)–(8.37) for the values $\gamma = 0.01, 0.05$ and 0.073.

black curve. While keeping all other parameters constant, we show three different scenarios as the parameter values for γ, the constant influx of immune cells from the

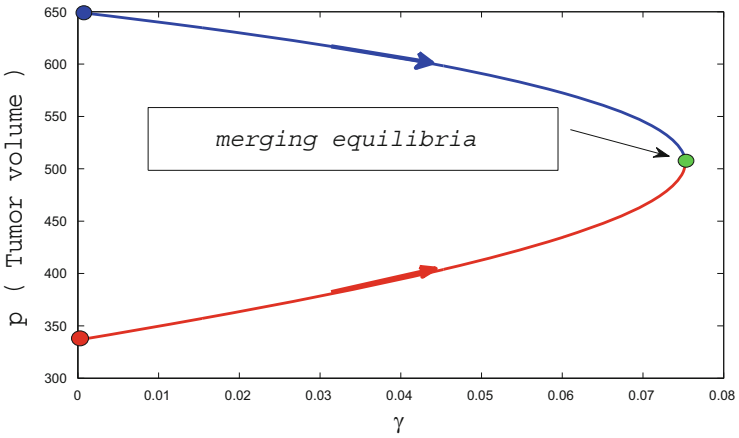

Fig. 8.18 Bifurcation diagram as γ is varied.

primary organs, is increased. The figures[3] illustrate how the unstable and malignant equilibrium points move toward each other and eventually, for $\gamma = 0.07524$, annihilate each other in a saddle-node bifurcation. For larger values of γ, the benign equilibrium point is globally asymptotically stable and the immune system is strong enough to control the cancer in a form of immunosurveillance. Figure 8.18 shows the corresponding bifurcation diagram.

Summarizing the dynamical properties, the model (8.35)–(8.37) exhibits a wide range of behavior that encompasses a variety of medically realistic scenarios. These range from cases when low-dose metronomic chemotherapy is able to completely eradicate the tumor (in the sense that all trajectories converge to the tumor free equilibrium point) to situations when tumor dormancy is induced (when a unique, globally asymptotically stable benign equilibrium point with small positive tumor volume exists) to multi-stable situations that have both persistent benign and malignant behaviors to situations when tumor growth simply is too dominant and cannot be affected by low-dose metronomic chemotherapy. Thus, *despite its simplicity, the model is able to capture the most important structural features of tumor development* under low-dose metronomic chemotherapy. On the other hand, precisely because of the model's simplicity, it is possible to give a complete mathematical analysis of its dynamic behavior.

8.4.5 Optimal Control Formulation for the Combined Model

We conclude this chapter with analyzing the optimal control problem when more generally time-varying administrations schedules are allowed. We are implicitly as-

[3] The numerical calculations were carried out by Behrooz Amini.

suming a set of parameter values for which the system is bistable and has both a benign and a malignant region of attraction. We take the objective to be minimized of the form

$$J(u) = Ap(T) + Bq(T) - Cr(T) + \int_0^T (Mu(t) + S)\, dt \tag{8.49}$$

where, as before, the weights $(A, B, -C)$ in the objective are chosen to induce the system to move from the malignant into the benign region. We have added a minus sign in the last coordinate so that all coefficients A, B and C are positive. One canonical choice is to take (A, B, C) as a multiple of the unstable eigenvector at the saddle point, oriented to point from the benign into the malignant region. Another natural choice would be to take a normal vector to the stable eigenspace of the saddle. For example, for the numerical values in Table 8.2, the saddle point is given by $(p_s, q_s, r_s) = (412.75, 558.41, 0.0105)$ and a properly oriented unstable eigenvector is $(A, B, C) = (0.9134, 0.4071, -0.0001)$. If the strength γ of the innate immune system is reduced to $\gamma = 0.01$, then these values change to $(p_s, q_s.r_s) = (349.65, 528.37, 0.0143)$ and $(A, B, C) = (0.9061, 0.4230, -0.0007)$. We consider the following optimal control problem:

[M] For a free terminal time T, minimize the objective (8.49) over all Lebesgue measurable (respectively, piecewise continuous) functions $u : [0, T] \to [0, 1]$ subject to the dynamics (8.7)–(8.8) with initial condition (p_0, q_0, r_0).

Now writing the state as $z = (p, q, r)^T$, the dynamics again takes the form $\dot{z} = f(z) + ug(z)$ with drift and control vector fields given by

$$f(z) = \begin{pmatrix} -\xi p \ln\left(\frac{p}{q}\right) - \theta pr \\ bp - (\mu + dp^{\frac{2}{3}})q \\ \alpha(p - \beta p^2)r + \gamma - \delta r \end{pmatrix} \quad \text{and} \quad g(z) = \begin{pmatrix} -\varphi_1 p \\ -\varphi_2 q \\ \varphi_3 r \end{pmatrix}. \tag{8.50}$$

First-order necessary conditions for optimality of a control u again follow from the maximum principle (Theorem A.3.1 in Appendix A). Extremals are all normal and thus, with a three-dimensional row-vector $\lambda = (\lambda_1, \lambda_2, \lambda_3) \in (\mathbb{R}^3)^*$ we already define the Hamiltonian $H = H(\lambda, p, q, r, u)$ as

$$\begin{aligned} H = Mu + S &+ \lambda_1 \left(-\xi p \ln\left(\frac{p}{q}\right) - \theta pr - \varphi_1 up \right) \\ &+ \lambda_2 \left(bp - (\mu + dp^{\frac{2}{3}})q - \varphi_2 uq \right) \\ &+ \lambda_3 \left(\alpha(p - \beta p^2)r + \gamma - \delta r + \varphi_3 ur \right). \end{aligned} \tag{8.51}$$

If u_* is an optimal control defined over an interval $[0, T]$ with corresponding trajectory $z_* = (p_*, q_*, r_*)^T$, then there exists an absolutely continuous covector λ defined on $[0, T]$ that satisfies the adjoint equations

$$\dot{\lambda_1} = -\frac{\partial H}{\partial p} = \lambda_1 \left(\xi \left(1 + \ln\left(\frac{p}{q}\right)\right) + \theta r + \varphi_1 u \right) \tag{8.52}$$
$$- \lambda_2 \left(b - \frac{2}{3} dq p^{-\frac{1}{3}} \right) - \lambda_3 \left(\alpha(1 - 2\beta p) r \right),$$

$$\dot{\lambda_2} = -\frac{\partial H}{\partial q} = -\lambda_1 \xi \frac{p}{q} + \lambda_2 (\mu + d p^{\frac{2}{3}} + \varphi_2 u), \tag{8.53}$$

$$\dot{\lambda_3} = -\frac{\partial H}{\partial r} = \lambda_1 \theta p - \lambda_3 \left(\alpha(p - \beta p^2) - \delta + \varphi_3 u \right), \tag{8.54}$$

with terminal condition $\lambda(T) = (A, B, -C)$ such that for almost every time $t \in [0, T]$ the optimal control $u_*(t)$ minimizes the Hamiltonian along $(\lambda(t), p_*(t), q_*(t), r_*(t))$ over the control set $[0, T]$ with minimal value given by 0.

Since the integral term of the objective does not depend on the state variables p, q and r, once more the adjoint equations can succinctly be expressed in the form (8.16) for a single-input u,

$$\dot{\lambda(t)} = -\lambda(t)(Df(z_*(t)) + u_*(t) Dg(z_*(t))),$$

and Proposition 8.2.2 applies to compute the derivatives of the switching function

$$\Phi(t) = M + \langle \lambda(t), g(z_*(t)) \rangle = M - \varphi_1 \lambda_1(t) p_*(t) - \varphi_2 \lambda_2(t) q_*(t) + \varphi_3 \lambda_3(t) r_*(t). \tag{8.55}$$

If an optimal control u_* is singular on an open interval I, then, as above, on I we have that $\Phi(t) \equiv 0$,

$$\dot{\Phi}(t) = \langle \lambda(t), [f, g](z_*(t)) \rangle \equiv 0,$$

and

$$H = \langle \lambda(t), f(z_*(t)) \rangle + S \equiv 0.$$

The Lie bracket $[f, g]$ is given by

$$[f, g](z) = Dg(z) f(z) - Df(z) g(z)$$
$$= \begin{pmatrix} -\varphi_1 & 0 & 0 \\ 0 & -\varphi_2 & 0 \\ 0 & 0 & \varphi_3 \end{pmatrix} \begin{pmatrix} -\xi p \ln\left(\frac{p}{q}\right) - \theta p r \\ \\ b p - (\mu + d p^{\frac{2}{3}}) q \\ \\ \alpha(p - \beta p^2) r + \gamma - \delta r \end{pmatrix}$$

$$
\begin{aligned}
&-\begin{pmatrix} -\xi\left(1+\ln\left(\frac{p}{q}\right)\right)-\theta r & \xi\frac{p}{q} & -\theta p \\ b-\frac{2}{3}dp^{-\frac{1}{3}}q & -(\mu+dp^{\frac{2}{3}}) & 0 \\ \alpha(1-2\beta p)r & 0 & \alpha(p-\beta p^2)-\delta \end{pmatrix}\begin{pmatrix} -\varphi_1 p \\ -\varphi_2 q \\ \varphi_3 r \end{pmatrix} \\
&=\begin{pmatrix} -(\varphi_1-\varphi_2)\xi p+\varphi_3\theta pr \\ (\varphi_1-\varphi_2)bp-\frac{2}{3}\varphi_1 dp^{\frac{2}{3}}q \\ \varphi_1\alpha(p-2\beta p^2)r+\varphi_3\gamma \end{pmatrix}
\end{aligned}
$$

and, except for a 2-dimensional surface, the vector fields f, g and $[f,g]$ are linearly independent. We therefore have the following result:

Proposition 8.4.5. *If an optimal control u_* is singular on an open interval I, then, away from the surface*

$$\mathscr{L}=\{z\in\mathbb{M}:\det(f(z),g(z),[f,g](z))=0\},$$

the associated multiplier $\lambda(t)$ is the unique solution of the equation

$$\lambda(t)\,(f(z_*(t)),g(z_*(t)),[f,g](z_*(t))=(-S,-M,0). \tag{8.56}$$

Thus, because of the dimension of the state-space, singular controlled trajectories are not constrained to lie on a priori specified lower dimensional submanifold, but, except for the set $\mathscr{L}$, solving equation (8.56) for $\lambda=\lambda_{\text{sing}}(z)$ and using the fact that $\ddot{\Phi}\equiv 0$, determines the singular control as the feedback function

$$u_{\text{sing}}(z)=-\frac{\langle\lambda_{\text{sing}}(z),[f,[f,g]](z)\rangle}{\langle\lambda_{\text{sing}}(z),[g,[f,g]](z)\rangle}. \tag{8.57}$$

Naturally, for optimality it needs to be checked that the Legendre-Clebsch condition is satisfied and that the values of the control are admissible. Away from the set $\mathscr{L}$ we can express the second-order Lie brackets $[f,[f,g]]$ and $[g,[f,g]]$ as linear combinations of the basis f, g, and $[f,g]$ in the form

$$[f,[f,g]](z)=\sigma_1(z)f(z)+\sigma_2(z)g(z)+\sigma_3(z)[f,g](z) \tag{8.58}$$

and

$$[g,[f,g]](z)=\omega_1(z)f(z)+\omega_2(z)g(z)+\omega_3(z)[f,g](z). \tag{8.59}$$

We then have that

$$\langle\lambda_{\text{sing}}(z),[f,[f,g]](z)\rangle=-\sigma_1(z)S-\sigma_2(z)M$$

and

$$\langle\lambda_{\text{sing}}(z),[g,[f,g]](z)\rangle=-\omega_1(z)S-\omega_2(z)M$$

so that the singular control is given by the feedback function

$$u_{\text{sing}}(z) = -\frac{\sigma_1(z)S + \sigma_2(z)M}{\omega_1(z)S + \omega_2(z)M}. \tag{8.60}$$

Note that if the emphasis is put on quick actions, i.e., if $S \gg M$, then

$$u_{\text{sing}}(z) \simeq -\frac{\sigma_1(z)}{\omega_1(z)}$$

and if the emphasis is more on side effects $M \gg S$, then

$$u_{\text{sing}}(z) \simeq -\frac{\sigma_2(z)}{\omega_2(z)}.$$

The vector field $[f,[f,g]]$ contains full and lengthy expressions that do not offer much insight, but $[g,[f,g]]$ reduces to the following simple form:

$$[g,[f,g]](z) = \begin{pmatrix} \varphi_3^2 \theta pr \\ -(\varphi_1 - \varphi_2)^2 bp + \frac{4}{9}\varphi_1^2 d p^{\frac{2}{3}} q \\ -\varphi_1^2 \alpha(p - 4\beta p^2)r - \varphi_3^2 \gamma \end{pmatrix}.$$

It is not difficult to compute these vector fields and hence also the singular control (8.60) numerically and to verify the Legendre-Clebsch condition. Figure 8.19 shows the graphs of the feedback functions $\langle \lambda_{\text{sing}}(z), [f,[f,g]](z) \rangle$ and $\langle \lambda_{\text{sing}}(z), [g,[f,g]](z) \rangle$ (the Legendre-Clebsch condition) for the parameter values from Table 8.2 with the one change that $\gamma = 0.01$; the coefficients in the objective were chosen as $S = 10$ and $M = 1$. Cross-sections through the graphs of the corresponding singular control $u_{\text{sing}}(z)$ are shown in Figure 8.20 for the value $r = 0.5$ on the top for the range considered in Figure 8.19 and on the bottom for the higher range $(p,q) \in [350,500] \times [350,500]$. Recall that the strengthened Legendre-Clebsch condition is satisfied if $\langle \lambda_{\text{sing}}(z), [g,[f,g]](z) \rangle$ is negative and this is the case for all points in the ranges shown here. However, the singular control is negative and thus inadmissible in the high range. Hence, in the malignant region the control will be at the maximum metronomic dose considered in the model. Once the system moves into the benign region, then singular controls keep decreasing and thus in this range it seems reasonable that the control rates will be lowered to control the benign equilibrium point.

In Figure 8.21 we still show the evolution of some sample controlled trajectories for a singular control over time from the initial condition $(p_0, q_0, r_0) = (200, 300, 0.1)$.

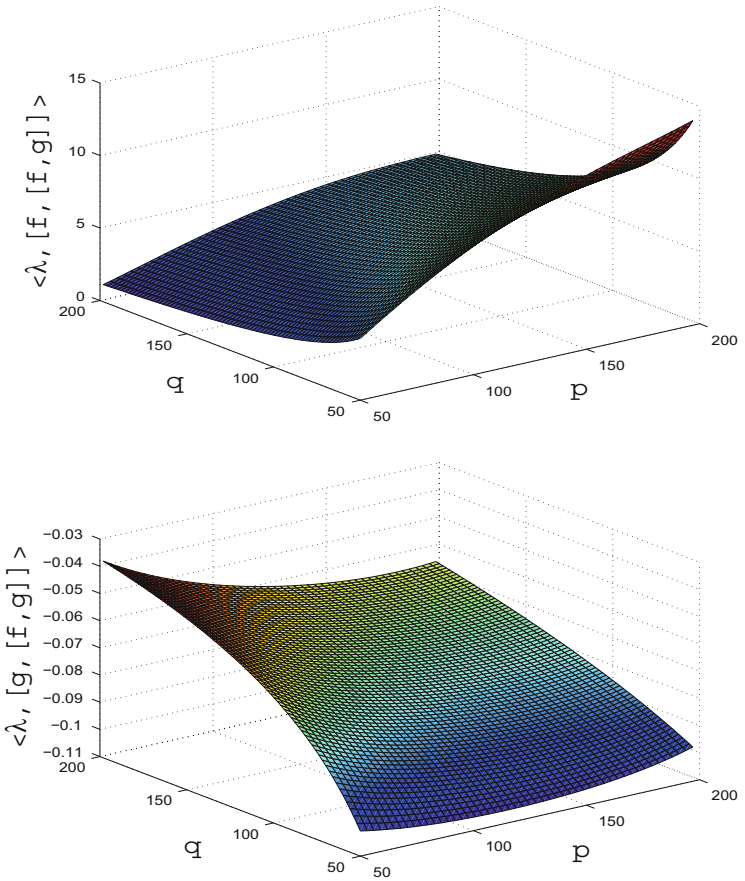

Fig. 8.19 Cross-section of the feedback functions $\langle \lambda(z), [f,[f,g]](z) \rangle$ (top) and $\langle \lambda(z), [g,[f,g]](z) \rangle$ (bottom) along a singular control for $r = 0.5$.

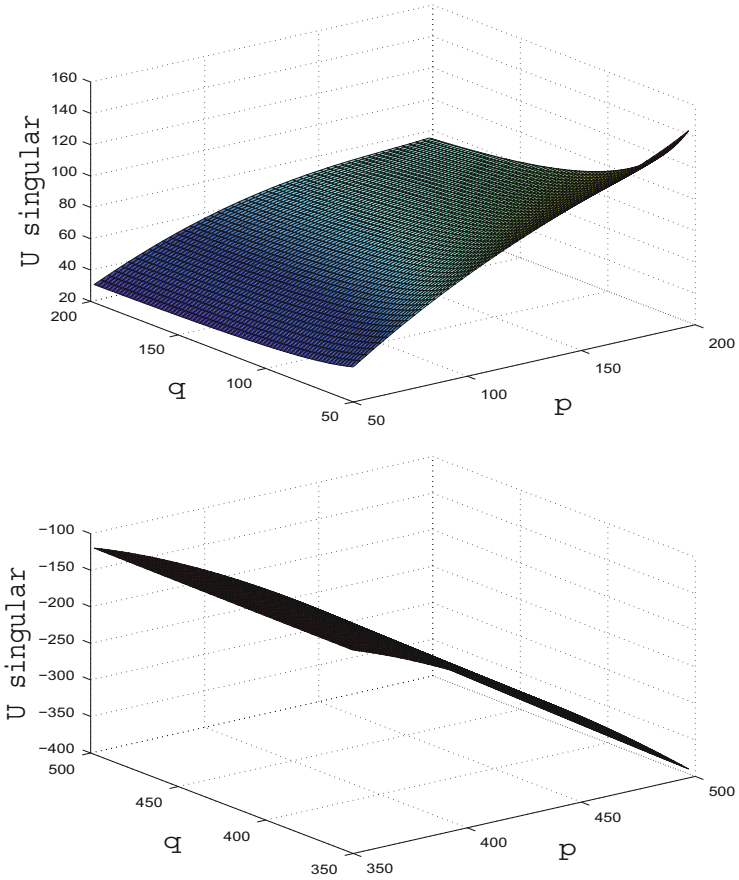

Fig. 8.20 Cross sections of the singular control u_{sing} as a feedback function of (p,q) for $r = 0.5$ for the ranges $[0,200] \times [0,200]$ (top) and $[350,500] \times [350,500]$ (bottom).

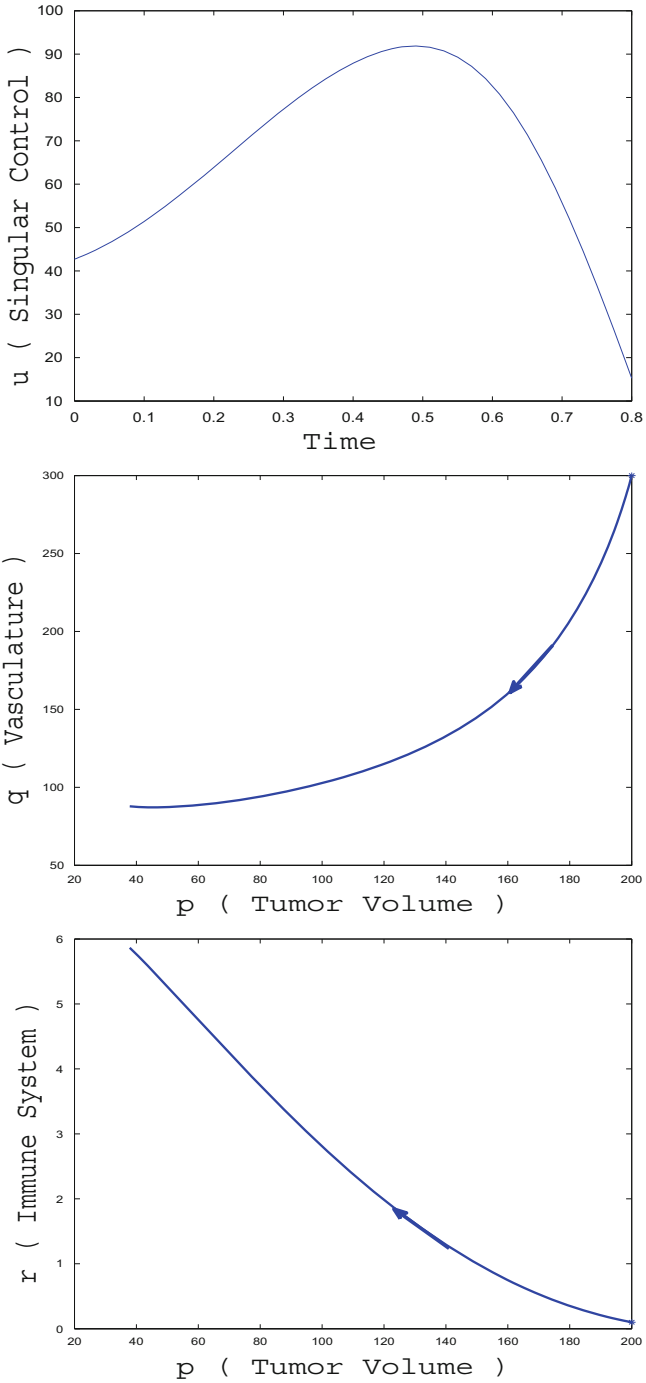

Fig. 8.21 Time evolution of some sample controlled trajectories for a singular control from the initial condition $(p_0, q_0, r_0) = (200, 300, 0.1)$.

Chapter 9
Concluding Remarks

The question how therapeutic agents should be administered in order to maximize their potential effects is of fundamental importance in medical treatments. In the administration of cancer treatments, these questions are still far from being answered conclusively. In this text, we have explored what can be said about this topic from an analysis of minimally parameterized models described by ordinary differential equations using an optimal control approach. Clearly, more precise and in this sense more realistic models exist. These range from the inclusion of spatial aspects in partial differential equations to the incorporation of random features in stochastic models to complex agent-based models. Becoming increasingly more precise, such models, however, are prone to the pitfalls of Borges's cartographers guild [33]. While current computer technologies enable large-scale computations and simulations, the number of parameters involved automatically carries with it uncertainty. Also, no matter how precise the data are that are available, the values of the parameters are for a particular case and numerical results pertain to a specific situation. On the other hand, the models considered here are all highly aggregated population based models, which, having small dimensions, allows to examine the underlying models analytically, not just numerically. Indeed, fairly robust qualitative features emerge from our analysis that we still would like to summarize.

The prevailing paradigm of giving as much of the drugs as possible as soon as possible clearly makes sense at the onset of discovery of the disease when quick and immediate actions are required. This is borne out in mathematical models for a homogeneous tumor population of chemotherapeutically sensitive cells. However, at an intercellular level, tumor cell populations act as ecosystems and many sources of complexity arise from internal cell-to-cell cooperative and competitive interactions which may generate great heterogeneity within a tumor. This can lead to the development of various degrees of chemotherapeutic resistance not just to one, but to several drugs. As these facts are taken into account, the picture of optimal drug administration schedules becomes blurry and MTD therapies no longer need to be the best overall options. Also, quiescent cells are immune from a cytotoxic attack

H. Schättler, U. Ledzewicz, *Optimal Control for Mathematical Models of Cancer Therapies*, Interdisciplinary Applied Mathematics 42,
DOI 10.1007/978-1-4939-2972-6_9

and this type of drug administration thus will be rather ineffective for tumors with small growth fractions. In such a case, MTD-based strategies may do more harm to the healthy tissue than good. For this reason, chemotherapy often is ruled out for slowly growing tumors. Even if MTD-type chemotherapy is initially successful, in the long run it is not uncommon that therapy fails because of drug resistance. A particularly difficult situation arises if a possibly tiny fraction of drug-resistant tumor cells has been present from the very beginning. While the sensitive cells are exceedingly being depleted by the MTD-type attack, in time (and possibly only after many years of seemingly remission of the cancer) the resistant cells become dominant leading to an eventual failure of therapy. Clearly, there do not yet exist well-developed strategies to deal with such situations and adaptive and metronomic chemotherapy are just two alternative scheduling protocols that have been proposed in the medical literature. The fact that conclusive answers remain elusive also in the mathematical analysis of such problems only reflects the complexities of the underlying real problem.

The question how chemotherapeutic agents should be scheduled to optimize their effects is a difficult one when the true system (patient) is considered and many systemic aspects need to be taken into account to give a satisfactory answer. This requires to consider not just the cancerous cells, but include also other aspects of the tumor microenvironment such as its vasculature or tumor-immune system interactions. The models analyzed in this text seem to point into the direction that it is not necessarily the better approach to give more. Clearly, robust conclusions can be drawn from the analysis of the mathematical models for angiogenic signaling that support the theory that an ideal balance between tumor size and tumor vasculature improves the efficacy of drug administration. There also exist well-founded biological considerations that would support such a notion. Tumor vasculature is highly irregular and large amounts of drugs simply are wasted in this leaky network since they never reach their intended target. Thus a properly calibrated dose of antiangiogenic agents can achieve a better overall effect than a purely maximum possible damage type of concept, certainly if agents are limited. Similarly, if tumor immune system interactions are taken into account, after some time optimal drug administration schedules tend to favor lower doses. The analysis of the models considered in this text consistently point to chemo-switch type protocols as optimal. Thus, *while the models that were considered are highly aggregated, they led to robust results about the qualitative structures of optimal protocols*.

Overall, our results are based on rudimentary, minimally parameterized models which still capture the essence of the underlying biology. Naturally, while these cannot include the more refined biological details, nevertheless the results obtained correlate positively with many approaches taken in medical practice and shed some light as to how these treatments should be administered in reality. As such the goal to obtain *qualitative information about the structure of optimal administration of treatment protocols* has been realized. On the other hand, clearly these models are limited. In modern medicine many promising avenues are pursued that fall outside of the realm of the models and procedures discussed here and that aim to overcome the limitations of these more conventional therapies. For example, the models for

chemotherapy considered here apply to a wide range of drugs that damage DNA or attempt to block synthesis that still form the staple of cancer treatment. In current medical research there is a strong attempt to develop drugs that target specific molecular pathways involved in carcinogenesis even to the extent of developing patient specific treatments. The mechanisms of actions and toxicities of such drugs are quite different from conventional approaches. For example, by being specifically targeted to particular molecular pathways, generally these drugs are less toxic to the healthy tissue. Yet, the issue of tumor heterogeneity still remains and specific pathways need not apply to all the cells in a tumor. These approaches require modeling approaches that are different from the fundamental principles that were considered here and since these pathways generally are highly complex, such models will be large scale. But from a mathematical modeling side little is known about these systems currently. While it is not likely that optimal control methods can be directly applied to large-scale models, numerical methods can always be undertaken. Yet, this leads us back to the discussions from the beginning of this chapter. Without a doubt, the ultimate question—*how to optimize the anti-tumor, antiangiogenic, and pro-immune effects of chemotherapy by modulating dose and administration schedule*—will still occupy both medical practitioners and modelers alike for many years to come.

Appendix A
Optimal Control: A Review of Main Results and Concepts

In this appendix, we review the main results and tools from optimal control. The presentation follows our book [292], but we forego generality to match the problem formulations closely to the ones considered in this text. Also, no proofs will be given. Some of the proofs are lengthy and difficult, but it is not necessary to know these proofs in order to follow the applications of the results. Generally, the main portion of the text is written in a self-contained manner and the appendix merely provides a convenient summary for the tools and techniques that we use.

In Section A.2 we formulate a general optimal control problem, establish standard terminology, and present the Pontryagin maximum principle, the fundamental necessary conditions for optimality. Then, in Section A.3 we specify these conditions further for systems that depend affinely on the controls. Such mathematical models are by far the most common models in practical applications of optimal control in engineering and the life sciences, and all the problems considered in this text have this structure. It simply reflects the fact that "controls" represent outside influences on a dynamical system and that one wants to set them up in a way so that these effects can be most easily understood and analyzed. For control-affine control systems, the analysis of the necessary conditions of the maximum principle leads to two classes of control functions as prime candidates for optimality, so-called bang and singular controls. We introduce the fundamental framework to analyze these controls consisting of switching functions and Lie-derivative based formulas for its derivatives and also state higher order necessary conditions for optimality of singular controls. Section A.4 concludes the appendix with an overview of sufficient conditions for optimality. We formulate the Hamilton-Jacobi-Bellman equation and briefly outline the method of characteristics as a procedure to construct a solution to this equation by means of integrating a field of extremals. In Appendix B.1 we shall explicitly carry out these technical constructions for the cancer chemotherapy model formulated in Section 2.1. We close with some results about a regular synthesis of optimal controls, the global solution of optimal control problems.

H. Schättler, U. Ledzewicz, *Optimal Control for Mathematical Models of Cancer Therapies*, Interdisciplinary Applied Mathematics 42,
DOI 10.1007/978-1-4939-2972-6

A.1 Notation and Terminology

We write the state x, $x \in \mathbb{R}^n$, of the system as a column vector, $x = (x_1, \ldots, x_n)^T$, but distinguish the state from the multipliers λ that arise in the necessary conditions for optimality and write these, consistent with their geometric meaning as covectors, as row vectors denoting the space of n-dimensional covectors or row vectors by $(\mathbb{R}^n)^*$. However, we do not distinguish between $\mathbb{R}$ and $\mathbb{R}^*$. We also interchangeably use the notations $\langle \lambda, x \rangle = \lambda x$ for the inner product of a row vector λ with a column vector x. For a scalar, continuously differentiable function $h : \mathbb{R}^n \to \mathbb{R}$, $x \mapsto h(x)$, we write the gradient with respect to x as a row vector and denote it by $\nabla h(x)$ or $\frac{\partial h}{\partial x}(x)$, i.e.,

$$\nabla h(x) = \frac{\partial h}{\partial x}(x) = \left(\frac{\partial h}{\partial x_1}(x), \ldots, \frac{\partial h}{\partial x_n}(x) \right).$$

For a vector-valued continuously differentiable map H,

$$H : \mathbb{R}^k \to \mathbb{R}^\ell, \qquad x \mapsto H(x) = \begin{pmatrix} h_1(x) \\ \ldots \\ h_k(x) \end{pmatrix},$$

we denote the Jacobian matrix of the partial derivatives of the components $h_i(x)$ with respect to the variables x_j by

$$DH(x) = \frac{\partial H}{\partial x}(x) = \begin{pmatrix} \frac{\partial h_1}{\partial x_1}(x) & \ldots & \frac{\partial h_1}{\partial x_k}(x) \\ \vdots & \frac{\partial h_i}{\partial x_j}(x) & \vdots \\ \frac{\partial h_k}{\partial x_1}(x) & \ldots & \frac{\partial h_k}{\partial x_k}(x) \end{pmatrix}_{1 \le i,j \le k},$$

with i as row index and j as column index. Thus, the Jacobian matrix is the matrix whose ith row is given by the gradient of the component h_i. The Hessian matrix of a twice continuously differentiable function $h : \mathbb{R}^n \to \mathbb{R}$, $x \mapsto h(x)$, is the matrix of the second-order partial derivatives of h and will be denoted by $D^2 h(x) = \frac{\partial^2 h}{\partial x^2}(x)$. With the convention above, the Hessian of h is the Jacobian matrix of the transpose of the gradient of h,

$$D^2 h(x) = \frac{\partial^2 h}{\partial x^2}(x) = \frac{\partial (\nabla h)^T}{\partial x}(x).$$

If $\Lambda = (\lambda_1, \ldots, \lambda_n)$ is a row vector of continuously differentiable functions $\lambda_j : \mathbb{R}^n \to \mathbb{R}$, $x \mapsto \lambda_j(x)$, $j = 1, \ldots, n$, then, and consistent with the notation just introduced, we denote the matrix of the partial derivatives $\left(\frac{\partial \lambda_j}{\partial x_i} \right)_{1 \le i,j \le n}$ with row index i and column index j by $\frac{\partial \Lambda}{\partial x}$, that is,

$$\frac{\partial \Lambda}{\partial x}(x) = \left(\frac{\partial \Lambda^T}{\partial x}(x) \right)^T \qquad \text{or} \qquad D\Lambda(x) = \left(D\left(\Lambda^T(x) \right) \right)^T.$$

Not only does this formalism properly distinguish the different geometric meanings of the variables involved, but it also allows us to write formulas without having to use transposes and this simplifies the notation considerably.

A.2 Optimal Control Problems and Necessary Conditions for Optimality

An optimal control problem is a dynamic optimization problem in which the state of a system, $x = x(t)$, is linked in time to the application of a control function, $u = u(t)$, by means of the solution to an ordinary differential equation that is shaped by the control, $\dot{x} = f(x, u(t))$, and then an objective $J = J(u)$ is optimized over all possible responses subject to external constraints. (More generally, the dynamics could be described by partial differential equations and/or stochastic effects may be included, but in this text we only consider so-called finite-dimensional deterministic problems.) We start with establishing some terminology and a precise formulation of the problems to be considered.

A.2.1 Formulation of an Optimal Control Problem

Definition A.2.1 (Control System). A control system is a 4-tuple $\Sigma = (M, U, f, \mathscr{U})$ consisting of a state space M, a control set U, a dynamics f, and a class $\mathscr{U}$ of admissible controls.

Throughout this text, we only consider the following simplified data structures defining control systems:

1. The *state space* M is an open and connected subset of $\mathbb{R}^n$.
2. The *control set* U is a compact and convex subset of $\mathbb{R}^m$.
3. The *dynamics*, $\dot{x} = f(x, u)$, is defined by a family of continuously differentiable vector fields f parameterized by the control values $u \in U$,

$$f : M \times U \to \mathbb{R}^n, \quad (x, u) \mapsto f(x, u),$$

   i.e., f assigns to every point $(x, u) \in M \times U$ a vector $f(x, u) \in \mathbb{R}^n$.
4. The class $\mathscr{U}$ of *admissible controls* consists of all Lebesgue measurable functions u defined on a compact interval $I \subset \mathbb{R}$ with values in the control set U, $u : I \to U$, $t \mapsto u(t)$. (This generality is needed to ensure the existence of solutions to optimal control problems and indeed, even for the problems considered in this text, optimal controls are not necessarily piecewise continuous.)

Given any admissible control $u \in \mathscr{U}$ defined over some open interval J, it follows from standard results about the local existence and uniqueness of ordinary differential equations that for any initial condition $x(t_0) = x_0$ with $t_0 \in J$, there exists a unique solution x to the initial value problem

$$\dot{x}(t) = f(x,u(t)), \qquad x(t_0) = x_0, \tag{A.1}$$

defined over some maximal interval $(\tau_-, \tau_+) \subset J$ that contains t_0.

Definition A.2.2 (Controlled Trajectory). Given an admissible control $u \in \mathscr{U}$ defined over an interval J, let x be the unique solution to the initial value problem (A.1) with maximal interval of definition $I = (\tau_-, \tau_+)$. We call this solution x the trajectory corresponding to the control u and call the pair (x,u) a controlled trajectory over the interval I.

An optimal control problem then consists in finding, among all admissible controlled trajectories, one that minimizes an objective, possibly subject to additional constraints. In this text, in addition to the control constraints that are implicit in the definition of the control set, we only consider *terminal constraints* in the form of a target set into which the controls need to steer the system. These may include a fixed terminal time T (e.g., chemotherapy over a prescribed therapy horizon) or limitations on the terminal state for a free final time T (e.g., optimizing in time the use of an a priori specified amount of therapeutic agents). We therefore describe the terminal set N in the form

$$N = \{(t,x) \in \mathbb{R} \times M : \Psi(t,x) = 0\}$$

where $\Psi : \mathbb{R} \times M \to \mathbb{R}^{n+1-k}$, $(t,x) \mapsto \Psi(t,x) = (\psi_0(t,x), \ldots, \psi_{n-k}(t,x))^T$, is a continuously differentiable mapping with the property that the matrix $D\Psi$ of the partial derivatives with respect to (t,x) is of full rank $n+1-k$ everywhere on N, (i.e., the gradients of the functions $\psi_0(t,x), \ldots, \psi_{n-k}(t,x)$ are linearly independent on N). A fixed terminal time simply will be modeled as the equation $\Psi_0(t,x) = t - T$ in the mapping Ψ defining the constraint in N. Geometrically, the terminal set is a k-dimensional embedded submanifold of $\mathbb{R} \times M$.

The *objective* is given in so-called Bolza form as the integral of a Lagrangian L plus a penalty term φ. Both the Lagrangian L, $L : M \times U \to \mathbb{R}$, $(x,u) \mapsto L(x,u)$, and the penalty term φ, $\varphi : \mathbb{R} \times M \to \mathbb{R}$, $(t,x) \mapsto \varphi(t,x)$, are continuously differentiable functions and the objective or cost functional is given as

$$\mathscr{J}(u) = \int_0^T L(x(s),u(s))ds + \varphi(T,x(T)), \tag{A.2}$$

where x is the unique trajectory corresponding to the control u. The initial time has been normalized to $t_0 = 0$ and the terminal time T can be fixed or free. In the latter case the possibility of penalizing long intervals is included in the function φ. The initial condition x_0 is fixed, but arbitrary. The optimal control problem then is the following one:

[OC] Minimize the objective $\mathscr{J}(u)$ over all admissible controlled trajectories (x,u) defined over an interval $[0,T]$ such that the terminal constraint $(T,x(T)) \in N$ is satisfied.

A.2.2 The Pontryagin Maximum Principle

The maximum principle of optimal control gives the fundamental necessary conditions for a controlled trajectory (x,u) to be optimal. It was developed in the mid 1950s in the Soviet Union by a group of mathematicians under the leadership of L.S. Pontryagin, also including V.G. Boltyanskii , R.V. Gamkrelidze, and E.F. Mishchenko, and is known as the Pontryagin maximum principle [29, 282]. On a formal level, it gives multiplier type necessary conditions for optimality, but its geometric significance lies quite a bit deeper.

Definition A.2.3 (Hamiltonian). The (control) *Hamiltonian* function H,

$$H : [0,\infty) \times (\mathbb{R}^n)^* \times \mathbb{R}^n \times \mathbb{R}^m \to \mathbb{R}, \quad (\lambda_0,\lambda,x,u) \mapsto H(\lambda_0,\lambda,x,u),$$

for the optimal control problem [OC] is defined as

$$H(\lambda_0,\lambda,x,u) = \lambda_0 L(x,u) + \lambda f(x,u). \tag{A.3}$$

Theorem A.2.1 (Pontryagin Maximum Principle [282]). *Let (x_*,u_*) be a controlled trajectory defined over the interval $[0,T]$. If (x_*,u_*) is optimal, then there exist a constant $\lambda_0 \geq 0$ and a covector $\lambda : [0,T] \to (\mathbb{R}^n)^*$, the so-called* adjoint variable*, such that the following conditions are satisfied:*

1. Nontriviality *of the multipliers: $(\lambda_0,\lambda(t)) \neq 0$ for all $t \in [0,T]$.*
2. Adjoint equation*: the adjoint variable λ is a solution to the time-varying linear differential equation*

$$\dot{\lambda}(t) = -\lambda_0 \frac{\partial L}{\partial x}(x_*(t),u_*(t)) - \lambda(t)\frac{\partial f}{\partial x}(x_*(t),u_*(t)). \tag{A.4}$$

3. Minimum condition: *almost everywhere in $[0,T]$ we have that*

$$H(\lambda_0,\lambda(t),x_*(t),u_*(t)) = \min_{v\in U} H(\lambda_0,\lambda(t),x_*(t),v) = \text{const.} \tag{A.5}$$

4. Transversality condition*: at the endpoint of the controlled trajectory, the covector $\left(H + \lambda_0\frac{\partial\varphi}{\partial t}, -\lambda + \lambda_0\frac{\partial\varphi}{\partial x}\right) \in \left(\mathbb{R}^{1+n}\right)^*$ is orthogonal to the terminal manifold N. This is equivalent to the existence of a multiplier $\nu \in (\mathbb{R}^{n+1-k})^*$ such that*

$$H + \lambda_0\frac{\partial\varphi}{\partial t} + \nu\frac{\partial\Psi}{\partial t} = 0, \qquad \lambda = \lambda_0\frac{\partial\varphi}{\partial x} + \nu\frac{\partial\Psi}{\partial x} \qquad \text{at } (T,x_*(T)). \tag{A.6}$$

The following statement is an immediate special case of the transversality condition.

Corollary A.2.1. *If the penalty function φ and the terminal constraint Ψ do not depend on t (and in this case the terminal time T necessarily is free), then the Hamiltonian H vanishes identically along the optimal controlled trajectory (x_*,u_*),*

$$H(\lambda_0, \lambda(t), x_*(t), u_*(t)) \equiv 0.$$

We introduce some useful terminology and give a brief, but somewhat informal description of the significance of each condition.

Definition A.2.4 (Extremals; Normal and Abnormal). Controlled trajectories (x,u) for which there exist multipliers λ_0 and λ such that the conditions of the maximum principle are satisfied are called *extremals* and the pair $((x,u),(\lambda_0,\lambda))$ consisting of the controlled trajectory and the multipliers is called an *extremal lift* (to the cotangent bundle in case of manifolds). If $\lambda_0 > 0$, then the extremal lift is called *normal* while it is called *abnormal* if $\lambda_0 = 0$.

(1) Normal and abnormal extremal lifts. The maximum principle takes the form of a multiplier rule with multiplier $(\lambda_0, \lambda(t))$. The nontriviality condition precludes a trivial solution of these conditions with $(\lambda_0, \lambda(t)) = (0,0)$. Since the conditions are linear in the multipliers (λ_0, λ), it is always possible to normalize this vector. For example, if $\lambda_0 > 0$, then the conditions do not change if we divide by λ_0 and instead consider as the new multiplier $(1, \tilde{\lambda}(t))$, where $\tilde{\lambda}(t) = \lambda(t)/\lambda_0$. Thus, without loss of generality, we may always assume that $\lambda_0 = 1$ if the extremal lift is normal. Note that it is a property of the extremal lift, not the controlled trajectory, to be normal or abnormal. It is possible that both normal and abnormal extremal lifts exist for a given controlled trajectory (x,u). For this reason, controlled trajectories for which only abnormal extremal lifts exist are sometimes called *strictly abnormal*.

(2) Adjoint system. As a solution to a linear time-varying ordinary differential equation, the adjoint variable $\lambda(\cdot)$ is well defined over the full interval $[0,T]$. Geometrically, and this is shown in the proof of the maximum principle, the multiplier $(\lambda_0, \lambda(t))$ represents a normal vector to a hyperplane in (t,x)-space (hence the nontriviality condition) that evolves in time according to the adjoint equation. This equation arises as the adjoint in the sense of linear ordinary differential equations of the so-called *variational equation*

$$\dot{y} = \frac{\partial f}{\partial x}(x_*(t), u_*(t))y, \tag{A.7}$$

which transports tangent vectors (that are generated by means of variations) along the reference controlled trajectory $t \mapsto (x_*(t), u_*(t))$. Solutions of the adjoint system provide the corresponding transport for covectors along this curve. In terms of the Hamiltonian H, the coupled system consisting of the dynamics and the adjoint equation can be written as

$$\dot{x}_*(t) = \frac{\partial H}{\partial \lambda}(\lambda_0, \lambda(t), x_*(t), u_*(t)) \quad \text{and} \quad \dot{\lambda}(t) = -\frac{\partial H}{\partial x}(\lambda_0, \lambda(t), x_*(t), u_*(t)) \tag{A.8}$$

and thus forms a *Hamiltonian system* that is coupled with the control u_* through the minimization condition (A.5).

(3) Minimum condition. In the original formulation of the theorem by Pontryagin et al. [282], this condition was formulated as a maximum condition and gave

the result its name. In fact, depending on the choice of the signs associated with the multipliers λ_0 and λ, the maximum principle can be stated in four equivalent versions. Here, since most of the problems we will be considering are cast as *minimization* problems, we prefer this more natural formulation, but retain the classical name. The minimum condition (A.5) states that in order to solve the minimization problem on the function space of controls, the control u_* needs to be chosen so that for some extremal lift, it minimizes the Hamiltonian H pointwise over the control set U, i.e., for almost every $t \in [0,T]$, the control $u_*(t)$ is a minimizer of the function $v \mapsto H(\lambda_0, \lambda(t), x_*(t), v)$ over the control set U. Note that it is not just required that the control satisfy the necessary conditions for minimality—and this is how a weak version of the maximum principle is formulated—but that the control $u_*(t)$ be a true minimizer over the control set U. This condition generally is the starting point for any analysis of an optimal control problem. Formally, we may try to "solve" the minimization condition (A.5) for the control u as a function of the other variables, $u = u(t, x_*, \lambda_0, \lambda)$, and then substitute the "result" into the differential equations for dynamics and adjoint variable to get

$$\begin{aligned} \dot{x} &= f(x, u(t, x_*; \lambda_0, \lambda)), & x(t_0) &= x_0, \\ \dot{\lambda}(t) &= -\lambda_0 \frac{\partial L}{\partial x}(x_*(t), u(t, x_*; \lambda_0, \lambda)) - \lambda(t) \frac{\partial f}{\partial x}(x_*(t), u(t, x_*; \lambda_0, \lambda)). \end{aligned}$$

Multiple solutions to the minimization problem can exist and in general this is not a unique specification of the control. Even when the minimization problem has a unique solution, this solution depends on the multiplier, i.e., lives in the cotangent bundle. It is possible that there exist multiple solutions and thus this need not give rise to unique controlled trajectories. In fact, two extremals projecting onto the same point in the state space is the typical geometric picture that arises when trajectories lose local optimality properties near conjugate points.

(4) Transversality conditions. Equations (A.1) and (A.4) form a system in $2n+1$ variables (the state x, the multiplier λ, and the terminal time T) with the initial condition x_0 specified. Information about the remaining $n+1$ conditions is contained in the transversality conditions at the endpoint. The requirement that the terminal state lie on the manifold N, $(T, x(T)) \in N$, imposes $n+1-k$ conditions and thus leaves k degrees of freedom. The adjoint variable $\lambda(T) \in (\mathbb{R}^n)^*$ at the terminal time T is determined on the k-dimensional tangent space to N at $(T, x_*(T))$ by the relation

$$\lambda(T) = \lambda_0 \frac{\partial \varphi}{\partial x}(T, x_*(T)) + \nu \frac{\partial \Psi}{\partial x}(T, x_*(T))$$

and the multiplier $\nu \in \left(\mathbb{R}^{n+1-k}\right)^*$ in this equation accounts for $n-(n+1-k) = k-1$ degrees of freedom. The last degree of freedom is taken up by the equation

$$H(\lambda_0, \lambda(T), x_*(T), u_*(T)) + \lambda_0 \frac{\partial \varphi}{\partial t}(T, x_*(T)) + \nu \frac{\partial \Psi}{\partial t}(T, x_*(T)) = 0$$

if the terminal time T is free. Overall, there thus are $2n+1$ equations for the boundary values $x(T)$, $\lambda(T)$ and T. Hence, at least in nondegenerate situations, the

transversality conditions provide the required information about the missing boundary conditions for both the adjoint variable and the terminal time T. The geometric statement that the vector $(H+\lambda_0\frac{\partial\varphi}{\partial t}, -\lambda+\lambda_0\frac{\partial\varphi}{\partial x})$ is orthogonal to the terminal constraint N at the endpoint of the controlled trajectory is equivalent to the formulation given in the theorem.

Corollary A.2.2. *If there are no constraints on the terminal state $x(T)$, then all extremals are normal.*

Proof. In this case the transversality conditions reduce to the equations

$$H(\lambda_0,\lambda(T),x_*(T),u_*(T))+\lambda_0\frac{\partial\varphi}{\partial t}(T,x_*(T))=0$$

and

$$\lambda(T)=\lambda_0\frac{\partial\varphi}{\partial x}(T,x_*(T)).$$

If $\lambda_0=0$, then the adjoint equation (A.4) is a time-varying homogeneous linear differential equation with terminal condition $\lambda(T)=0$. Hence $\lambda(t)\equiv 0$ contradicting the nontriviality of the multipliers. □

Summarizing, in order to solve an optimal control problem, in principle, we need to *find all solutions to a boundary value problem on state and costate, coupled by a minimization condition, and then compare the costs that the projections of these solutions onto the controlled trajectories give*. This is not an easy task.

A.3 Control Affine Systems as Mathematical Models for Biomedical Models

We say a control system is *control-affine* with drift vector field f and control vector fields g_i, $i=1,\dots,m$, if the dynamics takes the following form:

$$\dot{x}=f(x)+\sum_{i=1}^{m}g_i(x)u_i,\qquad x\in M,\qquad u\in U. \tag{A.9}$$

Here the vector field f represents the uncontrolled dynamics while the vector fields g_i model the influence of the ith control on the system. In the biomedical models considered in this text, the controls represent dose rates or concentrations of some agents and these are nonnegative values that lie in prescribed ranges. We therefore take the control set U as an m-dimensional interval of the form

$$U=[0,u_1^{\max}]\times\cdots\times[0,u_m^{\max}] \tag{A.10}$$

and the class $\mathscr{U}$ of *admissible controls* is given by Lebesgue measurable functions $u=(u_1,\dots,u_m)^T$ defined on some interval I with values in U, $u_i: I\to[0,u_i^{\max}]$, $t\mapsto$

$u_i(t)$. In this section, we only consider terminal constraints on the final state $x(T)$ of the system, but once more assume that such constraints have a regular geometric structure and are given in the form $N = \{x \in M : \psi(x) = 0\}$ with $\psi : M \to \mathbb{R}^{n-k}$ a continuously differentiable mapping and the matrix $D\psi$ of the partial derivatives of ψ with respect to x of full rank everywhere on N. We also adjust the functional form of the objective to be consistent with the control-affine structure of the dynamics, i.e., we take the functional to be minimized in the form

$$\mathscr{J}(u) = \int_0^T \left(L(x(s)) + \sum_{i=1}^m \theta_i u_i(s) \right) ds + \varphi(x(T)). \tag{A.11}$$

with $L : M \to \mathbb{R}$, $x \mapsto L(x)$, and $\varphi : N \to \mathbb{R}$, $x \mapsto \varphi(x)$, continuously differentiable functions. The terminal time T can be fixed or free. Not only does this form agree with the general structure of a control-affine control systems, but, more importantly, the integrals $\int_0^T u_i(t)dt$ have an immediate interpretation in terms of the total dose of agents given if the control represents dose rates or the AUC (area under the curve), a commonly used pharmacological quantity, if the controls denote concentrations. Thus these quantities are biomedically meaningful. The optimal control problem is the same as before:

[OC] minimize the objective $\mathscr{J}(u)$ over all admissible controlled trajectories (x,u) subject to the terminal constraint $x(T) \in N$.

A.3.1 Bang-Bang and Singular Controls

For a control-affine system the *Hamiltonian* function H takes the form

$$H = \lambda_0 \left(L(x) + \sum_{i=1}^m \theta_i u_i \right) + \left\langle \lambda,\ f(x) + \sum_{i=1}^m g_i(x) u_i \right\rangle \tag{A.12}$$

and the conditions of the Pontryagin maximum principle reduce to the following statement:

Theorem A.3.1 (Pontryagin Maximum Principle for Control-Affine Systems). *Let (x_*, u_*) be a controlled trajectory for the problem [OC] defined over the interval $[0,T]$. If (x_*, u_*) is optimal, then there exist a constant $\lambda_0 \geq 0$, a multiplier $\nu \in (\mathbb{R}^{n-k})^*$ and a co-vector $\lambda : [0,T] \to (\mathbb{R}^n)^*$ such that the following conditions are satisfied:*

1. Nontriviality *of the multipliers: $(\lambda_0, \lambda(t)) \neq 0$ for all $t \in [0,T]$;*
2. Adjoint equation: *the adjoint variable λ is a solution to the time-varying linear differential equation*

$$\dot{\lambda}(t) = -\lambda_0 \frac{\partial L}{\partial x}(x_*(t)) - \lambda(t) \left(\frac{\partial f}{\partial x}(x_*(t)) + \sum_{i=1}^{m} u_i^*(t) \frac{\partial g_i}{\partial x}(x_*(t)) \right) \tag{A.13}$$

with terminal condition

$$\lambda(T) = \lambda_0 \frac{\partial \varphi}{\partial x}(x_*(T)) + \nu \frac{\partial \psi}{\partial x}(x_*(T)); \tag{A.14}$$

3. Minimum condition: *almost everywhere in* $[0,T]$ *we have that*

$$H(\lambda_0, \lambda(t), x_*(t), u_*(t)) = \min_{v \in U} H(\lambda_0, \lambda(t), x_*(t), v) = \text{const.} \tag{A.15}$$

If the terminal time T is free, the value of this constant is 0.

For this problem, since U is an m-dimensional interval, $U = [0, u_1^{\max}] \times \cdots \times [0, u_m^{\max}]$, the minimum condition splits into m scalar minimization problems that are easily solved. Defining the functions $\Phi_i(t) = \lambda_0 \theta_i + \langle \lambda(t), g_i(x_*(t)) \rangle$, it follows that the optimal controls satisfy

$$u_i^*(t) = \begin{cases} 0 & \text{if } \Phi_i(t) > 0, \\ u_i^{\max} & \text{if } \Phi_i(t) < 0. \end{cases} \tag{A.16}$$

Definition A.3.1 (Switching Function). The function $\Phi_i : [0,T] \to \mathbb{R}$,

$$t \mapsto \Phi_i(t) = \frac{\partial H}{\partial u_i}(\lambda_0, \lambda(t), x_*(t), u_*(t)) = \lambda_0 \theta_i + \langle \lambda(t), g_i(x_*(t)) \rangle, \tag{A.17}$$

is called the switching function corresponding to the control u_i.

A priori, the control u_i is not determined by the minimum condition at times when $\Phi_i(\tau) = 0$. In such a case, all control values trivially satisfy the minimum condition and thus, in principle, all are candidates for optimality. However, the switching functions are absolutely continuous and if the derivative $\dot{\Phi}_i(\tau)$ does not vanish, then the control switches at time τ from $u_i = 0$ to $u_i = u_i^{\max}$ if $\dot{\Phi}_i(\tau)$ is negative and from $u_i = u_i^{\max}$ to $u_i = 0$ if $\dot{\Phi}_i(\tau)$ is positive. Such a time τ is called a bang-bang switch. On the other hand, if $\Phi_i(t)$ were to vanish identically on an open interval I, then, although the minimization property by itself gives no information about the control, in this case also all the derivatives of $\Phi_i(t)$ must vanish and this condition puts strong limitations on the controls. Extremal controls for which the switching function vanishes identically over an open interval I are called *singular* while the constant controls $u_i = 0$ and $u_i = u_i^{\max}$ are called *bang* controls; controls that only switch between 0 and the maximum control values are called *bang-bang controls*. If the control represents dose rates for the application of some therapeutic agent, then bang-bang controls correspond to treatment strategies that switch between maximum dose therapy sessions and rest periods, the typical MTD (maximum tolerated dose) type applications of chemotherapy. Singular controls, on the other hand, correspond to time-varying administrations of the agent at intermediate

and often significantly lower dose rates. There is growing interest in such structures in the medical community because of mounting evidence that "more is not necessarily better" [118, 273] and that a biologically optimal dose (BOD) with the best overall response should be sought. The question whether optimal controls are bang-bang or singular thus has an immediate interpretation and practical relevance for the structure of optimal treatment protocols.

Strictly speaking, to be singular is not a property of the control, but of the extremal lift, since it clearly also depends on the multiplier λ defining the switching function.

Definition A.3.2 (Singular Controls and Extremals). Let Γ be an extremal lift for the problem [OC] consisting of a controlled trajectory (x_*, u_*) defined over the interval $[0,T]$ with corresponding multiplier λ_0 and adjoint vector $\lambda : [0,T] \to (\mathbb{R}^n)^*$. The extremal lift Γ is said to be singular on an open interval $I \subset [0,T]$ if one of the switching functions Φ_i vanishes identically on I. We say the corresponding control u_i^* is singular on I and call the corresponding portion of the trajectory x a singular arc. The extremal lift Γ is said to be totally singular on an open interval $I \subset [0,T]$ if all of the switching functions Φ_i vanish identically on I.

This terminology has its historical origin in the following simple observation: in terms of the Hamiltonian H for problem [OC], the switching functions can be expressed as

$$\Phi_i(t) = \frac{\partial H}{\partial u_i}(\lambda_0, \lambda(t), x_*(t), u_*(t))$$

and thus, formally, the condition $\Phi_i(t) = 0$ is the first-order necessary condition for the Hamiltonian to have a minimum in the interior of the corresponding control interval. For a general optimal control problem, extremal lifts are called singular, respectively nonsingular, over an open interval I if the first-order necessary condition

$$\frac{\partial H}{\partial u}(\lambda_0, \lambda(t), x_*(t), u_*(t)) = 0$$

is satisfied for $t \in I$ and if the matrix of the second-order partial derivatives,

$$\frac{\partial^2 H}{\partial u^2}(\lambda_0, \lambda(t), x_*(t), u_*(t)),$$

is singular, respectively nonsingular, on I. For a control-affine problem [OC], this quantity is always zero, and thus any component u_i of an optimal control that takes values in the interior of the control set is necessarily singular. While the terminology may be a bit misleading, *singular controls* indeed *are often the more natural candidates for optimality* with bang controls only arising where singular controls are inadmissible or simply do not exist.

Bang and singular controls are thus the prime candidates for optimality in optimal control problems for control affine systems. It is clear that the zero sets $\mathscr{Z}_i$ of the switching functions, $\mathscr{Z}_i = \{t \in [0,T] : \ \Phi_i(t) = 0\}$, determine the structures of the optimal controls. Unfortunately, all that can be said about $\mathscr{Z}_i$ in general is

that it is a closed set (e.g., see [292, Proposition 2.8.1]). Even within the general class of control-affine optimal control problems, it is not difficult to construct examples (given by infinitely often differentiable drift and control vector fields) such that starting with an arbitrary (as weird as the reader can or cannot image) locally bounded, Lebesgue measurable control u, this control is the unique solution of the associated time-optimal control problem. No such results exist if the vector fields are real analytic. But also, except for the classical bang-bang theorem for linear systems [292, Theorems 3.4.1 and 3.6.1], no truly general results about regularity properties of optimal controls for analytic nonlinear systems are known either. Even for the models considered in this text, some optimal controls exhibit *chattering* or the so-called Fuller or Zeno phenomenon, i.e., switch infinitely many times on a finite interval. For example, such structures arise when the optimal concentrations of agents follow singular arcs and standard linear pharmacokinetic equations are included in the model (see Section 6.3). Thus, even for control-affine systems, it generally is a highly nontrivial mathematical problem to determine the precise structures of optimal controls.

A.3.2 Lie Brackets and High-Order Necessary Conditions for Optimality of Singular Controls

Optimal controls need to be synthesized from bang and singular controls, and the switching functions contain the information to unlock this structure. In order to study their zero sets, one needs to analyze the derivatives of the switching functions and in these calculations the Lie bracket of vector fields comes up naturally. We only remark that the Lie bracket is a natural generalization of the concept of the directional derivative from functions to vector fields. In fact, the Lie derivative of a function ϕ along a vector field X at a point p, $L_X(\phi)(p)$, is defined as the directional derivative of the function ϕ in the direction of $X(p)$, i.e., $L_X(\phi)(p) = \nabla\phi(p)\cdot X(p)$. This notion then extends in a unique way to arbitrary tensor fields and in this way the Lie bracket $[X,Y]$ can be thought of as a directional derivative of the vector field Y in the direction of X. For the purpose of this text, however, the simple coordinate wise definition given below suffices. We refer the interested reader to any textbook on differential geometry or the more specialized literature on optimal control (e.g., [2, 38, 31, 292]) for an intrinsic geometric set-up.

Definition A.3.3 (Lie Bracket of Vector Fields). Given two continuously differentiable vector fields f and g defined on some open set $G \subset \mathbb{R}^n$, $f,g : G \to \mathbb{R}^n$, their Lie bracket $[f,g]$ is another vector field defined on G by

$$[f,g](x) = Dg(x)f(x) - Df(x)g(x).$$

It is clear that the Lie bracket is anti-commutative, i.e., for all vector fields we have that $[f,g] = -[g,f]$. In addition, for arbitrary vector fields f, g and h, the Lie bracket satisfies the Jacobi identity

$$[f,[g,h]]+[g,[h,f]]+[h,[f,g]]\equiv 0. \tag{A.18}$$

Note that the Jacobi-identity can be re-written in the form

$$[f,[g,h]]=[[f,g],h]+[g,[f,h]]$$

and thus it merely expresses the fact that taking the Lie bracket of f with the product $[g,h]$ obeys the product rule and thus acts like a derivative. This property, which can be verified by a direct computation, is inherited from the definition of the Lie derivative as the directional derivative.

The importance of the Lie bracket in optimal control lies in the following formula for the derivatives of the switching function:

Proposition A.3.1. *Let $x(\cdot)$ be a solution of the dynamics (A.9) for the controls u_i and let λ be a solution of the corresponding adjoint equation (A.13). For any continuously differentiable vector field h, the derivative of the function*

$$\Psi(t)=\langle\lambda(t),h(x(t))\rangle=\lambda(t)h(x(t))$$

is given by

$$\dot{\Psi}(t)=\left\langle\lambda(t),\left[f+\sum_{i=1}^{m}u_i(t)g_i,h\right](x(t))\right\rangle-\lambda_0\left\langle\frac{\partial L}{\partial x}(x(t)),h(x(t))\right\rangle.$$

Proof. This is a direct verification:

$$\begin{aligned}
\dot{\Psi}(t)&=\dot{\lambda}(t)h(x(t))+\lambda(t)Dh(x(t))\dot{x}(t)\\
&=\left(-\lambda_0\frac{\partial L}{\partial x}(x(t))-\lambda(t)\left(Df(x(t))+\sum_{i=1}^{m}u_i(t)Dg_i(x(t))\right)\right)h(x(t))\\
&\quad+\lambda(t)Dh(x(t))\left(f(x(t))+\sum_{i=1}^{m}g_i(x(t))u_i(t)\right)\\
&=\langle\lambda(t),[f,h](x(t))\rangle+\sum_{i=1}^{m}u_i(t)\,\langle\lambda(t),[g_i,h](x(t))\rangle-\lambda_0\frac{\partial L}{\partial x}(x(t))h(x(t))\\
&=\left\langle\lambda(t),\left[f+\sum_{i=1}^{m}u_i(t)g_i,h\right](x(t))\right\rangle-\lambda_0\left\langle\frac{\partial L}{\partial x}(x(t)),h(x(t))\right\rangle.
\end{aligned}$$

□

Generally, singular controls are determined by differentiating the switching functions using the dynamics until the controls explicitly appear and then solving the resulting equations for the controls. Degenerate situations arise when such differentiation never leads to a term that explicitly depends on the control. In such a case, often all controls that otherwise satisfy the constraints of the problem are optimal

and such structures are almost always related to ill-posed problem formulations (e.g., see [317]). But typically, as all the examples analyzed in this text attest to, this procedure works fine. In the multi-input case the procedure may somewhat be hampered by the fact that controls appear that a priori are only known to be measurable and thus the procedure cannot be continued. In such a case, generally various cases that distinguish bang from singular controls needs to be considered (e.g., see Sections 2.2.2 and 2.2.3). The situation is more straightforward for a single-input control-affine system and we demonstrate the procedure for the system

$$\dot{x} = f(x) + g(x)u. \tag{A.19}$$

In this case $[g,g] \equiv 0$ and thus the first derivative of the switching function Φ is given by

$$\dot{\Phi}(t) = \langle \lambda(t), [f,g](x(t)) \rangle - \lambda_0 \left\langle \frac{\partial L}{\partial x}(x(t)), g(x(t)) \right\rangle. \tag{A.20}$$

This formula does not depend on the control and if the vector fields f and g and the Lagrangian L are twice continuously differentiable, we can differentiate $\dot{\Phi}$ once more to get

$$\begin{aligned}\ddot{\Phi}(t) = \langle \lambda(t), [f+ug,[f,g]](x(t)) \rangle - \lambda_0 \left\langle \frac{\partial L}{\partial x}(x(t)), [f,g](x(t)) \right\rangle \\ - \lambda_0 \frac{d}{dt} \left\langle \frac{\partial L}{\partial x}(x(t)), g(x(t)) \right\rangle\end{aligned}$$

$$\begin{aligned}= \langle \lambda(t), [f,[f,g]](x(t)) \rangle - \lambda_0 \left\langle \frac{\partial L}{\partial x}(x(t)), [f,g](x(t)) + Dg(x(t)f(x(t)) \right\rangle \\ - \lambda_0 \left\langle f^T(x(t)) \frac{\partial^2 L}{\partial x^2}(x(t)), g(x(t)) \right\rangle \\ + u(t) \left\{ \langle \lambda(t), [g,[f,g]](x(t)) \rangle - \lambda_0 \left\langle \frac{\partial L}{\partial x}(x(t)), Dg(x(t))g(x(t)) \right\rangle \right. \\ \left. -\lambda_0 \left\langle g(x(t))^T \frac{\partial^2 L}{\partial x^2}(x(t)), g(x(t)) \right\rangle \right\}.\end{aligned}$$

These formulas becoming increasingly more complex because of the derivatives of the terms multiplying λ_0, but the control u only appears linearly. Hence, if the term multiplying u is nonzero, the equation $\ddot{\Phi}(t) = 0$ formally can be solved for u and the result determines the singular control. But note that this formula depends on the state and the multipliers λ_0 and λ, i.e., on the extremal lift. In differential-geometric terms, it defines the singular control in the cotangent bundle, not as a feedback function in the state space. Naturally, the formula also in no way guarantees that the control bounds imposed by $u \in U$ are satisfied and generally whether a singular control is admissible needs to be verified on a case-by-case basis.

Formally, since $\Phi = \frac{\partial H}{\partial u}$, the term multiplying the control can be expressed as

$$\frac{\partial}{\partial u}\frac{d^2}{dt^2}\frac{\partial H}{\partial u}(\lambda_0, \lambda(t), x_*(t), u_*(t))$$

with the understanding that the outer derivative with respect to the control is taken ignoring the time-dependence in the derivative. Because of the anti-commutativity of the Lie bracket, the control cannot appear in the first derivative of the switching function and, in fact, in various situations, because of Lie-algebraic properties, the control can only occur for the first time in an even numbered derivative. This has led to the following definitions.

Definition A.3.4 (Order 1 Singular Control). Let Γ be a singular extremal lift for the problem [OC] consisting of a controlled trajectory (x_*, u_*) with corresponding multiplier λ_0 and adjoint vector λ. The control u_* is said to be of order 1 on an open interval I if

$$\frac{\partial}{\partial u}\frac{d^2}{dt^2}\frac{\partial H}{\partial u}(\lambda_0, \lambda(t), x_*(t), u_*(t))$$

does not vanish on I.

Definition A.3.5 (Higher-Order Singular Control). Let Γ be a singular extremal lift for the problem [OC] consisting of a controlled trajectory (x_*, u_*) with corresponding multiplier λ_0 and adjoint vector λ. The singular control is said to be of *intrinsic order k* over an open interval I if the first $2k-1$ derivatives of the switching function vanish identically and

$$\frac{\partial}{\partial u}\frac{d^{2k}}{dt^{2k}}\frac{\partial H}{\partial u}(\lambda_0, \lambda(t), x_*(t), u_*(t))$$

does not vanish on I.

Singular controls arise from the extremality conditions of the maximum principle when the minimization condition is satisfied trivially because $\frac{\partial H}{\partial u} = 0$. However, this condition does not distinguish between minimization and maximization and thus singular controls can be both minimizing or maximizing. It is the sign of the quantity $\frac{\partial}{\partial u}\frac{d^{2k}}{dt^{2k}}\frac{\partial H}{\partial u}(\lambda_0, \lambda(t), x_*(t), u_*(t))$ that distinguishes between these two cases and the following high-order necessary condition for optimality, the so-called generalized Legendre-Clebsch condition, holds.

Theorem A.3.2 (Generalized Legendre–Clebsch Condition). *Let Γ be a singular extremal lift for the problem [OC] consisting of a controlled trajectory (x_*, u_*) with corresponding multiplier λ_0 and adjoint vector $\lambda : [0,T] \to (\mathbb{R}^n)^*$. If the controlled trajectory (x_*, u_*) is optimal and the control u_* is singular of intrinsic order k over an open interval $I \subset [0,T]$, then*

$$(-1)^k \frac{\partial}{\partial u}\frac{d^{2k}}{dt^{2k}}\frac{\partial H}{\partial u}(\lambda_0, \lambda(t), x_*(t), u_*(t)) \geq 0 \quad \text{for all} \quad t \in I. \tag{A.21}$$

We say the Legendre-Clebsch condition for minimality of a singular control of order k is satisfied if equation (A.21) holds. If this quantity is positive, we say the *strengthened Legendre-Clebsch condition* holds.

A.3.3 Concatenations Between Optimal Bang and Singular Arcs

The order of a singular control is of importance when it comes to possible concatenations between singular and bang controls. In fact, for order 1 singular controls such concatenations are always locally optimal while they are never optimal for order 2 singular controls. These results will be used frequently in our text and we include this simple classical reasoning. We write *BS* for a concatenation of a trajectory corresponding to one of the constant controls $u = 0$ or $u = u_{\max}$ with a singular arc; i.e., for some $\varepsilon > 0$ the control is given by

$$u(t) = \begin{cases} 0 \text{ or } u_{\max} & \text{for} \quad t \in (\tau - \varepsilon, \tau), \\ u_{\text{sing}}(t) & \text{for} \quad t \in [\tau, \tau + \varepsilon). \end{cases}$$

Concatenations of the type *SB* are defined similarly. The time τ is called a *junction* time and $x(\tau)$ a junction (point).

Proposition A.3.2. *Let Γ be a singular extremal lift for the problem [OC] consisting of a controlled trajectory (x_*, u_*) with corresponding multiplier λ_0 and adjoint vector λ. Suppose the control u_* is singular of order 1 on an open interval I, takes values in the open interval $(0, u_{\max})$, and the strengthened Legendre-Clebsch condition is satisfied. Then, at every time $\tau \in I$, there exists an $\varepsilon > 0$ such that any concatenation of the singular control with a bang control $u = 0$ or $u = u_{\max}$ at time τ satisfies the necessary conditions of the maximum principle; i.e., concatenations of the types BS and SB are allowed.*

Proof. The singular control u_{sing} is defined by solving the equation $\ddot{\Phi}(t) = 0$ and is a continuous function. So trivially are the constant bang controls and thus the limits of the second derivative of the switching function at time τ are continuous from the left $(-)$ or right $(+)$ and have the form

$$\ddot{\Phi}(\tau_\pm) = \Theta(\tau_\pm) + u(\tau_\pm) \frac{\partial}{\partial u} \frac{d^2}{dt^2} \frac{\partial H}{\partial u}(\lambda_0, \lambda(t), x_*(t), u_*(t))$$

with Θ denoting the expression in $\ddot{\Phi}$ that does not multiply the control. The second derivative $\ddot{\Phi}$ vanishes identically along the singular control and since the strengthened Legendre-Clebsch condition is satisfied, we have that

$$\frac{\partial}{\partial u} \frac{d^2}{dt^2} \frac{\partial H}{\partial u}(\lambda_0, \lambda(t), x_*(t), u_*(t)) < 0.$$

Hence $\Theta(t)$ is positive along the singular control. Since $u_{\text{sing}}(\tau_\pm) > 0$, we also have that $\Theta(\tau_\pm) > 0$. If we switch to the constant control $u \equiv 0$, then it follows that

$$\ddot{\Phi}(\tau_\pm) = \Theta(\tau_\pm) > \Theta(\tau_\pm) + u_{\text{sing}}(\tau_\pm)\frac{\partial}{\partial u}\frac{d^2}{dt^2}\frac{\partial H}{\partial u}(\lambda_0, \lambda(t), x_*(t), u_*(t)) = 0$$

and for $u = u_{\max}$ we obtain

$$\begin{aligned}\ddot{\Phi}(\tau_\pm) &= \Theta(\tau_\pm) + u_{\max}\frac{\partial}{\partial u}\frac{d^{2k}}{dt^{2k}}\frac{\partial H}{\partial u}(\lambda_0, \lambda(t), x_*(t), u_*(t)) \\ &< \Theta(\tau_\pm) + u_{\text{sing}}(\tau_\pm)\frac{\partial}{\partial u}\frac{d^2}{dt^2}\frac{\partial H}{\partial u}(\lambda_0, \lambda(t), x_*(t), u_*(t)) = 0.\end{aligned}$$

In each case, these signs are consistent with both entry and exit from the singular arc, i.e., for example, if $u = 0$ on an interval $(\tau - \varepsilon, \tau)$, then the switching function has a local minimum at time $t = \tau$ with minimum value 0 and thus Φ is positive over this interval. This is consistent with the minimum condition of the maximum principle. □

Proposition A.3.3. *Let Γ be a singular extremal lift for the problem [OC] consisting of a controlled trajectory (x_*, u_*) with corresponding multiplier λ_0 and adjoint vector λ. Suppose the control u_* is singular of order 2 on an open interval I, takes values in the open interval $(0, u_{\max})$ and the strengthened Legendre-Clebsch condition is satisfied. Then, at no time $\tau \in I$ can the control u be concatenated with the bang controls $u = 0$ or $u = u_{\max}$. Concatenations of the types BS and SB violate the conditions of the maximum principle and are not optimal.*

Proof. The computations are analogous to the ones in the proof of Proposition A.3.2 and, without loss of generality, we consider the case when the control is singular over the interval $(\tau - \varepsilon, \tau)$ and is given by $u = 0$ over the interval $(\tau, \tau + \varepsilon)$. Since the singular control is of order 2, the first three derivatives of the switching function do not depend on the control and all vanish identically. Thus the fourth derivative takes the form

$$\Phi^{(4)}(t) = \Theta(t) + u(t)\frac{\partial}{\partial u}\frac{d^4}{dt^4}\frac{\partial H}{\partial u}(\lambda_0, \lambda(t), x_*(t), u_*(t))$$

with Θ again denoting the term that does not depend on the control. Here we have that $\frac{\partial}{\partial u}\frac{d^4}{dt^4}\frac{\partial H}{\partial u}(\lambda_0, \lambda(t), x_*(t), u_*(t)) > 0$ and thus $\Theta(t)$ is negative along the singular arc giving $\Theta(\tau_\pm) < 0$. Hence the fourth derivative of Φ at τ from the right is given by $\Phi^{(4)}(\tau) = \Theta(\tau_\pm) < 0$. Thus the switching function Φ has a local maximum for $t = \tau$ and is negative over the interval $(\tau, \tau + \varepsilon)$. But then the minimization property of the Hamiltonian implies that the control must be $u = u_{\max}$. The analogous contradiction arises for all concatenations of the type *SB* or *BS*. □

This result implies that an optimal singular control of order 2 cannot be concatenated with a bang control. In fact, an optimal control needs to switch infinitely many times between the bang controls $u = 0$ and $u = u_{\max}$ on any interval $(\tau, \tau \pm \varepsilon)$ if a

singular junction occurs at time τ. Corresponding trajectories are called *chattering arcs* and they indeed arise in optimal solutions. Also for the biomedical problems considered here for some initial conditions such structures become optimal once pharmacokinetic models are included in the equations.

A.3.4 The Goh Condition for Multi-Input Systems

The Goh condition is a specific necessary condition for optimality when more than one component of the control vector is singular. It follows from Proposition A.3.1 that the first derivatives of the switching function are given by

$$\dot{\Phi}_i(t) = \langle \lambda(t),\, [f,g_i](x(t))\rangle + \sum_{j\neq i} u_j(t)\left\langle \lambda(t),\, [g_j,g_i](x(t))\right\rangle \\ -\lambda_0\left\langle \frac{\partial L}{\partial x}(x(t)), g(x(t))\right\rangle .$$

In contrast to the single-input case, now the derivative $\dot{\Phi}_i$ depends on the controls; on the controls other than u_i, that is. The differentiability properties of these controls thus determine whether further derivatives can be computed. Clearly, there is no problem when controls are constant. If more than one component is singular at the same time, the following result, the so-called *Goh condition*, implies that these terms drop out from the computation.

Theorem A.3.3 (Goh Condition). *Let Γ be a singular extremal lift for the problem [OC] consisting of a controlled trajectory (x_*,u_*) with corresponding multiplier λ_0 and adjoint vector $\lambda : [0,T] \to (\mathbb{R}^n)^*$. If the controlled trajectory (x_*,u_*) is optimal and the controls u_i and u_j are simultaneously singular over an open interval I, then*

$$\left\langle \lambda(t),\, [g_i,g_j](x(t))\right\rangle \equiv 0 \quad \text{for all} \quad t \in I.$$

A.4 Sufficient Conditions for Optimality

The results discussed so far are only necessary conditions for optimality and do not guarantee that a controlled trajectory that satisfies them is optimal. The theory of sufficient conditions for optimality is more intricate. Essentially, to guarantee local optimality properties, it becomes necessary to embed a reference extremal (i.e., the controlled trajectory together with an associated multiplier) into a family of extremals in such a way that the controlled trajectories cover a neighborhood of the reference controlled trajectory. If this can be done globally in the form of what is called a *regular synthesis*, then the associated controls all are globally optimal. These concepts are related to classical ideas from the calculus of variations about fields of

extremals or, in a more modern language, to dynamic programming and solutions of the Hamilton-Jacobi-Bellman equations. We outline the main ideas and results for the optimal control problem [OC] in the formulation given in Section A.2.1.

A.4.1 The Hamilton-Jacobi-Bellman Equation and Value Function of an Optimal Control Problem

The key idea in studying sufficient conditions for optimality is to consider the value V of the optimal control problem as a function of variable initial conditions. In this context, it is customary and more convenient, although somewhat ambiguous, to denote the initial time by t and the initial value by x so that the value function is defined as

$$V(t,x) = \inf_{u \in \mathscr{U}} \mathscr{J}(u;t,x),$$

where the infimum is taken over all admissible controls $u \in \mathscr{U}$ whose corresponding trajectories start at the point x at time t and satisfy all other requirements of the optimal control problem. Essentially, the approach is to consider the optimal control problem for all possible initial conditions and determine the best possible action at time t if the state of the system is given by x. Note that, although the dynamics for the optimal control problem [OC] is time-invariant, the value function will depend on t if our problem formulation includes the terminal time T, either as a finite predetermined therapy horizon or through the penalty term $\varphi = \varphi(T, x(T))$. Intuitively, if the therapy horizon is specified, clearly it will matter how close to the end of the interval the current state of the system is. It is not difficult to see—and this is known as Bellman's *dynamic programming principle* (e.g., see [292, Proposition 5.1.1])—that, if the function V is differentiable at (t,x) with gradient $(\frac{\partial V}{\partial t}(t,x), \frac{\partial V}{\partial x}(t,x))$, then for all $u \in U$ the following inequality is satisfied:

$$\frac{\partial V}{\partial t}(t,x) + \frac{\partial V}{\partial x}(t,x) f(x,u) + L(x,u) \geq 0.$$

Furthermore, if u_* is an optimal control for the initial condition (t,x) which is continuous at the initial time t, then equality holds for $u = u_*(t)$. In this case the value V satisfies the so-called **Hamilton-Jacobi-Bellman** equation:

$$\frac{\partial V}{\partial t}(t,x) + \min_{u \in U} \left\{ \frac{\partial V}{\partial x}(t,x) f(x,u) + L(x,u) \right\} \equiv 0. \tag{A.22}$$

This is a first-order linear partial differential equation coupled with the optimal control u_* through the minimum condition. Generally, if it is possible to carry out this minimization and write the minimizer as a function of t, x, and $\frac{\partial V}{\partial x}(t,x)$, a highly nonlinear PDE results.

The importance of this equation lies in its significance as a sufficient condition for optimality. Indeed, if the pair (V, u_*) is a solution to this equation (in the sense

that V is a continuously differentiable function and $u_* = u_*(t,x)$ is an admissible control for which the minimum is realized), then u_* is an optimal control.

Definition A.4.1 (Admissible Feedback Controls). Let G be a region in the (t,x)-space. We call a feedback control $u : G \to U$, $(t,x) \mapsto u(t,x)$, admissible (on G) for the control problem $[OC]$ if for every initial condition $(t,x) \in G$ the initial value problem

$$\dot{\xi} = f(\xi, u(s,\xi)), \quad \xi(t) = x, \tag{A.23}$$

has a unique solution $\xi : [t,T] \to \mathbb{R}^n$ (forward in time) for which the corresponding open-loop control $\eta : [t,T] \to U$, $\eta(s) = u(s,\xi(s))$, lie in the class $\mathscr{U}$ of admissible controls.

If the feedback control u is smooth enough (e.g., continuous and Lipschitz in x), standard results on ODE's guarantee the existence and uniqueness of solutions to the initial value problem (A.23). However, in the presence of control constraints optimal feedbacks rarely are continuous and standard theory of ODEs is not potent enough to clarify the existence of solutions for piecewise continuous feedback functions. Rather than entering into the intricacies of when solutions to ordinary differential equations with discontinuous right-hand sides exist, we simply require the existence and uniqueness of solutions to (A.23) while, at the same time, demanding that the open-loop control that would give rise to this controlled trajectory is admissible. This will be satisfied for all the problems considered in this text.

Definition A.4.2 (Classical Solution to the Hamilton-Jacobi-Bellman Equation). Let G be a region in the (t,x)-space that contains the terminal manifold N in its boundary. We say the pair (V,u_*) is a classical solution to the Hamilton-Jacobi-Bellman equation for problem [OC] on G if *(i)* $V : G \to \mathbb{R}$ is continuously differentiable on G and extends continuously onto N, *(ii)* u_* is an admissible feedback control, *(iii)* we have

$$\frac{\partial V}{\partial t}(t,x) + \min_{u \in U} \left\{ \frac{\partial V}{\partial x}(t,x) f(x,u) + L(x,u) \right\} \equiv 0$$

with equality holding for the feedback control u_*, and *(iv)* the boundary condition $V(t,x) = \varphi(t,x)$ holds for all $(t,x) \in N$.

Theorem A.4.1. *If (V,u_*) is a classical solution to the Hamilton-Jacobi-Bellman equation on G, then the control u_* is optimal with respect to any other admissible control η for which the graph of the corresponding controlled trajectory ξ lies in G and V is the corresponding minimal value when taken over this class of controls. In particular, if a classical solution (V,u_*) exists on the full space, then u_* is an optimal control and V is the value function for the problem.*

Proof. Let $\eta : [t,T] \to U$ be any admissible control for initial condition $(t,x) \in G$ with corresponding trajectory ξ. By assumption, the graph of ξ lies in G for $s \in [t,T)$ and the function V is differentiable along the graph of ξ. Since ξ is an absolutely continuous curve, we have a.e. on $[t,T)$ that

$$\frac{d}{ds}V(s,\xi(s)) = \frac{\partial V}{\partial t}(s,\xi(s)) + \frac{\partial V}{\partial x}(s,\xi(s))f(s,\xi(s),\eta(s))$$

It thus follows from the Hamilton-Jacobi-Bellman equation that

$$\frac{d}{ds}V(s,\xi(s)) \geq -L(s,\xi(s),\eta(s)).$$

Integrating this inequality from t to some time $T-\varepsilon$ and then taking the limit as $\varepsilon \to 0$ therefore yields

$$V(T,\xi(T)) - V(t,x) \geq -\int_t^T L(s,\xi(s),\eta(s))ds.$$

The boundary condition for V demands that $V(T,\xi(T)) = \varphi(T,\xi(T))$ and thus it follows that

$$V(t,x) \leq \int_t^T L(s,\xi(s),\eta(s))ds + \varphi(T,\xi(T)) = \mathscr{J}(\eta;t,x).$$

Furthermore, for the control η_*, $\eta_*(s) = u_*(s,\xi_*(s))$, we have equality and thus $V(t,x) = \mathscr{J}(\eta_*;t,x)$. Hence V is the value function, $V(t,x) = \min_{\eta\in\mathscr{U}_{(t,x)}} \mathscr{J}(\eta;t,x)$. This proves the theorem. □

The solution of optimal control problems is thus closely related to finding solutions to the Hamilton-Jacobi-Bellman equation (A.22). It is the coupling of two aspects, first-order PDE and optimization problem, that makes this a challenge. As already mentioned, one possible approach is to try and solve the minimization problem for u and 'define' the control as a 'function' of the state and the gradient $\frac{\partial V}{\partial x}$, $u = u(t,x,\frac{\partial V}{\partial x})$, and then substitute the resulting relation into the partial differential equation. But there exist serious obstacles to this procedure: the minimum may not be unique and even if it is, (e.g., if the Hamiltonian of the associated control problem is strictly convex in u), then the resulting PDE typically becomes highly nonlinear and difficult to solve. In special cases, such as the linear-quadratic regulator in control theory (e.g., see [292, Example 5.1.1]) this procedure works to perfection and gives an explicit solution, but generally—and in particular for the problems considered in this text—this is not possible. An alternative procedure, that has its origin in the classical ideas of fields of extremals in the calculus of variations, is to construct a solution of the HJB-equation by adapting the *method of characteristics*, the standard procedure of solving first-order PDEs, to the optimal control problem. This also establishes the connections between necessary and sufficient conditions for optimality: the characteristic equations are given by the dynamics in the state-space and the adjoint equations on the multipliers. It is this procedure that we employ throughout this text. We briefly outline the main ideas below, but refer the reader to Chapters 5 and 6 of our text [292] for the mathematical details.

A.4.2 The Method of Characteristics

The key idea is to parameterize extremals by integrating the system and adjoint equation backward from the terminal manifold while maintaining the minimum condition of the maximum principle and then to investigate the mapping properties of the corresponding family of controlled trajectories. If the associated flow of controlled trajectories is one-to-one, then the objective evaluated along this family of trajectories, also sometimes called the *cost-to-go function*, will give rise to the desired solution of the Hamilton-Jacobi-Bellman equation. The construction itself clearly brings out the relationships between the necessary conditions of the maximum principle, Theorem A.2.1, and the dynamic programming principle, Theorem A.4.1.

For a typical control-affine optimal control problem with a bounded control set, as they are considered in this text, separate "patches" consisting of controlled extremals corresponding to smooth controls (e.g., the individual segments when a bang-bang control is constant or portions when the control is given by a differentiable singular control) need to be glued together to obtain the full solution. We first formalize the mathematical conditions for one such patch. Essential to the construction is some degree of smoothness on the parameter p that determines the family of controlled extremals.

Definition A.4.3 (C^r-Parameterized Family of Controlled Trajectories). Given an open subset P of $\mathbb{R}^d$ with $0 \le d \le n$, let

$$t_- : P \to \mathbb{R},\ p \mapsto t_-(p), \qquad \text{and} \qquad t_+ : P \to \mathbb{R},\ p \mapsto t_+(p),$$

be two r-times continuously differentiable functions, $t_\pm \in C^r(P)$, that satisfy $t_-(p) < t_+(p)$ for all $p \in P$. We call t_- and t_+ the initial and terminal times of the parametrization and define its domain as

$$D = \{(t,p) : p \in P, t_-(p) \le t \le t_+(p)\}.$$

Let $\xi_- : P \to \mathbb{R}^n$, $p \mapsto \xi_-(p)$, and $\xi_+ : P \to \mathbb{R}^n$, $p \mapsto \xi_+(p)$, be r-times continuously differentiable functions, $\xi_\pm \in C^r(P)$. A d-dimensional C^r-parameterized family $\mathscr{T}$ of controlled trajectories with domain D, initial conditions ξ_- and terminal conditions ξ_+ consists of:

1. admissible controls, $u : D \to U$, $(t,p) \mapsto u(t,p)$, that are continuous on D, r-times continuously differentiable in p on the interior of D with these partial derivatives extending continuously onto D, $(u \in C^{0,r}(D))$,
2. and corresponding trajectories $x : D \to \mathbb{R}^n$, $(t,p) \mapsto x(t,p)$, i.e., solutions of the dynamics
$$\dot{x}(t,p) = f(x(t,p),u(t,p)), \tag{A.24}$$
that exist over the full interval $[t_-(p),t_+(p)]$ and satisfy the initial condition $x(t_-(p),p) = \xi_-(p)$ and terminal condition $x(t_+(p),p) = \xi_+(p)$.

We shall be considering both time-dependent and time-independent formulations and always wish to separate between the time t and the state x in our notation (Figure A.1). For example, a time-dependent formulation arises if a fixed therapy horizon is considered (e.g., the models from Chapters 2 and 3) while time-independent formulations arise when the optimal administration of an a priori given amount of

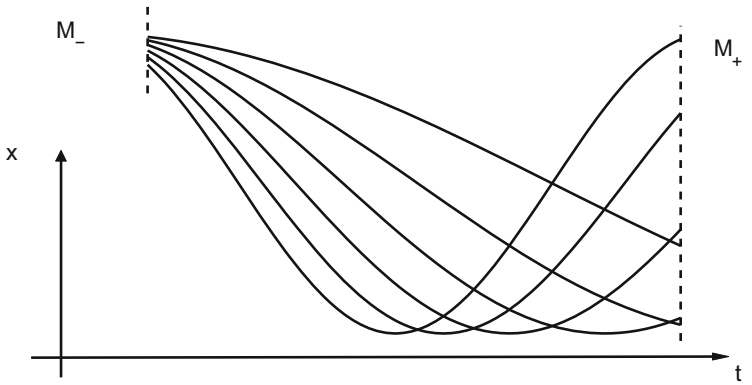

Fig. A.1 A parameterized family of controlled trajectories

agents is considered (e.g., see Chapter 5). It is convenient, however, to have a common notation for the associated flows.

Definition A.4.4 (Flow of Controlled Trajectories). Let $\mathscr{T}$ be a C^r-parameterized family of controlled trajectories. For a time-dependent optimal control problem, we define the associated flow as the map

$$F : D \to \mathbb{R} \times \mathbb{R}^n, \quad (t,p) \longmapsto F(t,p) = \begin{pmatrix} t \\ x(t,p) \end{pmatrix},$$

i.e., in terms of the graphs of the corresponding trajectories. For a time-independent optimal control problem, we define the associated flow as the flow of the trajectories,

$$F : D \to \mathbb{R}^n, \quad (t,p) \longmapsto F(t,p) = x(t,p).$$

We say the flow F is a $C^{1,r}$-mapping on some open set $Q \subset D$ if the restriction of F to Q is continuously differentiable in (t,p) and r times differentiable in p with derivatives that are jointly continuous in (t,p). If $F \in C^{1,r}(Q)$ is injective and the Jacobian matrix $DF(t,p)$ is nonsingular everywhere on Q, then we say F is a $C^{1,r}$-diffeomorphism onto its image $F(Q)$.

The boundary sections

$$M_- = \{(t,p) : \ p \in P,\ t = t_-(p)\} \qquad \text{and} \qquad M_+ = \{(t,p) : \ p \in P,\ t = t_+(p)\}$$

of a C^r-parameterized family of controlled trajectories are the graphs of the functions t_- and t_+, $M_- = \mathfrak{gr}(t_-)$ and $M_+ = \mathfrak{gr}(t_+)$. We call the images of these sections under the flow F, $N_\pm = F(M_\pm)$, the *source*, respectively the *target* of the parametrization. Thus

$$N_\pm = \{(t,x) : t = t_\pm(p),\ x = \xi_\pm(p), \quad p \in P\},$$

in the time-dependent case and

$$N_\pm = \{x : x = \xi_\pm(p),\ p \in P\}$$

for a time-independent problem. In the constructions, generally one of these is specified and the trajectories are defined as the solutions of the associated initial (or terminal) value problem. The other then simply is defined by the flow of these solutions. It is useful to be able to consider both the cases when trajectories are integrated forward in time (families of controlled trajectories with source N_-) and backward in time (families of controlled trajectories with target N_+).

Definition A.4.5 (C^r-Parameterized Family of Controlled Trajectories with Cost γ). Suppose $\mathscr{T}$ is a d-dimensional C^r-parameterized family $\mathscr{T}$ of controlled trajectories with domain D and initial and terminal values ξ_- and ξ_+. Given an r-times continuously differentiable function $\gamma_- : P \to \mathbb{R}$, $p \mapsto \gamma_-(p)$, (respectively, $\gamma_+ : P \to \mathbb{R}$, $p \mapsto \gamma_+(p)$,) we define the cost or cost-to-go function associated with $\mathscr{T}$ as

$$C(t,p) = \gamma_-(p) - \int_{t_-(p)}^{t} L(x(s,p),u(s,p))\,ds,$$

(respectively, as

$$C(t,p) = \int_{t}^{t_+(p)} L(s,x(s,p),u(s,p))\,ds + \gamma_+(p),$$

when the terminal value is specified) and call $\mathscr{T}$ a C^r-parameterized family of controlled trajectories with cost γ.

The functions γ_+ and γ_- propagate the cost along trajectories from patch to patch and $C(t,p)$ represents the value of the objective for the control $u = u(\cdot,p)$ if the initial condition at time t is given by $x(t,p)$. This specification is equally valid for a time-dependent or time-independent problem. Since the value of the optimal cost on the terminal manifold N is specified by the penalty term φ in the objective, integrating trajectories backward in time is the typical procedure. For syntheses where trajectories can be successively integrated backward from the terminal manifold, these functions are easily computed.

Definition A.4.6 (C^r-Parameterized Family of Extremals). As before, let P be an open subset of $\mathbb{R}^d$, $0 \le d \le n$, and let t_- and t_+, $t_\pm \in C^r(P)$, be the initial and terminal times for the parametrization and let $D = \{(t,p) : p \in P, t_-(p) \le t \le t_+(p)\}$. A d-dimensional C^r-parameterized family $\mathscr{E}$ of extremals (or extremal lifts) with domain D consists of

1. a C^r-parameterized family $\mathscr{T}$ of controlled trajectories (x,u) with domain D, initial and terminal conditions ξ_- and ξ_+, and cost γ_- (respectively, γ_+):

$$\dot{x}(t,p) = f(x(t,p),u(t,p)), \qquad x(t_\pm(p),p) = \xi_\pm(p);$$

2. a nonnegative multiplier $\lambda_0 \in C^{r-1}(P)$ and co-state $\lambda : D \to (\mathbb{R}^n)^*$, $\lambda = \lambda(t,p)$, so that $(\lambda_0(p),\lambda(t,p)) \neq (0,0)$ for all $(t,p) \in D$ and the adjoint equation

$$\dot{\lambda}(t,p) = -\lambda_0(p)\frac{\partial L}{\partial x}(x(t,p),u(t,p)) - \lambda(t,p)\frac{\partial f}{\partial x}(x(t,p),u(t,p)),$$

is satisfied on the interval $[\tau_-(p),\tau_+(p)]$ with boundary condition $\lambda_-(p) = \lambda(\tau_-(p),p)$ (respectively, $\lambda_+(p) = \lambda(\tau_+(p),p)$) given by an $(r-1)$-times continuously differentiable function of p,

such that the following conditions are satisfied:

3. defining $h(t,p) = H(\lambda_0(p),\lambda(t,p),x(t,p),u(t,p))$, the controls $u = u(t,p)$ solve the minimization problem

$$h(t,p) = \min_{v\in U} H(\lambda_0(p),\lambda(t,p),x(t,p),v);$$

4 (a). with $h_\pm(p) = h(t_\pm(p),p))$, the following transversality condition holds at the source (respectively, target)

$$\lambda_\pm(p)\frac{\partial \xi_\pm}{\partial p}(p) = \lambda_0(p)\frac{\partial \gamma_\pm}{\partial p}(p) + h_\pm(p)\frac{\partial t_\pm}{\partial p}(p); \tag{A.25}$$

4 (b). if the target N_+ is a part of the terminal manifold N, $N_+ \subset N$, then setting $T(p) = t_+(p)$, with $\xi_+(p) = x(T(p),p)$ we have that $\gamma_+(p) = \varphi(T(p),\xi_+(p))$; furthermore, there exists an $(r-1)$-times continuously differentiable multiplier $\nu : P \to \left(\mathbb{R}^{n+1-k}\right)^*$ so that the following transversality conditions are satisfied:

$$\lambda(T(p),p) = \lambda_0(p)\frac{\partial \varphi}{\partial x}(T(p),\xi_+(p)) + \nu(p)\frac{\partial \Psi}{\partial x}(T(p),\xi_+(p)), \tag{A.26}$$

$$-h(T(p),p) = \lambda_0(p)\frac{\partial \varphi}{\partial t}(T(p),\xi_+(p)) + \nu(p)\frac{\partial \Psi}{\partial t}(T(p),\xi_+(p)). \tag{A.27}$$

This definition merely formalizes that all controlled trajectories in the family $\mathscr{E}$ satisfy the conditions of the maximum principle while some smoothness properties are satisfied by the parametrization and natural geometric regularity assumptions are made at the terminal manifold N. It is not assumed that the parametrization $\mathscr{E}$ of extremals covers the state-space injectively. The degree r in the definition denotes the smoothness of the parametrization of the controls in the parameter p, $u \in C^{0,r}$, and it implies that $x \in C^{1,r}$. The condition $\lambda \in C^{1,r-1}$ is ensured by requiring that the multipliers λ_0 and the boundary values $\lambda_\pm(p)$, respectively ν, are

$(r-1)$-times continuously differentiable. In particular, for a C^1-parameterized family of extremals only continuity in p is required. If the data defining the problem $[OC]$ possess an additional degree of differentiability in x and if the multiplier λ_0 and the function $\lambda_\pm(p)$ are r-times continuously differentiable with respect to p, then it follows that $\lambda(t,p) \in C^{1,r}$ as well. In particular, this is true if $r=\infty$ or $r=\omega$ as it will be the case in all problems considered in this text. In such a case, we call $\mathscr{E}$ a *nicely* C^r-parameterized family of extremals (e.g., see Chapter 4). Also, if $\lambda_0(p) > 0$ for all $p \in P$, then all extremals are normal and by diving by $\lambda_0(p)$ we may assume that $\lambda_0(p) \equiv 1$ and we call such a family *normal*.

The transversality condition (A.25) ensures the proper relationship between the multiplier λ and the cost γ. Essentially, this condition is the propagation of the transversality condition (A.14) of Theorem A.3.1 from the terminal constraint along the parameterized family of extremals.

Lemma A.4.1 ([292, Lemma 5.2.1 and Corollary 5.2.1]). *For the optimal control problem $[OC]$, if the target N_+ is a part of the terminal manifold N, $N_+ \subset N$, then condition (A.25) follows from the transversality conditions of the maximum principle. Furthermore, given any continuously differentiable function $\tau : P \to \mathbb{R}$, $p \mapsto \tau(p)$, that satisfies $t_-(p) \le \tau(p) \le t_+(p)$, and defining $\xi(p) = x(\tau(p),p)$, $\gamma(p) = C(\tau(p),p)$, $\lambda(p) = \lambda(\tau(p),p)$ and $h(p) = h(\tau(p),p))$, we have that*

$$\lambda(p)\frac{\partial \xi}{\partial p}(p) = \lambda_0(p)\frac{\partial \gamma}{\partial p}(p) + h(p)\frac{\partial \tau}{\partial p}(p).$$

In particular, the transversality condition (A.25) propagates between source and target.

The following result establishes the key technical relation in making the transition from necessary to sufficient conditions for optimality.

Lemma A.4.2 (Shadow-Price Lemma [292, Lemma 5.2.2]). *Let $\mathscr{E}$ be a C^1-parameterized family of extremal lifts with domain D. Then for all $(t,p) \in D$ we have that*

$$\lambda_0(p)\frac{\partial C}{\partial p}(t,p) = \lambda(t,p)\frac{\partial x}{\partial p}(t,p). \tag{A.28}$$

If the parameterized family of extremals is normal and if the corresponding family of trajectories covers a region G injectively, then the Shadow-Price lemma implies that the associated cost-to-go function gives rise to a classical solution to the Hamilton-Jacobi-Bellman equation on G. Without loss of generality, we consider the time-dependent formulation, i.e., the flow F is given by $F(t,p) = (t, x(t,p))$.

Theorem A.4.2 ([292, Theorem 5.2.1]). *Let $\mathscr{E}$ be a C^r-parameterized family of normal extremals for a time-dependent optimal control problem and suppose the restriction of its flow F to some open set $Q \subset D$ is a $C^{1,r}$-diffeomorphism onto an*

open subset $G \subset \mathbb{R} \times \mathbb{R}^n$ of the (t,x)-space. Then the value $V^{\mathscr{E}}$ of the parameterized family $\mathscr{E}$ defined by

$$V^{\mathscr{E}} : G \to \mathbb{R}, \quad V^{\mathscr{E}} = C \circ F^{-1},$$

is continuously differentiable in (t,x) and r-times continuously differentiable in x for fixed t. The function

$$u_* : G \to \mathbb{R}, \quad u_* = u \circ F^{-1},$$

is an admissible feedback control that is continuous and r-times continuously differentiable in x for fixed t. Together, the pair $(V^{\mathscr{E}}, u_*)$ is a classical solution of the Hamilton-Jacobi-Bellman equation

$$\frac{\partial V}{\partial t}(t,x) + \min_{u \in U} \left\{ \frac{\partial V}{\partial x}(t,x) f(x,u) + L(x,u) \right\} \equiv 0$$

on G. Furthermore, the following identities hold in the parameter space on Q:

$$\frac{\partial V^{\mathscr{E}}}{\partial t}(t,x(t,p)) = -H(\lambda(t,p), x(t,p), u(t,p)), \tag{A.29}$$

$$\frac{\partial V^{\mathscr{E}}}{\partial x}(t,x(t,p)) = \lambda(t,p). \tag{A.30}$$

If $\mathscr{E}$ is nicely C^r-parameterized, then $V^{\mathscr{E}}$ is $(r+1)$-times continuously differentiable in x on G and we also have that

$$\frac{\partial^2 V^{\mathscr{E}}}{\partial x^2}(t,x(t,p)) = \frac{\partial \lambda^T}{\partial p}(t,p) \left(\frac{\partial x}{\partial p}(t,p) \right)^{-1}. \tag{A.31}$$

Outline. The identity $C = V^{\mathscr{E}} \circ F$ gives that

$$\frac{\partial C}{\partial p}(t,p) = \frac{\partial V^{\mathscr{E}}}{\partial x}(t,x(t,p)) \frac{\partial x}{\partial p}(t,p).$$

In view of Lemma A.4.2 and the fact that $\frac{\partial x}{\partial p}$ is nonsingular, equation (A.30) follows; furthermore,

$$\begin{aligned} -L(x(t,p),u(t,p)) &= \frac{\partial C}{\partial t}(t,p) = \frac{\partial V^{\mathscr{E}}}{\partial t}(t,x(t,p)) + \frac{\partial V^{\mathscr{E}}}{\partial x}(t,x(t,p)) \dot{x}(t,p) \\ &= \frac{\partial V^{\mathscr{E}}}{\partial t}(t,x(t,p)) + \lambda(t,p) f(x(t,p),u(t,p)) \end{aligned}$$

gives (A.29). But then the minimum condition in the definition of extremals implies that the pair $(V^{\mathscr{E}}, u_*)$ solves the Hamilton-Jacobi-Bellman equation: for $(t,x) = (t,x(t,p)) \in G$ and an arbitrary control value $v \in U$ we have that

$$\begin{aligned}
&\frac{\partial V^{\mathscr{E}}}{\partial t}(t,x)+\frac{\partial V^{\mathscr{E}}}{\partial x}(t,x)f(x,v)+L(x,v)\\
&=\frac{\partial V^{\mathscr{E}}}{\partial t}(t,x(t,p))+\frac{\partial V^{\mathscr{E}}}{\partial x}(t,x(t,p))f(x(t,p),v)+L(x(t,p),v)\\
&=\frac{\partial V^{\mathscr{E}}}{\partial t}(t,x(t,p))+\lambda(t,p)f(x(t,p),v)+L(x(t,p),v)\\
&=\frac{\partial V^{\mathscr{E}}}{\partial t}(t,x(t,p))+H(\lambda(t,p),x(t,p),v)\\
&\geq\frac{\partial V^{\mathscr{E}}}{\partial t}(t,x(t,p))+H(\lambda(t,p),x(t,p),u(t,p))=0
\end{aligned}$$

with equality for $v=u(t,p)$.

If $\mathscr{E}$ is nicely C^r-parameterized, then in addition λ also is C^r in p and thus, since on G we have $\frac{\partial V^{\mathscr{E}}}{\partial x}=\lambda\circ F^{-1}$, it follows that $\frac{\partial V^{\mathscr{E}}}{\partial x}$ is still r-times continuously differentiable in x. Differentiating the column vector $\lambda^T(t,p)=\left(\frac{\partial V^{\mathscr{E}}}{\partial x}\right)^T(t,x(t,p))$, we get that

$$\frac{\partial\lambda^T}{\partial p}(t,p)=\frac{\partial^2 V^{\mathscr{E}}}{\partial x^2}(t,x(t,p))\frac{\partial x}{\partial p}(t,p)$$

where, consistent with our notation, $\frac{\partial\lambda^T}{\partial p}$ is the matrix of partial derivatives of the column vector λ^T. □

If the problem is time-independent, then simply consider the autonomous version of the dynamics defined by

$$f'(x',u)=\begin{pmatrix}1\\ f(x',u)\end{pmatrix}$$

with the flow map given by $F(t,p)=x(t,p)$. For such a case, the terminal time T is necessarily free and thus the Hamiltonian H vanishes identically. Hence the value function is independent of t and the relation (A.30) reads

$$\frac{\partial V^{\mathscr{E}}}{\partial x}(x(t,p))=\lambda(t,p). \tag{A.32}$$

Definition A.4.7 (Local Field of Extremals). A C^r-parameterized local field of extremals, $\mathscr{F}$, is a C^r-parameterized family of normal extremals for which the associated flow $F:D\to\mathbb{R}\times\mathbb{R}^n$, $(t,p)\mapsto F(t,p)$, is a $C^{1,r}$-diffeomorphism from the interior of the set D, $\mathring{D}=\{(t,p):p\in P,t_-(p)<t<t_+(p)\}$, onto a region $G=F\left(\mathring{D}\right)$.

We do not require that the flow F is a diffeomorphism on the source or target of the parametrization. However, if these are hypersurfaces (codimension 1 embedded submanifolds) so that the flow F is transversal to them, then the flow extends

as a $C^{1,r}$-diffeomorphism onto a neighborhood of the full closed domain D. This is the typical scenario along switching surfaces and is satisfied in all the examples considered in Chapters 2 and 3. Combining Theorems A.4.1 and A.4.2 implies the following result about optimality (see Figure A.2):

Corollary A.4.1. *Let $\mathscr{F}$ be a C^r-parameterized local field of extremals with target N_T in the terminal manifold N, $N_T \subset N$, and assume its associated flow covers a domain G. Then, given any initial condition $(t_0, x_0) \in G$, $x_0 = x(t_0, p_0)$, the open-loop control $\bar{u}(t) = u(t, p_0)$, $t_0 \le t \le T(p_0)$, is optimal when compared with any other admissible control u for which the corresponding trajectory x (respectively, its graph) lies in G, i.e., $\mathscr{J}(\bar{u}) \le \mathscr{J}(u)$.*

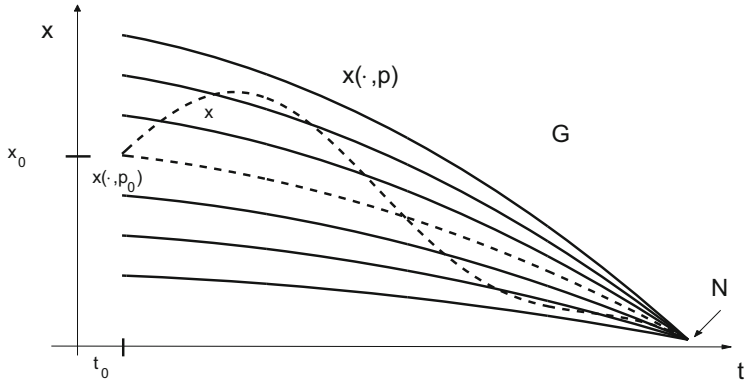

Fig. A.2 A relative minimum—$\mathscr{J}(u_{(t_0,x_0)}) \le \mathscr{J}(v)$.

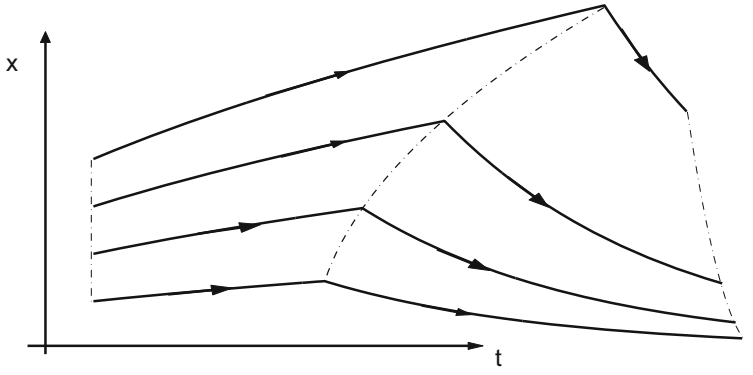

Fig. A.3 A parameterized family (field) of broken extremals.

A.4.3 Parameterized Families of Broken Extremals

The results above apply to a single patch (i.e., require a certain degree of smoothness in the parameterizations). In general, however, it is necessary to glue together various local fields of extremals to obtain a solution along a reference trajectory in order to construct a global synthesis. It is the minimization condition that generally determines when and where the control changes. This may happen because the value where the minimum of the Hamiltonian is achieved jumps and discontinuities arise in the optimal controls like at bang-bang junctions or where regularity properties of the parametrization break down as it occurs at junctions for the problems considered in Chapter 4. This naturally leads to the notion of parameterized families of broken extremals (Figure A.3).

Definition A.4.8 (Family of Broken Extremals). A C^r-parameterized family of broken extremals is a finite concatenation $\mathscr{E} = \mathscr{E}_1 * \cdots * \mathscr{E}_k$ of C^r-parameterized families of extremals.

In order to simplify the notation, and without loss of generality, we only describe the concatenation of two parameterized families of extremals. We keep the notation unambiguous by restricting the considerations to the time-dependent case, but the adjustments to the time-independent case are merely formal. Throughout this subsection, the flow F is thus defined in terms of the graphs of the controlled trajectories, $F(t,p) = (t, x(t,p))$. Let P be an open subset of $\mathbb{R}^d$ with $1 \le d \le n$ and let $\mathscr{E}_1$ be a C^r-parameterized family of extremals with domain

$$D_1 = \{(t,p) : p \in P, t_{1,-}(p) \le t \le t_{1,+}(p)\},$$

source

$$N_{1,-} = \{(t,x) :\ t = t_{1,-}(p),\ x = \xi_{1,-}(p), \quad p \in P\},$$

target

$$N_{1,+} = \{(t,x) :\ t = t_{1,+}(p),\ x = \xi_{1,+}(p), \quad p \in P\}$$

and cost $\gamma_{1,\pm} : P \to \mathbb{R}$, $p \mapsto \gamma_{1,\pm}(p)$, at the source, respectively, target. For the same parameter set P, let $\mathscr{E}_2$ be a C^r-parameterized families of normal extremals with domain

$$D_2 = \{(t,p) : p \in P, t_{2,-}(p) \le t \le t_{2,+}(p)\},$$

source

$$N_{2,-} = \{(t,x) :\ t = t_{2,-}(p),\ x = \xi_{2,-}(p), \quad p \in P\},$$

target

$$N_{2,+} = \{(t,x) :\ t = t_{2,+}(p),\ x = \xi_{2,+}(p), \quad p \in P\}$$

and cost $\gamma_{2,\pm} : P \to \mathbb{R}$, $p \mapsto \gamma_{2,\pm}(p)$, at the source, respectively, target. We denote the corresponding controls, trajectories, and multipliers by the corresponding subscript. For example, λ_2 denotes the adjoint variable for the family $\mathscr{E}_2$ and we denote the constant multiplier by $\lambda_{0,2}(p)$.

Two C^r-parameterized families $\mathscr{E}_1$ and $\mathscr{E}_2$ of extremals can be *concatenated* if for all $p \in P$ we have that (i) $t_{1,+}(p) = t_{2,-}(p)$, $\xi_{1,+}(p) = \xi_{2,-}(p)$, (ii) $\lambda_{0,1}(p) = \lambda_{0,2}(p)$, $\lambda_1(t_{1,+}(p),p) = \lambda_2(t_{2,-}(p),p)$, and (iii) $\gamma^1_+(p) = \gamma^2_-(p)$. Conditions (i) and (ii) enforce that the controlled trajectories of the two flows and their adjoint variables match at the junction $N_{1,+} = N_{2,-}$ while condition (iii) guarantees the agreement of the associated cost functions. In order to simplify the notation, we denote the functions defining the concatenation by

$$\tau(p) = t_{1,+}(p) = t_{2,-}(p), \quad \xi(p) = \xi_{1,+}(p) = \xi_{2,-}(p), \quad \gamma(p) = \gamma^1_+(p) = \gamma^2_-(p),$$

$$\lambda_0(p) = \lambda_{0,1}(p) = \lambda_{0,2}(p) \qquad \text{and} \qquad \lambda(p) = \lambda_1(t_{1,+}(p),p) = \lambda_2(t_{2,-}(p),p)$$

Furthermore, it follows from the fact that $\mathscr{E}_1$ and $\mathscr{E}_2$ are C^r-parameterized families of extremals that the controls $u_i = u_i(t,p)$ solve the minimization problems

$$\min_{v \in U} H(t,\lambda_i(t,p),x_i(t,p),v) = H(t,\lambda_i(t,p),x_i(t,p),u_i(t,p)).$$

Hence also the functions $h_i(t,p) = H(t,\lambda_i(t,p),x_i(t,p),u_i(t,p))$ remain continuous at the junction and we let

$$h(p) = h_1(t_{1,+}(p),p) = h_2(t_{2,-}(p),p).$$

The concatenated family $\mathscr{E} = \mathscr{E}_1 * \mathscr{E}_2$ is then defined as the family of extremals with domain

$$D = \{(t,p) : p \in P, t_{1,-}(p) \le t \le t_{2,+}(p)\},$$

source

$$N_{1,-} = \{(t,x) :\ t = t_{1,-}(p),\ x = \xi_{1,-}(p), \quad p \in P\},$$

target

$$N_{2,+} = \{(t,x) :\ t = t_{2,+}(p),\ x = \xi_{2,+}(p), \quad p \in P\}$$

and the controls u, trajectories x, and adjoint variable λ are defined piecewise as

$$u(t,p) = \begin{cases} u_1(t,p) & \text{for } (t,p) \in \mathit{int}\,(D_1), \\ u_2(t,p) & \text{for } (t,p) \in D_2, \end{cases} \qquad x(t,p) = \begin{cases} x_1(t,p) & \text{for } (t,p) \in D_1, \\ x_2(t,p) & \text{for } (t,p) \in D_2, \end{cases}$$

and

$$\lambda(t,p) = \begin{cases} \lambda_1(t,p) & \text{for } (t,p) \in D_1, \\ \lambda_2(t,p) & \text{for } (t,p) \in D_2. \end{cases}$$

The set $\mathscr{T} = \{(t,p) : t = \tau(p),\ p \in P\}$ is the graph of a continuously differentiable function τ and thus is a hypersurface in $(0,T) \times P$. We also want that the image $\mathscr{S}$ under the flow,

$$\mathscr{S} = F(\mathscr{T}) = \{t,x) :\ t = \tau(p),\ x = x(\tau(p),p),\ p \in P\},$$

is a hypersurface in $(0,T)\times\mathbb{P}$ and this requires some regularity condition. By construction, the two flows F_i, $i=1,2$ agree on the surface $\mathscr{T}$. However, their derivatives are discontinuous and we need to specify which flow is used when we differentiate at the switching parameters. Since the construction of extremals is done backward, we generally take the limits from the right, i.e., we consider the flow $\tilde{F}_2$. We call $\mathscr{T}$ the switching parameters and $\mathscr{S}$ the *switching surface*. A differentiable mapping $F:\mathbb{R}^m\to\mathbb{R}^m$ is said to be *regular* at a point x if the derivative $DF:\mathbb{R}^m\to\mathbb{R}^m$ is nonsingular at x.

Lemma A.4.3. *Let $\mathscr{T}=\{(t,p):t=\tau(p),\ p\in P\}$ with $P\subset\mathbb{R}^n$ an open set. If the flow map F_i, $i=1$ or $i=2$, is regular for $t=\tau(p)$, then near $(t,x)=(\tau(p),\xi(p))$ the switching surface*

$$\mathscr{S}=F(\mathscr{T})=\{(t,x):t=\tau(p),\ x=\xi(p),\ p\in P\}.$$

is an embedded n-dimensional hypersurface and the flow F_i is transversal to $\mathscr{S}$, i.e., the tangent vectors to the graphs of the trajectories, $(1,\dot{x}(t,p))^T$, do not lie in the tangent space to $\mathscr{S}$ at $F_i(t,p)$.

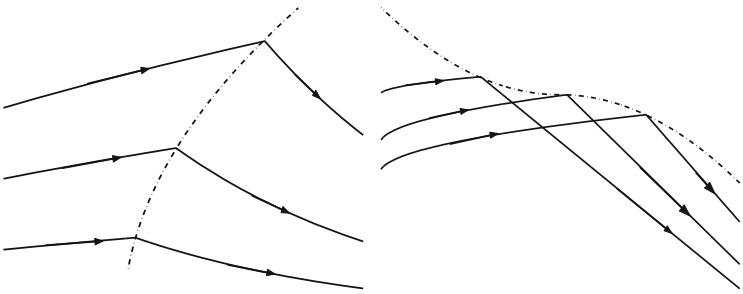

Fig. A.4 Transversal crossing (left) and fold (right) in a parameterized family of broken extremals.

Definition A.4.9 (Transversal Crossings and Folds). We say the C^r-parameterized family $\mathscr{E}=\mathscr{E}_1*\mathscr{E}_2$ of broken extremals has a regular switching point at $(t_0,p_0)=(\tau(p_0),p_0)$ if both flow maps F_1 and F_2 are regular at (t_0,p_0). We call such a switching point a transversal crossing if the graphs of the trajectories $t\mapsto x_i(t,p)$, $i=1,2$, cross the switching surface

$$\mathscr{S}=\{(t,x):t=\tau(p),\ x=\xi(p),\ p\in P\}$$

in the same direction and a transversal fold if they cross it in opposite directions (see Figure A.4).

Proposition A.4.1. *Suppose $\frac{\partial x_2}{\partial p}(t,p)$ is nonsingular for $t=\tau(p)$ and let*

$$k(p)=f(\xi(p),u_2(\tau(p),p))-f(\xi(p),u_1(\tau(p),p)).$$

The point $(\tau(p),p)$ is a regular switching point if and only if

$$1+\frac{\partial\tau}{\partial p}(p)\left(\frac{\partial x_2}{\partial p}(\tau(p),p)\right)^{-1}k(p)\neq 0. \tag{A.33}$$

The concatenated family $\mathscr{E}=\mathscr{E}_1*\mathscr{E}_2$ of broken normal extremals has a transversal crossing at $(\tau(p),p)$ if

$$1+\frac{\partial\tau}{\partial p}(p)\left(\frac{\partial x_2}{\partial p}(\tau(p),p)\right)^{-1}k(p)>0 \tag{A.34}$$

and a transversal fold if

$$1+\frac{\partial\tau}{\partial p}(p)\left(\frac{\partial x_2}{\partial p}(\tau(p),p)\right)^{-1}k(p)<0. \tag{A.35}$$

Recall that our formulations are for the time-dependent case, but analogous definitions and results apply to the time-independent formulation.

Proof. We show that the sign of the quantity (A.33) distinguishes between transversal folds and crossings. Since $\frac{\partial x_2}{\partial p}(t,p)$ is nonsingular at $t=\tau(p)$, the flow F_2 corresponding to the control u_2, $(t,p)\mapsto(t,x_2(t,p))$, is locally a $C^{1,r}$ diffeomorphism and hence invertible between some neighborhoods V of $(\tau(p),p)$ and W of $(\tau(p),x_2(\tau(p),p))$. Denote the inverse by $F_2^{-1}:W\to V$, $(t,x)\mapsto(t,\pi(t,x))$, and define a continuously differentiable function $\Psi:W\to\mathbb{R}$ by

$$\Psi(t,x)=t-\tau(\pi(t,x)). \tag{A.36}$$

This function Ψ then describes the switching surface in the state-space,

$$\mathscr{S}=\{(t,x)\in W:\Psi(t,x)=0\}.$$

The gradient $\nabla\Psi(t,x)$ is not zero on $\mathscr{S}$: for $(t,x)=(\tau(p),x_2(\tau(p),p))$, we have that

$$\begin{aligned}
\nabla\Psi(t,x)&=\big(1,\,-\nabla\tau(p)\big)\begin{pmatrix}1&0\\ \frac{\partial\pi}{\partial t}(t,x)&\frac{\partial\pi}{\partial x}(t,x)\end{pmatrix}\\
&=\big(1,\,-\nabla\tau(p)\big)\begin{pmatrix}1&0\\ \frac{\partial x_2}{\partial t}(t,p)&\frac{\partial x_2}{\partial p}(t,p)\end{pmatrix}^{-1}\\
&=\big(1,\,-\nabla\tau(p)\big)\begin{pmatrix}1&0\\ -\left(\frac{\partial x_2}{\partial p}(t,p)\right)^{-1}\frac{\partial x_2}{\partial t}(t,p)&\left(\frac{\partial x_2}{\partial p}(t,p)\right)^{-1}\end{pmatrix}\\
&=\left(1+\nabla\tau(p)\left(\frac{\partial x_2}{\partial p}(t,p)\right)^{-1}\frac{\partial x_2}{\partial t}(t,p),-\nabla\tau(p)\left(\frac{\partial x_2}{\partial p}(t,p)\right)^{-1}\right).
\end{aligned}$$

In particular, if $\frac{\partial \Psi}{\partial x}(t,x) = 0$, then $\frac{\partial \Psi}{\partial t}(t,x) = 1$ and therefore $\nabla \Psi(t,x) \neq 0$. Furthermore, by construction of Ψ we have on $\mathscr{S}$ that

$$\nabla \Psi(t,x) \cdot \begin{pmatrix} 1 \\ f(\xi(p), u_2(\tau(p),p)) \end{pmatrix} \equiv 1$$

and along the flow F_1 corresponding to the control u_1 we have that

$$\nabla \Psi(t,x) \cdot \begin{pmatrix} 1 \\ f(\xi(p), u_1(\tau(p),p)) \end{pmatrix} = 1 + \nabla \tau(p) \left(\frac{\partial x_2}{\partial p}(t,p) \right)^{-1} k(p).$$

The tangent plane to $\mathscr{S}$ at a point $(t,x) = (\tau(p), x_2(\tau(p),p))$ is given by

$$T_{(t,x)}\mathscr{S} = \left\{ (\alpha, z) \in \mathbb{R}^{n+1} : \frac{\partial \Psi}{\partial t}(t,x)\alpha + \frac{\partial \Psi}{\partial x}(t,x) z = 0 \right\},$$

and two vectors $(1,v)$ and $(1,w)$ point to the same side of $T_{(t,x)}\mathscr{S}$ at (t,x) if and only if $\nabla \Psi(t,x) \cdot \begin{pmatrix} 1 \\ v \end{pmatrix}$ and $\nabla \Psi(t,x) \cdot \begin{pmatrix} 1 \\ w \end{pmatrix}$ have the same sign. Hence it follows that the switching point at $(\tau(p),p)$ is a transversal crossing if and only if $1 + \nabla \tau(p) \left(\frac{\partial x_2}{\partial p}(\tau(p),p) \right)^{-1} k(p)$ is positive while it is a transversal fold if and only if this quantity is negative. □

The important feature of families of broken normal extremals is that the corresponding value in the state-space is a solution to the Hamilton-Jacobi-Bellman equation wherever the flow covers an open set in the state-space injectively. This even holds if for some intermediate segment this flow collapses onto lower dimensional manifolds, a common scenario both with bang-bang controls and when the controlled trajectories follow singular arcs. The key observation is that, since the trajectories, multipliers and the cost agree at the junctions, the transversality condition (A.25),

$$\lambda(p) \frac{\partial \xi}{\partial p}(p) = \lambda_0(p) \frac{\partial \gamma}{\partial p}(p) + h(p) \frac{\partial \tau}{\partial p}(p),$$

propagates from one family to the other. This directly follows from Lemma A.4.1. Hence the Shadow-Price lemma remains valid as one crosses from one parameterized family of extremals to the next and (A.28) holds on the domain D of the concatenated family $\mathscr{E}$ of extremals away from the junction $\mathscr{T} = \{(t,p) : t = \tau(p), p \in P\}$. On $\mathscr{T}$ the partial derivatives of C and x with respect to the parameter p generally are discontinuous, but their jumps cancel in the expression (A.28) and this allows to construct solutions to the Hamilton-Jacobi-Bellman equation for families of broken extremals. The formulas below are used in the constructions in Chapter 4 and in Section B.1 in Appendix B.

Lemma A.4.4 ([292, Lemma 6.1.1]). *The Shadow-Price identity (A.28) is valid for the concatenated family $\mathscr{E} = \mathscr{E}_1 * \mathscr{E}_2$ of broken extremals for all $(t,p) \in D \setminus \mathscr{T}$.*

Along the switching surface $\mathscr{T} = \{(t,p) : t = \tau(p),\ p \in P\}$*, it is valid in the limits as* $t \to \tau(p)$ *from the right and the left. Setting*

$$k_0(p) = L(\xi(p), u_2(\tau(p),p)) - L(\xi(p), u_1(\tau(p),p))$$

and

$$k(p) = f(\xi(p), u_2(\tau(p),p)) - f(\xi(p), u_1(\tau(p),p)),$$

we have that

$$\lambda_0(p)k_0(p) + \lambda(p)k(p) = 0$$

and

$$\frac{\partial C_2}{\partial t}(t,p) = \frac{\partial C_1}{\partial t}(t,p) - k_0(p)\left(1, -\frac{\partial \tau}{\partial p}(p)\right), \tag{A.37}$$

$$\frac{\partial x_2}{\partial p}(t,p) = \frac{\partial x_1}{\partial p}(t,p) + k(p)\left(1, -\frac{\partial \tau}{\partial p}(p)\right). \tag{A.38}$$

Recall that $\frac{\partial \tau}{\partial p}(p)$ denotes the gradient of τ written as a row vector. Hence $\frac{\partial x_2}{\partial p}(t,p)$ is a rank 1 correction of the matrix $\frac{\partial x_1}{\partial p}(t,p)$.

It seems geometrically intuitive that local optimality properties of the flow of extremals are preserved at transversal crossings where the combined flow remains one-to-one while optimality ceases at a switching surface that is a transversal fold where trajectories overlap. This indeed is the case and in the first case the value function $V^{\mathscr{E}}$ remains continuously differentiable at the switching surface $\mathscr{S}$ while this surface consists of so-called "conjugate points" in the latter scenario.

Definition A.4.10 (Field of Broken Extremals). We say the C^r-parameterized family $\mathscr{E} = \mathscr{E}_1 * \mathscr{E}_2$ of broken extremals defines a field of broken extremals over the domain D if each of the two flows $F_i : D_i \to G_i = F_i(D_i)$, is a $C^{1,r}$-diffeomorphism on the interior of the domains D_i and the combined flow map

$$F : D \to G = F(D), \quad (t,p) \mapsto (t, x(t,p)) = \begin{cases} (t, x_1(t,p)) & \text{for} \quad (t,p) \in D_1, \\ (t, x_2(t,p)) & \text{for} \quad (t,p) \in D_2, \end{cases}$$

is injective. The sets G and G_i are defined as the images under these flows and we have that $G = G_1 \cup \mathscr{S} \cup G_2$.

Theorem A.4.3. *[292, Theorem 6.1.1] Let* $\mathscr{E} = \mathscr{E}_1 * \mathscr{E}_2$ *be a* C^r*-parameterized field of broken normal extremals. If* $\mathscr{E}$ *has transversal crossings at all switching points in* $\mathscr{T} = \{(t,p) : t = \tau(p),\ p \in P\}$*, then the combined flow* $F : D \to G = F(D)$ *is a diffeomorphism and the associated value function* $V^{\mathscr{E}} : G \to \mathbb{R}$*,* $V^{\mathscr{E}} = C \circ F^{-1}$*, is a continuously differentiable solution to the Hamilton-Jacobi-Bellman equation on G.*

Corollary A.4.2. *Let* $\mathscr{E}$ *be a* C^1*-parameterized field of broken normal extremals with regular transversal crossings over its domain D. Let* $G = F(D)$*,* $\overline{G} = F(D) \cup N$ *and let* $V^{\mathscr{E}} : \overline{G} \to \mathbb{R}$*,* $V^{\mathscr{E}} = C \circ F^{-1}$*, be the corresponding value function and*

$u^* : G \to U$, $u^* = u \circ F^{-1}$, the corresponding feedback control. Then $V^{\mathscr{E}}$ is a continuously differentiable solution to the Hamilton-Jacobi-Bellman equation on G which has a continuous extension to the terminal manifold N. The feedback control is optimal on $\overline{G}$ (i.e., in comparison to any other control for which the corresponding trajectory lies in $\overline{G}$) and the corresponding value function is given by $V^{\mathscr{E}}$.

Transversal folds, on the other hand, correspond to surfaces where optimality of the combined flow ceases. In this case the switching surface $\mathscr{S}$ consists of controlled trajectories and if it can be argued that these trajectories cannot be optimal (e.g., if the associated controls need to be singular, but singular controls are known not to be optimal), then using the theory of envelopes [292, Sect. 6.1.3] it can be shown that $\mathscr{S}$ consists of "conjugate points" where optimality ceases. Rather than discussing this in general, in Appendix B.1 we shall carry out the full construction of a parameterized family of broken extremals and associated optimality considerations for the cell-cycle specific 2-compartment model considered in Section 2.1. There we also provide an efficient finite algorithm that allows to determine whether switching points are transversal crossings or folds.

A.4.4 A Regular Synthesis of Optimal Controlled Trajectories

We close this appendix with a verification theorem for proving the optimality of a family of extremal controlled trajectories that have been obtained by combining various local parameterized fields of extremals. The key feature is that a globally and piecewise defined value function $V^{\mathscr{E}} : G \to \mathbb{R}$ only needs to be differentiable on a sufficiently rich open subset of G. The result below will be used in Section B.4 in Appendix B to verify the optimality of a piecewise defined feedback control for the problem of antiangiogenic monotherapy considered in Chapter 5. For this reason we give the formulation here for a time-independent problem $[OC]$ with free terminal time.

Definition A.4.11 (Synthesis). A synthesis of controlled trajectories for the optimal control problem $[OC]$ over a domain $G \subset M$ consists of a family of controlled trajectories $\mathscr{S} = \{(x_z, u_z) : z \in G\}$ that start at the point $z \in G$, $x_z(0) = z$. A synthesis is called optimal (respectively, extremal) if each controlled trajectory in the family $\mathscr{S}$ is optimal (respectively, extremal).

Clearly, an optimal synthesis needs to be extremal and the aim of all the earlier constructions is to give conditions that guarantee that an extremal synthesis that has been found through an analysis of necessary conditions for optimality indeed is optimal. The result below provides such a statement. A union of sets $S_i \subset M$, $i \in I$, is said to be *locally finite* if every compact subset K of M only intersects a finite number of the sets S_i.

Theorem A.4.4 (Verification Theorem [292, Theorem 6.3.1]). *Let $G \subset M$ be a domain with N in its boundary and suppose $V : G \cup N \to \mathbb{R}$ is a continuous function*

defined on G that satisfies $V(z) \leq \varphi(z)$ for $z \in N$. Suppose there exists a locally finite union of embedded submanifolds M_i, $i \in \mathbb{N}$, of positive codimensions, such that the function V is continuously differentiable on the complement of these submanifolds in M, $M_g = M \setminus \cup_{i\in\mathbb{N}} M_i$, and satisfies the Hamilton-Jacobi-Bellman inequality

$$\frac{\partial V}{\partial z}(z) f(z,u) + L(z,u) \geq 0 \qquad \text{for all} \quad z \in M_g \quad \text{and} \quad u \in U. \tag{A.39}$$

Then, for every controlled trajectory (x,u) that starts at a point $z \in M$ whose trajectory lies in the region G over the interval $[0,T)$ and ends in N at time T, we have that

$$J(u) \geq V(z).$$

Generally, the function V of the theorem is defined by the value of the objective for some synthesis of controlled trajectories that has been constructed through an analysis of extremals as it has been described above. In particular, it then follows that the corresponding controls are optimal. However, in principle the function V could come from an arbitrary such selection of controlled trajectories (x_z, u_z) that steer the points $z \in G$ into N and it can even be allowed that there are multiple members of this family for some values $z \in G$ as long as they give the same value of the objective. This, for example, is of interest when optimal controls are not unique. Typically, however, the function V comes from a unique specification in terms of what is called a *memoryless* synthesis.

Definition A.4.12 (Memoryless Synthesis). A synthesis $\mathscr{S} = \{(x_z, u_z) : z \in G\}$ of controlled trajectories for the optimal control problem $[OC]$ over a domain $G \subset M$ is called memoryless, if whenever $(x_z, u_z) \in \mathscr{S}$ is defined on $[0,T]$ and $\tilde{z} = x(\tau)$ is a point on the trajectory for $\tau > 0$, then the controlled trajectory $(x_{\tilde{z}}, u_{\tilde{z}})$ in the family starting at the point $\tilde{z}$ is given by the restriction of the controlled trajectory to the interval $[\tau, T]$.

Parameterized families of extremals, $\mathscr{E}$, and their associated value functions $V^{\mathscr{E}}$ naturally give rise to the piecewise defined functions V that are needed for this verification theorem to apply. Differentiability properties of $V^{\mathscr{E}}$ on open subsets along with the fact that the Hamilton-Jacobi-Bellman equation is valid are automatic corollaries of our constructions while lower dimensional submanifolds M_i where differentiability fails arise naturally where the flow of parameterized families collapses to follow lower dimensional submanifolds (like it is often the case along singular trajectories in small dimensions), but can also include submanifolds where it is just inconvenient to verify differentiability of the value function. Being able to exclude these lower dimensional subsets from the differentiability requirement gives the result its *global* nature. Clearly, if the set G is small, the theorem provides sufficient conditions for a local minimum. At the same time, these constructions also provide us with a control $u = u_z$ in the parameterized family for which equality holds, $V(z) = J(u_z)$. Thus *the verification theorem implies the optimality of the controls in the synthesis*.

We close with a brief indication of the main argument for the proof of the verification theorem. We start with the observation that the result is trivial if V is differentiable everywhere on G and that this is simply the argument considered earlier in Theorem A.4.1: for any controlled trajectory defined over an interval $[0,T]$ we have that

$$\frac{d}{dt}V(x(t)) = \frac{\partial V}{\partial z}(x(t))f(x(t),u(t)) \geq -L(x(t),u(t))$$

and thus

$$V(x(T)) - V(x(0)) \geq -\int_0^T L(x(s),u(s))ds.$$

Hence

$$\begin{aligned} V(x(0)) &\leq \int_0^T L(x(s),u(s))ds + V(x(T)) \\ &\leq \int_0^T L(x(s),u(s))ds + \varphi(x(T)) = J(u). \end{aligned}$$

However, this reasoning breaks down if there exist lower dimensional submanifolds along which V is not differentiable. In principle, the set of times when a given controlled trajectory x lies in such a submanifold can be an arbitrary closed subset of the interval $[0,T]$ and it simply is no longer possible to differentiate the function V along such a trajectory. Dealing with this problem becomes a highly nontrivial technical matter. The idea, which goes back to Boltyansky's original approach of a so-called *regular synthesis* [29], is to perturb the given nominal trajectory in such a way that the resulting trajectory has a value that is close to the one of the original trajectory, but only intersects the manifolds where V is not differentiable for a finite set of times. Using Sard's theorem and various technical constructions, it can be shown that such an approximation is possible. Then the argument above can be carried out piecewise and the result follows in the limit as the approximations approach the given controlled trajectory (e.g., see [276] or [292, Sect. 6.3]). In Boltyansky's original definition, several, at times stringent, assumptions are made that guarantee these properties. Not all of these are necessary and in the theorem formulated here this approximation procedure is carried out using arguments of Sussmann that lead to continuity requirements on the value function V that are even weaker than we have stated them in Theorem A.4.4 [276].

Appendix B
Mathematical Proofs

In this appendix we collect some of the more mathematical constructions and proofs that have been omitted in the main portion of the text. In particular, we include a complete construction of the fields of bang-bang extremals for the cell-cycle specific models for chemotherapy from Chapter 2 and a verification of the synthesis of optimal controlled trajectories for model [H] in Chapter 5.

B.1 Construction of a Local Family of Broken Extremals for Cell-Cycle Specific Cancer Chemotherapy

The mathematical models for cell-cycle specific cancer chemotherapy considered in Section 2 all have optimal controls that are bang-bang. In this appendix, we give a detailed construction of the corresponding field of extremals for the 2-compartment model [CC2]. More generally, the same constructions apply for optimal control problems of the form [CC] for arbitrary multi-input bilinear systems as stated in Theorem 2.2.2.

B.1.1 Construction of a Parameterized Family of Broken Bang-Bang Extremals

We consider the optimal control problem [CC2] from Section 2, i.e.,

[CC2] for a fixed final time $T > 0$, minimize the objective

$$J(u) = rN(T) + \int_0^T qN(t) + su(t)dt \to \min \tag{B.1}$$

H. Schättler, U. Ledzewicz, *Optimal Control for Mathematical Models of Cancer Therapies*, Interdisciplinary Applied Mathematics 42,
DOI 10.1007/978-1-4939-2972-6

over all Lebesgue-measurable functions $u : [0,T] \to [0,u_{\max}]$, subject to the dynamics

$$\dot{N}(t) = (A + uB)N(t), \qquad N(0) = N_0, \tag{B.2}$$

with A and B given by the matrices

$$A = \begin{pmatrix} -a_1 & 2a_2 \\ a_1 & -a_2 \end{pmatrix} \qquad \text{and} \qquad B = \begin{pmatrix} 0 & -2a_2 \\ 0 & 0 \end{pmatrix}. \tag{B.3}$$

It is shown in Theorem 2.1.2 that optimal controls do not contain intervals where the control is singular and thus bang-bang controls are the prime candidates for optimality.

Let (N_*, u_*) be an extremal controlled trajectory, the *reference extremal*, such that u_* is a bang-bang control with switchings at times t_i, $i = 1,\dots,k$, $0 = t_0 < t_1 < \cdots < t_k < t_{k+1} = T$, and denote the corresponding adjoint variable by λ_*. We **assume** that all the switchings are *strict*, i.e., that the derivatives of the switching function at the switching times t_i do not vanish,

$$\dot{\Phi}_*(t_i) = \{\lambda_*(t_i)[A,B] - qB\}N_*(t_i) \neq 0. \tag{B.4}$$

In a first step, we embed this reference extremal into a *parameterized family of broken extremals* (see Definitions A.4.3 and A.4.8). Set $p_* = N_*(T)$ and for p in some neighborhood P of p_*, let $N(t,p)$ and $\lambda(t,p)$, $(t,p) \in [0,T] \times P$, denote the solutions to the terminal value problem for the system and adjoint equations given by

$$\dot{N}(t,p) = (A + u(t,p)B)N(t,p), \qquad x(T,p) = p, \tag{B.5}$$

$$\dot{\lambda}(t,p) = -\lambda(t,p)(A + u(t,p)B) - q, \qquad \lambda(T,p) = r, \tag{B.6}$$

while the control is chosen so that with

$$\Phi(t,p) = s + \lambda(t,p)BN(t,p) \tag{B.7}$$

we have that

$$\Phi(t,p)u(t,p) = \min_{v \in [0,u_{\max}]} \Phi(t,p)v. \tag{B.8}$$

In particular, for $p = p_*$, the control $u(\cdot,p_*)$ reduces to the reference control u_* and $N(\cdot,p_*)$ and $\lambda(\cdot,p_*)$ are the reference trajectory and corresponding multiplier,

$$N(t,p_*) = N_*(t), \qquad u(t,p_*) = u_*(t), \qquad \lambda(t,p_*) = \lambda_*(t).$$

Such a family is well defined near a strictly bang-bang extremal.

Proposition B.1.1. *Let $\Gamma = (N_*, u_*, \lambda_*)$ be a strictly bang-bang extremal lift and denote the switching times of the control u_* by t_i, $i = 1,\dots,k$, $0 = t_0 < t_1 < \cdots < t_k < t_{k+1} = T$. Then there exists a neighborhood P of $p_* = N_*(T)$ in $\mathbb{P}$ and real-analytic functions τ_i defined on P, $i = 1,\dots,k$, such that for $p \in P$ the controls*

$u(\cdot,p)$, which are defined as the bang-bang controls that have switchings at the times $0<\tau_1(p)<\cdots<\tau_k(p)<T$ in the same order as the reference control, satisfy the conditions of the maximum principle. If $N(\cdot,p)$ and $\lambda(\cdot,p)$ denote the corresponding state and costate defined as solutions to equations (B.5) and (B.6), then the triples $\Gamma_p=(N(\cdot,p),u(\cdot,p),\lambda(\cdot,p))$ for $p\in P$ are strictly bang-bang extremal lifts and the family $\mathscr{E}=\{\Gamma_p : p\in P\}$ is a real-analytic parameterized family of broken extremals over the domain $D=\{(t,p):\ 0\le t\le T,\ p\in P\}$.

Proof. We inductively define the controls $u=u(t,p)$, trajectories $N=N(t,p)$ and multipliers $\lambda=\lambda(t,p)$ backward from the terminal time. For all p in some open neighborhood P of p_* and $t\le T$, let $u=u(t,p)$ be constant given by the value of the reference control u_* on the interval $(t_k,T]$ and define $N(t,p)$ and $\lambda(t,p)$ as the solutions of (B.5) and (B.6), i.e.,

$$N(t,p)=\exp\left((t-T)(A+uB)\right)p,$$

and

$$\lambda(t,p)=\left(r+q\int_t^T\exp\left((s-T)(A+uB)\right)ds\right)\exp\left(-(t-T)(A+uB)\right).$$

Since the control is constant and independent of p, the solutions to these linear ODEs exist for all $t\in[0,T]$ and are real analytic functions. Furthermore, it follows from the uniqueness of solutions that

$$N(t,p_*)=N_*(t),\qquad u(t,p_*)=u_*(t),\qquad \lambda(t,p_*)=\lambda_*(t)\qquad \text{for}\quad t_k\le t\le T.$$

In terms of the parameterized switching function (B.7), we also have that

$$\Phi(t,p_*)=\Phi_*(t)=s+\lambda_*(t)BN_*(T)\qquad \text{for}\quad t_k\le t\le T.$$

In particular,

$$\frac{\partial\Phi}{\partial t}(t_k,p_*)=\dot\Phi_*(t_k)\neq 0$$

and thus, by the implicit function theorem, the equation $\Phi(t,p)=0$ can be solved uniquely for t as a function of p in a neighborhood of (t_k,p_*). This solution is given by a real analytic function $\tau_k=\tau_k(p)$ defined in a sufficiently small neighborhood of p_*. By choosing P small enough, we furthermore can ensure that $\Phi(t,p)$ has no additional zeros on the set $D_{k+1}=\{(t,p):\ \tau_k(p)\le t\le T,\ p\in P\}$ and is such that $\frac{\partial\Phi}{\partial t}(\tau_k(p),p)\neq 0$ for all $p\in P$. Hence $(N(\cdot,p),u(\cdot,p))$ is an extremal over $[\tau_k(p),T]$ with corresponding multiplier $\lambda(\cdot,p)$ that has a strict bang-bang junction at $\tau_k(p)$ with a switch in the control.

We now iterate this construction backward from switching surface to switching surface: Suppose $\tau_i=\tau_i(p)$ is given and $N(\tau_i(p),p)$ and $\lambda(\tau_i(p),p)$ are real-analytic functions on P. Define $u(t,p)$ by the constant value of the reference control u_* on the interval (t_{i-1},t_i) and integrate the corresponding system and adjoint equations

backward from $\{(t,p) : t = \tau_i(p)\}$ with boundary conditions given by $N(\tau_i(p),p)$ and $\lambda(\tau_i(p),p)$. It then again follows from the uniqueness of solutions to an ODE that

$$N(t,p_*) = N_*(t), \qquad u(t,p_*) = u_*(t), \qquad \lambda(t,p_*) = \lambda_*(t) \qquad \text{for} \quad t_{i-1} \le t \le t_i$$

and that N and λ are real-analytic functions given by analogous formulas as above: for $t \le \tau_i(p)$ we now have that

$$N(t,p) = \exp\left((t-\tau_i(p))(A+uB)\right)N(\tau_i(p),p)$$

and

$$\lambda(t,p) = \left(\lambda(\tau_i(p),p) + q\int_t^{\tau_i(p)} \exp\left((s-\tau_i(p))(A+uB)\right)ds\right)\exp\left(-(t-T)(A+uB)\right).$$

Consequently, by the implicit function theorem, the equation $\Phi(t,p) = 0$, now defined in terms of the newly constructed state and costate, can again be solved uniquely for t in a neighborhood of (t_{i-1},p_*) and the solution is given by a real analytic function $\tau_{i-1}(p)$ in a neighborhood of p_*. As before, by choosing P small enough, the resulting switching function will have no additional zeroes on $D_i = \{(t,p) : \tau_{i-1}(p) \le t \le \tau_i(p), p \in P\}$ and $\frac{\partial \Phi}{\partial t}(\tau_{i-1}(p),p) \neq 0$ holds for all $p \in P$.

The triples $\Gamma_p = (N(\cdot,p),u(\cdot,p),\lambda(\cdot,p))$ inductively constructed in this way are strictly bang-bang extremal lifts for $p \in P$. □

B.1.2 Transversal Crossings and Fields of Bang-Bang Extremals

For an optimal control problem over a prescribed time horizon, the flow F of trajectories associated with a parameterized family of extremals is defined in terms of the graphs of the controlled trajectories as

$$\begin{aligned} F : D = [0,T] \times P &\to [0,T] \times \mathbb{P}, \\ (t,p) &\mapsto F(t,p) = (t,N(t,p)). \end{aligned} \tag{B.9}$$

In general, this flow need not be injective: it is defined piecewise, and, if we denote its subdomains by

$$D_i = \{(t,p) : \tau_{i-1}(p) \le t \le \tau_i(p), p \in P\}, \qquad i = 1,\dots,k,k+1,$$

(with the convention that $\tau_0(p) \equiv 0$ and $\tau_{k+1}(p) \equiv T$), then the restrictions $F_i = F \restriction D_i$ of the flow map F to the domains D_i are diffeomorphisms, but overlaps can occur at the switching surfaces. The first statement is a consequence of the fact that the control is constant on each subdomain and thus standard results about uniqueness and differentiability of solutions to ODEs apply (also, see the proof of Theorem B.1.1 below) while the second one simply is due to the fact that different

controls before and after the switching are used. We thus need to analyze the mapping properties of the flow near the switching surfaces, i.e., determine whether the combined flow has a transversal crossing or a transversal fold (see Definition A.4.9). While the overall mapping remains injective in the case of a transversal crossing, near a transversal fold trajectories overlap and there exist two extremals for initial conditions near $\mathscr{S}_i$ prior to the switching. Intuitively, such a structure should no longer be optimal and this indeed is the case. As we shall show now, *for a flow of bang-bang trajectories, optimality is preserved between switching surfaces and at transversal crossings, but lost at transversal folds*.

Theorem B.1.1. *Given a strictly bang-bang extremal lift $\Gamma = (N_*, u_*, \lambda_*)$ with the switching times in the control u_* given by t_i, $i = 1, \dots, k$, $0 = t_0 < t_1 < \cdots < t_k < t_{k+1} = T$, let $\mathscr{E} = \{\Gamma_p = (N(\cdot,p), u(\cdot,p), \lambda(\cdot,p)) : p \in P\}$ be the real-analytic parameterized family of broken extremals constructed in Proposition B.1.1. If all the switchings (t_i, p_*) are transversal crossings, then there exists a neighborhood P of $p_* = N_*(t)$ such that the flow F restricted to $[0,T] \times P$ defines a field of broken extremals and the reference control u_* is optimal when compared with any other control u whose trajectory N lies in the region R covered by the flow F, $R = F([0,T] \times P)$.*

Proof. We first show inductively that, for a sufficiently small neighborhood P, the extensions $\tilde{F}_i$ of the restrictions of the flow map F to the subdomains D_i are diffeomorphisms, i.e., that they are injective mappings for which the Jacobian matrices $D\tilde{F}_i$ are nonsingular. It then follows from the inverse function theorem that these mappings have differentiable inverses and, in particular, that $\tilde{F}_i$ maps the hypersurface $\mathscr{T}_i$ diffeomorphically onto the switching surfaces $\mathscr{S}_i$.

Consider the last segment, i.e., $i = k+1$. Since the control is constant, all controlled trajectories satisfy the *same* differential equation, $\dot{N} = (A + uB)N$, and thus by the uniqueness result on ODEs different trajectories cannot intersect: suppose there exist times (s_1, p_1) and (s_2, p_2) in D_{k+1} such that $F_{k+1}(s_1, p_1) = F_{k+1}(s_2, p_2)$. Since the flow is defined in terms of the graphs of the trajectories, this immediately implies that $s_1 = s_2$ and thus the trajectories $N(\cdot, p_1)$ and $N(\cdot, p_2)$ are solutions to the differential equation $\dot{N} = (A + uB)N$ that have the same value $N(s_1, p_1) = N(s_2, p_2)$ at time $s_1 = s_2$. By standard uniqueness results about solutions to an ODE, these two trajectories agree for all times and thus $p_1 = N(T, p_1) = N(T, p_2) = p_2$. Hence the mapping $F \restriction D_{k+1}$ is injective. It remains to show that the Jacobian matrix,

$$DF(t,p) = \begin{pmatrix} 1 & 0 \\ \dot{N}(t,p) & \frac{\partial N}{\partial p}(t,p) \end{pmatrix},$$

is nonsingular. But the matrix $X(t,p) = \frac{\partial N}{\partial p}(t,p)$ is the fundamental solution to the variational equation

$$\dot{X} = (A + uB)X, \qquad X(T) = \mathrm{Id},$$

with Id denoting the identity matrix, and thus is nonsingular. In fact, we simply have that

$$\frac{\partial N}{\partial p}(t,p) = \exp\left((t-T)(A+uB)\right) \qquad \text{for } \tau_k(p) \le t \le T.$$

We only remark that the variational equation is obtained by formally differentiating the identity

$$\dot{N}(t,p) = (A+uB)N(t,p), \qquad N(T,p) = p,$$

with respect to p and interchanging differentiation with respect to time and parameter [145]. Since the dynamics is linear in N, this reproduces the same differential equation and differentiation of the terminal condition gives $\frac{\partial N}{\partial p}(T,p) = \mathrm{Id}$.

Inductively now assume the statement is correct over the interval $[\tau_{i+1}(p), T]$ with $i \le k-1$ and consider the previous section of the flow mapping, $\tilde{F}_i$. Injectivity of the map again follows from the uniqueness of solutions to ODEs, but also uses the fact that *switchings are transversal*. Suppose there exist times (s_1,p_1) and (s_2,p_2) in $D_{i+1} = \{(t,p) : \tau_i(p) \le t \le \tau_{i+1}(p), p \in P\}$ such that $F_i(s_1,p_1) = F_i(s_2,p_2)$; then, as above, this implies that $s_1 = s_2$ and that the two trajectories $N(\cdot,p_1)$ and $N(\cdot,p_2)$ agree on their common domain. Since all trajectories cross the switching surfaces transversally in the same direction, it follows that $\tau_{i+1}(p_1) = \tau_{i+1}(p_2)$ and thus, with $\tau = \tau_{i+1}(p_1) = \tau_{i+1}(p_2)$, we also have that $\tilde{F}_i(\tau,p_1) = \tilde{F}_i(\tau,p_2)$. The flow $\tilde{F}_i$ agrees with the flow $\tilde{F}_{i+1}$ on the hypersurface $\mathscr{T}_i$ and by inductive assumption, $\tilde{F}_{i+1}$ maps $\mathscr{T}_i$ diffeomorphically onto $\mathscr{S}_i$. Thus $p_1 = p_2$ follows. Furthermore, $X(t,p) = \frac{\partial N}{\partial p}(t,p)$ still is a solution of the differential equation $\dot{X} = (A+uB)X$, but now with terminal condition given by

$$X(\tau_{i+1}(p),p) = \frac{\partial N_-}{\partial p}(\tau_{i+1}(p),p)$$

with the notation N_- indicating that the partial derivatives are computed from the left. By assumption, all switchings are regular for both the flows before and after the switchings. Hence this matrix is nonsingular and so is then the solution $X(t,p)$. Now we have that,

$$\frac{\partial N}{\partial p}(t,p) = \exp\left((t-T)(A+uB)\right)\frac{\partial N_-}{\partial p}(\tau_{i+1}(p),p) \qquad \text{for} \quad t \le \tau_{i+1}(p).$$

This completes the inductive argument.

The reasoning used so far is valid whenever the junctions are regular for both flows involved in the switching: we only have used that the controls are constant and that all trajectories in each of the flows cross the switching surface in a unique direction. It is the fact that trajectories of both flows cross the switching surface in the same direction that makes the overall mapping $F : [0,T] \times P \to [0,T] \times \mathbb{P}$ one-to-one. This is clearly seen in Figure A.4 and can be proven as follows: suppose there exist times (s_1,p_1) and (s_2,p_2) in D such that $F(s_1,p_1) = F(s_2,p_2)$. Then, as above, $s_1 = s_2$ and, proceeding with a proof by contradiction, suppose that $p_1 \neq p_2$. By the previous argument, the points (s_1,p_1) and (s_2,p_2) cannot lie in the

same subdomain D_i since the flows $F_i = F \restriction D_i$ are diffeomorphisms. By choosing the neighborhood P small enough, if necessary, we can also assume that for all switching times τ_i we have that $\sup_{p\in P} \tau_i(p) < \inf_{p\in P} \tau_{i+1}(p)$. This then implies that (s_1,p_1) and (s_2,p_2) must lie in adjacent domains D_i and D_{i+1} since any hyperplane $t = s$ in $[0,T]\times P$ can at most intersect one of the hypersurfaces $\mathscr{T}_i$ and thus at most intersects two adjacent domains. Hence $F(s_1,p_1) = F(s_2,p_2) \in F(D_i)\cap F(D_{i+1})$. This is possible in case of a transversal fold, but in case of a transversal crossing the images $F(D_i)$ and $F(D_{i+1})$ lie to opposite sides of the switching surface $\mathscr{S}_i$. This is clear locally and follows for the full domains D_i and D_{i+1} from the fact that the flow is defined by the graphs of the trajectories. Contradiction.

Overall, the full, piecewise defined flow

$$F: \quad [0,T]\times\mathbb{P} \to R = F(D) \subset [0,T]\times\mathbb{P}, \quad (t,p) \mapsto F(t,p) = (t,N(t,p)),$$

is one-to-one and piecewise continuously differentiable on the interiors of the subdomains D_i, $i = 1,\dots,k,k+1$. Furthermore, the individual pieces $F_i : D_i \to R_i = F(D_i) \subset [0,T]\times\mathbb{P}$ have continuously differentiable extensions onto open neighborhoods $\tilde{D}_i$ of D_i. The flow thus has a globally well-defined inverse $F^{-1} : R \to D$, $(t,N) \mapsto F^{-1}(t,N)$, and the restrictions of F^{-1} to the regions $R_i = F(D_i)$ are continuously differentiable functions (i.e., with continuous limits at the bordering switching surfaces $\mathscr{S}_i$ and $\mathscr{S}_{i+1}$).

The parameterized cost $C = C(t,p)$ (see Definition A.4.5) associated with the parameterized family of $\mathscr{E} = \{\Gamma_p = (N(\cdot,p),u(\cdot,p),\lambda(\cdot,p)) : p \in P\}$ of broken extremals is defined as the *cost-to-go function* of the family, i.e.,

$$C(t,p) = rp + \int_t^T \{qN(z,p) + su(z,p)\}\,dz. \tag{B.10}$$

Thus $C(t,p)$ is the value of the objective of the optimal control problem [CC2] if the initial condition is given by $N(t,p)$ at time t. Recall that the parameterization is through the endpoints of the trajectories and thus $N(T,p) = p$. The value $V = V^{\mathscr{E}}$ of the parameterized family in the state-space is then simply given by

$$V = V^{\mathscr{E}} : R \to \mathbb{R}, \qquad V^{\mathscr{E}} = C \circ F^{-1}. \tag{B.11}$$

By construction, this function is continuous and continuously differentiable away from the switching surfaces $\mathscr{S}_i$, $i = 1,\dots,k$. It is a remarkable fact that, although the individual pieces of C and F are not continuously differentiable at the switchings, *in case of a transversal crossing, the value function remains continuously differentiable at the switching surfaces* $\mathscr{S}_i$. This is a consequence of the fact that the parameterized family of controlled trajectories that was used to define this value V consists of extremals and the conditions of the maximum principle. It follows from Lemma A.4.2 that the relation

$$\frac{\partial C}{\partial p}(t,p) = \lambda(t,p)\frac{\partial N}{\partial p}(t,p), \tag{B.12}$$

holds for all $(t,p) \in D_i$, $i = 1,\dots,k$, and, as a consequence, away from the switching surfaces $\mathscr{S}_i$, the derivatives of the parameterized value function $V^{\mathscr{E}}$ are given by

$$\frac{\partial V^{\mathscr{E}}}{\partial N}(t,N(t,p)) = \lambda(t,p)$$

and

$$\frac{\partial V^{\mathscr{E}}}{\partial t}(t,N(t,p)) = -H(\lambda(t,p),N(t,p),u(t,p))$$

(see Theorem A.4.2). But the multipliers and the Hamiltonian remain continuous at the switchings and thus these partial derivatives of $V^{\mathscr{E}}$ merge to a continuously differentiable function on the switching surfaces as well. Thus the function $V^{\mathscr{E}} = C \circ F^{-1}$ is continuously differentiable on all of R.

Theorem A.4.2 then implies that $V^{\mathscr{E}}$ together with the feedback control $u_* = u \circ F^{-1}$ is a classical solution of the so-called Hamilton-Jacobi-Bellman equation,

$$\frac{\partial V}{\partial t}(t,N) + \min_{u \in U}\left\{\frac{\partial V}{\partial N}(t,N)\,(A+uB)N + (qN+su)\right\} \equiv 0, \qquad V(T,N) = rN. \tag{B.13}$$

and optimality follows from Theorem A.4.1. □

B.1.3 Transversal Folds and Loss of Local Optimality

Theorem B.1.1 verifies that bang-bang extremals for the optimal control problem [CC2] are strongly local optimal if all switchings are transversal crossings. It remains to show that local optimality ceases at transversal folds.

Theorem B.1.2. *Given a strictly bang-bang extremal lift $\Gamma = (N_*,u_*,\lambda_*)$ with the switching times in the control u_* given by t_i, $i = 1,\dots,k$, $0 = t_0 < t_1 < \cdots < t_k < t_{k+1} = T$, let $\mathscr{E} = \{\Gamma_p = (N(\cdot,p),u(\cdot,p),\lambda(\cdot,p)) : p \in P\}$ be the real-analytic parameterized family of broken extremals constructed in Proposition B.1.1. If all the junctions are regular and there exists a switching (t_i,p_*) that is a transversal fold, then the reference control u_* is not locally optimal.*

Proof. Let ℓ be the largest index for which the switching surface is a transversal fold. It then follows from Theorem B.1.1 that the controlled trajectories $(N(\cdot,p), u(\cdot,p))$ are locally optimal over the domain $D_{opt} = \{(t,p) :\ \tau_\ell(p) < t \le T,\ p \in P\}$, i.e., for initial conditions that lie in $G_{opt} = F(D_{opt})$. We now show that the extremals of the field that start at points on the ℓ-th switching surface $\mathscr{S}_\ell$ are no longer optimal. Hence, these controlled trajectories are not optimal for initial times $t < \tau_\ell(p)$ and thus are not optimal over the full interval $[0,T]$.

The result follows using an *envelope* argument that shows that the ℓ-th switching surface consists of conjugate points where local optimality ceases [292, Theorem 6.1.2]. For the model considered here, all the necessary calculations can easily be

done and we give a self-contained derivation. Since $\mathscr{S}_\ell$ is a transversal fold, at every point $(t,N) \in \mathscr{S}_\ell$ the tangent vectors $(1,AN)$ and $(1,(A+u_{\max}B)N)$ to the graphs of the trajectories corresponding to the bang controls $u \equiv 0$ and $u \equiv u_{\max}$ are transversal to $\mathscr{S}_\ell$ and point to opposite sides of the surface $\mathscr{S}_\ell$ at (t,N). Hence there exists a unique value $\tilde{u} = \tilde{u}(t,N)$ that lies in the open interval $(0,u_{\max})$ such that the vector $(1,(A+\tilde{u}(t,N)B)N)$ is tangent to $\mathscr{S}_\ell$ at (t,N). By the implicit function theorem, this function $\tilde{u} = \tilde{u}(t,N)$ is continuously differentiable and by the theorem on existence of local solutions to ODEs, there exists a unique solution $\tilde{N} = \tilde{N}(t)$ to the initial value problem

$$\dot{N} = (A+\tilde{u}(t,N)B)N, \qquad N(t_\ell) = N_*(t_\ell),$$

over some small interval $[t_\ell, t_\ell+\kappa]$. The open-loop control $\tilde{u}$ defined as $\tilde{u}(t) = \tilde{u}(t,\tilde{N}(t))$ is continuous and takes values in the interior of the control set and thus is admissible. Hence $(\tilde{N},\tilde{u})$ is an admissible controlled trajectory. Furthermore, since the graph of the trajectory $\tilde{N} = \tilde{N}(t)$ is tangent to the switching surface $\mathscr{S}_\ell$ at every point along this trajectory, it follows that this graph lies in the switching surface $\mathscr{S}_\ell$.

We now use this controlled trajectory $(\tilde{N},\tilde{u})$ to construct a one-parameter family of controlled trajectories $(N_\varepsilon,u_\varepsilon)$ with initial point $(t_\ell,N_*(t_\ell))$ that all have the same value for the objective. Since the flow $F_{\ell+1}$ corresponding to the trajectories from the right is a diffeomorphism, given $\varepsilon \in [0,\kappa]$, there exists a unique parameter $p(\varepsilon) \in P$ given by a differentiable function of ε such that

$$\tilde{N}(t_\ell+\varepsilon) = N(t_\ell+\varepsilon, p(\varepsilon)), \tag{B.14}$$

i.e., there exists a unique trajectory in the family $\mathscr{E}$ of strictly bang-bang extremals that passes through the point $(t_\ell+\varepsilon,\tilde{N}(t_\ell+\varepsilon))$ and we denote the associated parameter by $p(\varepsilon)$. We now concatenate the controlled trajectory $(\tilde{N},\tilde{u})$ with the controlled trajectory $(N(\cdot,p(\varepsilon)),u(\cdot,p(\varepsilon)))$ at time $t_\ell+\varepsilon$ (see Figure B.1). Define the control u_ε over the interval $[t_\ell,T]$ as

$$u_\varepsilon(t) = \begin{cases} \tilde{u}(t) & \text{if} \quad t_\ell \le t < t_\ell+\varepsilon, \\ u(t,p(\varepsilon)) & \text{if} \quad t_\ell+\varepsilon \le t \le T, \end{cases}$$

so that the corresponding trajectory is given by

$$N_\varepsilon(t) = \begin{cases} \tilde{N}(t) & \text{if} \quad t_\ell \le t < t_\ell+\varepsilon, \\ N(t,p(\varepsilon)) & \text{if} \quad t_\ell+\varepsilon \le t \le T. \end{cases}$$

Note that for $\varepsilon = 0$ this reduces to the reference controlled trajectory,

$$u_0(t) = u(t,p_*) = u_*(t) \qquad \text{and} \qquad N_0(t) = N(t,p_*) = N_*(t) \qquad \text{for} \quad t_\ell \le t \le T.$$

The corresponding cost is given by

$$\Gamma(\varepsilon) = \int_{t_\ell}^{t_\ell+\varepsilon} \left\{ q\tilde{N}(z) + s\tilde{u}(z) \right\} dz + C(t_\ell+\varepsilon, p(\varepsilon))$$

where, as above,

$$C(t,p) = \int_t^T \{qN(z,p) + su(zx,p)\}\,dz + rp$$

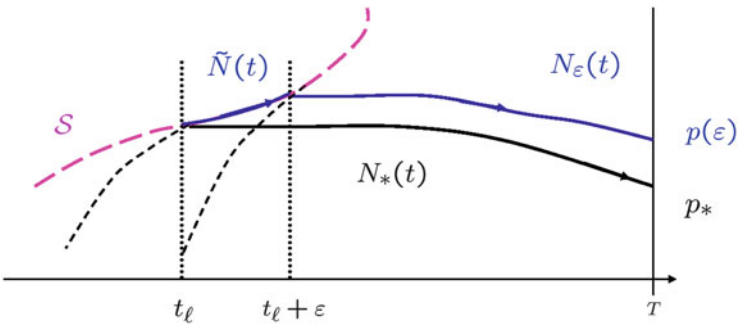

Fig. B.1 The 1-parameter family of controlled trajectories N_ε.

denotes the cost of the parameterized extremal with initial condition $N(t,p)$ at time t.

We will now show that all these trajectories have the same cost, i.e., that $\Gamma(\varepsilon) \equiv \Gamma(0)$ for all $\varepsilon \in [0,\kappa]$. (In the language of optimal control, the switching surface $\mathscr{S}_\ell$ is an envelope for the control system [292, Definition 5.4.5 and Theorem 6.1.2]). The function $\Gamma(\varepsilon)$ is differentiable in ε and it suffices to show that its derivative vanishes on $[0,\kappa]$. We have for almost every $\varepsilon \in [0,\kappa]$ that

$$\frac{d\Gamma}{d\varepsilon}(\varepsilon) = q\tilde{N}(t_\ell+\varepsilon) + s\tilde{u}(t_\ell+\varepsilon) + \frac{\partial C}{\partial t}(t_\ell+\varepsilon, p(\varepsilon)) + \frac{\partial C}{\partial p}(t_\ell+\varepsilon, p(\varepsilon))\frac{dp}{d\varepsilon}(\varepsilon). \tag{B.15}$$

By definition of $C(t,p)$, we have that

$$\frac{\partial C}{\partial t}(t_\ell+\varepsilon, p(\varepsilon)) = -qN(t_\ell+\varepsilon, p(\varepsilon)) - su(t_\ell+\varepsilon, p(\varepsilon))$$

and it follows from equation (B.12) that

$$\frac{\partial C}{\partial p}(t_\ell+\varepsilon, p(\varepsilon)) = \lambda(t_\ell+\varepsilon, p(\varepsilon))\frac{\partial N}{\partial p}(t_\ell+\varepsilon, p(\varepsilon))$$

where the partial derivatives of N with respect to p are evaluated from the right. The parameters $p(\varepsilon)$ are defined as solutions to equation (B.14), $N(t_\ell+\varepsilon, p(\varepsilon)) = \tilde{N}(t_\ell+\varepsilon)$, and thus (B.15) simplifies to

$$\frac{d\Gamma}{d\varepsilon}(\varepsilon) = s[\tilde{u}(t_\ell+\varepsilon) - u(t_\ell+\varepsilon, p(\varepsilon))] + \frac{\partial C}{\partial p}(t_\ell+\varepsilon, p(\varepsilon))\frac{dp}{d\varepsilon}(\varepsilon).$$

We need to compute $\frac{dp}{d\varepsilon}$. In terms of the flow $F_{\ell+1}$ defined for $t \geq \tau_\ell(p)$, equation (B.14) gives that

$$(t_\ell + \varepsilon, p(\varepsilon)) = F_\ell^{-1}(t_\ell + \varepsilon, \tilde{N}(t_\ell + \varepsilon))$$

and thus differentiating with respect to ε yields

$$\begin{pmatrix} 1 \\ \frac{dp}{d\varepsilon}(\varepsilon) \end{pmatrix} = (DF_\ell(t_\ell + \varepsilon, p(\varepsilon)))^{-1} \begin{pmatrix} 1 \\ \frac{d\tilde{N}}{d\varepsilon}(t_\ell + \varepsilon) \end{pmatrix}$$

$$= \begin{pmatrix} 1 & 0 \\ \frac{\partial N}{\partial t}(t_\ell + \varepsilon, p(\varepsilon)) & \frac{\partial N}{\partial p}(t_\ell + \varepsilon, p(\varepsilon)) \end{pmatrix}^{-1} \begin{pmatrix} 1 \\ \frac{d\tilde{N}}{d\varepsilon}(t_\ell + \varepsilon) \end{pmatrix}$$

$$= \begin{pmatrix} 1 & 0 \\ -\left(\frac{\partial N}{\partial p}(t_\ell + \varepsilon, p(\varepsilon))\right)^{-1} \left(\frac{\partial N}{\partial t}(t_\ell + \varepsilon, p(\varepsilon))\right) & \left(\frac{\partial N}{\partial p}(t_\ell + \varepsilon, p(\varepsilon))\right)^{-1} \end{pmatrix} \times \begin{pmatrix} 1 \\ \frac{d\tilde{N}}{d\varepsilon}(t_\ell + \varepsilon) \end{pmatrix}$$

Hence

$$\frac{dp}{d\varepsilon}(\varepsilon) = \left(\frac{\partial N}{\partial p}(t_\ell + \varepsilon, p(\varepsilon))\right)^{-1} \left[\frac{d\tilde{N}}{d\varepsilon}(t_\ell + \varepsilon) - \left(\frac{\partial N}{\partial t}(t_\ell + \varepsilon, p(\varepsilon))\right)\right].$$

Since $\tilde{N}$ is a trajectory of the system, we have that

$$\frac{d\tilde{N}}{d\varepsilon}(t_\ell + \varepsilon) = (A + \tilde{u}(t_\ell + \varepsilon)B)\tilde{N}(t_\ell + \varepsilon)$$

and from the parametrization of the extremals in the family $\mathscr{E}$ it follows that

$$\frac{\partial N}{\partial t}(t_\ell + \varepsilon, p(\varepsilon)) = (A + u(t_\ell + \varepsilon, p(\varepsilon))B)N(t_\ell + \varepsilon, p(\varepsilon)).$$

But $N(t_\ell + \varepsilon, p(\varepsilon)) = \tilde{N}(t_\ell + \varepsilon)$ and we therefore obtain that

$$\frac{dp}{d\varepsilon}(\varepsilon) = \left(\frac{\partial N}{\partial p}(t_\ell + \varepsilon, p_\varepsilon)\right)^{-1} [\tilde{u}(t_\ell + \varepsilon) - u(t_\ell + \varepsilon, p(\varepsilon))]\, BN(t_\ell + \varepsilon, p(\varepsilon)).$$

Hence

$$\begin{aligned} \frac{d\Gamma}{d\varepsilon}(\varepsilon) &= [\tilde{u}(t_\ell + \varepsilon) - u(t_\ell + \varepsilon, p(\varepsilon))]\, (s + \lambda(t_\ell + \varepsilon, q_\varepsilon)BN(t_\ell + \varepsilon, p(\varepsilon))) \\ &= [\bar{u}(t_\ell + \varepsilon) - u(t_\ell + \varepsilon, p(\varepsilon))]\, \Phi(t_\ell + \varepsilon, p(\varepsilon)), \end{aligned}$$

where, in the last line, $\Phi(t,p) = s + \lambda(t,p)BN(t,p)$ denotes the parameterized switching function (see Eq. (B.7)). But the points $(t_\ell + \varepsilon, N(t_\ell + \varepsilon, p(\varepsilon)))$ all lie on the switching surface $\mathscr{S}_\ell$ and therefore we have that

$$\Phi(t_\ell + \varepsilon, p(\varepsilon)) \equiv 0.$$

Hence $\frac{d\Gamma}{d\varepsilon}(\varepsilon) = 0$ and thus the function $\Gamma(\varepsilon)$ is constant.

The value of the objective for the reference controlled trajectory over the interval $[t_\ell, T]$, i.e., with initial condition $N_*(t_\ell)$ at time t_ℓ, is given by $\Gamma(0)$. If this trajectory is optimal, then so are all the other controlled trajectories $(N(\cdot, p(\varepsilon)), u(\cdot, p(\varepsilon)))$ in this one-parameter family since they have the same initial point and cost. But over the interval $(t_\ell, t_\ell + \varepsilon)$ the control $\tilde{u}$ takes values in the interior of the control set and thus this portion of the control is singular. But by Theorem 2.1.2 optimal controlled trajectories cannot have such an interval. Contradiction. Hence none of the controlled trajectories, including the reference, are optimal. □

B.1.4 Algorithmic Determination of Transversal Crossings and Folds

Theorems B.1.1 and B.1.2 decisively summarize the geometric properties that determine local optimality of a strictly bang-bang controlled trajectory: *if all switchings are transversal crossings, it is optimal, if there exists a switching that is a transversal fold, it is not*. These results apply to any single-input bilinear system and also to multi-input bilinear systems as long as only one of the controls switches at a particular switching surface. Locally, this of course is the typical (i.e., least degenerate) behavior. But it remains to provide an efficient numerical scheme that allows us to determine whether switchings are regular, and if so, whether they are transversal crossings or folds. For the 2-compartment model [CC2] we have that $B^2 = 0$, a relation generally not valid. We therefore derive these formulas in general without making this assumption.

For the moment, consider the following set-up: the controls have a strict bang-bang switching at time $t = \tau(p)$ defined by a differentiable function on P and we denote the constant controls for $t > \tau(p)$ and $t < \tau(p)$ by u_+ and u_-, respectively, with $\Delta u = u_+ - u_-$ the jump in the controls. For $p \in P$, let $N^+(t,p)$ and $N^-(t,p)$ denote the solutions to the dynamics

$$\dot{N} = (A + u_\pm B)N, \qquad N^\pm(\tau(p), p) = N(\tau(p), p).$$

Thus the trajectories of the system are given by $N^+(t,p)$ for $t \geq \tau(p)$ and by $N^-(t,p)$ for $t \leq \tau(p)$ and N^+ and N^- agree for the switching parameters $\mathscr{T} = \{(t,p) : t = \tau(p)\}$. Note that both functions N^+ and N^- are defined on a full neighborhood of $\mathscr{T}$. Later on, as above, our argument will proceed by induction backward from the terminal time. Recall that $\frac{\partial N^-}{\partial p}(T,p) \equiv \mathrm{Id}$ and that thus the matrix $\frac{\partial N^+}{\partial p}(\tau_k(p), p)$ at the last switching time is given by

$$\frac{\partial N^+}{\partial p}(\tau_k(p),p) = \exp\left((\tau_k(p)-T)(A+u_+B)\right)$$

with u_+ denoting the constant value of the reference control (0 or $u_{\max}$) over the interval $[t_k,T]$. In particular, this matrix is nonsingular. We thus inductively assume that the matrix $\frac{\partial N^+}{\partial p}(\tau(p),p)$ of the partial derivatives with respect to p taken from the right is nonsingular and first we need to determine whether the matrix $\frac{\partial N^-}{\partial p}(\tau(p),p)$, now with the partial derivatives with respect to p taken from the left along the trajectories corresponding to the control u_-, is nonsingular as well. If it is, the switching is regular.

While the states and costates remain continuous at the switching surface, their partial derivatives generally are discontinuous because of the two different controls used to the left and right of the switching surface. The jumps in these derivatives can be computed using the following elementary result. (For example, a proof is given in [292, Lemma 6.1.2]).

Lemma B.1.1. *Let $z_0 \in \mathbb{R}^n$ and let Z be an open neighborhood of z_0. Suppose $g : Z \to \mathbb{R}$ and $h : Z \to \mathbb{R}$ are continuously differentiable functions so that $h(z) = 0$ on $\{z \in Z : g(z) = 0\}$. If $g(z_0) = 0$ and $\nabla g(z_0) \neq 0$, then there exist a neighborhood W of z_0 contained in Z and a continuous function $k : W \to \mathbb{R}$ so that $h(z) = k(z)g(z)$ for $z \in W$ and $\nabla h(z_0) = k(z_0)\nabla g(z_0)$.*

We have that $h(t,p) = N^+(t,p) - N^-(t,p) = 0$ whenever $g(t,p) = t - \tau(p) = 0$ and $\nabla g(t,p) = (1, -\nabla\tau(p)) \neq 0$. Applying the Lemma, it follows that there exists a continuous real-valued function $k = k(t,p)$ defined near $\mathscr{T}$ such that for $(t,p) \in \mathscr{T}$ we have that

$$\nabla N^-(t,p) = \nabla N^+(t,p) + k(t,p)(1, -\nabla\tau(p)).$$

Considering the partial derivatives in t, it follows that

$$k(t,p) = (A+u_-B)N^-(t,p) - (A+u_+B)N^+(t,p) = -\Delta u B N(\tau(p),p)$$

and thus

$$\frac{\partial N^-}{\partial p}(\tau(p),p) = \frac{\partial N^+}{\partial p}(\tau(p),p) + \Delta u B N(\tau(p),p)\nabla\tau(p). \tag{B.16}$$

Hence $\frac{\partial N^-}{\partial p}(\tau(p),p)$ is a rank 1 correction of $\frac{\partial N^+}{\partial p}(\tau(p),p)$. The following fact from matrix algebra (e.g., see [292, Lemma 6.1.4]) gives us the desired update formulas.

Lemma B.1.2. *Suppose $A \in \mathbb{R}^{n\times n}$ is nonsingular and let u and v be vectors in $\mathbb{R}^n$. Then the matrix $B = A + uv^T$ is nonsingular if and only if $1 + v^T A^{-1} u \neq 0$. In this case*

$$(A+uv^T)^{-1} = A^{-1} - \frac{A^{-1}uv^TA^{-1}}{1+v^TA^{-1}u}.$$

Thus the matrix $\frac{\partial N^-}{\partial p}(\tau(p),p)$ is nonsingular if and only if

$$1+\Delta u\cdot\nabla\tau(p)\left(\frac{\partial N^+}{\partial p}(\tau(p),p)\right)^{-1}BN(\tau(p),p)\neq 0 \tag{B.17}$$

and in this case the inverse is given by

$$\left(\frac{\partial N^-}{\partial p}(\tau(p),p)\right)^{-1}=\left(\frac{\partial N^+}{\partial p}(\tau(p),p)\right)^{-1}\times\left(\mathrm{Id}-\frac{\Delta uBN(\tau(p),p)\nabla\tau(p)\left(\frac{\partial N^+}{\partial p}(\tau(p),p)\right)^{-1}}{1+\Delta u\nabla\tau(p)\left(\frac{\partial N^+}{\partial p}(\tau(p),p)\right)^{-1}BN(\tau(p),p)}\right).$$

The sign of the quantity in Eq. (B.17) determines whether a regular junction is a transversal crossing or a transversal fold. Recall from Proposition A.4.1 that the point $(\tau(p),p)$ is a regular switching point if and only if

$$1+\nabla\tau(p)\left(\frac{\partial N^+}{\partial p}(\tau(p),p)\right)^{-1}k(p)\neq 0. \tag{B.18}$$

The switching at $(\tau(p),p)$ is a transversal crossing if

$$1+\nabla\tau(p)\left(\frac{\partial N^+}{\partial p}(\tau(p),p)\right)^{-1}k(p)>0 \tag{B.19}$$

and a transversal fold if

$$1+\nabla\tau(p)\left(\frac{\partial N^+}{\partial p}(\tau(p),p)\right)^{-1}k(p)<0. \tag{B.20}$$

It remains to compute the quantity $\nabla\tau(p)\left(\frac{\partial N^+}{\partial p}(\tau(p),p)\right)^{-1}$. The function τ that defines the switchings is the solution of the equation

$$\Phi^+(t,p)=s+\lambda^+(t,p)BN^+(t,p)=0$$

for the parameterized switching function Φ^+ from the right with λ^+ denoting the adjoint variable corresponding to the control u_+. Since the reference extremal has strict bang-bang switchings it follows from the implicit function theorem that

$$\nabla\tau(p)=-\frac{\frac{\partial\Phi^+}{\partial p}(\tau(p),p)}{\frac{\partial\Phi^+}{\partial t}(\tau(p),p)}.$$

Differentiating $\Phi(t,p)$ with respect to p, it follows that

$$\frac{\partial \Phi^+}{\partial p}(t,p) = \lambda^+(t,p)B\frac{\partial N^+}{\partial p}(t,p) + \left(\frac{\partial \lambda^+}{\partial p}(t,p)BN^+(t,p)\right)^T.$$

By assumption, $\frac{\partial N^+}{\partial p}(t,p)$ is nonsingular near the parameterized switching set $\mathscr{T} = \{(t,p) : t = \tau(p)\}$ and thus the matrix

$$S^+(t,p) = \frac{\partial \lambda^{+T}}{\partial p}(t,p)\left(\frac{\partial N^+}{\partial p}(t,p)\right)^{-1} \tag{B.21}$$

is well-defined. Using it, we can write

$$\frac{\partial \Phi^+}{\partial p}(t,p) = \left\{\lambda(t,p)B + N^{+T}(t,p)B^T S^+(t,p)\right\}\frac{\partial N^+}{\partial p}(t,p)$$

and thus for $t = \tau(p)$ we have that

$$\begin{aligned}\nabla\tau(p)&\left(\frac{\partial N^+}{\partial p}(t,p)\right)^{-1} k(p) \\ &= -\frac{\Delta u}{\dot{\Phi}(t,p)}\left\{\lambda^+(t,p)B + N^{+T}(t,p)B^T S^+(t,p)\right\}BN^+(t,p)).\end{aligned} \tag{B.22}$$

Except for the matrix S^+, all the terms in this expression are known in a numerical computation of an extremal.

The matrix S^+ is easily computed. The partial derivatives $X = \frac{\partial N^+}{\partial p}$ and $Y = \frac{\partial \lambda^{+T}}{\partial p}$ are solutions of the corresponding variational equations for N and λ. But these equations are linear and thus X and Y are solutions of the matrix differential equations

$$\dot{X} = (A+uB)X \qquad \text{and} \qquad \dot{Y} = -(A+uB)^T Y.$$

But then the quotient $Z = YX^{-1}$ satisfies

$$\begin{aligned}\dot{Z} &= \dot{Y}X^{-1} + Y\frac{d}{dt}\left(X^{-1}\right) = \dot{Y}X^{-1} - YX^{-1}\dot{X}X^{-1} \\ &= -(A+uB)^T Z - Z(A+uB)\end{aligned}$$

and thus the matrix $S^+(t,p)$ is a solution to the linear Lyapunov equation

$$\dot{S} + S(A+uB) + (A+uB)^T S \equiv 0 \tag{B.23}$$

with constant coefficients. Over an interval $[t_0, t_1]$, this solution is given explicitly in the form

$$S(t) = \exp\left((A+uB)^T(t_1-t)\right) S(t_1) \exp\left((A+uB)(t_1-t)\right) \tag{B.24}$$

if the value at the terminal time t_1 is equal to $S(t_1)$.

Furthermore, the minimum condition of the maximum principle gives us that

$$\Delta u = u_+ - u_- = -u_{\max} \operatorname{sgn}\left(\dot{\Phi}(\tau(p), p)\right).$$

(For example, if $u_- = 0$ and $u_+ = u_{\max}$, then because of the minimization property of an extremal control the switching function decreases at a strict switching time $\tau(p)$ so that $\dot{\Phi}(\tau(p), p) < 0$.) Thus,

$$\frac{\Delta u}{\dot{\Phi}(t,p)} = -\frac{u_{\max}}{\left|\dot{\Phi}(t,p)\right|}.$$

It therefore follows from equation (B.22) that

$$\begin{aligned} &1 + \nabla\tau(p) \left(\frac{\partial N^+}{\partial p}(t,p)\right)^{-1} k(p) \\ &\quad = 1 + \frac{u_{\max}}{\left|\dot{\Phi}(t,p)\right|} \left\{\lambda^+(t,p)B + N^T(t,p)B^T S^+(t,p)\right\} BN(t,p). \end{aligned}$$

Equivalently, assuming that $\frac{\partial N^+}{\partial p}(\tau(p), p)$ is nonsingular, a switching is regular if and only if

$$\left|\dot{\Phi}(t,p)\right| + u_{\max} \left\{\lambda^+(t,p)B + N^T(t,p)B^T S^+(t,p)\right\} BN(t,p) \neq 0; \tag{B.25}$$

it is a transversal crossing if

$$\left|\dot{\Phi}(t,p)\right| + u_{\max} \left\{\lambda^+(t,p)B + N^T(t,p)B^T S^+(t,p)BN(t,p)\right\} > 0 \tag{B.26}$$

and a transversal fold if

$$\left|\dot{\Phi}(t,p)\right| + u_{\max} \left\{\lambda^+(t,p)B + N^T(t,p)B^T S^+(t,p)\right\} BN(t,p) < 0. \tag{B.27}$$

In particular, no partial derivatives of the state or costate with respect to the parameter p need to be calculated nor does one need to calculate an inverse. Everything is subsumed in the algorithmic computation of the matrix $S^+(t,p)$ at the switching points.

However, since the matrix S is defined in terms of the p-partials, it will no longer be continuous at switching times and we need to update formulas at the switchings. As above, let $S^+(t,p)$ and $S^-(t,p)$ denote the matrices S when constructed with $N^\pm$ and $\lambda^\pm$ respectively. The state N and costate λ are continuous at the switchings and so we simply write N and λ for these values. Then, and analogous to (B.16), we have that

$$S^-(\tau(p),p) = \frac{\partial\,(\lambda^-)^T}{\partial p}(\tau(p),p)\left(\frac{\partial N^-}{\partial p}(\tau(p),p)\right)^{-1}$$
$$= \left(-\Delta u B^T\lambda^T(\tau(p),p)\nabla\tau(p) + \frac{\partial\,(\lambda^+)^T}{\partial p}(\tau(p),p)\right)$$
$$\times\left(\Delta u BN(\tau(p),p)\nabla\tau(p) + \frac{\partial N^+}{\partial p}(\tau(p),p)\right)^{-1}.$$

To simplify the notation, set

$$G_\tau(p) = -\nabla\tau(p)\left(\frac{\partial N^+}{\partial p}(\tau(p),p)\right)^{-1}\Delta u$$
$$= \frac{\Delta u}{\dot\Phi(\tau(p),p)}\left\{\lambda(\tau(p),p)B + N^T(\tau(p),p)B^T S^+(\tau(p),p)\right\}.$$

Then, with all functions evaluated at $(\tau(p),p)$, it follows that

$$S^- = \left(B^T\lambda^T G_\tau + S^+\right)\frac{\partial N^+}{\partial p}\left((-BNG_\tau + \mathrm{Id})\frac{\partial N^+}{\partial p}\right)^{-1}$$
$$= \left(B^T\lambda^T G_\tau + S^+\right)(\mathrm{Id} - BNG_\tau)^{-1}$$
$$= \left(B^T\lambda^T G_\tau + S^+\right)\left(\mathrm{Id} + \frac{BNG_\tau}{1 - G_\tau BN}\right).$$

Recall that for a regular switching we have that

$$1 - G_\tau(p)BN(\tau(p),p) = 1 + \nabla\tau(p)\left(\frac{\partial N^+}{\partial p}(\tau(p),p)\right)^{-1}\Delta u BN(\tau(p),p) \neq 0$$

and thus this matrix is well defined. Summarizing, we have the following update formula for $S(t,p)$ at the switching $t = \tau(p)$:

Proposition B.1.2. *If the switching at $t = \tau(p)$ is regular, then with*

$$G_\tau(p) = \frac{\Delta u}{\dot\Phi(\tau(p),p)}\left\{\lambda(\tau(p),p)B + N^T(\tau(p),p)B^T S^+(\tau(p),p)\right\}$$

we have that $G_\tau(p)BN(\tau(p),p) \neq 1$ and

$$S^-(\tau(p),p) = \left(B^T\lambda^T(\tau(p),p)G_\tau(p) + S^+(\tau(p),p)\right)$$
$$\times\left(\mathrm{Id} + \frac{BN(\tau(p),p)G_\tau(p)}{1 - G_\tau(p)BN(\tau(p),p)}\right). \tag{B.28}$$

The algorithms presented in Theorem 2.1.5 for the 2-compartment optimal control problem [CC2] and in Theorem 2.2.2 for the general multi-input case then follow by propagating the flow of extremals between the various subdomains using this

update formula. At the terminal time T we have that $x(T,p) \equiv p$ and $\lambda(T,p) \equiv r$ so that

$$S^-(T,p) = \frac{\partial \lambda^T}{\partial p}(T,p)\left(\frac{\partial N}{\partial p}(T,p)\right)^{-1} \equiv 0.$$

Propagating the value of S through the last interval $[t_k, T]$, it follows from equation (B.24) that $S_k^+ = 0$ as well and thus the condition (B.25) for the last switching to be regular reduces to the following statement

$$\left|\dot{\Phi}_*(t_k)\right| + u_{\max}\lambda(t_k)B^2 N_*(t_k) \neq 0.$$

For the 2-compartment model [CC2] we have $B^2 = 0$ and thus the last switching is always a transversal crossing. The matrix S_k^- is then computed through the update-formula (B.28). In general, these updates are given by

$$S_i^- = \left(B^T\lambda_*^T(t_i)G_i + S_i^+\right)\left(\mathrm{Id} + \frac{BN_*(t_i)G_i}{1 - G_i B N_*(t_i)}\right)$$

where

$$G_i = -\frac{u_{\max}}{\left|\dot{\Phi}_*(t_i)\right|}\left(\lambda_*(t_i)B + N_*^T(t_i)B^T S_i^+\right).$$

In between the switching surfaces, the matrix S is simply propagated as the solution to a linear Lyapunov equation using equation (B.24). This verifies the algorithms presented in Chapter 2.

B.2 Proof of Theorem 2.2.8

We consider the optimal control problem [CC3b] from Section 2.2.3. The aim is to show that if (N_*, u_*, v_*) is an optimal controlled trajectory and

$$a_1 + a_2(1 - v_{\max}) - 2a_3 \geq 0,$$

then there also does not exist an interval on which the control u_* is singular.

Suppose u_* is singular on an open interval I, i.e., $\Phi_1(t) \equiv 0$ on I. It follows from Theorem 2.2.7 that v_* cannot be singular on any subinterval and thus, without loss of generality, we may assume that v_* is constant on I, $v_*(t) \equiv v$, given by either 0 or $v_{\max}$. The first and second derivatives of the switching function Φ_1 are thus given by

$$\dot{\Phi}_1(t) = \{\lambda(t)[A + vB_2, B_1] - qB_1\}N_*(t) \equiv 0$$

and

$$\begin{aligned}\ddot{\Phi}_1(t) = {} & \lambda(t)[A + u_*(t)B_1 + vB_2, [A + vB_2, B_1]]N_*(t) \\ & - q[A + vB_2, B_1]N_*(t) - qB_1(A + u_*(t)B_1 + vB_2)N_*(t).\end{aligned}$$

For this model we have that $B_1^2 = 0$ and thus

$$\ddot{\Phi}_1(t) = \{\lambda(t)[A+vB_2,[A+vB_2,B_1]] - q[A+vB_2,B_1] - qB_1(A+vB_2)\}N_*(t) + u_*(t)\lambda(t)[B_1,[A+vB_2,B_1]]N_*(t).$$

But for this system, the coefficient at the control u_* vanishes. Indeed,

$$[A+vB_2,B_1] = 2a_3\begin{pmatrix} 0 & -a_2(1-v) & a_3-a_1 \\ 0 & 0 & a_1 \\ 0 & 0 & 0 \end{pmatrix}$$

and this matrix commutes with B_1,

$$[B_1,[A+vB_2,B_1]] = [A+vB_2,B_1]B_1 - B_1[A+vB_2,B_1] \equiv 0.$$

Hence the second derivative of the switching function does not depend on the control u and it becomes necessary to differentiate further. In such a case it follows from general facts in Lie algebra that the control u cannot appear in the third derivative and we need to compute at least the fourth derivative. The singular control is at least of intrinsic order 2 in this case (c.f., Definition A.3.5).

In order to simplify the notation, it is convenient to switch to a formalism of Lie derivatives. Let

$$f(N) = (A+vB_2)N \qquad \text{and} \qquad g(N) = B_1N$$

denote the linear drift and control vector fields. For higher order derivatives the notation $\mathrm{ad}_X Y = [X,Y]$ for the Lie bracket (c.f., Definition A.3.3) becomes more convenient and we define $\mathrm{ad}_X^n Y$ inductively as

$$\mathrm{ad}_X^n Y = \mathrm{ad}_X \circ \mathrm{ad}_X^{n-1} Y.$$

For the linear vector fields $f(N)$ and $g(N)$ we have that

$$[f,g](N) = B_1(A+vB_2)N - (A+vB_2)B_1N = [A+vB_2,B_1]N$$

and the first two derivatives of the switching function Φ_1 can be expressed as

$$\dot{\Phi}_1(t) = \lambda(t)[f,g](N_*(t)) - qB_1N_*(t),$$
$$\ddot{\Phi}_1(t) = \lambda(t)[f+u_*g,[f,g]](N_*(t)) - q[A+vB_2,B_1]N_*(t) - qB_1(A+vB_2)N_*(t).$$

Hence

$$[g,[f,g]](N) = [B_1,[A+vB_2,B_1]]N \equiv 0$$

so that the vector field $[g,[f,g]]$ vanishes identically. In terms of the ad-notation, the formula for the second derivative can be rewritten more compactly as

$$\ddot{\Phi}_1(t) = \lambda(t)\left(\mathrm{ad}_f^2 g\right)(N_*(t)) - q\left(\mathrm{ad}_f g\right)(N_*(t)) - qB_1(A+vB_2)N_*(t) \qquad \text{(B.29)}$$

with

$$\left(\mathrm{ad}_f g\right)(N_*(t)) = [A + vB_2, B_1]N_*(t)$$

and

$$\left(\mathrm{ad}_f^2 g\right)(N_*(t)) = [A + vB_2, [A + vB_2, B_1]]\,N_*(t).$$

We now differentiate (B.29) once more, using Proposition 2.2.3 for the first term and the dynamics for all the terms with q. This yields that

$$\begin{aligned}
\Phi_1^{(3)}(t) &= \lambda(t)\left\{\left(\mathrm{ad}_f^3 g\right)(N_*(t)) + u_*(t)[g, \mathrm{ad}_f^2 g](N_*(t))\right\} - q\left(\mathrm{ad}_f^2 g\right)(N_*(t)) \\
&\quad - q[A + vB_2, B_1]\,(A + u_*(t)B_1 + vB_2)\,N_*(t) \\
&\quad - qB_1\,(A + vB_2)\,(A + u_*(t)B_1 + vB_2)\,N_*(t) \\
&= \lambda(t)\left(\mathrm{ad}_f^3 g\right)(N_*(t)) - q\left(\mathrm{ad}_f^2 g\right)(N_*(t)) \\
&\quad - q\left\{[A + vB_2, B_1]\,(A + vB_2) + B_1\,(A + vB_2)^2\right\}N_*(t) \\
&\quad + u_*(t)\left\{[g, \mathrm{ad}_f^2 g](N_*(t)) - q\left([A + vB_2, B_1]B_1 + B_1\,(A + vB_2)\,B_1\right)N_*(t)\right\}.
\end{aligned}$$

It follows from Lie algebraic facts about vector fields that the coefficient at the control u must vanish. In fact, since the vector field $[g,[f,g]]$ vanishes identically, the Jacobi identity and anticommutativity of the Lie bracket imply that

$$\begin{aligned}
[g, \mathrm{ad}_f^2 g](N_*(t)) &= [g,[f,[f,g]]] \\
&= -[f,[[f,g],g]] - [[f,g],[g,f]] \\
&= [f,[g,[f,g]]] = [f,0] \equiv 0.
\end{aligned} \tag{B.30}$$

Furthermore, as is easily verified, the matrices $[A + vB_2, B_1]\,B_1$ and $B_1\,(A + vB_2)\,B_1$ vanish as well. Thus the control u_* only appears in the fourth derivative $\Phi_1^{(4)}$. This occurs linearly and the term multiplying u_* is the coefficient that we need for the generalized Legendre-Clebsch condition. For a control of intrinsic order 2, the generalized Legendre-Clebsch condition (see Theorem A.3.2 in Appendix A) takes the form

$$(-1)^2 \frac{\partial}{\partial u}\frac{d^4}{dt^4}\frac{\partial H}{\partial u}(\lambda(t), N_*(t), u_*(t), v_*(t)) \geq 0 \qquad \text{for all } t \in I.$$

By differentiating (B.29) once more and taking the coefficient that arises at the control u_*, we obtain that the

$$\begin{aligned}
\frac{\partial}{\partial u}\frac{d^4}{dt^4}\frac{\partial H}{\partial u}(\lambda(t), N_*(t), u_*(t), v) &= \lambda(t)\left[g, \left(\mathrm{ad}_f^3 g\right)\right](N_*(t)) \\
&\quad - q\,[A + vB_2, [A + vB_2, B_1]]\,B_1 N_*(t) \\
&\quad - q[A + vB_2, B_1]\,(A + vB_2)\,B_1 N_*(t) \\
&\quad - qB_1\,(A + vB_2)^2\,B_1 N_*(t).
\end{aligned} \tag{B.31}$$

We first compute the term multiplying q. Since each matrix is multiplied with B_1 on the right, we only need the first rows of the other factors, but we need the commutator anyway to compute $\left[g, \left(\mathrm{ad}_f^3 g\right)\right]$. Somewhat longer, but nevertheless direct computations verify that the matrix

$$[A+vB_2,[A+vB_2,B_1]] = [A+vB_2,B_1](A+vB_2) - (A+vB_2)[A+vB_2,B_1]$$

is given by $2a_3$ times the matrix

$$\begin{pmatrix} -a_1a_2(1-v) & a_2^2(1-v)^2 + (a_3-2a_1)a_2(1-v) & -(a_3-a_1)^2 \\ 0 & 2a_1a_2(1-v) & -a_1(2a_3-a_1) + a_1a_2(1-v) \\ 0 & 0 & -a_1a_2(1-v) \end{pmatrix}$$

and upon multiplication with B_1 we get that

$$[A+vB_2,[A+vB_2,B_1]]B_1 = 4a_3^2 \begin{pmatrix} 0\,0 & a_1a_2(1-v) \\ 0\,0 & 0 \\ 0\,0 & 0 \end{pmatrix} = -2a_1a_2a_3(1-v)B_1.$$

In fact, it also holds that

$$[A+vB_2,B_1](A+vB_2)B_1 = 4a_3^2 \begin{pmatrix} 0\,0 & a_1a_2(1-v) \\ 0\,0 & 0 \\ 0\,0 & 0 \end{pmatrix} = -2a_1a_2a_3(1-v)B_1$$

and

$$B_1(A+vB_2)^2 B_1 = 4a_3^2 \begin{pmatrix} 0\,0 & a_1a_2(1-v) \\ 0\,0 & 0 \\ 0\,0 & 0 \end{pmatrix} = -2a_1a_2a_3(1-v)B_1$$

as well. All these matrices are equal and the term involving q is given by

$$\begin{aligned} &-q\left\{[A+vB_2,[A+vB_2,B_1]]B_1 + [A+vB_2,B_1](A+vB_2)B_1 + B_1(A+vB_2)^2 B_1\right\} N_*(t) \\ &\quad = 6a_1a_2a_3(1-v)qB_1N_*(t). \end{aligned} \tag{B.32}$$

It remains to compute the first term,

$$\left[g, \left(\mathrm{ad}_f^3 g\right)\right](N_*(t)) = [B_1,[A+vB_2,[A+vB_2,[A+vB_2,B_1]]]]N_*(t).$$

We only need the first column and last row of the matrix

$$[A+vB_2,[A+vB_2,[A+vB_2,B_1]]].$$

For, if this matrix has entries $(m_{ij})_{1\le i,j\le 3}$, then the commutator with B_1 is of the form

$$[B_1,[A+vB_2,[A+vB_2,[A+vB_2,B_1]]]] = 2a_3 \begin{pmatrix} m_{31} & m_{32} & m_{33}-m_{11} \\ 0 & 0 & -m_{21} \\ 0 & 0 & -m_{31} \end{pmatrix}.$$

A lengthier computation verifies that these entries are of the form

$$m_{ij} = 2a_1a_2a_3(1-v)\tilde{m}_{ij}$$

where

$$\begin{aligned} \tilde{m}_{11} &= -2a_1 + a_2(1-v) + a_3, \\ \tilde{m}_{21} &= 3a_1, \quad \tilde{m}_{31} = 0, \quad \tilde{m}_{32} = -3a_2, \\ \tilde{m}_{33} &= -a_1 - a_2(1-v) + 2a_3. \end{aligned}$$

Hence

$$\begin{aligned} &[B_1,[A+vB_2,[A+vB_2,[A+vB_2,B_1]]]] \\ &\quad = 12a_1a_2a_3^2(1-v) \begin{pmatrix} 0 & -a_2(1-v) & \frac{1}{3}(a_1-2a_2(1-v)+a_3) \\ 0 & 0 & -a_1 \\ 0 & 0 & 0 \end{pmatrix}. \end{aligned}$$

The generalized Legendre-Clebsch condition (B.31) therefore takes the form

$$\begin{aligned} &\frac{\partial}{\partial u}\frac{d^4}{dt^4}\frac{\partial H}{\partial u}(\lambda(t),N_*(t),u_*(t),v) \\ &= \lambda(t)\left[g,\left(\mathrm{ad}_f^3 g\right)\right](N_*(t)) + 6a_1a_2a_3(1-v)qB_1N_*(t) \\ &= 12a_1a_2a_3^2(1-v)\left\{\lambda(t)\begin{pmatrix} 0 & -a_2(1-v) & \frac{1}{3}(a_1-2a_2(1-v)+a_3) \\ 0 & 0 & -a_1 \\ 0 & 0 & 0 \end{pmatrix}\right. \\ &\qquad\qquad \left. +q\begin{pmatrix} 0 & 0 & -1 \\ 0 & 0 & 0 \\ 0 & 0 & 0 \end{pmatrix}\right\}N_*(t). \end{aligned}$$

The fact that $\dot{\Phi}_1(t) \equiv 0$ implies that we have $\{\lambda(t)[A+vB_2,B_1]-qB_1\}N_*(t) \equiv 0$, i.e.,

$$0 = 2a_3\left\{\lambda(t)\begin{pmatrix} 0 & -a_2(1-v) & a_3-a_1 \\ 0 & 0 & a_1 \\ 0 & 0 & 0 \end{pmatrix} - q\begin{pmatrix} 0 & 0 & -1 \\ 0 & 0 & 0 \\ 0 & 0 & 0 \end{pmatrix}\right\}N_*(t).$$

Multiplying this equation by $6a_1a_2a_3(1-v)$ and adding it to the first yields that

$$\frac{\partial}{\partial u}\frac{d^4}{dt^4}\frac{\partial H}{\partial u}(\lambda(t),N_*(t),u_*(t),v) = 24a_1a_2a_3^2(1-v) \times \lambda(t)\begin{pmatrix} 0 & -a_2(1-v) & -\frac{1}{3}(a_1+a_2(1-v)-2a_3) \\ 0 & 0 & 0 \\ 0 & 0 & 0 \end{pmatrix} N_*(t).$$

This quantity is negative (and in this case singular controls are not optimal) if and only if

$$-a_2(1-v)N_2(t) - \frac{1}{3}(a_1+a_2(1-v)-2a_3)N_3(t) < 0$$

or, equivalently, if and only if

$$-3a_2(1-v)\frac{N_2(t)}{N_3(t)} - a_1 - a_2(1-v) + 2a_3 < 0.$$

Since the states $N_i(t)$ are positive, an immediate sufficient condition for this to hold is that $-a_1 - a_2(1-v) + 2a_3 < 0$. This proves Theorem 2.2.8.

Although this argument does not exclude singular controls u altogether, they are highly unlikely to exist even if $a_1 + a_2(1-v) < 2a_3$. The reason is that generically the dimension of the state-space, $n = 3$, is too small for a singular arc to be of order 2. In fact, the condition $\Phi_1(t) \equiv 0$ determines the multiplier $\lambda_1(t)$ in terms of the state $N_3(t)$. Then the condition that $\dot{\Phi}_1(t) \equiv 0$ allows to solve for the multiplier $\lambda_2(t)$ in terms of the states $N(t)$. An additional necessary condition of the maximum principle is that the Hamiltonian function must be constant along the optimal controlled trajectory and the value of the constant is determined by the endpoint of the trajectory. It is then possible to determine the multiplier $\lambda_2(t)$ along the singular arc from this third condition. Having the multiplier, for an order 1 singular control, then the singular control is obtained by solving the equation $\ddot{\Phi}_1(t) \equiv 0$ for u and, if this control is admissible, in dimension 3 this forms a well-defined closed set of conditions. However, if the order is higher like it is the case here, then additional conditions need to be satisfied. Since the second derivative does not depend on the control, with the multipliers replaced by the conditions imposed by the switching function, its derivative and $H \equiv \text{const}$, the equation $\dddot{\Phi}_1(t) \equiv 0$ poses an additional constraint on the states of the system to be satisfied. Generically (i.e., under "typical" conditions) this defines a surface in the state-space on which the singular trajectories need to lie. But then the condition $\Phi_1^{(3)}(t) \equiv 0$ imposes a second such condition and thus generically singular trajectories can only be very special curves that lie in the intersections of these surfaces. Thus, a higher order singular control imposes severe additional requirements on the location where the corresponding trajectories can only lie. Therefore, typically, i.e., for most values of the parameters a_i and $v_{\max}$, optimal trajectories simply will not contain singular arcs.

B.3 Proof of Theorem 3.3.1

Recall that we consider a 3-compartment model consisting of chemotherapeutically sensitive, partially sensitive and resistant subpopulations with x, y and z denoting the proportions of the respective populations. The dynamics obeys the following Riccati differential equations:

$$\begin{aligned}
\dot{x} &= x(\alpha_1 - \rho_{12} - \rho_{13}) + y\rho_{21} + z\rho_{31} - x(\alpha_1 x + \alpha_2 y + \alpha_3 z),\\
\dot{y} &= x\rho_{12} + y(\alpha_2 - \rho_{21} - \rho_{23}) + z\rho_{32} - y(\alpha_1 x + \alpha_2 y + \alpha_3 z),\\
\dot{z} &= x\rho_{13} + y\rho_{23} + z(\alpha_3 - \rho_{32} - \rho_{33}) - z(\alpha_1 x + \alpha_2 y + \alpha_3 z).
\end{aligned}$$

and the aim is to show that there exists a unique equilibrium point $(x_*, y_*, z_*) \in \Sigma$ that is globally asymptotically stable, i.e., contains the entire simplex Σ in its region of attraction.

Because of symmetries in the differential equations, without loss of generality, i.e., by relabeling the states if necessary, we may assume that

$$\alpha_1 \geq \alpha_2 \geq \alpha_3.$$

Since $x+y+z \equiv 1$, the dynamics is 2-dimensional and we use x and y as the variables setting $z = 1-x-y$. We also consider Σ as a subset of (x,y)-space in $\mathbb{R}^2$,

$$\Sigma = \left\{(x,y) \in \mathbb{R}^2 : x \geq 0, y \geq 0, x+y+z \leq 1\right\}.$$

For $x = 0$ we have that $\dot{x}_{|x=0} = y\rho_{21} + z\rho_{31}$. At least one of y or z must be positive and thus it follows that $\dot{x}_{|x=0} > 0$. Analogously, we have that

$$\dot{y}_{|y=0} = x\rho_{12} + z\rho_{32} > 0 \qquad \text{and} \qquad \dot{z}_{|z=0} = x\rho_{13} + y\rho_{23} > 0.$$

Hence all trajectories starting at a point (x_0, y_0) in the boundary of Σ, $\partial\Sigma$, enter Σ forward in time, i.e., Σ is positively invariant.

Given an arbitrary initial condition $(x_0, y_0) \in \partial\Sigma$, the ω-limit set $\Omega(x_0, y_0)$ is defined as the set of all accumulation points of the positive semi-trajectory $\{(x(t;x_0,y_0), y(t;x_0,y_0)) : t > 0\}$ as $t \to \infty$. It is clear that, for all $(x_0, y_0) \in \partial\Sigma$ the ω-limit set $\Omega(x_0, y_0)$ is nonempty. It follows from Poincaré's theorem [145] that this limit set is a periodic orbit if it does not contain an equilibrium point. Since, by elementary index theory, any periodic orbit contains at least one equilibrium point (x_*, y_*) inside its trajectory [145], it follows that the dynamics (3.17)–(3.18) has at least one equilibrium point inside Σ. If (i) this equilibrium point is unique and if (ii) there exist no periodic orbits, then this implies that the system (3.17)–(3.18) is globally asymptotically stable with Σ its region of attraction. For, by (ii), for any initial condition (x_0, y_0) in the boundary of Σ, the ω-limit set $\Omega(x_0, y_0)$ consists of exactly one equilibrium point and thus, by (i), every trajectory $(x(t;x_0,y_0), y(t;x_0,y_0))$ converges to (x_*, y_*) as $t \to \infty$. It thus remains to establish these two properties.

Lemma B.3.1. *There exists exactly one equilibrium point in the unit simplex Σ.*

Proof. Using $z = 1 - x - y$, the equations defining the equilibria are given by

$$(\alpha_3 - \alpha_1)x^2 + (\alpha_1 - \alpha_3 - \rho_{12} - \rho_{13} - \rho_{31})x - (\alpha_2 - \alpha_3)xy + \rho_{21}y + \rho_{31}(1-y) = 0,$$

and

$$(\alpha_3 - \alpha_2)y^2 + (\alpha_2 - \alpha_3 - \rho_{21} - \rho_{23} - \rho_{32})y - (\alpha_1 - \alpha_3)xy + \rho_{12}x + \rho_{32}(1-x) = 0.$$

We begin with the solutions to the first equation, $\dot{x} = 0$. On the boundary of the unit simplex Σ, since $\dot{x}_{|x=0} = y\rho_{21} + (1-y)\rho_{31} > 0$, there are no solutions for $x = 0$. But it is easily seen that, and regardless of the values of the parameters, there exist unique solutions $(x_u, y_u) \in \partial\Sigma$ on the line $x + y = 1$ and $(x_\ell, 0) \in \partial\Sigma$ on the x-axis: for, we have that

$$\dot{x}_{|x+y=1} = (\alpha_2 - \alpha_1)x^2 + (\alpha_1 - \alpha_2 - \rho_{12} - \rho_{13} - \rho_{21})x + \rho_{21}$$

and

$$\dot{x}_{|y=0} = (\alpha_3 - \alpha_1)x^2 + (\alpha_1 - \alpha_3 - \rho_{12} - \rho_{13} - \rho_{31})x + \rho_{31}.$$

If $\alpha_1 > \alpha_2$, then $\dot{x}_{|x+y=1}$ and $\dot{x}_{|y=0}$ are concave quadratic functions that are positive for $x = 0$ and negative for $x = 1$. Hence there exist unique zeroes x_u and x_ℓ that lie in the open interval $(0,1)$. If $\alpha_1 = \alpha_2 > \alpha_3$, then this argument still applies to $\dot{x}_{|y=0}$ while we can simply solve $\dot{x}_{|x+y=1} = 0$ to get

$$x_u = \frac{\rho_{21}}{\rho_{12} + \rho_{13} + \rho_{21}} \qquad \text{and} \qquad y_u = \frac{\rho_{12} + \rho_{13}}{\rho_{12} + \rho_{13} + \rho_{21}}.$$

If all growth rates are equal, $\alpha_1 = \alpha_2 = \alpha_3$, we get that

$$x_\ell = \frac{\rho_{31}}{\rho_{12} + \rho_{13} + \rho_{31}}.$$

The same argumentation can be used to show that there are no solutions (x,y) of the equation $\dot{x} = 0$ for $y > y_u$ while there exists a unique solution $(x,y) = (x(y),y) \in \Sigma$ for $y \in [0, y_u]$: if $\alpha_1 = \alpha_2 = \alpha_3$, this follows by simply solving the equation $\dot{x} = 0$ for x as

$$x = x(y) = \frac{\rho_{21}y + \rho_{31}(1-y)}{\rho_{12} + \rho_{13} + \rho_{31}}.$$

These values are nonnegative for $y \in [0,1]$ and we have that $x(y_u) = y_u$. Since $x(1) > 0$, the points $(x(y),y)$ lie above the line $x + y = 1$ for $y > y_u$ and below it for $y < y_u$. If $\alpha_1 > \alpha_3$, then, as above, the restrictions $\dot{x}_{|y=\text{const}}$ are concave quadratic functions that are positive for $x = 0$ and are positive for $x = y$ if $y > y_u$ and negative if $y < y_u$. Hence, for $y > y_u$ these functions have no zero in $[0,y]$ while they have a unique zero $x = x(y) \in (0,y)$ if $y < y_u$. Furthermore, by the implicit function theorem, $x = x(y)$ is a continuously differentiable function. Overall, it therefore follows that the restriction Γ_x of the curve $\dot{x} = 0$ to Σ is the graph of a continuously differentiable function defined over the interval $[0, y_u]$.

We need to know more about the geometry of this curve Γ_x. It is not difficult to describe the set $\dot{x} = 0$ exactly, but, depending on the parameter values, several cases need to be distinguished. We content ourselves with describing a typical situation assuming that $\alpha_1 > \alpha_2 > \alpha_3$ and leave it to the interested reader to supply the calculus type details for the remaining cases. The formulas and the geometry of the resulting curves actually simplify if equality relations hold. Generically, the curve $\dot{x} = 0$ is the graph of the rational function

$$\begin{aligned} y = y(x) &= \frac{(\alpha_3 - \alpha_1)x^2 + (\alpha_1 - \alpha_3 - \rho_{12} - \rho_{13} - \rho_{31})x + \rho_{31}}{(\alpha_2 - \alpha_3)x + \rho_{31} - \rho_{21}} \\ &= Ax + B + \frac{C}{x + D} \end{aligned} \tag{B.33}$$

with simple pole $x_p = -D$ and slanted asymptote $y = Ax + B$. We have that

$$A = -\frac{\alpha_1 - \alpha_3}{\alpha_2 - \alpha_3} < 0 \qquad \text{and} \qquad D = \frac{\rho_{31} - \rho_{21}}{\alpha_2 - \alpha_3}$$

and, making the generic assumptions that $C \neq 0$, $D \neq 0$ and $D \neq -1$, the remaining constants B and C can easily be computed from the values

$$y(0) = \frac{\rho_{31}}{\rho_{31} - \rho_{21}} = B + \frac{C}{D}$$

and

$$y(1) = -\frac{\rho_{12} + \rho_{13}}{\alpha_2 - \alpha_3 + \rho_{31} - \rho_{21}} = A + B + \frac{C}{1 + D}.$$

Note that the following sign relations hold:

$$Dy(0) = \frac{\rho_{31}}{\alpha_2 - \alpha_3} > 0 \qquad \text{and} \qquad (1 + D)y(1) = -\frac{\rho_{12} + \rho_{13}}{\alpha_2 - \alpha_3} < 0$$

Depending on the location of the pole x_p, three cases need to be distinguished: $x_p < 0$, $0 < x_p < 1$ and $x_p > 1$. The reasoning in each case is similar and we only describe the geometry for the second subcase $x_p \in (0, 1)$, i.e., for $-1 < D < 0$. (We refer the interested reader to [175] where an alternative argument is fully carried out.) The condition $\rho_{21} > \rho_{31}$ corresponds to the realistic case that the transition rate ρ_{21} from the partially resistant to the sensitive compartment is higher than the transition rate ρ_{31} from the fully resistant to the sensitive compartment. In this case, both $y(0)$ and $y(1)$ are negative. But depending on whether C is positive or negative, there still exist two subcases: if $C > 0$, the graph of y lies above the slanted asymptote for $x > x_p$ and below it for $x < x_p$ while these relations are reversed if $C < 0$. As a result, and using that $y(0) < 0$, if $C > 0$, there is no segment of $\dot{x} = 0$ that lies in Σ for $x < x_p$ while there exists a unique such segment for $x > x_p$. For $C < 0$, these relations are reversed and now there exists a unique segment of $\dot{x} = 0$ in Σ for $x < x_p$. We illustrate the

geometry of the corresponding rational functions in Figure B.2 and show blow-ups of the resulting segments of the curve $\dot{x} = 0$ that lie in Σ in Figure B.3.

In each case, the curve Γ_x (the segment of $\dot{x} = 0$ that lies in Σ) is the graph of either a strictly increasing function $y = \varphi(x)$ defined over the interval $[x_\ell, x_u]$ or a strictly decreasing function defined over $[x_u, x_\ell]$ with range given by $[0, y_u]$. This condition can be verified as well for all other cases (generic or nongeneric). For example, in the most degenerate case when $\alpha_2 = \alpha_3$ and $\rho_{21} = \rho_{31}$, Γ_x is simply the segment of the vertical line $y \equiv x_\ell = x_u$ inside Σ.

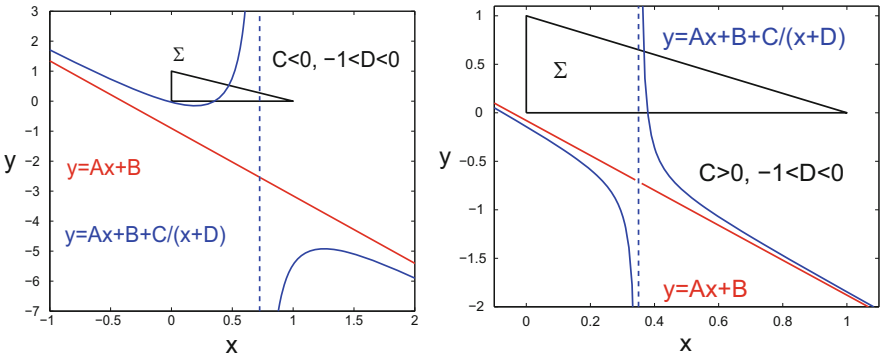

Fig. B.2 The graphs of the rational function $y(x) = Ax + B + \frac{C}{x+D}$ for $-1 < D < 0$ and $C < 0$ (left) and $C > 0$ (right).

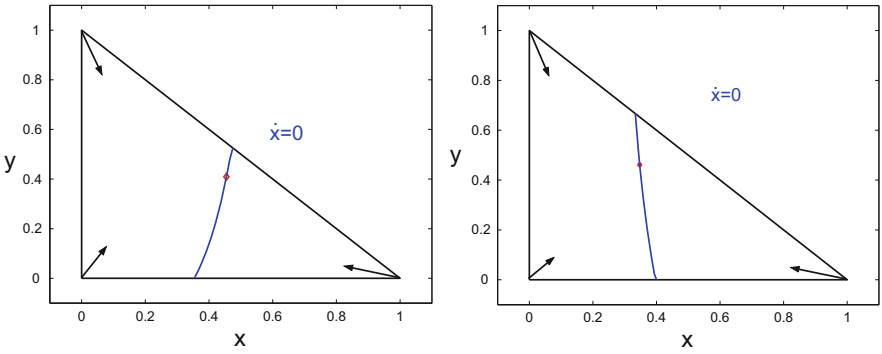

Fig. B.3 The segments Γ_x of the graphs of $y(x) = Ax + B + \frac{C}{x+D}$ in the unit simplex Σ.

It is clear, i.e., it follows by arguments invoking symmetry, that the geometry of solving the equation $\dot{y} = 0$ is entirely the same, only with the roles of x and y interchanged. Now we have $\dot{y}_{|y=0} = x\rho_{12} + (1-x)\rho_{32} > 0$ and thus there is no intersection with the x-axis in Σ, but there exist unique points $(0, \tilde{y}_\ell) \in \Sigma$ on the y-axis and $(\tilde{x}_h, \tilde{y}_h)$ on the line $x + y = 1$ that solve $\dot{y} = 0$. It is a matter of verification

to show that $\tilde{x}_h > x_u$ or, equivalently, that $y_u > \tilde{y}_h$. Here the curve $\dot{y} = 0$ is generically the graph of the rational function

$$x = x(y) = \frac{(\alpha_3 - \alpha_2)\,y^2 + (\alpha_2 - \alpha_3 - \rho_{21} - \rho_{23} - \rho_{32})\,y + \rho_{32}}{(\alpha_1 - \alpha_3)\,y + \rho_{32} - \rho_{12}} = \mathfrak{A}x + \mathfrak{B} + \frac{\mathfrak{C}}{x + \mathfrak{D}}$$

and the curve Γ_y (the segment of $\dot{y} = 0$ that lies in Σ) is the graph of either a strictly increasing function $x = \psi(y)$ defined over the interval $[\tilde{y}_\ell, \tilde{y}_h]$ or a strictly decreasing function defined over $[\tilde{y}_h, \tilde{y}_\ell]$ with range given by $[0, \tilde{x}_h]$. In the most degenerate case when $\alpha_1 = \alpha_3$ and $\rho_{12} = \rho_{32}$, this again simply becomes the segment of the horizontal line $x \equiv \tilde{y}_\ell = \tilde{y}_h$ in Σ. We illustrate the geometric shape of the curve Γ_y for the two most typical scenarios in Figure B.4.

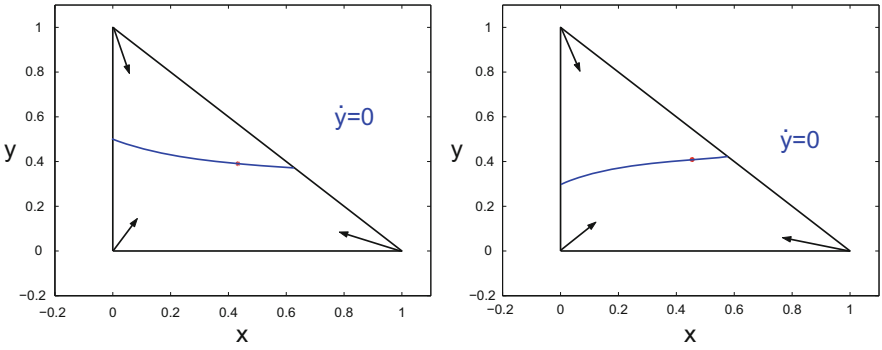

Fig. B.4 The segments Γ_y of the graphs of $y(x) = Ax + B + \frac{C}{x+D}$ in the unit simplex Σ.

Intersecting the graphs of the strictly monotonic function $y = \varphi(x)$ describing the curve Γ_x with the graph of the strictly monotonic function $x = \psi(y)$ describing the curve Γ_y results in at most one intersection point. Since $y_u > \tilde{y}_h$, or, since we already know that such an intersection point must exist, the result follows. □

Lemma B.3.2. *There do not exist periodic orbits in the unit simplex Σ.*

Proof. Unfortunately, Bendixson's criterion is not conclusive here and we need to resort to a more direct and technical argument. It follows from elementary index theory that any periodic orbit γ must contain the equilibrium point (x_*, y_*) in the region encircled by γ. No periodic orbit can therefore exist if there exists a trajectory $\{(x(t;x_0,y_0), y(t;x_0,y_0)) : t > 0\}$ that starts at a point (x_0, y_0) in the boundary of Σ and converges to the equilibrium point (x_*, y_*) as $t \to \infty$. (This simply is a consequence of uniqueness of solutions). This and similar arguments can be used in each case to preclude the existence of a periodic orbit. Here we only present two cases that are based on the geometric properties of the curves Γ_x or Γ_y for the generic cases.

Figure B.5 depicts the main geometric scenarios that arise. Both $\dot{x}$ and $\dot{y}$ are positive at the origin and we have $\dot{x} > 0$ and $\dot{y} < 0$ at the vertex $(0,1)$ and $\dot{x} < 0$

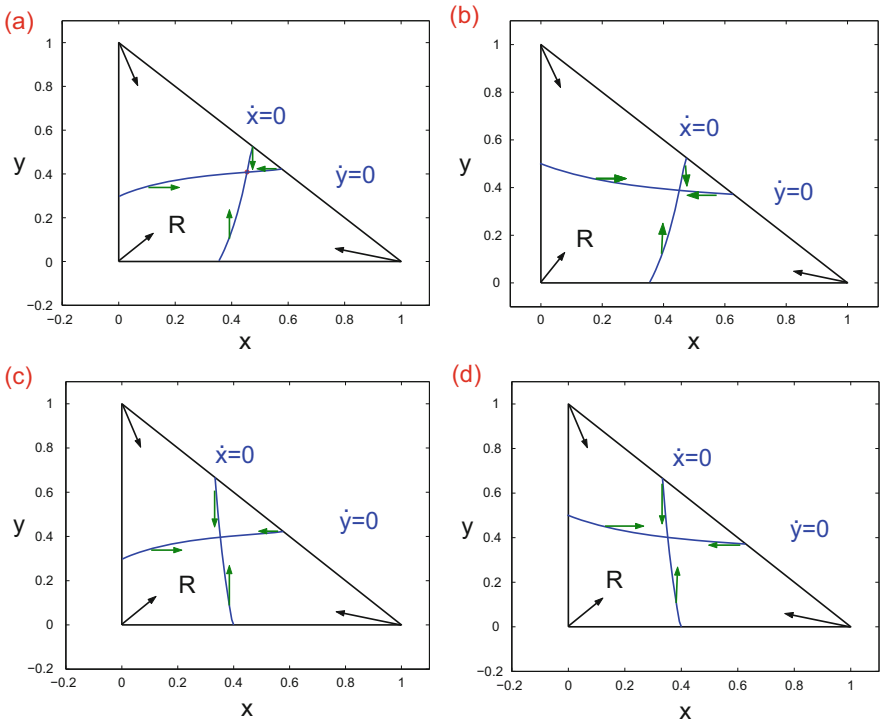

Fig. B.5 The main geometric scenarios that determine the regions bounded by the curves Γ_x and Γ_y and the directions of the vector field defining the dynamics (3.17) and (3.18).

and $\dot{y} > 0$ at the vertex $(1,0)$. This determines the directions of the vector fields in each of the subregions of Σ bounded by the curves Γ_x and Γ_y. Let R denote the subregion that has the origin in its boundary, so that both $\dot{x}$ and $\dot{y}$ are positive in R. All trajectories are inflowing into R in case (a) and outflowing from region R in case (d). Hence in these cases no periodic orbit γ can exist since it would need to both enter and leave this region R. Cases (b) and (c) are more intricate. Now the directions of the vector field in principle would allow for circular motions, but the geometry of the curves Γ_x and Γ_y actually prevents a return. This can be seen by setting up a simple dynamical system that bounds the solutions. Consider case (b) and let (x_0, y_0) be an initial condition on the curve Γ_x that lies below the equilibrium point (x_*, y_*). In particular, we have that

$$y_0 = Ax_0 + B + \frac{C}{x_0 + D}.$$

Then define the next point (x_1, y_1) by keeping $x_1 = x_0$ and defining y_1 to lie on the curve Γ_y, i.e., by solving

$$x_0 = \mathfrak{A}y_1 + \mathfrak{B} + \frac{\mathfrak{C}}{y_1 + \mathfrak{D}}$$

for y_1. Continuing this procedure, (x_2, y_2) is the point on the curve Γ_x for $y_2 = y_1$, i.e.,

$$y_1 = Ax_2 + B + \frac{C}{x_2 + D}$$

and (x_3, y_3) is the point on the curve Γ_y for $x = x_2$, i.e.,

$$x_2 = \mathfrak{A}y_3 + \mathfrak{B} + \frac{\mathfrak{C}}{y_3 + \mathfrak{D}}.$$

Finally, (x_4, y_4) is the return point on the curve Γ_x for $y_4 = y_3$, i.e.,

$$y_3 = Ax_4 + B + \frac{C}{x_4 + D}.$$

It follows from the geometric properties of the curves Γ_x and Γ_y that this return point is closer to the equilibrium point than the initial condition was. But a solution to the differential equations, if it were to return at all, needs to lie above the point (x_4, y_4). Thus no periodic orbits are possible. This proves the lemma. □

This concludes the proof of Theorem 3.3.1.

B.4 Synthesis of Optimal Controlled Trajectories for Antiangiogenic Therapy

We prove Theorem 5.3.1 and construct the synthesis of optimal controlled trajectories for model [H].

B.4.1 Analysis of Bang-Bang Junctions

We begin with the analysis of optimal bang-bang junctions. We first carry out a strictly local analysis of switchings that establishes the regions in (p, q)-space where optimal switchings from $u = u_{\max}$ to $u = 0$ or from $u = 0$ to $u = u_{\max}$ are possible. The singular base curve $\mathscr{S}_0$ and the diagonal $\mathscr{D}_0 = \{(p, q) : p = q\}$ form boundary curves to these regions. Denote by $\mathscr{S}_+$ the region outside of the singular loop $\mathscr{S}_0$ and by $\mathscr{S}_-$ the region inside this loop and then define the following regions (see Figure B.6)

$$I = \mathscr{D}_+ \cap \mathscr{S}_+, \quad II = \mathscr{D}_+ \cap \mathscr{S}_-, \quad III = \mathscr{D}_- \cap \mathscr{S}_-, \quad IV = \mathscr{D}_- \cap \mathscr{S}_+.$$

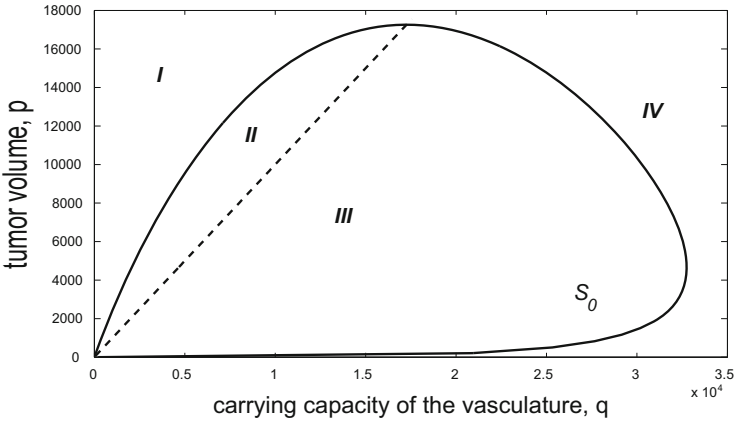

Fig. B.6 Definition of the regions *I*, *II*, *III*, and *IV*.

Proposition B.4.1. *Let u_* be an optimal control and denote the corresponding trajectory by (p_*,q_*). If $(p_*(t),q_*(t))$ lies in regions I or III, u_* can switch at time t only from $u=0$ to $u=u_{\max}$ and if $(p_*(t),q_*(t))$ lies in regions II or IV, u_* can only switch from $u=u_{\max}$ to $u=0$.*

Proof. Suppose an optimal control switches at time τ. At the junction the multiplier $\lambda(\tau)$ vanishes against $g(z_*(\tau))$ and $f(z_*(\tau))\equiv 0$. Except for points on the diagonal $\mathscr{D}_0=\{(p,q):p=q\}$, the vector fields f, g and the constant coordinate vector field $h=(0,0,1)^T$ are linearly independent and thus the Lie bracket $[f,g]$ can be written as a linear combination of these vector fields in the form

$$[f,g](z)=\rho(z)f(z)+\sigma(z)g(z)+\zeta(z)h,$$

namely,

$$\gamma p\begin{pmatrix}\xi\\ -b\\ 0\end{pmatrix}=\rho(z)\begin{pmatrix}-\xi p\ln\left(\frac{p}{q}\right)\\ bp-\left(\mu+dp^{\frac{2}{3}}\right)q\\ 0\end{pmatrix}+\sigma(z)\begin{pmatrix}0\\ -\gamma q\\ 1\end{pmatrix}+\zeta(z)\begin{pmatrix}0\\ 0\\ 1\end{pmatrix}.$$

This gives

$$\rho(z)=-\frac{\gamma}{\ln\left(\frac{p}{q}\right)}\quad\text{and}\quad\sigma(z)=\frac{b\frac{p}{q}\left(\ln\left(\frac{p}{q}\right)-1\right)+\left(\mu+dp^{\frac{2}{3}}\right)}{\ln\left(\frac{p}{q}\right)}=-\zeta(z).$$

Thus we have that

$$\begin{aligned}\dot{\Phi}(\tau) &= \langle \lambda(\tau), [f,g](z_*(\tau))\rangle \\ &= \rho(z_*(\tau))\,\langle \lambda(\tau), f(z_*(\tau))\rangle + \sigma(z_*(\tau))\,\langle \lambda(\tau), g(z_*(\tau))\rangle - \sigma(z_*(\tau))\lambda_3 \\ &= -\sigma(z_*(\tau))\lambda_3. \end{aligned} \tag{B.34}$$

Without loss of generality, by Lemma 5.2.3 we may assume that $\lambda_3 > 0$ and thus $\dot{\Phi}(\tau)$ and $\sigma(z_*(\tau))$ have opposite signs. The denominator of σ is positive in $\mathscr{D}_+ = \{(p,q) \in \mathscr{D} : p > q\}$ and negative in $\mathscr{D}_- = \{(p,q) \in \mathscr{D} : p < q\}$ while the zero set of the numerator of σ is the locus where the vector fields f and $[f,g]$ are linearly dependent, i.e., the singular base curve $\mathscr{S}_0$ (see (5.42)). We have labeled the regions so that the numerator is positive in $\mathscr{S}_+$ and negative in $\mathscr{S}_-$. Hence $\dot{\Phi}(\tau)$ is negative in regions *I* and *III* and positive in regions *II* and *IV*. Thus, whenever the switching function has a zero and $(p_*(\tau), q_*(\tau))$ lies in region *I* or *III*, then the switching function changes sign at time τ from positive to negative values and thus the control switches from $u = 0$ to $u = u_{\max}$. Analogously, whenever the switching function has a zero and $(p_*(\tau), q_*(\tau))$ lies in region *II* or *IV*, then the switching function changes sign at time τ from negative to positive values and thus the control switches from $u = u_{\max}$ to $u = 0$. □

We proceed to the analysis of bang-bang controls over the full interval. For the reader's convenience, we restate the form of the Hamiltonian and the adjoint equations for the model [H]:

$$\begin{aligned} H &= -\lambda_1 \xi p \ln\left(\frac{p}{q}\right) + \lambda_2\left(bp - \left(\mu + dp^{\frac{2}{3}}\right)q - \gamma u q\right) + \lambda_3 u, \\ &= -\lambda_1 \xi p \ln\left(\frac{p}{q}\right) + \lambda_2\left(bp - \left(\mu + dp^{\frac{2}{3}}\right)q\right) + \Phi u, \end{aligned}$$

and

$$\dot{\lambda}_1 = \xi\lambda_1\left(\ln\left(\frac{p}{q}\right) + 1\right) + \lambda_2\left(\frac{2}{3}d\frac{q}{p^{\frac{1}{3}}} - b\right), \qquad \lambda_1(T) = 1, \tag{B.35}$$

$$\dot{\lambda}_2 = -\xi\lambda_1\frac{p}{q} + \lambda_2\left(\mu + dp^{\frac{2}{3}} + \gamma u\right), \qquad \lambda_2(T) = 0. \tag{B.36}$$

We begin with some simple, but useful facts.

Lemma B.4.1. *Optimal controlled trajectories have no switching points on the diagonal.*

Proof. If $\Phi(\tau) = 0$ and $(p(\tau), q(\tau)) \in \mathscr{D}_0$, then the Hamiltonian reduces to

$$H = \lambda_2(\tau)p_*(\tau)\left(b - \mu - dp_*(\tau)^{\frac{2}{3}}\right) \equiv 0.$$

In the domain $\mathscr{D}$, i.e., for $0 < p < \bar{p} = \left(\frac{b-\mu}{d}\right)^{\frac{3}{2}}$, we have that

$$b - \mu - dp^{\frac{2}{3}} = d\left(\frac{b-\mu}{d} - p^{\frac{2}{3}}\right) = d\left(\bar{p}^{\frac{2}{3}} - p^{\frac{2}{3}}\right) > 0$$

and thus $\lambda_2(\tau) = 0$. Hence $\Phi(\tau) = \lambda_3 > 0$. Contradiction. □

We recall (see Figure B.7) the notation

$$\mathscr{N}_+ = \{(p,q) \in \mathscr{D} : bp > (\mu + dp^{\frac{2}{3}})q\},$$
$$\mathscr{N}_0 = \{(p,q) \in \mathscr{D} : bp = (\mu + dp^{\frac{2}{3}})q\}$$

and

$$\mathscr{N}_- = \{(p,q) \in \mathscr{D} : bp < (\mu + dp^{\frac{2}{3}})q\}.$$

It was shown in Lemma 5.3.1 that all controlled trajectories cross $\mathscr{N}_0$ from $\mathscr{N}_-$ into $\mathscr{N}_+$.

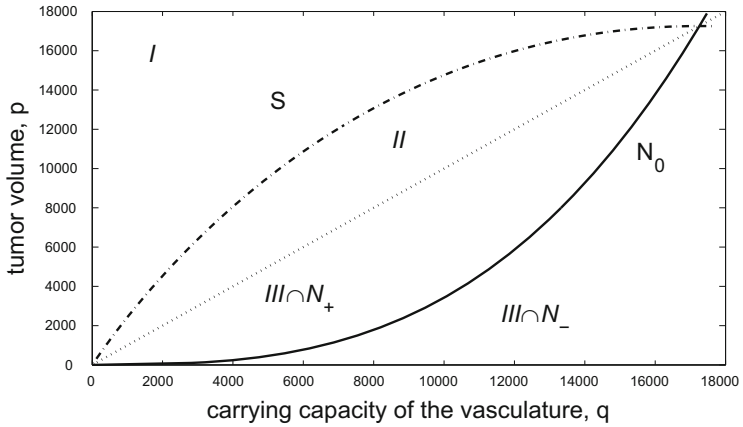

Fig. B.7 The region $III \cap \mathscr{N}_+$.

Proposition B.4.2. *Optimal controlled trajectories do not have switching points in the region $III \cap \mathscr{N}_+$ or on its boundary curve $\mathscr{N}_0$. If a state $(p,q;y)$ is well posed and the projection (p,q) lies in $(III \cap \mathscr{N}_+) \cup \mathscr{N}_0$, then the optimal control at $(p,q;y)$ is given by a maximum dose rate treatment, i.e., $u_{\text{opt}} = u_{\text{opt}}(p,q;y) \equiv u_{\max}$.*

Recall that a point $(p,q;y)$ in the state-space $\mathscr{D} \times [0,A]$ is well posed if it is possible to reach a final state $(\tilde{p},\tilde{q};A)$ with $\tilde{p} < p$ (see Section 5.2.1). We only consider well-posed states.

Proof. Let u_* be an optimal control with corresponding trajectory (p_*, q_*) defined over $[0,T]$ and suppose there exists a time $\alpha \in (0,T)$ when the corresponding trajectory has a switching point in $(III \cap \mathscr{N}_+) \cup \mathscr{N}_0$. It then follows from the fact that the Hamiltonian H vanishes identically that

$$-\lambda_1(\alpha)\xi p_*(\alpha)\ln\left(\frac{p_*(\alpha)}{q_*(\alpha)}\right) + \lambda_2(\alpha)\left(bp_*(\alpha) - \left(\mu + dp_*(\alpha)^{\frac{2}{3}}\right)q_*(\alpha)\right) = 0.$$

Without loss of generality, again we only consider extremals with $\lambda_3 > 0$ and thus $\lambda_2(t)$ is positive whenever the switching function $\Phi(t) = \lambda_3 - \lambda_2(t)\gamma q_*(t)$ vanishes. Hence $\lambda_2(\alpha) > 0$ and $\lambda_1(\alpha) \leq 0$. It follows from Proposition B.4.1 that a switch at time α must be from $u = 0$ to $u = u_{\max}$. Since optimal controls end with an interval along which $u_*(t) \equiv 0$, there exists another switching time $\beta < T$ such that $u_*(t) \equiv u_{\max}$ on (α, β). The switching function is negative on this interval with zeros at α and β, $\Phi(\alpha) = \Phi(\beta) = 0$. Hence Φ has a minimum over the interval $[\alpha, \beta]$ at some time $\sigma \in (\alpha, \beta)$ and by (5.45) we have that

$$\dot{\Phi}(\sigma) = \langle \lambda(\sigma), [f,g](z(\sigma))\rangle = \gamma p_*(\sigma)\left(\xi\lambda_1(\sigma) - b\lambda_2(\sigma)\right) = 0.$$

In particular, $\lambda_1(\sigma)$ and $\lambda_2(\sigma)$ have the same sign. But $\lambda_2(\sigma)$ is positive (the switching function is negative) and thus $\lambda_1(\sigma) > 0$. Hence there exists a last zero for λ_1 in the interval $[\alpha, \sigma)$, say $\lambda_1(\rho) = 0$. At this zero, the adjoint equation (B.35) reads

$$\dot{\lambda}_1(\rho) = \lambda_2(\rho)\left(\frac{2}{3}d\frac{q_*(\rho)}{\sqrt[3]{p_*(\rho)}} - b\right).$$

By Lemma 5.3.1, the controlled trajectory lies in $\mathscr{N}_+$ for all times $t > \alpha$, i.e., we have that

$$q_*(t) < \frac{bp_*(t)}{\mu + dp_*(t)^{\frac{2}{3}}},$$

and thus

$$\frac{2}{3}d\frac{q_*(\rho)}{\sqrt[3]{p_*(\rho)}} - b \leq \frac{2}{3}d\frac{bp_*(\rho)^{\frac{2}{3}}}{\mu + dp_*(\rho)^{\frac{2}{3}}} - b = b\left(\frac{2}{3}\frac{dp_*(\rho)^{\frac{2}{3}}}{\mu + dp_*(\rho)^{\frac{2}{3}}} - 1\right) < -\frac{1}{3}b < 0.$$

Since the multiplier $\lambda_2(\rho)$ is positive, we therefore get that $\dot{\lambda}_1(\rho) < 0$ and thus λ_1 is negative for $t > \rho$. Contradiction.

This argument implies that whenever $(p,q;y) \in (III \cap \mathscr{N}_+) \cup \mathscr{N}_0$ is well posed, then any associated switching function is nonzero. At this point the control cannot be $u = 0$ since then there would need to be a switch to $u = u_{\max}$ at some later time, but the entire forward orbit for $u = 0$ lies in the set $III \cap \mathscr{N}_+$ and thus this is not possible. Hence at any such point the optimal control is given by $u_{\text{opt}}(p,q;y) \equiv u_{\max}$. □

Corollary B.4.1. *Optimal controlled trajectories cannot cross from $\mathscr{D}_+$ into $\mathscr{D}_-$.*

Proof. Let u_* be an optimal control defined over $[0,T]$ and suppose there exists a time $\tau \in (0,T)$ such that the corresponding trajectory crosses from $\mathscr{D}_+$ into $\mathscr{D}_-$. It follows from Lemma B.4.1 that the switching function does not vanish at time τ and thus the control u_* is given by $u_*(t) \equiv 0$ in some neighborhood of τ. The diagonal $\mathscr{D}_0$ lies in the set $\mathscr{N}_+$,

$$bp - \left(\mu + dp^{\frac{2}{3}}\right) p = dp\left(\frac{b-\mu}{d} - p^{\frac{2}{3}}\right) > 0 \qquad \text{for } 0 < p < \bar{p} = \left(\frac{b-\mu}{d}\right)^{\frac{3}{2}},$$

and thus, as long as the control $u = 0$ is used, the corresponding controlled trajectory for $t > \tau$ lies in $III \cap \mathscr{N}_+$. But by Proposition B.4.2 no more switchings are thus possible. Clearly, then the optimal time to terminate the trajectory is $T = \tau$. □

Proposition B.4.3. *For points $(p,q;y) \in \mathscr{D} \times [0,A]$ whose projection (p,q) lies in the region II, the optimal control is given by*

$$u_{\text{opt}}(p,q;y) = \begin{cases} u_{\max} & \text{if } y < A, \\ 0 & \text{if } y = A. \end{cases}$$

Proof. In region II, whenever the switching function Φ vanishes at some time τ, by Proposition B.4.1 only changes from $u = u_{\max}$ to $u = 0$ are possible. Such switchings arise whenever the antiangiogenic agents run out and clearly $u_{\text{opt}}(p,q;A) \equiv 0$. We thus only need to argue that an optimal control cannot switch to $u = 0$ as long as antiangiogenic agents are available. Suppose it did. Then, since the control cannot switch back to $u = u_{\max}$ while the trajectory lies in region II, the corresponding trajectory reaches the diagonal $\mathscr{D}_0$ with antiangiogenic inhibitors remaining. This is not optimal by Lemma 5.2.1. But it also cannot cross into $\mathscr{D}_-$ by Corollary B.4.1. Contradiction. □

Coupled with Lemma B.4.1, Propositions B.4.2 and B.4.3 imply that

$$u_{\text{opt}}(p,q;y) \equiv u_{\max} \quad \text{in the region} \quad \mathscr{S}_- \cap \mathscr{N}_+$$

inside the singular loop provided the state $(p,q;y)$ is well posed.

Corollary B.4.2. *Suppose $(p,q;y)$ is a well-posed point with antiangiogenic agents still available, $y < A$, whose projection (p,q) lies in $\mathscr{S}_- \cap \mathscr{N}_+ = (II \cup \mathrm{D}_0 \cup III) \cap \mathscr{N}_+$ or on $\mathscr{N}_0$. Then the optimal control at $(p,q;y)$ is given by a maximum dose rate treatment, i.e., $u_{\text{opt}}(p,q;y) \equiv u_{\max}$.*

We close this section with an important qualitative statement about controlled trajectories that lie in $\mathscr{D}_+$. Note that initial conditions $(p_0,q_0) \in \mathscr{D}_+$ are automatically well posed and that these trajectories remain in $\mathscr{D}_+$ until they reach the diagonal at the optimal terminal time T (Corollary B.4.1).

Proposition B.4.4. *Let (α,β) be a maximal open interval on which the optimal control is given by $u_* \equiv 0$ with corresponding trajectory $(p_*(\cdot),q_*(\cdot))$ lying in $\mathscr{D}_+$.*

Then α and β cannot both be switching times. If α is a switching time, then $\beta = T$, the final time, and if β is a switching time, then $\alpha = 0$, the initial time.

Proof. On the interval (α,β), we have that

$$H = -\lambda_1(t)\xi p_*(t)\ln\left(\frac{p_*(t)}{q_*(t)}\right) + \lambda_2(t)\left(bp_*(t) - \left(\mu + dp_*(t)^{\frac{2}{3}}\right)q_*(t)\right) \equiv 0$$

with $\xi p \ln(\frac{p}{q}) > 0$ and $bp - \left(\mu + dp^{\frac{2}{3}}\right)q > 0$ on $\mathscr{D}_+$. Neither λ_1 nor λ_2 can vanish in this case and therefore λ_1 and λ_2 have the same sign over (α,β). Since λ_2 is positive at switchings times, it follows that both λ_1 and λ_2 are positive over the compact interval $[\alpha,\beta]$ if at least one of the endpoints is a switching time. Along $u = 0$ the derivatives of the switching function are given by $\dot{\Phi}(t) = \langle \lambda(t), [f,g](z_*(t))\rangle$ and $\ddot{\Phi}(t) = \langle \lambda(t), [f,[f,g]](z_*(t))\rangle$. If there exists a time $\tau \in (\alpha,\beta)$ where $\dot{\Phi}(\tau) = 0$, then it follows from (5.48) and (5.46) that

$$\begin{aligned}\ddot{\Phi}(\tau) &= \left(\xi + b\frac{p_*(\tau)}{q_*(\tau)}\right)\dot{\Phi}(\tau) + \psi(p_*(\tau),q_*(\tau))\,\langle \lambda(\tau), [g,[f,g]](z_*(\tau))\rangle \\ &= -\psi(p_*(\tau),q_*(\tau))b\gamma^2 p_*(\tau)\lambda_2(\tau).\end{aligned}$$

Recall that

$$\psi(p,q) = -\frac{1}{\gamma}\left(\xi\ln\left(\frac{p}{q}\right) + b\frac{p}{q} + \frac{2}{3}\xi\frac{d}{b}\frac{q}{p^{\frac{1}{3}}} - \left(\mu + dp^{\frac{2}{3}}\right)\right)$$

and on the set $\mathscr{D}_+$ we have that

$$b\frac{p}{q} - \left(\mu + dp^{\frac{2}{3}}\right) > b - \mu - dp^{\frac{2}{3}} > b - \mu - d\left(\frac{b-\mu}{d}\right) = 0.$$

Hence $\psi(p_*(\tau),q_*(\tau)) < 0$ and $\ddot{\Phi}(\tau) > 0$.

Suppose α is a switching time. Since the control changes to $u = 0$ at α, the switching function becomes positive for $t > \alpha$ near α and therefore $\dot{\Phi}(\alpha) \geq 0$. Hence there exists an $\varepsilon > 0$ so that $\dot{\Phi}$ is positive in $(\alpha,\alpha+\varepsilon)$. This is clear by continuity if $\dot{\Phi}(\alpha) > 0$ and even if $\dot{\Phi}(\alpha) = 0$, then the argument just made shows that $\ddot{\Phi}(\alpha) > 0$ and thus $\dot{\Phi}$ will be positive on some interval $(\alpha,\alpha+\varepsilon)$ as well. If $\dot{\Phi}$ has zeroes in (α,β), then there thus exists a smallest one, say τ. Then we have $\dot{\Phi}(t) > 0$ on the interval (α,τ) and so Φ cannot have a local minimum at τ contradicting $\ddot{\Phi}(\tau) > 0$. Hence Φ is strictly increasing over (α,β) and there does not exist another zero at β. Hence $\beta = T$, the terminal time. Similarly, if β is a switching time, then Φ is strictly decreasing over (α,β) and again there cannot exist another zero at α so that $\alpha = 0$. □

It thus follows that once optimal controlled trajectories cross from $\mathscr{D}_-$ into $\mathscr{D}_+$ (and this happens along the control $u = u_{\max}$), the corresponding controls can only switch to $u \equiv 0$ as all antiangiogenic agents have been exhausted.

B.4.2 Analysis of Junctions of Singular and Bang Arcs

The important and nontrivial aspect of the synthesis arises if controlled trajectories reach the admissible portion of the singular arc, $\mathscr{S}_{ad}$, with antiangiogenic agents left. At such a time, in principle the trajectory could continue with the control $u \equiv u_{\max}$ or it could switch to the singular control and follow the corresponding singular trajectory. The derivative $\dot{p}$ does not depend on the control and thus, for $(p,q) \in \mathscr{S}_{ad}$ and setting $x = \frac{p}{q}$, we have that

$$\ddot{p} = -\xi\, \dot{p} \ln x - \xi q \dot{x} \qquad \text{with} \qquad \dot{x} = x(\gamma u - (\xi + bx)\ln x).$$

If the singular control u_{sing} is admissible, then $\dot{x}$ is maximized for $u \equiv u_{\max}$ and the tumor volume decays the fastest along the maximum dose rate control. But agents are limited and as long as the singular control is admissible, these values lie below $u_{\max}$, in some cases significantly, and thus agents can be administered for a longer time along the singular curve. The question then becomes which of these two behaviors wins out in the end. This depends on the remaining amount of agents and where on the singular curve $\mathscr{S}_{ad}$ the point (p,q) lies.

We first show that concatenations of bang controls with the admissible singular arc $\mathscr{S}_{ad}$ are locally extremal whenever the singular control at the junction point takes values in the interior of the control set. This is the statement of Proposition A.3.2 for this particular problem. We denote the relative interior of $\mathscr{S}_{ad}$ by $\mathring{\mathscr{S}}_{ad}$.

Proposition B.4.5. *Let I be an open interval on which the optimal control u_* is singular and takes values in the interior of the control set. Then concatenations of both the forms* **bs** *and* **sb** *where* **b** *stands for any of the two bang controls, $u = 0$ or $u = u_{\max}$, are extremal.*

Proof. Let $(\tau - \varepsilon, \tau + \varepsilon)$ be a small interval with the property that the optimal control is singular on $(\tau - \varepsilon, \tau)$ or $(\tau, \tau + \varepsilon)$ and constant on the complementary interval, $u = 0$ or $u = u_{\max}$. We show that the conditions of the maximum principle are satisfied. To see this, recall that, by (5.29), for any control u that is continuous from the left $(-)$ or right $(+)$, the second derivative of the switching function is given by

$$\ddot{\Phi}(\tau_\pm) = \langle \lambda(\tau), [f,[f,g]](z_*(\tau))\rangle + u(\tau_\pm)\,\langle \lambda(t), [g,[f,g]](z_*(\tau))\rangle$$

and along the singular control this derivative vanishes identically. Since the strengthened Legendre-Clebsch condition is satisfied, we have that

$$\langle \lambda(t), [g,[f,g]](z_*(t))\rangle < 0.$$

By assumption, the singular control takes values in the interior of the control set $[0, u_{\max}]$ and thus

$$\langle \lambda(t), [f,[f,g]](z_*(t))\rangle > 0.$$

Hence, for $u = 0$ we get $\ddot{\Phi}(\tau) > 0$ and for $u = u_{\max}$ we have that $\ddot{\Phi}(\tau) < 0$. These signs are consistent with entry and exit from the singular arc for each control, i.e.,

for example, if $u = 0$ on an interval $(\tau - \varepsilon, \tau)$, then Φ is positive over this interval consistent with the choice $u = 0$ as minimizing control. The remaining cases are analogous. □

Thus, as long as the singular control has not saturated, it is possible to concatenate it with the constant controls $u = 0$ or $u = u_{\max}$ at any point without violating the conditions of the maximum principle locally (in a neighborhood of the junction point). Optimality over longer time-intervals is not guaranteed and needs to be analyzed. For example, it follows from Proposition B.4.4 that the singular arc can only be left with the control $u = 0$ when all inhibitors have been exhausted. Similarly, if the remaining amount of agents is too small so that it would be impossible to reach the region $II = \mathscr{D}_+ \cap \mathscr{S}_-$ along the constant control $u = u_{\max}$ (for only in this region a switching from $u = u_{\max}$ to $u = 0$ can be optimal), then optimal controlled trajectories will follow the singular arc until all inhibitors are exhausted. On the other hand, if an ample amount of antiangiogenic agents is available and prolonged use of the singular control would lead to saturation, then, as we shall show now, optimal controlled trajectories must leave the singular arc before this happens.

Proposition B.4.6. *Let u_* be an optimal control with the property that u_* is singular over an interval $[\sigma, \tau]$. If the singular control saturates at time τ, then all inhibitors become exhausted at time τ, $y_*(\tau) = A$. Optimal controlled trajectories for which the singular control would saturate with agents remaining, must leave the singular arc prior to the saturation point $(\tilde{p}, \tilde{q})$ with the control $u = u_{\max}$.*

While this result may seem somewhat counterintuitive, this indeed is the generic behavior at saturation points in low dimensions (e.g., see [32, 291, 292]).

Proof. We use the same notation as in Proposition 5.3.5: $(\tilde{p}, \tilde{q})$ denotes the point on $\mathscr{S}_{ad}$ where the singular control saturates at its upper limit $u_{\max}$ and $x_u^* = \frac{\tilde{p}}{\tilde{q}}$. Also recall from the proof of this result that the value of the singular control is strictly increasing along the singular arc and thus that there exists a unique time when the singular control saturates.

Consider a trajectory that follows the singular arc, saturates at the upper control limit at time τ, and continues with the constant control $u_{\max}$. It follows from equations (5.29) and (5.47) that

$$\ddot{\Phi}(t) = \left(\xi + b\frac{p(t)}{q(t)}\right)\dot{\Phi}(t) + (u(t) + \psi(p(t), q(t)))\,\langle \lambda(t), [g,[f,g]](z(t))\rangle\,.$$

The derivative of the switching function, $\dot{\Phi}(t)$, vanishes along the singular arc and at the saturation point we also have that $\ddot{\Phi}(\tau-) = 0$ since $\psi(p(\tau), q(\tau)) = -u_{\max}$. Hence, along the control $u = u_{\max}$ from the right we obtain that

$$\begin{aligned}\Phi^{(3)}(\tau+) &= \left(\frac{d}{dt}_{|t=\tau+}\psi(p(t), q(t))\right)\langle \lambda(t), [g,[f,g]](z(t))\rangle \\ &= -\left(\frac{d}{dt}_{|t=\tau+}\psi(p(t), q(t))\right) b\gamma^2\lambda_2(\tau)p(\tau).\end{aligned}$$

At the saturation point, the control remains continuous and thus the function $t \mapsto \psi(p(t),q(t))$ is continuously differentiable at τ. We can therefore replace the derivative from the right with the derivative from the left. Furthermore,

$$-\psi(p(t),q(t)) = \Psi(x(t)), \qquad x = \frac{p}{q},$$

with Ψ defined by (5.50) in Proposition 5.3.5. We thus have that

$$-\frac{d}{dt}_{|t=\tau}\psi(p(t),q(t)) = \Psi'(x_u^*)\dot{x}(\tau).$$

It follows from the proof of Proposition 5.3.5 that $\Psi'(x_u^*) > 0$ and in general we have that

$$\dot{x} = \frac{\dot{p}q - p\dot{q}}{q^2} = -\xi x \ln x - bx^2 + (\mu + dp^{\frac{2}{3}})x + \gamma u x.$$

Substituting $(\mu + dp^{\frac{2}{3}}) = bx(1-\ln x)$ along the singular arc (c.f., (5.41)), we obtain that

$$\dot{x} = x\left(\gamma u_{\text{sing}} - (\xi + bx)\ln x\right).$$

But at the saturation point we also have that

$$\gamma u_{\max} = \gamma u_{\text{sing}}(\tau) = \left(\frac{1}{3}\xi + bx(\tau)\right)\ln x(\tau) + \frac{2}{3}\xi\left(1 - \frac{\mu}{bx(\tau)}\right)$$

and thus, again using (5.41),

$$\dot{x}(\tau) = \frac{2}{3}\frac{\xi}{b}\left(bx(\tau)\left(1-\ln x(\tau)\right) - \mu\right) = \frac{2}{3}\frac{\xi}{b}dp(\tau)^{\frac{2}{3}} > 0.$$

Hence $\Phi^{(3)}(\tau+)$ is positive. But then Φ is positive for $t > \tau$, t near τ, and this contradicts the minimization property for $u = u_{\max}$. Thus it follows that optimal controlled trajectories need to leave the singular arc $\mathscr{S}_{ad}$ prior to saturation. As long as inhibitors are still available, by Proposition B.4.4 this is only possible with the control $u = u_{\max}$.

An analogous computation with $u = 0$ for $t > \tau$ shows that it is possible to switch to $u = 0$ at saturation if all inhibitors have been exhausted. In this case, we have that

$$\ddot{\Phi}(\tau+) = -u_{\max}\langle \lambda(\tau), [g,[f,g]](z(\tau))\rangle$$

and since the strengthened Legendre-Cebsch condition is satisfied along the singular arc, this quantity is positive. Hence Φ is positive for $t > \tau$ near τ consistent with the choice of $u = 0$ as the minimizing control. □

When precisely optimal controlled trajectories leave the singular arc depends on the amount of inhibitors left. We now have sufficiently reduced the possible structures of optimal controls and trajectories and can reduce the computation of this time to a 1-dimensional optimization problem that can be solved numerically. Suppose

(p,q) is a point on the admissible portion of the singular base curve different from the saturation point and let $y < A$. Consider the controlled trajectory that starts at (p,q) at time $t = 0$ and follows the singular control u_{sing}. Along this trajectory, let $\theta_{sat} = \theta_{sat}(p,q)$ denote the time when the singular control saturates at its upper value $u_{\max}$ (ignoring the constraint on the amount of agents) and let $\theta_A = \theta_A(p,q;y)$ denote the time when all antiangiogenic agents are used up along the singular arc (ignoring saturation). For $0 \le \varepsilon \le \theta = \min\{\theta_A, \theta_{sat}\}$, define a 1-parameter family of controlled trajectories

$$\Gamma_\varepsilon = (p_\varepsilon(\cdot), q_\varepsilon(\cdot); y_\varepsilon(\cdot)), \qquad \varepsilon \in [0,\theta],$$

that follows the singular arc for time ε, then switches to a full dose rate trajectory with $u = u_{\max}$ until all agents have been exhausted at time $\tau(\varepsilon)$, and ends with a segment for $u = 0$ until the minimum tumor volume is realized as the diagonal $\mathscr{D}_0$ is crossed at time $T(\varepsilon)$. Thus the control is given by

$$u_\varepsilon(t) = \begin{cases} u_{\text{sing}}(t) & \text{for } \tau \le t \le \varepsilon, \\ u_{\max} & \text{for } \varepsilon \le t \le \tau(\varepsilon), \\ 0 & \text{for } \tau(\varepsilon) \le t \le T(\varepsilon). \end{cases} \tag{B.37}$$

Note that the amount of agents used up along the singular portion of the control is

$$\sigma(\varepsilon) = \int_0^\varepsilon u_{\text{sing}}(t)dt \tag{B.38}$$

and thus

$$\tau(\varepsilon) = \varepsilon + \frac{A - y - \sigma(\varepsilon)}{u_{\max}}. \tag{B.39}$$

The terminal time $T(\varepsilon)$ is defined implicitly by the fact that the trajectory ends on the diagonal.

Proposition B.4.7. *For an initial condition $(p,q;y)$ with $(p,q) \in \mathring{\mathscr{S}}_{ad}$ (the admissible portion of the singular base curve, but not at saturation) and $y < A$, the controlled trajectories Γ_ε, $0 \le \varepsilon \le \theta$, are the only possible extremals.*

Proof. The control $u(t) = 0$ is not optimal unless all agents have been used up. For, in this case the corresponding trajectory enters the region II where switchings from $u = 0$ to $u = u_{\max}$ are not optimal by Proposition B.4.1. Hence the diagonal is reached with antiangiogenic agents to spare. Contradiction. Thus, initially the control must be singular or $u = u_{\max}$. On the other hand, once the control $u(t) = u_{\max}$ is used at any point on the segment $\mathring{\mathscr{S}}_{ad}$ of the singular base curve, the corresponding trajectory enters the region I where switchings from $u = u_{\max}$ to $u = 0$ are not optimal. No change in the control is therefore possible until the corresponding trajectory has crossed over into the region II. This can only happen in the inadmissible portion of the singular base curve $\mathscr{S}_0$. Once in II, it is again only possible to switch to $u = 0$ when all antiangiogenic agents have been used up. Summarizing, once an extremal

controlled trajectory leaves the singular arc with $u = u_{\max}$, this control must be used until all available agents have been used up. Since, by Proposition B.4.6, it is not optimal to continue with $u = u_{\max}$ at the saturation point, the family Γ_ε exhausts all possibilities. □

Thus, optimal controlled trajectories from a point of the singular arc are at most concatenations of the form $\mathbf{su}_{\max}\mathbf{0}$. The family Γ_ε, $0 \le \varepsilon \le \theta$, contains the extreme situations when optimal controlled trajectories are of the form $\mathbf{u}_{\max}\mathbf{0}$ ($\varepsilon = 0$) and $\mathbf{s0}$ ($\varepsilon = \theta = \theta_A$) for the limits of the parameters. The value of the objective along this family of controlled trajectories is given by

$$\upsilon(\varepsilon) = p_\varepsilon(T(\varepsilon)).$$

It is clear from the definition of the family Γ_ε that υ is a continuously differentiable function of ε. (This follows from the fact that solutions to an ordinary differential equation defined by continuously differentiable functions themselves are continuously differentiable functions of initial conditions and parameters. It is also used that the functions τ and T are continuously differentiable functions. For τ, this is immediate from its definition and for T this follows from the implicit function theorem and the fact that the trajectories cross the diagonal $\mathscr{D}_0$ transversally.) It is not difficult to compute the values $\upsilon(\varepsilon)$ numerically and then to minimize over $[0, \theta]$.

Figure B.8 illustrates the family of controlled trajectories $(p_\varepsilon(\cdot), q_\varepsilon(\cdot))$ for the case when $\theta = \theta_A < \theta_{sat}$. The trajectory that follows the singular arc until all inhibitors are exhausted is shown in blue and some sample trajectories of Γ_ε are shown in black. The red curve is the curve of endpoints for the full dose rate segments when all inhibitors are exhausted. For the data used to generate the figure, the amount of available agents is too small to reach region II inside the loop $\mathscr{S}$ using the control $u = u_{\max}$ and thus the only extremal is the trajectory Γ_θ. The optimal control is of the type $\mathbf{s0}$ and given for the final parameter, $\varepsilon_{\min} = \theta$, i.e., it is optimal to follow the singular arc until all agents have been used up. The figure on the right shows the corresponding values υ which are strictly decreasing in ε.

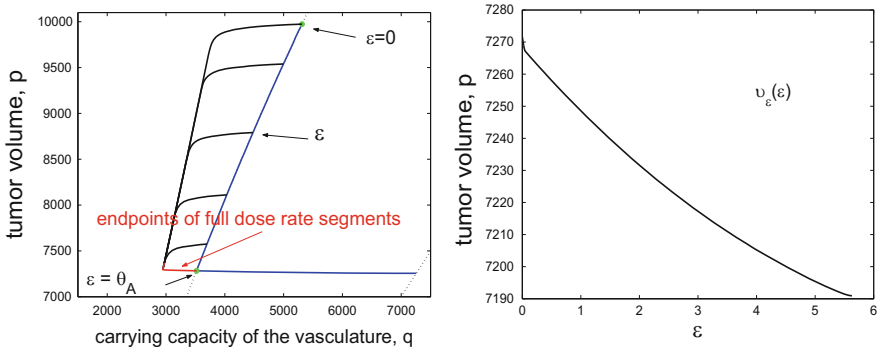

Fig. B.8 The 1-parameter family of controlled trajectories $(p_\varepsilon(\cdot), q_\varepsilon(\cdot))$ is shown on the left. The endpoints of the variation are represented by the red curve. The graph of the corresponding value $\varepsilon \mapsto \upsilon_\varepsilon(\varepsilon)$ is shown on the right. In this case, the optimal control is of the form $\mathbf{s0}$.

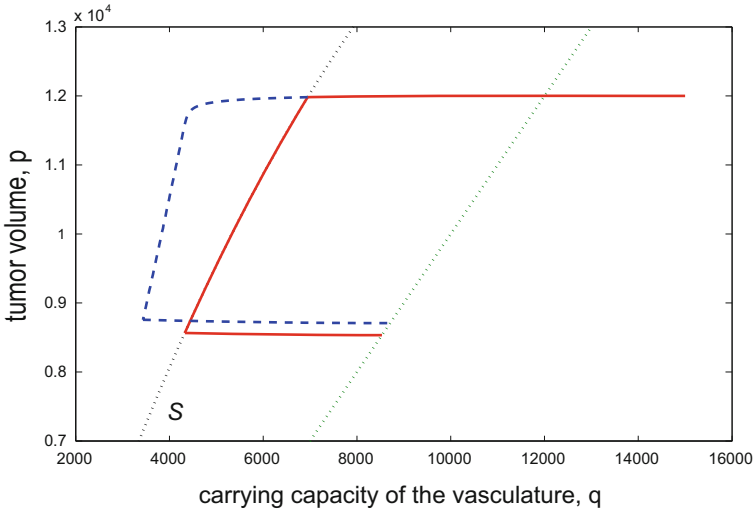

Fig. B.9 Comparison of a $\mathbf{u}_{\max}\mathbf{0}$-trajectory (dashed blue curve) with an optimal $\mathbf{u}_{\text{sing}}\mathbf{0}$-trajectory (solid red curve).

Figure B.9 still shows a comparison of an optimal trajectory that follows the singular arc with the nonoptimal $\mathbf{u}_{\max}\mathbf{0}$-trajectory. The initial conditions are given by $p_0 = 12{,}000\ [mm^3]$ and $q_0 = 15{,}000\ [mm^3]$. For comparison, the optimal minimum tumor volume is $p_*(T) = 8533.4\ [mm^3]$ while the terminal value for the trajectory which applies all available inhibitors in one full dose rate session is $8707.4\ [mm^3]$.

In order to determine whether $u = u_{\max}$ or the singular control is better at the initial point $(p,q;y)$, we can also consider ε as a variational parameter and compute the derivative

$$\upsilon'(0) = \frac{d\upsilon}{d\varepsilon}_{|\varepsilon=0}.$$

As long as this derivative is negative, the optimal control is given by $u_{\text{sing}}(p,q)$ and the point to leave the singular arc with $u = u_{\max}$ occurs when $\upsilon'(0) = 0$. By the chain rule,

$$\upsilon'(\varepsilon) = \frac{\partial p_\varepsilon}{\partial \varepsilon}(T(\varepsilon)) + \frac{\partial p_\varepsilon}{\partial t}(T(\varepsilon))T'(\varepsilon).$$

Since the endpoint lies on the diagonal, $p_\varepsilon(T(\varepsilon)) \equiv q_\varepsilon(T(\varepsilon))$, the second term in this expression vanishes,

$$\frac{\partial p_\varepsilon}{\partial t}(T(\varepsilon)) = \dot{p}_\varepsilon(T(\varepsilon)) \equiv 0,$$

and thus

$$\upsilon'(\varepsilon) = \frac{\partial p_\varepsilon}{\partial \varepsilon}(T(\varepsilon)). \tag{B.40}$$

Proposition B.4.8. *Given $z = (p,q;y) \in \mathring{\mathscr{S}}_{ad}$, let $(p_0(\cdot), q_0(\cdot))$ be the controlled trajectory for $\varepsilon = 0$ in the 1-parameter family Γ_ε and denote the corresponding*

terminal time by T_0 (i.e., the available antiagiogenic agents are used up along an initial full dose segment and T_0 is the time when the subsequent trajectory for $u \equiv 0$ crosses the diagonal.) Let λ be the solution of the corresponding adjoint equation with terminal value $\lambda(T_0) = (1,0,0)$ and set $\eta = \lambda(0)$. The derivative $\upsilon'(0)$ of the value of the 1-parameter family Γ_ε along at $\varepsilon = 0$ is then given by

$$\upsilon'(0) = \left(1 - \frac{u_{\text{sing}}(p,q)}{u_{\max}}\right) \langle \eta, f(z) \rangle .$$

The optimal control at $(p,q;y)$ is given by

$$u_{\text{opt}}(p,q;y) = u_{\text{sing}}(p,q) \qquad \text{if} \quad \langle \eta, f(z) \rangle < 0.$$

Proof. The computation of the derivative of the family Γ_ε with respect to the parameter ε involves differentiations of a solution of an ODE with respect to initial conditions and parameters and is more involved. Customarily, the solution at time t to an initial value problem of the form $\dot{z} = X(z)$, $z(0) = z_0$, is denoted by $z(t;z_0)$ or, if the emphasis is on the flow, by $z(t;z_0) = \Phi_t^X(z_0)$. The flow along these solutions is then defined by $\Phi_{s,t}^X(z) = \left(\Phi_t^X \circ \Phi_{-s}^X\right)(z)$ and it simply denotes the value of the solution to the ODE at time t with initial condition z at time s. Using this notation, and denoting the singular vector field by $S = f + u_{\text{sing}} g$ and setting $Y = f + u_{\max} g$, then, with $e_1 = (1,0,0)$ the covector for the first coordinate vector field in the variable $z = (p,q,y)$, we can represent the function $\upsilon(\varepsilon)$ in the form[1]

$$\upsilon(\varepsilon) = p_\varepsilon(T(\varepsilon)) = \left\langle e_1, \Phi^f_{\tau(\varepsilon),T(\varepsilon)} \left(\Phi^Y_{\varepsilon,\tau(\varepsilon))} \left(\Phi^S_{0,\varepsilon}(z) \right) \right) \right\rangle .$$

At this point, a good computational framework for the flows of vector fields becomes helpful. Such a framework is provided by an exponential formalism for solutions to differential equations (e.g., see [292, Sect. 4.5]) and we therefore deviate from conventional usage and we write the solution to the above initial value problem, $\dot{z} = X(z)$, $z(0) = z_0$, in the form

$$z(t) = z_0 \exp(tf).$$

Different from customary notation, here the operator acts on the right side. With this notation, we can express the endpoint of the variation in the equivalent form

$$\begin{aligned} \varsigma(\varepsilon) &= \Phi^f_{\tau(\varepsilon),T(\varepsilon)} \left(\Phi^Y_{\varepsilon,\tau(\varepsilon))} \left(\Phi^S_{0,\varepsilon}(z) \right) \right) \\ &\simeq z \exp(\varepsilon S) \exp\left((\tau(\varepsilon) - \varepsilon) Y \right) \exp\left((T(\varepsilon) - \tau(\varepsilon)) f \right). \end{aligned}$$

The advantage of the exponential formalism is that differentiation rules using exponential calculus apply not only to the flow of solutions, but also to all versions of variational equations derived from it. For example, using the product rule, the derivative with respect to ε can simply be expressed in the form

[1] Note the reverse order in the switching times along the trajectory that this customary notation induces.

$$\begin{aligned}\varsigma'(\varepsilon) = {} & z\exp(\varepsilon S)\,\mathrm{S}\exp((\tau(\varepsilon)-\varepsilon)Y)\exp((T(\varepsilon)-\tau(\varepsilon))f) \\ & + z\exp(\varepsilon S)\exp((\tau(\varepsilon)-\varepsilon)Y)\,\mathrm{Y}\left(\tau'(\varepsilon)-1\right)\exp((T(\varepsilon)-\tau(\varepsilon))f) \\ & + z\exp(\varepsilon S)\exp((\tau(\varepsilon)-\varepsilon)Y)\exp((T(\varepsilon)-\tau(\varepsilon))f)\,\mathrm{f}\left(T'(\varepsilon)-\tau'(\varepsilon)\right)\end{aligned}$$

where we have used a Roman font (S,Y,f) to distinguish vectors from the flows represented by the exp-terms. This is a formal expression for complicated mathematical objects: For example, the term

$$z\exp(\varepsilon S)\,\mathrm{S}\exp((\tau(\varepsilon)-\varepsilon)Y)\exp((T(\varepsilon)-\tau(\varepsilon))f)$$

denotes the vector obtained by moving the tangent vector $z\exp(\varepsilon S)\,\mathrm{S}$ at the endpoint of the singular portion of the variation forward along the remaining portions of the trajectory to the endpoint of the trajectory by integrating the corresponding variational equations. The time derivatives $\tau'(\varepsilon)-1$ and $T'(\varepsilon)-\tau'(\varepsilon)$ are scalar quantities that can be moved freely along the flows. Similarly,

$$z\exp(\varepsilon S)\exp((\tau(\varepsilon)-\varepsilon)Y)\exp((T(\varepsilon)-\tau(\varepsilon))f)\,\mathrm{f}$$

denotes the vector field f evaluated at the endpoint of the trajectory. As before, since $p_\varepsilon(T(\varepsilon)) \equiv q_\varepsilon(T(\varepsilon))$, we have that

$$\langle e_1, z\exp(\varepsilon S)\exp((\tau(\varepsilon)-\varepsilon)Y)\exp((T(\varepsilon)-\tau(\varepsilon))f)\,\mathrm{f}\rangle\, T'(\varepsilon) \equiv 0$$

and thus this term, which is equivalent to $\frac{\partial p_\varepsilon}{\partial t}(T(\varepsilon))T'(\varepsilon)$, vanishes. Although the exponential notation may seem cumbersome, it is anything but and offers tremendous computational advantages when dealing with the variational equations since the same exponential formalisms applies to both the underlying system and these variational equations. This is what is needed here. For example, vectors can be moved backward and forward along their own flows, i.e.,

$$z(t) = z\exp(tf)\mathrm{f} = z\mathrm{f}\exp(tf).$$

Since $\upsilon'(\varepsilon) = \langle e_1, \varsigma'(\varepsilon)\rangle$ where $e_1 = (1,0,0)$ denotes the covector for the first coordinate, we can express $\upsilon'(\varepsilon)$ in the form

$$\begin{aligned}\upsilon'(\varepsilon) &= \left\langle e_1, \varsigma'(\varepsilon)\right\rangle \\ &= \left\langle e_1, z\exp(\varepsilon S)\left\{\mathrm{S} + \mathrm{Y}\left(\tau'(\varepsilon)-1\right)\right\}\right. \\ &\qquad \left.\times \exp((\tau(\varepsilon)-\varepsilon)Y)\exp((T(\varepsilon)-\tau(\varepsilon))f)\right\rangle.\end{aligned}$$

The tangent vector $z\exp(\varepsilon S)\left\{\mathrm{S} + \mathrm{Y}\left(\tau'(\varepsilon)-1\right)\right\}$ is easily computed:

$$\begin{aligned}S + (f + u_{\max}g)\left(\tau'(\varepsilon)-1\right) &= f + u_{\mathrm{sing}}g + (f+u_{\max}g)\left(-\frac{u_{\mathrm{sing}}}{u_{\max}}\right) \\ &= f\left(1 - \frac{u_{\mathrm{sing}}}{u_{\max}}\right)\end{aligned}$$

and thus, for $\varepsilon = 0$, we have that

$$\upsilon'(0) = \left\langle e_1, zf\left(1 - \frac{u_{\text{sing}}}{u_{\max}}\right)\exp(\tau_A Y)\exp(\tau_0 f)\right\rangle$$

where $\tau_A = \frac{A-y}{u_{\max}}$ denotes the time along the $u_{\max}$-trajectory starting at z until all agents are exhausted and τ_0 denotes the subsequent time along $u = 0$ until the diagonal is reached.

This equation can be simplified by moving the two operators $\exp(\tau_0 f)$ and $\exp(\tau_A Y)$ to the covector e_1 using the adjoint operators. The derivatives of the flow of a differential equation are computed by integrating the variational equation and the adjoint of this equation is precisely the adjoint equation of the maximum principle, hence its name (e.g., see [292, Proposition 4.2.2]). The value of the inner product is constant under this operation and we obtain

$$\upsilon'(0) = \left\langle e_1 \left(\exp(\tau_0 f)\right)^* \left(\exp(\tau_A Y)\right)^*, zf\left(1 - \frac{u_{\text{sing}}}{u_{\max}}\right)\right\rangle.$$

With $(p_0(\cdot), q_0(\cdot))$ denoting the $\mathbf{u}_{\max}\mathbf{0}$-trajectory that, starts at $z = (p, q, y)$, and λ the solution of the corresponding adjoint equation with terminal condition $\lambda(T_0) = (1, 0, 0)$, the result follows. □

If one ignores the saturation limit on the control, the variation Γ_ε can be made anywhere on the singular base curve $\mathscr{S}_0$. At the saturation point we have that $u_{\text{sing}}(p, q) = u_{\max}$ and thus $\upsilon'(0) = 0$. Hence the changes in the value υ near the saturation point will be of higher order and indeed, the point when optimal trajectories leave the singular arc will be very close to the saturation point. From a practical point of view, the difference in the values is negligible. Thus *the errors made by replacing optimal controlled trajectories with the simpler ones that follow the singular arc until saturation and then use a full dose control are insignificant*. Figure B.10 shows an example of the function $\upsilon(\varepsilon)$ when saturation occurs. The differences in

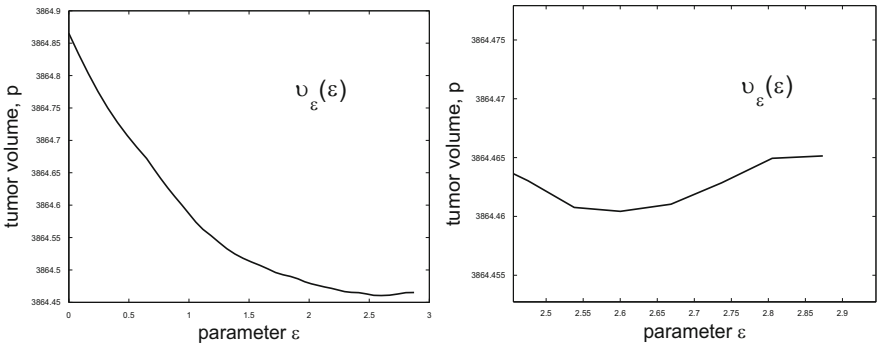

Fig. B.10 A smoothed (averaged) graph of the function $\varepsilon \mapsto \upsilon_\varepsilon(\varepsilon)$ for a case when the singular control saturates (left) and a blow-up near the saturation values (right).

the terminal values are minute and the graph on the left has been smoothed out by averaging close-by values. The graph on the right shows a blow-up near the parameter values corresponding to the saturation point.

As these computations indicate, the precise structure of optimal trajectories that pass close to the saturation point is rather involved. In [291], a theoretical analysis of time-optimal controls near a saturation point of a singular arc is developed and it can also be found in the context of a specific application from the chemical industry in [32]. In these papers, a general local synthesis of optimal controls of the type *bbsb* or *bsbb* where *b* denotes a bang arc and *s* a singular arc, is established and for our problem here the same structure is valid near the saturation point: optimal controls follow the concatenation structure $\mathbf{bsu}_{\max}\mathbf{0}$ with **b** denoting an arc corresponding to the control $u = 0$ or $u = u_{\max}$ depending on from which side trajectories meet the singular arc.

B.4.3 Synthesis of Optimal Controlled Trajectories

We combine the pieces and construct a synthesis of optimal controlled trajectories on the subset $\tilde{\mathscr{X}} = \tilde{\mathscr{D}} \times [0,A]$ of the state space $\mathscr{X} = \mathscr{D} \times [0,A]$. Formally, the fact that the range in the variable y is closed represents a state space constraint. But this analysis is straightforward. Initial conditions lie on the boundary segment $\tilde{\mathscr{X}}_0 = \tilde{\mathscr{D}} \times \{0\}$ and terminal conditions (for well-posed initial data) all lie on $\mathscr{D}_0 \times \{A\} \subset \tilde{\mathscr{X}}_A = \tilde{\mathscr{D}} \times \{A\}$. The structure of any admissible controlled trajectory is such that it will lie on $\tilde{\mathscr{X}}_0$ for some interval $[0, \tau_0]$ if the control $u \equiv 0$ is applied, but as soon as antiangiogenic agents are administered, the controlled trajectory enters the interior of the region $\tilde{\mathscr{X}}$ where it will remain as long as agents are still available. Only as all agents have been used up, the state enters $\tilde{\mathscr{X}}_A$ and then remains there over a final interval $[\tau_A, T]$ until the diagonal is reached along the control $u \equiv 0$. The control $u \equiv 0$ indeed is optimal in some regions of the sets $\tilde{\mathscr{X}}_0$ and $\tilde{\mathscr{X}}_A$ and becomes part of the optimal synthesis, but there is no need to consider the formulation as an optimal control problem with state space constraints. Formally, if one would, all additional structures caused by this formulation, will be trivial.

The singular base curve $\mathscr{S}_0$ divides the set $\tilde{\mathscr{D}}$ into a region E that lies below $\mathscr{S}_0$ (in direction of p) and a region F that lies above $\mathscr{S}_0$. The region E is the union of the diagonal $\mathscr{D}_0$, the region $II = \mathscr{D}_+ \cap \mathscr{S}_-$, and the portion of $III = \mathscr{D}_- \cap \mathscr{S}_-$ that lies above the nullcline $\mathscr{N}_0$; the region E is the same as $I = \mathscr{D}_+ \cap \mathscr{S}_+$ (see Figure B.11).

We now determine the optimal control for an arbitrary well-posed point $(p,q;y)$ with $(p,q) \in \tilde{\mathscr{D}}$ and $y < A$. Recall that the point $(p,q;y)$ is well posed if it is possible to reach a tumor volume lower than p with the remaining amount of antiangiogenic agents $y_r = A - y$. This will always be true if $(p,q) \in \mathscr{D}_+$.

(i) Optimal controlled trajectories for points $(p,q) \in \mathscr{S}_0^+ = \mathscr{S}_0 \cap \mathscr{D}_+$: If $(p,q) \in \mathring{\mathscr{S}}_{ad}$, the interior of the admissible singular arc, this structure has just been determined and we have seen that optimal controlled trajectories starting from such a point are at most of the form $\mathbf{su}_{\max}\mathbf{0}$. For points $(p,q) \in \mathscr{S}_0^+$ that are inadmissible or at the lower saturation point $(\tilde{p},\tilde{q})$, the optimal control is given by

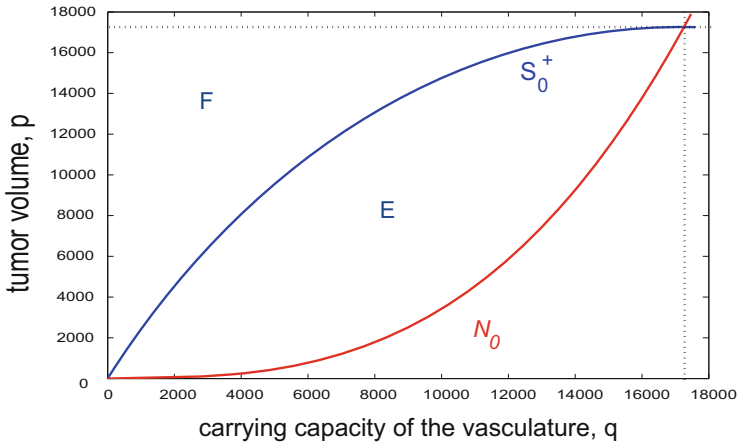

Fig. B.11 Partition of the set $\tilde{\mathscr{D}}$.

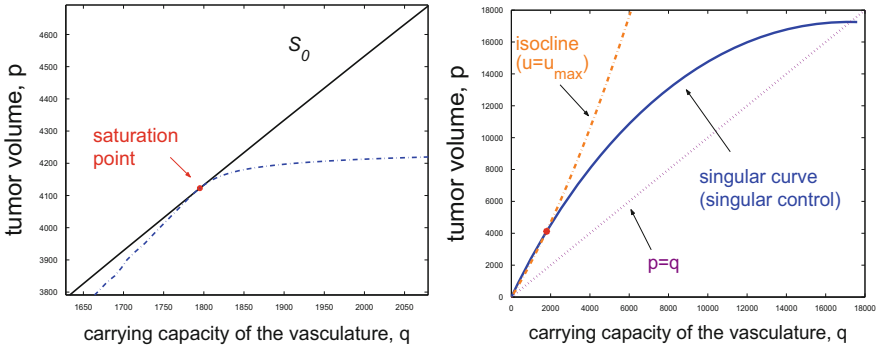

Fig. B.12 A blow-up of the trajectory for $u \equiv u_{\max}$ near the saturation point. On the right, the $\dot{q}$ nullcline for $u \equiv u_{\max}$ is shown. After the saturation point has been passed, $u_{\max}$ trajectories closely follow this nullcline which represents the slow manifold for the corresponding differential-algebraic system.

$$u_{\text{opt}}(p,q,y) = u_{\max}, \qquad (p,q) \in \mathscr{S}_0^+ \setminus \mathring{\mathscr{S}}_{ad},\ y < A, \tag{B.41}$$

and optimal controlled trajectories are of the type $\mathbf{u}_{\max}\mathbf{0}$. For, controlled trajectories corresponding to the control $u(t) \equiv u_{\max}$ cross the curve $\mathring{\mathscr{S}}_{ad}$ transversally from region II inside the singular loop into region I outside the singular loop. At the saturation point $(\tilde{p},\tilde{q})$ the value of the singular control is given by $u_{\max}$ and the corresponding trajectory through the saturation point is tangential to the singular base curve $\mathscr{S}_0^+$. It has order of contact 1 and immediately reenters region II. At all the points on the singular base curve $\mathscr{S}_0^+$ that are not admissible, the directions are reversed and here $u_{\max}$-trajectories cross the curve $\mathscr{S}_0^+$ from region I outside the singular loop into region II inside the singular loop. Figure B.12 shows a blow-up of the $u_{\max}$ trajectory that passes through the saturation point $(\tilde{p},\tilde{q})$ and also shows the $\dot{q}$-nullcline for $u \equiv u_{\max}$. Note how close it is to the inadmissible portion of the

singular arc. If at any such point the control would be $u = 0$, then the corresponding trajectory would lie in the region II as long as $u = 0$ and could have no more switching by Proposition B.4.1. But then it would reach the diagonal with antiangiogenic agents left. Contradiction. This proves (B.41). Hence the $\dot{q}$-nullcline for $u \equiv u_{\max}$ represents the optimal response of the system for low tumor volumes.

(ii) Optimal controls for points $(p,q) \in E = III \cup \mathscr{D}_0 \cup (III \cap \mathscr{D}_+)$: Let $\Gamma_{\max}$ denote the curve that is obtained by integrating the dynamics for p and q and the control $u(t) \equiv u_{\max}$ backward from the saturation point $(\tilde{p},\tilde{q})$. This curve divides E into a region E_+ that lies above $\Gamma_{\max}$ (in the sense of higher p-values) and a region E_- that lies below $\Gamma_{\max}$ (see Figure B.13). For a well-posed state $(p,q;y)$ with $(p,q) \in E_-$, the corresponding optimal control is given by

$$u_*(t) = \begin{cases} u_{\max} & \text{if } 0 \le t \le \tau = \frac{A-y}{u_{\max}}, \\ 0 & \text{if } \tau < t \le T. \end{cases}$$

with τ the time when all remaining antiangiogenic agents have been used up and T the time when the trajectory corresponding to $u = 0$ reaches the diagonal. This

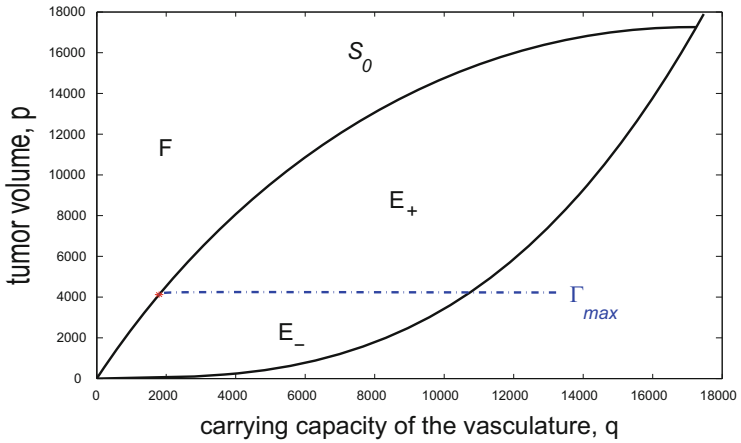

Fig. B.13 Subdivision of the regions E and F: the curve $\Gamma_{\max}$ is the trajectory obtained by integrating $u \equiv u_{\max}$ backward from the saturation point $(\tilde{p},\tilde{q})$.

directly follows from Corollary B.4.2 which implies that the optimal control is given by the feedback function

$$u_{\text{opt}}(p,q,y) \equiv u_{\max}, \qquad (p,q) \in E,$$

whenever the base point (p,q) lies in the interior of E (or on $\mathscr{N}_0$). For initial conditions in E_-, the entire forward orbit of the controlled trajectory with $u \equiv u_{\max}$ lies in E_- for all times $t > 0$. Once the diagonal has been crossed (this happens since the state is well posed), the remaining trajectory lies in the region $II \cap E_-$ until all agents have been used up. The same holds for initial conditions (p,q) that lie on the curve Γ with the possible exception that the trajectory may touch $\mathscr{S}_0^+$ in the

saturation point $(\tilde{p},\tilde{q})$. This form also is the structure of optimal controls for initial conditions (p,q) that lie in E_+ if the remaining amount of inhibitors $y_r = A - y$ simply is too small to reach the singular base curve $\mathscr{S}_0^+$, but still the data are well posed. In this case, antiangiogenic agents run out as the state is moving toward $\mathscr{S}_0$ in region II, but just never reaches this curve. For such points and all points on $\Gamma_{\max}$ and in E_-, optimal controlled trajectories again are simply of the type $\mathbf{u}_{\max}\mathbf{0}$. If, for a state $(p,q) \in E_+$ there are enough agents left to reach the admissible portion $\mathring{\mathscr{S}}_{ad}$ of the singular arc, then from the junction point onward, the above analysis applies and overall optimal controlled trajectories are of the type $\mathbf{u}_{\max}\mathbf{s}\mathbf{u}_{\max}\mathbf{0}$. This is the longest concatenation sequence that can arise for an initial condition $(p,q;0)$ with $(p,q) \in E$.

(iii) Optimal controls for points $(p,q) \in F = I = \mathscr{D}_+ \cap \mathscr{S}_+$: For states $(p,q;y)$ with base point (p,q) in F, the only nontrivial situation arises at the initial condition when $y = 0$. For, if $0 < y < A$, then we have that

$$u_{\text{opt}}(p,q,y) \equiv u_{\max}, \qquad (p,q) \in F,\ 0 < y < A.$$

This immediately follows from Proposition B.4.4: Suppose the optimal control at such a point were given by $u = 0$. Since $y > 0$, agents have already been administered in the past and thus, integrating $u \equiv 0$ backward from this point, at some time α there must be a switching time to $u = 0$. But this backward trajectory entirely lies in $\mathscr{D}_+$ and thus, by Proposition B.4.4, there cannot exist another switching forward in time. Hence, once more the diagonal is reached with agents left over. Contradiction. This result simply expresses the fact that, once controlled trajectories have entered into the region F during treatment, this only can happen along the terminal portion when $u = u_{\max}$.

The synthesis at the initial point, $y = 0$, is more involved. In such a case, initially both $u = 0$ and $u = u_{\max}$ are possible. We already know that the optimal control is given by $u_{\max}$ on the inadmissible part of $\mathscr{S}_0^+$ and thus it is to be expected that this is the optimal control near such points in F. On the other hand, once the control starts with $u_{\max}$, by Proposition B.4.1 it cannot switch any more in the region F. Thus, if the value of p is high and the amount of agents is too small to reach the region II inside the singular loop, the initial control must be $u = 0$. Thus there exists a curve Γ_{cut}, a so-called *cut locus*, that divides the regions where the controls $u = 0$ and $u = u_{\max}$ are optimal. Similarly as for initial points on the admissible portion of the singular arc, we set up a 1-parameter family of controlled trajectories and minimization of the objective along this family determines the optimal control at the initial time.

For $(p,q) \in F$, let $\varsigma = \varsigma(p,q)$ denote the trajectory along the control $u = 0$ that starts at (p,q) and denote by $\theta = \theta(p,q)$ the time when this trajectory reaches the singular base curve $\mathscr{S}_0^+$. Since this trajectory converges to the equilibrium point $(\bar{p},\bar{q})$ along the nullcline $\mathscr{N}_0$ from within $\mathscr{D}_-$, it is clear that this time is finite. For $0 \le \delta \le \theta$, consider the controlled trajectories

$$\Theta_\delta = (p_\delta(\cdot), q_\delta(\cdot); y_\delta(\cdot)), \qquad \varepsilon \in [0,\theta],$$

that follow the trajectory ς for time δ and then switch to the full dose rate trajectory with $u = u_{\max}$ until all agents have been exhausted. The time along these full dose rate trajectories is constant and given by $\tau = \frac{A}{u_{\max}}$. The endpoint of this trajectory lies in $\mathscr{D}_+$ and thus, as before, the minimum tumor volume is realized as the subsequent trajectory for $u = 0$ crosses the diagonal at time $T = T(\delta)$. Hence the control is given by

$$u_\delta(t) = \begin{cases} 0 & \text{for } \tau \le t \le \delta, \\ u_{\max} & \text{for } \delta \le t \le \tau + \delta, \\ 0 & \text{for } \tau + \delta \le t \le T(\delta). \end{cases}$$

Switchings from $u = 0$ to $u = u_{\max}$ are feasible in the region F, but the second switching must be in E for such a structure to be optimal. As before, the corresponding value $\upsilon(\delta) = p_\delta(T(\delta))$ is a continuously differentiable function and attains its minimum on the compact interval $[0, \theta]$. If this minimum is attained for $\theta = 0$, optimal controlled trajectories are simply of the form $\mathbf{u}_{\max}\mathbf{0}$ and this is the structure for initial points near the inadmissible portion of the singular arc. If the minimum is attained in the interior of the interval, $0 < \delta_{\min} < \theta$, then optimal controls are bang-bang with two switchings in the order $\mathbf{0u}_{\max}\mathbf{0}$. While this may appear odd, it can arise for initial conditions with low carrying capacities, $q \ll p$. Intuitively, if the optimal tumor reductions arise along the $\dot{q}$-nullcline for $u = u_{\max}$, then it is optimal to let the vasculature grow to get close to this nullcline and only then apply agents to reduce the tumor volume. While clearly possible as optimal controls for such an initial condition, the initial condition itself is not medically realistic and we do not discuss this scenario further. The minimum of $\upsilon(\delta)$ is attained for the right end point $\delta = \theta$ only if ς meets the singular arc in its admissible portion. (It is not difficult to see that there cannot be a switch from $u = 0$ to $u = u_{\max}$ anywhere on $\mathscr{S}_0^+$.) In this case, the analysis of Section B.4.2 applies and overall the optimal control is of the form $\mathbf{0su}_{\max}\mathbf{0}$. However, also these initial conditions are not realistic for the underlying problem. This concludes the mathematical proof of Theorem 5.3.1.

(iv) Initial conditions (p,q) that lie in $\mathscr{D}$, but not in E or F, are even less relevant. It is possible to carry on the mathematical analysis and, for example, it easily follows from the results that have already been established that optimal controls are concatenations of at most the form $\mathbf{0u}_{\max}\mathbf{su}_{\max}\mathbf{0}$ if the initial condition lies in the region *III*. (Proposition B.4.1 allows for one more switch from $u = 0$ to $u = u_{\max}$ in the region *III* before the system enters the region E.) For initial conditions that lie in region *IV*, in principle one more switch could occur, but such conditions are totally unrealistic. In fact, in view of Lemma 5.3.1, any such initial conditions are not viable steady states and would never occur as initial conditions for the medical problem. These are the ones in the region $III \cap \mathscr{N}_+$.

B.4.4 On the Mathematical Verification of the Optimal Synthesis

We close with some comments on the construction of the synthesis. For every possible initial condition $(p,q;0)$ with $(p,q) \in \tilde{\mathscr{D}} = E \cup \mathscr{D}_0 \cup F$, the reasoning above

shows that optimal controls are at most concatenations of the form $\mathbf{bsu}_{\max}\mathbf{0}$ with $\mathbf{b}$ denoting an arc corresponding to the control $u = 0$ or $u = u_{\max}$ and, in each case, if the structure of a unique extremal is not clear a priori, a simple one-dimensional minimization allows to compute the optimal control. This, for all means and purposes, solves the optimal control problem.

An *optimal synthesis* for an optimal control problem provides a decomposition of the state space into a finite (or possibly even countably infinite) collection of embedded submanifolds, $\mathscr{M} = \{M_i\}_{i\in\mathbb{N}}$, sometimes also called *strata*, together with (i) a well-defined flow of trajectories corresponding to admissible controls on each stratum and (ii) regular transitions between the strata that generate (iii) a memoryless flow of extremal trajectories, i.e., there exist unique solutions forward in time and the resulting controlled trajectories satisfy the conditions of the Pontryagin maximum principle (c.f., Theorem A.4.4). Modulo minor technical arguments that have not been given, our construction above does precisely that. Basically, it would still need to be established rigorously that there exists a unique curve Γ_{cut} in the set $F \times \{0\}$ that separates the regions where $u = 0$ and $u = u_{\max}$ and it would need to be shown that there is a well-defined curve $\Psi : \mathscr{S}_{ad} \to [0,A]$, $p \mapsto \Upsilon(p)$, defined over $\mathscr{S}_{ad}$, the admissible portion of the singular base curve, that separates points where the optimal control is singular (and this will happen for points that have y-values below the curve) from those points where $u = u_{\max}$ (above this curve). This curve passes through the lower saturation point $(\tilde{p},\tilde{q})$ when $y = A$ and increases along the singular arc $\mathscr{S}_{ad}$ to reach this terminal value for $\tilde{p}$. These arguments become even more technical and do not add new insights into the structure of optimal controlled trajectories. We therefore do not carry them out here.

It is clear from our proofs that all constructed controlled trajectories are extremal and thus satisfy the conditions of the maximum principle. This is essential in the verification that the cost-to-go function, i.e., the cost evaluated along the trajectories in the synthesis, is a solution to the Hamilton-Jacobi-Bellman equation. It is not difficult to verify that the cost is a continuous functions and, in fact, is continuously differentiable away from some lower dimensional submanifolds which are related to structural changes in the optimal controls (like the cut-locus Γ_{cut} where optimal concatenation sequences change from $\mathbf{0u}_{\max}\mathbf{0}$ to $\mathbf{0su}_{\max}\mathbf{0}$ or near the saturation point where changes from $\mathbf{bs0}$ to $\mathbf{bsu}_{\max}\mathbf{0}$ occur). We refer the interested reader to Section 6.2 of our textbook [292] where a detailed proof of the differentiability of the value has been carried out for the case of an optimal controlled trajectory of the form $\mathbf{u}_{\max}\mathbf{s0}$ for an initial condition in the region $III \cap \mathscr{N}_+$. These, and further analogous verifications simply make sure that the technical assumptions for an optimal synthesis are met. Specifically, the conditions of Theorem 6.3.3. in [292] hold. We only mention that not all of the requirements imposed on a regular synthesis as defined originally by Boltyansky [29] are satisfied. Indeed, there exist tangential intersections of some of the strata at the saturation point for the singular control. However, such transversal intersections are not required in Sussmann's approach [276] (also, see [292, Section 6.3]).

References

1. New Applications of Cancer Immunotherapy, *Seminars in Oncology*, S.A. Agarwala, Ed., Special Issue **29-3**, Suppl. 7, (2003).
2. A.A. Agrachev and Y. Sachkov, *Control Theory from the Geometric Viewpoint*, Springer, 2004.
3. Z. Agur, R. Arnon and B. Schechter, Reduction of cytotoxicity to normal tissues by new regimens of phase-specific drugs, *Mathematical Biosciences*, **92**, (1988), pp. 1–15.
4. Z. Agur, L. Arakelyan, P. Daugulis and Y. Ginosar, Hopf point analysis for angiogenesis models, *Discrete and Continuous Dynamical Systems, Series B*, **4**(1), (2004), pp. 29–38.
5. B. Alberts, A. Johnson, J. Lewis, M. Raff, K. Roberts, P. Walter, *Molecular Biology of the Cell*, Fourth Edition, Garland Science, Talor and Francis, New York, 2002.
6. M.R. Alison and C.E. Sarraf, *Understanding Cancer-From Basic Science to Clinical Practice*, Cambridge University Press, 1997.
7. K. Alitalo, Amplification of cellular oncogenes in cancer cells, *Trends Biochemical Science*, **10** (1985), pp. 194–197.
8. A. Anderson and M. Chaplain, Continuous and discrete mathematical models of tumor-induced angiogenesis, *Bulletin of Mathematical Biology*, **60**, (1998), pp. 857–899.
9. N. André, L. Padovani, E. Pasquier, Metronomic scheduling of anticancer treatment: the next generation of multitarget therapy? *Future Oncology*, **7**(3), (2011), pp. 385–394.
10. M. Andreef, A. Tafuri, P. Bettelheim, P. Valent, E. Estey, R. Lemoli, A. Goodacre, B. Clarkson, F. Mandelli, and A. Deisseroth, Cytokinetic resistance in acute leukemia: Recombinant human granulocyte colony-stimulating factor, granulocyte macrophage colony stimulating factor, interleukin 3 and stem cell factor effects in vitro and clinical trials with granulocyte macrophage colony stimulating factor, *Haematolology and Blood Transfusion*,**4**, (1992), pp. 108-117.
11. D. Angeli, J.E. Ferrell, and E.D. Sontag, Detection of multistability, bifurcations, and hysteresis in a large class of biological positive-feedback systems, *Proceedings of the National Academy of Sciences*, **101**(7), (2004), pp. 1822–1827.
12. S. Anita, V. Arnăutu and V. Capasso, *An Introduction to Optimal Control Problems in Life Sciences and Economics*, Birkhäuser, New York, 2010.
13. L. Arakelyan, V. Vainstain and Z. Agur, A computer algorithm describing the process of vessel formation and maturation, and its use for predicting the effects of anti-angiogenic and anti-maturation therapy on vascular tumour growth, *Angiogenesis*, **5**(3), (2003), pp. 203–214.
14. D.R. Beil and L.M. Wein, Sequencing surgery, radiotherapy, and chemotherapy: insights from a mathematical analysis, *Breast Cancer Research and Treatment*, **74**, (2002), pp. 279–286.

H. Schättler, U. Ledzewicz, *Optimal Control for Mathematical Models of Cancer Therapies*, Interdisciplinary Applied Mathematics 42,
DOI 10.1007/978-1-4939-2972-6

15. D.J. Bell and D.H. Jacobson, *Singular Optimal Control Problems*, Academic Press, New York, 1975.
16. J. Bellmunt, J.M. Trigo, E. Calvo, J. Carles, J.L. Pérez-Garcia, J.A. Virizuela, R. Lopez, M. Lázaro and J. Albanell, Activity of a multi-targeted chemo-switch regimen (sorafenib, gemcitabine, and metronomic capecitabine) in metastatic renal-cell carcinoma: a phase-2 study (SOGUG-02-06), *Lancet Oncology*, 2010.
17. N. Bellomo, N. Delitala, From the mathematical kinetic, and stochastic game theory for active particles to modelling mutations, onset, progression and immune competition of cancer cells, *Physics of Life Reviews*, **5**, (2008), pp. 183–206.
18. N. Bellomo and L. Preziosi, Modelling and mathematical problems related to tumor evolution and its interaction with the immune system, *Mathematical and Computer Modelling*, **32**, (2000), pp. 413–452.
19. D.A. Benson, A Gauss pseudospectral transcription for optimal control, Ph.D. dissertation, Dept. of Aeronautics and Astronautics, MIT, November 2004.
20. D.A. Benson, G.T. Huntington, T.P. Thorvaldsen, and A.V. Rao, Direct trajectory optimization and costate estimation via an orthogonal collocation method, *Journal of Guidance, Control, and Dynamics*, **29** (6), (2006), pp. 1435–1440.
21. S. Benzekry, N. André, A. Benabdallah, J. Ciccolini, C. Faivre, F. Hubert and D. Barbolosi, Modeling the impact of anticancer agents on metastatic spreading, *Mathematical Modeling of Natural Phenomena*, **7**(1), 2012, pp. 306–336, doi: 10.1051/mmnp/20127114.
22. S. Benzekry, D. Barbolosi, A. Benabdallah, F. Hubert and D. Barbolosi, Quantitative analysis of the tumor/metastasis system and its optimal therapeutic control,
23. S. Benzekry and P. Hahnfeldt, Maximum tolerated dose versus metronomic scheduling in the treatment of metastatic cancers, *J. Theoretical Biology*, **335**, (2013), pp. 235—244.
24. G. Bocci, K. Nicolaou and R.S. Kerbel, Protracted low-dose effects on human endothelial cell proliferation and survival in vitro reveal a selective antiangiogenic window for various chemotherapeutic drugs, *Cancer Research*, **62**, (2002), pp. 6938–6943.
25. S. Benzekry, C. Lamont, A. Beheshti, A. Tracz, Classical mathematical models for description and prediction of experimental tumor growth, *PLoS Computational Biology*, **10**(8), (2014), e1003800, doi:10.1371/journal.pcbi.1003800.
26. F. Billy, J. Clairambault and O. Fercoq, Optimisation of cancer drug treatments using cell population dynamics, in: *Mathematical Methods and Models in Biomedicine*, (U. Ledzewicz, H. Schättler, A. Friedman and E. Kashdan, Eds.), Lecture Notes on Mathematical Modeling in the Life Sciences, Springer Verlag, 2012, pp. 265–309.
27. M. Bodnar and U. Forys, Hahnfeldt angiogenesis model with time delays, Proceedings of the 13th National Conference on Applications of Mathematics in Biology and Medicine, Serpelice nad Bugiem, Poland, September 2007, pp. 19–24.
28. T. Boehm, J. Folkman, T. Browder and M.S. O'Reilly, Antiangiogenic therapy of experimental cancer does not induce acquired drug resistance, *Nature*, 390, (1997), pp. 404–407.
29. V.G. Boltyansky, Sufficient conditions for optimality and the justification of the dynamic programming method, *SIAM J. Control*, **4**, (1966), pp. 326–361.
30. G. Bonadonna, M. Zambetti and P. Valagussa, Sequential of alternating Doxorubicin and CMF regimens in breast cancer with more then 3 positive nodes. Ten years results, *JAMA-The Journal of the American Medical Association*, **273**, (1995), pp. 542–547.
31. B. Bonnard and M. Chyba, *Singular Trajectories and their Role in Control Theory*, Springer, Series: Mathematics and Applications, Vol. 40, 2003.
32. B. Bonnard and J. de Morant, Toward a geometric theory in the time-minimal control of chemical batch reactors, *SIAM J. Control and Optimization*, **33** (1995), pp. 1279–1311.
33. J. Borges, On rigor in science, in: *Dreamtigers*, University of Texas Press, Austin, 1964.
34. W.E. Boyce and R.C. di Prima, *Elementary Differential Equations and Boundary Value Problems*, Wiley, 9th ed., 2009
35. F. Brauer and C. Castillo-Chavez, *Mathematical Models in Population Biology and Epidemiology*, Springer, 2001.

36. D.J. Brenner, E.J. Hall, Y. Huang and R.K. Sachs, Optimizing the time course of brachytherapy and other accelerated radiotherapy protocols, *Int. J. of Radiation Oncology and Biological Physics*, **29**, (1994), pp. 893–901.
37. D.J. Brenner, L.R. Hlatky, P.J. Hahnfeldt, Y. Huang and R.K. Sachs, The linear-quadratic model and most other common radiobiological models result in similar predictions of time-dose relationships, *Radiation Research*, **150**, (1998), pp. 83–91.
38. A. Bressan and B. Piccoli, *Introduction to the Mathematical Theory of Control*, American Institute of Mathematical Sciences (AIMS), 2007.
39. T. Browder, C.E. Butterfield, B.M. Kräling, B. Shi, B. Marshall, M.S. O'Reilly and J. Folkman, Antiangiogenic scheduling of chemotherapy improves efficacy against experimental drug-resistant cancer, *Cancer Research*, **60**, (2000), pp. 1878–1886.
40. B.W. Brown and J.R. Thompson, A rationale for synchrony strategies in chemotherapy, *Epidemiology*, SIAM Publications, Philadelpia, (1975), pp. 31–48.
41. A.E. Bryson and Y.C. Ho, *Applied Optimal Control*, Hemisphere Publishing, 1975.
42. T. Burden, J. Ernstberger and K.R. Fister, Optimal control applied to immunotherapy, *Discrete and Continuous Dynamical Systems - Series B*, **4**, (2004), pp. 135–146.
43. C. Büskens, Optimierungsmethoden und Sensitivitätsanalyse für optimale Steuerprozesse mit Steuer- und Zustands-Beschränkungen, Dissertation, Institut für Numerische Mathematik, Universität Münster, Germany, 1998.
44. C. Bskens and H. Maurer, Sensitivity analysis and real–time optimization of parametric nonlinear programming problems, in: Online Optimization of Large Scale Systems, M. Grtschel et al., Eds., Springer–Verlag, Berlin, 2001, pp. 3–16.
45. C. Bskens and H. Maurer, SQP–methods for solving optimal control problems with control and state constraints: adjoint variables, sensitivity analysis and real–time control, *J. of Computational and Applied Mathematics*, **120**, (2000), pp. 85–108.
46. P. Calabresi and P.S. Schein, *Medical Oncology, Basic Principles and Clinical Management of Cancer*, Mc Graw-Hill, New Yok, 1993.
47. G. Caravagna, A. d'Onofrio, P. Milazzo and R. Barbuti, Antitumour immune surveillance through stochastic oscillations, *J. of Theoretical Biology*, **265**, (2010), pp. 336–345.
48. A. Cappuccio, F. Castiglione and B. Piccoli, Determination of the optimal therapeutic protocols in cancer immunotherapy, *Mathematical Biosciences*, **209**, (2007), pp. 1-13.
49. F. Castiglione and B. Piccoli, Optimal control in a model of dendritic cell transfection cancer immunotherapy, *Bulletin of Mathematical Biology*, **68**, (2006), pp. 255–274.
50. F. Castiglione and B. Piccoli, Cancer immunotherapy, mathematical modeling and optimal control, *J. of Theoretical Biology*, **247**, (2007), pp. 723–732.
51. L. Cesari, *Optimization - Theory and Applications*, Springer Verlag, New York, 1983.
52. B.A. Chabner and D.L. Longo, *Cancer Chemotherapy and Biotherapy*, Lippencott-Raven, 1996.
53. K.H. Chadwick and H.P. Leenhouts, *The Molecular Theory of Radiation Biology*, Springer-Verlag, Berlin, 1981.
54. M.A.J. Chaplain, Avascular growth, angiogenesis and vascular growth in solid tumours: The mathematical modelling of the stages of tumour development, *Mathematical and Computer Modeling*, **23**, (1996), pp. 47–87.
55. M. Chaplain and A. Anderson, The mathematical modelling, simulation and prediction of tumour-induced angiogenesis, *Invasion and Metastasis*, **16**, (1997), pp. 222–234.
56. D. Chen, J.M. Roda, C.B. Marsh, T.D. Eubank and A. Friedman, Hypoxia inducible factors mediate the inhibition of cancer by GM-CSF: a mathematical model, *Bulletin of Mathematical Biology*, **74**(11), (2012), pp. 2752-2777, doi: 10.1007/s11538-012-9776-3.
57. J. Clairambault, Modeling physiological and pharmacological control on cell proliferation to optimize cancer treatments, *Mathematical Modelling of Natural Phenomena*, **4**, (2009), pp. 12–67.
58. S.E. Clare, F. Nahlis, J.C. Panetta, Molecular biology of breast cancer metastasis. The use of mathematical models to determine relapse and to predict response to chemotherapy in breast cancer, *Breast Cancer Res.*, **2**, (2000), pp. 396–399.

59. L. Cojocaru and Z. Agur, A theoretical analysis of interval drug dosing for cell-cycle-phase-specific drugs, *Mathematical Biosciences*, **109**, (1992), pp. 85–97.
60. A.J. Coldman and J.H. Goldie, A model for the resistance of tumor cells to cancer chemotherapeutic agents, *Mathematical Biosciences*, **65**, (1983), pp. 291–307.
61. A.J. Coldman and J.H. Goldie, A stochastic model for the origin and treatment of tumors containing drug-resistant cells, *Bulletin of Mathematical Biology*, 48, (1986), pp. 279–292.G
62. L.P. Coly, D.W. van Bekkum and A. Hagenbeek, Enhanced tumor load reduction after chemotherapy induced recruitment and synchronization in a slowly growing rat leukemia model (BNML) for human acute myelonic leukemia, *Leukemia Research*, **8**, (1984), pp. 953–963.
63. M.I. Costa and J.L. Baldrini, Conflicting objectives in chemotherapy with drug resistance, *Bulletin of Mathematical Biology*, **59**, (1997), pp. 707–724.
64. M.I.S. Costa, J.L. Boldrini and R.C. Bassanezi, Drug kinetics and drug resistance in optimal chemotherapy, *Mathematical Biosciences*, **125**, (1995), pp. 191–209.
65. G. Craciun, B. Aguda and A. Friedman, Mathematical analysis of a modular network coordinating the cell cycle and apoptosis, *Mathematical Biosciences and Engineering*, **2**, (2005), pp. 473–485.
66. S. Davis and G.D. Yancopoulos, The angiopoietins: Yin and Yang in angiogenesis, *Current Topics in Microbiology and Immunology*, **237**, (1999), pp. 173–185.
67. B.F. Dibrov, A.M. Zhabotynsky, A.M. Krinskaya, A.V. Neyfakh, A. Yu and L.I. Churikova, Mathematical model of cancer chemotherapy. Periodic schedules of phase-specific cytotoxic agent administration increasing the selectivity of therapy, *Mathematical Biosciences*, **73**, (1985), pp. 1–31.
68. B.F. Dibrov, A.M. Zhabotinsky, A. Yu, M.P. Orlova, Mathematical model of hydroxyurea effects on cell populations in vivo (in Russian), *Chem-Pharm J.*, **20**, (1986), pp. 147–153.
69. T.A. Drixler, I.H. Borel Rinkes, E.D. Ritchie, T.J. van Vroonhoven, M.F. Gebbink and E.E. Voest, Continuous administration of angiostatin inhibits accelerated growth of colorectal liver metastasies after partial hepatectomy, *Cancer Research*, **60**, (2000), pp. 1761–1765.
70. Z. Duda, A gradient method for application of chemotherapy models, *J. of Biological Systems*, **3**, (1995), pp. 3–11.
71. Z. Duda, Numerical solutions to bilinear models arising in cancer chemotherapy, *Nonlinear World*, **4**, (1997), pp. 53–72.
72. G.P. Dunn, L.J. Old and R.D. Schreiber, The three ES of Cancer Immunoediting, *Annual Review of Immunology*, **22**, (2004), pp. 322–360.
73. R. Eidukevicius, D. Characiejus, R. Janavicius, N. Kazlauskaite, V. Pasukoniene, M. Mauricas and W.D. Otter, A method to estimate cell cycle time and growth fraction using bromodeoxyuridine-flow cytometry data from a single sample, *BMC Cancer*, (2006), 6:184.
74. M. Eisen, *Mathematical Models in Cell Biology and Cancer Chemotherapy*, Lecture Notes in Biomathematics, Vol. 30, Springer Verlag, Berlin, 1979.
75. M. Eisen and J. Schiller, Stability analysis of normal and neoplastic growth, *Bulletin of Mathematical Biology*, **66**, (1977), pp. 799–809.
76. D. Elliott, *Bilinear Control Systems - Matrices in Action*, Applied Mathematical Sciences, Vol. 169, Springer, New York, 2009.
77. A. Ergun, K. Camphausen and L.M. Wein, Optimal scheduling of radiotherapy and angiogenic inhibitors, *Bulletin of Mathematical Biology*, **65**, (2003), pp. 407–424.
78. J.H. Eschenburg and E. Heintze, Comparison theory for Riccati equations, *Manuscripta Matematicae*, **68**, (1990), pp. 209–214.
79. A. Fasano and A. Gandolfi, The steady state of multicellular tumour spheroids: a modelling challenge, in: *Mathematical Methods and Models in Biomedicine*, (U. Ledzewicz, H. Schättler, A. Friedman and E. Kashdan, Eds.), Lecture Notes on Mathematical Modeling in the Life Sciences, Vol. 1, Springer Verlag, 2012, pp. 171–194.
80. U. Felgenhauer, L. Poggiolini, and G. Stefani, Optimality and stability result for bang-bang optimal controls with simple and double switch behaviour. in: 50 Years of Optimal Control, A. Ioffe, K. Malanowski, F. Tröltzsch, Eds., *Control and Cybernetics*, **38**, (2009), pp. 1305–1325.

81. M.M. Ferreira, U. Ledzewicz, M. do Rosario de Pinho and H. Schättler, A model for cancer chemotherapy with state space constraints, *Nonlinear Analysis*, **63**(5), 2005, pp. 2591–2602.
82. K.R. Fister and J. Hughes Donnelly, Immunotherapy: an optimal control approach, *Mathematical Biosciences and Engineering (MBE)*, **2**(3), (2005), pp. 499–510.
83. K.R. Fister and J.C. Panetta, Optimal control applied to cell-cycle-specific cancer chemotherapy, *SIAM J. of Applied Mathematics*, **60**, (2000), pp. 1059–1072.
84. W.H. Fleming and R.W. Rishel, *Deterministic and Stochastic Optimal Control*, Springer Verlag, 1975.
85. J. Folkman, Tumor angiogenesis: therapeutic implications, *New England J. of Medicine*, **295**, (1971), pp. 1182–1196.
86. J. Folkman, Antiangiogenesis: new concept for therapy of solid tumors, *Annals of Surgery*, **175**, (1972), pp. 409–416.
87. J. Folkman, The vascularization of tumors, *Scientific American*, **234**, (1976), pp. 58–73.
88. J. Folkman, Angiogenesis inhibitors generated by tumors, *Molecular Medicine*, **1**, (1995), pp. 120–122.
89. J. Folkman, Opinion - Angiogenesis: an organizing principle for drug discovery? *Nature Reviews Drug Discovery*, (2007), **6**, pp. 273–286.
90. J. Folkman and M. Klagsburn, Angiogenic factors, *Science*, **235**, (1987), pp. 442–447.
91. U. Forys, Y. Keifetz and Y. Kogan, Critical-point analysis for three-variable cancer angiogenesis models, *Mathematical Biosciences and Engineering-MBE*, **2**(3), (2005), pp. 511–525.
92. U. Forys, J. Waniewski and P. Zhivkov, Anti-tumor immunity and tumor anti-immunity in a mathematical model of tumor immunotherapy, *J. of Biological Systems*, **14**, (2006), pp. 13–30.
93. R. Fourer, D.M. Gay, and B.W. Kernighan, "AMPL: A Modeling Language for Mathematical Programming", Duxbury Press, Brooks-Cole Publishing Company, 1993.
94. J.F. Fowler, The linear-quadratic formula and progress in fractionated radiotherapy, *British J. of Radiology*, **62**, (1989), pp. 679–694.
95. D. Frame, New strategies in controlling drug resistance. *J. of Managed Care Pharmacy*, **13**, (2007), pp. 13–17.
96. A. Friedman, A hierarchy of cancer models and their mathematical challenges, *Discrete and Continuous Dynamical Systems, Series B*, **4**, (2004), pp. 147–160.
97. A. Friedman, Cancer models and their mathematical analysis, in: *Tutorials in Mathematical Biosciences III*, Lecture Notes in Mathematics, Vol. 1872, pp. 223–246, 2006.
98. A. Friedman, Mathematical analysis and challenges arising from models of tumor growth, *Mathematical Models & Methods in Applied Sciences*, **17**, Suppl. (2007), pp. 1751–1772.
99. A. Friedman and Y. Kim, Tumor cell proliferation and migration under the influence of their microenvironment, *Mathematical Biosciences and Engineering - MBE*, **8**(2), (2011), pp. 371–383.
100. A. Friedman, J.P. Tian, G. Fulci, E.A. Chocca and J. Wang, Glioma virotherapy: the effects of innate immune suppression and increased viral replication capacity, *Cancer Research*, **66**(4), (2006), pp. 2314–2319.
101. H. Gaff and E. Schaefer, Optimal control applied to vaccination and treatment strategies for various epidemiologic models, *Mathematical Biosciences and Engineering (MBE)*, **6**, (2009), pp. 469–492.
102. R.A. Gatenby, A.S. Silva, R.J. Gillies, and B.R. Frieden, Adaptive therapy, *Cancer Research*, **69**, 4894–4903, (2009).
103. H. Gardner-Moyer, Sufficient conditions for a strong minimum in singular control problems, *SIAM J. Control*, **11** (1973), pp. 620–636.
104. J.H. Goldie, Drug resistance in cancer: a perspective, *Cancer and Metastasis Review*, **20**, (2001), pp. 63–68.
105. J.H. Goldie and A. Coldman, A model for resistance of tumor cells to cancer chemotherapeutic agents, *Mathematical Biosciences*, **65**, (1983), pp. 291–307.
106. J.H. Goldie and A. Coldman, Quantitative model for multiple levels of drug resistance in clinical tumors, *Cancer Treatment Reports*, **67**, (1983), pp. 923–931.

107. J.H. Goldie and A. Coldman, *Drug Resistance in Cancer*, Cambridge University Press, 1998.
108. R. Goodman, *Introduction to Stochastic Models*, Benjamin Cummings, Menlo Park, CA, 1988.
109. R. Grantab, S. Sivananthan and I.F. Tannock, The penetration of anticancer drugs through tumor tissue as a function of cellular adhesion and packing density of tumor cells, *Cancer Research*, **66**, (2006), pp. 1033–1039.
110. J. Greene, O. Lavi, M.M. Gottesman and D. Levy, The impact of cell density and mutations in a model of multidrug resistance in solid tumors, *Bulletin of Mathematical Biology*, **74**, (2014), pp. 627–653, doi:10.1007/s11538-014-9936-8.
111. J. Guckenheimer and P. Holmes, *Nonlinear Oscillations, Dynamical Systems, and Bifurcations of Vector Fields*, Springer Verlag, New York, 1983.
112. C. Guiot, P.G. Degiorgis, P.P. Delsanto, P. Gabriele, and T.S. Deisboecke, Does tumor growth follow a 'universal law'?, *J. of Theoretical Biology*, **225**, (2003), pp. 147–151.
113. J.D. Hainsworth and F.A. Greco, Paclitaxel administered by 1-hour infusion, *Cancer*, **74**, (1994), pp. 1377–1382.
114. W. Hahn, *Stability of Motion*, Springer Verlag, New York, 1967.
115. P. Hahnfeldt and L. Hlatky, Cell resensitization during protracted dosing of heterogeneous cell populations, *Radiation Research*, **150**, (1998), pp. 681–687.
116. P. Hahnfeldt, D. Panigrahy, J. Folkman and L. Hlatky, Tumor development under angiogenic signaling: a dynamical theory of tumor growth, treatment response, and postvascular dormancy, *Cancer Research*, **59**, (1999), pp. 4770–4775.
117. P. Hahnfeldt, J. Folkman and L. Hlatky, Minimizing long-term burden: the logic for metronomic chemotherapeutic dosing and its angiogenic basis, *J. of Theoretical Biology*, **220**, (2003), pp. 545–554.
118. D. Hanahan, G. Bergers and E. Bergsland, Less is more, regularly: metronomic dosing of cytotoxic drugs can target tumor angiogenesis in mice, *J. Clinical Investigations*, **105**(8), (2000), pp. 1045–1047.
119. D. Hanahan and R.A. Weinberg, Hallmarks of Cancer: The Next Generation, *Cell*, 144, (2011), pp. 646–674.
120. L.G. Hanin and M. Zaider, Cell-survival probability at large doses: an alternative to the linear-quadratic models, *Physics in Medicine and Biology*, **55**, (2010), pp. 4687–4702.
121. Y.B. Hao, S.Y. Yi, J. Ruan, L. Zhao and K.J. Nan, New insights into metronomic chemotherapy-induced immunoregulation, *Cancer Letters*, **354**(2),(2014) pp. 220–226.
122. L.E. Harnevo and Z. Agur, The dynamics of gene amplification described as a multitype compartmental model and as a branching process, *Mathematical Biosciences*, **103** (1991), pp. 115–138.
123. L.E. Harnevo and Z. Agur, Drug resistance as a dynamic process in a model for multistep gene amplification under various levels of selection stringency, *Cancer Chemotherapy and Pharmacology*, **30**, (1992), pp. 469–476.
124. D. Hart, E. Shochat, and Z. Agur, The growth law of primary breast cancer as inferred from mammography screening trials data, *British J. of Cancer*, **78**, (1999), pp. 382–387.
125. H. Hethcote, The Mathematics of Infectious Diseases, *SIAM Review*, **42**, (2000), pp. 599–653.
126. B.T. Hill, Cancer chemotherapy. The relevance of certain concepts of cell cycle kinetics, *Biochimica et Biophysica Acta*, **516**(4), (1979), pp. 389–417.
127. T. Hillen, G. de Vries, J. Gong and C. Finlay, From cell population models to tumor control probability: including cell cycle effects, *Acta Oncologica*, 2010; doi: 10.3109/02841861003631487.
128. L. Holmgren, M.S. OReilly and J. Folkman, Dormancy of micrometastases: balanced proliferation and apoptosis in the presence of angiogenesis suppression, *Nature Medicine*, **1**, (1995), pp. 149–153.
129. G.T. Huntington, Advancement and Analysis of a Gauss Pseudospectral Transcription for Optimal Control, Ph.D. dissertation, Dept. of Aeronautics and Astronautics, MIT, May 2007.

130. T.L. Jackson and H. Byrne, A mathematical model to study the effects of drug resistance and vascularization on the response of solid tumors to chemotherapy, *Mathematical Biosciences*, **164**, (2000), pp. 17–38.
131. R.K. Jain, Normalizing tumor vasculature with anti-angiogenic therapy: a new paradigm for combination therapy, *Nature Medicine*, **7**, (2001), pp. 987–989.
132. R.K. Jain and L.L. Munn, Vascular normalization as a rationale for combining chemotherapy with antiangiogenic agents, *Principles of Practical Oncology*, **21**, (2007), pp. 1–7.
133. E. Jung, S. Lenhart and Z. Feng, Optimal control of treatments in a two strain tuberculosis model, *Discrete and Continuous Dynamical Systems, Series B*, **2**, (2002), pp. 473–482.
134. V. Jurdjevic, *Geometric Control Theory*, Cambridge Studies in Advanced Mathematics, Vol. 51, Cambridge University Press, 1977.
135. S. Karlin and H.M. Taylor, *A First Course in Stochastic Processes*, Academic Press, San Diego, 1975.
136. B. Kamen, E. Rubin, J. Aisner, and E. Glatstein, High-time chemotherapy or high time for low dose? *J. Clinical Oncology*, **18**, (2000), editorial, pp. 2935–2937.
137. J.M. Kaminski , J.B. Summers, M.B. Ward, M.R. Huber and B. Minev, Immunotherapy and prostate cancer, *Cancer Treatment Review*, **29**, (2004), pp. 199–209.
138. R.J. Kaufman, P.C. Brown, and R.T. Schimke, Loss and stabilization of amplified dihydrofolate reductase genes in mouse sarcoma S-180 cell lines, *Molecular Cell Biology*, **1** (1981), pp. 1084–1093.
139. A.M. Kellerer and H.H. Rossi, The theory of dual radiation action, *Current Topics in Radiation Research Quarterly*, **8**, (1972), pp. 85–158.
140. B.J. Kennedy, Cyclic leukocyte oscillations in chronic myelogenous leukemia during hydroxyurea therapy, *Blood*, **35**, (1970), pp. 751–760.
141. R.S. Kerbel, A cancer therapy resistant to resistance, *Nature*, **390**, (1997), pp. 335–336.
142. R.S. Kerbel, Tumor angiogenesis: past, present and near future, *Carcinogensis*, **21**, (2000), pp. 505–515.
143. R. Kerbel and J. Folkman, Clinical translation of angiogenesis inhibitors, *Nature Reviews Cancer*, **2**, (2002), pp. 727–739.
144. T.J. Kindt, B.A. Osborne and R.A. Goldsby, *Kuby Immunology*, W.H. Freeman 2006.
145. H.K. Khalil, *Nonlinear Systems*, 3rd. ed. Prentice Hall, 2002.
146. Y. Kim and A. Friedman, Interaction of tumor with its microenvironment: a mathematical model, *Bulletin of Mathematical Biology*, **72**, (2010), pp. 1029–1068.
147. M. Kim, K.B. Woo and S. Perry, Quantitative approach to the design of antitumour drug dosage schedule via cell cycle kinetics and systems theory, *Annals of Biomedical Engineering*, **5**, (1977), pp. 12–33.
148. M. Kimmel and D.E. Axelrod, Mathematical models of gene amplification with applications to cellular drug resistance and tumorigenicity, *Genetics*, **125** (1990), pp. 633–644.
149. M. Kimmel and D.E. Axelrod, *Branching Processes in Biology*, Springer Verlag, New York, NY, 2002.
150. M. Kimmel and A. Swierniak, An optimal control problem related to leukemia chemotherapy, *Scientific Bulletins of the Silesian Technical University*, **65**, (1983), pp. 120–130.
151. M. Kimmel and A. Swierniak, Control theory approach to cancer chemotherapy: benefitting from phase dependence and overcoming drug resistance, in: Tutorials in Mathematical Biosciences III: Cell Cycle, Proliferation, and Cancer, Lecture Notes in Mathematics, Mathematical Biosciences Subseries, Springer, Heidelberg, 2006.
152. M. Kimmel, A. Swierniak and A. Polanski, Infinite-dimensional model of evolution of drug resistance of cancer cells, *J. of Mathematical Systems, Estimation and Control*, **8**, (1998), pp. 1–16.
153. M. Kimmel and A. Swierniak, Control theory approach to cancer chemotherapy: benefiting from phase dependence and overcoming drug resistance, in: *Tutorials in Mathematical Biosciences III: Cell Cycle, Proliferation, and Cancer*, A. Friedman, ed., *Lecture Notes in Mathematics, Vol. 1872*, Springer, New York, (2006), pp. 185-221.
154. M. Kimmel and F. Traganos, Estimation and prediction of cell cycle specific effects of anticancer drugs, *Mathematical Biosciences*, **80**, (1986), pp. 187–208.

155. J.P. Kirkpatrick, J.P. Meyer and L.B. Marks, The linear-quadratic model is inappropriate to model high dose per fraction effects in radiosurgery, *Seminars in Radiation Oncology*, **18**(4), (2008), pp. 240–243.
156. D. Kirschner, Using mathematics to understand HIV immune dynamics, *Notices of the American Mathematical Society*, **43**, (1996), pp. 191–202.
157. D. Kirschner, S. Lenhart, and S. Serbin, Optimal control of chemotherapy of HIV, *J. of Mathematical Biology*, **35**, (1997), pp. 775–792.
158. D. Kirschner and J.C. Panetta, Modeling immunotherapy of the tumor-immune interaction, *J. of Mathematical Biology*, **37**, (1998), pp. 235–252.
159. D.E. Kirschner and G.F. Webb, A mathematical model of combined drug therapy of HIV infection, *J. of Theoretical Medicine*, **1**, (1997), pp. 25–34.
160. O. Kisker, C.M. Becker, D. Prox, M. Fannon, R. d'Amato, E. Flynn, W.E. Fogler, B.K. Sim, E.N. Allred, S.R. Pirie-Shepherd and J. Folkman, Continuous administration of endostatin by intraperitoneally implanted osmotic pump improves the efficacy and potency of therapy in a mouse xenograft tumor model, *Cancer Research*, **61**, (2001), pp. 7669–7674.
161. M. Klagsburn and S. Soker, VEGF/VPF: the angiogenesis factor found?, *Current Biology*, **3**, (1993), pp. 699–702.
162. G. Klement, S. Baruchel, J. Rak, S. Man, K. Clark, D.J. Hicklin, P. Bohlen and R.S. Kerbel, Continuous low-dose therapy with vinblastine and VEGF receptor-2 antibody induces sustained tumor regression without overt toxicity, *J. Clinical Investigations*, **105**(8), (2000), R15–R24.
163. H.W. Knobloch and F. Kappel, *Gewöhnliche Differentialgleichungen*, B.G. Teubner, Stuttgart, 1974.
164. C.M. Koebel, W. Vermi, J.B. Swann, N. Zerafa, S.J. Rodig, L.J. Old, M.J. Smyth and R.D. Schreiber, Adaptive immunity maintains occult cancer in an equilibrium state, *Nature*, **450**, (2007), pp. 903–907.
165. Y. Kogan, U. Forys, O. Shukron, N. Kronik and Z. Agur, Cellular immunotherapy for high grade gliomas: mathematical analysis deriving efficacious infusion rates based on patient requirements, *SIAM J. Applied Mathematics*, **70**, (2010), pp. 1953–1976.
166. M. Kohandel, M. Kardar, S. Sivaloganathan and M. Milosevic, Dynamics of tumor growth and combination of anti-angiogenic and cytotoxic therapies, *Physics in Medicine and Biology*, **52**, (2007), pp. 3665–3667.
167. N.L. Komarova, E. Barnes, P. Klenerman and D. Wodarz, Boosting immunity by anti-viral drug therapy: a simple relationship between timing, efficacy and success, *Proceedings of the National Academy of Sciences*, **100**, (2003), pp. 1855–1860.
168. N.L. Komarova and D. Wodarz, *Targeted Cancer Treatment in Silico-Small Molecule Inhibitors and Oncolytic Viruses*, Birkhäuser, 2014.
169. E.L. Korn, S.G. Arbuck, J.M. Pluda, R. Simon, R.S. Kaplan and M.C. Christian, Clinical trial designs for cytostatic agents: are new approaches needed? *J. Clinical Oncology*, **19**, (2001), pp. 265–272.
170. F. Kozusko, P. Chen, S.G. Grant, B.W. Day, J.C. Panetta, A mathematical model of in vitro cancer cell growth and treatment with the antimitotic agent curacin A, *Mathematical Biosciences*, **170**, (2001), pp. 1–16.
171. V.A. Kuznetsov, I.A. Makalkin, M.A. Taylor and A.S. Perelson, Nonlinear dynamics of immunogenic tumors: parameter estimation and global bifurcation analysis, *Bulletin of Mathematical Biology*, **56**, (1994), pp. 295–321.
172. B.C. Lampkin, T. Nagao and A.M. Mauer, Synchronization and recruitment in acute leukemia, *J. of Clinical Investigations*, **50**, (1971), pp. 2204–2214.
173. O. Lavi, J. Greene, D. Levy, and M. Gottesman, The role of cell density and intratumoral heterogeneity in multidrug resistance, *Cancer Research*, **73**, (2013), pp. 7168–7175.
174. U. Ledzewicz, B. Amini and H. Schaettler, Dynamics and control of a mathematical model for metronomic chemotherapy, *Mathematical Biosciences and Engineering-MBE*, **12**(6), (2015), to appear

175. U. Ledzewicz, K. Bratton, and H. Schättler, A 3-compartment model for chemotherapy of heterogeneous tumor populations, *Acta Applicandae Matematicae*, **135**(1), (2014), pp. 191–207, doi:10.1007/s10440-014-9952-6
176. U. Ledzewicz, M.S. Faraji Mosalman, and H. Schättler, On optimal protocols for combinations of chemo- and immunotherapy, Proc. 51st IEEE Conference on Decision and Control, Maui, Hawaii, USA (2012), pp. 7492–7497.
177. U. Ledzewicz, M.S. Faraji Mosalman, and H. Schättler, Optimal controls for a mathematical model of tumor-immune interactions under targeted chemotherapy with immune boost, *Discrete and Continuous Dynamical Systems, Series B*, 18, (2013), pp. 1031–1051, doi:10.3934/dcdsb.2013.18.1031.
178. U. Ledzewicz, J. Marriott, H. Maurer and H. Schättler, The scheduling of angiogenic inhibitors minimizing tumor volume, *J. of Medical Informatics and Technologies*, **12**, (2008), pp. 23–28.
179. U. Ledzewicz, J. Marriott, H. Maurer and H. Schättler, Realizable protocols for optimal administration of drugs in mathematical models for anti-angiogenic treatment, *Mathematical Medicine and Biology*, **27**, (2010), pp. 157–179, doi:10.1093/imammb/dqp012.
180. U. Ledzewicz, H. Maurer and H. Schättler, Bang-bang and singular controls in a mathematical model for combined anti-angiogenic and chemotherapy treatment, Proc. 48th IEEE Conference on Decision and Control, Shanghai, China, (2009), pp. 2280–2285.
181. U. Ledzewicz, H. Maurer and H. Schättler, Minimizing tumor volume for a mathematical model of anti-angiogenesis with linear pharmacokinetics, in: *Recent Advances in Optimization and its Applications in Engineering*, M. Diehl, F. Glineur, E. Jarlebring and W. Michiels, Eds., (2010), pp. 267–276.
182. U. Ledzewicz, H. Maurer and H. Schättler, Optimal and suboptimal protocols for a mathematical model for tumor anti-angiogenesis in combination with chemotherapy, *Mathematical Biosciences and Engineering*, **8**(2), (2011), pp. 3-7–323, doi:10.3934/mbe.2011.8.307.
183. U. Ledzewicz, J. Munden and H. Schättler, Scheduling of anti-angiogenic inhibitors for Gompertzian and logistic tumor growth models, *Discrete and Continuous Dynamical Systems, Series B*, **12**, (2009), pp. 415–439.
184. U. Ledzewicz, M. Naghnaeian and H. Schättler, Dynamics of tumor-immune interactions under treatment as an optimal control problem, Proc. of the 8th AIMS Conference on Dynamical Systems, Differential Equations and Applications, Dresden, Germany, 2010, pp. 971–980.
185. U. Ledzewicz, M. Naghnaeian and H. Schättler, Bifurcation of singular arcs in an optimal control problem for cancer immune system interactions under treatment, Proc. of the 49th IEEE Conference on Decision and Control, Atlanta, USA, (2010), pp. 7039–7044.
186. U. Ledzewicz, M. Naghnaeian and H. Schättler, Optimal response to chemotherapy for a mathematical model of tumor-immune dynamics, *J. of Mathematical Biology*, **64**, (2012), pp. 557–577, doi 10.1007/s00285-011-0424-6.
187. U. Ledzewicz, O. Olumoye and H. Schättler, On optimal chemotherapy with a strongly targeted agent for a model of tumor-immune system interactions with generalized logistic growth, *Mathematical Biosciences and Engineering - MBE*, 10(3), (2012), pp. 787–802, doi:10.3934/mbe.2013.10.787.
188. U. Ledzewicz, A. d'Onofrio and H. Schättler, Tumor development under combination treatments with anti-angiogenic therapies, in: *Mathematical Methods and Models in Biomedicine*, (U. Ledzewicz, H. Schättler, A. Friedman and E. Kashdan, Eds.), Lecture Notes on Mathematical Modeling in the Life Sciences, Springer Verlag, 2012, pp. 301–327.
189. U. Ledzewicz, V. Oussa and H. Schättler, Optimal solutions for a model of tumor anti-angiogenesis with a penalty on the cost of treatment, *Applicationes Mathematicae*, **36**(3), (2009), pp. 295–312.
190. U. Ledzewicz and H. Schättler, On a synthesis of controls for a mathematical model of cancer chemotherapy, Proc. of the 39th IEEE Conference on Decision and Control, Sydney, Australia, (2000), pp. 4845–4850.
191. U. Ledzewicz and H. Schättler, Optimal bang-bang controls for a 2-compartment model in cancer chemotherapy, *J. of Optimization Theory and Applications - JOTA*, **114**, (2002), pp. 609–637.

192. U. Ledzewicz and H. Schättler, Analysis of a cell-cycle specific model for cancer chemotherapy, *J. of Biological Systems*, **10**, (2002), pp. 183–206.
193. U. Ledzewicz and H. Schättler, Optimal control for a bilinear model with recruiting agent in cancer chemotherapy, Proc. of the 42nd IEEE Conference on Decision and Control, Maui, Hawaii, December 2003, pp. 2762–2767.
194. U. Ledzewicz and H. Schättler, Controlling a model for bone marrow dynamics in cancer chemotherapy, *Mathematical Biosciences and Engineering*, **1**, (2004), pp. 95–110.
195. U. Ledzewicz and H. Schättler, The influence of PK/PD on the structure of optimal control in cancer chemotherapy models, *Mathematical Biosciences and Engineering (MBE)*, **2**(3), (2005), pp. 561–578.
196. U. Ledzewicz and H. Schättler, A synthesis of optimal controls for a model of tumor growth under angiogenic inhibitors, Proc. of the 44th IEEE Conference on Decision and Control, Sevilla, Spain, December 2005, pp. 934–939.
197. U. Ledzewicz and H. Schättler, Optimal control for a system modelling tumor anti-angiogenesis, Proc. of the ICGST International Conference on Automatic Control and System Engineering, ACSE-05, Cairo, Egypt, December 2005, pp. 147–152.
198. U. Ledzewicz and H. Schättler, Drug resistance in cancer chemotherapy as an optimal control problem, *Discrete and Continuous Dynamical Systems, Series B*, **6**, (2006), pp. 129–150.
199. U. Ledzewicz and H. Schättler, Analysis of models for evolving drug resistance in cancer chemotherapy, *Dynamics of Continuous, Discrete and Impulsive Systems - DCDIS*, Proceedings **2**, (2006), pp. 291–304.
200. U. Ledzewicz and H. Schättler, Application of optimal control to a system describing tumor anti-angiogenesis, Proc. of the 17th International Symposium on Mathematical Theory of Networks and Systems (MTNS), Kyoto, Japan, July 2006, pp. 478-484.
201. U. Ledzewicz and H. Schättler, Antiangiogenic therapy in cancer treatment as an optimal control problem, *SIAM J. on Control and Optimization*, **46**(3), (2007), pp. 1052–1079.
202. U. Ledzewicz and H. Schättler, Optimal controls for a model with pharmacokinetics maximizing bone marrow in cancer chemotherapy, *Mathematical Biosciences*, **206**, (2007), pp. 320–342.
203. U. Ledzewicz and H. Schättler, Optimal and suboptimal protocols for a class of mathematical models of tumor anti-angiogenesis, *J. of Theoretical Biology*, **252**, (2008), pp. 295–312.
204. U. Ledzewicz and H. Schättler, Analysis of a mathematical model for tumor anti-angiogenesis, *Optimal Control, Applications and Methods*, **29**(1), (2008), pp. 41–57.
205. U. Ledzewicz and H. Schättler, Effect of the Objective on Optimal Controls for a System Describing Tumor Anti-Angiogenesis, in: New Aspects of Systems, Part II, Proc. of the 12th WSEAS International Conference on Systems, Heraklion, Greece, July 2008, pp. 483-490
206. U. Ledzewicz and H. Schättler, On the optimality of singular controls for a class of mathematical models for tumor anti-angiogenesis, *Discrete and Continuous Dynamical Systems, Series B*, **11** (3), (2009), pp. 691–715.
207. U. Ledzewicz and H. Schättler, Singular controls and chattering arcs in optimal control problems arising in biomedicine, *Control and Cybernetics*, **38**, (2009), pp. 1501–1523.
208. U. Ledzewicz and H. Schättler, On a mathematical model of combined anti-angiogenic and radiotherapy treatment, Proc. of the 16th National Conference on Applications of Mathematics in Biology and Medicine, Krynica, Poland, September 2010, pp. 76–81.
209. U. Ledzewicz and H. Schättler, Multi-input optimal control problems for combined tumor anti-angiogenic and radiotherapy treatments, *J. of Optimization Theory and Applications - JOTA*, **153**, (2012), pp. 195–224, doi: 10.1007/s10957-011-9954-8.
210. U. Ledzewicz and H. Schättler, On optimal chemotherapy for heterogeneous tumors, *J. of Biological Systems*, **22**(2), (2014), pp. 1-21, doi: 1142/s0218339014400014.
211. U. Ledzewicz and H. Schättler, A review of optimal chemotherapy protocols: from MTD towards metronomic therapy, *Mathematical Modeling of Natural Phenomena*, **9**(4), 2014, pp. 131-152, doi: 10.1051/mmnp/20149409.
212. U. Ledzewicz and H. Schättler, Tumor microenvironment and anticancer therapies: an optimal control approach, in: Mathematical Oncology (A. d'Onofrio and A. Gandolfi, Eds.,), Springer, (2014), pp. 295–334.

213. U. Ledzewicz and H. Schättler, An optimal control approach to cancer chemotherapy with tumor-immune system interactions, in: Mathematical Models of Tumor-Immune System Dynamics (Eladaddi and P. Kim, Eds.), Springer, New York, (2014), pp. 153–193, doi:10.1007/978-1-4939-1793-8-7.
214. U. Ledzewicz, H. Schättler, A. Friedman and E. Kashdan, (Eds.), Mathematical Methods and Models in Biomedicine, Springer, New York, 2013.
215. U. Ledzewicz, H. Schättler, M. Reisi Gahrooi and S. Mahmoudian Dehkordi, On the MTD paradigm and optimal control for multi-drug cancer chemotherapy, *Mathematical Biosciences and Engineering (MBE)*, **10**(3), (2013), pp. 803–819, doi:10.3934/mbe.2013.10.803.
216. S. Lenhart and J.T. Workman, *Optimal Control Applied to Biological Models*, Chapman & Hall/CRC, Mathematical & Computational Biology, 2007.
217. D. Liberzon, *Calculus of Variations and Optimal Control Theory*, Princeton University press, Princeton, 2012.
218. C. de Lisi and A. Rescigno, Immune surveillance and neoplasia: a minimal mathematical model, *Bull. of Mathematical Biology*, **39**, (1977), pp. 201–221.
219. P. Lista, M.F. Brizzi, G. Avanzi, F. Veglia, L. Resegotti and L. Pegoraro, Induction of proliferation of acute myeloblastic leukemia (AML) cells with hemopoietic growth factors, *Leukemia Research*, **12**, (1988), pp. 441–447.
220. L.A. Loeb, A mutator phenotype in cancer, *Cancer Research*, **61**, (2001), pp. 3230–3239.
221. A. Lorz, T. Lorenzi, M.E. Hochberg, J. Clairambault and B. Perthame, Population adaptive evolution, chemotherapeutic resistance and multiple anti-cancer therapies, *ESAIM: Mathematical Modelling and Numerical Analysis*, **47**, (2013) pp. 377-399, doi:10.1051/m2an/2012031.
222. A. Lorz, T. Lorenzi, J. Clairambault, A. Escargueil and B. Perthame, Effects of space structure and combination therapies on phenotypic heterogeneity and drug resistance in solid tumors, preprint
223. A.P. Lyss, Enzymes and random synthetics, in: *Chemotherapy Source Book*, (M.C. Perry ed., 1992), Williams & Wilkins, Baltimore, pp. 403–408.
224. K.J. Luzzi, I.C. MacDonald, E.E. Schmidt, N. Kerkvliet, V.L. Morris, A.F. Chambers, A.C. Groom, Multistep nature of metastatic inefficiency: dormancy of solitary cells after successful extravasation and limited survival of early micrometastases, *American J. of Pathology*, **153**, (1998), pp. 865–873.
225. M.C. Mackey, Unified hypothesis for the origin of aplastic anemia and periodic hematopoeisis, *Blood*, **51**, (1978), pp. 941–956.
226. N.V. Mantzaris, S. Webb and H. Othmer, Mathematical modeling of tumor-induced angiogenesis, *J. of Mathematical Biology*, **49**, (2004), pp. 111-187, doi:10.1007/s00285-003-0262-2.
227. M. Marusic, A. Bajzer, J.P. Freyer, and S. Vuk-Povlovic, Analysis of growth of multicellular tumor spheroids by mathematical models, *Cell Proliferation*, **27**(2), (1994), pp. 73–94.
228. K. Margolin, M.S. Gordon, E. Holmgren, J. Gaudreault, W. Novotny, G. Fyfk, D. Adelman, S. Stalter and J. Breed, Phase Ib trial of intravenous recombinant humanized monoclonal antibody to vascular endothelial cell growth factor in combination with chemotherapy in patients with advanced cancer, *J. of Clinical Oncology*, **19**(3), (2001), pp. 851–856.
229. R.B. Martin, Optimal control drug scheduling of cancer chemotherapy, *Automatica*, **28**, (1992), pp. 1113–1123.
230. R. Martin and K.L. Teo, *Optimal Control of Drug Administration in Cancer Chemotherapy*, World Scientific Press, Singapore, 1994.
231. A. Matveev and A. Savkin, Optimal control applied to drug administration in cancer chemotherapy: the case of several toxicity constraints, Proc. of the 39th IEEE Conference on Decision and Control, Sydney, Australia, (2000), pp. 4833–4838.
232. A. Matzavinos, M. Chaplain and V.A. Kuznetsov, Mathematical modelling of the spatio-temporal response of cytotoxic T-lymphocytes to a solid tumour, *Mathematical Medicine and Biology*, **21**, (2004), pp. 1–34.

233. A.M. Mauer, S.B. Murphy and F.A. Hayes, Evidence for recruitment and synchronization in leukemia and solid tumors, *Cancer Treatment Reports*, **60**, (1976), pp. 1841–1844.
234. H. Maurer, C. Büskens, J.-H. Kim and Y. Kaja, Optimization techniques for the verification of second-order sufficient conditions for bang-bang controls, *Optimal Control, Applications and Methods*, **26**, (2005), pp. 129-156.
235. A. McAneney and S.F.C. O'Rourke, Investigation of various growth mechanisms of solid tumor growth within the linear-quadratic model for radiotherapy, *Physics in Medicine and Biology*, **52**, (2006), pp. 1039–1054.
236. S.R. McDougall, A.R.A. Anderson, M.A. Chaplain, Mathematical modelling of dynamic adaptive tumour-induced angiogenesis: Clinical implications and therapeutic targeting strategies, *J. of Theoretical Biology*, **241**, (2006), pp. 564–589.
237. E. Mehrara, E. Forssell-Aronsson, H. Ahlman, and P. Bernhardt, Specific growth rate versus doubling time for quantitative characterization of tumor growth rate, *Cancer Research*, **67**, (2007), pp. 3970–3975.
238. R.R. Mohler, *Bilinear Control Systems*, Academic Press, (1973).
239. J.C.M. Mombach, N. Lemke, B.E.J. Bodmann, and M.A.P. Idiart, A mean-field theory of cellular growth, *Europhysics Letters*, **59**, (2002), pp. 923–928.
240. J.D. Murray, *Mathematical Biology I: An Introduction*, Interdisciplinary Applied Mathematics, Springer, New York, 2001.
241. J.D. Murray, *Mathematical Biology II: Spatial Models and Biomedical Applications*, Interdisciplinary Applied Mathematics, Springer, New York, 2003.
242. J.M. Murray, Optimal control for a cancer chemotherapy problem with general growth and loss functions, *Mathematical Biosciences*, **98**, (1990), pp. 273–287.
243. J.M. Murray, Some optimal control problems in cancer chemotherapy with a toxicity limit, *Mathematical Biosciences*, **100**, (1990), pp. 49–67.
244. L. Norton and R. Simon, Growth curve of an experimental solid tumor following radiotherapy, *J. of the National Cancer Institute*, **58**, (1977), pp. 1735–1741.
245. L. Norton and R. Simon, Tumor size, sensitivity to therapy, and design of treatment schedules, *Cancer Treatment Reports*, **61**, (1977), pp. 1307–1317.
246. L. Norton and R. Simon, The Norton-Simon hypothesis revisited, *Cancer Treatment Reports*, **70**, (1986), pp. 41–61.
247. L. Norton, A Gompertzian model of human breast cancer growth, *Cancer Research*, **48**, (1988), pp. 7067–7071.
248. A. d'Onofrio, A general framework for modelling tumor-immune system competition and immunotherapy: Mathematical analysis and biomedial inferences, *Physica D*, **208**, (2005), pp. 202–235.
249. A. d'Onofrio, Tumor-immune system interaction: modeling the tumor-stimulated proliferation of effectors and immunotherapy, *Mathematical Models and Methods in Applied Sciences*, **16**, (2006), pp. 1375–1401.
250. A. d'Onofrio, Tumor evasion from immune control: strategies of a MISS to become a MASS, *Chaos, Solitons and Fractals*, **31**, (2007), pp. 261–268.
251. A. d'Onofrio, Rapidly acting antitumoral anti-angiogenic therapies, *Physical Review E*, **76**(3), art. no. 031920, (2007).
252. A. d'Onofrio, Metamodeling tumor-immune system interaction, tumor evasion and immunotherapy, *Mathematical and Computer Modelling*, **47**, (2008), pp. 614–637.
253. A. d'Onofrio, Fractal growth of tumors and other cellular populations: Linking the mechanistic to the phenomenological modeling and vice versa, *Chaos, Solitons and Fractals*, **41**, (2009), pp. 875–880.
254. A. d'Onofrio, Fractal growth of tumors and other cellular populations: Linking the mechanistic to the phenomenological modeling and vice versa, *Chaos, Solitons and Fractals*, **41**, (2009), pp. 875–880.
255. A. d'Onofrio, Bounded-noise-induced transitions in a tumor-immune system interplay, *Physics Reviews E*, **81**, (2010), art. no. 021923, doi: 10.1103/PhysRevE.81.021923.

256. A. d'Onofrio, A. Fasano, and B. Monechi, A generalization of Gompertz law compatible with the Gyllenberg-Webb theory for tumour growth *Mathematical Biosciences*, **230**(1), (2011), pg. 45–54.
257. A. d'Onofrio and A. Gandolfi, Tumour eradication by antiangiogenic therapy: analysis and extensions of the model by Hahnfeldt et al. (1999), *Mathematical Biosciences*, **191**, (2004), pp. 159–184.
258. A. d'Onofrio, and A. Gandolfi, The response to antiangiogenic anticancer drugs that inhibit endothelial cell proliferation, *Applied Mathematics and Computation*, **181**, (2006), pp. 1155–1162.
259. A. d'Onofrio and A. Gandolfi, A family of models of angiogenesis and anti-angiogenesis anti-cancer therapy, *Mathematical Medicine and Biology*, **26**, (2009), pp. 63–95, doi:10.1093/imammb/dqn024.
260. A. d'Onofrio and A. Gandolfi, Resistance to anti-tumor chemotherapy due to bounded-noise transitions, *Physics Reviews E*, **82**, (2010) art. no. 061901.
261. A. d'Onofrio, and A. Gandolfi, Chemotherapy of vascularised tumours: role of vessel density and the effect of vascular "pruning", *J. of Theoretical Biology*, **264**, (2010), pp. 253–265.
262. A. d'Onofrio, and A. Gandolfi, *Mathematical Oncology 2013*, Birkhäuser, New York, 2014.
263. A. d'Onofrio, A. Gandolfi and A. Rocca, The dynamics of tumour-vasculature interaction suggests low-dose, time-dense antiangiogenic schedulings, *Cell Proliferation*, **42**, (2009), pp. 317–329.
264. A. d'Onofrio, U. Ledzewicz, H. Maurer and H. Schättler, On optimal delivery of combination therapy for tumors, *Mathematical Biosciences*, **222**, (2009), pp. 13-26, doi:10.1016/j.mbs.2009.08.004.
265. A. d'Onofrio, U. Ledzewicz and H. Schättler, On the dynamics of tumor immune system interactions and combined chemo- and immunotherapy, in: New Challenges for Cancer Systems Biomedicine (A. d'Onofrio, P. Cerrai and A. Gandolfi, Eds.), SIMAI Springer series, Vol. 1, 2012, pp. 249–266.
266. M.S. O'Reilly, T. Boehm, Y. Shing, N. Fukai, G. Vasios, W.S. Lane, E. Flynn, J.R. Birkhead, B.R. Olsen, and J. Folkman, Endostatin: an endogenous inhibitor of angiogenesis and tumour growth, *Cell*, **88**, (1997), pp. 277–285.
267. S.F.C. O'Rourke, H. McAneney and T. Hillen, Linear quadratic and tumour control probability modelling in external beam radiotherapy, *J. of Mathematical Biology*, **58**, (2009), pp. 799–817, doi: 10.1007/s00285-008-0222-y.
268. J.C. Panetta, A mathematical model of breast and ovarian cancer treated with paclitaxel, *Mathematical Biosciences*, **146**, (1997), pp. 83–113.
269. J.C. Panetta, A. Wall, C.H. Pui, M.V. Relling, W.E. Evans, Methotrexate intracellular disposition in acute lymphoblastic leukemia: a mathematical model of gammaglumatyl hydrolase activity, *Clinical Cancer Research*, **8**, (2002), pp. 2423–2439.
270. J.C. Panetta, Y. Yanishevski, C.H. Pui, J.T. Sandlund, J. Rubnitz, G.K. Rivera, R. Ribeiro, W.E. Evans, M.V. Relling, A mathematical model of in vivo methotrexate accumulation in acute lymphoblastic leukemia, *Cancer Chemotherapy and Pharmacology*, **50**, (2002), pp. 419–428.
271. D. Pardoll, Does the Immune System see Tumors as foreign or self? *Annual Review of Immunology*, **21**, (2003), pp. 807–839.
272. E. Pasquier, M. Kavallaris and N. André, Metronomic chemotherapy: new rationale for new directions, *Nature Reviews|Clinical Oncology*, **7**, (2010), pp. 455–465.
273. E. Pasquier, and U. Ledzewicz, Perspective on "More is not necessarily better": Metronomic Chemotherapy, Newsletter of the Society for Mathematical Biology, **26**(2), (2013), pp. 9–10.
274. M. Peckham, H.M. Pinedo, and U. Veronesi, *Oxford Textbook of Oncology*, Oxford Medical Publications, Oxford, 1995.
275. A.S. Perelson, Mathematical approaches to immunology, in: Theory and Control of Dynamical Systems: Applications to Systems in Biology, (S.I. Andersson, A.E. Andersson, and U. Ottoson, Eds.), World Scientific Press, Singapore, (1992), pp. 200–230.
276. B. Piccoli and H. Sussmann, Regular synthesis and sufficient conditions for optimality, *SIAM J. on Control and Optimization*, **39**, (2000), pp. 359-410

277. K. Pietras and D. Hanahan, A multi-targeted, metronomic and maximum tolerated dose "chemo-switch" regimen is antiangiogenic, producing objective responses and survival benefit in a mouse model of cancer, *J. of Clinical Oncology*, **23**, (2005), pp. 939–952.
278. L.G. de Pillis, W. Gu and A. Radunskaya, Mixed immunotherapy and chemotherapy of tumors: modeling, applications and biological interpretations, *J. of Theoretical Biology*, **238**, (2006), pp. 841–862.
279. L.G. de Pillis and A. Radunskaya, A mathematical tumor model with immune resistance and drug therapy: an optimal control approach, *J. of Theoretical Medicine*, **3**, (2001), pp. 79–100.
280. L.G. de Pillis, A. Radunskaya and C.L. Wiseman, A validated mathematical model of cell-mediated immune response to tumor growth, *Cancer Research*, **65**, (2005), pp. 7950–7958.
281. J. Poleszczuk and U. Forys, Derivation of the Hahnfeldt et al. model (1999) revisited, Proc. of the 16th National Conference on Applications of Mathematics in Biology and Medicine, Krynica, Poland, September 2010, pp. 87–92.
282. L.S. Pontryagin, V.G. Boltyanskii, R.V. Gamkrelidze and E.F. Mishchenko, *The Mathematical Theory of Optimal Processes*, MacMillan, New York, 1964.
283. D.Z. Qian, X. Wang, S.K. Kachhap, Y. Kato, Y. Wei, L. Zhang, P. Atadja and R. Pili, The histone deacetylase inhibitor NVP-LAQ824 inhibits angiogenesis and has a greater antitumor effect in combination with the vascular endothelial growth factor receptor tyrosine kinase inhibitor PTK787/ZK222584, *Cancer Research*, **64**(18), (2004), pp. 6626–6634.
284. A.V. Rao, D.A. Benson, G.T. Huntington, C. Francolin, C.L. Darby, and M.A. Patterson, User's Manual for GPOPS: A MATLAB Package for Dynamic Optimization Using the Gauss Pseudospectral Method, University of Florida Report, 2008.
285. R. Retsky, Metronomic Chemotherapy was originally designed and first used in 1994 for early stage cancer - why is it taking so long to proceed?, *Bioequivalence and Bioavailability*, (editorial), **3**(4), http://dx.doi.org/10.4172/jbb.100000e6.
286. R.K. Sachs, P. Hahnfeldt and D.J. Brenner, The link between low-LET dose-response relations and the underlying kinetics of damage production/repair/misrepair, *Int. J. Radiation Biology*, **72**(4), (1997), pp. 351–374.
287. R.K. Sachs, L.R. Hlatky and P. Hahnfeldt, Simple ODE models of tumor growth and anti-angiogenic or radiation treatment, *Mathematical and Computer Modelling*, **33**, (2001), pp. 1297–1305.
288. E. Sackmann, *Biological Membranes Architecture and Function*, Handbook of Biological Physics, (R. Lipowsky and E. Sackmann, Eds.), Vol. 1, Elsevier, 1995
289. H. Sbeity and R. Younes, Review of optimization methods for cancer chemotherapy treatment planning, *Computational Biology Journal*, (2015), to appear.
290. H. Schättler, U. Ledzewicz and B. Amini, Dynamical properties of a minimally parameterized mathematical model for metronomic chemotherapy, *J. of Mathematical Biology*, (2015), doi: 10.1007s/00285-015-0907y
291. H. Schättler and M. Jankovic, A Synthesis of time-optimal controls in the presence of saturated singular arcs, *Forum Mathematicum*, **5**, (1993), pp. 203–241.
292. H. Schättler and U. Ledzewicz, *Geometric Optimal Control*, Springer, New York, 2012.
293. H. Schättler, U. Ledzewicz and B. Cardwell, Robustness of optimal controls for a class of mathematical models for tumor anti-angiogenesis, *Mathematical Biosciences and Engineering- MBE*, **8**(2), (2011), pp. 355–369.
294. H. Schättler, U. Ledzewicz, S. Mahmoudian Dehkordi and M. Reisi Gahrooi, A geometric analysis of bang-bang extremals in optimal control problems for combination cancer chemotherapy, Proc. of the 51st IEEE Conference on Decision and Control, Maui, Hawaii, December 2012, pp. 7691–7696.
295. H. Schättler, U. Ledzewicz and H. Maurer, Sufficient conditions for strong local optimality in optimal control problems with L_2-type objectives and control constraints, *Discrete and Continuous Dynamical Systems, Series B*, **19**(8), (2014), pp.
296. R.T. Schimke, Gene amplification, drug resistance and cancer, *Cancer Research*, **44**, (1984), pp. 1735–1742.

297. J. Schmielau and O.J. Finn, Activated granulocytes and granulocyte-derived hydrogen peroxide are the underlying mechanism of suppression of T-cell function in advanced cancer patients, *Cancer Research*, **61**, (2001), pp. 4756–4760.
298. H.E. Skipper, On mathematical modeling of critical variables in cancer treatment (goals: better understanding of the past and better planning in the future), *Bulletin of Mathematical Biology*, **48**, (1986), pp. 253–278.
299. R.V. Sole, Phase transitions in unstable cancer cell populations, *European J. Physics B*, **35**, (2003), pp. 117–124.
300. J.A.M. Felippe de Souza, M.A.L. Caetano and T. Yoneyama, Optimal control theory applied to the anti-viral treatment of AIDS, Proc. of the 39th IEEE Conference on Decision and Control, Sydney, Australia, (2000), pp. 4839–4844.
301. E. Sontag. Some new directions in control theory inspired by systems biology, *IET Systems Biology*, **1**, (2004), pp. 9–18.
302. E. Sontag, Molecular Systems Biology and Control, *European J. of Control*, **11**, (2005), pp. 1–40.
303. N.V. Stepanova, Course of the immune reaction during the development of a malignant tumour, *Biophysics*, **24**, (1980), pp. 917–923.
304. T.J. Stewart and S.I. Abrams, How tumours escape mass destruction, *Oncogene*, **27**, (2008), pp. 5894–5903.
305. J. Stoer and R. Bulirsch, *Introduction to Numerical Analysis*, Springer-Verlag, New York, 1990.
306. G.W. Swan, *Applications of Optimal Control Theory in Medicine*, Marcel Dekker, New York, 1984.
307. G.W. Swan, General applications of optimal control theory in cancer chemotherapy, *IMA J. of Mathematical Applications in Medicine and Biology*, **5**, (1988), pp. 303–316.
308. G.W. Swan, Role of optimal control in cancer chemotherapy, *Mathematical Biosciences*, **101**, (1990), pp. 237–284.
309. J.B. Swann and M.J. Smyth, Immune surveillance of tumors, *J. Clinical Investigations*, **117**, (2007), pp. 1137–1146.
310. M.A. Swartz, N. Iida, E.W. Roberts, S. Sangaletti, M.H. Wong, F.E. Yull, L.M. Coussens, and Y.A. DeClerck, Tumor microenvironment complexity: Emerging roles in cancer therapy, *Cancer Research*, **72**, (2012), pp. 2473–2480.
311. A. Swierniak, Optimal treatment protocols in leukemia - modelling the proliferation cycle, Proc. of the 12th IMACS World Congress, Paris, **4**, (1988), pp. 170–172.
312. A. Swierniak, Some control problems for simplest differential models of proliferation cycle, *Applied Mathematics and Computer Science*, **4**, (1994), pp. 223–232.
313. A. Swierniak, Cell cycle as an object of control, *Journal of Biological Systems*, **3**, (1995), pp. 41–54.
314. A. Swierniak, Direct and indirect control of cancer populations, *Bulletin of the Polish Academy of Sciences*, Technical Sciences, **56**(4), (2008), pp. 367–378.
315. A. Swierniak, Modelling combined angiogenic and chemotherapy, Proc. of the 14th National Conf. on Applications of Mathematics in Biology and Medicine, Leszno, Poland, (2008), pp. 127–133.
316. A. Swierniak, Comparison of control theoretic properties of models of antiangiogenic therapy, Proc. of the 6th International IASTED Conference on Biomedical Engineering, Acta Press, (2008), pp. 156–160.
317. A. Swierniak and Z. Duda, Singularity of optimal control in some problems related to optimal chemotherapy, *Mathematical and Computational Modelling*, **19**, (1994), pp. 255–262.
318. A. Swierniak and Z. Duda, Bilinear models of cancer chemotherapy-singularity of optimal solutions, in: Mathematical Population Dynamics, **2**, (1995), pp. 347–358.
319. A. Swierniak, A. d'Onofrio, A. Gandolfi, Optimal control problems related to tumor angiogenesis, Proc. IEEE-IECON'2006, pp. 667–681.
320. A. Swierniak, G. Gala, A. Gandolfi and A. d'Onofrio, Optimization of angiogenic therapy as optimal control problem, Proc. of the 4th IASTED Conference on Biomechanics, Acta Press, (M. Doblare, Ed.), (2006), pp. 56–60.

321. A. Swierniak, U. Ledzewicz and H. Schättler, Optimal control for a class of compartmental models in cancer chemotherapy, *Int. J. Applied Mathematics and Computer Science*, **13**, (2003), pp. 357–368.
322. A. Swierniak, A. Polanski and Z. Duda, "Strange" phenomena in simulation of optimal control problems arising in cancer chemotherapy, Proc. of the 8th Prague Symposium on Computer Simulation in Biology, Ecology and Medicine, (1992), pp. 58–62.
323. A. Swierniak, A. Polanski and M. Kimmel, Optimal control problems arising in cell-cycle-specific cancer chemotherapy, *Cell proliferation*, **29**, (1996), pp. 117–139.
324. A. Swierniak, A. Polanski, M. Kimmel, A. Bobrowski and J. Smieja, Qualitative analysis of controlled drug resistance model - inverse Laplace and semigroup approach, *Control and Cybernetics*, **28**, (1999), pp. 61–75.
325. A. Swierniak and J. Smieja, Cancer chemotherapy optimization under evolving drug resistance, *Nonlinear Analysis*, **47**, (2000), pp. 375–386.
326. A. Tafuri and M. Andreeff, Kinetic rationale for cytokine-induced recruitment of myeloblastic leukemia followed by cycle-specific chemotherapy in vitro, *Leukemia*, **4**, (1990), pp. 826–834.
327. I. Tannock, Cell kinetics and chemotherapy: a critical review, *Cancer Treatment Reports*, **62**(8), (1978), pp. 1117–1133.
328. D. Tee and J. DiStefano III, Simulation of tumour-induced angiogenesis and its response to anti-angiogenic drug treatment: mode of drug delivery and clearance rate dependencies, *J. of Cancer Research and Clinical Oncology* **130**, (2004), pp. 15–24.
329. H.D. Thames and J.H. Hendry, *Fractionation in Radiotherapy*, Taylor and Francis, London, 1987.
330. C.A. Tobias, E.A. Blakeley, F.Q.H. Ngo and T.C.H. Yang, The repair-misrepair model of cell survival, in: *Radiation Biology and Cancer Research*, (R.E. Meyn and H.R. Withers, Eds.), Raven Press, New York, 1980, pp. 195–230.
331. C. Tomasetti and D. Levy, An elementary approach to modeling drug resistance in cancer, *Mathematical Biosciences and Engineering*, **7**, (2010), pp. 905–918.
332. E. Toyota, T. Ohtsuki, N. Kamiyama, T. Fukushima, L. Shirato, A. Kanzaki, O. Yamada and Y. Yawata, Hypoplastic leukemia successfully treated with low-dose aclarubicin: a case report, *Rinsho Ketsueki*, **32**, (1991), pp. 996–1000 [in Japanese].
333. M. Villasana, G. Ochoa and S. Aguilar, Modeling and optimization of combined cytostatic and cytotoxic cancer chemotherapy, *Artificial Intelligence in Medicine*, **50**, (2010), pp. 163–173.
334. H.P. de Vladar and J.A. González, Dynamic response of cancer under the influence of immunological activity and therapy, *J. of Theoretical Biology*, **227**, (2004), pp. 335–348.
335. H. Vodopick, E.M. Rupp, C. L. Edwards, F.A. Goswitz and J.J. Beauchamp, Spontaneous cyclic leukocytosis and thrombocytosis in chronic granulocytic leukemia, *New England J. of Medicine*, **286**, (1972), pp. 284–290.
336. G. de Vries, T. Hillen, M. Lewis, J. Müller, and B. Schönfisch, *A Course in Mathematical Biology: Quantitative Modeling with Mathematical & Computational Methods*, SIAM, Mathematical Modeling and Computation, Vol. 12, 2006.
337. A. Wächter and L.T. Biegler, On the implementation of an interior-point filter line-search algorithm for large-scale nonlinear programming, *Mathematical Programming*, **106**, (2006), pp. 25–57.
338. G.F. Webb, Resonance phenomena in cell population chemotherapy models, *Rocky Mountain J. of Mathematics*, **20**, (1990), pp. 1195–1216.
339. G.F. Webb, Resonance in periodic chemotherapy scheduling, Proc. of the First World Congress of Nonlinear Analysts, Vol. 4, (V. Lakshmikantham, Ed.), Walter DeGruyter, Berlin, 1995, pp. 3463–3747.
340. L.M. Wein, J.E. Cohen, J.T. Wu, Dynamic optimization of a linear-quadratic model with incomplete repair and volume-dependent sensitivity and repopulation, *Int. J. of Radiation Oncology*, **47**(4), (2000), pp. 1073–1083.
341. S.D. Weitman, E. Glatstein and B.A. Kamen, Back to the basics: the importance of concentration $\times$ time in oncology, *J. of Clinical Oncology*, **11**, (1993), pp. 820–821.

342. J.J. Westman, B.R. Fabijonas, D.L. Kern and F.B. Hanson, Cancer treatment using multiple chemotherapeutic agents subject to drug resistance, Proc. of the 15th International Symposium of Mathematical Theory of Networks and Systems (MTNS), August 2002.
343. T.E. Wheldon, *Mathematical Models in Cancer Research*, Boston-Philadelphia: Hilger Publishing, 1988.
344. T.L. Whiteside, Tumor-induced death of immune cells: its mechanisms and consequences, *Seminars in Cancer Biology*, **12**, (2002), pp. 43–50.
345. N.S. Wijeratne and K.A. Hoo, Understanding the role of the tumour vasculature in the transport of drugs to solid cancer tumors, *Cell Proliferation*, **40**, (2007), pp. 283–301.
346. J.L. Yu and J.W. Rak, Host microenvironment in breast cancer development: Inflammatory and immune cells in tumour angiogenesis and arteriogenesis, *Breast Cancer Research* **5**, (2003), pp. 83–88.
347. B. Yu, S. Kusmartsev, F. Cheng, M. Paolini, Y. Nefedova, E. Sotomayor and D. Gabrilovich, Effective combination of chemotherapy and dendritic cell administration for the treatment of advanced-stage experimental breast cancer, *Clinical Cancer Research*, **9**, (2003), pp. 285–294.
348. M.I. Zelikin and V.F. Borisov, *Theory of Chattering Control with Applications to Astronautics, Robotics, Economics and Engineering*, Birkhäuser, Boston, 1994.

Index

H. Schättler, U. Ledzewicz, *Optimal Control for Mathematical Models of Cancer Therapies*, Interdisciplinary Applied Mathematics 42,
DOI 10.1007/978-1-4939-2972-6